



**PHYTOCHEMICAL INVESTIGATION AND BIOLOGICAL
STUDIES OF SOME SOUTH AFRICAN PLANT SPECIES
(ASTERACEAE AND HYACINTHACEAE)**

By

FUNSHO MARY OYETUNDE-JOSHUA

2021

**PHYTOCHEMICAL INVESTIGATION AND BIOLOGICAL STUDIES OF SOME
SOUTH AFRICAN PLANT SPECIES (ASTERACEAE AND HYACINTHACEAE)**

By

FUNSHO MARY OYETUNDE-JOSHUA (216077005)

2021

A thesis submitted in fulfilment of the requirements for the degree of Doctor of Philosophy in the School of Chemistry and Physics, College of Agriculture, Engineering and Science, University of KwaZulu-Natal, Westville. This thesis has been prepared according to **Format 4** as outlined in the guidelines from the College of Agriculture, Engineering and Science.

Supervisor:

Signed:



Name: Professor Roshila Moodley

Date: 14/10/2021

ABSTRACT

Plants used in conventional medicine for the treatment of different ailments have been the bedrock for modern therapeutics. *Scilla nervosa* from the Hyacinthaceae family and *Helichrysum panduratum* and *Helichrysum actutaum* from the Asteraceae family are plants used in traditional medicine in South Africa. However, limited information exists on the biological potential and safety of these plants. This research aimed to phytochemically investigate these plants by isolating and characterizing their secondary metabolites and testing their biological activities.

The phytochemical investigation of *S. nervosa* yielded eleven compounds, including two novel homoisoflavonoids, two novel lanostane-type triterpenes, five known homoisoflavonoids, one stilbene and one sterol glucoside. The cytotoxicity of the homoisoflavonoids was good against the Caco-2 tumor cell line but moderate against the HepG2 cell line and the methanol extract of the leaves showed promising activity against Caco-2 and HepG2 cell lines, giving IC₅₀ values of 7.79 and 9.29 µg/mL, respectively. For homoisoflavonoids, polarity influenced activity, with the least polar compounds being more active. Likewise, saturation between the benzopyrone ring and ring C contributed to activity. The homoisoflavonoids with methoxy substituents displayed better antibacterial activity than those with hydroxy substituents but these were still lower than flavonoids. Molecular docking using MraY phospho-MurNAc-pentapeptide translocase was conducted on the bioactive homoisoflavonoids to rationalize their antibacterial activity. The results showed isolates to bind in the same active site of the substrate, with a slight difference due to the presence of the hydroxy group.

The phytochemical investigation of *H. panduratum* led to the isolation of a sterol, a sterol glucoside, three triterpenes, a phenolic glucoside, and one homoisoflavonoid, which is the first

report of this group of flavonoids from *Helichrysum* genus. The plant was shown to have moderate antibacterial activity. Screening of the quorum sensing-controlled phenotype of bioluminescence in *Vibrio harveyi* BB120 was conducted. The methanol extract of the leaves could inhibit Gram-negative N-acyl homoserine lactone-based and global crosstalk autoinducer-2-based quorum sensing. The cytotoxicity assay showed reduced activity towards Caco-2, HepG2 and the regular cell line Hek 293, making it safe for human use.

H. acutatum yielded three compounds, a sterol, a sterol glucoside and a cinnamic acid derivative. The plant showed no antibacterial activity and no cytotoxicity towards the normal cell line, Hek 293, making it safe for human consumption. The ethyl acetate extract of the root demonstrated good antioxidant activity, which could be attributed to the cinnamic acid derivative. The leaves of *H. panduratum* are rich in arbutin, a natural hydroquinone form, making it valuable in cosmetology.

The antibacterial potential of the isolated homoisoflavonoids could be enhanced by synthetic manipulations of the molecular framework. These modifications could also improve selectivity towards tumor cell lines. The findings from this study provide scientific evidence for the use of the plants in traditional medicine, especially *H. acutatum*, for which there are no reports on its use or biological activity.

LIST AND STRUCTURES OF ISOLATED COMPOUNDS

Compounds **A1**–**A11** isolated from *Scilla Nervosa* (Burch.) Jessop:

A1 - 3-(4-Methoxybenzyl)-5,7-dimethoxychroman-4-one

A2 - 3-(4-Methoxybenzyl)-6-hydroxy-5,7-dimethoxychroman-4-one

A3 - 3-(4-Hydroxybenzyl)-6-hydroxy-5,7-dimethoxychroman-4-one

A4 - 3-(4-Hydroxy-3-methoxybenzyl)-5-hydroxy-7-methoxychroman-4-one

A5 - 3-(4-Hydroxy-3-methoxybenzyl)-5,7-dihydroxy-6-methoxychroman-4-one

A6 - 3-(4-Hydroxy-3-methoxybenzyl)-5,6,7-trihydroxychroman-4-one

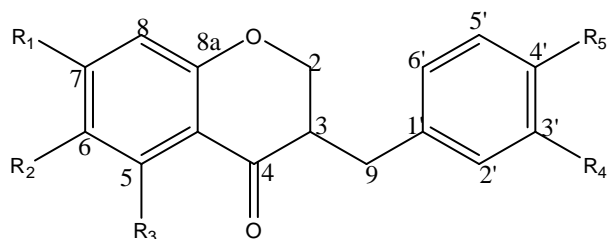
A7 - 3-Benzylidienechroman-4-one

A8 - Rhapontigenin

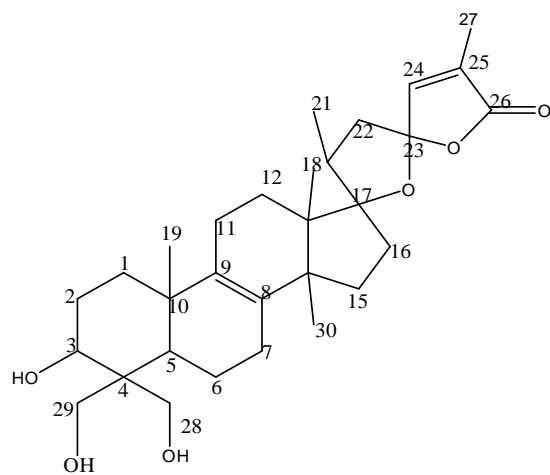
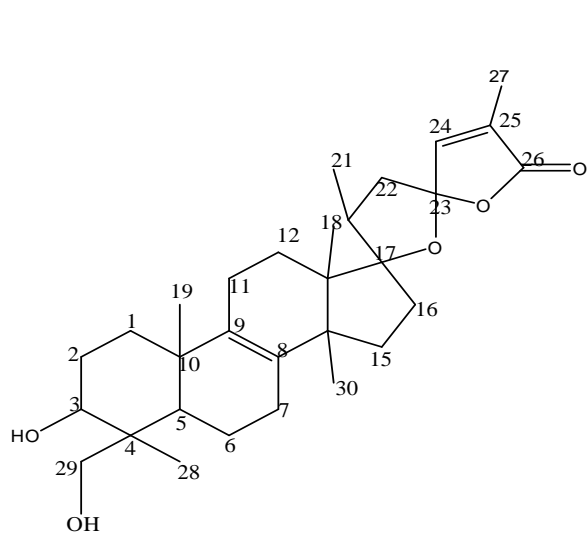
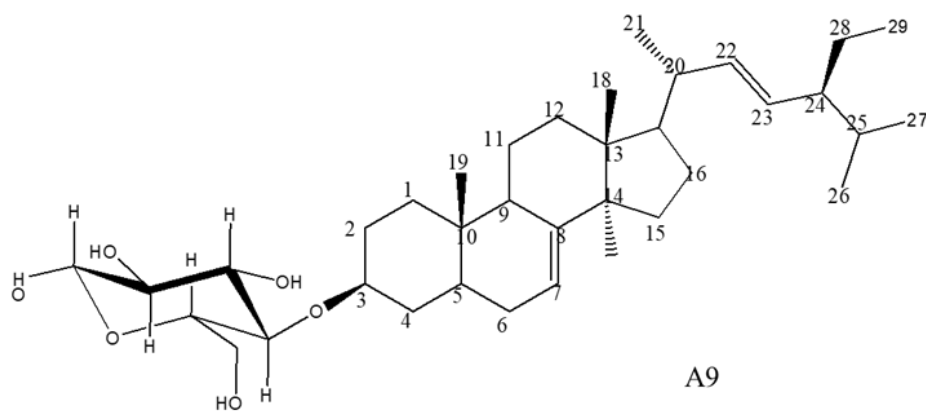
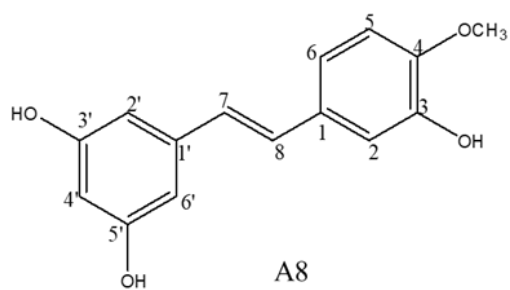
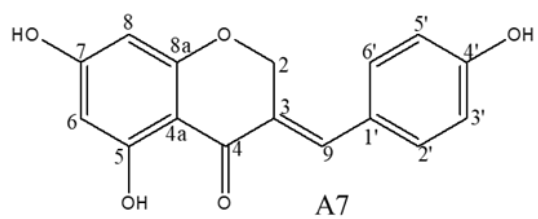
A9 - Spinasterol-3-*O*- β -d-glucopyranoside

A10 - 17 α ,23 α -Epoxy-3 β ,29-dihydroxy-nor-lanost-8,24-dien-26-one

A11 - 17 α ,23 α -Epoxy-3 β ,28,29-trihydroxy-nor-lanost-8,24-dien-26-one



	R ₁	R ₂	R ₃	R ₄	R ₅
A1	OCH ₃	H	OCH ₃	H	OCH ₃
A2	OCH ₃	OH	OCH ₃	H	OCH ₃
A3	OCH ₃	OH	OCH ₃	H	OH
A4	OCH ₃	H	OH	OCH ₃	OH
A5	OH	OH	OH	OCH ₃	OH
A6	OCH ₃	OH	OH	OCH ₃	OH



Compounds **B1–B7** isolated from *Helichrysum panduratum* O.Hoffm.:

B1 - Stigmasterol

B2 - Stigmasterol glucoside

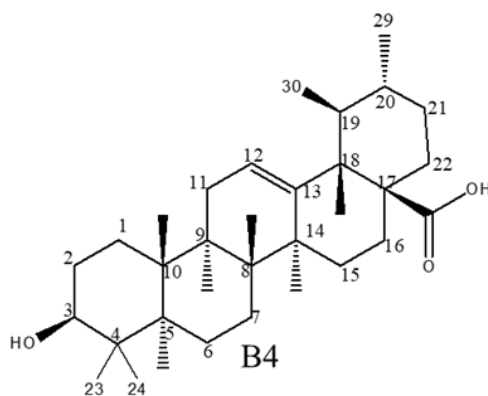
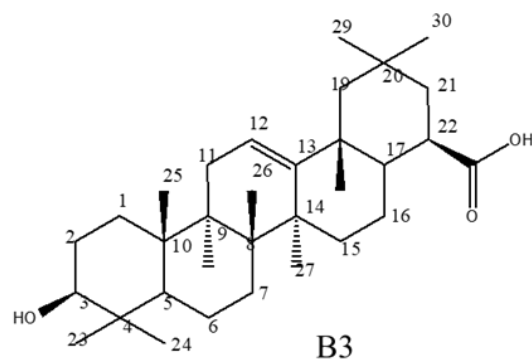
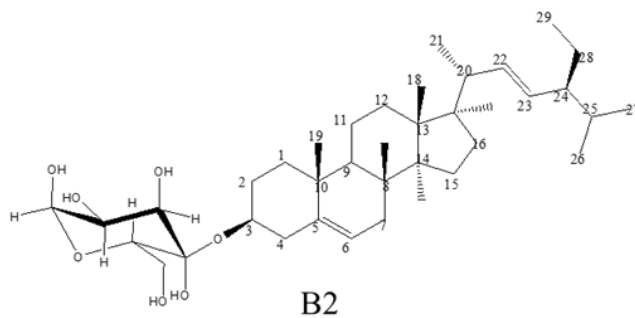
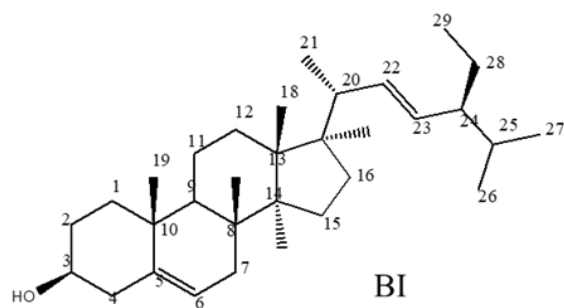
B3 - Oleanolic acid

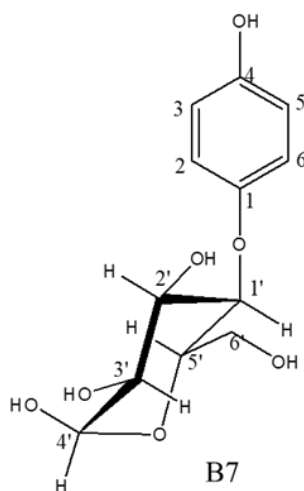
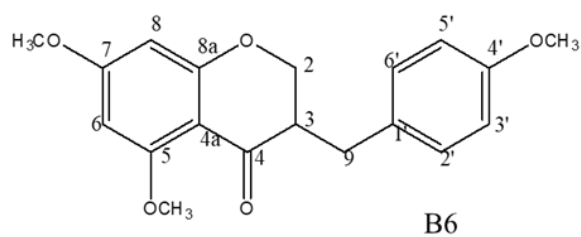
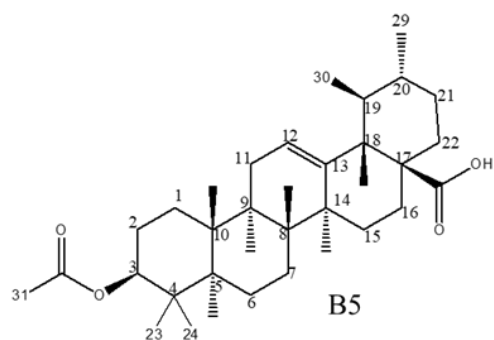
B4 - Ursolic acid

B5 - 3-Acetyl ursolic acid

B6 - 3-(4-Methoxybenzyl)-5,7-dimethoxychroman-one

B7 - α -Arbutin



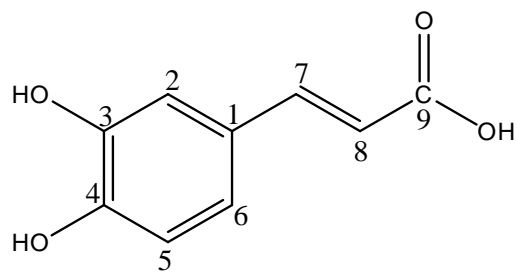
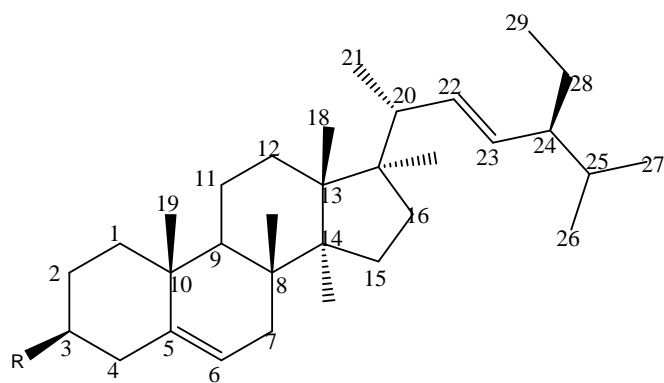


Compounds **C1–C3** isolated from *Helichrysum acutatum* DC:

C1 - Stigmasterol

C2 - Stigmasterol glucoside

C3 - Caffeic acid



C1: R=H

C2: R= Glucoside

LIST OF ABBREVIATIONS

^{13}C -NMR	C-13 nuclear magnetic resonance spectroscopy
^1H -NMR	proton nuclear magnetic resonance spectroscopy
ATP	adenosine triphosphate
Caco-2	colorectal adenocarcinoma cells
CCM	complete culture media
COSY	correlated spectroscopy
d	doublet
dd	double doublet
DEPT	distortionless enhancement by polarization transfer
DMEM	Dulbecco's modified eagle medium
DPPH	2,2-diphenyl-1-picrylhydrazyl
FRAP	ferric reducing antioxidant potential
FTIR	Fourier-transform infrared
Hek 293	human embryonic kidney cell
HepG2	liver hepatocellular carcinoma cell
HMBC	heteronuclear multiple bond coherence
HRMS	high resolution mass spectrometry

HSQC	heteronuclear single quantum coherence
IR	infrared
LDH	lactate dehydrogenase
m	multiplet
MMP	mitochondrial membrane potential
MTT	3-(4,5-dimethylthiazol-2-yl)-2,5-diphenyltetrazolium bromide
NOESY	nuclear overhauser effect spectroscopy
PBS	phosphate buffered saline
s	singlet
TLC	thin layer chromatography

DECLARATIONS

Declaration 1: Plagiarism

I, Funsho Mary Oyetunde-Joshua, declare that:

1. The research reported in this thesis is my original research.
2. The work described in this thesis has not been submitted to UKZN or other tertiary institution for purposes of obtaining an academic qualification, whether by myself or any other party.
3. This thesis does not contain other persons' data, pictures, graphs or other information, unless specifically acknowledged as being sourced from other persons.
4. This thesis does not contain other persons' writing, unless specifically acknowledged as being sourced from other researchers. Where other written sources have been quoted, then:
 - a. Their words have been re-written, but the general information attributed to them has been referenced.
 - b. Where their exact words have been used, then their writing has been placed in italics and inside quotation marks and referenced.
5. This thesis does not contain text, graphics or tables copied and pasted from the Internet, unless specifically acknowledged, and the source being detailed in the thesis and in the References sections.

Signe 

Funsho Mary Oyetunde-Joshua

Declaration 2: Publications and Conferences

Publication 1

Title: Phytochemical, antibacterial and docking studies of *Scilla nervosa* (Burch.) Jessop **Authors:** Funsho Mary Oyetunde-Joshua and Roshila Moodley

Journal: Manuscript prepared for submission to Journal of Ethnopharmacology.

Publication 2

Title: Evaluation of the cytotoxic potential of homoisoflavonoids and extracts from *Scilla nervosa* (Burch.) Jessop

Authors: Funsho Mary Oyetunde-Joshua and Roshila Moodley

Journal: Manuscript prepared for submission to Anticancer Agents in Medicinal Chemistry.

Publication 3

Title: Phytochemical, antibacterial and cytotoxicity studies of *Helichrysum panduratum* O.Hoffm.

Authors: Funsho Mary Oyetunde-Joshua and Roshila Moodley

Journal: Manuscript prepared for submission to Scientific Reports.

Publication 4

Title: Phytochemical and biological studies of *Helichrysum acutatum* DC.

Authors: Funsho Mary Oyetunde-Joshua and Roshila Moodley.

Journal: Manuscript prepared for submission to South African Journal of Botany.

Title: Postgraduate Research and Innovative Symposium. University of KwaZulu-Natal, Westville Campus, Durban. October 2019.

Poster: Phytochemical analysis of *Helichrysum panduratum* by Funsho Mary Oyetunde-Joshua and Roshila Moodley.

In all the publications, I have performed all the experimental work and written the manuscripts. The co-authors were involved in discussion of the results and were responsible for verifying the scientific content and accuracy of the results as well as editing the manuscripts.

Signed: 

Funsho Mary Oyetunde-Joshua

ACKNOWLEDGEMENTS

Foremost, my gratitude goes to the Almighty God, my Sustainer, and my Stay for seeing me through this journey.

My unreserved thanks to my supervisor, Professor Roshila Moodley, for believing in me and accepting to supervise me, also for her love and unflinching support from the beginning till the completion of this work. You are amazing.

I am also indebted to Dr Hafizah Cheniah for the antibacterial and anti-quorum sensing assays, and Dr Rene Myburg for the cytotoxicity assay. Thank you for guiding me through and making your laboratory available.

I acknowledge my colleagues in the Natural Product Research group, Amanda, Thabile, Dr Paul and those who have graduated from the group Dr Sunday, Dr Nomfundo, Dr Esther, Dr Neal and Dr Kemi for their help and support. Thanks to Mr. Theophilus Adedokun for his support.

Thanks to my parents who started me on a good path academically, and my siblings for their love. My appreciation to my spiritual parents who never stopped praying for me; Pastor Yomi and Dr Tayo Ajayi, Rev. Adesina and Mrs. Grace Adediran, Rev. Chucks and Mrs. Pat Obiechie, Pastor Peace and Mrs. Elizabeth Olanisinmi.

Lastly, I would like to thank my husband for his love, prayers, and support. You never stopped believing in me even when I did not believe in myself. Thank you for pushing, thank you for working hard to make us comfortable, God bless you really good and I love you. And my children, Gloria and Doxa, thank you for bearing and understanding with mummy as she did her program. I love you guys.

CONTENTS

ABSTRACT.....	iii
LIST AND STRUCTURES OF ISOLATED COMPOUNDS	v
DECLARATIONS.....	xi
ACKNOWLEDGEMENTS	xiii
LIST OF FIGURES	xvi
LIST OF TABLES.....	xix
CHAPTER ONE	1
1.1 INTRODUCTION.....	1
1.2 RATIONALE FOR THE RESEARCH.....	2
1.3 AIMS AND OBJECTIVES.....	3
1.4 STRUCTURE OF THE THESIS	4
REFERENCES.....	5
CHAPTER TWO	8
LITERATURE REVIEW	8
2.1 NATURAL PRODUCTS AS THERAPEUTIC AGENTS.....	8
2.2 TRADITIONAL MEDICINE IN SOUTH AFRICA.....	10
2.3 PLANTS AS A SOURCE OF THERAPEUTICS	11
2.4 SECONDARY METABOLITES.....	12
2.5 THE GENUS <i>HELICHRYSUM</i>	20
2.6 THE GENUS <i>SCILLA</i>	24
2.7 BIOLOGICAL ASSAYS	27
CHAPTER 3	54
Phytochemical, antibacterial and docking studies of <i>Scilla nervosa</i> (Burch.) Jessop	54
ABSTRACT	54
3.1 INTRODUCTION.....	55
3.2. MATERIALS AND METHODS	57
3.3 RESULTS AND DISCUSSION	61
3.4 CONCLUSION	75
REFERENCES.....	76
CHAPTER 4	87

Evaluation of the cytotoxic potential of homoisoflavonoids and extracts from <i>Scilla nervosa</i> (Burch.) Jessop.....	87
ABSTRACT	87
4.1 INTRODUCTION.....	88
4.2 MATERIALS AND METHODS	90
4.3 RESULTS.....	93
4.3 DISCUSSION	100
4.4 CONCLUSION	107
REFERENCES.....	108
CHAPTER 5	114
Phytochemical, antibacterial and cytotoxicity studies of <i>Helichrysum panduratum</i> O.Hoffm. .	114
ABSTRACT	114
5.1 INTRODUCTION.....	115
5.2 MATERIALS AND METHODS	117
5.3 RESULTS.....	124
5.4 DISCUSSION	138
5.5 CONCLUSION	143
REFERENCES.....	144
CHAPTER 6	153
Phytochemical and biological studies of <i>Helichrysum acutatum</i> DC.....	153
ABSTRACT	153
6.1 INTRODUCTION.....	154
6.2 MATERIALS AND METHODS	155
6.3 RESULTS.....	161
6.4 DISCUSSION	169
6.5 CONCLUSION	173
REFERENCES.....	174
CHAPTER SEVEN	179
OVERALL SUMMARY.....	179
CONCLUSION	180
RECOMMENDATIONS FOR FUTURE WORK.....	181
APPENDICES	182

LIST OF FIGURES

Figure 2.1 Different extraction methods.....	13
Figure 2.2 The principal of separation in column chromatography.....	14
Figure 2.3 Structures of eucomin and eucomol, the first homoisoflavonoids isolated from <i>E. bicolor</i>	15
Figure 2.4 General structure of a flavonoid and homoisoflavonoid.	15
Figure 2.5 Carbon skeletons of homoisoflavonoids.	16
Figure 2.6 Four groups with the 3-benzyl chromane skeleton: (A) 3-benzyl-4-chromanones, (B) 3-hydroxy-3-benzyl-4-chromanones, (C) 3-benzylidene-4-chromanones and (D) 3-benzyl-chrom-2-en-4-ones.....	16
Figure 2.7 Scheme showing proposed biosynthetic routes of sappanin-type homoisoflavonoids, starting from 2'-methoxychalcones (Castelli and Lopez, 2017).	17
Figure 2.8 The biogenetic pathway of sterols showing the cyclization and rearrangement of the acyclic precursor, 2,3-oxidosqualene, catalyzed oxidosqualene cyclases.	19
Figure 2.9 Structure of eucosterol.....	20
Figure 2.10 Picture of <i>Helichrysum acutatum</i>	23
Figure 2.11 Compounds previously isolated from the aerial parts and roots of <i>H. acutatum</i> . A thiophene derivative (1) and chalcone (2).	23
Figure 2.12 Picture of <i>Helichrysum panduratum</i>	24
Figure 2.13 Helipandurin from <i>Helichrysum panduratum</i>	24
Figure 2.14 <i>Scilla nervosa</i> leaves and bulbs.....	26
Figure 2.15 Skeletal structures of homoisoflavonoids isolated from <i>S. nervosa</i> (Silayo et al., 1999).	27
Figure 2.16 Reaction of DPPH and hydrogen donating substrate (Singh and Singh, 2008).	28
Figure 2.17 Reaction for FRAP assay (Prior et al., 2005).	29
Figure 2.18 Schematic showing quorum sensing (QS) and the formation of bacterial biofilms. QS signals (purple circles) are produced by the enzyme synthase and is released into the extracellular environment. These signals re-enter the cell if their concentration is high in the extracellular medium and are sensed by a receptor in bacterial cell that then activates the transcription of QS-	

regulated genes. Signal number is proportional to cell density (Adapted from <u>Muras</u> et al. 2020).	30
Figure 2. 19 Some cytotoxicity assays and the agents used for detection of cell viability.....	32
Figure 2.20 Conversion of MTT to formazan (Riss et al., 2013).	33
Figure 2.21 Reaction between the adenosine triphosphate (ATP) reagent and luciferin and scheme showing the conversion of ATP to adenosine diphosphate ADP (Promega) (Riss et al., 2003).	34
Figure 2.22 The reaction catalyzed by lactate dehydrogenase (LDH) (Adapted from Kumar et al., 2018).	35
Figure 2.23 Mechanism of cell death measuring different markers of cell viability and apoptosis <i>in-vitro</i> (Adapted from Riss et al., 2003).	38
Figure 3.1: Structures of compounds A1-6 isolated from the bulbs and leaves of <i>S. nervosa</i>	61
Figure 3.2: Structures of compounds A7 and A8 isolated from the bulbs and leaves of <i>S. nervosa</i>	65
Figure 3.3: Structure of compound A9 isolated from the bulbs and leaves of <i>S. nervosa</i>	66
Figure 3.4: Structures of compounds A10 and A11 isolated from the bulbs and leaves of <i>S.</i> <i>nervosa</i>	67
Figure 3.5. 3D representation of the modeled MraY complexes of SNL-17 (a) and SNL-34 (b).	74
Figure 4.1. Dose-response curve for viability using MTT assay in Caco-2, HepG2, and Hek-293 cells exposed to test samples for 24 h.	94
Figure 4.2 Effect of IC ₈₀ and IC ₅₀ concentrations of tested samples on the mitochondrial membrane potential (MMP) of Caco-2, HepG2 and Hek-293 cell lines.	96
Figure 4.3. Effect of IC ₈₀ and IC ₅₀ concentrations of tested samples on the intracellular ATP levels of Caco-2, HepG2 and Hek-293 cell lines.	98
Figure 4.4. Effect of IC ₈₀ and IC ₅₀ concentrations of tested samples on the plasma membrane of Caco-2, HepG2 and Hek-293 cell lines.	99
Figure 4.5 Structure of compounds 1-3.	101
Figure 5.1: Chemical structures of compound B1-B7 isolated from the leaves and stems of <i>Helichrysum panduratum</i>	124

Figure 5.2. Quantitative analysis of the concentration-dependent, violacein production inhibitory effects of isolated compounds from <i>H. panduratum</i> at 200–1000 µg mL ⁻¹ against <i>Chromobacterium violaceum</i> ATCC 12472 (long-chain AHL inhibition) and CV017 (short-chain AHL inhibition).	128
Figure 5.3. Quantitative analysis of the concentration-dependent, violacein production inhibitory effects of four <i>Helichrysum panduratum</i> crude extracts and three isolated compounds at 200–1000 µg mL ⁻¹ against <i>Chromobacterium violaceum</i> ATCC 12472 (long-chain AHL inhibition) and CV017 (short-chain AHL inhibition).....	129
Figure 5.4. Inhibitory effect of extract and isolates from <i>H. panduratum</i> against QS-controlled phenotype of bioluminescence, with cinnamaldehyde as a positive control.	130
Figure 5.5 Dose-dependent decrease in cell viability of Caco-2, HepG2, and Hek-293 cell lines after exposure to varying concentrations of tested samples using MTT assay.....	133
Figure 5.6: Results of the ATP assay.....	135
Figure 5.7: Results for the mitochondrial membrane potential (MPP).....	136
Figure 5.8: Results for LDH (lactate dehydrogenase) release.	137
Figure 6.1: Compounds C1-C3 isolated from the root of <i>H. acutatum</i>	162
Figure 6.2: Free radical scavenging activity of selected crude extracts measured by DPPH method.....	163
Figure 6.3: Ferric reducing antioxidant power (FRAP) of selected crude extracts.	163
Figure 6.4: MTT graphs; Effect of different concentrations of <i>H. acutatum</i> extracts on the viability of three cell lines; Caco-2, HepG2 and Hek293.	165
Figure 6.5: LDH graphs; Effect of IC ₈₀ and IC ₅₀ concentrations of <i>H. acutatum</i> extracts on the plasma membrane of Caco-2, HepG2 and Hek-293 cell lines.....	166
Figure 6.6: MMP graphs; Effect of IC ₈₀ and IC ₅₀ concentrations of <i>H. acutatum</i> extracts on the mitochondrial membrane potential of Caco-2, HepG2 and Hek-293 cell lines.....	167
Figure 6.7: ATP graphs. Effect of IC ₈₀ and IC ₅₀ concentrations of <i>H. acutatum</i> extracts on ATP levels of Caco-2, HepG2 and Hek-293 cell lines.....	168

LIST OF TABLES

Table 3.1: ^1H and ^{13}C NMR data for compound A5 and A6 compared to literature.-----	64
Table 3.2: ^1H , ^{13}C , COSY and HMBC data for compound A10 . -----	68
Table 3.3: ^1H , ^{13}C , COSY and HMBC data for compound A11 . -----	69
Table 3.4: Antibacterial susceptibility test of <i>S. nervosa</i> compounds and crude extracts against selected Gram-negative and Gram-positive bacterial strains. -----	72
Table 3.5. Molecular docking results of homoisoflavones with MraY.-----	73
Table 4.1: Analysis of the results obtained for the cytotoxicity assays (LDH, MMP and ATP) after treatment with the IC_{80} and IC_{50} concentrations of pure compounds and extracts (DCM, EtOAc and MeOH) of <i>S. nervosa</i> using the cell lines, Caco-2, HepG2 and Hek-293.-----	106
Table 5.1: Antibacterial susceptibility assay against selected Gram-positive bacteria. -----	127
Table 5.2: Antibacterial susceptibility assay against selected Gram-negative bacteria. -----	127
Table 5.3: Autoinducer inhibitory profile of compounds and extracts from <i>H. panduratum</i> against Gram-negative AHL-based quorum sensing inhibition (QSI). -----	131
Table 5.4: IC_{50} values in $\mu\text{g mL}^{-1}$ of tested compounds and extracts of <i>H. panduratum</i> .-----	133
Table 5.5: Mitochondria membrane potential (MPP) result for tested samples.-----	135
Table 6.1: Results obtained for the cytotoxicity assays (LDH, MMP and ATP) after treatment with the IC_{80} and IC_{50} concentrations of the extracts (DCM, EtOAc and MeOH) using the cell lines, Caco-2, HepG2 and Hek-293.-----	171

CHAPTER ONE

1.1 INTRODUCTION

Nature is a vast reserve of many biologically relevant products derived from various sources, including terrestrial plants, microorganisms, vertebrates and invertebrates, and marine organisms (Newman et al., 2000). The chemical entities from natural sources provided the foundation for early medicines used in treating and preventing diseases, and they still serve as lead molecules for drug discovery programs. Additionally, natural products are consistently being used as supplements (nutritional and medicinal), flavoring agents, pesticides, and cosmetics (Kunin and Lawton, 1996; Pleroni et al., 2004).

The use of plants in traditional medicine dates back to the Paleolithic age (Solecki et al., 1975), and currently, many ethnic groups still depend on plants as their primary source of medicine. It has been reported that, between 1981-2000, natural product-derived drugs constituted 28% of all new chemical entities (NCEs) (Newman et al., 2003), with many of these drugs being developed from plant sources, including morphine (Benyhe et al., 1994), artemisinin (Klayman, 1985), paclitaxel (Wani et al., 1971), and camptothecin (Wall et al., 1966).

Furthermore, empirical evidence suggests that nature is the primary source for new structural templates and effective drug development. The World Health Organization (WHO) estimated that about 80% of 400 million of the world's population depends on plant-derived traditional medicine for their primary health care as of 1985 (Fransworth et al., 1985). For instance, it was estimated that about 80% of the black population in South Africa still consults traditional healers to treat their ailments (Jager et al., 1996). This phenomenon can be attributed to the rich diversity of the country's indigenous flora, which houses about 30 000 plant species that makeup 10% of the world's higher plant species, of which approximately 3 000 are used

medicinally (Van Wyk and Gericke, 2000; Louw et al., 2002). Due to the considerable use of plants in traditional medicine, there is a high potential for discovering novel compounds (Van Wyk et al., 1997).

Phytochemistry plays an essential role in the study of plants used in traditional medicine as it provides a rationale for the use of plants in the treatment and management of diseases (Efferth et al., 2007; Folashade et al., 2012). Advancements in natural product research have also enabled discovering an array of secondary metabolites from terrestrial and marine sources. Secondary metabolites are not intrinsically essential for plants' growth but perform certain physiological functions such as defense against predators. These secondary metabolites have pharmacological significance and are used as is or are synthetically modified to produce drugs with enhanced activities (Efferth et al., 2007).

1.2 RATIONALE FOR THE RESEARCH

Since the isolation of the first alkaloid, morphine, from the poppy plant in 1802 to the more recently approved drugs derived from plants, higher plants have been recognized as an invaluable source of pharmaceutical products. The search for cost-effective therapeutics with minimal side effects for the management of life-threatening diseases such as cancer, malaria, and infectious diseases is gaining momentum. In this regard, secondary metabolites from plants have been recruited as leads in drug discovery. Advancements in science and technology have also increased the understanding of the chemical constituents and toxicity profiles of the different plant species used in traditional medicine. Consequently, the discovery of structurally diverse pharmacophores has led to advances in treating and mitigating some life-threatening diseases.

This study focused on three South African medicinal plants from two families, *Helichrysum acutatum* and *Helichrysum panduratum* from Asteraceae and *Scilla nervosa* from Hyacinthaceae. A phytochemical study of the root of *H. acutatum* has been conducted by Bohlmann and Abraham (1979), while Heyman (2009) presented antifungal and antibacterial findings. However, the antioxidant and toxicity profiling to justify the plants use and safety in traditional medicine remains unexplored. *H. panduratum* was studied by Chapman and Hall (2009), and a thiophene derivative known as helipandurin was the only compound isolated from the plant. The leaves and stems need further exploration to isolate and identify other secondary metabolites that may be present. Extensive work has been done on *Scilla nervosa*, and several homoisoflavanones and stilbenoids have been isolated. However, there is a dearth of information on its cytotoxicity towards tumor and normal cell lines. Previous work evaluated the cytotoxic effect of the aqueous extract on HepG2 (hepatocellular carcinoma) cell lines (Pillay et al., 2013), however, the cytotoxic effect of the isolates and organic extracts on Caco-2 (human colorectal cancer cell), HepG2 (hepatocellular carcinoma tumor cell) and Hek-293 (normal human epithelial kidney cell) cell lines, which are the primary organs the plant will have contact with when taken orally are yet to be established. In addition, it has been hypothesized that greater efficacy would be achieved by the extracts from *S. nervosa* and medicinal plants, in general, than the individual biomolecules. This assumed that the phytocompounds present in the extracts would reciprocally potentiate the activity of the individual biomolecules (du Toit, 2011; van Vuuren, 2008)

1.3 AIMS AND OBJECTIVES

The primary aim of this study was to investigate the three South African medicinal plants, namely *Scilla nervosa*, *Helichrysum acutatum*, and *Helichrysum panduratum* to validate their

use in ethnomedicine and to determine their biological activities, especially the cytotoxicity of the extracts and isolates.

The specific research objectives were:

- To extract, isolate and identify the secondary metabolites from each plant using spectroscopic techniques (nuclear magnetic resonance spectroscopy (NMR), Fourier-transform infrared spectroscopy (FTIR), and high-resolution mass spectroscopy (HRMS),
- To evaluate the isolated compounds and crude extracts for their antioxidant, and antibacterial activities, and to determine for synergistic effects,
- To determine the cytotoxic activities using different assays such as ATP to evaluate intracellular energy levels, LDH release to evaluate plasma integrity, and mitochondrial membrane potential to evaluate the release of cytosol C to initiate apoptotic death.

1.4 STRUCTURE OF THE THESIS

The findings reported in this thesis are as follows: Chapter 3 describes the extraction, isolation, and identification of secondary metabolites from the bulbs and leaves of *S. nervosa*, together with an evaluation of their antibacterial activity and molecular docking.

Chapter 4 reports on the anticancer potential of isolated homoisoflavonoids and crude extracts from *S. nervosa*.

Chapter 5 describes the extraction, isolation, and identification of secondary metabolites from the stem and leaves of *H. panduratum*, followed by evaluating the antibacterial and cytotoxic activity of the compounds and extracts.

Chapter 6 describes the extraction, isolation, and identification of the bioactive constituents from the roots of *H. acutatum*, and subsequent determination of their antioxidant, antibacterial, and cytotoxic activity.

A concise summary of the findings and conclusions for the study are presented in chapter 7.

REFERENCES

- Bohlmann, F., Abraham W-R. (1979). Neue diterpene aus *Helichrysum acutatum*. PHYTOCHEMISTRY 18, 1754-1756.
- Chapman & Hall/CRC. (2009). Dictionary of Natural Products. Vol 12:3. HDS Software Copyright © Hampden Data Service Ltd.
- Efferth, T., Li, P.C., Konkimalla, V.S.B., Kaina, B. (2007). From traditional Chinese medicine to rational cancer therapy. TRENDS IN MOLECULAR MEDICINE 13, 353-361.
- Farnsworth, N. R., Akerele, R. O., Bingel, A. S., Soejarto, D.D., Guo, Z. (1985). Medicinal plants in therapy, Bull. World Health Organization. 63, 965–981.
- Folashade, O., Omoregie, H., Ochogu, P. (2012). Standardization of herbal medicines – A review. INTERNATIONAL JOURNAL OF BIODIVERSITY AND CONSERVATION 4, 101-112.
- Heyman, H. (2009). Metabolomic comparison of selected *Helichrysum* species to predict their antiviral properties, M. Sc thesis, University of Pretoria, Pretoria, South Africa.
- Jäger, A.K., Hutchings, A., and Van Staden, J. (1996). Screening of Zulu medicinal plants from prostaglandin-synthesis inhibitors. JOURNAL OF ETHNOPHARMACOLOGY 52, 95-100.

- Klayman, D.L. (1985). Qinghaosu (Artemisinin): An antimalarial drug from China. *SCIENCE* 228, 1049-1055.
- Kunin, W.E. and Lawton, J. (1996) Does biodiversity matter? Evaluating the case for conserving species. In K.J. Gaston (ed.) *BIODIVERSITY. A BIOLOGY OF NUMBERS AND DIFFERENCE*, 283–308. Oxford. Blackwell.
- Kunin, W.E., and Lawton, J.H. (1996). Does biodiversity matter? Evaluating the case for conserving species. In: *Biodiversity*, (Editor Gaston, K.J.), Blackwell Science LTD, UK. pp. 283-308.
- Louw, C. A. M., Regnier, T. J. C. and Korsten, L. (2002). Medicinal bulbous plants of South Africa and their traditional relevance in the control of infectious diseases, *JOURNAL OF ETHNOPHARMACOLOGY* 82, 147–154.
- Newman D. J., Cragg G. M., & Snader, K. M. (2000). The influence of natural products upon drug discovery. *NATURAL PRODUCT REPORTS*. 17, 215 – 234.
- Newman D. J., Cragg G. M., & Snader, K. M. (2003). Natural products as sources of new drugs over the period 1981-2002. *JOURNAL OF NATURAL PRODUCT*. 66, 1022 - 1037. B. E.
- Peroni, A., Quare, C.L., Villanelli, M.L., Mangino, P., Sabbatini, G., Santini, L., Boccetti, T., Profili, M., Ciccioli, T., Rampa, L.G., Antonini, G., Girolamini, C., Cecchi, M, and Tomasi, M. (2004). Ethnopharmacognostic survey on the natural ingredients used in folk cosmetics, cosmeceuticals and remedies for healing sting diseases in the inland Marches, Central-Eastern Italy. *JOURNAL OF ETHNOPHARMACOLOGY*, 9, 331- 344.
- Pillay, P., Phulukdaree, A., Chuturgoon, A. A., Du Toit, K., & Bodenstein, J. (2013). The cytotoxic effects of *Scilla nervosa* (Burch.) Jessop (Hyacinthaceae) aqueous extract on

- cultured HepG2 cells. JOURNAL OF ETHNOPHARMACOLOGY, 145(1), 200–204. doi: 10.1016/j.jep.2012.10.053.
- Solecki, R., and Shanidar, I.V. (1975). A Neanderthal flower burial in northern Iraq. SCIENCE, 190, 880 -881.
- Van Wyk and Gericke, N., People's Plants. A Guide to Useful Plants of Southern Africa, Briza Publications, 2000.
- Van Wyk, B., Van Oudtshoorn, B., Gericke, N. (1997). Medicinal Plants of South Africa. Briza, Pretoria.
- Wall, M.E., Wani, M.C., Cook, C.E., Palmer, K.H, Mcphail, A.T., & Sim, G.A. (1966). Plant Antitumor Agents I. The isolation and structure of camptothecin, a novel alkaloidal leukemia and tumor inhibitor from *Camptotheca acuminata*. JOURNAL OF AMERICAN CHEMICAL SOCIETY, 88, 3888-3890.
- Wani, M.C., Taylor, H.L., Wall, M.E., Coggon, P., and McPhail, A.T. (1971). Plant Antitumor Agents VI. The isolation and structure of Taxol, a novel antileukemic and antitumor agent from *Taxus brevifolia*. JOURNAL OF AMERICAN CHEMICAL SOCIETY, 93: 2325-2327.

CHAPTER TWO

LITERATURE REVIEW

2.1 NATURAL PRODUCTS AS THERAPEUTIC AGENTS

Humans have always depended on nature to care for their basic needs such as food, shelter and clothing. Nature presents us with an assembly of different types of chemical entities from diverse sources. Natural products are the chemical substances produced by the living organisms found in nature, also defined as small molecules produced by a biological source (Nature, 2007). They have served as a foundation for new inventions in drug discovery; it has also been indicated that most of the drugs in the market have their origin from nature (Chin et al., 2006, Newman et al., 2003). Natural product research focuses on the chemical properties, biosynthesis, and biological functions of secondary metabolites (Nature, 2007).

The discovery of therapeutic agents from natural sources started with the isolation of morphine from poppy plants (*Papaver somniferum*) in 1804 (Lockemann, 1951). Thereafter, bioactive compounds have been isolated from medicinal plants such as cinchona (quinine). Research for therapeutic agents expanded after the second world war to include the screening of microorganisms for new antibacterial agents, which led to the discovery of penicillin (Li and Vederas, 2009). While the evolution of drug resistance in clinically essential infections has limited the use of many natural antibiotics, their discovery and commercialization laid the scientific and financial foundation of the modern pharmaceutical industry (Beutler, 2009).

The study of natural products made it possible to scientifically establish the safety and efficacy of plants used in traditional medicine in the diagnosis, treatment, and prevention of diseases and validate their therapeutic properties and constituents. Chemical, pharmacological, and clinical studies of natural products have led to the discovery of drugs, and also provided leads

for semi or total synthesis of drugs to treat life-threatening diseases. Natural products have been used as a starting point for drug discovery, followed by a synthetic modification to improve efficacy, minimize side effects, and increase bioavailability. Natural products include a large and diverse group of substances, including extracts and isolated compounds. The natural sources include marine organisms, fungi, bacteria, and higher plants. However, drug discovery from natural products has received less attention in the 21st Century attributed to cost, intellectual property, compositional variation due to seasons or soil types, loss of sources due to high extinction rates, access, and supply (Li and Vederas, 2009). Others are the complexity of the structures of isolated compounds (Beutler, 2009), and lab-intensive and time-consuming extraction and isolation processes. However, the advent of automated and rapid techniques has helped overcome these challenges.

It was reported by Newman and Cragg (2012) that the drugs developed between 1981 and 2002 were natural product-derived and comprised 28% of all the new chemical entities (NCE) launched into the market. Computational chemistry, sequencing of the human genome and high throughput screening (HTS) has resulted in the decline of research in this field; nevertheless, natural products still serve as drug leads. The advantages of natural products over drugs are that they have high structural diversity and unique pharmacological or biological activities and synergy, due to the natural selection and evolutionary processes that have shaped their utility over hundreds of thousands of years. Also, natural products introduce novel molecular skeletons and functionalities that humans have not previously conceived, such as ivermectin, mitomycin, bleomycin and espiamicin (Beutler, 2009).

2.2 TRADITIONAL MEDICINE IN SOUTH AFRICA

Traditional medicine has played an essential role in the primary health care of South Africans, with about 80% of the black population reported to have consulted traditional healers for their health care needs (Jager et al., 1996). Traditional healers are more easily accessible for a more significant part of the population due to the high cost of medical services; hence profiling and proper documentation of the safety and use of these medicinal plants is essential (Mahomoodally, 2013). South Africa is home to about 30,000 flowering plants, and it is estimated that about 700,000 tons of plant materials are consumed annually (Street and Prinsloo, 2013). With the sizeable botanical diversity, only a few plants have been commercialized into medicinal products.

Plants indigenous to South Africa used in traditional medicines include *Agathosma betulina* (buchu), used internally for digestive issues and externally for wounds, *Aloe ferox*, used as a laxative, *Artemisia afra* (African wormwood), used to treat fevers and stomach-ache, *Aspalathus linearis* (rooibos tea), consumed as a tea for its antioxidant and anti-aging properties, *Eucomis autumnalis*, used as an enema for lower back pains and healing of fractures, and *Hypoxis hemerocallidea* (African potato), used to treat benign prostate hyperplasia (Van Wyk, 2011).

Traditional medicine, as opposed to evidence-based medicine, was not recognized during the colonial times in South Africa because of the belief that diagnosis is often by spiritism or mediums since it was not scientific-based. Reports showed that in sub-Saharan Africa, the ratio of traditional healers to the population is approximately 1:500, while western-trained medical doctors present a 1:40 000 ratio (Semenya et al., 2012). The large population of people using traditional medicine has made the World Health Organization (WHO) encourage promoting

and integrating conventional medical practices into the primary health care system (Mothibe and Sibanda, 2019).

Despite the extensive use of plants in African traditional medicine, there is no proper documentation of these plants compared to other countries such as China and India. Most of the knowledge that exists is fragmented and has been passed down from generation to generation. Cock and Van Vuuren (2020) reported that the antibacterial activity of most South Africa plant species is yet to be verified. For example, a study on the ethnobotanical knowledge of herbal medicine used by Bapedi healers in Limpopo for reproductive ailments showed that, of the thirty-six plants evaluated, most were not scientifically validated for their ethnomedicinal use (Semenya et al., 2012). Therefore, there is need to analyze plants used in traditional medicine to evaluate their health-promoting potential and their interaction with known conventional drugs. In addition, these findings need to be appropriately documented.

2.3 PLANTS AS A SOURCE OF THERAPEUTICS

The birth of drug discovery is closely connected to the study of natural products from plants as was seen with morphine over 200 years ago; a discovery that initiated an era whereby plant extracts could be purified, and pure compounds isolated, elucidated, and formulated into drugs (Yuan et al., 2016). Plants have served as food, spices, flavoring agents, ornaments, and medicines for man since antiquity; they have a long history of therapeutics in the traditional medicine system, with the earliest documentation dating around 2900-2600BCE (Borchardt, 2002). From as early as the 18th century, bioactive constituents of plants have been isolated and used for medical treatments. The use of the Cinchona bark was long used to treat malaria before chemical investigation led to the isolation of quinine. Artemisinin, a sesquiterpene lactone from the Chinese plant *Artemisia annua* for treating chloroquine-resistant malaria, is one of the

breakthroughs recorded in plant research. Recently, it was reported that artemisinin could be used in the treatment of covid-19. Taxol, used to treat solid tumors, is another isolate from the bark of the pacific yew (*Taxus brevifolia*). Aspirin, one of the most used analgesics by humans, is a derivative of the naturally occurring salicin isolated from willows (*Salix* spp.).

Pharmaceutical companies abandoned natural product research in the 1970s, but this was reversed when cancer chemotherapeutics such as vinblastine, Taxol and etoposide were discovered. Additionally, the inability of synthetic and computational chemists to design structural diversity compounds such as those isolated from natural sources has revived natural product research (Houghton, 1995).

2.4 SECONDARY METABOLITES

Plants produce primary and secondary metabolites. Primary metabolites are used for a cell's intrinsic functions such as reproduction and growth. The biosynthesis of secondary metabolites is from the fundamental processes of photosynthesis, glycolysis, and the Krebs cycle to afford biosynthetic intermediates, which, ultimately, results in their formation (Dias et al., 2012). Secondary metabolites are not essential for the plants growth but have an extrinsic function such as to deter predation and ensure the plants survival in its ecosystem (Zahner, 1979). Plants contain secondary metabolites that may act individually, additively, or in synergy to improve its survival. These secondary metabolites have been perceived to show more drug-likeness and biological friendliness than totally synthetic molecules, making them good candidates for further drug development. Secondary metabolites from nature can be active compounds in prescription and non-prescription drugs, cosmetics, dietary supplements, and natural health products.

2.4.1 Extraction, Purification and Identification

All secondary metabolites exist as complex mixtures in the natural source, from which they have to be obtained. The initial step in natural product research is extraction that is a method of removing the molecules of the plant by using appropriate solvents and extraction methods. Extraction methods include maceration, infusion, decoction, percolation, digestion, and use of Soxhlet, ultrasound, and microwave (Abubakar and Haque, 2020) (Figure 2.1). Extraction is of two types; the first is the conventional method that requires a large volume of solvent and is time-consuming. The second is a greener technique that involves using costly equipment, high temperatures or pressures, and short extracting times (Njila et al., 2017). Grinding or crushing plant material helps create a large surface area for extraction. Different solvents are employed in the extraction process and the choice of solvent depends on the polarity and solubility of the target metabolites (Jones and Kinghorn, 2012). Multiple solvents are generally used sequentially, starting from the least polar to the most polar solvent. A solute will extract into a solvent of similar polarity; this principle is employed in the use of different solvents in extraction.

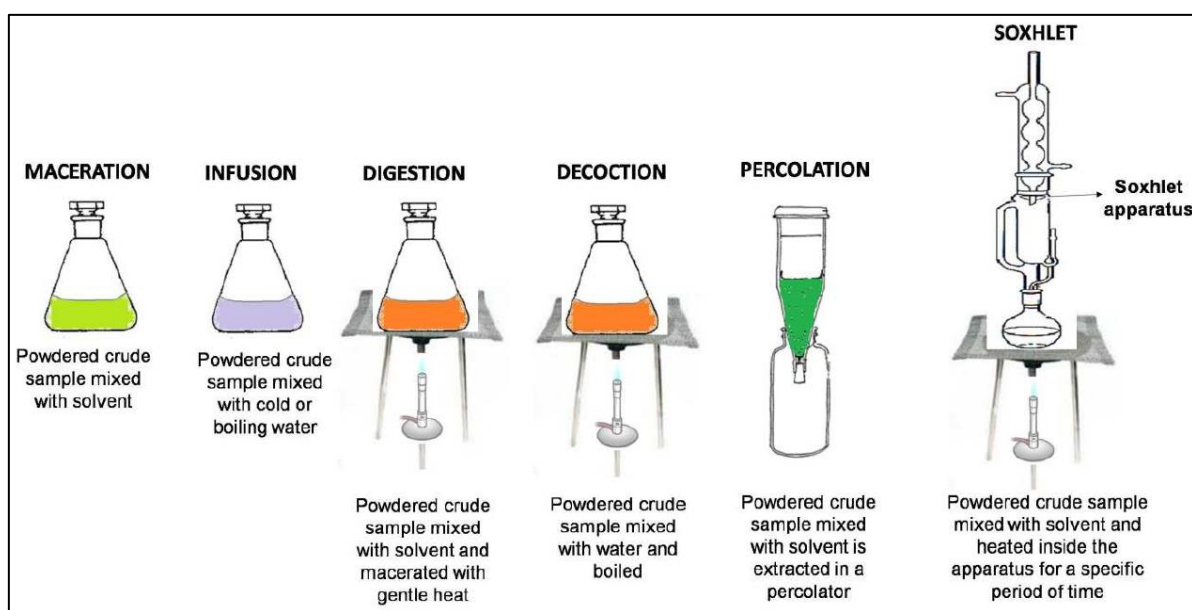


Figure 2.1 Different extraction methods.

Chromatographic techniques are usually used to separate and purify secondary metabolites from the crude extracts, with column chromatography being the primary separation method (Altemimi et al., 2017). The principle of separation in column chromatography (solid-liquid chromatography) is based on the adsorption affinities of the molecules for either the mobile or stationary phases (Figure 2.2). Selecting an appropriate stationary phase (adsorbent) and mobile phase (eluent) is crucial in achieving well resolved bands (individual molecules) and good separation. Silica gel, a polar adsorbent, is commonly used in column chromatography to separate crude extracts from plant sources; thus, polar substances are retained more in silica gel than non-polar substances. The polarity of the adsorbent also determines the polarity of the mobile phase. For silica gel, the mobile phase employed during chromatography is more non-polar since the adsorbent is polar (normal phase). For a non-polar adsorbent, an opposite mobile phase will be used (reversed-phase). Thin-layer chromatography (TLC) is used for visualization of eluted molecule identification. TLC has the advantage of showing which group of secondary metabolites is present by using the suitable spray reagent.

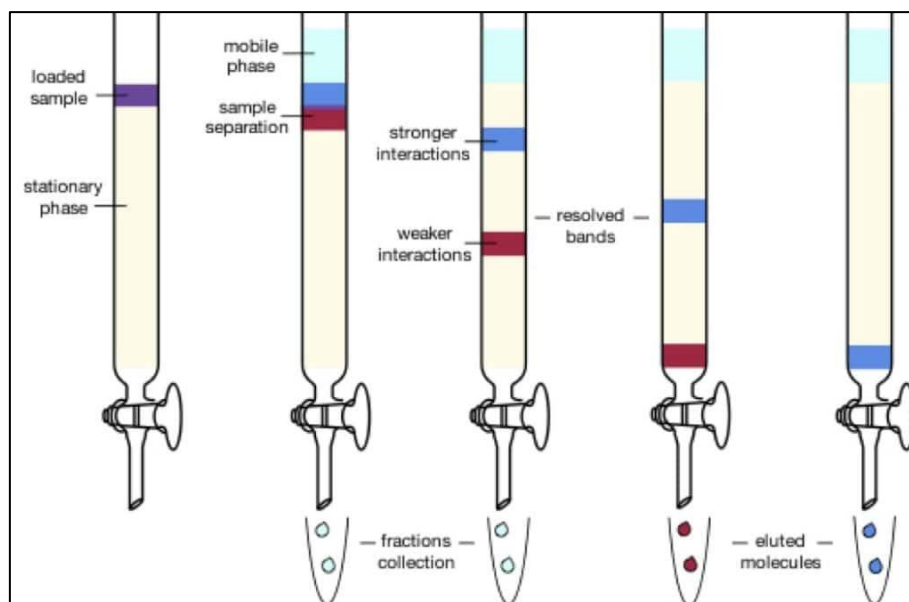


Figure 2.2 The principal of separation in column chromatography.

A wide range of spectroscopic techniques such as nuclear magnetic resonance spectroscopy (NMR), ultraviolet-visible spectroscopy (UV-Vis), infrared spectroscopy (IR), and mass spectrometry (MS) can be used for identification of isolated molecules.

2.4.2 Classes of Secondary metabolites in this study

Homoisoflavonoid

The term homoisoflavonoids was first used by Bohler and Tamm to refer to a group of secondary metabolites first isolated from *Eucomis autumnalis*. The secondary metabolites were eucomin and eucomol (Figure 2.3) (Castelli and Lopez, 2017).

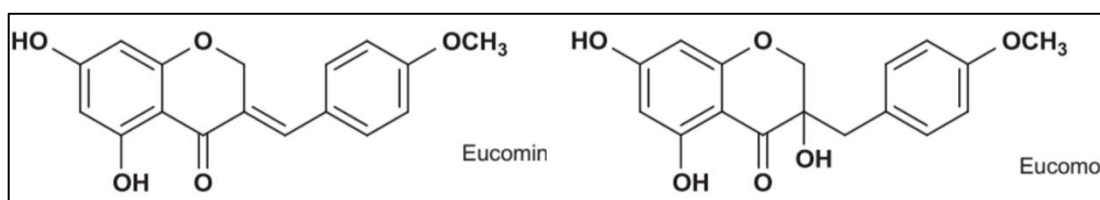


Figure 2.3 Structures of eucomin and eucomol, the first homoisoflavonoids isolated from *E. bicolor*.

Homoisoflavonoids are a subclass of flavonoids; they differ from other flavonoids (Figure 2.4) with a carbon linking the benzopyrone ring to ring C. They are limited in their occurrence in nature and have been reported to be biosynthesized mainly by the Fabaceae and Asparagaceae family, and are less common in Polygonaceae, Portulacaceae, Orchidaceae, and Gentianaceae families (Lin et al., 2014).

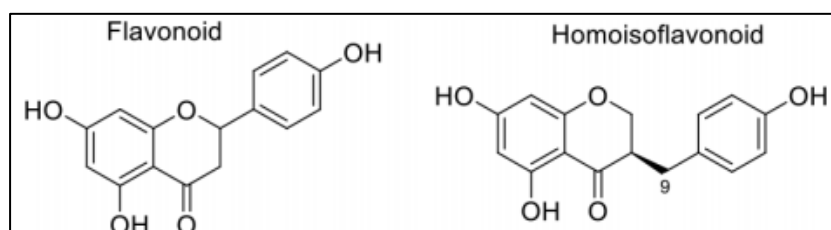


Figure 2.4 General structure of a flavonoid and homoisoflavonoid.

Structurally, homoisoflavonoids are classified into five groups (Figure 2.5). Among the 240 reported naturally occurring homoisoflavonoids, the sappanin-type accounts for 190. They are

characterized with a 3-benzyl chromane skeleton and can be further divided into 3-benzyl-4-chromanones (Figure 2.6A), the 3-hydroxy-3-benzyl-4-chromanones (Figure 2.6B), the 3-benzylidene-4-chromanones (*E* or *Z*) (Figure 2.6C) and the 3-benzyl-chrom-2-en-4-ones (Figure 2.6D) (Mulholland et al., 2013). The Hyacinthaceae are known to biosynthesize the sappanin-type homoisoflavonoids. Homoisoflavanones exhibit a vast range of bioactivities such as antibacterial, anti-cancer, antioxidant, anti-inflammatory, and anti-mutagenic activities (El-Elimat et al., 2018; Li et al., 2012; Schwikkard et al., 2018; Machala et al., 2001).

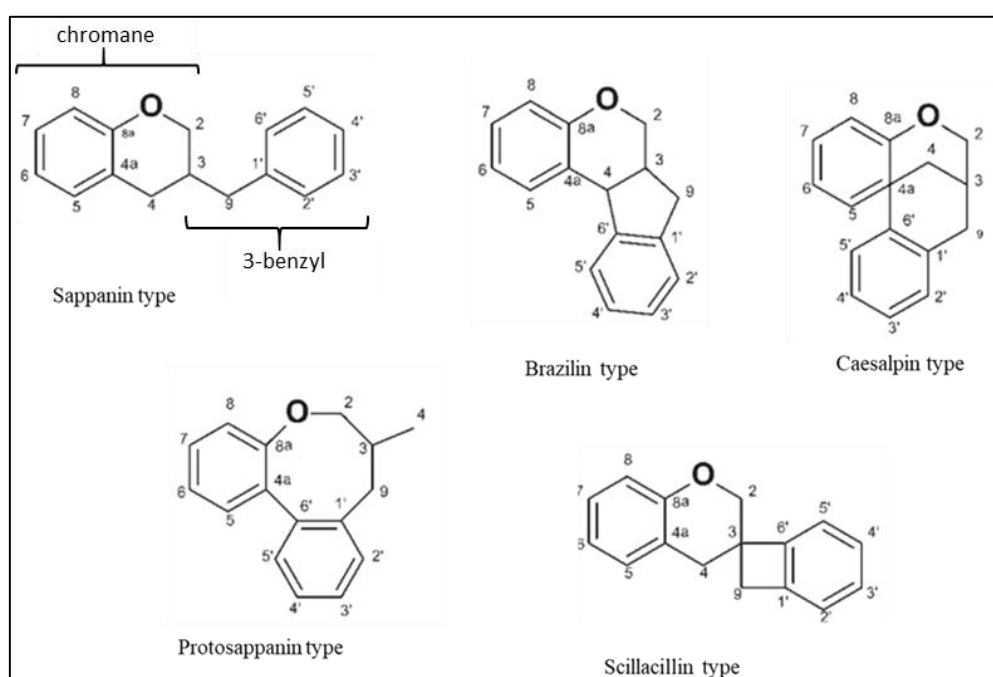


Figure 2.5 Carbon skeletons of homoisoflavonoids.

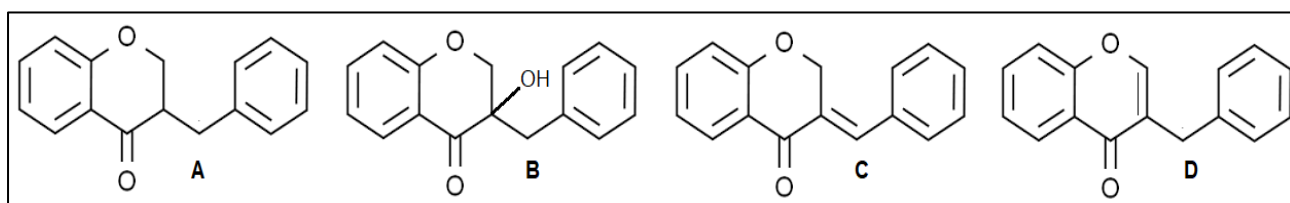


Figure 2.6 Four groups with the 3-benzyl chromane skeleton: (A) 3-benzyl-4-chromanones, (B) 3-hydroxy-3-benzyl-4-chromanones, (C) 3-benzylidene-4-chromanones and (D) 3-benzyl-chrom-2-en-4-ones.

Biosynthetic pathway of homoisoflavonoids

The labeling pattern from feeding experiments indicated that eucomin was biosynthesized by the addition of a carbon atom derived from methionine onto a C₁₅ chalcone-type carbon skeleton (Dewick, 1975). The first step in the biosynthesis of homoisoflavonoids involves forming a chalcone, which is a direct precursor of homoisoflavonoids (Figure 2.7).

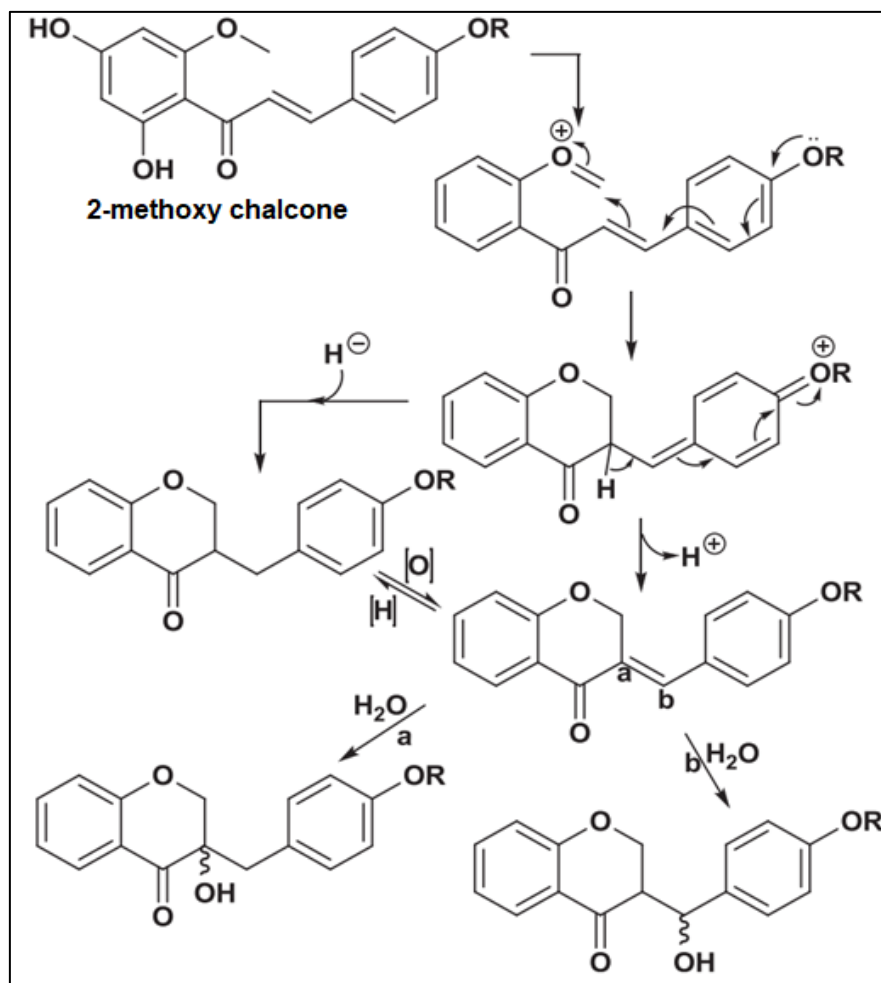


Figure 2.7 Scheme showing proposed biosynthetic routes of sappanin-type homoisoflavonoids, starting from 2'-methoxychalcones (Castelli and Lopez, 2017).

The 2-methoxy group undergoes oxidation and then cyclization to produce three basic types of homoisoflavonoids. A loss of a proton from the cyclization product produces 3-benzalchroman-4-one, while the addition of a hydride ion will produce 3-benzylchroman-4-one. Hydration or oxidation at the C-3 position of a 3-benzylchroman-4-one leads to a 3-

benzyl-3-hydroxychroman-4-one (Dewick, 1975; Moodley, 2001). The feeding experiment established that eucomin and other compounds containing the 3-benzylchroman-4-one skeleton are biosynthesized by modifying the C₆-C₃-C₆ chalcone skeleton with an extra carbon atom (Dewick, 1975).

Triterpenes

Triterpenes are one of the largest secondary metabolites, with more than 100 different scaffolds described as natural products (Domingo et al., 2008). They are metabolites of isopentenyl pyrophosphate and are found in all parts of higher plants; they are also found in mosses, liverworts, algae, and lichens. Triterpenes and sterols are synthesized *via* the mevalonate pathway. The biogenetic pathway of triterpenes and sterols starts with the cyclization and rearrangement of the acyclic precursor squalene and 2,3-oxidosqualene, catalyzed by enzymes known as oxidosqualene cyclases. Animals and fungi have one oxidosqualene cyclase and lanosterol synthase for sterol biosynthesis, while plants have oxidosqualene cyclases for both sterols and triterpenes biosynthesis. The oxidosqualene cyclases enable the various skeletal variations of triterpenes in plants (Sawai and Saito, 2011). In sterols, 2,3-oxidosqualene is cyclized to lanosterol or cycloartenol *via* the chair-boat-chair (CBC) conformation (Figure 2.8).

In triterpenes, the substrate assumes a different conformation (CCC, chair-chair-chair) before cyclization into different types of triterpenes. Triterpene cyclization can lead to different triterpene structures, all derived from 2,3-oxidosqualene (Thimmappa et al., 2014; Philips et al., 2006).

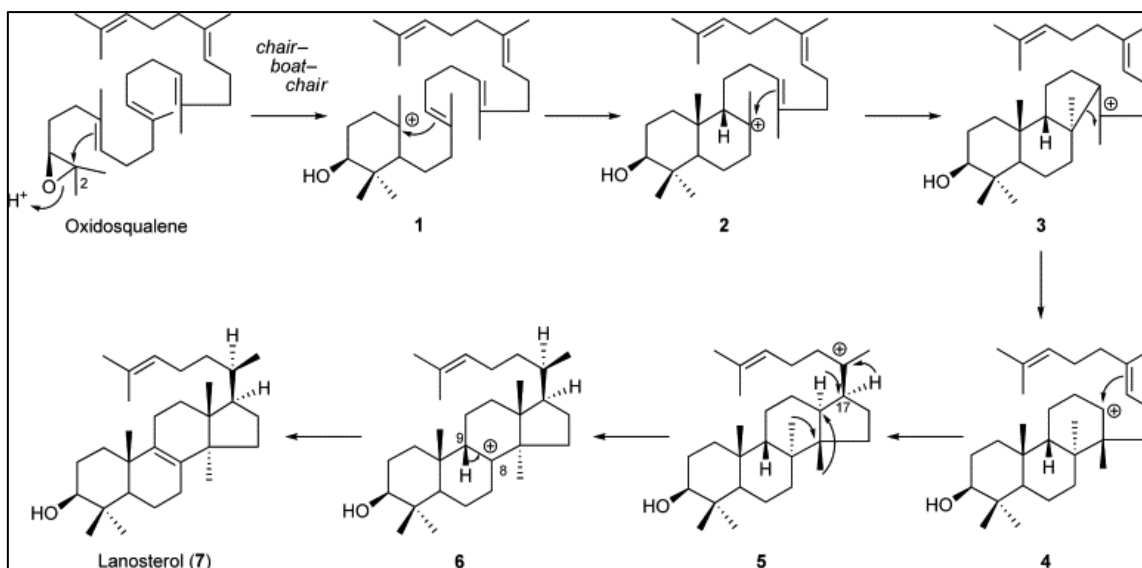


Figure 2.8 The biogenetic pathway of sterols showing the cyclization and rearrangement of the acyclic precursor, 2,3-oxidosqualene, catalyzed oxidosqualene cyclases.

Nortriterpenoids are derived from lanostane-type triterpenoids by degradation of the side chain. Spirocyclic nortriterpenoids have been isolated from the Hyacinthaceae family (Ziegler et al., 1976; Moodley et al., 2004). The first report of a nortriterpene was eucosterol from *Eucomis bicolor* (Sidwell et al., 1975). Eucosterols have a spiro-fused furanoic system with an ether linkage between C-17 and C-23 that forms the heterocyclic ring (Figure 2.9), which are common in the diterpenes and sesterterpenes such as ophiobolin A. Eucosterols are interesting triterpenes with their missing side chain carbon atom that represents biosynthetically uncommon nortriterpenes. The ^1H NMR of eucosterol-type triterpenes have the following characteristic peaks; a pair of doublets at δ_{H} 3.30-3.50 and δ_{H} 4.0-4.20 for the methylene protons at the CH_2OH of C-29, a multiplet at δ_{H} 3.40-3.60 for the proton at C-3, a triplet at δ_{H} 4.64-4.80 for the methine proton at C-23 and six methyl resonances between δ_{H} 0.90-1.5. The ^{13}C NMR spectrum shows resonance for the fully substituted C-O of C-17 at δ_{C} 91-100, two substituted alkene carbons at δ_{C} 133.0-135.2 and δ_{C} 133.1-137.0 for C-8 and C-9 and a carbonyl. The structure of eucosterol showed an ether linkage between C-17 and C-23, forming a heterocyclic ring.

2.5.2. *Ethnobotany and biological activities of the genus Helichrysum*

Helichrysum species treat infection-related diseases, from skin infections to sexually transmitted and respiratory infections (Hutchings et al. 1996; Afolayan and Meyer, 1997). Some of the species have demonstrated good *in vitro* antimicrobial, antioxidant, mutagenic and cytogenic activity (Eroğlu et al., 2009; Yagura et al., 2008; Aiyegoro and Okoh, 2009; Süzgeç-Selçuk and Birteksöz, 2011). In southern Africa, *Helichrysum* species are used mainly to treat wounds, infections, and respiratory conditions such as circumcision wounds that are wrapped with crushed leaves of *Helichrysum pedunculatum*, *Helichrysum appendiculatum* or *Helichrysum longifolium* (Van Wyk et al., 1997). The Sotho people inhale smoke from the burnt plant of *Helichrysum caespititium* to treat headaches and chest colds (Van Wyk et al., 1997). *Helichrysum psilolepis* is used to treat menstrual cramps and *Helichrysum cooperi* is used as an aphrodisiac (Hutchings et al. 1996; Watt & Breyer-Brandwijk. 1962). Essential oils from the Mediterranean *Helichrysum italicum* are used for their antimicrobial activity (Bougatsos et al., 2004).

Helichrysum caespititium, used by traditional healers to treat gonorrhea, was tested against four gonorrhea strains, which showed good or better activity than gentamicin and amoxicillin (Mamabolo et al. 2018). Seven *Helichrysum* species exhibited MIC values lower than 0.1 mg/mL against *Bacillus cereus* and *Staphylococcus aureus* (Lourens et al., 2011). *Helichrysum zivojinii* showed dose-dependent cytotoxicity against selected cancer cell lines and induced apoptosis in HeLa cells through the activation of the intrinsic and extrinsic pathways (Matić et al., 2013). *Helichrysum arenarium* demonstrated synergism with the standard drug ciprofloxacin against *S. aureus*, *S. pneumoniae* and *M. catarrhalis* (Adina et al., 2014).

2.5.3 Phytochemistry of the genus *Helichrysum*

Plants from the genus *Helichrysum* have different biosynthetic routes and secondary metabolites, including flavonoids, chalcones, phloroglucinol, pyrones, triterpenoids, diterpenoids and sesquiterpenes (Jakupovic et al., 1989). Ten phloroglucinols and one triterpene was isolated from methanolic extract of the aerial parts of *Helichrysum niveum* (Popoola et al., 2015). Three novel flavonoids were isolated from the aerial parts of *Helichrysum forskahlii* (Al-Rehaily et al., 2008). Chalcones, flavonoids and flavonoid glycosides were isolated from the methanol leaf extracts of *Helichrysum foetidum* and *Helichrysum mechowianum* (Malolo et al., 2015). A known flavonoid and acylphloroglucinol were isolated from the DCM extract of the flowers of *Helichrysum gymnocomum* (Drewes and van Vuuren, 2008). Two new pyrone derivatives were isolated from the aerial parts of *Helichrysum italicum* (Werner et al., 2018). Three unusual amino-phloroglucinols were isolated from *Helichrysum italicum* (D'Abrosca et al., 2016). Galangin was isolated from the aerial parts of *H. aureonitens* and apigenin was isolated from *H. graveolens* (Afolayan and Meyer, 1997; Suntar et al., 2013).

2.5 4 *Helichrysum acutatum* DC

Helichrysum acutatum (Figure 2.10) is in group 21 according to Hillard (1983) classification. It grows in grasslands and can be found in KwaZulu Natal, Swaziland, Mpumalanga, and the northern parts of the Limpopo. The plant's root is widely sold in the muthi market, but no documented specific use is recorded in the literature. Bohlmann and Abraham investigated the roots and aerial parts of the plant. The roots gave a thiophene derivative (Figure 2.11), dimethyl ether and pinocembrin, while the aerial parts gave a chalcone (Figure 2.11) and diterpenes.



Figure 2.10 Picture of *Helichrysum acutatum*.

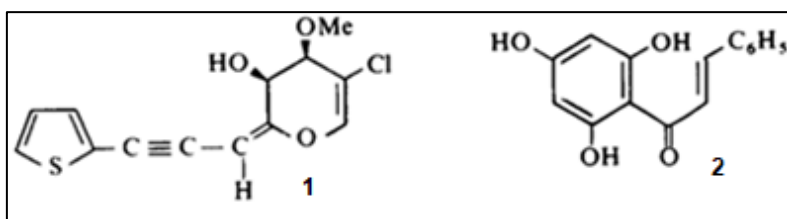


Figure 2.11 Compounds previously isolated from the aerial parts and roots of *H. acutatum*. A thiophene derivative (1) and chalcone (2).

2.5.5 *Helichrysum panduratum* var. *panduratum* O. Hoffm

H. panduratum falls in group 18 (Figure 2.12). It is a soft-wooded sub-shrub with loose stems. The leaves are panduriform, sessile, base thinly grey woolly above, and densely below. It can be found in the Eastern Cape and KwaZulu-Natal. Common names are *H. auriculatum* Less. var. *panduratum* Harv. (Hilliard, 1983). A decoction from the leaves is used to treat febrile convulsions in children, while the plant sap is used to treat malaria used to make herbal tea (Lourens et al., 2008). Helipandurin (Figure 2.13), a thio-derivative, is the only compound that has been isolated from the plant (Chapman and Hall, 2009).



Figure 2.12 Picture of *Helichrysum panduratum*.

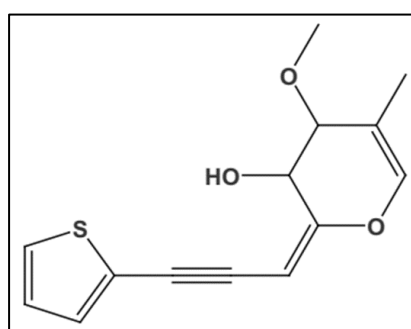


Figure 2.13 Helipandurin from *Helichrysum panduratum*.

2.6 THE GENUS *SCILLA*

The genus *Scilla* has recently been classified under the Asparagaceae family and subfamily Scilloideae. Prior to that *Scilla* was placed in the Hyacinthaceae family (Liliaceae). *Scilla* is a large genus with most species found in Europe, North Africa and western to central Africa. There are also species from tropical Africa, India, and South Africa. Some are winter growing, and some are summer growing. There are six *Scilla* species in southern Africa; *S. plumbea*, *S. nervosa*, *S. natalensis*, *S. dracomontana*, *S. kraussi* and *S. firmifolia* (Du Plessis and Duncan, 1989). Other plants in this genus that are not indigenous to southern Africa are *S. maritima*, *S. scilloides*, *S. indica* and *S. peruviana* (Du Plessis and Duncan, 1989). The taxonomy adopted here is based on the family and subfamily arrangements for Hyacinthaceae by *sensu* APGII. A subsequent arrangement based on molecular analyses whereby

Hyacinthaceae is included under the Asparagaceae (APGIII) family was not used because most work cited in our study was done with the old taxonomy.

2.6.1 Ethnobotany and biological activities of the genus *Scilla*

Only *S. nervosa* (*Schizocarpus nervosus* (Burch.) van der Merwe) and *S. natalensis* of the six *Scilla* species have their traditional uses documented (Bangani, 1999). *S. nervosa* bulbs are used in Zulu traditional medicine to treat dysentery and relieve nervous conditions in children, while in Botswana, it is used to treat infection and infertility (Bangani, 1999). Decoctions from *S. natalensis* are administered for rheumatic fever, menstrual cramps and to facilitate labor in women ((Gerstner, 1941; Hutchings, 1989; Hutchings, 1996). Toxicity in sheep has been reported for *S. natalensis* (Watt and Breyer-Brandwijk, 1962). The bulbs of *S. natalensis* are sold at the muthi market to treat gastrointestinal ailments, including stomach aches, constipation, intestinal worms, diarrhea, dysentery, nausea, and indigestion (Hutchings, 1989; van Wyk et al., 1997). Decoctions are also taken as enemas for female fertility and enhance male potency and libido (van Wyk et al., 1997). In Botswana, *Scilla* species are used to prevent witchcraft, while in Malawi, a gluey substance called *ulimo* from *Scilla* species is used as an insect trap (Bangani, 1999).

The dichloromethane and methanol extracts of *S. natalensis* showed good inhibition against COX-1 and COX-2 while the aqueous extract showed good activity against *Schistosoma haematobium*, (Sparg et al., 2002). Results from a mouse model showed that the methanol extract of *S. nervosa* had potent anti-inflammatory activity on oil-induced auricular contact dermatitis. The same study showed that the non-polar fraction of *S. nervosa* had better antibacterial than antifungal activity, while the polar fraction had better antifungal than antibacterial activity (Du Toit et al., 2011). Cultured HepG2 cells was demonstrated to be sensitive to the aqueous extract of *S. nervosa*. (Pillay et al., 2013).

2.6.2 *Phytochemistry of Scilla species*

Homoisoflavonoids, stilbenoids and spirocyclic triterpenes have been reported from the *Scilla* species in South Africa (Bangani, Crouch, Mulholland, 1999; Crouch, Bangani, Mulholland, 1999; Moodley, 2001; Nishida et al., 2013).

2.6.3 *Scilla nervosa (schizocarpus nervosus) (Burch.) Jessop*

Scilla nervosa (Burch.) Jessop (Hyacinthaceae) [*Schizocarpus nervosus* (Burch.) Van der Merwe] (Figure 2.14) is the most widely distributed *Scilla* species in Southern Africa. It is known as *ingcino* by the Zulus. The Zulus use it to treat pain associated with rheumatic fever; the bulbs are used by the Tswana people to treat infertility in women; the Sotho people use it to treat gallstones in livestock, constipation, dysentery, and nervous conditions in children (Bangani et al., 1999). About 20 homoisoflavonoids (Figure 2.15) and stilbenes have been reported from the bulbs and the yellow deposit on the surface of the bulbs (Bangani et al., 1999; Silayo et al., 1999, Famuyiwa et al., 2012).



Figure 2.14 *Scilla nervosa* leaves and bulbs.

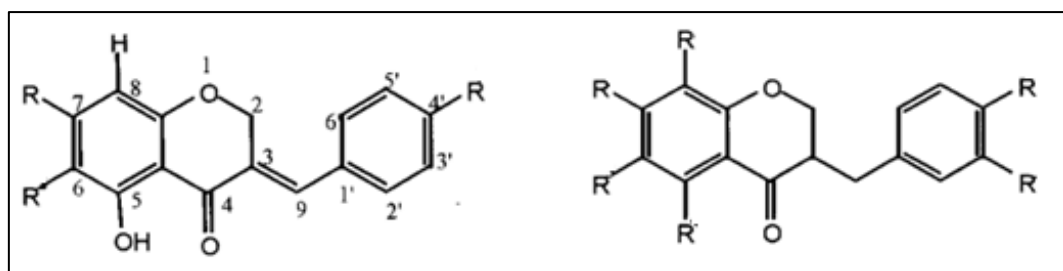


Figure 2.15 Skeletal structures of homoisoflavonoids isolated from *S. nervosa* (Silayo et al., 1999).

2.7 BIOLOGICAL ASSAYS

In natural products research, plants and their isolates are screened for their safety and pharmacological activity. Different assays are employed depending on the activity targeted. These tests are done *in-vitro* in the laboratory, and offer some advantages compared to *in-vivo* testing.

2.7.1 Antioxidant Activity

Biological processes such as respiration generate free radicals due to the incomplete reduction of oxygen. Free radicals partially reduce oxygen, and its derivatives such as superoxide, hydrogen peroxide and hydroxyl ion constitute reactive oxygen species (ROS) (Singh and Singh, 2008). ROS are highly reactive and cause damages to cell structures and alter their function. The human body has an integrated antioxidant system, which is enzymatic or non-enzymatic and is usually effective in preventing the harmful effects of ROS. In some pathological conditions, the natural antioxidant systems could become overwhelmed, creating an imbalance between the oxidants (ROS) and the antioxidants. This shift in balance leads to oxidative stress. Oxidative stress contributes to many diseases, including cancer, hypertension, atherosclerosis, asthma, diabetes, chronic obstructive pulmonary diseases, and Alzheimer's (Birben et al., 2012). ROS has two sources, endogenous and exogenous. An antioxidant is any substance that can significantly delay or prevent oxidation at a low concentration (Singh and

Singh, 2008). Different methods exist to determine the antioxidant capacity of molecules including the 2,2-diphenyl-1-picrylhydrazyl (DPPH) radical scavenging and ferric reducing antioxidant power (FRAP) assays. Both were used in this research.

DPPH (2,3-diphenyl-1-picrylhydrazyl) assay

This method was developed by Blois (1953). The molecule, 2,3-diphenyl-1-picrylhydrazyl (DPPH), is a stable free radical. It has a deep violet color due to the delocalization of a spare electron on the molecule and absorbs UV at 520 nm in ethanol solution (Kedare and Singh, 2011). The assay measures the scavenging ability of the antioxidants, which is observed as a color change for the DPPH from deep violet to yellow. The nitrogen atom in the DPPH radical that is deficient, acquires an electron from the hydrogen radical (Figure 2.16) from the antioxidant (test sample) to form hydrazine (Contreras-Guzman and Srong 1982). The antioxidant ability of the test sample is evaluated by measuring the change in optical density of the DPPH radical.

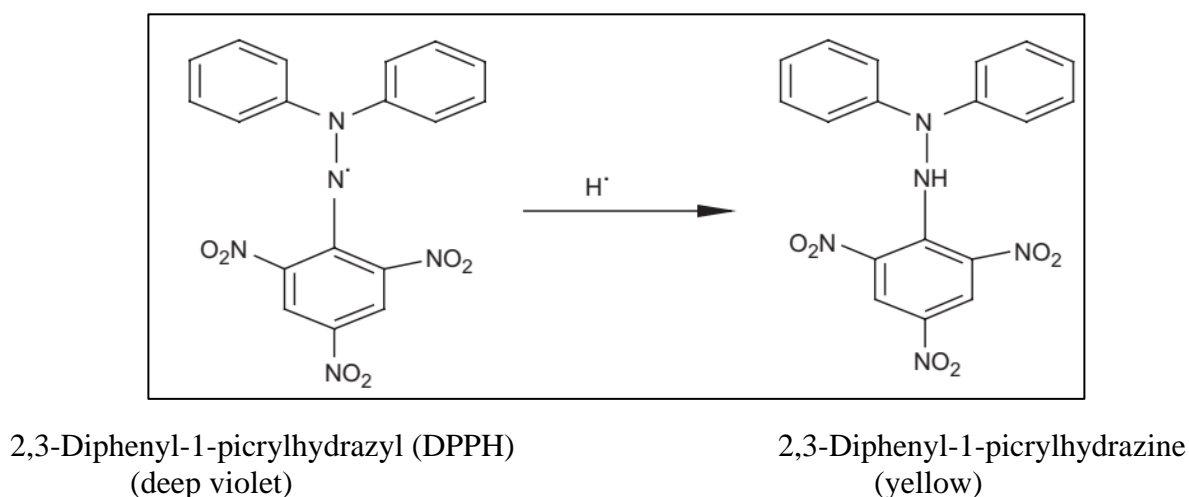
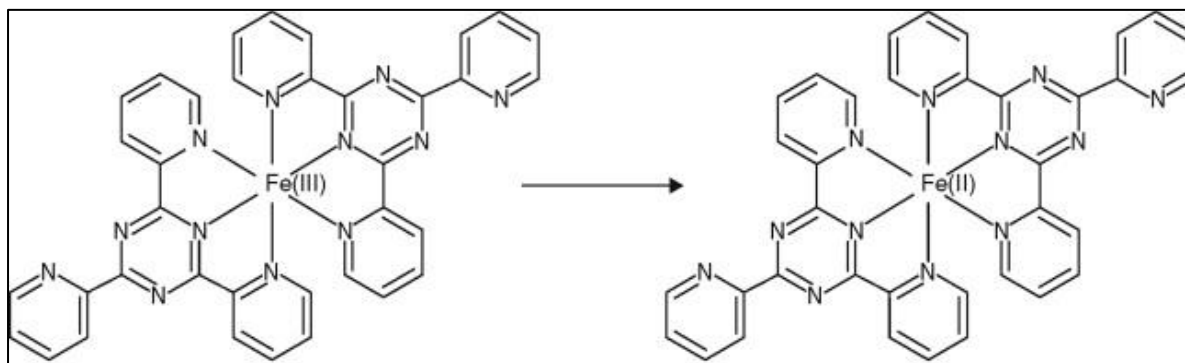


Figure 2.16 Reaction of DPPH and hydrogen donating substrate (Singh and Singh, 2008).

Ferric reducing antioxidant power (FRAP) assay

The principle of the FRAP assay is the ability of the antioxidant to reduce the ferric iron complex (ferric 2,4,6-tripyridyl-*s*-triazine) to its ferrous form at low pH (Figure 2.17). The assay was developed by Benzie and Strain to measure reducing power in plasma, but the assay has been adapted and used for plant extracts (Prior et al., 2005).



Ferric 2,4,6-tripyridyl-*s*-triazine (colorless) Ferrous 2,4,6-tripyridyl-*s*-triazine (blue)

Figure 2.17 Reaction for FRAP assay (Prior et al., 2005).

2.7.2 Antimicrobial Susceptibility Testing

Infectious diseases, according to WHO, account for about 45% of all deaths in low-income countries (Shetty and Shetty, 2009). Drug-resistant microbes pose a challenge to global health. Therefore, in recent years, there has been growing interest in the research and development of new antimicrobial agents to tackle the menace of drug resistance (Balouiri et al., 2016). Antibiotics act by targeting the inhibition of cell wall (peptidoglycan) synthesis, protein synthesis (ribosome) or deoxyribonucleic acid (DNA) or ribonucleic acid (RNA) synthesis (DNA topoisomerase or RNA polymerase). Bacteria develop resistance to antimicrobial drugs by reduced penetration of the drug *via* limited permeability and efflux pumps, mutations or modifications of the binding target, and degradation of the drug itself (Rossiter et al., 2017).

Antimicrobial susceptibility testing can be used to investigate the antibacterial potential of molecules *in-vitro*. The standard methods are the disk-diffusion and broth or agar dilution methods (Balouiri et al., 2016; Schumacher et al., 2018). Bacteria possess the ability to communicate. This process is known as quorum sensing. Quorum sensing is cell to cell communication amongst bacteria, which involves secretion of signaling molecules known as autoinducers (AIs), detecting the change in the concentration of signaling molecules, and regulating gene transcription (Rutherford and Bassler, 2012) (Figure 2.18). Both Gram-positive and Gram-negative bacteria use quorum sensing but with different mechanisms. For Gram-positive bacteria, the signaling molecule is an autoinducing peptide (AIP), while N-Acyl homoserine lactone (AHL) is the signaling molecule for Gram-negative bacteria. Bacteria use quorum sensing communication circuits to control and regulate physiological processes such as virulence, genetic competence, movement, and biofilm formation. This intra and inter species communication allows bacteria to coordinate the gene expression, and therefore the behavior of the entire community, which is akin to some of the qualities of higher organisms.

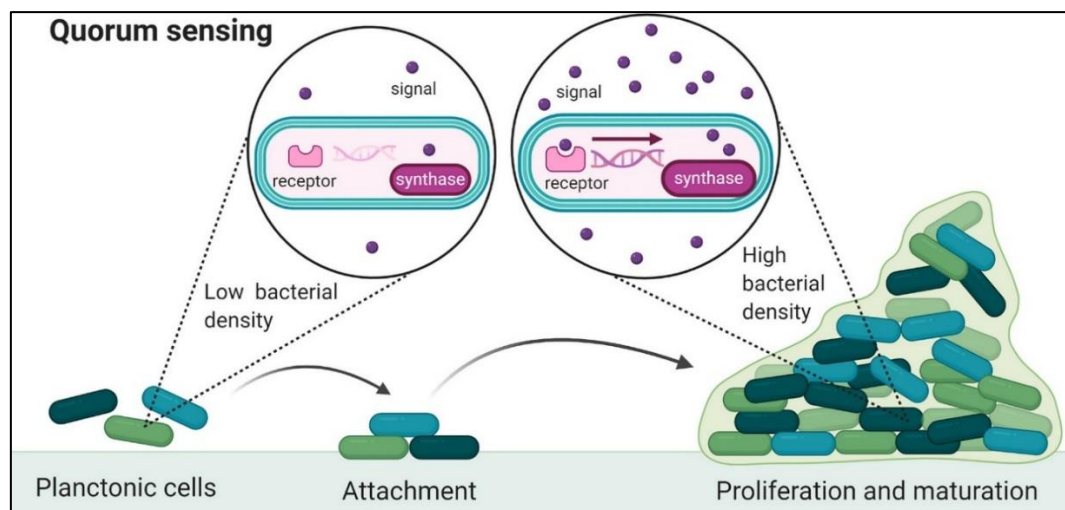


Figure 2.18 Schematic showing quorum sensing (QS) and the formation of bacterial biofilms. QS signals (purple circles) are produced by the enzyme synthase and is released into the extracellular environment. These signals re-enter the cell if their concentration is high in the extracellular medium and are sensed by a receptor in bacterial cell that then activates the transcription of QS-regulated genes. Signal number is proportional to cell density (Adapted from [Muras](#) et al. 2020).

Due to the ability of bacteria to build resistance as an adaptive feature after surviving antimicrobial agent attacks, research is now gearing towards the development of antibiotics that can shut down the communication among bacteria known as quorum sensing inhibition. *Chromobacterium violaceum*, a Gram-negative bacterium, is a known bioindicator used to identify substances that inhibit quorum sensing. The ability of biomolecules to inhibit quorum sensing can be evaluated as a function of capacity to inhibit or reduce *violacein* and biofilm biomass in *C. violaceum* (Wang et al., 2019).

2.7.3 Cytotoxicity Testing

Cell division occurs in all living cells and this is essential to monitor cell growth and death. Normal cell division causes proliferation of single-celled organisms, development, and tissue repair in a multi-celled organism, but uncontrolled cell division leads to the formation of tumors (Istifli et al., 2019). Cancer is a term used to define several diseases characterized by the uncontrollable proliferation of cells due to dysfunction in the regulatory signaling pathway (McCauley et al., 2013).

Cytotoxicity is caused by the adverse reaction of chemical, biological or physical agents on cells. Testing is done *in-vitro* to measure the effect of a test compound on cell viability after incubation for a specific time. There are different assays to measure the number of viable cells; these assays are done with cultured cells for cytotoxicity tests of chemicals and drug screening. In addition, these assays are used in oncology research to measure both compound toxicity and tumor cell growth inhibition during drug development. Cytotoxic agents are known to be toxic to the cells, prevent their growth and eventually cause death. These agents, which may be chemical or biological, exert their effect by destroying cell membranes, preventing protein synthesis, and binding to receptors irreversibly (Aslantürk, 2018). They also affect cellular energy production pathways (mitochondrial effect) or by attenuating the integrity of the

membrane in the cell (plasma membrane or intracellular organelles that have membranes) (Istifli et al., 2019).

Different assays have been developed for *in-vitro* toxicity testing of compounds; these assays could measure viability or toxicity in four different ways: proliferation (direct viable cell count), cell division (DNA synthesis by ³H thymidine uptake), metabolism (MTT, Alamar blue, ATP production) membrane (leakage of lactate dehydrogenase from dead cells) (Figure 2.19) (Istifli et al., 2019). The choice of the assay depends on the number of cells used and the expected outcome.

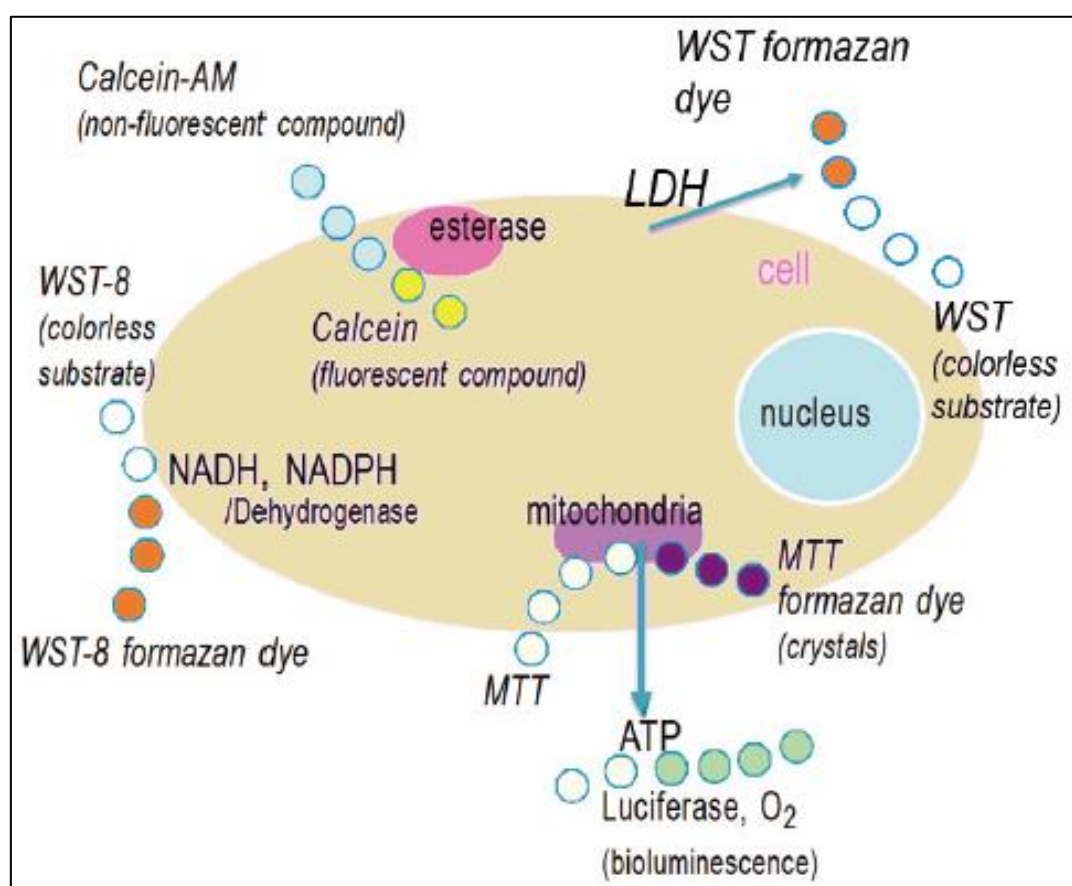


Figure 2. 19 Some cytotoxicity assays and the agents used for detection of cell viability.

MTT (3-(4,5-dimethylthiazol-2-yl)-2,5-diphenyltetrazolium bromide) assay

The molecule, 3-(4,5-dimethylthiazol-2-yl)-2,5-diphenyltetrazolium bromide or MTT, is a water-soluble yellow tetrazolium salt that is reduced by the mitochondria of viable cells to the insoluble purple formazan crystal by cleavage of the tetrazolium ring by dehydrogenase enzymes. The water-insoluble formazan crystal is solubilized using DMSO, isopropanol or acidic ethanolic reagents. The solubilized solution is measured using a plate reading spectrophotometer, using absorbances at 500 and 600 nm wavelengths as a function of the concentration of converted dye. Non-viable cells lose the ability to convert MTT to formazan, so the color formation indicates viable cells (Riss et al., 2013). The MTT assay is usually used in cytotoxicity studies due to its ease of use, accuracy, and rapid indication of toxicity. The mechanism by which cells convert MTT to formazan is still not well understood. The possible explanation is the reaction with NADH or similar reducing molecules that transfer electrons to MTT. The NADH is produced by mitochondrial dehydrogenase enzymes, reducing the tetrazolium salt (Figure 2.20) (McCauley et al., 2013).

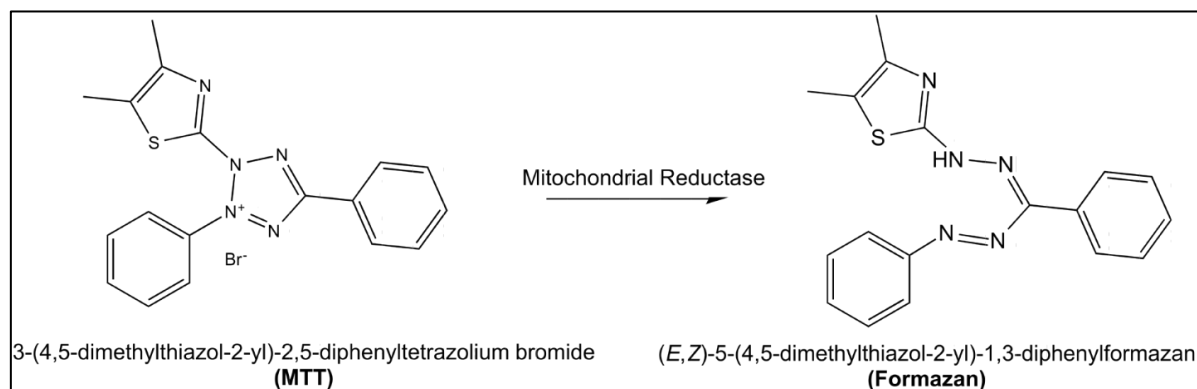


Figure 2.20 Conversion of MTT to formazan (Riss et al., 2013).

ATP (adenosine triphosphate) assay

The ATP assay is based on adenosine triphosphate (ATP) measurement using the firefly luciferase-luciferin system. Measuring ATP levels is the most sensitive, reliable, and

convenient method for monitoring active cell metabolism (Riss et al., 2011). Since ATP degrades rapidly after cell death, its concentration is proportional to cell number. It can be used to evaluate cytotoxicity and as a marker for apoptotic or a necrotic death (Zamaraeva et al., 2005; Tsujimoto, 1997). In addition, the measurement of mitochondrial ATP can be used to probe cellular energy metabolism because mitochondria generate more ATP than those generated *via* glycolysis in the cytoplasm (Manfredi et al., 2001). Unlike the tetrazolium assay, where cells are still intact after addition of the MTT reagent, the ATP reagent ruptures the cell. Therefore, there is no need for an incubation period. The CellTiter-Glo® luminescent cell viability assay is used to determine the number of viable cells in culture. Detection is based on using the luciferase reaction to measure the amount of ATP in viable cells (Figure 2.20). The mechanism of action of the CellTiter-Glo® Reagent is to lyse the cell membrane to release ATP, inhibit endogenous ATPases, and produce luciferin and luciferase necessary to measure ATP using a bioluminescent reaction (Riss et al., 2003) (Figure 2.21).

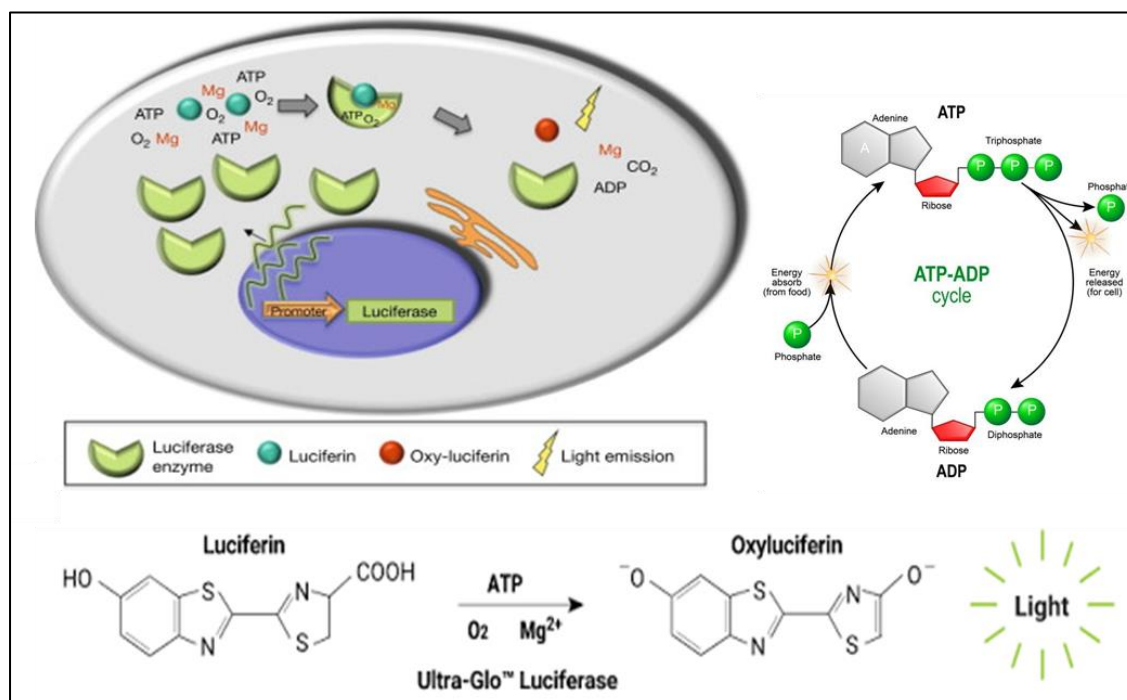


Figure 2.21 Reaction between the adenosine triphosphate (ATP) reagent and luciferin and scheme showing the conversion of ATP to adenosine diphosphate ADP (Promega) (Riss et al., 2003).

LDH (lactate dehydrogenase) assay

This assay measures the activity of cytoplasmic enzymes released during cell lysis. Lactate dehydrogenase (LDH) is released and used as a marker of membrane integrity. Plasma membrane damage, which is a crucial feature of a cell undergoing apoptosis and necrosis, leads to the release of LDH to the cell culture supernatant. LDH from dead cells that leak into the culture medium catalyzes the conversion of lactate to pyruvate and, in the process, generates nicotinamide adenine dinucleotide plus hydrogen (NADH). NADH then reduces the yellow tetrazolium salt into the red, water-soluble formazan-class dye, which has an absorbance at 492 nm (Figure 2.22). The amount of formazan is directly proportional to the amount of LDH in the culture, which in turn, is directly proportional to the number of dead or damaged cells (Kumar et al., 2018). The LDH assay is done using the supernatant of the cell culture.

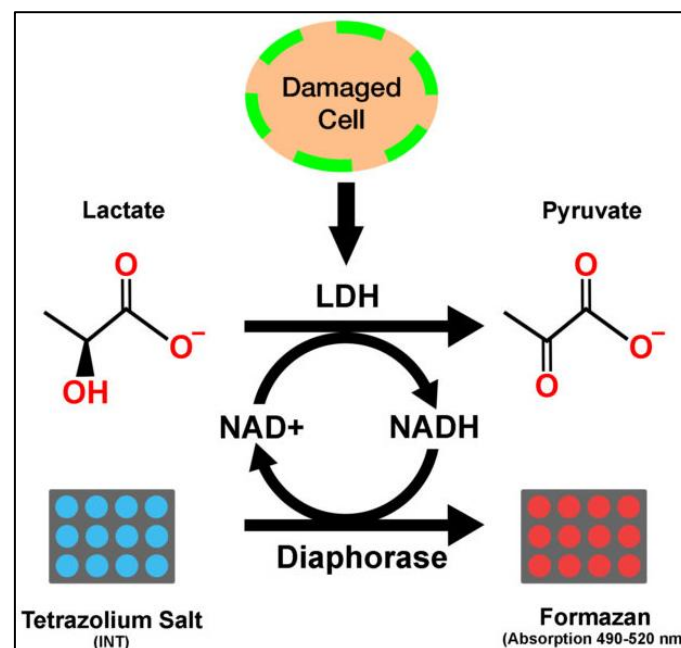


Figure 2.22 The reaction catalyzed by lactate dehydrogenase (LDH) (Adapted from Kumar et al., 2018).

Mitochondria membrane potential (MMP) ($\delta\psi_m$) assay

The mitochondria are regarded as the powerhouse of the cell; they regulate metabolism and cell death pathways. Other functions of the mitochondria are the production of ATP through oxidative phosphorylation and the citric acid cycle, regulation of calcium homeostasis and modulation of apoptosis through the release of several cell death-inducing molecules (Acton et al., 2004). The mitochondria use oxidizable substrates to produce an electrochemical proton gradient across the mitochondrial membrane, which produces ATP; this involves electron transfer between an electron donor and an electron acceptor. The mitochondrial electron transport chain creates an electrochemical gradient that drives the synthesis of ATP and generates the mitochondrial membrane potential (MMP) (Sakamuru et al., 2016). Loss of electron transport means a drop in ATP production; although the loss of mitochondrial ATP could lead to cell death, it is unlikely a mechanism in apoptosis. A decrease in MMP is associated with opening the mitochondrial permeability pores and loss of the electrochemical gradient. Since mitochondria are involved in apoptosis, MMP could be used as a marker for cell health (Sivandzade et al., 2019). Cytotoxic agents can have a direct or secondary effect on mitochondrial function. Many of these compounds reduce MMP by perturbing a variety of macromolecules in the mitochondria, affecting different mitochondrial functions (Sakamuru et al., 2016).

Florescent cationic dyes are used to study MMP in both healthy and apoptotic cells. These dyes are available commercially and are cell membrane permeable. Examples are rhodamine-123, DiOC₆, 5,5,6,6'-tetrachloro-1,1',3,3'-tetraethylbenzimidazolylcarbocyanine iodide (JC-1) and tetramethyl rhodamine methyl and ethyl esters (TMRM and TMRE) (Sakamuru et al., 2016). The JC-1 dye has a problem of solubility, which makes it precipitate in aqueous buffers when used in high concentrations. The JC-10 dye offers better solubility even at higher concentrations compared to JC-1. MMP is negatively charged, so in healthy cells, JC-10

accumulates in the mitochondria to form a red-fluorescence aggregate, with an excitation wavelength of 540 nm and emission wavelength at 590 nm. In apoptotic cells with low negatively charged MMP due to MMP collapse, the mitochondria cannot retain JC-10 dye, the green aggregates are formed with excitation wavelength at 490 nm and emission wavelength at 525nm. The JC-10 dye can be used to monitor apoptosis and for screening apoptosis inhibitors and activators (Sigma-Aldrich JC-10 product information).

Fluorescent dye accumulation in mitochondria can be optically detected by flow cytometry, fluorescent microscopy, confocal microscopy, and through the use of a fluorescence plate reader. Mitochondria polarization or depolarization is indicated by the red/green fluorescence intensity ratio of the dye. Polarization means higher MMP and high red shift of the dye, while depolarization is lower MMP of the mitochondria and lower red to green ratio of the fluorescent marker (Sivandaze et al., 2019; Elefantova et al., 2018). During apoptosis, some events take place in the mitochondria, which includes the opening of the mitochondria pores, with the release of cytochrome c, which initiates some apoptotic pathway, changes in electron transport, loss of mitochondrial transmembrane potential, altered cellular oxidation-reduction, and participation of pro-and anti-apoptotic Bcl-2 family proteins (Green and Reed, 1998).

Cell death occurs either by necrosis or apoptosis. Necrosis, which is ATP-independent, is characterized by cell and organelle swelling, increased permeability with loss of cell membrane integrity, and the release of intracellular contents to the extracellular environment. In contrast, apoptosis is ATP dependent, characterized by cell shrinkage, maintenance of plasma membrane integrity, chromatin condensation, nuclear fragmentation, and activation of a family of cysteine-containing, aspartate-directed proteases called caspases (Cummings and Schnellmann, 2004). The presence of ATP favors apoptosis, while necrosis prevails in its absence (Tatsumi et al., 2003). Studies have shown that necrosis and apoptosis represent

different outcomes of the same pathway. Figure 2.23 shows the mechanism of cell death measuring different markers of cell viability and apoptosis *in-vitro*.







	Time Zero	30 minutes–4 hours	24 hours		Time Zero	30 minutes–4 hours	24 hours
Apoptosis				Necrosis			
	Viable Cell		2° Necrosis		Viable Cell		Cell Debris
LDH Release	0	+	+++	LDH Release	0	+++	++
Caspase	0	+++	++	Caspase	0	0	0
ATP	+++	++	0	ATP	+++	0	0
MTS	+++	++	0	MTS	+++	0	0
Resazurin	+++	++	0	Resazurin	+++	0	0

Figure 2.23 Mechanism of cell death measuring different markers of cell viability and apoptosis *in-vitro* (Adapted from Riss et al., 2003).

REFERENCES

- Abubakar, A. R., & Haque, M. (2020). Preparation of medicinal plants: basic extraction and fractionation procedures for experimental purposes. *JOURNAL OF PHARMACY & BIOALLIED SCIENCES*, 12(1), 1–10. https://doi.org/10.4103/jpbs.JPBS_175_19.
- Adina C. Gradinaru, Mihaela Silion, Adriana Trifan, Anca Miron & Ana C. Aprotosoae (2014) *Helichrysum arenarium* subsp. *arenarium*: phenolic composition and antibacterial activity against lower respiratory tract pathogens, *NATURAL PRODUCT RESEARCH*, 28:22, 2076-2080, DOI: 10.1080/14786419.2014.924931.
- Afolayan, A., & Meyer, J. J. (1997). The antimicrobial activity of 3,5,7-trihydroxyflavone isolated from the shoots of *Helichrysum aureonitens*. *JOURNAL OF ETHNOPHARMACOLOGY*, 57(3), 177–181. doi:10.1016/s0378-8741(97)00065-2.
- Aiyegoro, O. A., & Okoh, A. I. (2010). Preliminary phytochemical screening and *in vitro* antioxidant activities of the aqueous extract of *Helichrysum longifolium* DC. *BMC COMPLEMENTARY AND ALTERNATIVE MEDICINE*, 10, 21. <https://doi.org/10.1186/1472-6882-10-21>.
- Aiyegoro, O., & Okoh, A. (2009). Phytochemical screening and polyphenolic antioxidant activity of aqueous crude leaf extract of *Helichrysum pedunculatum*. *INTERNATIONAL JOURNAL OF MOLECULAR SCIENCES*, 10(11), 4990–5001. doi:10.3390/ijms10114990.
- Al-Rehaily, A. J., Albishi, O. A., El-Olemy, M. M., & Mossa, J. S. (2008). Flavonoids and terpenoids from *Helichrysum forskahlii*. *PHYTOCHEMISTRY*, 69(9), 1910–1914. doi: 10.1016/j.phytochem.2008.03.025.

- Altemimi, A., Lakhssassi, N., Baharlouei, A., Watson, D. G., & Lightfoot, D. A. (2017). Phytochemicals: extraction, isolation, and identification of bioactive compounds from plant extracts. *PLANTS (BASEL)*, 6(4), 42. doi:10.3390/plants6040042.
- Aslantürk, Ö. S. (2018). *In vitro* cytotoxicity and cell viability assays: principles, advantages, and disadvantages. *GENOTOXICITY - A PREDICTABLE RISK TO OUR ACTUAL WORLD*. doi:10.5772/intechopen.71923.
- Balouiri, M., Sadiki, M., & Ibnsouda, S. K. (2016). Methods for *in vitro* evaluating antimicrobial activity: A review. *JOURNAL OF PHARMACEUTICAL ANALYSIS*, 6(2), 71–79. doi:10.1016/j.jpha.2015.11.005.
- Bangani Vuyisile, (1998). Homoisoflavonoids and stilbenoids from *Scilla* species. MSc thesis, School of Chemistry and Physics, University of KwaZulu Natal.
- Bangani, V., Crouch, N. R., & Mulholland, D. A. (1999). Homoisoflavanones and stilbenoids from *Scilla nervosa*. *PHYTOCHEMISTRY*, 51(7), 947–951. doi:10.1016/s0031-9422(99)00155-7.
- Bayer, R. J., Puttock, C. F., & Kelchner, S. A. (2000). Phylogeny of South African *Gnaphalieae* (Asteraceae) based on two noncoding chloroplast sequences. *AMERICAN JOURNAL OF BOTANY*, 87(2), 259–272. doi:10.2307/26569140.
- Beutler JA. (2009) Natural products as a foundation for drug discovery. *Current protocols in pharmacology / editorial board*, SJ Enna. 2009 Sep 1;46:9 11 1-9 21. PubMed PMID: 20161632. PUBMED CENTRAL PMCID: 2813068.
- Birben, E., Sahiner, U. M., Sackesen, C., Erzurum, S., & Kalayci, O. (2012). Oxidative stress and antioxidant defense. *WORLD ALLERGY ORGANIZATION JOURNAL*, 5(1), 9–19. doi:10.1097/wox.0b013e3182439613.

- Bohlmann, F., Abraham W-R., (1979). Neue diterpene aus *Helichrysum acutatum*. PHYTOCHEMISTRY 18, 1754-1756.
- Bougatsos, C., Ngassapa, O., Runyoro, D. K. B., & Chinou, I. B. (2004). Chemical composition and *in vitro* antimicrobial activity of the essential oils of two *Helichrysum* species from Tanzania. ZEITSCHRIFT FÜR NATURFORSCHUNG C, 59(5-6), 368–372. doi:10.1515/znc-2004-5-614.
- Castelli, M. V., & López, S. N. (2017). Homoisoflavonoids: occurrence, biosynthesis, and biological activity. STUDIES IN NATURAL PRODUCTS CHEMISTRY, 315–354. doi:10.1016/b978-0-444-63929-5.00009-7.
- Chapman & Hall/CRC., (2009). Dictionary of Natural Products. Vol 12:3. HDS Software Copyright © Hampden Data Service Ltd.
- Chin Y.W., Balunas M. J., Chai H. B., Kinghorn A. D. (2006) Drug discovery from natural sources. THE AAPS JOURNAL. 2006;8(2): E239-53. PubMed PMID: 16796374. PUBMED CENTRAL PMCID: 3231566.
- Cock, I. E., & Van Vuuren, S. F. (2020). The traditional use of southern African medicinal plants for the treatment of bacterial respiratory diseases: A review of the ethnobotany and scientific evaluations. JOURNAL OF ETHNOPHARMACOLOGY, 263, 113204. <https://doi.org/10.1016/j.jep.2020.113204>.
- Contreras-Guzman ES, Strong FC (1982) Determination of tocopherols (Vitamin E) by reduction of cupric ion. JOURNAL OF THE ASSOCIATION OF OFFICIAL ANALYTICAL CHEMIST (JAOAC) 65:1215– 1222.
- Crouch, N.R., Bangani, V., Mulholland, D.A. (1999). Homoisoflavanones from three South African *Scilla* species. PHYTOCHEMISTRY 51, 943/946.

- Cummings, B. S., & Schnellmann, R. G. (2004). Measurement of cell death in mammalian cells. *CURRENT PROTOCOLS IN PHARMACOLOGY*, Chapter 12, 10.1002/0471141755.ph1208s25. <https://doi.org/10.1002/0471141755.ph1208s25>.
- D'Abrosca, B., Buommino, E., Caputo, P., Scognamiglio, M., Chambery, A., Donnarumma, G., & Fiorentino, A. (2016). Phytochemical study of *Helichrysum italicum* (Roth) G. Don: Spectroscopic elucidation of unusual amino-phlorogucinols and antimicrobial assessment of secondary metabolites from medium-polar extract. *PHYTOCHEMISTRY*, 132, 86–94. doi: 10.1016/j.phytochem.2016.09.012.
- Dewick, P. M. (1975). Biosynthesis of the 3-benzylchroman-4-one eucomin in *Eucomis bicolor*. *PHYTOCHEMISTRY*, 14(4), 983–988. doi:10.1016/0031-9422(75)85172-7.
- Dias, D. A., Urban, S., & Roessner, U. (2012). A historical overview of natural products in drug discovery. *METABOLITES*, 2(2), 303–336. doi:10.3390/metabo2020303.
- Domingo, V., Arteaga, J. F., Quílez del Moral, J. F., & Barrero, A. F. (2009). Unusually cyclized triterpenes: occurrence, biosynthesis and chemical synthesis. *NATURAL PRODUCT REPORT*, 26(1), 115–134. doi:10.1039/b801470c.
- Drewes, S. E., & van Vuuren, S. F. (2008). Antimicrobial acylphloroglucinols and dibenzylxy flavonoids from flowers of *Helichrysum gymnocomum*. *PHYTOCHEMISTRY*, 69(8), 1745–1749. doi: 10.1016/j.phytochem.2008.02.022.
- Du Plessis, N. and Duncan, G. (1989) Bulbous plants of Southern Africa: a guide to their cultivation and propagation, Tafelberg Publishers, Cape Town, p.71.
- Du Toit, K., Kweyama, A., & Bodenstein, J. (2011). Anti-inflammatory and antimicrobial profiles of *Scilla nervosa* (Burch.) Jessop (*Hyacinthaceae*). *SOUTH AFRICAN JOURNAL OF SCIENCE*, 107(5/6). doi:10.4102/sajs. v107i5/6.259.

- Elefantova, K., Lakatos, B., Kubickova, J., Sulova, Z., & Breier, A. (2018). Detection of the mitochondrial membrane potential by the cationic dye JC-1 in 11210 cells with massive overexpression of the plasma membrane ABCB1 drug transporter. *INTERNATIONAL JOURNAL OF MOLECULAR SCIENCES*, *19*(7), 1985. doi:10.3390/ijms19071985.
- El-Elimat T, Rivera-Chávez J, Burdette JE, Czarnecki A, Alhawarri MB, Al-Gharaibeh M, et al. (2018) Cytotoxic homoisoflavonoids from the bulbs of *Bellevia flexuosa*. *FITOTERAPIA*. 127:201-6.
- Eroğlu, H. E., Aksoy, A., Hamzaoglu, E., Budak, Ü., & Albayrak, S. (2009). Cytogenetic effects of nine *Helichrysum* taxa in human lymphocytes culture. *CYTOTECHNOLOGY*, *59*(1), 65–72. doi:10.1007/s10616-009-9193-0.
- Famuyiwa, S. O., Ntuny, A. N., Andrae-Marobela, K., & Yeboah, S. O. (2013). A new homoisoflavonoid and the bioactivities of some selected homoisoflavonoids from the inter-bulb surfaces of *Scilla nervosa* subsp. *rigidifolia*. *SOUTH AFRICAN JOURNAL OF BOTANY*, *88*, 17–22. doi: 10.1016/j.sajb.2013.04.009.
- Green and John C. Reed, D. R. (1998). Mitochondria and apoptosis. *SCIENCE*, *281*(5381), 1309–1312. doi:10.1126/science.281.5381.1309.
- Hilliard, O. M., (1983). Flora of Southern Africa, Vol. 33, Part 7, Fascicle 2, 61-310. Botanical Research Institute, Department of Agriculture, South Africa.
- Hilliard, O.M., (1983). Asteraceae. In: Leistner, O.A. (Ed.), Flora of Southern Africa, vol. 33, part 7 (Inuleae). Botanical Research Institute of South Africa, Pretoria, pp. 7-2:61–7-2:317.

- Houghton, P. J. (1995). The role of plants in traditional medicine and current therapy. *THE JOURNAL OF ALTERNATIVE AND COMPLEMENTARY MEDICINE*, 1(2): 131–143. doi:10.1089/acm.1995.1.131.
- Hutchings, A, Scott, A.H., Lewis, G. and Cunningham, A.B., (1996), *Zulu Medicinal Plants an Inventory*, University of Natal Press: Pietermaritzburg.
- Hutchings, A. (1989). A survey and analysis of traditional medicinal plants as used by the Zulu, Xhosa and Sotho. *BOTHALIA* 19, 111/ 123.
- Jäger, A.K., Hutchings, A., and Van Staden, J. (1996). Screening of Zulu medicinal plants from prostaglandin-synthesis inhibitors. *JOURNAL OF ETHNOPHARMACOLOGY* 5(2): 95-100. Doi:10.1016/0378-8741(96)01395-5.
- Jakupovic J, Zdero C, Grenz M et al (1989). Twenty-one acylphloroglucinol derivatives and further constituents from South African *Helichrysum* species. *PHYTOCHEMISTRY* 28:1119–1131.
- Jones, W. P., & Kinghorn, A. D. (2012). Extraction of plant secondary metabolites. *NATURAL PRODUCTS ISOLATION*, 341–366. doi:10.1007/978-1-61779-624-1_13.
- Kedare, S. B., & Singh, R. P. (2011). Genesis and development of DPPH method of antioxidant assay. *JOURNAL OF FOOD SCIENCE AND TECHNOLOGY*, 48(4), 412–422. <https://doi.org/10.1007/s13197-011-0251-1>.
- Kumar, P., Nagarajan, A., & Uchil, P. D. (2018). Analysis of cell viability by the lactate dehydrogenase assay. *COLD SPRING HARBOR PROTOCOLS*, (6), 10.1101/pdb.prot095497. <https://doi.org/10.1101/pdb.prot095497>.

- Li N, Zhang J-Y, Zeng K-W, Zhang L, Che Y-Y, Tu P-F. (2012) Anti-inflammatory homoisoflavonoids from the tuberous roots of *Ophiopogon japonicus*. FITOTERAPIA. 83(6):1042-5.
- Li, J. W., & Vederas, J. C. (2009). Drug discovery and natural products: end of an era or an endless frontier? SCIENCE (New York, N.Y.), 325(5937), 161–165. <https://doi.org/10.1126/science.1168243>.
- Lin, L.-G., Liu, Q.-Y., & Ye, Y. (2014). Naturally Occurring Homoisoflavonoids and their pharmacological activities. PLANTA MEDICA, 80(13), 1053–1066. doi:10.1055/s-0034-1383026.
- Lockermann, G. (1951). Friedrich Wilhelm Serturmer, the discoverer of morphine. JOURNAL OF CHEMICAL EDUCATION, 28(5): 277. doi:10.1021/ed028p277.
- Lourens, A. C. U., Van Vuuren, S. F., Viljoen, A. M., Davids, H., & Van Heerden, F. R. (2011). Antimicrobial activity and *in vitro* cytotoxicity of selected South African *Helichrysum* species. SOUTH AFRICAN JOURNAL OF BOTANY, 77(1): 229–235. doi: 10.1016/j.sajb.2010.05.006.
- Lourens, A. C. U., Viljoen, A. M., & van Heerden, F. R. (2008). South African *Helichrysum* species: A review of the traditional uses, biological activity and phytochemistry. *Journal of ETHNOPHARMACOLOGY*, 119(3): 630–652. doi: 10.1016/j.jep.2008.06.011.
- Machala, M., Kubínová, R., Hořavová, P., & Suchý, V. (2001). Chemoprotective potentials of homoisoflavonoids and chalcones of *Dracaena cinnabari*: modulations of drug-metabolizing enzymes and antioxidant activity. PHYTOTHERAPY RESEARCH, 15(2): 114–118. doi:10.1002/ptr.697.

- Mahomoodally, M. F. (2013). Traditional medicines in Africa: An appraisal of ten potent African medicinal plants. EVIDENCE-BASED COMPLEMENTARY AND ALTERNATIVE MEDICINE, 2013, 1–14. doi:10.1155/2013/617459.
- Malolo, F. A. E., Bissoue Nougba, A., Kakam, A., Franke, K., Ngah, L., Flausino, O., ... Wessjohann, L. (2015). Protease-inhibiting, molecular modeling and antimicrobial activities of extracts and constituents from *Helichrysum foetidum* and *Helichrysum mechowianum* (compositae). CHEMISTRY CENTRAL JOURNAL, 9(1). doi:10.1186/s13065-015-0108-1.
- Mamabolo MP, Muganza FM, Olivier MT, Olaokun OO, Nemutavhanani LD (2018) Evaluation of antigonorrhea activity and cytotoxicity of *Helichrysum caespititium* (DC) Harv. whole plant extracts. BIOLOGY AND MEDICINE (Aligarh) 10: 422. DOI: 10.4172/0974-8369.1000422.
- Manfredi, G., Spinazzola, A., Checcarelli, N., & Naini, A. (2001). Assay of mitochondrial ATP synthesis in animal cells. MITOCHONDRIA, 133–145. doi:10.1016/s0091-679x(01)65008-8.
- Matić, I. Z., Aljančić, I., Žižak, Ž., Vajs, V., Jadranin, M., Milosavljević, S., & Juranić, Z. D. (2013). *In vitro* antitumor actions of extracts from endemic plant *Helichrysum zivojinii*. BMC COMPLEMENTARY AND ALTERNATIVE MEDICINE, 13(1). doi:10.1186/1472-6882-13-36.
- McCauley, J., Zivanovic, A. & Skropeta, D. (2013). Bioassays for anti-cancer activities. METHODS IN MOLECULAR BIOLOGY, 1055 191-205.
- Moodley, N., Mulholland, D. A., & Crouch, N. R. (2004). Eucosterol-type nortriterpenoids from *Merwillia natalensis*. JOURNAL OF NATURAL PRODUCTS, 67(5), 918–920. doi:10.1021/np0204803.

- Moodley. N. (2001) The chemical investigation of *Ledebouria zebrina* and *Scilla natalensis*. MSc thesis university of Natal, Durban, South Africa.
- Mothibe, M., & Sibanda, M. (2019). African traditional medicine: South African perspective. TRADITIONAL AND COMPLEMENTARY MEDICINE. doi:10.5772/intechopen.83790.
- Mulholland, D.A., Schwikkard S.L., and Crouch N.R. (2013) The chemistry and biological activity of the Hyacinthaceae. NATURAL PRODUCT REPORT, 2013, 30, 1165.
- Muras, A., Mallo, N., Otero-Casal, P., Pose-Rodríguez, J. M., Otero, A. (2020). Quorum sensing systems as a new target to prevent biofilm-related oral diseases. ORAL DISEASES. DOI: (10.1111/odi.13689)
- Nature: All natural (Editorial) (2007) NATURE CHEMICAL BIOLOGY.
- Newman D. J., Cragg G. M., Snader K. M. (2003). Natural products as sources of new drugs over the period 1981-2002. JOURNAL OF NATURAL PRODUCT. 66: 1022 - 1037.
- Newman DJ, Cragg GM. (2012) Natural products as sources of new drugs over the 30 years from 1981 to 2010. JOURNAL OF NATURAL PRODUCTS. 2012 Mar 23;75(3):311-35. PubMed PMID:22316239.
- Njila, M., Mahdi, E., Lembè, D., Nde, Z., Doriane, & Nyonseu (2017). Review on Extraction and Isolation of Plant Secondary Metabolites.
- P. Shetty, N., & S. Shetty, P. (2009). Epidemiology of disease in the tropics. MANSON'S TROPICAL DISEASES, 19–34. <https://doi.org/10.1016/B978-1-4160-4470-3.50007-0>.
- Phillips, D. R., Rasbery, J. M., Bartel, B., & Matsuda, S. P. (2006). Biosynthetic diversity in plant triterpene cyclization. CURRENT OPINION IN PLANT BIOLOGY, 9(3), 305–314. doi: 10.1016/j.pbi.2006.03.004.

- Pillay, P., Phulukdaree, A., Chuturgoon, A. A., Du Toit, K., & Bodenstein, J. (2013). The cytotoxic effects of *Scilla nervosa* (Burch.) Jessop (Hyacinthaceae) aqueous extract on cultured HepG2 cells. JOURNAL OF ETHNOPHARMACOLOGY, 145(1), 200–204. doi: 10.1016/j.jep.2012.10.053.
- Pooley, E., 2003. Mountain flowers: a field guide to the flora of the drakensberg and Lesotho, 1st ed. The Flora Publications Trust, Durban, pp. 44, 102–110, 146–157, 222–225.
- Popoola O. K., Marnewick J. L., Rautenbach F., Ameer F., Iwuoha E. I., Hussein A. A. (2005) inhibition of oxidative stress and skin aging-related enzymes by prenylated chalcones and other flavonoids from *Helichrysum teretifolium*. MOLECULES. 2015;20(4):7143-7155.
- Popoola, O. K., Marnewick, J. L., Rautenbach, F., Iwuoha, E. I., & Hussein, A. A. (2015). Acylphloroglucinol derivatives from the South African *Helichrysum niveum* and their biological activities. MOLECULES (BASEL, SWITZERLAND), 20(9),17309–17324. <https://doi.org/10.3390/molecules200917309>.
- Popoola, O., Marnewick, J., Rautenbach, F., Iwuoha, E., & Hussein, A. (2015). Acylphloroglucinol derivatives from the South African *Helichrysum niveum* and their biological activities. MOLECULES, 20(9), 17309–17324. doi:10.3390/molecules200917309.
- Prior, R. L., Wu, X., & Schaich, K. (2005). Standardized methods for the determination of antioxidant capacity and phenolics in foods and dietary supplements. JOURNAL OF AGRICULTURAL AND FOOD CHEMISTRY, 53(10), 4290–4302. <https://doi.org/10.1021/jf0502698>.
- Riss TL, Moravec RA, Niles AL, et al. Cell Viability Assays. 2013 May 1 [Updated 2016 Jul 1]. In: Markossian S, Grossman A, Brimacombe K, et al., editors. Assay Guidance Manual

- [Internet]. Bethesda (MD): Eli Lilly & Company and the National Center for Advancing Translational Sciences; 2004-. Available from: <https://www.ncbi.nlm.nih.gov/books/NBK144065/>.
- Riss, T. L., Moravec, R. A., & Niles, A. L. (2011). Cytotoxicity testing: measuring viable cells, dead cells, and detecting mechanism of cell death. *MAMMALIAN CELL VIABILITY*, *103–114*. doi:10.1007/978-1-61779-108-6_12.
- Rossiter, S. E., Fletcher, M. H., & Wuest, W. M. (2017). Natural products as platforms to overcome antibiotic resistance. *CHEMICAL REVIEWS*, *117(19)*, *12415–12474*. doi:10.1021/acs.chemrev.7b00283.
- Rutherford, S. T., & Bassler, B. L. (2012). Bacterial quorum sensing: its role in virulence and possibilities for its control. *COLD SPRING HARBOR PERSPECTIVES IN MEDICINE*, *2(11)*, *a012427–a012427*. doi:10.1101/cshperspect. a012427.
- Sakamuru, S., Attene-Ramos, M. S., & Xia, M. (2016). Mitochondrial membrane potential assay. *METHODS IN MOLECULAR BIOLOGY*, *1473*, *17–22*. https://doi.org/10.1007/978-1-4939-6346-1_2.
- Salih Istifli, E., Tahir Hüsünet, M., & Basri İla, H. (2019). Cell division, cytotoxicity, and the assays used in the detection of cytotoxicity. *Cytotoxicity - DEFINITION, IDENTIFICATION, AND CYTOTOXIC COMPOUNDS*. doi:10.5772/intechopen.88368.
- Sawai, S., & Saito, K. (2011). Triterpenoid biosynthesis and engineering in plants. *FRONTIERS IN PLANT SCIENCE*, *2*, *25*. <https://doi.org/10.3389/fpls.2011.00025>.
- Schumacher, A., Vranken, T., Malhotra, A., Arts, J. J. C., & Habibovic, P. (2017). *In vitro* antimicrobial susceptibility testing methods: agar dilution to 3D tissue-engineered models.

- EUROPEAN JOURNAL OF CLINICAL MICROBIOLOGY & INFECTIOUS DISEASES, 37(2), 187–208. doi:10.1007/s10096-017-3089-2.
- Schwikkard, S. L., Whitmore, H., Corson, T. W., Sishtla, K., Langat, M. K., Carew, M., & Mulholland, D. A. (2018). Antiangiogenic activity and cytotoxicity of triterpenoids and homoisoflavonoids from *Massonia pustulata* and *Massonia bifolia*. PLANTA MEDICA, 84(9/10), 638–644. <https://doi.org/10.1055/a-0577-5322>.
- Semenya, S., Maroyi, A., Potgieter, M., & Erasmus, L. (2012). Herbal medicines used by Bapedi traditional healers to treat reproductive ailments in the Limpopo Province, South Africa. AFRICAN JOURNAL OF TRADITIONAL, COMPLEMENTARY, AND ALTERNATIVE MEDICINES: AJTCAM, 10(2), 331–339. <https://doi.org/10.4314/ajtcam.v10i2.19>.
- Sidwell, W. T. L., Tamm, C., Ziegler, R., Finer, J., & Clardy, J. (1975). Eucosterol, a novel spirocyclic nortriterpene isolated from bulbs of *Eucomis* species. JOURNAL OF THE AMERICAN CHEMICAL SOCIETY, 97(12), 3518–3519. doi:10.1021/ja00845a041.
- Silayo, A., Ngadjui, B. T., & Abegaz, B. M. (1999). Homoisoflavonoids and stilbenes from the bulbs of *Scilla nervosa subsp. rigidifolia*. PHYTOCHEMISTRY, 52(5), 947–955. doi:10.1016/s0031-9422(99)00267-8.
- Singh, S., & Singh, R. P. (2008). *In vitro* methods of assay of antioxidants: An overview. FOOD REVIEWS INTERNATIONAL, 24(4), 392–415. doi:10.1080/87559120802304269.
- Sivandzade, F., Bhalerao, A. and Cucullo, L. (2019). Analysis of the mitochondrial membrane potential using the cationic jc-1 dye as a sensitive fluorescent probe. BIO-PROTOCOL 9(1): e3128. DOI: 10.21769/BioProtoc.3128.

- Sparg, S. G., van Staden, J., & Jäger, A. K. (2002). Pharmacological and phytochemical screening of two Hyacinthaceae species: *Scilla natalensis* and *Ledebouria ovatifolia*. JOURNAL OF ETHNOPHARMACOLOGY, 80(1), 95–101. doi:10.1016/s0378-8741(02)00007-7.
- Street, R. A., & Prinsloo, G. (2013). Commercially important medicinal plants of South Africa: A review. JOURNAL OF CHEMISTRY, 2013, 1–16. doi:10.1155/2013/205048.
- Sudhakar Singh & R.P. Singh (2008): *In vitro* methods of assay of antioxidants: An overview, FOOD REVIEWS INTERNATIONAL, 24:4, 392-415.
- Süntar . I., Esra Küpeli Akkol a,n, Hikmet Keles b, Erdem Yesilada c, Satyajit D. Sarker (2013) Exploration of the wound healing potential of *Helichrysum graveolens* (Bieb.) Sweet: Isolation of apigenin as an active component. JOURNAL OF ETHNOPHARMACOLOGY 149 (2013) 103–110.
- Süzgeç-Selçuk, S., & Birteksöz, A. S. (2011). Flavonoids of *Helichrysum chasmolycicum* and its antioxidant and antimicrobial activities. SOUTH AFRICAN JOURNAL OF BOTANY, 77(1), 170–174. doi:10.1016/j.sajb.2010.07.017.
- Tatsumi T., Shiraishi J., Keira N., Akashi, K., Mano A., Yamanaka S., Nakagawa. M. (2003). Intracellular ATP is required for mitochondrial apoptotic pathways in isolated hypoxic rat cardiac myocytes. CARDIOVASCULAR RESEARCH, 59(2), 428–440. doi:10.1016/s0008-6363(03)00391-2.
- THE ANGIOSPERM PHYLOGENY GROUP, An update of the Angiosperm Phylogeny Group classification for the orders and families of flowering plants: APG II, BOTANICAL JOURNAL OF THE LINNEAN SOCIETY, 141(4), 399–436.

THE ANGIOSPERM PHYLOGENY GROUP, An update of the angiosperm phylogeny group classification for the orders and families of flowering plants: APG III, BOTANICAL JOURNAL OF THE LINNEAN SOCIETY, 161(2), 105–121.

Thimmappa, R., Geisler, K., Louveau, T., O'Maille, P., & Osbourn, A. (2014). Triterpene biosynthesis in plants. ANNUAL REVIEW OF PLANT BIOLOGY, 65(1), 225–257. doi:10.1146/annurev-arplant-050312-120229.

Tsujimoto, Y. (1997). Apoptosis and necrosis: Intracellular ATP level as a determinant for cell death modes. CELL DEATH AND DIFFERENTIATION, 4(6), 429–434. doi:10.1038/sj.cdd.4400262.

Van Wyk B.E., Van Oudtshoorn B., Gericke N. (1997). Medicinal Plants of South Africa. Briza Publications, Pretoria.

Van Wyk, B.-E. (2011). The potential of South African plants in the development of new medicinal products. SOUTH AFRICAN JOURNAL OF BOTANY, 77(4), 812–829. doi: 10.1016/j.sajb.2011.08.011.

Wang, W., Li, D., Huang, X., Yang, H., Qiu, Z., Zou, L., Liang, Q., Shi, T., Wu, Y., Wu, S., Yang, C., Li, Y. (2019). Study on antibacterial and quorum-sensing inhibition activities of *Cinnamomum camphora* leaf essential oil. MOLECULES, 24(20), 3792. doi:10.3390/molecules24203792.

Watt, J.M. and Breyer-Brandwijk, M.G. (1962) Medicinal and Poisonous Plants of East and Southern and Eastern Africa, 2nd edition, E and S Livingstone, Edinburgh, p.713.

- Werner, J., Ebrahim, W., Özkaya, F. C., Mándi, A., Kurtán, T., El-Neketi, M., Liu, Z., Proksch, P. (2018). Pyrone derivatives from *Helichrysum italicum*. FITOTERAPIA. doi: 10.1016/j.fitote.2018.12.018.
- Yagura, T., Motomiya, T., Ito, M., Honda, G., Iida, A., Kiuchi, F., Tokuda, H., Nishino, H. (2008). Anticarcinogenic compounds in the Uzbek medicinal plant, *Helichrysum maracandicum*. JOURNAL OF NATURAL MEDICINES, 62(2), 174–178. doi:10.1007/s11418-007-0223-y.
- Yuan, H., Ma, Q., Ye, L., & Piao, G. (2016). The traditional medicine and modern medicine from natural products. MOLECULES, 21(5), 559. doi:10.3390/molecules21050559.
- Zähner H. What are secondary metabolites? (1979) FOLIA MICROBIOLOGICA, 24(5), 435-43.
- Zamaraeva, M. V., Sabirov, R. Z., Maeno, E., Ando-Akatsuka, Y., Bessonova, S. V., & Okada, Y. (2005). Cells die with increased cytosolic ATP during apoptosis: a bioluminescence study with intracellular luciferase. CELL DEATH AND DIFFERENTIATION, 12(11), 1390–1397. doi: 10.1038/sj.cdd.4401661.
- Ziegler, R., & Tamm, C. (1976). Isolation and structure of eucosterol and 16-hydroxyeucosterol, two novel spirocyclic nortriterpenes, and of a new 24- nor-5-chola-8, 16-diene-23-oic acid from bulbs of several *Eucomis* species. HELVETICA CHIMICA ACTA, 59(6), 1997–2011. doi:10.1002/hlca.19760590613.

CHAPTER 3

Phytochemical, antibacterial and docking studies of *Scilla nervosa* (Burch.) Jessop

ABSTRACT

Scilla nervosa (Burch.) Jessop is a plant used in traditional medicine as an analgesic and to treat infections. This study aimed to phytochemically study the bulbs and leaves of *S. nervosa*, test the antibacterial potential of biomolecules and extracts, and determine the structure-activity relationships using molecular docking. From the bulbs and leaves, two novel homoisoflavonoids, namely 3-(4-hydroxy-3-methoxybenzyl)-5,7-dihydroxy-6-methoxychroman-4-one, and 3-(4-hydroxy-3-methoxybenzyl)-5,6,7-trihydroxychroman-4-one, two novel lanostane-type triterpenes, namely 17 α ,23 α -epoxy-3 β ,29-dihydroxy-nor-lanost-8,24-dien-26-one and 17 α ,23 α -epoxy-3 β ,28,29-trihydroxy-nor-lanost-8,24-dien-26-one, five known homoisoflavanones, namely 3-(4-methoxybenzyl)-5,7-dimethoxychroman-4-one, 3-(4-methoxybenzyl)-6-hydroxy-5,7-dimethoxychroman-4-one, 3-(4-hydroxybenzyl)-6-hydroxy-5,7-dimethoxychroman-4-one, 3-(4-hydroxy-3-methoxybenzyl)-5-hydroxy-7-methoxychroman-4-one, and 3-(4-hydroxybenzylidene)-5,7-dihydroxychroman-4-one, a stilbene (rhapontigenin) and a spinasterol glucopyranoside, were isolated. The structures of the isolated compounds were established by nuclear magnetic resonance spectroscopy and mass spectrometry. The crude extracts and isolates were screened against Gram-positive and Gram-negative bacterial strains. The antibacterial activities of the biomolecules were better than those of the extracts with biomolecule activity being proportional to the number of methoxy groups; the 5,7,4'-trisubstituted homoisoflavonoids demonstrated better activity than the disubstituted or unsubstituted ones. Homoisoflavonoids showed minimal antibacterial activity, both *in-vitro*

and by computational study. However, synthetic manipulations of their molecular structure could ameliorate their activity. *S. nervosa* was shown to biosynthesize lanostane-type triterpenes similar to other species in the genus.

Keywords: Homoisoflavonoids; molecular docking, nuclear magnetic resonance, phytochemistry

3.1 INTRODUCTION

Plants have been a storehouse of various secondary metabolites, some of which have found therapeutic use as antimicrobial, antidiabetic, antimalarial, and anticancer agents. Naturally occurring bioactive compounds have been a significant source of lead compounds in drug discovery and development (Newman and Cragg, 2003). Infectious diseases have been described as a significant burden to many societies, according to the World Health Organization (WHO) (Boutayeb, 2010). Antimicrobial resistance, which results from a change in the gene of pathogens that allows it to evade the action of antibiotics, has been seen as a public health threat (Simpkin et al., 2017). Additionally, it has been projected that by 2050 the total number of deaths from antimicrobial resistance would rise to 10 million per year worldwide (Cattoir and Felden, 2019). Antimicrobial resistance has necessitated the need for new antibiotics that can tackle the burden of antibiotic resistance. There is a need for new pharmacophores for antibacterial drug development due to the increasing resistance to conventional antibiotics. Antimicrobial agents act by interfering with essential processes needed for the growth or division of microorganisms. Interference could be by inhibiting cell wall synthesis, inhibition of plasma membrane integrity, interference with nucleic acid synthesis, inhibition of ribosome function, or folate synthesis (Baron, 1996).

The cell wall provides rigidity and stability for the bacteria, and it is crucial for its survival. The cell wall consists of a peptidoglycan layer that prevents osmotic lysis. Peptidoglycan is a polymer consisting of interlocking chains of identical peptidoglycan monomers, a β -1,4-linked glycan of alternating N-acetylglucosamine (GlcNAc), and N-acetylmuramic acid (MurNAc) sugars. There are different stages in the biosynthetic pathway of peptidoglycan (Kimura and Bugg, 2003). The enzyme catalyst, phospho-iMurNAc-pentapeptide translocase (MraY), is essential for the initial step of the lipid-linked chain of reactions in the synthesis of peptidoglycan (Bugg et al., 2006). Certain antibiotics such as penicillin (ampicillin), cephalosporins (cefixime), carbapenems (loracarbef), and glycopeptides (vancomycin) work by inhibiting the synthesis of peptidoglycan; interference in the process of peptidoglycan synthesis leads to a weak cell wall and lysis of the bacterium from osmotic pressure. The biosynthetic pathway of peptidoglycan is a good target for the development of novel antibacterial agents. Several antibacterial natural products and one protein antibacterial agent that targets translocase have been identified (Bugg et al., 2006).

Scilla nervosa (Burch.) Jessop [syn. *Schizocarphus rigidifolia* Kunth] from the Hyacinthaceae family is an indigenous medicinal plant in Southern Africa that is a rich source of homoisoflavanones (Silayo et al., 1999). It is known as igncino in isiZulu, and inkwitelu by the Xhosa people of South Africa. It is widely distributed in the Eastern Cape, Free State, Gauteng, KwaZulu-Natal, Limpopo, Mpumalanga, Northwest, and Northern Cape. *S. nervosa* forms rounded clumps with large, buried bulbs with fibrous sheaths; there are tiny flowers on a stalk, white or creamy yellow with green or blackish ovaries (Hutchings, 1996). In Southern African, *S. nervosa* is used as an analgesic and to treat infections (Du Toit et al., 2011). *Scilla* species have demonstrated cytotoxic effects against AGS cell lines (Salar et al., 2016), as well as anti-tumor (Lee et al., 2002), antioxidant (Nishida et al., 2013), antimicrobial, and anti-inflammatory activities (Du Toit et al., 2011).

Several studies on *Scilla* species have shown them to be rich sources of homoisoflavonoids (Bangani et al., 1999; Silayo et al., 1999; Famuyiwa et al., 2012; Hafez-Ghoran et al., 2015). *Scilla* species also contain other secondary metabolites such as stilbenoids, cardiac glycosides, and triterpenes (Bangani et al., 1999; Crouch, Bangani, Mulholland, 1999; Mimaki et al., 1993; Nishida et al., 2008). Lanostane-type triterpenoids and their glycosides have also been isolated from some *Scilla* species, such as *Scilla scilliodes*, *Scilla perisca*, and *Scilla natalensis* (Amschler et al., 1998; Ono et al., 2012).

du Toit (2011), postulated that the extracts from *S. nervosa* would exhibit better antibacterial activity as the compounds present in them would reciprocally potentiate the activity of the individual molecules. In a review article on the antimicrobial activity of South African medicinal plants, van Vuuren (2008) suggested that individual biomolecules conferring activity was improbable and greater efficacy would be achieved by a combination thereof. Therefore, in this study, we compare the antibacterial potential of the crude extracts and individual biomolecules from *S. nervosa* against selected strains of Gram-negative and Gram-positive bacteria to determine for additive effects. We also phytochemically investigated the leaves of the plant that have not previously been studied.

3.2. MATERIALS AND METHODS

3.2.1 General Experimental Procedure

^1H , ^{13}C and 2D NMR were obtained on Bruker Avance III 400 MHz spectrophotometer using either deuterated chloroform (CDCl_3) or methanol (MeOD) at room temperature. High-resolution mass spectrometry (HRMS) was done on a Waters Micromass LCT Premier TOF-MS instrument. Infrared (IR) spectra were recorded on a Perkin Elmer Spectrum 100 Fourier transform infrared spectrophotometer (FT-IR). Ultraviolet-visible (UV-Vis) spectra were

recorded on a Varian Cary UV-Vis spectrophotometer. Column chromatography was performed using Merck silica gel 60 (0.040-0.063 mm), a R CH-20 (Merck) Sephadex column, and 20 × 20 aluminum sheets coated with silica gel 60 F245 was used for thin-layer chromatography (TLC). TLC plates were viewed under UV light at wavelengths of 254 nm and 366 nm. Further visualization was done by spraying with 10% sulfuric acid in MeOH solution followed by heating. All reagents were supplied by either Merck (Darmstadt, Germany) or Sigma (St. Louis, USA) chemical companies.

3.2.2 Plant Materials

Fresh bulbs and leaves of *Scilla nervosa* were purchased from the Berea muthi (herbal) market in Durban and were identified by the taxonomist, Mr. Edward Khathi of the School of Life Sciences, University of KwaZulu Natal (UKZN, Westville). A voucher specimen, 18272 02 1086000, was deposited in the ward herbarium in the School of Life Sciences.

3.2.3 Extraction, Isolation, and Purification

Plant material was air-dried and crushed. Crushed bulbs (300 g) and leaves (1 kg) were successively extracted using MeOH, ethyl acetate (EtOAc), and dichloromethane (DCM) by cold maceration on a shaker for 48 h at room temperature. Each crude extract was evaporated under reduced pressure to remove excess solvent and concentrated to give 5 g from DCM, 3 g from EtOAc, and 24 g from MeOH for the bulbs and 3 g from MeOH for the leaves. Extracts were subjected to column chromatography, using hexane and EtOAc gradient starting with 100% hexane that was stepped by 10 % to 100 % EtOAc. After that, 10 % MeOH was added to EtOAc. Fingerprinting using TLC was done for each of the chromatographic fractions. Fractions that gave the same retention factor (R_f) were pooled together.

From the DCM extract of the bulbs (65 × 100 mL fractions), fractions 17 and 18 presented compound **A1** (350 mg), a yellow and oily gum, fractions 23 and 24 presented compound **A2**

(100 mg), while fraction 34 presented compound **A3** (11 mg). Fraction 14 was purified to obtain compound **A4** (10 mg). The MeOH extract of the leaves (30 × 100 mL fractions) resulted in the isolation of compound **A1** from fraction 17, a mixture of compounds **A1** and **A5** from fraction 18 (6 mg), and compound **A6** (5 mg) from fraction 19. From the EtOAc extract of the bulbs (50 × 100 mL fractions), compound **7** (20 mg), a yellow powder was precipitated out of fraction 25 using DCM, and compound **A8** (12 mg), a yellow powder was obtained from fraction 28. Compound **A9** (10 mg) was obtained as white flakes from fractions 41-44 of the DCM extract of the bulbs after cleaning with MeOH. Compound **A10** was obtained as brown spikes from fraction 26 of the DCM extract of the bulbs, while compound **A11**, a brown powder, was obtained from fraction 31 of the same extract.

3.2.4 Evaluation of Antibacterial Activity

Antibacterial activity of the crude extracts (DCM and MeOH extracts of the bulbs, and MeOH extract of the leaves) and isolated phytochemicals (**A1**, **A2**, **A4** and **A7**) was evaluated using the agar-well diffusion method (CLSI, 2012) against three Gram-positive bacteria (*Bacillus subtilis* ATCC 6653, methicillin-resistant *Staphylococcus aureus* ATCC 43000 and *Mycobacterium smegmatis* mc² 155) and four Gram-negative bacteria, (beta-lactam-resistant *Escherichia coli* ATCC 35218, multidrug-resistant *Pseudomonas aeruginosa* ATCC 27853, extended-spectrum beta-lactamase-producing *Klebsiella pneumoniae* ATCC 700603 and the quorum sensing indicator *Chromobacterium violaceum* ATCC 12472). Test samples were dissolved in MeOH to a final concentration of 20 mg mL⁻¹ for the crude extracts and 10 mg mL⁻¹ for the pure compounds. The wells were loaded with 25 µL and 50 µL of the test samples, respectively. Susceptibility or resistance to compounds tested was assigned based on the following zone diameter criteria: Susceptible (S) ≥ 15 mm, Intermediate (I) = 11–14 mm, and Resistant (R) ≤ 10 mm (Chenia, 2013). The criteria for assigning susceptibility or resistance to

ampicillin was as follows: (S) ≥ 17 mm, (I) = 14–16 mm, (R) ≤ 13 mm, while those for tetracycline were: (S) ≥ 19 mm, (I) = 15–18 mm, (R) ≤ 14 mm (CLSI, 2012).

3.2.5 Molecular Docking Protocol

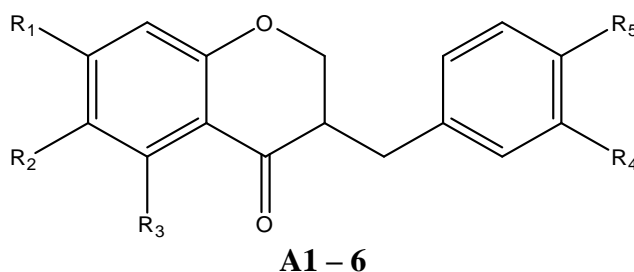
All calculations were performed with the Schrodinger molecular modeling suite (version 2019-4) using the OPLS_2005 forcefield. The minimized 3D geometries of the ligands were generated with LigPrep (2019), and their protonation states were assigned at pH 7.0 ± 2.0 using Epik (2019). The X-ray crystal structure of MraY (PDB ID: 6OYH) was retrieved from the RCSB database and processed with the Protein Preparation Wizard using the default workflow, including filling in the missing protein side chains and loops with Prime (2019). Subsequently, the ligand-receptor complexes were modeled with the induced fit docking protocol (Induced, 2019) using the standard protocol. The receptor grid was defined as the centroid of cognate ligand, and the first stage of glide docking was performed with a brief constrained refinement of the protein structure to a root mean square deviation of $\leq 0.18\text{\AA}$, followed by auto trimming of ≤ 3 residues within 5\AA of the active site and B-factor > 40 . The requisite implicit membrane for the Prime refinement stage was modeled by aligning the protein structure and loading the membrane coordinates from the OPM database (Iomisei). Then, glide redocking was performed using the extra-precision mode, and the best poses were selected based on docking score, glide emodel value, and IFD score. The binding affinity of the ligands to MraY was also estimated with Prime Molecular Mechanics and Generalized Born Surface Area (MM-GBSA) (prime) using the best poses as input structures and a Variable-dielectric Generalized Born (VSGB) model as implicit solvation model.

3.3 RESULTS AND DISCUSSION

3.3.1 Structure Elucidation

3-Benzylchroman-4-ones (compounds A1-6)

This class of compounds is characterized by the appearance of two pairs of double doublets at δ_H 4.2/4.0 (C-2) and δ_H 3.1/2.6 (C-9) due to the geminal proton resonances, and a multiplet at δ_H 2.7-2.6 (C-3). Resonances for C-2, C-3 and C-9 were consistent in all these compounds, and they appeared at δ_C 69, 48, and 32, respectively.



Compound	R ₁	R ₂	R ₃	R ₄	R ₅
A1	OCH ₃	H	OCH ₃	H	OCH ₃
A2	OCH ₃	OH	OCH ₃	H	OCH ₃
A3	OCH ₃	OH	OCH ₃	H	OH
A4	OCH ₃	H	OH	OCH ₃	OH
A5	OH	OH	OH	OCH ₃	OH
A6	OCH ₃	OH	OH	OCH ₃	OH

Figure 3.1: Structures of compounds **A1-6** isolated from the bulbs and leaves of *S. nervosa*.

The 1H NMR spectra of compounds **A1-3** showed a centrosymmetric multiplet indicating a 4'-oxygen substituted AA'BB' system in the B-ring. For compound **A1**, two meta-coupled proton signals at δ_H 6.1 and δ_H 6.0, indicated a 5,7-disubstituted ring A, with three methoxy signals at δ_H 3.79 (H-7), 3.77 (H-5) and 3.73 (H-4'). From the ^{13}C NMR spectrum, the placement of the methoxy group at C-5 was further supported by the upfield chemical shift of the carbonyl to δ_C 193.7 (C-4) compared to its chemical shift (δ_C 197-198) when a hydroxy group is at C-5. The upfield shift of (C-4) can also be due to the absence of chelation between the OH group at C-5

and C=O (C-4). Compound **A1** has previously been isolated from *S. nervosa*, and the reported spectra compare well with those in literature; therefore, compound **A1** was identified as 3-(4-methoxybenzyl)-5,7-dimethoxychroman-4-one (Figure 3.1) (Silayo et al., 1999; Bangani et al., 1999; Bezahib et al., 2009).

Compounds **A2** and **A3** differed from compound **A1** in that there was only one proton resonance in ring A at δ_H 6.38. The ^{13}C NMR spectrum of compound **A2** agrees with the spectra of the previously isolated compound 11 from *S. nervosa* (Silayo et al., 1999), and of compound **A3** agrees with the data reported for zebrinin C, which was isolated from *Scilla zebrina* (Mulholland et al., 2005) and compound 1 from *S. nervosa* (Bezabih et al., 2009). Therefore, compound **A2** was identified as 3-(4-methoxybenzyl)-6-hydroxy-5,7-dimethoxychroman-4-one and compound **A3** as 3-(4-hydroxybenzyl)-6-hydroxy-5,7-dimethoxychroman-4-one (Figure 3.1).

The 1H NMR spectra of compounds **A4-6** indicated that they all contain a chelated OH group at C-5 due to resonances at $\delta_H \sim 12$. The chelated hydroxy group was also confirmed by the carbonyl signals observed in the ^{13}C NMR at δ_C 197-198. The 1H NMR spectra also indicated an ABC system of protons in the B-ring. This system was confirmed by the ^{13}C NMR spectra, which showed two non-protonated carbon resonances at δ_C 145.4 and 145.7, a characteristic of a 3',4'-dioxxygenated ring B. Compound **A4** has previously been reported, and our spectral data compare well with those in literature (Bangani et al., 1999; Silayo et al., 1999). Therefore, compound **A4** was identified as 3-(4-hydroxy-3-methoxybenzyl)-5-hydroxy-7-methoxychroman-4-one (Figure 3.1).

Compounds **A5** and **A6** were isolated from the MeOH extract of the leaves. The ^{13}C NMR spectra had similarities with that reported for compound **A8** by Silayo et al. (1999) (Table 3.1), with differences in the number of methoxy groups. Compound **A5** has one methoxy, while

compound **6** had two compared to three reported for compound **8** by Silayo et al. (1999). For compound **A6**, ring A has three substituents, 2 OHs, and one OCH₃. One OH substituent was placed at C-5 for two reasons; one is due to a phenolic proton resonance at δ_H 12.3 and 12.2 for compounds **A5** and **A6**, respectively. Secondly, the C-4 carbonyl group occurred downfield at δ_C 198.7 for both compounds. The appearance of the resonance due to H-8 downfield of δ_H 6.00 is an indication of a methoxy substituent at C-7. In addition, it has been established that resonances for C-6 and C-8 appear at δ_C 97.1-97.3 and δ_C 95.8-96 with an OH group at C-7 and a higher field (-1.3 ppm) if it carried an OCH₃ substituent (Adinolfi et al., 1986). Therefore, the OCH₃ was placed at C-7. The second OH group was placed at C-6 due to the HMBC correlation of the only proton in the ring with C-7 and C-8a; the proton was assigned to C-8 and the OH to C-6. Ring B had an ABX system, for compound **A5**, the following chemical shifts were observed δ_H 6.78 (d, J = 2.0 Hz), 6.76 (d, J = 8.0 Hz), 6.60 (dd, J = 8.0, 2.0 Hz) for H-2', H-5', H-6', respectively, while resonances at δ_H 6.82 (d, J = 2.0 Hz), 6.78 (d, J = 8.2 Hz), and 6.67 (dd, J = 8.2, 2.0 Hz), which were assigned to H-2', H-5', H-6', respectively was observed for compound **A6**. Both compounds had two substituents in the ring B, an OH, and an OCH₃. The OCH₃ was placed at C-3 due to its HMBC correlation with δ_C 145.4 for both compounds, while OH was placed at C-4.

Based on the spectral data, compounds **A5** and **A6** were identified as 3-(4-hydroxy-3-methoxybenzyl)-5,6,7-trihydroxychroman-4-one, and 3-(4-hydroxy-3-methoxybenzyl)-5,7-dihydroxy-6-methoxychroman-4-one respectively (Figure 3.1). From the literature survey, we found no compounds to have the same chemical shifts as ours. Although the proposed structures for our compounds are similar to that of compound **1** isolated from *Scilla zebrina* (Mulholland et al., 2006), the chemical shifts are slightly different.

Table 3.1: ^1H and ^{13}C NMR data for compound **A5** and **A6** compared to literature.

	Compound A5 in CDCl_3		Compound A6 in CDCl_3		Reference ^b (Silayo et al., 1999)	
	^1H	^{13}C	^1H	^{13}C	^1H	^{13}C
C-2	a, 4.21, 1H, dd, 11.3, 4.14 b, 4.08, 1H, dd, 11.3, 8.3	69.0	a 4.20 (1H, dd, 12.6, 4.17) b 4.06 (1H, dd, 12.6, 7.25)	69.0	a, 4.27 (dd, 11.4, 4.2) b, 4.11 (dd, 11.4, 7.2)	69.4
C-3	2.68, 1H, m	46.7	2.76, 1H, m	46.7	2.82 (m)	46.9
C-4		198.7		198.7		198.7
C-4a		102.5		102.5		102.8
C-5		158.2		158.7		161.0
C-6		130.2		130.1		130.2
C-7		157.4		157.3		159.0
C-8	6.01, 1H, s	94.2	6.01, 1H, s	94.1	6.02 (s)	91.4
C-8a		154.7		154.7		155.3
C-9	A, 3.12, 1H, dd, 13.6, 4.3 b.2.61, 1H, dd, 13.6, 10.5	31.9	a3.26, 1H, (dd, 13.9, 4.3) b2.63, 1H, (dd, 13.9, 10.3)	31.9	a 3.17 (dd, 13.8, 4.2) b 2.64 (dd, 13.8, 10.5)	32.3
C-1'		130.6		130.9		131.1
C-2'	6.78, 1H, d, 1.92	115.1	6.80, 1H, d, 2.04	115.1	6.81 (d, 21)	115.3
C-3'		145.4		145.4		145.6
C-4'		145.7		145.7		145.8
C-5'	6.76, 1H, d, 8.05	110.8	6.70, 1H, (d, 8.2)	110.8	6.80 (d, 8.1)	111.0
C-6'	6.65, 1H, dd, 8.05, 2.06	120.6	6.67, 1H, (dd, 8.2, 2.04)	120.6	6.70 (dd, 8.4, 2.1)	120.8
C-5-OMe		-		-		-
C6-OMe		-		61.1	3.88	61.1
C-7OMe		-	3.90, 3H, s	-	3.83	56.4
C-8OMe		-		-		-
C-3'OMe	3.89, 3H, s	61.1	3.85, 3H, s	56.2	3.80	56.2
C-4'OMe		-		-		-

3-Benzylidienechroman-4-one (A7) and rhapontigenin (A8)

This group of homoisoflavonoids has two configurations, *E* or *Z*, which can be determined from the ^1H NMR. For the *E*-geometry, the proton for C-9 resonates downfield at δ_{H} 7.6-7.9, while it resonates upfield at $\sim\delta_{\text{H}}$ 5.5 for *Z*-geometry (Silayo et al., 1999). Compound **A7** had a

resonance for H-9 at δ_H 7.67, establishing that it has an *E* configuration. It also presented with an AA'BB' system for the B-ring and one downfield proton at δ_H 12.85 that indicates a chelated 5-OH group. The 1H NMR spectrum of compound **A8** showed two vinylic proton signals with a *trans* geometry due to the large coupling constant ($J=16.2$ Hz). Comparison with literature showed compound **A7** to be 3-benzylidenechroman-4-one and compound **A8** to be rhapontigenin, a stilbene (Figure 3.2).

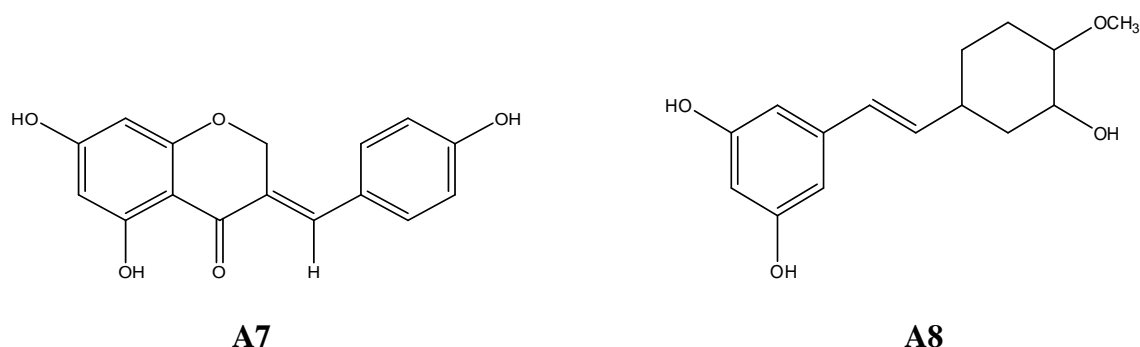


Figure 3.2: Structures of compounds **A7** and **A8** isolated from the bulbs and leaves of *S. nervosa*.

Structure elucidation of spinasterol-3-O-D-glucopyranoside (A9)

Compound **A9** was obtained as white flakes, having a molecular formula of $C_{35}H_{58}O_6$. The 1H NMR showed resonance for five methyls at δ 0.54, 0.79, 0.80, 0.85 and 1.02, each integrating to 3 protons. Two double bonds were observed between C7 and C8, and C22 and C23. This is supported by the resonance of the 1H chemical shift at δ 5.14 (H-7), δ 5.20 (H-22) and δ 5.09 (H-23). The ^{13}C NMR showed resonances due to an anomeric carbon at δ_c 101.0, which correlates to a doublet at δ_H 4.24 in the 1H NMR. Other resonances are a methylene for the sugar moiety at δ_c 61.4, four methine between δ_c 70.4-76.9, and a quaternary at δ_c 139.1 (C-8). The HMBC experiment showed the chemical shift for C-3 to correlate to the anomeric protons and this established the sugar linkage at position 3. By comparing the spectral data with those in literature, it was concluded that compound **A9** is spinasterol-3-O- β -D-glucopyranoside (Figure 3.3) (Henry and Chantalat-Dublanche, 1985).

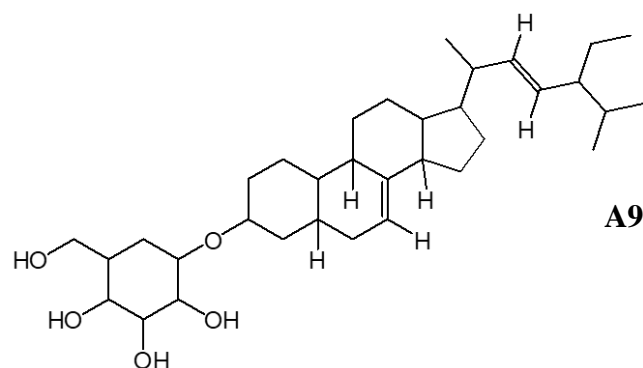


Figure 3.3: Structure of compound **A9** isolated from the bulbs and leaves of *S. nervosa*.

Compound A10 and A11

Compound **A10** was isolated as brown spikes with its HRMS calculated as m/z 483.31 (M-H) and its molecular formula was determined to be $C_{30}H_{44}O_5$. The IR spectrum showed absorption bands at 3282 and 1686 cm^{-1} for hydroxyl and carbonyl functional groups. In the 1H NMR spectrum (Table 3.2), six methyl signals at δ_H 0.72 (s), 0.93 (s), 1.01 (s), 1.22 (s) and 1.89 (s), two oxygenated methylene protons (δ_H 3.40, d, $J = 11.1$ Hz; 4.18, d, $J = 11.1$ Hz), one oxygenated methine proton (δ_H 3.36), and a non-oxygenated methine proton (δ_H 6.5, dd, $J = 10.5, 7.9$ Hz) were observed.

The ^{13}C and DEPT spectrum (Table 3.2) showed 30 carbon signals, which includes two methine carbons at δ_C 81.2 (C-3) and δ_C 145.0 (C-24), a methylene carbon at δ_C 65.1 (C-29), an ether linkage δ_C 97.0 (C-17) and δ_C 115.4 (C-23) forming a heterocyclic ring, two substituted alkene carbons at δ_C 135.8 and 135.7, and an ester carbonyl at δ_C 171.5. The HBMBC spectrum showed a correlation from the resonance of the methyl protons at H-27 to the carbonyl at C-26, the methine carbon at C-24 and the quaternary carbon at C-25. The spectral data is consistent with lanostane-type triterpenes that have been isolated from *Scilla natalensis* (Moodley, 2011; Moodley et al, 2004) and *Scilla scilliodes* (Ren et al, 2015). The first report of lanostane-triterpenes from the Hyacinthaceae family was from *Eucomis autumnalis* (Sidwell et al, 1975; Ziegler and Tamm, 1976), and this was used as the basis for the analysis of the

isolated triterpenes from our plant. The only difference was that our compound had a double bond between C-24 and C-25. A literature survey showed that lanostane-type triterpenes from the *Abies* family (Wang et al., 2015), have a double bond at that position, which helped in our elucidation. Compound **A10** was determined to be the novel 17 α ,23 α -epoxy-3 β ,29-dihydroxy-nor-lanost-8,24-dien-26-one (Figure 3.4).

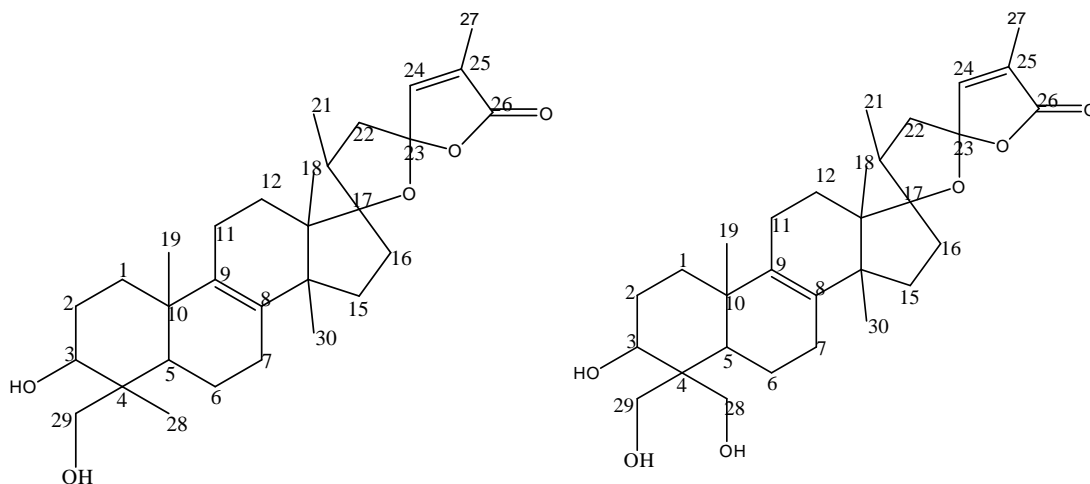


Figure 3.4: Structures of compounds **A10** and **A11** isolated from the bulbs and leaves of *S. nervosa*.

Compound **A11** was isolated as a brown powder; five methyl protons at δ_H 0.90, 0.96, 0.99, 1.13 and 1.79 were detected from its 1H NMR spectrum as well as two pairs of oxygenated methylene protons for H-28 and H-29 (Table 3.3). Compound **A11** was similar to compound **A10**, the major difference being the presence of two pairs of oxygenated methylene protons in **A11** as opposed to one pair in **A10**, that was placed at C-28 and C-29 due to the HMBC experiment showing correlations by H-28 and H-29 with C-3. Therefore, compound **A11** was determined to be 17 α ,23 α -epoxy-3 β ,28,29-trihydroxy-nor-lanost-8,24-dien-26-one (Figure 3.4). Similar to compound **A10**, this compound has not previously been isolated and identified.

Table 3.2: ^1H , ^{13}C , COSY and HMBC data for compound **A10**.

NMR spectroscopic data for compound A10 in DMSO				
No	δ_{H} (ppm)	δ_{C} (ppm)	COSY	HMBC
1	H-1 α 1.22 (m) H-1 β 1.79 (m)	32.3	H3	3H-19
2	2H 1.77 (m)	29.5	H-3	
3	3. 37 (d)	81.2	H-2	3H-28, H-29, H-1
4		43.6		H-5
5	1.57 (m)	52.4		3H-19, H-22
6	H-6 α 18.0 (m) H-6 β 1.49 (m)	19.6		
7	2H 2.02 (m)	29.0		
8		135.8		H-30
9		135.9		H-19, H-11
10		38.0		H-1, H-19
11	2H 2.08 (m)	22.1		
12	H-12 α 2.07 (m) H-12 β 1.76 (m)	27.9		
13		45.7		H-18, 3H-30
14		51.0		H-18, 3H-30
15	H-15 α 1.23 (m) H-15 β 1.66 (m)	31.9	H-16 α , β	
16	H-16 α 1.79 (m) H-16 β 1.24 (m)	36.7	H-15 α , β	
17		97.0		3H-18
18	1.01 (s)	20.3		
19	1.01 (s)	20.2		
20	1.36 (m)	34.9		
21	0.72 (s)	16.3		H-21
22	H-22 α 1.42 (m) H-22 β 1.67 (m)	44.9		
23		115.4		
24	6.5 (dd, $J = 10.5, 7.9$ Hz)	145.0		3H-27
25		129.6		3H-27
26		171.5		3H-27, H-24
27	1.89 (s)	13.1		
28	1.22 (s)	23.1		
29	H29 α 4.18 (d, $J = 11.1$ Hz) H29 β 3.40 (d, $J = 11.1$ Hz)	65.1	H29 β H29 α	
30	0.93 (s)	24.6		3H-18

Table 3.3: ^1H , ^{13}C , COSY and HMBC data for compound **A11**.

NMR spectroscopic data for compound A11 in DMSO				
No	δH (ppm)	δC (ppm)	COSY	HMBC
1	H1 α 1.84 (m) H1 β 2.38 (m)	36.5		3H-19, H-2
2	1.69 (m)	27.5	H-3	
3	3.59 (m)	71.7	H-2	
4		45.5		
5	1.49 (m)	42.3		H-28, 3H-19
6	H6 α 1.45(m) H6 β 1.69 (m)	18.4		
7	1.91 (m)	25.8		
8		134.3		3H-30
9		134.2		3H-19
10		36.2		
11	2.02	20.1		
12	H12 α 1.41 () H12 β 2.08 ()	24.2		3H-18
13		47.9		3H-18; 3H-30
14		50.0		3H-18; 3H-30
15	H15 α 1.27 (m) H15 β 1.66 (m)	31.2	H16 β	
16	H16 α 1.92 (m) H16 β 2.29 (m)	36.7	H15 β	
17		97.8		3H-18
18	0.96 (s)	19.3		
19	0.90 (s)	17.8		
20	2.36	43.8		3H-21
21	1.14, d, 7.14	14.7		
22	H22 α 1.08 (d, 6.9) H22 β 1.64 (d, 6.9)	35.2		3H-21
23		113.2		H-24
24	7.1, d, 1.6	148.4	H-27	3H-27
25		129.2		3H-27
26		171.4		
27	1.79, s	9.7	H-24	
28	H28 α 3.47 (dd, 10.9, 6.3 Hz) H28 β 3.82 (dd, 10.9, 5.9 Hz)	60.7	H28 β H28 α	H-29
29	3.89, dd, 11.3, 2.66 Hz 3.38, dd, 11.3, 4.2 Hz	61.6	H29 β H29 α	H-5, H-28
30	1.02, d, 6.9	25.5		

3.3.2 Chemotaxonomy Significance

Homoisoflavonoids, first reported from *Eucomis bicolor*, are a small group of secondary metabolites that are restricted in their distribution (Bohler, 1967; Castelli and Lopez, 2017).

These compounds are divided into five categories, 3-benzyl-4-chromanones, 3-hydroxy-3-

benzyl-4-chromanones, 3-benzylidene-4-chromanones (*E* or *Z*), 3-benzyl-chrom-2-en-4-ones, and scillascillins (Mulholland et al., 2013). They have been reported in all species of the *Scilla* genus, making them excellent taxonomic markers for the genus. They have also been reported in other families, including the Fabaceae, but remain a powerful taxonomic marker for the Hyacinthaceae family because most reported outside this family lack oxygenation at C-5, such as intricatin and bonducelin from *Caesalpinia bonducella* (Fabaceae). The isolation of 3-benzyl-4-chromanones from *S. nervosa* is consonant with other work that has been done on this plant (Bangani et al., 1999; Silayo et al., 1999). The *Scilla* species indigenous to South Africa contain mostly the 3-benzyl-4-chromanone-type homoisoflavonoids, and few contain 3-benzylidene-4-chromanones and 3-hydroxybenzyl-4-chromanones. Additionally, of the *Scilla* species indigenous to South Africa, only *S. nervosa* has been reported to biosynthesize the 3-benzylidene-4-chromanone-type homoisoflavonoids.

3.3.3 Antibacterial Activity

The antibacterial susceptibility results for the DCM and MeOH extracts of the bulbs, and MeOH extracts of the leaves, and isolated compounds are presented in Table 3.4. Only those compounds that exhibited antibacterial activity are presented. Test samples were screened against three Gram-positive bacterial strains (*B. subtilis* ATCC 6653, *S. aureus* ATCC 43000 and *M. smegmatis* mc² 155). No significant antibacterial activity against the methicillin-resistant *S. aureus* was observed for the MeOH leaf extracts. In contrast, antibacterial activity was observed against *B. subtilis* and *M. smegmatis* for the bulb extracts with the MeOH extract showing higher activity than the DCM extract. Compound **A2** (3-(4-methoxybenzyl)-6-hydroxy-5,7-dimethoxychroman-4-one) demonstrated greater efficacy against *B. subtilis* and *M. smegmatis* compared to compound **A1** (3-(4-methoxybenzyl)-5,7-dimethoxychroman-4-one), which could be attributed to the additional hydroxy substituent in compound **A1**.

Test samples were screened against four Gram-negative bacterial strains (*E. coli* ATCC 35218, *P. aeruginosa* ATCC 27853, *K. pneumoniae* ATCC 700603, and *C. violaceum* ATCC 12472). Although antimicrobial activity against *C. violaceum* was observed with the MeOH and EtOAc extracts from the bulbs and compounds **A1** and **A2**, no quorum sensing inhibition was observed. Antibacterial activity was observed against the β -lactam resistant *E. coli* for the DCM extract of the bulbs and compound **A1**. No antibacterial activity was observed with extracts and phytochemicals against multidrug-resistant *P. aeruginosa* and extended-spectrum beta-lactamase-producing *K. pneumoniae* therefore the results were omitted from the table.

The structures of the isolated compounds that showed moderate antibacterial activity (compounds **A1** and **A2**) were observed to have three methoxy substituents each, also at the same positions, C-5, C-7, and C-4' while the compounds without activity showed methoxy substitutions at C-7 and C-3' (compound **A4**) or no methoxy substitution (compound **A7**). In isoflavones, hydroxy groups at C-5 or C-7 increase their antibacterial activity (Mukne et al., 2011), but this was not observed in homoisoflavanones. The results indicate that 5,7,4'-trisubstituted homoisoflavanones ameliorated the antibacterial activity as disubstituted and unsubstituted homoisoflavanones exhibited no antibacterial activity. Nevertheless, our findings indicate that homoisoflavanones that are one carbon more than the ubiquitous flavonoids, in general, have lower antibacterial activity compared to flavonoids (Mukne et al., 2011).

Previous studies have shown that the MeOH and DCM extracts of *S. nervosa* inhibited certain strains of microorganisms (*S. aureus* and *K. pneumoniae*) in a dose-dependent manner with average MIC values of 40 μ g/mL (du Toit, 2011). du Toit (2011), postulated that the extracts would exhibit better activity as the compounds present in them would likely work synergistically to potentiate the bacteriostatic or bactericidal activity of the individual molecules. Our study counters this assumption as, in all cases, the individual molecules demonstrated greater antibacterial activity than their extracts (Table 1). Famuyiwa et al. (2013)

also demonstrated that 3-(4'-methoxybenzyl)-6-hydroxy-5,7-dimethoxychroman-4-one isolated from the yellow deposit on the surface of *S. nervosa* bulbs has significant antibacterial activity against *E. coli* when screened.

Table 3.4: Antibacterial susceptibility test of *S. nervosa* compounds and crude extracts against selected Gram-negative and Gram-positive bacterial strains.

Test Sample	Conc	<i>B. subtilis</i>		<i>M. smegmatis</i>		<i>S. aureus</i>		<i>C. violaceum</i>		<i>E. coli</i>	
		25 µl	50 µL	25 µl	50 µL	25 µL	50 µL	25 µL	50 µL	25 µL	50 µL
MeOH Bulb	20	10	14	8	16	0	10	7	12	0	10 (hazy)
DCM Bulb	20	8	10	10	16	0	10 (hazy)	0	0	7	17
MeOH Leaves	20	0	8	0	0	0	0	0	0	0	0
Compound A1	10	8	11	9	19	0	10 (hazy)	9	16	15	21
Compound A2	10	18	22	14	18	0	8 (hazy)	9	14	0	0
CONTROL (µg per disc)											
Ampicillin	10	12	12	0	0	0	0	0	0	0	0
Tetracyclin	30	18.9	18.9	22	22	19	19	30	30	23	23

B. subtilis ATCC 6653, *M. smegmatis* mc² 155, *S. aureus* ATCC 43300, *C. violaceum* ATCC 12472, *E. coli* ATCC 35218. Compound A1 - 3-(4-methoxybenzyl)-5,7-dimethoxychroman-4-one, Compound A2 - 3-(4-methoxybenzyl)-6-hydroxy-5,7-dimethoxychroman-4-one. MeOH – methanol extract, DCM – dichloromethane extract. Hazy indicates that activity is not bactericidal but bacteriostatic.

3.3.4 Molecular Docking

In order to rationalize the antibacterial effects displayed by 3-(4-methoxybenzyl)-5,7-dimethoxychroman-4-one (A1) and 3-(4-methoxybenzyl)-6-hydroxy-5,7-dimethoxychroman-4-one (A2), the homoisoflavones were docked into the cytoplasmic active site of integral membrane protein, phospho-MurNAc-pentapeptide translocase (MraY) (Figure 3.5). The choice of MraY for docking studies was hinged on its role as a catalyst for the first step in the second stage of lipid-linked reaction cascade for the biosynthesis of the bacterial cell wall peptidoglycan layer (Egan et al., 2020; Chung et al., 2013). The docking calculations predict that the ligands (Figure 3.2) bind in the same active site region, highlighting the similarity in

their structure and antibacterial potency. Nonetheless, slight differences in the binding pattern exist, attributed to the hydroxy unit in compound **A2** and consequently, the positioning of ring-A in the active site. The polarity of the hydroxy unit seems to impair the fitness and stability of the molecule in the active site, as evidenced by the ligand's inferior docking results compared to compound **A1** (Table 3.5).

Table 3.5. Molecular docking results of homoisoflavones with MraY.

Ligand	Docking score	XPG score	IFD score	Glide emodel	Glide energy (kcal mol ⁻¹)	MM-GBSA ΔG_{bind} (kcal mol ⁻¹)
Compound A1	-6.909	-6.909	-668.50	-53.353	-44.413	-68.87
Compound A2	-5.173	-5.173	-665.85	-50.541	-40.280	-51.54

A1: 3-(4-methoxybenzyl)-5,7-dimethoxychroman-4-one, **A2**: 3-(4-methoxybenzyl)-6-hydroxy-5,7-dimethoxychroman-4-one.

Analysis of the MraY-3-(4-methoxybenzyl)-5,7-dimethoxychroman-4-one complex revealed the hydrogen bond (H-b) interactions of the A-ring with Lys70, Asp196, Asn255, and Met263 *via* its methoxy groups as well as aromatic H-b and π - π stacking interactions with Asp196 and Phe262, respectively. The carbonyl oxygen of the B-ring also furnishes H-b interaction with Gly264 while the C-ring engages in π -cation and hydrophobic interactions with Lys133 and Asp265, respectively. On the other hand, the MraY-3-(4-methoxybenzyl)-6-hydroxy-5,7-dimethoxychroman-4-one complex is characterized by H-b interactions of the A-ring methoxy groups with Thr75 and Lys121, the hydroxy unit with Asp118 as well as the B-ring carbonyl oxygen with Gly264. The A- and C-rings also provided π -cation and π - π stacking interactions with Lys121 and Phe262, while hydrophobic contacts with Leu195, Asp196, and Asp262 presumably stabilized the complex in the active site.

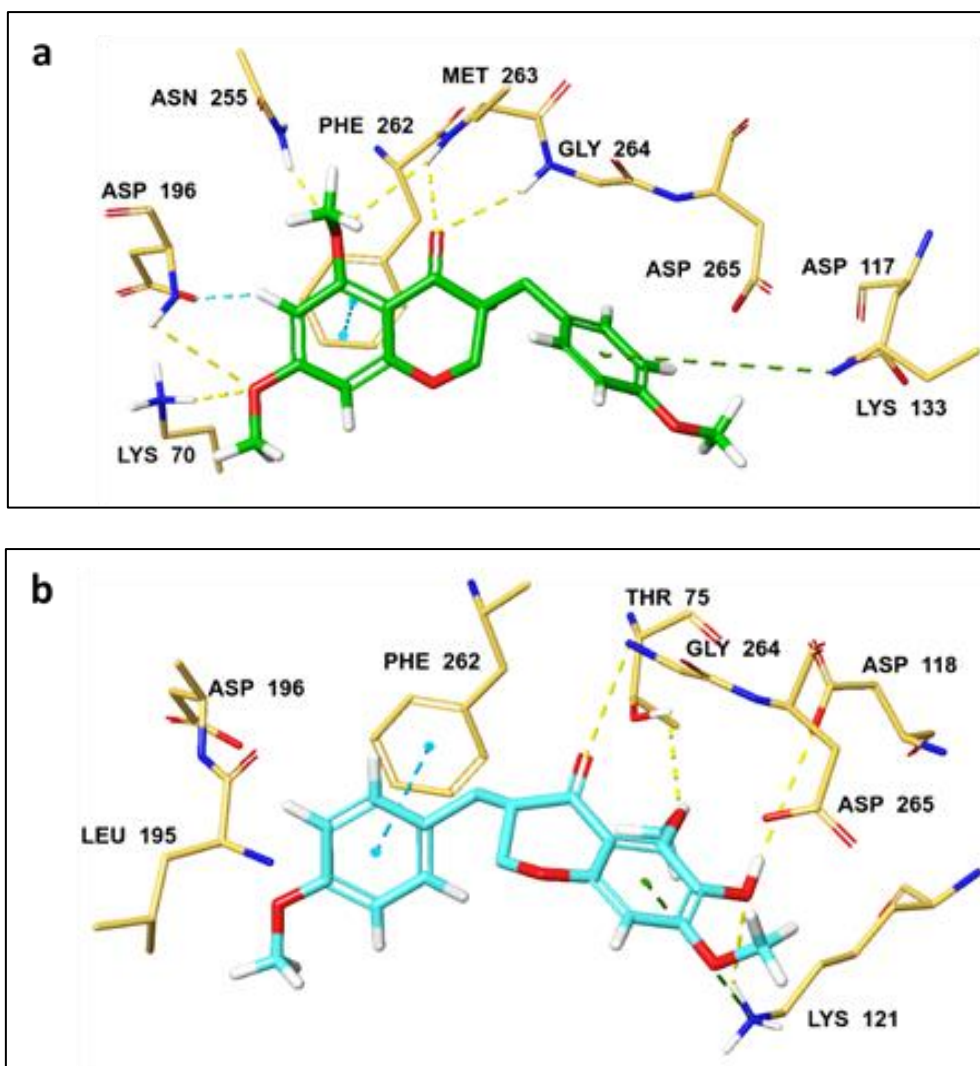


Figure 3.5. 3D representation of the modeled MraY complexes of SNL-17 (a) and SNL-34 (b).

Protein interactions are shown as dashed lines; H-bond (yellow), aromatic H-bond (cyan), π - π stacking (light blue), and π -cation (green). Atoms: carbon (3-(4-methoxybenzyl)-5,7-dimethoxychroman-4-one: green; 3-(4-methoxybenzyl)-6-hydroxy-5,7-dimethoxychroman-4-one.: cyan; protein: orange), nitrogen (blue), oxygen (red), hydrogen (white).

Furthermore, the modest antibacterial potency of these biomolecules is traceable to their lack of solid and requisite interactions with active site residues, particularly the aspartic triad (Asp117, Asp118, and Asp265), His324 (of the HHH motif), and Leu191 in the hydrophobic groove (Chung et al., 2013; Fer et al., 2015). We believe that synthetic manipulations of the homoisoflavanones framework would help attenuate these shortcomings for enhanced antibacterial potency.

3.4 CONCLUSION

This report described the isolation of two new homoisoflavonoids from the leaves, five known homoisoflavonoids, one stilbene, and a sterol glucoside from the bulbs of *S. nervosa*, thus confirming that all the plant parts are rich in homoisoflavonoids. The screening of the organic extracts and isolated compounds for antibacterial activity showed that homoisoflavonoids do not have good antibacterial activity compared to other classes of flavonoids but their activity was better than that of extracts. Furthermore, this study explored the potential of homoisoflavonoids that showed moderate antibacterial activity. The result showed poor binding with the active site of the protein. Although homoisoflavonoids have been isolated from different plant families, little information exists on their biological activities concerning their structures. Future work will be to synthetically modify the structures of homoisoflavonoids reported to have moderate antibacterial activity to enhance their activity and study their structure-activity relationships.

REFERENCES

- Adinolfi, M., Lanzetta, R., Laonigro, G., Parrilli, M. and Breitmaier, E. (1986), ^1H and ^{13}C chemical shift assignments of homoisoflavanones. *MAGNETIC RESONANCE CHEMISTRY*, 24: 663-666.
- Amschler, G., Frahm, A. W., Müller-Doblies, D., & Müller-Doblies, U. (1998). Spirocyclic nortriterpenes from the bulbs of *Veltheimia viridifolia*. *PHYTOCHEMISTRY*, 47(3): 429–436. doi:10.1016/s0031-9422(97)00584-0.
- Bangani, V., Crouch, N. R., & Mulholland, D. A. (1999). Homoisoflavanones and stilbenoids from *Scilla nervosa*. *PHYTOCHEMISTRY*, 51(7): 947–951. doi:10.1016/s0031-9422(99)00155-7.
- Baron S, editor. (1996). *Medical Microbiology*. 4th edition. Galveston (TX): University of Texas Medical Branch at Galveston.
- Bezabih, M., Famuyiwa, S.O., Abegaz, B.M., (2009). HPLC analysis and NMR identification of homoisoflavonoids and stilbenoids from the inter-bulb surfaces of *Scilla nervosa*. *NATURAL PRODUCT COMMUNICATIONS* 4, 1367–1370.
- Bohler, P. and Tamm, C. (1967). The homo-isoflavones, a new class of natural product. Isolation and structure of eucomin and eucomol. *TETRAHEDRON LETTERS*, 3479.
- Boutayeb A. (2010). The impact of infectious diseases on the development of Africa. In: Preedy V.R., Watson R.R. (eds) *Handbook of Disease Burdens and Quality of Life Measures*. Springer, New York, NY. https://doi.org/10.1007/978-0-387-78665-0_66.
- Bugg, T. D., Lloyd, A. J., & Roper, D. I. (2006). Phospho-MurNAc-pentapeptide translocase (MraY) as a target for antibacterial agents and antibacterial proteins. *INFECTIOUS DISORDERS DRUG TARGETS*, 6(2): 85–106.

- Castelli, M. V., & López, S. N. (2017). Homoisoflavonoids: Occurrence, biosynthesis, and biological activity. *STUDIES IN NATURAL PRODUCTS CHEMISTRY* (Vol. 54, pp. 315-354). Elsevier.
- Cattoir, V., & Felden, B. (2019). Future antibacterial strategies: from basic concepts to clinical challenges. *THE JOURNAL OF INFECTIOUS DISEASES*, 220(3): 350–360.
- Chenia HY, (2013). Anti-quorum sensing potential of crude *Kigelia africana* fruit extracts. *SENSORS* 13: 2802–2817.
- Chung, B. C. et al. (2003). Crystal structure of MraY, an essential membrane enzyme for bacterial cell wall synthesis. *SCIENCE* 341, 1012-1016, doi:10.1126/science.1236501.
- Clinical and Laboratory Standards Institute, (2012). Performance standards for antimicrobial susceptibility testing; twenty-second informational supplement. CLSI Document M100-S22. Clinical and Laboratory Standards Institute, Wayne, PA, USA.
- Crouch, N.R., Bangani, V., Mulholland, D.A. (1999). Homoisoflavanones from three South African *Scilla* species. *PHYTOCHEMISTRY* 51: 943/946.
- Du Toit, K., Kweyama, A., Bodenstein, J. (2011). Anti-inflammatory and antimicrobial profiles of *Scilla nervosa* (Burch.) Jessop (Hyacinthaceae). *SOUTH AFRICAN JOURNAL OF SCIENCE*, 107:96-100.
- Egan, A. J. F., Errington, J. & Vollmer, W. (2020). Regulation of peptidoglycan synthesis and remodeling. *NATURE REVIEWS MICROBIOLOGY* 18: 446-460, doi:10.1038/s41579-020-0366-3
- Epik, Schrödinger. (2019). LLC, New York, NY. 2019.
- Famuyiwa, S. O., Ntummy, A. N., Andrae-Marobela, K., & Yeboah, S. O. (2013). A new homoisoflavonoid and the bioactivities of some selected homoisoflavonoids from the inter-

- bulb surfaces of *Scilla nervosa* subsp. *rigidifolia*. SOUTH AFRICAN JOURNAL OF BOTANY, 88: 17–22. doi: 10.1016/j.sajb.2013.04.009.
- Famuyiwa, S.O., Sichilongo, K.F., Yeboah, S.O., Abegaz, B.M., (2012). Homoisoflavonoids from the inter-bulb surfaces of *Scilla nervosa* subsp. *rigidifolia*. PHYTOCHEMISTRY LETTERS 5: 591–595.
- Fer, M. J. et al. (2015). 5'-Methylene-triazole-substituted-aminoribosyl uridines as *MraY* inhibitors: synthesis, biological evaluation and molecular modeling. ORGANIC BIOMOLECULE CHEMISTRY. 13: 7193-7222, doi:10.1039/C5OB00707K.
- Hafez-Ghoran, S., Ebrahimi, P., Mighani, H., & Saeidnia, S. (2015). Isolation and characterization of homoisoflavonoids from *Scilla persica* HAUSSKN. BRAZILIAN JOURNAL OF PHARMACEUTICAL SCIENCES, 51(4): 949–955. doi:10.1590/s1984-82502015000400020.
- Henry, M., & Chantalat-Dublanche, I. (1985). Isolation of spinasterol and its glucoside from cell suspension cultures of *Saponaria officinalis*: ¹³C-NMR Spectral Data and Batch Culture Production. PLANTA MEDICA, 51(04): 322–325. doi:10.1055/s-2007-969502.
- Hutchings, A, Scott, A.H., Lewis, G. and Cunningham, A.B., (1996). Zulu medicinal plants an inventory, University of Natal Press: Pietermaritzburg, 41.
- Induced Fit Docking protocol (2019). Glide, Schrödinger, LLC, New York, NY, 2019; Prime, Schrödinger, LLC, New York, NY. 2019.
- Kimura, K. I., & Bugg, T. D. H. (2003). Recent advances in antimicrobial nucleoside antibiotics targeting cell wall biosynthesis. NATURAL PRODUCT REPORTS, 20(2): 252-273. doi:10.1039/B202149H

- Lee S. M., Chun H. K., Lee C. H., Min B. S., Lee E. S., Kho Y. H. (2002). Eucosterol oligoglycosides isolated from *Scilla scilloides* and their anti-tumor activity. CHEMICAL AND PHARMACEUTICAL BULLETIN. 50:1245–1249.
- LigPrep. (2019). Schrödinger, LLC, New York, NY.
- Lomize, M. A., Pogozheva, I. D., Joo, H., Mosberg, H. I. & Lomize, A. L. (2012). OPM database and PPM web server: resources for positioning of proteins in membranes. NUCLEIC ACIDS RESEARCH. 40: D370-D376, doi:10.1093/nar/gkr703.
- Mimaki, Y., Ori, K., Sashida, Y., Nakaido, T., Song, L., & Ohmoto, T. (1993). Peruvianosides A and B, novel triterpene glycosides from the bulbs of *Scilla peruviana*. BULLETIN OF THE CHEMICAL SOCIETY OF JAPAN. Vol 66, No. 4. doi.org/10.1246/bcsj.66.1182.
- Moodley Nivan, (2001). The chemical investigation of *Ledebouria zebrina* and *Scilla natalensis*. MSc thesis, School of Chemistry, University of KwaZulu Natal.
- Moodley, N., Mulholland, D. A., & Crouch, N. R. (2004). Eucosterol-type nortriterpenoids from *Merwillia natalensis*. JOURNAL OF NATURAL PRODUCTS, 67(5): 918–920. doi:10.1021/np0204803.
- Mukne, A. P., Viswanathan, V., & Phadatare, A. G. (2011). Structure pre-requisites for isoflavones as effective antibacterial agents. PHARMACOGNOSY REVIEWS, 5(9): 13–18. doi:10.4103/0973-7847.79095.
- Mulholland, D. A., Crouch, N. R., Koorbanally, C., Moodley, N., & Pohl, T. (2006). Intraspecific chemical variation in *Scilla zebrina* (Hyacinthaceae). BIOCHEMICAL SYSTEMATICS AND ECOLOGY, 34(3): 251–255. doi: 10.1016/j.bse.2005.10.005.

- Mulholland, D. A., Schwikkard, S. L., & Crouch, N. R. (2013). The chemistry and biological activity of the Hyacinthaceae. *NATURAL PRODUCT REPORTS*, 30(9): 1165. doi:10.1039/c3np70008a.
- Newman, D.J., Cragg, G.M., Snader, K.M., (2003). Natural products as sources of new drugs over the period 1981–2002. *JOURNAL OF NATURAL PRODUCTS* 66: 1022–1037.
- Nishida, Y., Wada, K., Toyohisa, D., Tanaka, T., Ono, M., Yasuda, S. H. (2013). Homoisoflavones as the antioxidants responsible from bulbs of *Scilla scilloides*. *NATURAL PRODUCT. RESEARCH*, v.27, n.24, p.2360-2362.
- Nishida, Yoichiro; Eto, Masashi; Miyashita, Hiroyuki; Ikeda, Tsuyoshi; Yamaguchi, Koki; Yoshimitsu, Hitoshi; Nohara, Toshihiro; Ono, Masateru (2008). A new homostilbene and two new homoisoflavones from the bulbs of *Scilla scilloides*. *CHEMICAL AND PHARMACEUTICAL BULLETIN* 56 (7): 1022–1025. doi:10.1248/cpb.56.1022. PMID 18591825.
- Ono, M., Takatsu, Y., Ochiai, T., Yasuda, S., Nishida, Y., Tanaka, T., Okawa, M., Kinjo, J., Yoshimitsu, H., Nohara, T. (2012). Two new nortriterpenoid glycosides and a new phenylpropanoid glycoside from the bulbs of *Scilla scilloides*. *CHEMICAL AND PHARMACEUTICAL BULLETIN*, 60(10): 1314–1319. doi:10.1248/cpb.c12-00457.
- Prime. (2019). Prime MM-GBSA, Schrödinger, LLC, New York, NY.
- Protein Preparation Wizard. (2019). Epik, Schrödinger, LLC, New York, NY; Impact, Schrödinger, LLC, New York, NY, 2019; Prime, Schrödinger, LLC, New York, NY.
- Ren, F.-C., Wang, L.-X., Yu, Q., Jiang, X.-J., & Wang, F. (2015). Lanostane-type triterpenoids from *Scilla scilloides* and structure revision of drimiopsin D. *NATURAL PRODUCTS AND BIOPROSPECTING*, 5(5): 263–270. doi:10.1007/s13659-015-0076-0

- Salar Hafez Ghoran, Soodabeh Saeidnia, Esmaeil Babaei, Fumiyuki Kiuchi & Hidayat Hussain (2016) Scillapersicene: a new homoisoflavonoid with cytotoxic activity from the bulbs of *Scillapersica* HAUSSKN, NATURAL PRODUCT RESEARCH, 30:11, 1309-1314, DOI: 10.1080/14786419.2015.1054286.
- Sidwell, W. T. L., Tamm, C., Ziegler, R., Finer, J., & Clardy, J. (1975). Eucosterol, a novel spirocyclic nortriterpene isolated from bulbs of *Eucomis* species. JOURNAL OF THE AMERICAN CHEMICAL SOCIETY, 97(12): 3518–3519. doi:10.1021/ja00845a041.
- Silayo, A., Ngadjui, B. T., & Abegaz, B. M. (1999). Homoisoflavonoids and stilbenes from the bulbs of *Scilla nervosa subsp. rigidifolia*. PHYTOCHEMISTRY, 52(5): 947–955. doi:10.1016/s0031-9422(99)00267-8.
- Simpkin, V. L., Renwick, M. J., Kelly, R., & Mossialos, E. (2017). Incentivising innovation in antibiotic drug discovery and development: progress, challenges, and next steps. THE JOURNAL OF ANTIBIOTICS, 70(12): 1087–1096. Society of Japan, 66, 1182.
- Wang, G.-W., Lv, C., Yuan, X., Ye, J., Jin, H.-Z., Shan, L., ... Zhang, W.-D. (2015). Lanostane-type triterpenoids from *Abies faxoniana* and their DNA topoisomerase inhibitory activities. PHYTOCHEMISTRY, 116: 221–229. doi: 10.1016/j.phytochem.2015.04.012.
- Ziegler, R., & Tamm, C. (1976). Isolation and structure of eucosterol and 16-hydroxyeucosterol, two novel spirocyclic nortriterpenes, and of a new 24- nor-5-chola-8, 16-diene-23-oic acid from bulbs of several *Eucomis* species. HELVETICA CHIMICA ACTA, 59(6): 1997–2011. doi:10.1002/hlca.19760590613.

SUPPORTING INFORMATION

NMR data of isolated compounds

Compound **A1** (3-(4-methoxybenzyl)-5,7-dimethoxychroman-4-one): Yellow sticky oil.

IR ν_{\max} (cm^{-1}): 2934 (C-H); 1636 (C=O); 1602, 1568, 1510, 1453 (C=C); 212 (C-O).

HR-ESI-MS m/z 351.1213 (measured) for $[\text{M}+\text{Na}]^+$ corresponding to $\text{C}_{19}\text{H}_{20}\text{O}_5\text{Na}$ and 351.1208 (calculated) with a mass error of 1.4 ppm.

^1H -NMR (CD_3OD , 400 MHz) δ_{H} ppm 7.10 (2H, d, H-2', H-6', $J=8.35$ Hz), 6.83 (2H, d, H-3', H-5', $J=8.35$ Hz), 6.10 (1H, d, H-6, $J=2.10$ Hz), 6.04 (1H, d, H-8, $J=2.10$ Hz), 4.21 (1H, dd, H-2a, $J=15.52$ Hz, 7.07 Hz), 4.03 (1H, dd, H-2b, $J=15.52$ Hz, 3.71 Hz), 3.06 (1H, dd, H-9a, $J=18.29$ Hz, 9.15 Hz), 2.69 (1H, m, H-3), 2.59 (1H, dd, H-9b, $J=18.29$ Hz, 3.77 Hz), 3.79 (3H, s, OCH_3 -7), 3.77 (3H, s, OCH_3 -5), 3.73 (3H, s, OCH_3 -4')

^{13}C -NMR (CD_3OD , 400 MHz) δ_{C} ppm 193.7 (C-4), 167.7 (C-7), 166.5 (C-5), 163.9 (C-8a), 159.8 (C-4'), 131.8 (C-1'), 131.1 (C-5', 3'), 115.1 (C-6', 2'), 94.6 (C-6), 93.8 (C-8), 70.1 (C-2), 49.6 (C-3), 33.1 (C-9), 56.3 (OCH_3 -5), 56.2 (OCH_3 -7), 55.7 (OCH_3 -C4').

Compound **A2** (3-(4-methoxybenzyl)-6-hydroxy-5,7-dimethoxychroman-4-one): Brown gum

IR ν_{\max} (cm^{-1}): 3326 (-OH), 2941, 1646 (C=O), 1607 (C=C), 1513, 1453 (C-H).

LRMS m/z 367.1070 (measured) for $[\text{M}+\text{Na}]^+$ corresponding to $\text{C}_{19}\text{H}_{20}\text{O}_6\text{Na}$ and 367.11576 (calculated) with a mass error of -22.360828 ppm

^1H -NMR (DMSO , 400 MHz) δ_{H} ppm 7.00 (2H, d, H-2', 6', $J=8.46$ Hz), 6.69 (2H, d, H-3', 5', $J=8.46$ Hz), 6.38 (1H, s, H-8), 4.20 (1H, dd, H-2a, $J=11.32$ Hz, 4.28 Hz), 4.00 (1H, dd, H-2b, $J=11.32$ Hz, 8.32 Hz), 2.71 (1H, m, H-3), 2.97 (1H, dd, H-9a, $J=13.89$ Hz, 5.16 Hz), 2.54 (1H, dd, H-9b, $J=13.89$ Hz, 9.42 Hz), 3.81 (3H, s, OCH_3 -5), 3.71 (3H, s, OCH_3 -7), 3.68 (3H, s, OCH_3 -4')

^{13}C -NMR (DMSO, 400 MHz) δ_{C} ppm 191.1 (C-4), 158.9 (C-5), 156.3 (C-7), 155.2 (C-4'), 147.2 (C-8a), 134.8 (C-6), 130.3 (C-2', 6'), 129.0 (C-1'), 115.6 (C-3', 5'), 108.4 (C-4a), 96.3 (C-8), 69.3 (C-2), 31.7 (C-9), 60.7 (C-5 OCH₃), 56.4 (C-7 OCH₃), 56.0 (C-4' OCH₃).

Compound **A3** (3-(4-hydroxybenzyl)-5,7-dimethoxy-6-hydroxychroman-4-one): Orange

IR ν_{max} (cm⁻¹): 3345 (-OH), 2936 (C-H), 1744 (C=O), 1652 (C=C), 1606 (C=C), 1514, 1496, 1452 (C-H).

LRMS m/z 331.0805 (measured) for $[\text{M}+\text{H}]^+$ corresponding to C₁₈H₁₈O₆H and 331.1103

^1H NMR (MeOD, 400 MHz) δ_{H} ppm 7.01 (2H, d, H-2', 6', $J=8.1$ Hz), 6.73 (2H, d, H-3', 5', $J=8.2$ Hz), 6.29 (1H, s, H-8), 4.18 (1H, dd, H-2a, $J=11.3$ Hz, 3.8 Hz), 4.12 (1H, dd, H-2b, $J=11.3$ Hz, 7.0 Hz), 3.02 (1H, dd, H-9a, $J=13.2$ Hz, 4.0 Hz), 2.58 (1H, dd, H-9b, $J=13.2$ Hz, 10.0 Hz), 3.84 (3H, s, OCH₃-7), 3.78 (3H, s, OCH₃-5)

^{13}C -NMR (MeOD, 400 MHz) δ_{C} ppm 192.9 (C-4), 157.1 (C-8a), 155.5 (C-4'), 155.3 (C-7), 146.6 (C-5), 134.3 (C-6), 129.8 (C-2', 6'), 129.1 (C-1'), 115.0 (C-3', 5'), 107.7 (C-4a), 95.6 (C-8), 68.8 (C-2), 48.3 (C-3), 31.8 (C-9), 60.2 (C-5 OCH₃), 55.4 (C-7 OCH₃).

Compound **A4** (5-hydroxy-7-methoxy-3-(3'-hydroxy-4'-methoxybenzyl)chroman-4-one): Light yellow

IR ν_{max} (cm⁻¹): 3426 (-OH), 2917 (C-H), 1636 (C=O), 1574, 1512 (C=C), 1462 (C-H).

HR-ESI-MS m/z 353.1003 (measured) for $[\text{M}-\text{H}]^+$ corresponding to C₁₈H₁₈O₆Na and 353.1001 (calculated) with a mass error of 0.6 ppm.

^1H -NMR (CDCl₃, 400 MHz) δ_{H} ppm 12.08 (1H, s, OH-5), 6.78 (1H, broad s, H-2'), 6.76 (1H, s, H-5'), 6.68 (1H, dd, H-6', $J=10.24$ Hz, 6.12 Hz), 6.03 (1H, d, H-6, $J=2.30$ Hz), 5.94 (1H, d, H-8, $J=2.30$ Hz), 4.26 (1H, dd, H-2a, $J=15.63$ Hz, 7.21 Hz), 4.10 (1H, dd, H-2b, $J=15.63$ Hz, 4.2

Hz), 3.15 (1H, dd, H-9a, $J=18.49$ Hz, 9.48 Hz), 2.79 (1H, m, H-3), 2.64 (1H, dd, H-9b, $J=18.49$ Hz, 3.37 Hz)

^{13}C -NMR (CDCl_3 , 400 MHz) δ_{H} ppm 197.9 (C-4), 167.8 (C-7), 164.4 (C-5), 162.8 (C-8a), 145.7 (C-4'), 145.4 (C-3'), 131.0 (C-1'), 120.6 (C-6'), 115.2 (C-5'), 102.6 (C-4a), 94.9 (C-6), 93.8 (C-8), 69.0 (C-2), 46.6 (C-3), 31.9 (C-9), 55.9 (OCH_3 -7), 55.6 (OCH_3 -3').

Compound **A5** (5,6,7-trihydroxy-3-(4'-hydroxy-3'-methoxybenzyl) chroman-4-one): Light yellow. IR ν_{max} (cm^{-1}): 3606(-OH) 2916 (C-H), 1720 (C=O), 1668, 1606 (C=C), 1573, 1512, 1475, 1462 (C-H).

HR-ESI-MS m/z 331.0802 (measured) for $[\text{M}]^+$ corresponding to $\text{C}_{17}\text{H}_{15}\text{O}_7$ and 331.0818 (calculated) with a mass error of -4.8 ppm.

^1H -NMR (CDCl_3 , 400 MHz) δ_{H} ppm 6.78 (1H, H-2', d, $J=1.92$ Hz), δ 6.76 (1H, H-5', d, $J=$), 6.6 (1H, H-6', dd, $J=8.05$ Hz, 2.06 Hz), 6.01 (1H, s, H-8), 4.21 (1H, dd, H-2a, $J=11.3$ Hz, 4.14 Hz), 4.06 (1H, dd, H-2b, $J=11.3$ Hz, 8.3 Hz), 3.12 (1H, dd, H-9a, $J=13.6$ Hz, 4.3 Hz), 2.6 (1H, dd, H-9b, $J=13.6$ Hz, 10.5 Hz), 2.68 (1H, m, H-3), 3.89 (3H, s, OCH_3 -3').

^{13}C -NMR (CDCl_3 , 400 MHz) δ 198.7 (C-4), 158.2 (C-5), 157.4 (C-7), 154.7 (C-8a), 145.7 (C-4'), 145.4 (C-3'), 130.6 (C-1'), 130.2 (C-6), 120.6 (C-6'), 110.8 (C-5'), 102.5 (C-4a), 94.2 (C-8), 69.0 (C-2), 46.7 (C-3), 31.9 (C-9), 61 (OCH_3 -3'). IR $\nu_{\text{max}}^{\text{KBr}}$ (cm^{-1}): 3606(-OH) 2916, 1720 (C=O), 1668, 1606, 1573, 1512, 1475, 1462, 1246, 1214

Compound **A6** (5,6-dihydroxy-7-methoxy-3-(4'-hydroxy-3'-methoxybenzyl)chroman-4-one): Light yellow. IR ν_{max} (cm^{-1}): 3602 (-OH), 2915, 2849 (C-H), 1729 (C=O), 1607 (C=C), 1512, 1469 (C-H).

HR-ESI-MS m/z 347.1114 (measured) for $[\text{M}]^+$ corresponding to $\text{C}_{18}\text{H}_{19}\text{O}_7$ and 347.1131 (calculated) with a mass error of -4.9 ppm.

^1H -NMR (CDCl_3 , 400MHz) δ_{H} ppm 6.81 (1H, d, H-2', $J=2.0$ Hz), 6.7 (1H, d, H-5', $J=8.2$ Hz), 6.67 (1H, dd, H-6', $J=8.2$ Hz, 2.0 Hz), 6.01 (1H, s, H-8), 4.20 (1H, dd, H-2a, $J=12.6$ Hz, 4.17 Hz), 4.06 (1H, dd, H-2b, $J=12.6$ Hz, 7.2 Hz), 3.12 (1H, dd, H-9a, $J=13.9$ Hz, 4.3 Hz), 2.63 (1H, dd, H-9b, $J=13.9$ Hz, 10.3 Hz), 2.76 (1H, m, H-3), 3.90 (3H, s, OCH_3 -6), 3.85 (3H, s, OCH_3 -3'), 12.2 (1H, s, OH-5)

^{13}C -NMR (CDCl_3 , 400MHz) δ_{C} ppm 198.7 (C-4), 158.7 (C-5), 157.3 (C-7), 154.7 (C-8a), 145.7 (C-4'), 145.4 (C-3'), 130.1 (C-6), 120.6 (C-6'), 115.1 (C-2'), 110.8 (C-5'), 102.5 (C-4a), 94.1 (C-8), 69.0 (C-2), 46.7 (C-3), 31.9 (C-9), 61.0 (OCH_3 -6), 56.2 (OCH_3 -3').

Compound **A7** (3-(4'-hydroxybenzylidene)-5,7-dihydroxychroman-4-one: Yellow powder

IR ν_{max} (cm^{-1}): 3399 (OH), 1638 (C=C), 1464 (C-H).

HR-ESI-MS m/z 283.0607 (measured) for $[\text{M}]^+$ corresponding to $\text{C}_{16}\text{H}_{11}\text{O}_5$ and 283.0606 (calculated) with a mass error of 0.4 ppm.

^1H -NMR (DMSO , 400MHz) δ_{H} ppm 7.32 (2H, dd, H-2', 6' $J=8.6$ Hz), 7.67 (1H, d, H-9, $J=2.0$ Hz), 6.88 (2H, dd, H-3' 5', $J=8.6$ Hz), 5.9 (1H, d, H-6, $J=2.0$ Hz), 5.8 (1H, d, H-8, $J=2.0$ Hz), 5.31 (1H, d, H-2a, $J=1.7$ Hz), 5.31 (1H, d, H-2b, $J=1.7$ Hz), 12.85 (1H, s, OH-5)

^{13}C -NMR (DMSO , 400 MHz) δ_{C} ppm 184.8 (C-4), 167.2 (C-7), 164.9 (C-5), 162.3 (C-8a), 159.8 (C-4'), 137.1 (C-9), 133.3 (C-2' 6'), 126.5 (C-1'), 125.2 (C-3), 116.3 (C-3', 5'), 102.1 (C-4a), 96.6 (C-6), 95.2 (C-8), 67.6 (C-2).

Compound **A8** (Rhapontigenin): Yellow powder

IR ν_{max} (cm^{-1}): 3443 (OH), 2251 (C-H), 1661 (C=O), 1224 (C=C).

HR-ESI-MS m/z 259.0972 (measured) for $[\text{M}]^+$ corresponding to $\text{C}_{15}\text{H}_{15}\text{O}_4$ and 259.0970 (calculated) with a mass error of 0.8 ppm.

^1H NMR (MeOD, 400MHz) δ_{H} ppm 3.82 (3H, s, OMe), 6.14 (1H, d, $J = 1.8$ Hz, H-4'), 6.41 (2H, br, $J = 1.8$ Hz, H-2' and H-6'), 6.85 (1H, d, $J = 8.3$ Hz, H-5), 6.94 (1H, d, $J = 16.2$ Hz, H-a), 7.02 (1H, dd, $J = 8.3, 1.8$ Hz, H-6), 7.04 (1H, d, $J = 16.2$ Hz, H-b), 7.17 (1H, d, $J = 1.8$ Hz, H-2);

^{13}C NMR (MeOD) δ_{C} ppm 158.9 (C-3', C-5'), 148.2 (C-3), 147.0 (C-4), 139.6 (C-1'), 130.5 (C-1), 128.3 (C-a), 126.9 (C-b), 120.6 (C-6), 116.0 (C-5), 110.3 (C-2), 104.9 (C-2' and C-6'), 102.3 (C-4'), 56.0 (OMe).

Compound **A9** (Spinasterol-3-*O*- β -D-glucopyranoside): white flakes

IR ν_{max} (cm^{-1}): 3403.06 (OH), 2939.08 (CH_2 -CH), 1377.54 (C=C), 1027.70 (CH).

^1H NMR (400 MHz, DMSO) δ 5.14 (1H, br s, H-7), 5.20 (1H, dd, $J = 15.4, 8.5$ Hz, H-22), 5.09 (1H, dd, $J = 15.4, 8.5$ Hz, H-23), 4.25 (1H, d, $J = 7.6$ Hz, H-1'), 3.57 (1H, br s, H-3'), 3.68 (1H, d, $J = 5.6$ Hz, H- β -6'), 3.47 (1H, d, $J = 5.6$ Hz, H- α -6'), 3.17 (1H, m, H-5'), 3.10 (1H, m, H-3), 3.10 (1H, m, H-4'), 2.94 (1H, m, H-2'), 0.54 (3H, s, H-18), 0.79 (3H, s, H-19), 1.02 (3H, d, $J = 6.7$ Hz, H-21), 0.80 (3H, s, H-26, 29), 0.85 (3H, d, $J = 6.7$ Hz, H-27).

^{13}C -NMR (100MHz, DMSO), δ 36.7 (C1), 29.1 (C2), 76.6 (C3), 34.1 (C4), 40.2 (C5), 29.3 (C6), 117.1 (C7), 139.1 (C8), 48.9 (C9), 33.9 (C10), 21.1 (C11), 38.9 (C12), 42.9 (C13), 54.5 (C14), 22.5 (C15), 27.8 (C16), 55.5 (C17), 11.8 (C18), 12.6 (C19), 40.2 (C20), 21.0 (C21), 137.6 (C22), 129.2 (C23), 50.5 (C24), 31.2 (C25), 18.8 (C26), 20.7 (C27), 24.6 (C28), 11.9 (C29). 101.0 (C-1'), 73.6 (C-2'), 76.6 (C-3'), 70.4 (C-4'), 76.9 (C-5'), 61.4 (C-6').

CHAPTER 4

Evaluation of the cytotoxic potential of homoisoflavonoids and extracts from *Scilla nervosa* (Burch.) Jessop

ABSTRACT

Scilla nervosa (Burch.) Jessop is a bulbous plant indigenous to South Africa with various uses in traditional medicine, especially as an anti-inflammatory. A phytochemical investigation of *S. nervosa* has led to the isolation of more than twenty homoisoflavonoids. This study investigated the *in-vitro* cytotoxicity of isolated homoisoflavonoids and crude extracts from the plant against two cancer cell lines, Caco-2 (human colorectal adenocarcinoma) and HepG2 (human hepatoma), and the normal cell line, Hek-293 (human embryonic kidney), using the MTT assay. Cells were treated with half-maximal inhibitory concentrations (IC₅₀) of the samples to investigate ATP, LDH, and mitochondrial membrane potential by JC-1 staining. All tested samples decreased the viability of Caco-2 and HepG2 cell lines in a dose-dependent manner, with a U-shaped cytotoxicity graph in some cases. The IC₅₀ values were between 13-71 µg/mL in Caco-2 cell lines and 36-520 µg/mL in HepG2 cell lines for the homoisoflavonoids. The methanol extract of leaves also demonstrated promising activity in both Caco-2 and HepG2 cell lines with an IC₅₀ value of 7.79 and 9.29 µg/mL, respectively. Treating the different cell lines at the IC₈₀ and IC₅₀ concentrations of the pure compounds and crude extracts resulted in a decrease in intracellular ATP level for the compounds and crude extracts, an increase in LDH releases, and no significant change in mitochondrial membrane potential for HepG2 and Hek-293 cell lines. These results showed that homoisoflavonoids and organic extracts of *S. nervosa* induced cytotoxicity via ATP depletion and disruption of plasma.

In addition, their effect on mitochondrial membrane potential is concentration and cell line dependent.

Keywords: cytotoxicity, homoisoflavonoids, MTT, ATP, LDH, MMP

4.1 INTRODUCTION

Traditional medicine has proven valuable in the treatment and management of different kinds of ailments among South Africans. The World Health Organization (WHO) reported that 80% of the world's population still rely on traditional medicine for their primary healthcare needs. While in South Africa, about three million people are reported to be using indigenous, traditional medicine for primary healthcare purposes (Van Wyk and Gericke, 2000). The country is a host to 30 000 flowering plants, which account for 10% of the world's higher plant species (Street and Prinsloo, 2013); among these, only a few have been exploited and studied for their pharmacological potential. There is a growing interest in screening traditionally used medicinal plants for pharmacological activities and their chemical profiling. Plants herbal preparations have been used since antiquity to treat different ailments, including cancer. Despite the success recorded in exploring natural products in drug research, most plant species have not been researched (Amaral et al., 2009).

About 25% of drugs in the modern pharmacopeia are derived from plants, while 60% of drugs used as anticancer agents are from nature (Ramawat and Goyal, 2009). Cancer is the second leading cause of death globally and accounts for 8.8 million deaths annually in humans (Om et al., 2019). The search for cancer therapeutics with good efficacy with minimal side effects and toxicity is an integral part of drug discovery and development. Also, bioactive constituents of plants have served as leads in the development of new drug candidates due to their structural

diversity. Additionally, their biological activities could be ameliorated by modification of their molecular structure.

The genus *Scilla* (Hyacinthaceae), sub-family Hyacinthoideae, represents about 80 taxa globally, of which six species are native to South Africa (Crouch et al., 1999), including *Scilla krausii* Bak., *Scilla natalensis* Planch., *Scilla nervosa* Burch., and *Scilla dracomontana* Hilliard and Burch. *S. nervosa* is one of the bulbous plants that are of importance to traditional healers in South Africa (Louw et al., 2002). *Scilla* species are widely used in traditional medicine; a decoction from the bulb is used as an enema for internal tumors by the Sotho's (Hutchings et al., 1996) and as an antimicrobial (Lee and Lee, 2013). Phytochemical investigations of *S. nervosa* have been carried out extensively; however, there is a dearth of information on the scientific evaluation of the anticancer potential of the homoisoflavonoids and organic extracts of the plant.

Homoisoflavonoids are a naturally occurring form of flavonoids, and unlike the other forms of flavonoids, they are limited in occurrence (Castelli and Lopez, 2017). They differ from other flavonoids by an additional carbon (C₆-C₄-C₆) to the C₆-C₃-C₆ carbon skeleton of flavonoids. They have been reported to possess good antioxidant (Youichirou et al., 2013), antiangiogenic (Schwikkard et al., 2018), antibacterial (Du Toit et al., 2007), and chemoprotective properties (Machala et al. 2001).

In our previous work, we isolated and identified the major constituents of *S. nervosa* and screened selected isolated homoisoflavonoids and crude extracts for their antibacterial activity against various Gram-positive and Gram-negative bacteria. This study explored the anticancer potential of the crude extracts and selected homoisoflavonoids previously isolated from the plant on two tumor cell lines (Caco-2 and HepG2) and one standard cell line (Hek-293).

4.2 MATERIALS AND METHODS

4.2.1 Plant Material and Isolation of Compounds

S. nervosa was purchased from the Berea muthi market. The taxonomist in the School of Life Sciences, University of KwaZulu Natal, authenticated the species, and a voucher specimen was lodged in the ward herbarium of the School. Extraction, isolation, purification, and identification of pure compounds was conducted, as previously reported.

4.2.2 Chemicals and Reagents

Dulbecco's minimum essential medium (DMEM), L-Glutamine, penstrep-fungizone, and trypsin were procured from Whitehead Scientific. The lactate dehydrogenase (LDH) cytotoxicity detection kit and CellTitre-Glo ® reagent were purchased from Merck and prepared according to the manufacturer's instructions.

4.2.3 Cell Lines and Cultures

Human CaCo-2, HepG2 tumor cell lines, and Hek-293 normal kidney cell lines were procured from America Tissue Culture Collection (ATCC) (Virginia, USA). The cells were propagated in 25 mL tissue culture flasks in complete culture medium (CCM) which consists of 500 mL DMEM supplemented with 1% L-glutamine, 1% penicillin-streptomycin-fungizone and 10% FCS at 37°C and 5% CO₂ until 100% confluence. The cells were rinsed three times with phosphate buffer saline (PBS), Caco-2, and Hek-293 were harvested by trypsinizing with 1 mL of trypsin-EDTA. Cells were counted using the trypan blue method.

4.2.4 Cell Viability

MTT (3-[4,5-Dimethylthiazol-2-yl]-2,5-diphenyl tetrazolium bromide) assay

Test samples (25 mg of pure compounds and 50 mg of crude extracts) were dissolved in 100 µL of dimethyl sulfoxide (DMSO), then made up to 10 mL with dichloromethane (DCM) to

make stock solutions of 2.5 mg/mL and 5 mg/L, respectively. The final concentration of DMSO in the stock solution was 1%. Working concentrations of 50 µg/mL - 5 mg/mL were prepared from the stock solutions for the MTT cell viability assay, while IC₈₀ and IC₅₀ concentrations from the MTT assay were used for other assays. The ability of the cells to reduce MTT (3-(4, 5-dimethylthiazol-2-yl) 2, 5-diphenyltetrazolium bromide) after exposure to test samples was used to evaluate their cytotoxicity. Briefly, CaCo-2, HepG2, and Hek-293 cells were seeded in a 96-well microtiter plate (2×10^5 cells/ well) and incubated overnight (37°C in 5% CO₂) to allow cells to adhere to the well. Cells were treated with varying concentrations of test samples at a volume of 100 µL for 24 h. After cultivation for 24 h, the media was removed, and 10 µl MTT solution at a concentration of 5 mg/mL and 100 µL of phosphate buffer saline (PBS) were added to each well. The plates were incubated at 37°C for 4 h. Thereafter, the MTT solution was removed, and DMSO (100 µL) was added to solubilize the formed formazan crystal. The cell viability was measured using a Bio-Tek µQuant plate spectrophotometer at 540 nm (Winooski, Vermont, United States). All experiments were done in triplicate.

$$\text{Cell viability (\%)} = (\text{Average OD of treated cells} / \text{Average OD of control cells}) \times 100$$

Mitochondria membrane potential (MMP) assay

Cells were cultured in a humid environment at 37°C and 5% CO₂, 2×10^5 were plated into each well of a 96-well plate reader. Cells were treated with the concentration of IC₈₀ and IC₅₀ values obtained from the MTT assay for each test sample and incubated for 24 h to induce apoptosis. JC-10 dye was prepared according to the manufacturer's description. Treatment media was removed and stored for other assays. Thereafter, 50 µL of PBS and 25 µL of JC-10 dye were added to each well and incubated at 37°C for 1 h. The plates were protected from light by wrapping in foil before being placed into the incubator. After incubation, fluorescent intensity was read at 490 nm excitation and 525 nm emission for green fluorescent monomers, and 540

nm excitation and 590 nm emission for red fluorescence aggregates. Data were presented as a ratio of red (590 nm) to green (525 nm) fluorescence.

Adenosine triphosphate (ATP) assay

The effect of the IC₅₀ and IC₈₀ doses of test samples obtained from the MTT assay against the viability of Caco-2, HepG2, and Hek-293 cell lines after 24 h treatment was evaluated using the CellTiter-Glo[®] reagent (Promega), which was prepared according to the manufacturer's instructions. Immediately after the mitochondria membrane potential assay was carried out, 25 µL of CellTiter-Glo[®] reagent was added to each well after 50 µL of PBS. Luminescent reading was done on a Modulus[™] microplate luminometer (Turner Bio-Systems, California, USA).

Lactate dehydrogenase (LDH) release

LDH is released into the culture medium when cell lysis occurs during apoptosis and necrosis, and this can be used as a measure of cytotoxicity. IC₅₀ and IC₈₀ concentrations obtained from the MTT cell viability assay for each test sample were used to evaluate their cytotoxicity after exposure in Caco-2, HepG2, and Hek-293 cell lines. A volume of 50 µL of supernatant of cell treatment was pipetted into a 96-well plate in triplicate. After that, 25 µL of a reagent consisting of catalyst (diaphorase) and the INT/sodium lactate dye solution was added to each well and kept at room temperature for 30 min then 12.5 µL of stop solution was added. Readings were recorded on a spectrophotometer (Biotek µQuant spectrophotometer, Winooski, Vermont, United States) at a wavelength of 480 nm.

4.2.8 Statistical Analysis

Data analyses were done on Microsoft Excel. IC₅₀ values were calculated using the non-linear regression dose versus response curve on GraphPad Prism 5 software (GraphPad Software Inc., San Diego, California, United States). IC₈₀ values were extrapolated from the graph. Statistical difference ($p < 0.05$) from control was determined by student t-test.

4.3 RESULTS

MTT (3-[4,5-Dimethylthiazol-2-yl]-2,5-diphenyl tetrazolium bromide) assay

The cells were treated with different working concentrations ($50\ \mu\text{g mL}^{-1}$ to $5\ \text{mg mL}^{-1}$) of the test samples (3 homoisoflavonoids and 3 crude extracts) for 24 h. The viability of the cells was determined using the MTT assay. Cell viability was presented relative to the untreated cells (control). The toxic effects were observed at IC_{50} concentrations that were extrapolated from the graph. Cell viability was reduced following 3-(4-methoxybenzyl)-5, 7-dimethoxychroman-4-one (compound 1) administration from 100% in the control to 48% at $25\ \mu\text{g mL}^{-1}$ in Caco-2, 69% in HepG2, and 14% in Hek-293 cell lines at the same concentration, giving an IC_{50} concentration of $17.65\ \mu\text{g mL}^{-1}$, $51.66\ \mu\text{g mL}^{-1}$ and $8.577\ \mu\text{g mL}^{-1}$, respectively. A U-shaped cytotoxicity curve was observed for compound 1 across all cell lines (Figure 4.1).

A stimulatory effect was observed after treatment with 3-(4-methoxybenzyl)-6-hydroxy-5,7-dimethoxychroman-4-one (compound 2), in HepG2 cells (Figure 4.1). Cell viability increased from 100% to 118% at $25.12\ \mu\text{g mL}^{-1}$. Thereafter, cell viability decreased to 110% at $50.12\ \mu\text{g mL}^{-1}$ and 76% at $251.19\ \mu\text{g mL}^{-1}$. Cell viability was reduced to 55% and 35% in Caco-2 and Hek-293 at $25.12\ \mu\text{g mL}^{-1}$, respectively. Furthermore, it was reduced to 35% and 14% at $50.12\ \mu\text{g mL}^{-1}$ for both cell lines. After the administration of 3-(4-hydroxybenzylidene)-5,7-dihydroxychroman-4-one (compound 3), cell viability in Caco-2 was reduced to 44% at $25.12\ \mu\text{g mL}^{-1}$ and 8% at $50\ \mu\text{g mL}^{-1}$; a dose-dependent reduction was observed with an IC_{50} value of $13.57\ \mu\text{g mL}^{-1}$. In HepG2 cells, there was no decrease in cell viability across the concentrations from 0- $25\ \mu\text{g mL}^{-1}$. A sharp decrease in cell viability from 100% to 11% was observed at $50.12\ \mu\text{g mL}^{-1}$, and the IC_{50} value was $36.34\ \mu\text{g mL}^{-1}$. Cytotoxicity was observed in Hek-293 cells at a concentration of $25.12\ \mu\text{g mL}^{-1}$, where cell viability was reduced from 100% to 11% with a generated IC_{50} value of $6.71\ \mu\text{g mL}^{-1}$.

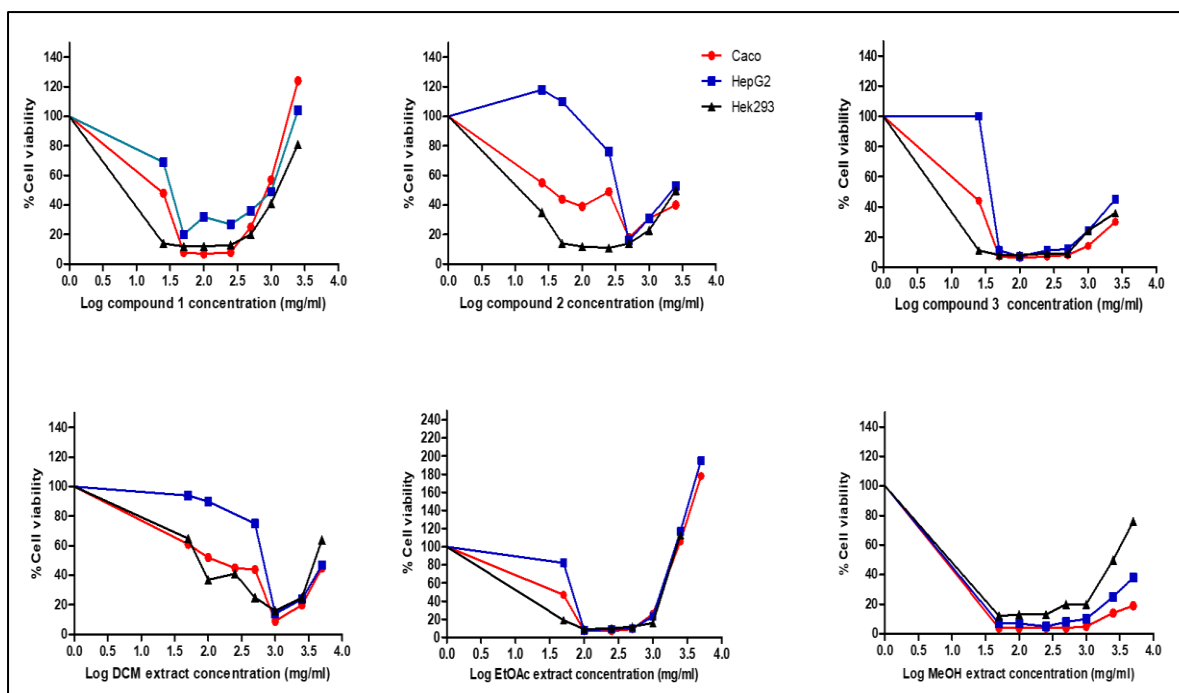


Figure 4.1. Dose-response curve for viability using MTT assay in Caco-2, HepG2, and Hek-293 cells exposed to test samples for 24 h.

Compound 1: 3-(4-methoxybenzyl)-5,7-dimethoxychroman-4-one, Compound 2: 3-(4-methoxybenzyl)-6-hydroxy-5,7-dimethoxychroman-4-one, Compound 3: 3-(4-hydroxybenzylidene)-5,7-dihydroxychroman-4-one. DCM – dichloromethane, EtOAc – ethyl acetate and MeOH – methanol.

A reduction in cell viability for Caco-2 (61%), HepG2 (95%), and Hek-293 (65%) were observed after treatment with the DCM extract ($50.12 \mu\text{g mL}^{-1}$) (Figure 4.1). At a higher concentration ($1000 \mu\text{g mL}^{-1}$), a further reduction in cell viability was observed; Caco-2 (9%), HepG2 (14%), and Hek-293 (6%). Cell viability reduced from 100% (control) to 47% (Caco-2), 82% (HepG2), and 19% (Hek-293) after treatment with the ethyl acetate (EtOAc) extract ($50.12 \mu\text{g mL}^{-1}$). The cytotoxicity profile for the EtOAc extract was U-shaped, similar to the DCM extract (Figure 4.1). Cytotoxicity was most prominent with the methanol (MeOH) extract against Caco-2 and HepG2 cells, with IC_{50} concentrations of $7.79 \mu\text{g mL}^{-1}$ and $9.29 \mu\text{g mL}^{-1}$, respectively. Additionally, a reduction in cell viability from 100% (control) to 4% (Caco-2), 7% (HepG2), and 12% (Hek-293) was noted at a concentration of $50.12 \mu\text{g mL}^{-1}$.

Mitochondrial membrane potential (MMP, $\Delta\Psi_m$)

Caco-2, HepG2, and Hek-293 cells were treated with IC₈₀ and IC₅₀ concentrations of the three homoisoflavonoids and three crude extracts. The results are expressed as fold change (Figure 4.2). The MMP did not significantly decrease in Caco-2 (1.01-fold) and the increase in HepG2 (1.09-fold), and Hek-293 (1.07-fold) was also not significant after treatment with an IC₈₀ dose of compound 1. At the IC₅₀ concentration of compound 1, 1.01 and 1.05-fold increase in MMP was observed in Caco-2 and HepG2 cell lines respectively, while a 1.02-fold decrease was seen in Hek-293. Treatment with an IC₈₀ dose of compound 2 resulted in a 1.09, 1.52 ($p = 0.023$) and 1.03-fold increase in Caco-2, HepG2, and Hek-293. In addition, the IC₅₀ dose showed a 1.40 ($p = 0.0436$) and 2.19 ($p = 0.0008$) fold increase in Caco-2 and HepG2 cells, with a 1.03-fold decrease in Hek-293 cells. The IC₈₀ dose of compound 3 showed a 1.05-fold increase in Hek-293 but a 1.45 ($p = 0.0061$) and 1.02-fold decrease in Caco-2 and HepG2 cells. Furthermore, the IC₅₀ dose showed a 1.15, a 1.01, and 1.14-fold decrease in Caco-2, HepG2, and Hek-293 cells. Among the three pure compounds, compound 2 showed a significant increase in the MMP of HepG2 cell lines at both IC₈₀ and IC₅₀ concentration, while compound 3 significantly decrease MMP in Caco-2 cell at IC₈₀ concentration.

The DCM extract at an IC₈₀ dose showed a significant decrease in Caco-2 (1.82-fold, $p = 0.0337$), no significant decrease in Hek-293 (1.02-fold), but a significant increase ($p = 0.0173$) was observed in HepG2 (1.44-fold). At the IC₅₀ dose, a decrease was observed in Caco-2 (1.11-fold), a significant increase ($p = 0.0285$) in HepG2 (1.52-fold) and 1.05-fold increase in Hek-293. Exposure to the EtOAc extract at an IC₈₀ dose showed a decrease in MMP in Caco-2 (1.30-fold), a significant increase ($p = 0.0056$) in HepG2 (1.20-fold) and a 1.01-fold increase in Hek-293 cell lines. The IC₅₀ dose showed a significant decrease ($p = 0.0377$) in Caco-2 (1.32-fold) a significant increase ($p = 0.0013$) in HepG2 (1.40-fold) and a 1.04-fold increase in Hek-293. Treatment with the methanol extract at the IC₈₀ dose showed a significant

decrease ($p = 0.0135$) in Caco-2 (1.64-fold), 1.03-fold decrease in HepG2, and a significant increase ($p = 0.0369$) in Hek-293 (1.10-fold) and at the IC_{50} dose, an increase in MMP was observed in Caco-2 (1.02-fold) and Hek-293 (1.02-fold), but a significant decrease ($p = 0.0306$) in the HepG2 (1.04-fold).

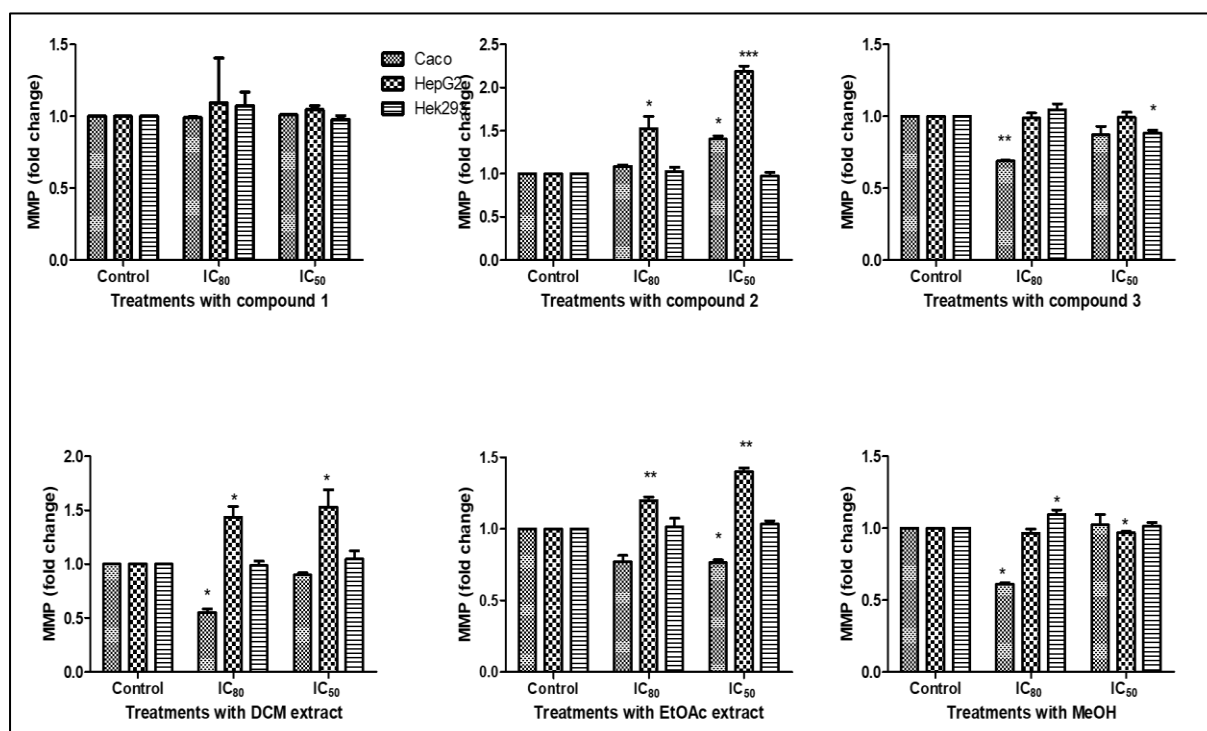


Figure 4.2 Effect of IC_{80} and IC_{50} concentrations of tested samples on the mitochondrial membrane potential (MMP) of Caco-2, HepG2 and Hek-293 cell lines.

Compound 1: 3-(4-methoxybenzyl)-5,7-dimethoxychroman-4-one, Compound 2: 3-(4-methoxybenzyl)-6-hydroxy-5,7-dimethoxychroman-4-one, Compound 3: 3-(4-hydroxybenzylidene)-5,7-dihydroxychroman-4-one. DCM – dichloromethane, EtOAc – ethyl acetate and MeOH – methanol.

Adenosine triphosphate (ATP) assay

Caco-2, HepG2, and Hek-293 cells were treated with IC_{80} and IC_{50} concentrations of the three homoisoflavonoids and three crude extracts. The ATP value for the controls was calculated to be 1, and those for treated cells were calculated as a ratio against the control (Figure 4.3). ATP

decreased to 91% in Caco-2, and 74% in HepG2 ($p = 0.0270$), but a significant increase to 144% in Hek-293 ($p = 0.0706$) after exposure to the IC_{80} concentration of compound 1. At the IC_{50} concentration, a significant reduction to 66% ($p = 0.0080$) and 61% ($p = 0.0028$) was observed in Caco-2 and HepG2, respectively, while a significant increase ($p = 0.0014$) to 120% was seen in Hek-293. Treatment with an IC_{80} concentration of compound 2 decreased ATP to 95% in Caco-2, and 83% in HepG2, while an increase ($p = 0.0322$) to 131% was observed in Hek-293. The IC_{50} concentration decreased ATP in Caco-2 to 70% ($p = 0.0115$) and 32% ($p = 0.0008$) in HepG2, with a 122% ($p = 0.0396$) increase for Hek-293. For treatment with the IC_{80} dose of compound 3 (Figure 3), a 6% and 19% decrease in ATP was observed in Caco-2 and HepG2, respectively, with a 40% ($p = 0.0339$) increase for Hek-293. The IC_{50} concentration of the same compound resulted in a 19% ($p = 0.0229$) and 29% ($p = 0.0103$) decrease of ATP in Caco-2 and HepG2, respectively, and 30% increase in ATP for Hek-293.

Treatment with the DCM extract at IC_{80} concentration decreased ATP to 77% in Caco-2 and 68% ($p = 0.0176$) in HepG2, but increased ATP to 175% ($p = 0.0180$) in Hek-293, while IC_{50} treatment decreased ATP to 81% ($p = 0.0251$) in Caco-2 and 39% ($p = 0.0010$) in HepG2 but increased to 142% in Hek-293. The EtOAc extract at IC_{80} concentration decreased ATP to 95% in Caco-2 and 70% ($p = 0.0163$) in HepG2 but increased it to 216% in Hek-293. At the IC_{50} concentration, ATP was reduced to 72% ($p = 0.0075$) in Caco-2 and 65% ($p = 0.0044$) in HepG2 but increased to 216% in Hek-293. ATP decreased to 71% ($p = 0.0168$) in HepG2 after treatment with the MeOH extract at the IC_{80} concentration but increased to 105%, and 337% ($p = 0.0422$) in Caco-2 and Hek-293, respectively. At the IC_{50} concentration, ATP decreased to 72% ($p = 0.0051$) in Caco-2 and 67% ($p = 0.0106$) in HepG2 but increased to 167% ($p = 0.0087$) in Hek-293.

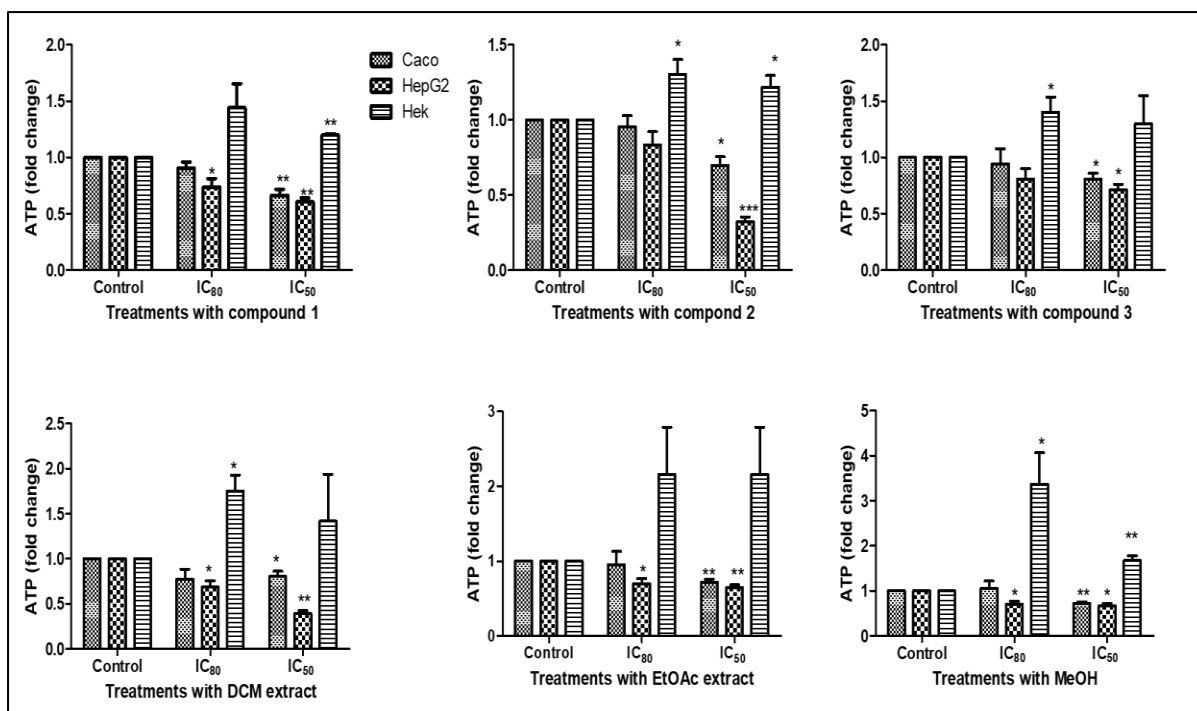


Figure 4.3. Effect of IC₈₀ and IC₅₀ concentrations of tested samples on the intracellular ATP levels of Caco-2, HepG2 and Hek-293 cell lines.

Compound 1: 3-(4-methoxybenzyl)-5,7-dimethoxychroman-4-one, Compound 2: 3-(4-methoxybenzyl)-6-hydroxy-5,7-dimethoxychroman-4-one, Compound 3: 3-(4-hydroxybenzylidene)-5,7-dihydroxychroman-4-one. DCM – dichloromethane, EtOAc – ethyl acetate and MeOH – methanol.

Lactate dehydrogenase (LDH) release assay

Caco-2, HepG2, and Hek-293 cells were treated with IC₈₀ and IC₅₀ concentrations of the three homoisoflavonoids and three crude extracts (Figure 4.4). An increase in LDH level from 100% in the control to 143%, 259% ($p = 0.0469$) and 148% ($p = 0.0173$) was observed in Caco-2, HepG2 and Hek-293 cell lines after treatment with compound 1 at IC₈₀ concentration. At IC₅₀ concentration the increase was 225% ($p = 0.0158$) in Caco-2, 133% ($p = 0.0311$) in HepG2 and 160% ($p = 0.0251$) in Hek-293 cell lines. Treatment with compound 2 IC₈₀ concentration caused significant increase ($p = 0.0218$) in LDH released to 217% in Caco-2, and non-significant increase to 103% and 127% in HepG2 and Hek-293 cell lines, respectively. At IC₅₀ treatment of compound 2, significant increase of 295% ($p = 0.0243$) and 168% ($p = 0.0199$) was observed in Caco-2 and HepG2 cell lines, and non-significant increase of 162% in Hek-

293. Treatment with IC₈₀ value of compound 3 significantly reduced LDH in Caco-2 to 88% ($p = 0.0498$) and in HepG2 to 48% ($p = 0.0047$) but an increase to 116% was observed in Hek-293.

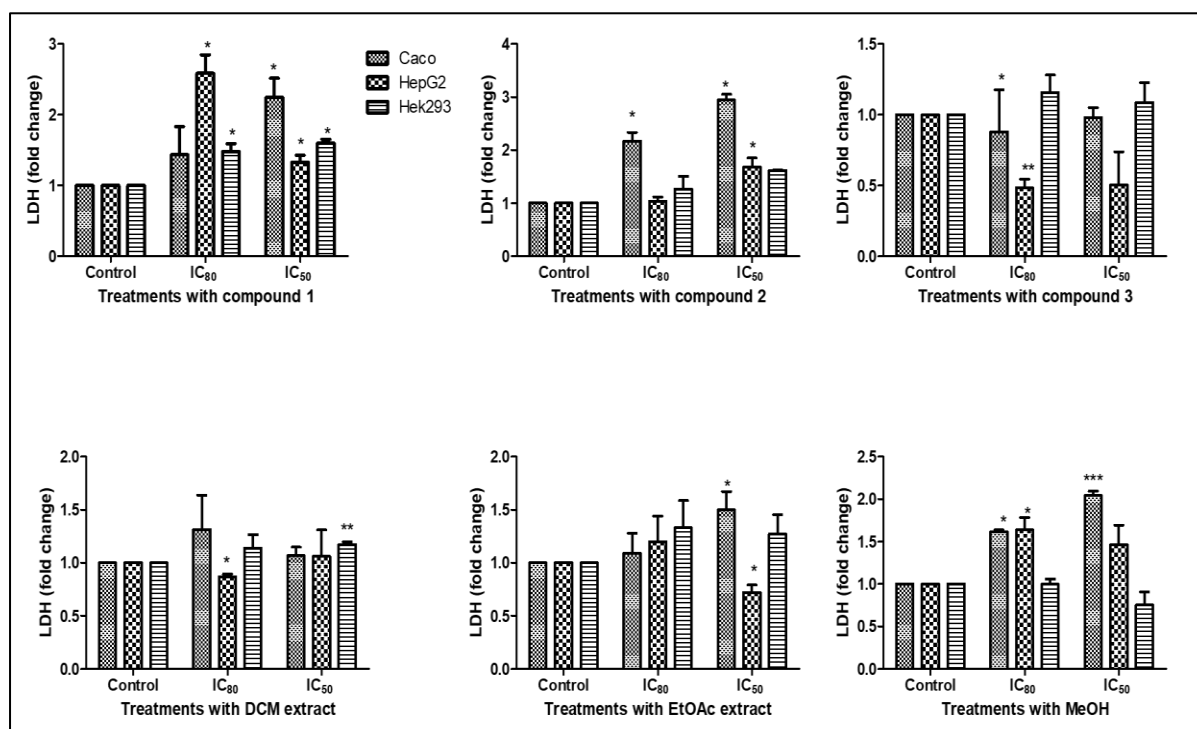


Figure 4.4. Effect of IC₈₀ and IC₅₀ concentrations of tested samples on the plasma membrane of Caco-2, HepG2 and Hek-293 cell lines.

Compound 1: 3-(4-methoxybenzyl)-5,7-dimethoxychroman-4-one, Compound 2: 3-(4-methoxybenzyl)-6-hydroxy-5,7-dimethoxychroman-4-one, Compound 3: 3-(4-hydroxybenzylidene)-5,7-dihydroxychroman-4-one. DCM – dichloromethane, EtOAc – ethyl acetate and MeOH – methanol.

Treatment with the DCM extract at the IC₈₀ concentration resulted in 132% increase in LDH for Caco-2, 87% significant decrease ($p = 0.0113$) in HepG2, and 114% increase in Hek-293 cell lines. At IC₅₀ DCM extract treatment, LDH was increased to 107% in Caco-2, 106% in HepG2 and a significant increase ($p = 0.0067$) of 117% in Hek-293. IC₈₀ concentration of EtOAc increased LDH to 109%, 120% and 133% in Caco-2, HepG2 and Hek-293 cell lines, respectively. At IC₅₀ treatment LDH was significantly increased ($p = 0.0377$) to 150% in Caco-2, significantly reduced ($p = 0.0190$) to 72% in HepG2 and non-significant increase to 127% in

Hek-293. Treatment with IC₈₀ concentration of MeOH extract significantly increase LDH in Caco-2 ($p = 0.0185$) to 161% and in HepG2 ($p = 0.0174$) to 164%. No change was observed in LDH level in Hek-293 at the same concentration. IC₅₀ concentration significantly increase ($p = 0.0008$) LDH to 204% in Caco-2, with non-significant increase of 146% in HepG2 and a non-significant decrease to 75% in Hek-293. All tested samples showed an increase in LDH for Hek-293 at both IC₈₀ and IC₅₀ except for the methanol extract.

4.3 DISCUSSION

A phytochemical investigation of *Scilla nervosa* revealed it to be rich in homoisoflavonoids (Bangani, 1998; Crouch et al., 1999). The cytotoxic potential of *Scilla* species indigenous to South Africa has not been well studied. *Scilla* species from other regions have demonstrated potential cytotoxic activity against different cell lines (Mimaki et al., 1994; Lee et al., 2002). Therefore, this report describes the *in vitro* cytotoxic effect of homoisoflavonoids and crude extracts from *S. nervosa* on three different cell lines.

The MTT assay revealed the cytotoxic potential of homoisoflavonoids and extracts against Caco-2 with IC₅₀ values within the NCI (US National Cancer Institute) recommendation (IC₅₀ < 30 $\mu\text{g/mL}$) for anticancer activity (Begüm and Emine, 2013). For the pure compounds, the IC₅₀ values against Caco-2 were in the order compound 3 (13.57 $\mu\text{g/mL}$) > compound 1 (17.65 $\mu\text{g/mL}$) > compound 2 (70.79 $\mu\text{g/mL}$) while for the crude extracts, it was MeOH (7.79 $\mu\text{g/mL}$) > EtOAc (37.96 $\mu\text{g/mL}$) > DCM (178.4 $\mu\text{g/mL}$). The MeOH extract displayed synergism due to the attenuation of cell viability for Caco-2 and HepG2 compared to the individual compounds and antagonism for the DCM and EtOAc extracts.

All tested homoisoflavonoids showed good activity against Caco-2 compared to HepG2. This selective activity was also reported for (3S)-3,5,7-trihydroxy-3-(3'-hydroxy-4'-

methoxybenzyl)-4-chromanone, isolated from *Pseudoprospero firmifolium* (Sihra et al., 2020). The IC₅₀ value of scillasillin, a homoisoflavonone isolated from *Ledebouria hyderabadensis*, was significant against MCF-7 (breast cancer cell line, 9.59 µg/mL) and DU-145 (prostate cancer cell line, 11.32 µg/mL), compared to the IC₅₀ value of the MeOH extract, 36.22 µg/mL and 44.86 µg/mL, respectively (Chinthala *et al.*, 2014). Scillasillin was also shown to significantly reduce DU-145 compared to the standard doxorubicin (Chinthala *et al.*, 2014).

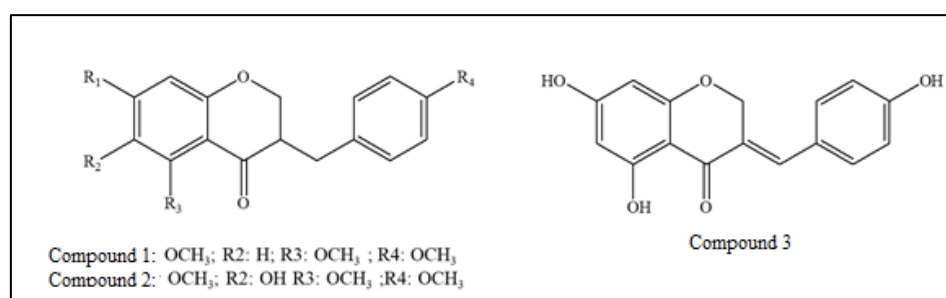


Figure 4.5 Structure of compounds 1-3.

An investigation of the cytotoxicity of homoisoflavonoids isolated from *Scilla persica* led to the ascription of cytotoxic activity to the low energy gaps between the first ionization potentials and highest occupied molecular orbital (Salar et al., 2016). The cytotoxicity of several homoisoflavonoids against various cancer cell lines demonstrated the influence of the substitution pattern on the B-ring with the 4'-OH group reducing cytotoxicity and the 3',4'-dihydroxy substituents improving activity (El Elimat et al., 2018). Likewise, reducing the polarity of the B-ring substitution enhances activity. Homoisoflavonoids isolated from the bulbs of *Bellevalia eigii* showed that highly oxygenated homoisoflavonoids with high polarity are less active against colon cancer cell lines than those with methoxy substituents (Alali et al., 2015). The presence of exocyclic double bonds also increased activity against Caco-2 and HepG2 cell lines (Alali et al., 2015). Introduction of the hydroxy group to position 3', methoxy group to position 7 or methoxy/hydroxy groups to position 4' of 3-benzylidene chromanone derivatives were found to increase tumor specificity, which was found to be better than

doxorubicin and 5- fluorouracil (5-FU) (Yoshihiro et al., 2016). Studies done by Dai et al. (2013) showed that methylation and hydroxylation at position 3 of homoisoflavonoids increased their cytotoxicity. Compound 3 which is a 3-benzylidenechroman-4-one with OH substituent at 4'showed a good cytotoxicity activity against Caco-2 and HepG2 cell lines compared to other two compounds which are 3-benzylchroman-4-one type homoisoflavonoids (Figure 4.5).

Other evidence that homoisoflavonoids can be considered as anticancer drug candidates could be seen in isobonducellin, a homoisoflavonoid that showed good cytotoxic activity in Jurkat and HepG2 cells but moderate activity in colon205 cells (Rao et al., 2007). In addition, naturally occurring homoisoflavonoids have showed estrogen inhibition, while another study using synthesized homoisoflavonoids showed that it is inactive against MCF-7 cell lines at 50 μ M after 24 h treatment (Gan et al., 2017).

A stimulatory effect at a low dose of compound 2 was observed in HepG2, with compound 1 and the EtOAC extract giving a U-shaped curve. U-shaped cytotoxicity was also observed for compound 2, compound 3, the DCM extract, and MeOH extract. This observation has been described as hormesis. Hormesis is when a toxic substance to a biological system at high doses produces a stimulatory effect at low doses (Borriello et al., 2013). The hormesis curve is an optimality trajectory of a multi-dimensional homeostatic system responding to rising perturbation intensity, which is manifested by a change in structure (Wan et al. 2015). Several *in vitro* studies have reported hormesis in different compounds and plant extracts. Toxic effects are monitored as inhibition of some biological processes above a threshold level occurs with increasing concentration of the chemical agent. However, in some cases, it has been reported that harmful or inhibiting biological processes at high concentrations could also be stimulatory at lower concentrations. The hormetic reaction was first observed with antibiotics, where a low dose of antibiotics caused cell growth; it was also observed in yeast and was later observed and

confirmed in other substances. Some reports also suggested resveratrol can stimulate cell growth at a low concentration (Adrianna et al., 2013).

In contrast to the linear dose-response curve, hormesis is usually represented by a J, U, or inverted U-shaped curve. For the determination of treatment dosage, its biphasic function needs to be understood. Regulatory bodies such as the Food and Drug Administration (FDA) and Environmental Protection Agency (EPA) in the USA have implemented guidelines to consider the hermetic effects of therapeutics. A cell or organism's hormesis effects could be an adaptive response to stress induced by a physical, chemical, or biological stressor (factors). Though hormetic effects have been shown to have some health benefits, including enhanced immunity and injury resistance, it also has potential adverse effects in cancer treatment (Bao et al., 2015). In a study carried out by Bao et al. (2015), it was noted that berberine, a phytochemical with promising anticancer activity, caused cell proliferation at a low dose but inhibited cell growth at a higher concentration. Further, it was observed that co-treatment of a low dose of berberine attenuates the anticancer activity of cancer chemotherapeutics such as 5-FU, camptothecin (CPT), and paclitaxel (TAX).

ATP is a measure of cell viability and proliferation, and a change of intracellular ATP could also be a biomarker for cellular proliferation. A decrease in intracellular ATP was observed in Caco-2 and HepG2 across all tested samples at both IC₈₀ and IC₅₀ concentrations, but more significantly at IC₅₀ concentrations for both cell lines (Table 4.1 and 4.2). The depletion in ATP observed in Caco-2 and HepG2 cell lines, correlated with decrease in cell viability (Plackal et al., 2015). In contrast to our result, Pillay et al., (2013), reported an increase in intracellular ATP of HepG2 after treatment with aqueous extract of *S. nervosa*. In Hek-293, an increase in intracellular ATP was observed, this means cell proliferation was observed at both IC₈₀ and IC₅₀ concentrations of all tested samples. Studies have shown that the level of intracellular ATP determines if a cell dies by necrosis or apoptosis. Apoptosis is programmed cell death that plays

an important role in the elimination of cancerous cells. This process requires energy, depletion of cellular ATP has been shown to switch cell death from apoptosis to necrosis. Lower concentrations of glucose cause ATP to decrease and cell death *via* necrosis. As the glucose level is increased, apoptosis replaces necrosis as a form of cell death (Tsujimoto, 1997; Tatsumi et al., 2003; Leist et al., 1997).

The LDH assay was used to measure cytotoxicity, membrane integrity and necrosis. An increase in the release of LDH was observed for all tested samples in Caco-2 and HepG2 cell lines (Table 4.1. and 4.2). When the cell membrane is compromised or damaged due to external stressors, LDH, a soluble enzyme found in the cytoplasm, is released into the surrounding extracellular environment. Cells undergoing necrosis are known to swell and lose membrane integrity before releasing their intracellular content into the surrounding environment. Therefore, the release of LDH can be used to quantify necrosis, as well as cytotoxicity (Chan, Moriwaki, De Rosa., 2013; Maes et al., 2015). Increase in LDH release was observed for tested samples at both IC₈₀ and IC₅₀ concentrations, except for compound 3, that showed a decrease in LDH at both concentrations. The same effect was observed in HepG2 cell lines after treatment with compound 3. In Hek-293, all tested samples increased LDH at IC₈₀ and IC₅₀, except MeOH extract, which showed a decrease.

Apoptosis and necrosis are two forms of cell death; an increase in intracellular oxidation may determine the selection between the two (Vairetti et al., 2005). In our study, loss of ATP with an increase in LDH released was observed for the cancerous cells. This phenomenon could mean that the tested samples induced cell death *via* necrosis instead of apoptosis. Treatment of MCF-7 and HFS cell lines with the aqueous extract of *Lepidium sativum* seed was observed to induce apoptosis at low concentrations (25 and 50%) and necrosis at high concentrations (75%) (Mahassni and Al Reemi, 2013).

Mitochondria are involved in apoptosis (Wang and Youle, 2009); in some apoptotic cells, loss of membrane potential is thought to be an early event in the apoptotic process. The mitochondrial membrane potential (MMP, $\Delta\Psi_M$) can be used to evaluate cell health and apoptosis. Disruption of mitochondrial function such as changes that leads to the loss of MMP could be an early apoptotic event in some apoptotic systems (Ly, Grubb and Lawen, 2003). The opening of the mitochondria, which leads to a reduction in the electrochemical gradient, decreases MMP and activates the pro-apoptotic factor. The MMP is investigated using cationic fluorescent dyes that accumulate in the negative mitochondrial matrix. A healthy cell accumulates more dye to emit a red fluorescence, while an apoptotic cell accumulates less to emit green fluorescence. Mitochondrial depolarization is indicated by a decrease in the red: green fluorescence intensity ratio. However, some studies suggest that the MMP may either decrease or increase (Ly, Grubb and Lawen, 2004).

In this study, the homoisoflavonoids and crude extracts tested did not significantly reduce the MMP in Hek-293 cell lines, while increase in MMP was observed in HepG2 cell lines (Table 4.1). In agreement with our findings, a previous study showed that the aqueous extract from *S. nervosa* decreased cell viability in HepG2 in a concentration-dependent manner with an IC_{50} value of 30 $\mu\text{g/mL}$, with no significant change in the MMP (Pillay et al., 2013). In Caco-2 cell lines, compound 3 significantly reduced MMP at the IC_{80} concentration, while the reduction at IC_{50} was not significant. The same was observed for the DCM and MeOH extracts. All extracts caused MMP depolarization in Caco-2 cells, but among the pure compounds, only compound 3 depolarized MMP. Curcumin was reported to inhibit the growth of HepG2 and cause disruption of MMP (Wang et al., 2011). Depolarization of MMP, with the release of cytochrome c has been reported to be an early event in apoptosis, however, some data also suggests that MMP may decrease, increase, or remain unchanged during apoptosis (Pillay et al., 2013).

Table 4.1: Analysis of the results obtained for the cytotoxicity assays (LDH, MMP and ATP) after treatment with the IC₈₀ and IC₅₀ concentrations of pure compounds and extracts (DCM, EtOAc and MeOH) of *S. nervosa* using the cell lines, Caco-2, HepG2 and Hek-293.

Cell Lines	Assay	Compound 1	Compound 2	compound 3	DCM	EtOAc	MeOH
IC₈₀							
Caco-2	<i>LDH</i>	increase	increase	decrease	increase	increase	increase
	<i>MMP</i>	no change	increase	decrease	decrease	decrease	decrease
	<i>ATP</i>	Decrease	decrease	decrease	decrease	decrease	decrease
HepG2	<i>LDH</i>	increase	increase	decrease	decrease	increase	increase
	<i>MMP</i>	increase	increase	No change	increase	increase	Slight decrease
	<i>ATP</i>	decrease	decrease	decrease	decrease	decrease	decrease
Hek-293	<i>LDH</i>	increase	increase	increase	increase	increase	no change
	<i>MMP</i>	increase	Slight increase	Slight increase	No change	No change	increase
	<i>ATP</i>	increase	increase	increase	increase	increase	increase
IC₅₀							
Caco-2	<i>LDH</i>	increase	increase	decrease	increase	increase	increase
	<i>MMP</i>	no change	increase	decrease	decrease	decrease	slight increase
	<i>ATP</i>	decrease	decrease	decrease	decrease	decrease	decrease
HepG2	<i>LDH</i>	increase	increase	decrease	increase	decrease	increase
	<i>MMP</i>	increase	increase	Slight decrease	increase	increase	Slight decrease
	<i>ATP</i>	decrease	decrease	decrease	decrease	decrease	decrease
Hek-293	<i>LDH</i>	increase	increase	increase	increase	increase	decrease
	<i>MMP</i>	Slight decrease	Slight decrease	decrease	increase	Slight increase	Slight increase
	<i>ATP</i>	increase	increase	increase	increase	increase	increase

LDH - Lactate dehydrogenase, MMP – Mitochondrial membrane potential, ATP - Adenosine triphosphate.

Compound 1– 3-(4-methoxybenzyl)-5,7-dimethoxychroman-4-one, compound 2– 3-(4-methoxybenzyl)-6-hydroxy-5,7-dimethoxychroman-4-one, compound 3 – 3-(4-hydroxybenzylidene)-5,7-dihydroxychroman-4-one, DCM – Dichloromethane, EtOAc – Ethyl acetate, MeOH – Methanol.

The DCM, EtOAc and MeOH extracts induced cytotoxicity on Caco-2 cell lines by the depletion of intracellular ATP, depolarization of MMP, disruption of plasma membrane with the release of LDH at both IC₈₀ and IC₅₀ concentrations (Table 4.1). Among the pure compounds, compound 3 induced cytotoxicity on Caco-2 cell lines by depletion of ATP, dissipation of MMP, and LDH release. This agrees with the report on eugenol, a secondary metabolite from cloves, which decreased viability in MCF-7 cell lines, caused ATP depletion

in intracellular ATP and dissipation of the MMP with a release of cytochrome c into the culture media. Additionally, a release of LDH indicating a disruption of plasma membrane integrity was observed (Al-wafai et al., 2017).

4.4 CONCLUSION

Homoisoflavonoids and different organic extracts from *S. nervosa* showed good to moderate cytotoxic activity towards Caco-2 and HepG2 tumor cell lines using the MTT assay. The low IC₅₀ concentrations for some plant extracts indicated potential anticancer properties, but there is a need for some modification in the structure of the homoisoflavonoids to improve their efficacy and selectivity, without toxicity on normal cell lines. ATP and LDH assays showed that the tested samples can exert cytotoxicity through depletion of intracellular ATP, increase ATP to facilitate apoptotic death, disrupt plasma membrane for LDH release as well as support necrotic and late apoptotic death.

REFERENCES

- Al Wafai, R., El-Rabih, W., Katerji, M., Safi, R., El Sabban, M., El-Rifai, O., & Usta, J. (2017). Chemosensitivity of MCF-7 cells to eugenol: release of cytochrome-c and lactate dehydrogenase. *SCIENTIFIC REPORTS*, 7(1): 43730 doi:10.1038/srep43730.
- Alali, F., El-Elimat, T., Albataineh, H., Al-Balas, Q., Al-Gharaibeh, M., Falkinham, J. O., Oberlies, N. H. (2015). Cytotoxic homoisoflavones from the bulbs of *Bellevallia eigii*. *JOURNAL OF NATURAL PRODUCTS*, 78(7), 1708–1715.
- Amaral R. G., dos Santos S. A., Andrade L. N., Severino P., Carvalho A. A. (2009). Natural products as treatment against cancer: A historical and current vision. *CLINICAL ONCOLOGY*. 4: 1562.
- Bangani Vuyisile, (1998). Homoisoflavonoids and stilbenoids from *Scilla* species. MSc thesis, School of Chemistry and Physics, University of KwaZulu Natal.
- Bao, J., Huang, B., Zou, L., Chen, S., Zhang, C., Zhang, Y., Chen, M., Wan, J. B., Su, H., Wang, Y., & He, C. (2015). Hormetic effect of berberine attenuates the anticancer activity of chemotherapeutic agents. *PLOS ONE*, 10(9), e0139298. <https://doi.org/10.1371/journal.pone.0139298>.
- Begüm Yurdakök & Emine Baydan (2013) Cytotoxic effects of *Eryngium kotschyi* and *Eryngium maritimum* on Hep2, HepG2, Vero and U138 MG cell lines, *PHARMACEUTICAL BIOLOGY*, 51:12, 1579-1585.
- Borriello, A., Bencivenga, D., Caldarelli, I., Tramontano, A., Borgia, A., Pirozzi A. V., Oliva, A., and Della Ragione, F. (2013) Resveratrol and cancer treatment: is hormesis a yet unsolved matter? *CURRENT PHARMACEUTICAL DESIGN*. 19(30): 5384-5393. Doi:10.2174/138161281131930.

- Castelli, M. V., & López, S. N. (2017). Homoisoflavonoids: Occurrence, biosynthesis, and biological activity. *STUDIES IN NATURAL PRODUCTS CHEMISTRY* (Vol. 54, pp. 315-354). Elsevier.
- Chan, F. K., Moriwaki, K., & De Rosa, M. J. (2013). Detection of necrosis by release of lactate dehydrogenase activity. *METHODS IN MOLECULAR BIOLOGY* (Clifton, N.J.), 979, 65–70. https://doi.org/10.1007/978-1-62703-290-2_7.
- Chinthala, Y., Chinde, S., Kumar, A. N., Srinivas, K. V., Kumar, J. K., Sastry, K. P., Grover, P., & Ramana, M. V. (2014). Anticancer active homoisoflavanone from the underground bulbs of *Ledebouria hyderabadensis*. *PHARMACOGNOSY RESEARCH*, 6(4), 303–305.
- Crouch, N.R., Bangani, V., Mulholland, D.A., (1999). Homoisoflavanones from three South African *Scilla* species. *PHYTOCHEMISTRY* 51 (7), 943/946.
- Dai, Y., Harinantenaina, L., Brodie, P. J., Goetz, M., Shen, Y., TenDyke, K., & Kingston, D. G. (2013). Antiproliferative homoisoflavonoids and bufatrienolides from *Urginea depressa*. *JOURNAL OF NATURAL PRODUCTS*, 76(5), 865–872.
- Du Toit, K., Elgorashi, E. E., Malan, S. F., Mulholland, D. A., Drewes, S. E., & Van Staden, J. (2007). Antibacterial activity and QSAR of homoisoflavanones isolated from six Hyacinthaceae species. *SOUTH AFRICAN JOURNAL OF BOTANY*, 73(2), 236–241. doi: 10.1016/j.sajb.2007.01.002.
- El-Elimat, T., Rivera-Chávez, J., Burdette, J. E., Czarnecki, A., Alhawarri, M. B., Al-Gharaibeh, M., ... Oberlies, N. H. (2018). Cytotoxic homoisoflavonoids from the bulbs of *Bellevalia flexuosa*. *FITOTERAPIA*, 127, 201–206. doi: 10.1016/j.fitote.2018.02.022
- Gan, L.-S., Zeng, L.-W., Li, X.-R., Zhou, C.-X., & Li, J. (2017). New homoisoflavonoid analogues protect cells by regulating autophagy. *BIOORGANIC & MEDICINAL CHEMISTRY LETTERS*, 27(6), 1441–1445.

- Hutchings, A, Scott, A.H., Lewis, G. and Cunningham, A.B., (1996), Zulu Medicinal Plants an Inventory, University of Natal Press: Pietermaritzburg, 41.
- Lee, Hyang Burm., Lee, Sang-Myung. (2013). Antimicrobial activity of eucosterol oligosaccharides isolated from bulb of squill (*Scilla scilloides*). PHARMACOLOGY & PHARMACY, 04, 110-114. doi:10.4236/pp.2013.41016.
- Lee, Sang-Myung., Chun, Hyo., Lee, Choong.-Hwan., Min, Byung.-Sun., Lee, Eun.-Sook., & Kho, Yung.-Hee. (2002). Eucosterol oligoglycosides isolated from *Scilla scilloides* and their anti-tumor activity. CHEMICAL & PHARMACEUTICAL BULLETIN, 50, 1245-1249
- Leist, M., Single, B., Castoldi, A. F., Kühnle, S., & Nicotera, P. (1997). Intracellular adenosine triphosphate (ATP) concentration: a switch in the decision between apoptosis and necrosis. THE JOURNAL OF EXPERIMENTAL MEDICINE, 185(8), 1481–1486. <https://doi.org/10.1084/jem.185.8.1481>.
- Louw, C. A., Regnier, T. J., & Korsten, L. (2002). Medicinal bulbous plants of South Africa and their traditional relevance in the control of infectious diseases. JOURNAL OF ETHNOPHARMACOLOGY, 82(2-3), 147–154.
- Ly, J.D., Grubb, D.R. & Lawen, A. (2003). The mitochondrial membrane potential ($\Delta\psi_m$) in apoptosis; an update. APOPTOSIS 8, 115–128 <https://doi.org/10.1023/A:1022945107762>.
- Machala, M., Kubínová, R., Hořavová, P., & Suchý, V. (2001). Chemoprotective potentials of homoisoflavonoids and chalcones of *Dracaena cinnabari*: modulations of drug-metabolizing enzymes and antioxidant activity. PHYTOTHERAPY RESEARCH, 15(2), 114–118. doi:10.1002/ptr.697.
- Maes, M., Vanhaecke, T., Cogliati, B., Yanguas, S. C., Willebrords, J., Rogiers, V., & Vinken, M. (2015). Measurement of apoptotic and necrotic cell death in primary hepatocyte cultures. METHODS IN MOLECULAR BIOLOGY (Clifton, N.J.), 1250, 349–361. https://doi.org/10.1007/978-1-4939-2074-7_27.

- Mahassni, S. H., & Al-Reemi, R. M. (2013). Apoptosis and necrosis of human breast cancer cells by an aqueous extract of garden cress (*Lepidium sativum*) seeds. SAUDI JOURNAL OF BIOLOGICAL SCIENCES, 20(2), 131–139. doi: 10.1016/j.sjbs.2012.12.002.
- Mimaki, Y., Nishino, H., Ori, K., Kuroda, M., Matsui, T., Sashida, Y., (1994). Lanosterol oligosaccharides from the plants of the subfamily Scilloideae and their antitumor-promoter activity. CHEMICAL AND PHARMACEUTICAL BULLETIN 42 (2), 327/332.
- Om Prakash, Shazia Usmani, Ruchi Singh, Debarshi K. Mahapatra and Amresh Gupta. (2019). Cancer chemotherapy by novel bio-active natural products: looking towards the future. CURRENT CANCER THERAPY Reviews 15(1). doi:10.2174/157339471466618032115
- Pillay, P., Phulukdaree, A., Chuturgoon, A. A., Du Toit, K., & Bodenstein, J. (2013). The cytotoxic effects of *Scilla nervosa* (Burch.) Jessop (Hyacinthaceae) aqueous extract on cultured HepG2 cells. JOURNAL OF ETHNOPHARMACOLOGY, 145(1), 200–204. doi: 10.1016/j.jep.2012.10.053.
- Plackal, A. G. B., Tynga, I. M., & Abrahamse, H. (2015). *In vitro* antiproliferative effect of the acetone extract of *Rubus fairholmianus* Gard. Root on human colorectal cancer cells. BIOMED RESEARCH INTERNATIONAL, 2015, 1–8. doi:10.1155/2015/165037.
- Ramawat K., Goyal S. (2009) Natural products in cancer chemoprevention and chemotherapy. In: Ramawat K. (eds) Herbal Drugs: Ethnomedicine to Modern Medicine. Springer, Berlin, Heidelberg.
- Rao, Y. K., Geethangili, M., Fang, S.-H., & Tzeng, Y.-M. (2007). Antioxidant and cytotoxic activities of naturally occurring phenolic and related compounds: A comparative study. FOOD AND CHEMICAL TOXICOLOGY, 45(9), 1770–1776.
- Salar Hafez Ghoran, Soodabeh Saeidnia, Esmaeil Babaei, Fumiyuki Kiuchi & Hidayat Hussain (2016) Scillapersicene: a new homoisoflavonoid with cytotoxic activity from the bulbs of

- Scillapersica* HAUSSKN, NATURAL PRODUCT RESEARCH, 30:11, 1309-1314, DOI: 10.1080/14786419.2015.1054286.
- Schwikkard, S. L., Whitmore, H., Corson, T. W., Sishtla, K., Langat, M. K., Carew, M., & Mulholland, D. A. (2018). Antiangiogenic activity and cytotoxicity of triterpenoids and homoisoflavonoids from *Massonia pustulata* and *Massonia bifolia*. PLANTA MEDICA, 84(9/10), 638–644. <https://doi.org/10.1055/a-0577-5322>.
- Sihra, J. K., Crouch, N. R., Nawrot, D. A., Mas-Claret, E., Langat, M. K., & Mulholland, D. A. (2020). Anti-leukaemic and anti-melanoma activities of homoisoflavonoids from *Pseudoprospero firmifolium* subsp. *natalensis* (Hyacinthaceae). SOUTH AFRICAN JOURNAL OF BOTANY, 135, 404–407.
- Street, R. A., & Prinsloo, G. (2013). Commercially important medicinal plants of South Africa: A review. JOURNAL OF CHEMISTRY. doi:10.1155/2013/205048.
- Tatsumi, T., Shiraishi, J., keira, N., Akashi, K., Mano, A., Yamanaka, S., Matoba, S., Fushiki, S., Fliss, H., Nakagawa, M. (2003). Intracellular ATP is required for mitochondrial apoptotic pathways in isolated hypoxic rat cardiac myocytes. CARDIOVASCULAR RESEARCH, 59(2), 428–440. doi:10.1016/s0008-6363(03)00391-2.
- Tsujimoto, Y. (1997). Apoptosis and necrosis: Intracellular ATP level as a determinant for cell death modes. CELL DEATH AND DIFFERENTIATION, 4(6), 429–434. doi: 10.1038/sj.cdd.4400262.
- Vairetti, M., Ferrigno, A., Bertone, R., Richelmi, P., Bertè, F., & Freitas, I. (2005). Apoptosis vs. necrosis: glutathione-mediated cell death during rewarming of rat hepatocytes. BIOCHIMICA ET BIOPHYSICA ACTA (BBA) - MOLECULAR BASIS OF DISEASE, 1740(3), 367–374. doi: 10.1016/j.bbadis.2004.11.022.
- van Wyk, B. and Gericke, N. (2000) People's Plants. A Guide to Useful Plants of Southern Africa. Briza Publications, Pretoria, 352 pp. ISBN 1-875093-19-2.

- Wang, C., & Youle, R. J. (2009). The role of mitochondria in apoptosis. *ANNUAL REVIEW OF GENETICS*, 43, 95–118. <https://doi.org/10.1146/annurev-genet-102108-134850>.
- Wang, M., Ruan, Y., Chen, Q., Li, S., Wang, Q., & Cai, J. (2011). Curcumin induced HepG2 cell apoptosis-associated mitochondrial membrane potential and intracellular free Ca²⁺ concentration. *EUROPEAN JOURNAL OF PHARMACOLOGY*, 650(1), 41–47. doi: 10.1016/j.ejphar.2010.09.049.
- Yoshihiro, U., Hiroshi, S., Hajime K., Marimo, Y., Koichi, T., and Yoshiaki, S. (2016.) Quantitative structure-cytotoxicity relationship of 3-benzylidenechromanones. *ANTICANCER RESEARCH* 36, 5803-5812.
- Youichirou Nishida, Kensuke Wada, Daiki Toyohisa, Toshiharu Tanaka, Masateru Ono & Shin Yasuda (2013) Homoisoflavones as the antioxidants responsible from bulbs of *Scillascilloides*, *NATURAL PRODUCT RESEARCH*, 27(24), 2360-2362, DOI:10.1080/14786419.2013.830218.

CHAPTER 5

Phytochemical, antibacterial and cytotoxicity studies of

Helichrysum panduratum O.Hoffm.

ABSTRACT

The leaves of the medicinal plant, *Helichrysum panduratum*, are used in traditional medicine to treat febrile convulsions, while the sap is used to treat malaria in children. In this study, we aimed to isolate and identify the bioactive constituents in the plant, which we found to be the homoisoflavanone (3-(4-methoxybenzyl)-5,7-dimethoxychroman-4-one), which is a class previously unreported in the species, two sterols (stigmasterol, and stigmasterol glucoside), three triterpenes (oleanolic acid; ursolic acid; and 3-acetyl ursolic), and a phenol glucoside (α -arbutin). The cytotoxic activity of selected compounds and extracts were assayed *in vitro* against two human cancer cell lines, liver hepatoblastoma (HepG2) and colorectal adenocarcinoma (Caco-2), with the human embryonic kidney cell line (Hek-293) as the non-transformed control. The mitochondrial membrane potential, lactate dehydrogenase (LDH) release, and adenosine triphosphate (ATP) levels were also evaluated using IC₈₀ and IC₅₀ concentrations obtained from the 3-(4,5-dimethylthiazol-2-yl)-2,5-diphenyl-2H-tetrazolium bromide (MTT) assay. The cytotoxicity assay showed a dose-dependent response. Ursolic acid demonstrated moderate cytotoxic effects at 24 h with a half inhibitory concentration (IC₅₀) of 132.2 $\mu\text{g mL}^{-1}$ in Caco-2, 350.9 $\mu\text{g mL}^{-1}$ in HepG2, and 107.8 $\mu\text{g mL}^{-1}$ in Hek-293 compared to the other test samples. The dichloromethane extract from the leaves and ethyl acetate extract from the stems were toxic to Hek-293, with IC₅₀ values of 52.76 $\mu\text{g mL}^{-1}$ and 54.86 $\mu\text{g mL}^{-1}$, respectively. Isolated compounds and crude extracts demonstrated insufficient antibacterial

activity to Gram-positive and Gram-negative bacteria and weak quorum sensing (QS) inhibition. The methanol extract from the leaves was most effective at inhibiting both short-chain (45.3%) and long-chain (35.7%) N-acyl homoserine lactone (AHL)-mediated QS and showed potential at inhibiting Gram-negative AHL-based QS. The results demonstrated moderate antibacterial and anticancer activity for *H. panduratum*, with the methanol extract from the stems showing promising anti-QS ability.

Keywords: phytochemistry; quorum sensing inhibition; cytotoxicity; spectroscopy; arbutin; homoisoflavonoid

5.1 INTRODUCTION

The dearth of therapeutic agents in treating and managing diseases and the emergence of new diseases is a significant threat to the human population. This paucity necessitated the need to search for new drugs with better efficacy and low side effects or make the existing ones more effective. Bacteria possess the ability to act individually and collectively (Windsor, 2020). Quorum sensing (QS) is cell-to-cell communication, and it regulates some coordinated processes such as bioluminescence, virulence factor production, biofilm formation, production of secondary metabolites, and competence for DNA uptake (Muhkerge and Bassler, 2019; Rutherford and Bonnie, 2012).

Autoinducers (AI) are chemical signal molecules produced by bacteria and released into the environment, which can be detected at high cell density. At low cell density, AIs are present in low concentrations that are below the detection threshold. Gram-negative bacteria use acylated homoserine lactones (AHLs) as AIs, and Gram-positive bacteria use processed oligopeptides or auto-inducing peptides (AIPs) to communicate (Miller and Bassler, 2001). QS allows intra-species and inter-species communication between bacteria with the help of AIs.

Transmembrane domains that connect the inside of the cell to the environment detect the AIs at high cell density. This information initiates a phosphorylation cascade within the cell, which activates the response gene that regulates various characteristics such as virulence, biofilm formation, and horizontal gene transfer (Hugo, 2016). QS-controlled virulence has been considered a new target for therapeutic development in the fight against infectious diseases (Jiang et al., 2019). In the quest for developing novel and alternative antibacterial therapeutics, there is a need to explore other mechanisms of bacterial control, such as QS inhibition rather than bacteriostatic or bactericidal control.

Nature has remained one of the primary sources of structurally diverse chemical compounds for humankind, facilitating the discovery and development of novel and potent therapeutics to combat different ailments plaguing the human population. Traditional medicinal plants provide an alternate source of therapeutic modalities, from artemisinin for the treatment of malaria to paclitaxel for cancer management.

The *Helichrysum* genus of about 400 species is widely distributed in South Africa, with over 234 species naturalized in South Africa. It is well known for various secondary metabolites, including flavonoids, triterpenes, diterpenoids, phloroglucinol, pyrone, sterols, and sesquiterpenoids. Likewise, several biological activities have been reported for plants in the genus (Lourens, Viljoen, & Van Heerden, 2008; Aiyegoro & Okoh, 2010; Meyer, Afolayan, Taylor, & Engelbrecht, 1996; Matic et al., 2013). *Helichrysum panduratum* O.Hoffm. var. *panduratum* is a shrub that grows on grasslands. The leaves of the plant have been reported to be used in traditional medicine to treat febrile convulsions in children, and the sap for treating malaria (Lourens, Viljoen, & Van Heerden, 2008). The leaves are also used as herbal tea. According to Hilliard (1983) morphological classification of *Helichrysum* genus, *H. panduratum* is in group 18 with other plants including *H. pantulum*, *H. pandurifolium*, and *H. petiolare*.

Previously, a thio-derivative, helipandurin, was isolated from *H. panduratum* (Bohlman and Abraham, 1979), and the antibacterial activity of its essential oil was evaluated. There is no literature report on the phytochemistry, antibacterial activity, and cytotoxicity of *H. panduratum*. Therefore, in this study, we phytochemically investigate *H. panduratum* and assess the extracts and isolated secondary metabolites for their antibacterial activity and cytotoxicity.

5.2 MATERIALS AND METHODS

5.2.1 General Experimental Procedures

¹H, ¹³C and 2D NMR were recorded using either deuterated chloroform (CDCl₃), methanol (MeOD), and dimethyl sulfoxide (DMSO) at room temperature on a Bruker Avance^{III} 400 MHz spectrometer, standardized against tetramethyl silane (TMS). Infrared spectroscopy (IR) was performed using a Perkin Elmer Spectrum 100 Fourier-transform infrared spectrophotometer with ATR sampling techniques. High-resolution mass spectra were obtained on a Waters Micromass LCT Premier TOF-MS instrument. Separation was done using Merck silica gel 60 (0.040-0.063 mm) packed in column. Fractions were monitored with Merck 20 cm × 20 cm silica gel 60 F₂₅₄ aluminum sheets TLC plates, visualization was done with UV at 254 and 366 nm before spraying with 5% sulfuric acid in methanol (MeOH) solution followed by heating.

5.2.2 Materials

Plant material was collected from the botanic garden University of KwaZulu Natal (UKZN), Pietermaritzburg campus, in May 2019. Authentication was performed by the curator Mr. E Khathi from the School of Life Sciences, UKZN, Westville Campus, Durban, and a voucher specimen (18273 03 9006000) was lodged in the herbarium.

5.2.3 Extraction and Isolation of Compounds

Dried and crushed leaves (350 g) and stems (530 g) of *H. panduratum* were exhaustively extracted with hexane, dichloromethane (DCM), ethyl acetate (EtOAc), and methanol (MeOH) at room temperature using an orbital shaker. The extracts were concentrated using a rotary evaporator under reduced pressure, and excess solvent was recovered. All crude extracts were subjected to column chromatography using Merck silica gel 60. Thin-layer chromatography (TLC) was carried out using Merck 20 cm × 20 cm silica gel 60 F₂₅₄ aluminum sheets to monitor collected fractions. Visualization was done under UV with 254 and 366 nm wavelength lamp and spraying with 5% sulfuric acid in a 95% MeOH solution heated with a hot air jet.

The DCM extract from the leaves (5.05 g) was loaded on silica and eluted with hexane: EtOAc gradient (100:0 - 0:100, v/v) to give 60 fractions of 100 mL each. Fraction 15 was crystallized to give compound **B1** (24 mg), while fractions 21-23 were purified to give compound **B3** (10 mg). The MeOH extract of the leaves (27 g) was subjected to column chromatography; elution was done using hexane: EtOAc, starting with 100% hexane that was stepped by 10% to 100% EtOAc. Fractions of 100 mL each were collected, and fractions with similar TLC profiles (retention factor) were combined. Fractions 14-18 gave compound **B1**, and compound **B4** (15 mg) was obtained from fractions 31-33. The MeOH extract of the leaves was rich in compound **B7** (7 g), which was obtained from fractions 61-90 as crystals.

The MeOH extract (5.36 g) from the stems was purified using hexane: EtOAc, starting with 100% hexane that was stepped by 10% EtOAc to 100% EtOAc to give 70 fractions of 100 mL each. Fractions 24-26 gave a purple color after treatment with acid and heat on TLC; these were combined to give compound **B6**. Compound **B4** was obtained from fractions 35-40. Compound **B2** (6 mg) was obtained from fractions 64-65 after purifying with MeOH while

fractions 69-70 gave compound B7 (5 mg) in low yield. The EtOAc extract of the stem (4.9 g) was purified using column chromatography, with silica gel as stationary phase and hexane: EtOAc as mobile phase. Fraction 14 gave compound **B5** (5 mg), while fractions 21-23 yielded **B6** also.

5.2.4 Antibacterial Susceptibility Test

Plants extracts and isolated compounds at a concentration of 400 µg and 800 µg were tested against different strains of Gram-negative (*Escherichia coli* ATCC 25922, *E. coli* ATCC 35218, *Klebsiella pneumoniae* ATCC 70063, *Pseudomonas aeruginosa* ATCC 27583) and Gram-positive (*Staphylococcus aureus* ATCC 29213, *S. aureus* ATCC 43300, *S. aureus* ATCC700698, *Staphylococcus epidermidis* ATCC12228, *Enterococcus faecalis* ATCC 29212, *E. faecalis* ATCC 51299). Pure compounds and crude extracts of *H. panduratum* were subjected to antibacterial screening using the agar well diffusion method. Test samples were dissolved in 10% DMSO to a final concentration of 20 mg mL⁻¹.

5.2.5 Gram-negative Quorum Sensing Inhibition (QSI)

The QS inhibition activity of the four extracts and three phytochemicals were quantified using the quantitative violacein inhibition assay with *Chromobacterium violaceum* ATCC 12472 (long-chain AHL inhibition) and CV017 (short-chain AHL inhibition) as the bio-indicator organisms (McLean *et al.*, 2004; Wang *et al.*, 2016). *C. violaceum* was cultured in Luria-Bertani broth (3 mL) at 30 °C with the addition of increasing concentrations of test samples (200; 400; 600; 800; 1000 µg/mL). Vanillin was used as the QS inhibition-positive control (Chenia, 2013).

For this assay, growth (OD_{600 nm}) and violacein production (OD_{585 nm}) was determined following overnight incubation using the Glomax Multi+ Detection System (microtiter plate reader) (Promega). An overnight culture of *C. violaceum* ATCC 12472/CV017 (1 mL) was

then centrifuged (13 000 rpm; 10 min) to precipitate insoluble violacein. The culture supernatant was discarded, and the pellet was evenly resuspended in 1 mL of DMSO (Chenia, 2013). The solution was then centrifuged again at 13 000 rpm for 10 min to remove cells, and the percentage violacein inhibition was calculated as follows:

$$\% \text{ Violacein inhibition} = \left(\frac{\text{control OD560 nm} - \text{test OD560 nm}}{\text{control OD560 nm}} \right) \text{ (Chenia, 2013).}$$

The assays were performed in triplicate on two separate occasions. Samples at any given concentration that exhibited a percentage growth inhibition $\geq 40\%$ were considered bactericidal rather than QS inhibitors. Samples that exhibited violacein inhibition (VI) $\geq 50\%$ with $\leq 40\%$ growth inhibition were taken as suitable QS inhibitors.

5.2.6 Autoinducer-2 Inhibition Assay

Extracts and phytochemicals were screened for their ability to inhibit the QS-controlled phenotype of bioluminescence in *Vibrio harveyi* BB120 as described by Teasdale et al. (2011). Marine soft agar (8 mL) was seeded with 150 μL of an overnight culture of *V. harveyi* BB120 and poured over a pre-warmed LB agar plate. Blank discs (6 mm; Oxoid) were loaded with 400 and 800 μg (20 and 40 μL of 20 mg/mL stock, respectively) of the extracts and phytochemicals. Cinnamaldehyde, a known AI-2 inhibitor, was used as the positive inhibition control. Plates were incubated at 30 °C for 16 h. Using the Syngene GBOX F3 in chemiluminescence mode, the luminescence from each agar plate was captured. The appearance of zones lacking luminescence but not growth inhibition was indicative of autoinducer-2 inhibition (AI-2) inhibition

5.2.7 Cytotoxicity Assay

In-vitro growth inhibition of human cancer cell lines is usually done on natural products or isolated pure compounds to test for their cytotoxic activities. Cytotoxicity assay was conducted

on pure compounds and extracts using the 3-(4,5-dimethylthiazol-2-yl)-2,5-diphenyl-2H-tetrazolium bromide (MTT), lactate dehydrogenase (LDH), and adenosine triphosphate (ATP) assays.

Cell culture

Cryopreserved Caco-2 and HepG2 tumor cells and Hek-293 normal kidney cells were recovered by thawing and centrifugation. Cells were cultured in the laboratory in a 25 mL tissue culture flask in CCM (complete culture medium) consisting of (DMEM) Dulbecco's modified eagle's medium (Lonza Biowhittaker, Walkersville, USA), 1% L-glutamine, 1% penicillin-streptomycin-fungizone and 10% fetal calf serum (FCS) at 37⁰C and 5% CO₂ until they were at 100% confluence. Cells were washed thrice with phosphate buffered saline (PBS) and detached from the flask using trypsin.

MTT (3-(4,5-dimethylthiazol-2-yl)-2-5-diphenyltetrazolium bromide) assay

MTT is a colorimetric assay that assesses cell metabolic activity, which can be MTT (yellow) to formazan (purple) (Riss et al, 2016). This color change can be explored to measure cell viability. MTT assay measures the metabolic activity of cells and their ability to reduce MTT salt to formazan. Cells in 100 μ L DMEM were plated in a 96-well microtiter plate at a density of 2×10^4 cells per well and then incubated overnight at 37⁰C and 5% CO₂ for the cells to attach to the plate. The medium was removed, and test compounds (100 μ L) were added to each well in triplicate. Test compounds were prepared by first dissolving in DMSO, before making it up to 10 mg/mL using CCM. The final concentration of DMSO was less than 0.5%. Different working concentration between 50 μ g/mL to 5 mg/mL was prepared from the stock before treatment. Untreated cells in CCM served as control. After 24 h incubation, the medium was removed, and 20 μ L of MTT at 5 mg/mL in PBS and 100 μ L of CCM was added to each well and incubated for 4 h. The formazan salt from the reduction of MTT was solubilized with 100

μL DMSO and reading was done on a microplate reader, a Bio-Tek μQuant plate spectrophotometer (Winooski, Vermont, United States) at 570 nm with a reference wavelength of 690nm. The tests were conducted in triplicate, and IC₅₀ values were generated using GraphPad Prism V5.0 software (GraphPad Software Inc., La Jolla, USA).

Mitochondrial membrane potential (MMP) assay ($\Delta\psi_m$)

Mitochondria regulate metabolism and cell death and are involved in the apoptotic process of cells. During apoptosis, the collapse of the mitochondrial membrane potential (MMP, $\Delta\psi_m$) correlates with the opening of the mitochondrial permeability transition pore. Mitochondrial function can be accessed for cell health by monitoring changes in the MPP (Sakamuru et al, 2016). The effect of chemicals on the mitochondrial function can be assessed by measuring the MPP using a cationic dye. JC-10, a cationic, lipophilic dye, which is preferable to JC-1 due to its solubility, was used in this study. Cells were seeded to a 96-well microplate and incubated overnight in a humid environment (37°C and 5% CO₂). Treatment was done using a concentration of the IC₈₀ and IC₅₀ doses obtained from the MTT assay for 24 h. After that, the treatment was removed and stored for other assays. Approximately 50 μL of PBS and 25 μL of JC-10 dye were added to each well. The plate was protected from light and incubated at 37°C for 1 h. After incubation, JC-10 dye and PBS solution were removed, and 80 μL of PBS was added before reading was done.

JC-10 dye enters the mitochondria due to its lipophilicity, where it accumulates to form J-aggregates, a reversible complex. JC-10 forms reversible red-fluorescent aggregates in healthy cells, while in apoptotic cells with MMP collapse, failure to retain JC-10 in the mitochondria leads to the formation of green-fluorescent aggregates (Sivandzade et al, 2019). The green aggregates have absorption/emission of 510/527 nm, and the red aggregates have absorption/emission of 585/590 nm. Results were analyzed using the red-green ratio.

Adenosine triphosphate (ATP) assay

ATP is produced in the mitochondria. Immediately after taking reading for the MMP assay, CellTitre-Glo® for ATP assay was used to evaluate cell viability in all three cell lines. According to the manufacturer's instructions, the reagent was prepared; 25 µL CellTitre-Glo® and 50 µL of PBS were added to each well. The plates were protected from light and incubated at room temperature for 30 mins. The luminescent signal was measured on a Modulus™ microplate luminometer (Turner Bio-Systems, California, USA).

Lactate dehydrogenase (LDH) assay

LDH is a stable enzyme found in the cell cytoplasm released when cell plasma is damaged (Kumar et al, 2018), which is used to measure cytotoxicity. The supernatant of the treatment done during the MPP assay was stored for use in the LDH assay. The treatment was thawed at room temperature, and 50 µL was pipetted into a non-sterile 96-well plate reader in triplicate. The LDH cytotoxicity detection kit was prepared according to the manufacturer's instruction, and 25 µL was added to each well and incubated at room temperature before 12.5 µL stop reagent was added. Reading was done at 490 nm using a Biotek µQuant spectrophotometer (Winooski, Vermont, United States).

5.2.8 Statistical Analysis

Data were expressed as mean and standard deviation of the mean from three readings. Linear regression was used to calculate the IC₅₀ and IC₈₀ on GraphPad prism. Statistical differences between the control and treated cells were determined using the Student t-test and $P < 0.05$ were considered significant.

5.3 RESULTS

5.3.1 Identification of Isolated Compounds from *H. panduratum*

Seven compounds were isolated from the leaves and stem of *H. panduratum* (Figure 5.1). The compounds, which are a sterol, sterol glucoside, triterpenes, homoisoflavanone, and phenol glucoside, were identified using their ^1H , ^{13}C , and 2D-NMR spectra and comparison with literature values. The DCM and MeOH extract of the leaves yielded stigmasterol **B1** (Habib et al., 2007), ursolic acid **B3** (Labib et al., 2016), and oleanolic acid **B4** (Seebacher et al., 2003). Stigmasterol glucoside **B2** was obtained from the MeOH extract of the stem (Khatun, 2012). The EtOAc and MeOH extract of the stem both yielded compound **B6**, a homoisoflavanoids, 3-(4-methoxybenzyl)-5,7-dimethoxychroman-one, which is the first report of this class of secondary metabolite from *Helichrysum* species (Silayo et al., 1999). Compound **B5**, 3-acetyl ursolic acid, was obtained from the EtOAc extract of the stem (Endo et al., 2019). Both the MeOH extract of the stem and leaves yielded compound **B7**, α -arbutin, but the leaves had a higher yield than the stem.

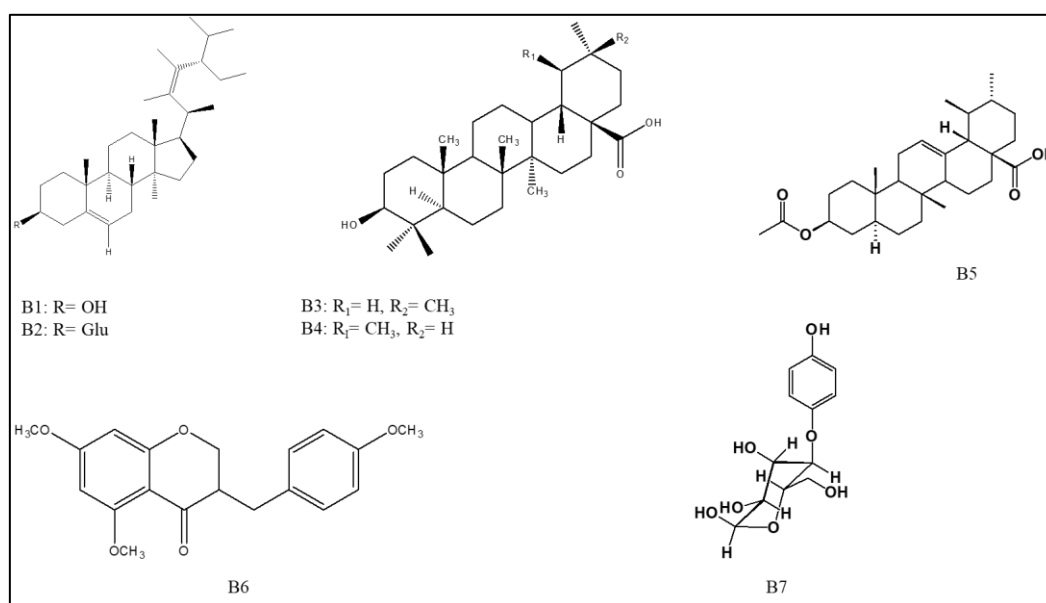


Figure 5.1: Chemical structures of compound **B1**-**B7** isolated from the leaves and stems of *Helichrysum panduratum*.

Compound **B6**, 3-(4-methoxybenzyl)-5,7-dimethoxychroman-4-one (Silayo et al., 1999), was obtained as sticky yellow oil. Its molecular formula $C_{19}H_{20}O_5$ was established by NMR spectroscopy and HRMS, which massed as 351.1213 (calc. for $C_{19}H_{20}O_5Na$ 351.1208). The 1H -NMR spectrum showed characteristic peaks of a 3-benzylchroman-4-one homoisoflavanone with a pair of double doublets at δ_H 4.24-4.06 and δ_H 3.16-2.60 for protons at H-2 and H-9, respectively. The signal for aromatic protons resonated at δ_H 6.84 ($J=8.75$ Hz H2', 6') and δ_H 7.13 ($J=8.75$, H3', 5') for the B-ring; their integration and coupling constant showed that the ring is 1,4 di-substituted. The peak at δ_H 6.04 ($J=2.34$ Hz, H6, 8), a doublet, integrated to two protons on the A-ring, indicating that the ring is di-substituted at positions C-5 and C-7. Three methoxy signals were observed between δ_H 3.7-3.9, each integrating to 3 protons each. The ^{13}C NMR spectrum showed 17 peaks for 19 carbons; the carbonyl peak resonating at δ_c 191.46 indicated that C-5 has a methoxy substituent as downfield resonance between δ_c 198-200, would indicate a hydroxy substituent at C-5. Resonances at δ_c 114.05 are due to C2' and 6'; δ_c 93.25 (C-6), 93.0 (C-8), 68.95 (C-2), 48.56 (C-3), 32.02 (C-9), 105.47 (C-4a), 165.84 (C-5), 164.98 (C-7), 162.62 (C-8a), and 158.30 (C-4'). Resonances due to three methoxy carbons were found at δ_c 56.06, 55.53 and 55.26. HMBC correlations confirmed the placement of the methoxy groups at positions 5, 7, and 4'.

Compound **B7** (β -hydroquinone glucoside), known as α -arbutin (Nycz et al., 2010), was obtained as a crystal. The 1H NMR spectrum for α -arbutin showed a para-disubstituted aromatic ring with the appearance of a doublet at δ_H 6.72 ($J= 8.92$ Hz), which integrated to two protons assigned to H-2 and H-6 and another doublet at δ_H 6.87 ($J= 8.92$ Hz), which integrated to two protons assigned to H-3 and H-5. The resonances for H-3 and H-5 appeared downfield, indicating that they are deshielded, so they were placed in an electron-deficient environment where the hydroxyl is attached to the aromatic ring. Resonances for H-2 and H-6 were upfield so they were placed close to the sugar moiety. The sugar moiety presented a doublet at δ_H 4.76

($J=7.12$ Hz), assigned as 1' (anomeric proton). The signals due to the four methine carbons and one methylene carbon on the sugar moiety were assigned the δ_C 76.6 (CH, C-3'), 76.5 (CH, C-5'), 73.4 (CH, C-2'), 70.0 (CH, C-4') and 61.2 (CH₂, C-6'). The ^{13}C NMR spectrum showed 2 quaternary carbons (δ_C 151.0 (C-1) and δ_C 152.4 (C-4)), and two aromatic carbons (δ 118.01 (C3, 5), δ 115.3 (C2, 6)) that correlated with the aromatic protons at δ_H 6.98, and 6.72, respectively. The methine protons resonated between δ_H 3.33-3.45, while the methylene protons resonated at δ_H 3.90 (1H, dd, $J=12.1, 1.8$ Hz), 3.72 (1H, dd, $J=12.1, 4.5$ Hz). The spectral data corresponds with that in literature (Nycz et al., 2010).

5.3.2 Antibacterial Activity

The result of the susceptibility test for the isolated compounds and crude extract are presented in Table 5.1 and 5.2. Tested samples of compounds and crude extracts did not demonstrate any notable antimicrobial activity at 400 and 800 $\mu\text{g/mL}$ against antimicrobial-sensitive and antimicrobial-resistant bacterial isolates.

Homoisoflavonoids showed an intermediated activity against susceptible Gram-positive *S. aureus* ATCC 29213, while both susceptible *E. faecalis* ATCC 29212 and resistant *E. faecalis* ATCC 51299 were resistant to it. Methicillin-resistant *S. aureus* ATCC 43300 demonstrated intermediate susceptibility to EtOAc extract of the stems but resistance to both the MeOH extract of the leaves and stems. Resistant *E. faecalis* ATCC 51299 demonstrated an intermediate susceptibility to α -arbutin and the DCM extract of the leaves but resistance to other extracts, MeOH and EtOAc. All tested samples showed no activity at 400 $\mu\text{g/mL}$ against all Gram-negative strains. The MeOH extract of both stems and leaves showed intermediate susceptibility towards *E. coli* ATCC 25922 at 800 $\mu\text{g/mL}$.

Table 5.1: Antibacterial susceptibility assay against selected Gram-positive bacteria.

Test samples	<i>S. aureus</i> ^b		<i>S. aureus</i> ^c		<i>S. aureus</i> ^d		<i>S. epidermidis</i>		<i>E. faecalis</i> ^e		<i>E. faecalis</i> ^f	
	Concentration (µg/mL)											
20 mg/mL	400	800	400	800	400	800	400	800	400	800	400	800
Homoisoflavanone ^a	0	12	0	0	0	0	0	0	0	10	0	10
α-Arbutin	0	0	0	0	0	0	0	0	0	0	8	12
DCM extract leaves	8	10	0	0	8	11	0	0	0	10	8	12
EtOAc acetate extract stems	7	10	0	10	8	10	0	0	0	10	7	10
MeOH extract leaves	0	7	0	8	0	7	0	0	0	0	0	10
MeOH extract stems	0	7	0	8	0	7	0	0	0	0	0	10
Controls												
Amoxicillin-clavulanate AMC 30	13.5		13		0		14		20		15 with RC	
Gentamicin CN10	21.5		10		0		29		14		8	
Norfloxacin NOR10	23		23		0		30		15		19.5 RC	
Tetracycline TE30	20		19		7		0		7		28	
10% DMSO	0											

^a - 3-(4-methoxybenzyl)-5,7-dimethoxychroman-4-one, Resistant ≤ 10 mm, Intermediate 11-15, Susceptible >15,

^b - *S. aureus* ATTC 29213, ^c - *S. aureus* ATCC 43300, ^d - *S. aureus* ATCC 700698, ^e - *E. faecalis* ATCC 29212,

^f - *E. faecalis* ATCC 51299, *S. epidermidis* ATCC12228.

DCM – dichloromethane, EtOAc – ethyl acetate, MeOH – methanol.

Table 5.2: Antibacterial susceptibility assay against selected Gram-negative bacteria.

Test samples	<i>E. coli</i> ^b		<i>E. coli</i> ^c		<i>K. pneumoniae</i> ^d		<i>P. aeruginosa</i>	
	Concentration (µg/mL)							
20 mg/mL	400	800	400	800	400	800	400	800
Homoisoflavanone ^a	0	7	0	0	0	8	0	0
α-Arbutin	0	8	0	0	0	8	0	0
DCM extract leaves	0	7	0	7	0	0	0	7
EtOAc acetate extract stems	0	8	0	7	0	8	0	8
MeOH extract leaves	0	10	0	0	0	9	0	0
MeOH extract stems	0	11	0	0	0	7	0	0
Controls								
Amoxicillin-clavulanate AMC 30	0		0		11		0	
Gentamicin CN10	17		20		12		19	
Norfloxacin NOR10	32		18		20		30	
Tetracycline TE30	8		31		9		0	
10% DMSO	0							

^a - 3-(4-methoxybenzyl)-5,7-dimethoxychroman-4-one, ^b - *E. coli* ATCC 25922, ^c - *E. coli* ATCC 35218,

^d - *K. pneumoniae* ATCC 700603, ^e - *P. aeruginosa* ATCC 27583.

DCM – dichloromethane, EtOAc – ethyl acetate, MeOH – methanol.

5.3.3 Quantitative QSI Assay

Neither the extracts nor the isolated phytochemicals were potent QS inhibitors (Figure 5.2 and 5.3). Varying levels of inhibition were observed for short-chain (CV017) and long-chain (ATCC 12472) AHL inhibition. The MeOH leaf extract was the most effective at inhibiting both short and long-chain AHL-mediated QS, with .45.26% and 35.68%, respectively.

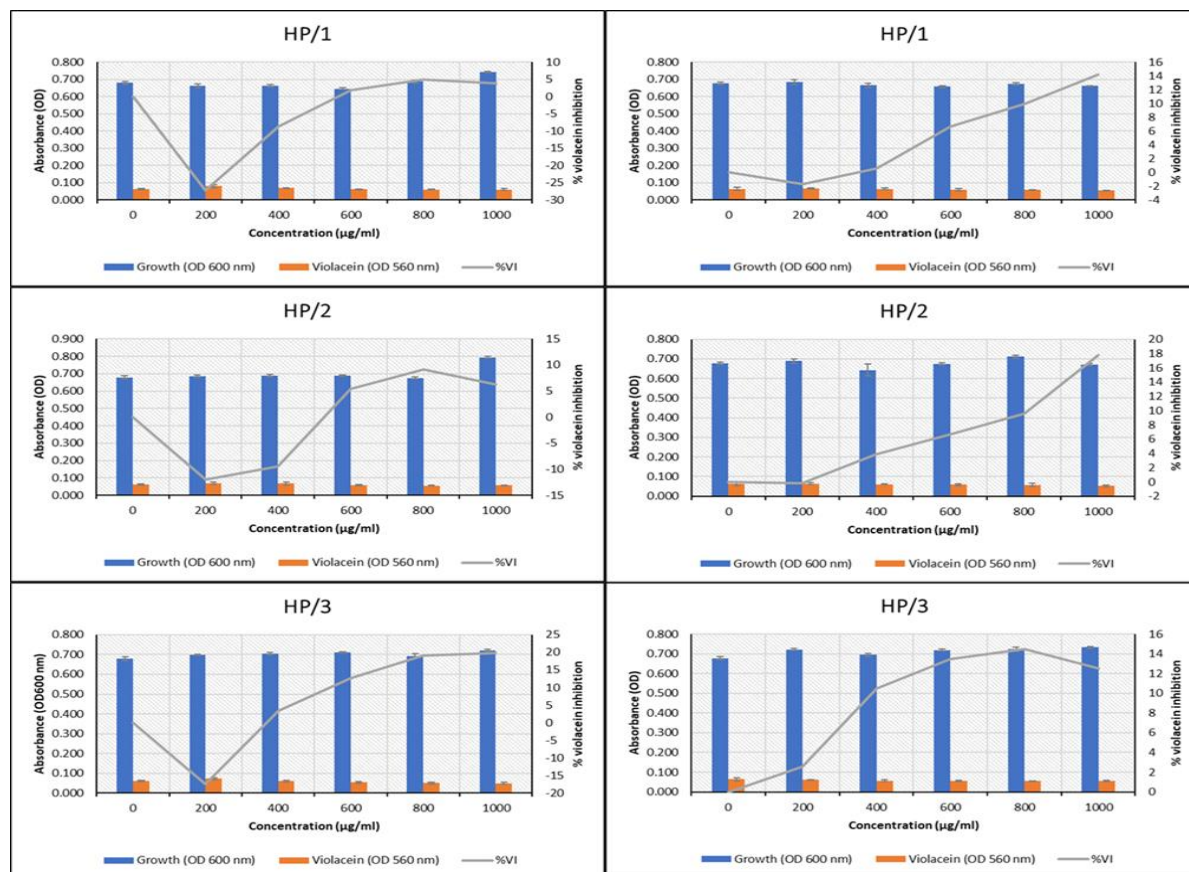


Figure 5.2. Quantitative analysis of the concentration-dependent, violacein production inhibitory effects of isolated compounds from *H. panduratum* at 200–1000 µg mL⁻¹ against *Chromobacterium violaceum* ATCC 12472 (long-chain AHL inhibition) and CV017 (short-chain AHL inhibition).

HP/1 - ursolic acid, HP/2 - 3-(4-methoxybenzyl)-5,7-dimethoxychroman-4-one, HP/3 - arbutin. Bacterial growth at OD 600 nm; violacein production at OD 560 nm and blue line graph represents percentage violacein inhibition. Data represents the mean of two independent experiments done in triplicate.

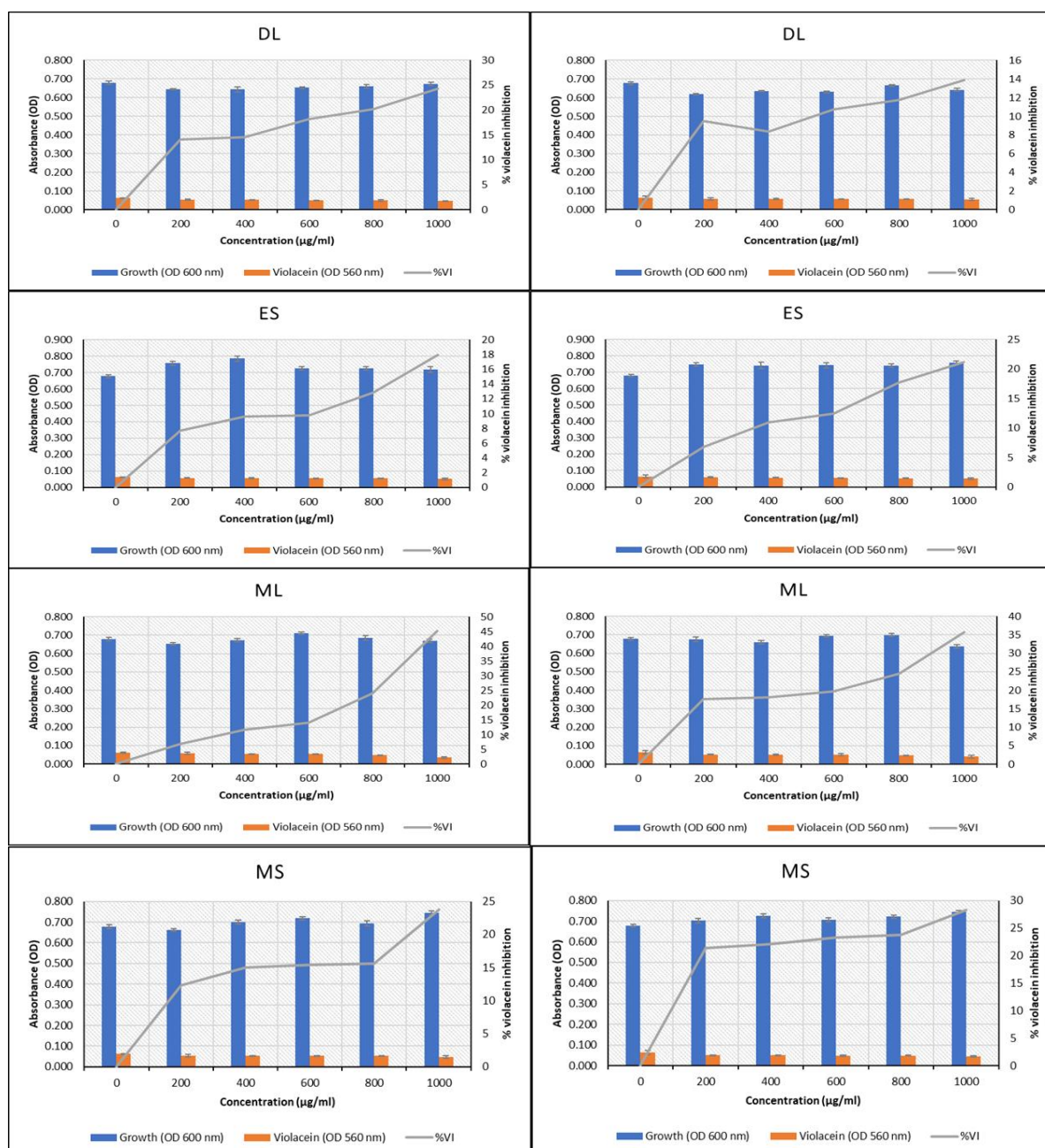


Figure 5.3. Quantitative analysis of the concentration-dependent, violacein production inhibitory effects of four *Helichrysium panduratum* crude extracts and three isolated compounds at 200–1000 $\mu\text{g mL}^{-1}$ against *Chromobacterium violaceum* ATCC 12472 (long-chain AHL inhibition) and CV017 (short-chain AHL inhibition).

DL - DCM leaves extract, ES - EtOAc stem extract, ML - MeOH leaves extract, MS - MeOH stem extract. Bacterial growth at OD 600 nm; violacein production at OD 560 nm and blue line graph represents percentage violacein inhibition. Data represents the mean of two independent experiments done in triplicate.

For short-chain inhibition, the order of inhibition of extracts was MeOH extract leaves > DCM extract leaves > MeOH extract stems > EtOAc acetate extract stems, while for long-

chain inhibition it was MeOH extract leaves > MeOH extract stems > EtOAc acetate extract stems > DCM extract leaves. With respect to the isolated phytochemicals, short-chain AHL inhibition was observed as follows α -arbutin > 3-(4-methoxybenzyl)-5,7-dimethoxychroman-4-one > ursolic acid, while for long chain inhibition: 3-(4-methoxybenzyl)-5,7-dimethoxychroman-4-one > ursolic acid > α -arbutin.

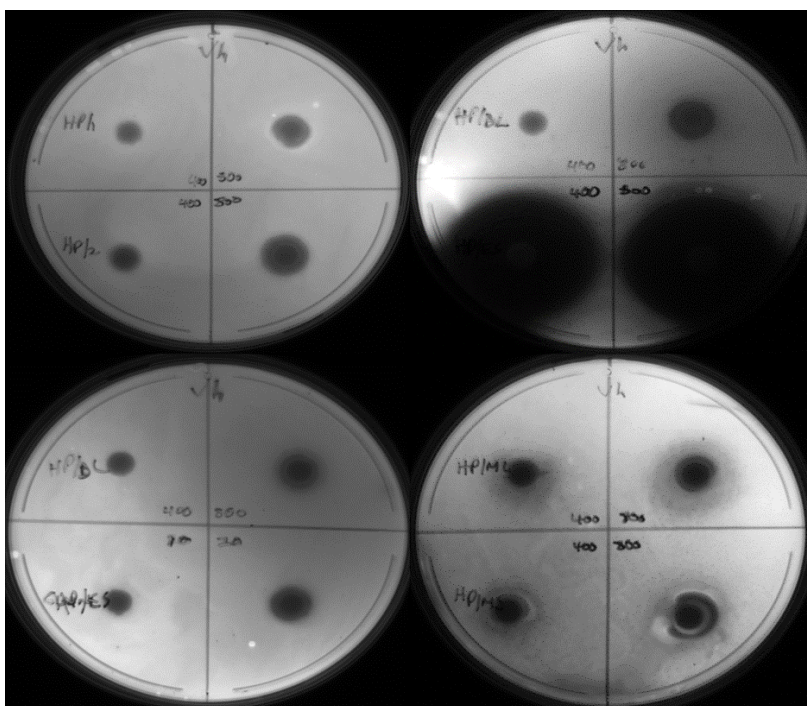


Figure 5.4. Inhibitory effect of extract and isolates from *H. panduratum* against QS-controlled phenotype of bioluminescence, with cinnamaldehyde as a positive control.

HP/1 = ursolic acid, HP/2 = 3, HP/3 = α -arbutin, HP/DL = DCM (dichloromethane) leaves extract, HP/ES = EtOAc (ethyl acetate) stem extract, HP/ML = MeOH (methanol) leaves extract, HP/SM = MeOH (methanol) stem extract.

Of the four extracts, the MeOH extract leaves appears to have compounds that might be able to inhibit autoinducer-2, as evidenced by the halo of decreased bioluminescence (both 400 and 800 μ g) (Figure 5.4). The DCM extract leaves and EtOAc extract stems also exhibited minor AI-2 inhibition at 800 μ g (Table 5.3). However, the MeOH extract stems were bactericidal. Of the three phytochemicals, the homoisoflavonone (3-(4-methoxybenzyl)-5,7-

dimethoxychroman-4-one) and α -arbutin exhibited minor inhibition at 800 μg , with some bactericidal activity. The MeOH extract leaves might be a promising source of compounds with the ability to inhibit not only Gram-negative AHL-based QS but may also be inhibitory to global crosstalk AI-2-based QS.

Table 5.3: Autoinducer inhibitory profile of compounds and extracts from *H. panduratum* against Gram-negative AHL-based quorum sensing inhibition (QSI).

Test sample	<i>Vibrio harveyi</i> B120					
	400 μg			800 μg		
	Total zone	Clear zone	QSI zone	Total zone	Clear zone	QSI zone
Ursolic acid	0	0	0	9	0	9
Homoisoflavanone ^a	0	0	0	11	7	4
α -Arbutin	0	0	0	10	8	2
DCM extract leaves	0	0	0	8	0	8
EtOAc acetate extract stems	0	0	0	8	0	8
MeOH extract leaves	8	0	8	12	0	12
MeOH extract stems	0	0	0	10	10	0
Cinnamaldehyde	26	25	1	38	28	10

^a - 3-(4-methoxybenzyl)-5,7-dimethoxychroman-4-one

DCM – dichloromethane, EtOAc – ethyl acetate, MeOH – methanol.

5.3.4 Cytotoxicity Assay

Caco-2, HepG2, and Hek-293 cells were treated with different concentrations of the tested samples, including some selected compounds and crude extracts for 24 h. The MTT assay was used to determine cell viability and obtain IC_{50} values. Also, a dose-dependent curve was generated from the plate reader data. Their cell viability results were presented relative to the untreated cells (control).

MTT cell viability assay

Exposure to ursolic acid after 24 h showed no significant decline in viability at a concentration of 0 - 100 $\mu\text{g mL}^{-1}$ for HepG2 and 0 - 25.11 $\mu\text{g mL}^{-1}$ for Caco-2 cell lines. At a concentration of 100 $\mu\text{g mL}^{-1}$, cell viability was reduced to 43% and 32% for Caco-2 and Hek-293, respectively, and 49% for HepG2 at 251.19 $\mu\text{g mL}^{-1}$. Results from Figure 5.5 showed that cell

viability was reduced in proportion to administered dose in all cell lines, with a pronounced U-shaped curve for Hek-293, while Caco-2 and HepG2 showed slight U-shaped toxicity. α -Arbutin (Figure 5.5) showed insufficient activity across all cell lines, even at higher concentrations. At a concentration of $2511.89 \mu\text{g mL}^{-1}$, cell viability was reduced to 78%, 94%, and 87% for Caco-2, HepG2, and Hek-293, respectively. A stimulatory effect was observed in Caco-2 and HepG2 cell lines after treatment with the DCM extract leaves at a concentration of $50.12 \mu\text{g mL}^{-1}$. Cell viability increased from 100% in the control to 124% and 114% for Caco-2 and HepG2 cell lines. Between $100 - 1000 \mu\text{g mL}^{-1}$, there was a significant decrease in cell viability to 29% for Caco-2 and 49% for Hek-293. Cell viability was reduced to 53% in Hek-293 at a treatment concentration of $50.12 \mu\text{g mL}^{-1}$ for the DCM extract leaves. The lowest cell viability was observed at $2511.89 \mu\text{g mL}^{-1}$ for the three cell lines, 6% for Caco-2 and HepG2, and 5% for Hek-293. The dose-response curve showed that the DCM extract leaves decreased viability in a dose-dependent manner.

Treatment with the MeOH extract stems increased cell viability from 100% in the control to 118% in HepG2 at a concentration of $50.12 \mu\text{g mL}^{-1}$ but was reduced to 95% in Caco-2 and 84% in Hek-293 at the same concentration. At $1000 \mu\text{g mL}^{-1}$, cell viability was reduced by 96%, 58%, and 37% in Caco-2, HepG2, and Hek-293, respectively. The lowest viability was observed at $2511.89 \mu\text{g mL}^{-1}$, 40% for HepG2, 37% for Caco-2, and 17% for Hek-293. Between concentrations of $0 - 31.62 \mu\text{g mL}^{-1}$, there was no significant change in cell viability after treatment with the MeOH extract leaves. At $50.12 \mu\text{g mL}^{-1}$, a stimulatory effect was observed, cell viability was increased from 100% in the control to 105% in Caco-2 and 107% in hepG2 cell lines, while no effect was observed in Hek-293, the cell viability was still at 100% at the same concentration. A sharp decline in cell viability was observed from $1000 - 2511.89 \mu\text{g mL}^{-1}$; cell viability was reduced to 27% in Caco-2, 64% in HepG2, and 24% in Hek-293.

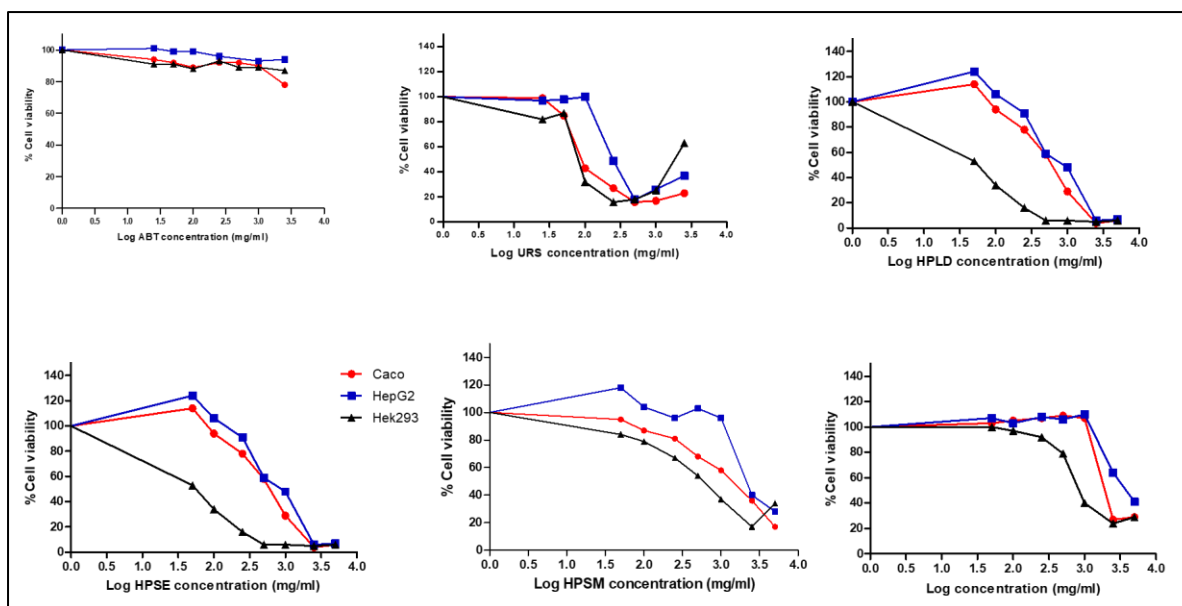


Figure 5.5 Dose-dependent decrease in cell viability of Caco-2, HepG2, and Hek-293 cell lines after exposure to varying concentrations of tested samples using MTT assay.

ABT – α -arbutin, URS - ursolic acid, HPLD - DCM leaves extract, HPSE - EtOAc stem extract, HPSM - MeOH stem extract, HPLM - MeOH leaves extract.

ATP assay

The number of viable cells after exposure to IC_{80} and IC_{50} (Table 5.4) doses of each test was evaluated using the CellTitre-Glo[®]. ATP fold change value for the control in all the cell lines was 100%. The result for all tested samples is presented in Figure 5.6.

Table 5.4: IC_{50} values in $\mu g mL^{-1}$ of tested compounds and extracts of *H. panduratum*.

Test samples	Caco-2	HepG2	Hek-293
α -Arbutin	8016	28863	11408
Ursolic acid	132.2	350.9	107.8
DCM extract leaves	604	868.1	52.76
EtOAc acetate extract stems	3196	5945	1181
MeOH extract leaves	1056	1699	54.86
MeOH extract stems	1207	3155	583.8

DCM – dichloromethane, EtOAc – ethyl acetate, MeOH – methanol.

After treatment with IC₈₀ concentrations of ursolic acid, ATP was reduced from 100% in the control to 78% in Caco-2 and 70% in HepG2 but increased to 126% in Hek-293. At the IC₅₀ dose of ursolic acid, ATP was reduced to 54% in Caco-2, 36% in HepG2, and increased to 137% in Hek-293. Exposure to IC₈₀ concentrations of α -arbutin reduced ATP to 99%, 50%, and 98% in Caco-2, HepG2, and Hek-293, respectively. IC₅₀ concentrations reduced ATP in Caco-2 and HepG2 to 75% and 32%, respectively, with an increase observed in Hek-293 to 132%.

A decrease in ATP from 100% in the control to 89%, 73%, and 80% in Caco-2, HepG2, and Hek-293, respectively was observed after treatment with IC₈₀ concentrations of the DCM extract leaves. While at IC₅₀ concentrations, ATP reduction was observed in Caco-2 to 65% and HepG2 to 58% but increased to 125% in Hek-293. Treatment with an IC₈₀ dose of the EtOAc extract stems, reduced ATP to 99% and 70% in Caco-2 and HepG2, respectively but was increased to 126% in Hek-293. At the IC₅₀ dose in Caco-2 and HepG2, ATP was reduced to 53% and 60%, while a significant increase in ATP to 212% was observed in Hek-293. A slight decrease in ATP from 100% in the control to 94% and 93% in Caco-2 and HepG2 and an increase to 156% in Hek-293 was observed after treatment with the IC₈₀ dose of the MeOH extract stems. At IC₅₀ concentrations, ATP decreased to 58% in Caco-2 and 75% in HepG2 and a significant increase to 227% in Hek-293. The IC₈₀ dose of MeOH extract leaves extract decreased ATP to 85% in Caco-2 and 89% in HepG2, but an increase to 166% was observed in Hek-293. The IC₅₀ dose reduced ATP to 54% and 36% in Caco-2 and HepG2, respectively, while an increase to 159% was seen in Hek-293.

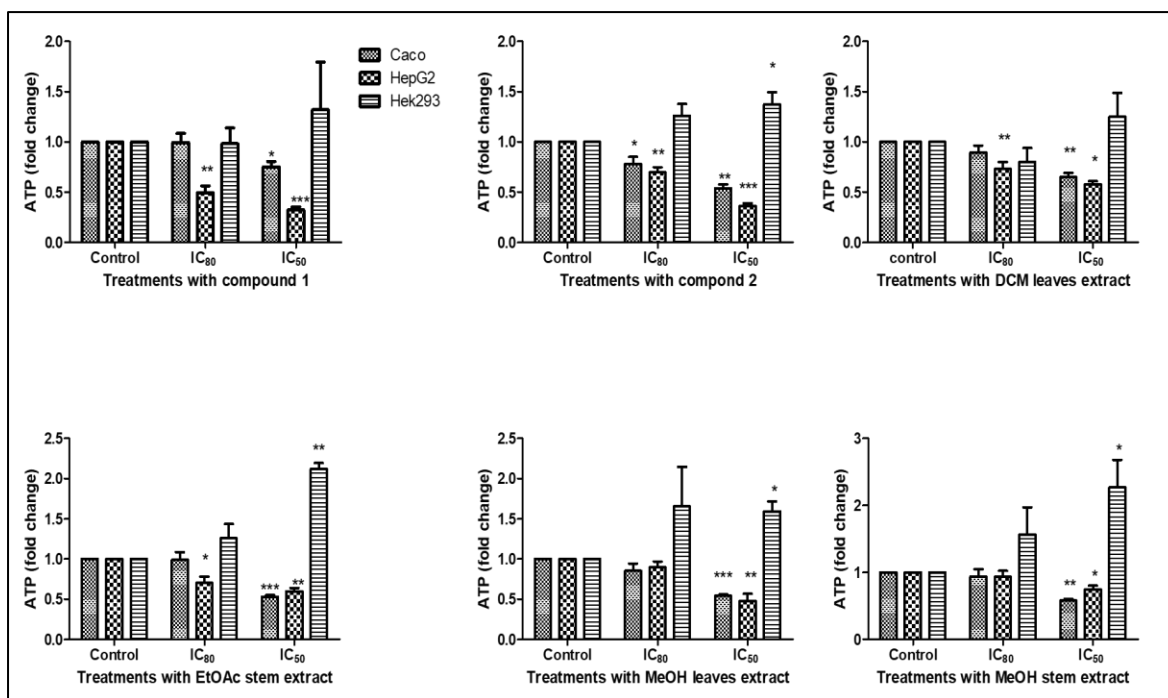


Figure 5.6: Results of the ATP assay.

Compound 1: α -Arbutin, compound 2: ursolic acid, DCM (dichloromethane) leaves extract, EtOAc (ethyl acetate) stem extract, MeOH (methanol) leaves extract, MeOH (methanol) stem extract.

Mitochondrial membrane potential (MMP) evaluation

The mitochondrial membrane potential was used to evaluate mitochondrial toxicity by the test samples using JC-10 dye. The ratio of the red and green aggregate in the control was 1 using fold change. Treatment was done at IC₈₀ and IC₅₀ of tested samples. Results are presented in Table 5.5 and Figure 5.7.

Table 5.5: Mitochondria membrane potential (MPP) result for tested samples.

Treatment	IC ₈₀			IC ₅₀		
	Caco-2	HepG2	Hek-293	Caco-2	HepG2	Hek-293
Ursolic acid	80%	177%	222%	154%	179%	246%
α -Arbutin	96%	127%	99%	98%	153%	108%
DCM extract leaves	94%	121%	104%	118%	159%	102%
EtOAc acetate extract stems	57%	193%	99%	95%	271%	113%
MeOH extract leaves	102%	169%	108%	56%	222%	128%
MeOH extract stems	78%	194%	96%	137%	210%	108%

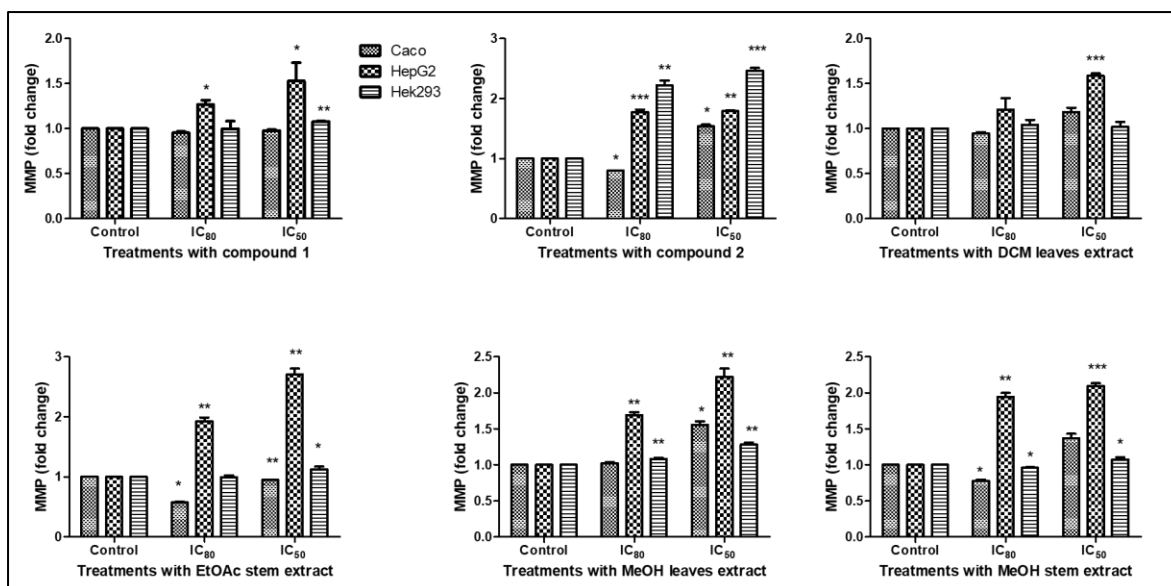


Figure 5.7: Results for the mitochondrial membrane potential (MPP).

Compound 1: α -Arbutin, compound 2: ursolic acid, DCM - dichloromethane, EtOAc – ethyl acetate, MeOH - methanol.

Quantification of LDH released

LDH released into the medium was monitored with the LDH detection kit. IC₈₀ and IC₅₀ concentrations of test samples were used. Results are presented in Figure 5.8. After exposure to IC₈₀ concentrations of ursolic, LDH increased in all cell lines compared to the control. An increase to 169%, 137%, and 144% was observed in Caco-2, HepG2, and Hek-293, respectively. IC₅₀ concentrations also increased LDH for the three cell lines; 190%, 171%, and 199% for Caco-2, HepG2, and Hek-293, respectively. Treatment with the IC₈₀ dose of α -arbutin increased LDH to 116% in Caco-2 and decreased HepG2 to 50% and Hek-293 to 87%. IC₅₀ concentrations increased LDH to 121% in Caco-2 and decreased it to 51% and 67% in HepG2 and Hek-293, respectively.

Exposure to IC₈₀ concentrations of the DCM extract leaves reduced LDH to 89% and 91% in Caco-2 and HepG2 and increased it to 126% in Hek-293. At IC₅₀ concentrations, an increase in LDH was observed for Caco-2, HepG2, and Hek-293 to 127%, 137%, and 149%,

respectively. LDH was significantly increased in Hek-293 to 257% after treatment with IC₈₀ concentrations of the EtOAc extract stems. At the same treatment, a slight increase to 126% was observed for Caco-2 cells and a slight decrease to 98% for HepG2. At IC₅₀ treatment, a significant increase to 290% was also observed for Hek-293, 135% for Caco-2, and a decrease to 78% for HepG2. At IC₈₀ and IC₅₀ concentrations of the MeOH extract leaves, treatment significantly increased LDH to 254% and 253% in Hek-293, a slight increase for Caco-2 cell lines to 102% and 139%, and a decrease to 96% at IC₈₀ treatment was observed for HepG2, but an increase to 159% at IC₅₀ treatment. Treatment with IC₈₀ concentrations of the MeOH extract stems, increased LDH to 118% and 115% in Caco-2 and HepG2 and decreased it to 66% in Hek-293. IC₅₀ concentrations increased LDH in all cell lines; 139% for Caco-2, 159% for HepG2 but a significant increase to 253% was observed for HepG2.

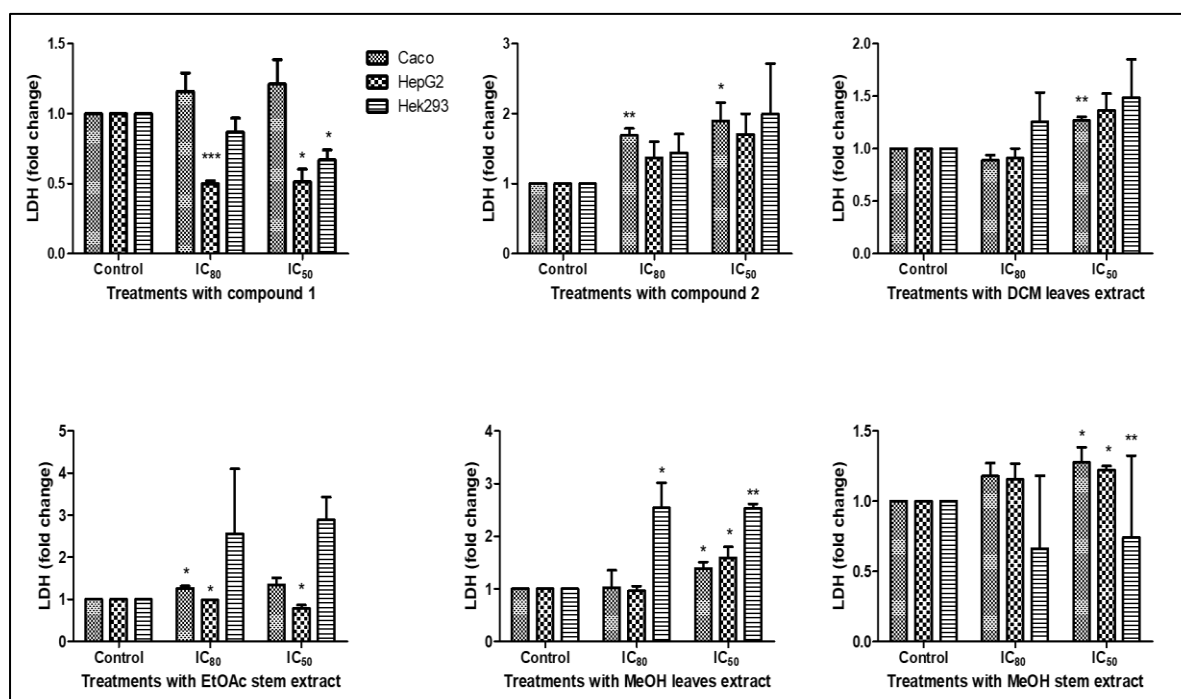


Figure 5.8: Results for LDH (lactate dehydrogenase) release.

Compound 1: α -Arbutin, compound 2: ursolic acid, DCM - dichloromethane, EtOAc – ethyl acetate, MeOH - methanol.

5.4 DISCUSSION

The phytochemical investigation of *H. panduratum* led to the isolation of seven compounds: the ubiquitous triterpenes, a homoisoflavonoid, and α -arbutin, a natural form of hydroquinone. These were identified based on their spectra and comparison to literature data. The DCM and MeOH extract of the leaves both yielded stigmasterol. The MeOH extract of the stem yielded stigmasterol glucoside and 3-(4-methoxybenzyl)-5,7-dimethoxychroman-4-one. Other compounds from the DCM extract of the leaves were oleanolic acid and ursolic acid. The EtOAc extract of the stems yielded acetyl ursolic acid and 3-(4-methoxybenzyl)-5,7-dimethoxychroman-4-one (6). The MeOH extract of the leaves yielded α -arbutin in large quantities, more than the MeOH extract of the stem. This is the first report of a homoisoflavonoid in *Helichrysum* species. Chalcones and phloroglucinol are precursors to homoisoflavonoids and have been reported in the *Helichrysum* genus (Rawal and Cava, 1983; Jakupovic, 1986; Mathekga, 2001). The homoisoflavanone, 3-(4-methoxybenzyl)-5,7-dimethoxychroman-4-one, has been isolated from other plants such as *Eucomis*, *Scilla*, and *Ledebouria* (Du Toit et al., 2010; Castelli and Lopez, 2017;). α -Arbutin has been isolated from *H. patulum* (Swartz, 2006) in the same morphological group with *H. panduratum*.

Antibiotic resistance occurs when pathogens acquire genes that make them evade antimicrobial action. These genes are transferred to other members of the same species leading to a public health concern. Plants and their constituents have been explored as a source of new and effective antimicrobials. Inhibiting the activity of disease-causing bacteria could be achieved by QS inhibition. Our study showed that *H. panduratum* and its isolates have minimal antibacterial activity against Gram-positive and Gram-negative bacteria. Ursolic acid is a pentacyclic triterpene found in plants and has been reported to exert some biological activities such as antibacterial, anticancer, antioxidant (Do Nascimento et al., 2014), anti-inflammatory, hepatoprotective (Sultana et al., 2010), and antimycobacterial (Wolska et al, 2010). Chandramu

et al (2003) reported that ursolic acid has no activity against *E. coli* but showed minimal effect against *B. subtilis* with a zone diameter of 30.6 mm at a high concentration of 1000 µg/disc compared to the standard kanamycin, with an inhibitory zone of 207.2 mm at a concentration of 0.05 µg mL⁻¹. This finding agrees with our findings. Antibacterial activity of pentacyclic triterpenoids is dependent on a double bond in the γ or β-position to a carboxylic group and a ketone functional group in ring A of an oleanane-skeleton. In ursolic acid, a double bond is present at the γ-position of the carboxylic group, but no keto group in ring A, a hydroxy group is present instead. This could be the reason for the low antibacterial activity of ursolic acid. Derivatives of ursolic acid have proven to have better antibacterial activity than ursolic acid itself.

Ursolic acid demonstrated better cytotoxic activity against Caco-2 and HepG2 cell lines among all tested samples with an IC₅₀ of 132.2 and 350.9 µg mL⁻¹ respectively. Its mechanism of action in cancer treatment has been reported to suppress nuclear factor kappa B signaling in cancer cells (Seo et al., 2018). It was also reported that it inhibits the growth of some cancer cell lines by inhibiting the signal transducer and activator of the transcription (STAT3) activation pathway (Ashutosh et al., 2007). Good cytotoxic activity in triterpenes has been linked to the presence of hydroxy or monosaccharide groups at the C-3 position, hydroxy at C-19, or conjugation with the double bond at C-12, 13 (Shou et al., 2018).

α-Arbutin is a natural polyphenol and a natural form of hydroquinone making it an essential and preferable ingredient in cosmetology due to its non-toxic properties, as it inhibits melanin production *via* tyrosinase inhibition. α-Arbutin has demonstrated good anti-inflammatory and antioxidant activity *in vitro* (Lee and Kim, 2012; Khadir et al., 2015). In our study, we observed deficient cytotoxic activity against Caco-2 and HepG2 cell lines. Tilak et al. (2011) reported that α-arbutin did not induce cytotoxicity at a concentration of 2 mM against HepG2, neither was there any LDH release at the same concentration compared to hydroquinone. They also

reported that cytotoxicity of α -arbutin is noticeable when it is metabolized to hydroquinone. A cytotoxicity study on UVB-irradiated α -arbutin and its derivative, deoxyarbutin, on Detroit 551 human fibroblast cells and B16-F10 mouse melanoma cells, showed that both have strong cytotoxicity towards the fibroblast cell (Chang et al., 2017). α -Arbutin at a concentration between 400-5000 μ M showed no cytotoxic effect on fibroblast cells (Chang et al., 2017). For α -arbutin to be cytotoxic, intestinal bacteria play a major role in metabolizing it to hydroquinone (Kang et al., 2011). After 72 h of treatment, acetylated α -arbutin was reported to induce cell viability at a concentration of \sim 3.85 mM, while at a concentration of 5.4 mM, α -arbutin reduced cell viability to 45.8%, and its acylated form reduced viability to 89.9% (Jiang et al., 2017). From our study, no significant cytotoxic effect was observed after 24 h treatment. The reduced cytotoxicity could mean that time is a factor in the cytotoxic activity of α -arbutin against Caco-2 and HepG2 cell lines (Jiang et al., 2017).

Antibacterial activity of α -arbutin has been reported to be enhanced by polymerization. The MICs of α -arbutin and its polymer, poly(arbutin) and its 10% octylated derivative [poly(arb)-C₈]₁₀ against *E. coli* were reported to be 111, 15.2, and 52.6 mg/mL and 111, 1.00, and 1.00 mg/mL against *S. aureus*; this shows selectivity towards Gram-negative bacteria (Rika et al., 2019). This selectivity may be due to the difference in the cell wall structure of Gram-negative and Gram-positive bacteria.

More is known about the chemistry of homoisoflavonoids than their biological activities and structure-activity relationships (Castelli and Lopez, 2017). From our findings, 3-(4-methoxybenzyl)-5,7-dimethoxychroman-4-one demonstrated moderate antibacterial activity against *S. aureus* ATTC 29213 compared to other isolated compounds and crude extracts but was resistant to all Gram-negative bacteria tested. The crude extracts demonstrated resistance and intermediate activity towards both Gram-positive and Gram-negative bacteria. Mathekga and Meyer (1998) investigated the antibacterial activity of the acetone extract of *H.*

callicomum, *H. glomeratum*, *H. hypoleucum*, *H. odoratissimum*, *B. subtilis*, *H. pilosellum* and *H. rugulosum* against *E. coli*, *K. pneumonia*, and *P. aeruginosa*. The result showed that all extracts were active against *E. coli* and *B. subtilis*, except for *H. glomeratum* and *H. pilosellum*; both had no activity against all tested Gram-positive and Gram-negative bacteria. This data indicates that some plants in the *Helichrysum* genus have no antibacterial activity.

The results of the violacein inhibition assay using *C. violaceum* ATCC 12472 showed a concentration-dependent inhibition of violacein produced by the bacterium. Growth inhibition at $\leq 40\%$ and violacein inhibition $\geq 50\%$ are taken as suitable QS inhibitors. All isolated compounds demonstrated quorum sensing inhibition (QSI) at 1000 μg between 5-18%, except for ursolic acid that demonstrated QSI of 20% for the short-chain AHL-mediated QS and 12% for the long-chain AHL-mediated QS at 1000 μg . Flavonoids, coumarins, sulfur-containing compounds, benzoic acid derivatives, phenylpropanoids, and monoterpenes have been indicated as plant-derived compounds possessing good AHL-mediated QS in bacteria (Dervabin et al., 2019).

The crude extracts were better than the isolated compounds in inhibiting violacein, with QSI between 18-45% for the short-chain AHL-mediated QS and 14-35% for the long-chain AHL-mediated QS, with MeOH extract of the leaves demonstrating the highest with 45.26% and 35.68%. Similarly, crude extract of *S. nigrescens* inhibited QS-regulated violacein production in *C. violaceum* in a concentration-dependent manner, with a 28-48% QSI at 700 μg and 27-39% growth inhibition (Bodede et al., 2017). Crude plant extracts are more effective than their isolates at the same concentration; this could be attributed to synergies between the plant constituents. This synergy was seen in the MeOH extract of the leaves; the constituents in the extract played a synergistic role in its antibacterial activity and QSI. Different pathways exist for QSI, including inhibition of the AI pathway, AI receptor antagonism, and degradation of AIs using catalytic antibodies (Asfour, 2018).

LDH release is a marker for cytotoxicity and could also indicate apoptotic or necrotic cell death. Likewise, a reduction in MPP could indicate the initiation of the mitochondrial apoptotic pathway. ATP depletion has been implicated in the necrotic death of cells. A study showed that an elevated level of ATP is a requisite for apoptotic death (Zamaraeva et al., 2005).

α -Arbutin and ursolic acid demonstrated a decrease in ATP and mitochondrial membrane potential and LDH release. The reduction of the MMP was dose-dependent. Depolarization of the MMP may cause a reduction in ATP levels. Some secondary metabolites have demonstrated the ability to disrupt MMP, accompanied by reduced ATP levels after exposure to some cell lines. Eugenol, a secondary metabolite from cloves, decreases viability in MCF-7, caused ATP depletion (decrease in intracellular ATP), dissipation of membrane potential, and a release of cytochrome c into the culture media. Also, a release of LDH indicating disruption of plasma membrane integrity was observed (Al-wafai et al., 2017). Treatment with 1-(2-hydroxyphenyl)-4-methylpentan-1-one and 2-[(3-methylbutoxy) carbonyl] benzoic acid, two bioactive compounds from *Rubus fairholmianus* against MCF-7 breast cancer cell lines, resulted in changes in MMP accompanied by the release of cytosol-c, supporting intrinsic apoptotic death (George and Abrahmase, 2019). Curcumin, an active metabolite from the rhizome of turmeric inhibited the growth of HepG2 and disrupt the MMP; this resulted in the release of mitochondrial membrane apoptin and cell apoptosis (Wang et al., 2011).

Among the extracts, EtOAc disrupted the MMP, which led to ATP depletion. The integrity of the plasma membrane was compromised by the release of LDH by the extract. Methanolic and hexane extracts of *Bulbine frutescens* showed the same activity by disrupting the MMP of breast cancer cells, MDA-MB-231 and T47D (Prem et al, 2019). Loss of MMP happens during apoptosis due to the opening of the mitochondrial permeability pore and loss of electron gradient in the membrane (Sivandzade et al., 2019; Isenberg and Klaunig, 1999). The study showed that a decrease in MPP causes apoptosis by matrix condensation, exposure of

cytochrome c to the intermembrane space, which causes the release of cytochrome c and cell death (Gottlieb et al. 2003). Depolarization of MPP is due to collapse or decrease in the electrochemical gradient of the mitochondrial membrane. Our findings showed that the cytotoxicity of most of the test samples towards Caco-2 is necrotic due to increases in ATP levels and elevated LDH release due to disruption of the plasma membrane.

5.5 CONCLUSION

The isolation of seven secondary metabolites from *H. panduratum* was reported, including 3-(4-methoxybenzyl)-5,7-dimethoxychroman-4-one, a homoisoflavonoid, which was isolated for the first time from *Helichrysum* species. Our study showed that *H. panduratum* is rich in triterpenes and α -arbutin. α -Arbutin, a natural form of hydroquinone with no cytotoxic effect, would make the leaves of *H. panduratum* a potential source of the compound for the cosmetic industry. The isolated compounds and extract demonstrated low antibacterial activity to both Gram-positive and Gram-negative bacteria, with the methanol extract of the leaves showing potential as an effective inhibitor of short and long-chain AHL-mediated QS. The cytotoxic activity showed that the plant is relatively safe for consumption due to the selectivity of isolated compounds and some crude extracts towards the untransformed cell lines.

REFERENCES

- Aiyegoro, O.A., Okoh, A.I. (2010) Preliminary phytochemical screening and *in vitro* antioxidant activities of the aqueous extract of *Helichrysum longifolium* DC. BMC COMPLEMENT ALTERNATIVE MEDICINE 10, 21.doi:10.1186/1472-6882-10-21
- Al Wafai, R., El-Rabih, W., Katerji, M., Safi, R., El Sabban, M., El-Rifai, O., & Usta, J. (2017). Chemosensitivity of MCF-7 cells to eugenol: release of cytochrome-c and lactate dehydrogenase. SCIENTIFIC REPORTS, 7(1), 43730. doi:10.1038/srep43730.
- Asfour H. Z. (2018). Anti-quorum sensing natural compounds. JOURNAL OF MICROSCOPY AND ULTRASTRUCTURE, 6(1), 1–10.
- Bodede, O., Shaik, S., Chenia, H., Singh, P., & Moodley, R. (2018). Quorum sensing inhibitory potential and in silico molecular docking of flavonoids and novel terpenoids from *Senegalia nigrescens*. JOURNAL OF ETHNOPHARMACOLOGY, 216,134-146.
- Bohlmann Ferdinand, Abraham Wolf-Rainer. (1979) Neue, chloresubstituierte thiophenacetylenverbindungen mit ungewöhnlicher struktur aus *Helichrysum-arten*, PHYTOCHEMISTRY, Volume 18, Issue 5, Pages 839-842, ISSN 0031-9422.
- Castelli, M.V., López, S.N. (2017) Chapter 9 - Homoisoflavonoids: Occurrence, biosynthesis, and biological activity, Editor(s): Atta-ur-Rahman, STUDIES IN NATURAL PRODUCTS CHEMISTRY, ELSEVIER, Volume 54, Pages 315-354, ISSN 1572-5995, ISBN 9780444639295.
- Chandramu, C., Manohar, R.D., Krupadanam, D.G.L. and Dashavantha, R.V. (2003), Isolation, characterization and biological activity of betulinic acid and ursolic acid from *Vitex negundo* L. PHYTOTHERAPY RESEARCH 17: 129-134

- Chang, N. F., Chen, Y. S., Lin, Y. J., Tai, T. H., Chen, A. N., Huang, C. H., & Lin, C. C. (2017). Study of hydroquinone mediated cytotoxicity and hypopigmentation effects from UVB-irradiated arbutin and deoxy arbutin. *INTERNATIONAL JOURNAL OF MOLECULAR SCIENCES*, 18(5), 969
- Chenia HY, (2013). Anti-quorum sensing potential of crude *Kigelia africana* fruit extracts. *SENSORS* 13: 2802–2817.
- Deryabin, D., Galadzhieva, A., Kosyan, D., & Duskaev, G. (2019). Plant-derived inhibitors of ahl-mediated quorum sensing in bacteria: Modes of action. *INTERNATIONAL JOURNAL OF MOLECULAR SCIENCES*, 20(22), 5588.
- Do Nascimento, P., Lemos, T., Bizerra, A., Arriaga, Â., Ferreira, D., Santiago, G., Costa, J. (2014). Antibacterial and antioxidant activities of ursolic acid and derivatives. *MOLECULES*, 19(1), 1317–1327.
- Du Toit, Karen; Drewes, Siegfried E.; Bodenstein, Johannes (2010). The chemical structures, plant origins, ethnobotany, and biological activities of homoisoflavanones. *NATURAL PRODUCT RESEARCH*. 24 (5), 457–490.
- Endo, M., Shigetomi, K., Mitsuhashi, S., Igarashi, M., & Ubukata, M. (2019). Isolation, structure determination and structure–activity relationship of anti-toxoplasma triterpenoids from *Quercus crispula* Blume outer bark. *JOURNAL OF WOOD SCIENCE*, 65(1). doi:10.1186/s10086-019-1782-
- George, B. P., & Abrahamse, H. (2019). Increased oxidative stress induced by *Rubus* bioactive compounds induce apoptotic cell death in human breast cancer cells. *OXIDATIVE MEDICINE AND CELLULAR LONGEVITY*, 2019, 1–18. doi:10.1155/2019/6797921.

- Gottlieb, E., Armour, S. M., Harris, M. H., & Thompson, C. B. (2003). Mitochondrial membrane potential regulates matrix configuration and cytochrome c release during apoptosis. *CELL DEATH & DIFFERENTIATION*, 10(6), 709–717. doi: 10.1038/sj.cdd.4401231.
- Habib MR, Nikkon F, Rahman M, Haque ME, Karim MR. (2007) Isolation of stigmasterol and beta-sitosterol from methanolic extract of root bark of *Calotropis gigantea* (Linn). *Pakistan JOURNAL OF BIOLOGICAL SCIENCES: PJBS*. 2007 Nov;10(22):4174-4176. DOI:10.3923/pjbs.2007.4174.4176.
- Hilliard, O. M., 1983. Flora of Southern Africa, Vol. 33, Part 7, Fascicle 2, 61-310. Botanical Research Institute, Department of Agriculture, South Africa.
- Isenberg, J. S., Klaunig, J. E. (1999). Role of the mitochondrial membrane permeability transition (MPT) in rotenone-induced apoptosis in liver cells. *TOXICOLOGICAL SCIENCES*, 53(2), 340–351. doi:10.1093/toxsci/53.2.340.
- Jakupovic, J., Kuhnke, J., Schuster, A., Metwally, M. A., Bohlmann, F., 1986. Phloroglucinol derivatives and other constituents from South African *Helichrysum* species. *PHYTOCHEMISTRY* 25, 1133-1142.
- Jiang, L., Wang, D., Zhang, Y., Li, J., Wu, Z., & Wang, Z. (2017). Investigation of the pro-apoptotic effects of arbutin and its acetylated derivative on murine melanoma cells. *INTERNATIONAL JOURNAL OF MOLECULAR MEDICINE*, 41, 1048-1054. <https://doi.org/10.3892/ijmm.2017.3256>.

- Jiang, Q., Chen, J., Yang, C., Yin, Y., & Yao, K. (2019). Quorum sensing: A prospective therapeutic target for bacterial diseases. *BIOMED RESEARCH INTERNATIONAL*, 2019, 2015978. <https://doi.org/10.1155/2019/2015978>.
- Kang Mi Jeong, Hyun Woo Ha, Hyung Gyun Kim, Dae Hun Lee, Min Jeong Kong, Young Tae Ahn, Dong Hyun Kim, Beom Soo Shin, Wonku Kang, Hye Gwang Jeong, Tae Cheon Jeong (2011). Role of metabolism by intestinal bacteria in arbutin-induced toxicity *in vitro*. *ARCHIVES OF PHARMACEUTICAL RESEARCH* 34, 687–693 (2011).
- Khadir, F., Pouramir, M., Joorsaraee, S. G., Feizi, F., Sorkhi, H., & Yousefi, F. (2015). The effect of arbutin on lipid peroxidation and antioxidant capacity in the serum of cyclosporine-treated rats. *CASPIAN JOURNAL OF INTERNAL MEDICINE*, 6(4), 196–200.
- Khatun, M., Billah, M., & Quader, M. A. (2012). Sterols and sterol glucoside from *Phyllanthus* species. *DHAKA UNIVERSITY JOURNAL OF SCIENCE*, 60(1). doi:10.3329/dujs.v60i1.10327.
- Kumar, P., Nagarajan, A., & Uchil, P. D. (2018). Analysis of cell viability by the lactate dehydrogenase assay. *COLD SPRING HARBOR PROTOCOLS*, 2018(6), 10.1101/pdb.prot095497.
- Kushwaha, P. P., Vardhan, P. S., Kapewangolo, P., Shuaib, M., Prajapati, S. K., Singh, A. K., & Kumar, S. (2019) *Bulbine frutescens* phytochemical inhibits notch signalling pathway and induces apoptosis in triple negative and luminal breast cancer cells. *LIFE SCIENCES*, Volume 234, 116783. doi.org/10.1016/j.lfs.2019.116783

- Labib, R. M., Ebada, S. S., Youssef, F. S., Ashour, M. L., & Ross, S. A. (2016). Ursolic acid, a natural pentacyclic triterpene from *Ochrosia elliptica* and its role in the management of certain neglected tropical diseases. *PHARMACOGNOSY MAGAZINE*, 12(48), 319–325. <https://doi.org/10.4103/0973-1296.192207>.
- Lee, H.J., & Kim, K.W. (2012). Anti-inflammatory effects of arbutin in lipopolysaccharide stimulated BV2 microglial cells. *INFLAMMATION RESEARCH*, 61(8), 817–825. doi:10.1007/s00011-012-0474-2
- Lourens, A. C., Viljoen, A. M., & van Heerden, F. R. (2008). South African *Helichrysum* species: a review of the traditional uses, biological activity and phytochemistry. *JOURNAL OF ETHNOPHARMACOLOGY*, 119(3), 630–652.
- Mathekga, A. D. M., 2001. Antimicrobial activity of *Helichrysum* species and the isolation of a new phloroglucinol from *Helichrysum caespititium*. PhD dissertation. University of Pretoria, South Africa
- Mathekga, A., & Meyer, J. (1998). Antibacterial activity of South African *Helichrysum* species. *SOUTH AFRICAN JOURNAL OF BOTANY*, 64, 293-295.
- Matić, I. Z., Aljančić, I., Žižak, Ž., Vajs, V., Jadranin, M., Milosavljević, S., & Juranić, Z. D. (2013). *In vitro* antitumor actions of extracts from endemic plant *Helichrysum zivojinii*. *BMC COMPLEMENTARY AND ALTERNATIVE MEDICINE*, 13, 36.
- McLean, R. J., Pierson, L. S., Fuqua C. A. (2004). Simple screening protocol for the identification of quorum signal antagonists. *JOURNAL OF MICROBIOLOGY METHODS*. Sep;58(3):351-60. doi: 10.1016/j.mimet.2004.04.016.

- Meyer, J. J., Afolayan, A. J., Taylor, M. B., & Engelbrecht, L. (1996). Inhibition of herpes simplex virus type 1 by aqueous extracts from shoots of *Helichrysum aureonitens* (Asteraceae). *JOURNAL OF ETHNOPHARMACOLOGY*, 52(1), 41–43.
- Miller, M. B., & Bassler, B. L. (2001). Quorum sensing in bacteria. *ANNUAL REVIEW OF MICROBIOLOGY*, 55, 165–199.
- Mukherjee, S., & Bassler, B.L. (2019). Bacterial quorum sensing in complex and dynamically changing environments. *NATURAL REVIEW MICROBIOLOGY* 17, 371–382.
- Nycz, J. E., Malecki, G., Morag, M., Nowak, G., Ponikiewski, L., Kusz, J., & Switlicka, A. (2010). Arbutin: Isolation, X-ray structure and computational studies. *JOURNAL OF MOLECULAR STRUCTURE*, 980(1-3), 13–17. doi: 10.1016/j.molstruc.2010.06.026
- Pathak, A. K., Bhutani, M., Nair, A. S., Ahn, K. S., Chakraborty, A., Kadara, H., Guha, S., Sethi, G., & Aggarwal, B. B. (2007). Ursolic acid inhibits stat3 activation pathway leading to suppression of proliferation and chemosensitization of human multiple myeloma cells. *MOLECULAR CANCER RESEARCH* 5 (9), 943-955. doi:10.1153/1541-7786.MCR-06-0348.
- Rawal, V. H., & Cava, M. P. (1983). Synthesis of scillascillin, a naturally occurring benzocyclobutene. *TETRAHEDRON LETTERS*. 24 (50): 5581–5584.
- Rika, K., Ayaka, S., Hisayoshi, K., Yoko, S., Yoshiyuki, O., & Yuji, S. (2019) Enhanced antimicrobial activities of polymerized arbutin and its derivatives prepared by oxidative polymerization of arbutin. *REACTIVE AND FUNCTIONAL POLYMERS*, 138, Pages 39-45, ISSN 1381-5148.

- Riss, T.L., Moravec, R. A., Niles, A. L., et al. Cell Viability Assays. 2013 May 1 [Updated 2016 Jul 1]. In: Markossian S, Grossman A, Brimacombe K, et al., editors. Assay Guidance Manual [Internet]. Bethesda (MD): Eli Lilly & Company and the National Center for Advancing Translational Sciences; 2004-. Available from: <https://www.ncbi.nlm.nih.gov/books/NBK144065/>
- Rutherford, S. T., & Bassler, B. L. (2012). Bacterial quorum sensing: its role in virulence and possibilities for its control. COLD SPRING HARBOR PERSPECTIVES IN MEDICINE, 2(11), a012427.
- Sakamuru, S., Attene-Ramos, M. S., & Xia, M. (2016). Mitochondrial membrane potential assay. METHODS IN MOLECULAR BIOLOGY (Clifton, N.J.), 1473, 17–22.
- Seebacher, W., Simic, N., Weis, R., Saf, R., & Kunert, O. (2003). Complete assignments of ¹H and ¹³C NMR resonances of oleanolic acid, 18-oleanolic acid, ursolic acid and their 11-oxo derivatives. MAGNETIC RESONANCE IN CHEMISTRY, 41(8), 636–638. doi:10.1002/mrc.1214
- Seo, D. Y., Lee, S. R., Heo, J. W., No, M. H., Rhee, B. D., Ko, K. S., Kwak, H. B., & Han, J. (2018). Ursolic acid in health and disease. THE KOREAN JOURNAL OF PHYSIOLOGY & PHARMACOLOGY: OFFICIAL JOURNAL OF THE KOREAN PHYSIOLOGICAL SOCIETY AND THE KOREAN SOCIETY OF PHARMACOLOGY, 22(3), 235–248.
- Shuo, S., Wei, L., Ming-an, O., & Jian, W. (2018) Structure-activity relationship of Triterpenes and derived Glycosides against cancer cells and mechanism of apoptosis induction, NATURAL PRODUCT RESEARCH, 32:6, 654-661.

- Sivandzade, F., Bhalerao, A., & Cucullo, L. (2019). Analysis of the mitochondrial membrane potential using the cationic JC-1 Dye as a sensitive fluorescent probe. *BIO-PROTOCOL*, 9(1). doi:10.21769/bioprotoc.3128.
- Sultana, T., Rashid, M., Ali, M., & Mahmood, S. (2010). Hepatoprotective and antibacterial activity of ursolic acid extracted from *Hedyotis corymbos* (L). *BANGLADESH JOURNAL OF SCIENTIFIC AND INDUSTRIAL RESEARCH*, 45(1), 27-34.
- Teasdale, M.E., Donovan, K.A., Forschner-Dancause, S.R. *et al.* (2011). Gram-Positive marine bacteria as a potential resource for the discovery of quorum sensing inhibitors. *MARINE BIOTECHNOLOGY* 13, 722–732. <https://doi.org/10.1007/s10126-010-9334-7>.
- Tilak Khanal, Hyung Gyun Kim, Yong Pil Hwang, Min Jeong Kong, Mi Jeong Kang, Hee Kyung Yeo, Dong Hyun Kim, Tae Cheon Jeong, Hye Gwang Jeong. (2011). Role of metabolism by the human intestinal microflora in arbutin-induced cytotoxicity in HepG2 cell cultures. *BIOCHEMICAL AND BIOPHYSICAL RESEARCH COMMUNICATIONS*, Volume 413, Issue 2, Pages 318-324, ISSN 0006-291X.
- Vuyiswa Gladys Swartz (2006) Phytochemical studies of *Helichrysum patulum* MSc thesis. University of the Western Cape, South Africa.
- Wang X., Hinshaw K. C., Macdonald S. J., Chandler, J. R. (2016). Draft genome sequence of *Chromobacterium violaceum* strain CV017. *GENOME ANNOUNC.* Mar 3;4(2):e00080-16. doi: 10.1128/genomeA.00080-16.
- Wang, M., Ruan, Y., Chen, Q., Li, S., Wang, Q., & Cai, J. (2011). Curcumin induced HepG2 cell apoptosis-associated mitochondrial membrane potential and intracellular free Ca²⁺

concentration. EUROPEAN JOURNAL OF PHARMACOLOGY, 650(1), 41–47. doi: 10.1016/j.ejphar.2010.09.049

Windsor Jon. (2020). How quorum sensing works. AMERICAN SOCIETY FOR MICROBIOLOGY.

Wolska, K.I., Grudniak, A.M., Fiecek, B. *et al.* (2010). Antibacterial activity of oleanolic and ursolic acids and their derivatives. CENTRAL EUROPEAN JOURNAL OF BIOLOGY. 5, 543–553.

Yen, H. (2016). Quorum sensing. ENCYCLOPEDIA BRITANNICA. <https://www.britannica.com/science/quorum-sensing>.

Zamaraeva, M. V., Sabirov, R. Z., Maeno, E., Ando-Akatsuka, Y., Bessonova, S. V., & Okada, Y. (2005). Cells die with increased cytosolic ATP during apoptosis: a bioluminescence study with intracellular luciferase. CELL DEATH AND DIFFERENTIATION, 12(11), 1390–1397. doi: 10.1038/sj.cdd.4401661.

CHAPTER 6

Phytochemical and biological studies of *Helichrysum acutatum* DC.

ABSTRACT

Helichrysum acutatum from the Asteraceae family is a shrub that is indigenous to Southern Africa. The plant is used in traditional medicine as an enema for newborn babies. This study aimed to isolate and identify the bioactive constituents from *H. acutatum*. In addition, the crude extracts and isolated compounds were tested for their antioxidant, antibacterial and cytotoxic activities. The phytochemical investigation afforded the known compounds stigmasterol, stigmasterol glucoside, and caffeic acid. The antioxidant activity of the ethyl acetate extract was higher compared to other extracts, ascorbic acid, and butylated hydroxytoluene. Antibacterial profiling of all the extracts showed no activity against both Gram-negative and Gram-positive bacterial strains. The cytotoxic activity of the crude extracts was assayed *in vitro* against two human cancer cell lines, liver hepatoblastoma (HepG2) and colorectal adenocarcinoma (Caco-2). The human embryonic kidney cell line (Hek-293) was used as the non-transformed control. The plant extracts showed insufficient antiproliferative or cytotoxic activity to the tumor and regular cell lines tested, which signifies suitably for human consumption. Overall, this plant had better antioxidant activity than other plants in the genus, which needs to be explored further.

Keywords: caffeic acid, cytotoxicity, nuclear magnetic resonance, antioxidant.

6.1 INTRODUCTION

Plants are a storehouse for different therapeutic molecules, and they have played a significant and crucial role in modern drug discovery and development. The search for safe, effective, and affordable healthcare has made many trust traditional medicines. Coming from a natural source, people believe that these medicines are relatively safe for use. Also, the search for new molecular compounds in the treatment and management of diseases has led to research in natural products leads in drug discovery. Natural products account for more than 50% of modern drugs used clinically, with some possessing the ability to inhibit cancer cells (Rajendra et al., 2010)

Oxidative stress has been implicated in some degenerative diseases such as Parkinson's, Alzheimer's, and cancer. Oxidative stress occurs when there is a shift in the production and removal of reactive oxygen species (ROS), favoring the production rather than the removal. The National Cancer Institute (NCI) defined ROS as unstable molecules that contain oxygen that quickly reacts with other molecules in the cell. They are free radicals and could be referred to as oxygen radicals. Examples include peroxide, superoxide, hydroxyl radicals, and singlet oxygen species (Hayyan et al., 2006). The build-up of ROS in the cell may cause damage to the DNA, RNA, proteins, and even cell death. The imbalance of antioxidants and free radicals in the body leads to oxidative stress. Antioxidants react with free radicals in the body and terminate their chain reaction.

Helichrysum species are known to possess antimicrobial, antifungal, antiviral, and antioxidant activities. There are approximately 600 species in the genus *Helichrysum* (Asteraceae). Compounds including chalcones, diterpenes, phloroglucinol, and its derivatives have been isolated from the aerial parts and roots of some *Helichrysum* species (Jakupovic et al., 1985). Traditionally some of the species have found use in the treatment of diarrhea, wounds, colds, coughs, and

infection of the respiratory tract (Lourens et al., 2008). Essential oils from *Helichrysum* species have been used, with the most widely used essential oil being from *Helichrysum italicum*. *Helichrysum acutatum* DC. is a perennial woody herb with a flowering stem that grows in grasslands; Hillard (1983) classified it morphologically into group 21. Other plants in this group are *H. dasymallum* and *H. oreophyllum*. Although *H. acutatum* is widely sold at the Muthi market, there is no literature for its ethnopharmacology relevance. The locals in the market provided anecdotal information on its use in traditional medicine, as an enema for newborns. Bohlmann and Abraham (1979) investigated the plant's roots and isolated fourteen compounds that included chalcones and diterpenes. In the current study, the roots of *Helichrysum acutatum*, widely sold at the Muthi market in Durban, were investigated to establish a rationale for its traditional use by the locals as no biological studies have previously been done on the plant.

6.2 MATERIALS AND METHODS

6.2.1 General Experimental Procedures

Infra-red spectra were obtained using Perkin Elmer Spectrum 100 FT-IR spectrometer with universal ATR sampling. NMR spectra (^1H , ^{13}C , and 2D) were recorded on Bruker Avance^{III} 400Hz spectrometer, using deuterated chloroform, methanol or DMSO at room temperature, with TMS as internal standard. Column chromatography was carried out using Merck silica gel 60 (0.040-00063mm) as a stationary phase and solvents of different polarities as a mobile phase. Examination of separated fractions was done using Merck 20 cm \times 20 cm silica gel 60 F₂₅₄ aluminum sheets for TLC. The TLC plates were first visualized under UV (254 and 366 nm) before spraying with 10% H₂SO₄ in methanol (MeOH) solution, followed by heating for the second

visualization. High-resolution mass spectra (HR-MS) were recorded on the Waters Micromass LCT Premier TOF-MS instrument. All reagents were of analytical grade and were sourced from either Merck (Darmstadt, Germany) or Sigma (St. Louis, USA) chemical companies.

6.2.2 Plant Collection

Plant material (root) of *H. acutatum* was purchased from Berea Muthi market. The taxonomist in the School of Life Sciences, UKZN, authenticated the sample, and a voucher specimen (18271 01 900600) was deposited in the ward herbarium. The plant was air-dried and then crushed with a metal mortar and pestle to a smaller fragment for extraction.

6.2.3 Extraction and Isolation

The roots of *H. acutatum* (1.3 kg) were oven-dried, crushed, and extracted sequentially with organic solvents of varying polarities, starting with the least polar to the most polar solvent in the order; DCM, EtOAc, and MeOH with the aid of a mechanical shaker. Each solvent was filtered and concentrated under reduced pressure using a rotary evaporator to give 5.4 g of DCM, 4.5 g of EtOAc, and 20 g of MeOH extracts.

The DCM extract was subjected to separation on a silica gel column, with hexane and EtOAc as solvents using gradient elution to give 50 fractions of 100 mL monitored on TLC. Fraction 18 gave compound **C1** (20 mg) as white flakes. The MeOH extract was purified on a packed silica gel column using hexane: EtOAc as the mobile phase similar to the DCM extract. Fraction 20 gave compound **C1**, and fractions 40-45 were further purified by washing with MeOH to give compound **C2** (5 mg), an orange powder. The EtOAc extract was fractionated on silica gel and eluted sequentially with hexane and EtOAc, starting from 100% hexane that was stepped by 10%

to 100% EtOAc. A total of 40 fractions of 100 mL were obtained. Fractions 26-28 gave compound **C3** (15 mg), a yellowish powder.

6.2.4 Antioxidant Activity

2,2-Diphenyl-1-picryl-hydrazyl (DPPH) radical scavenging activity

The DPPH radical scavenging ability was determined using an established procedure (Rajurkar and Hande, 2011) with minor modifications. Approximately 1 mL of 0.1 mM of DPPH solution was added to an equal volume of the plant extracts at varying concentrations of 7.5-250 μ L. Methanol and DPPH were used as blanks, while ascorbic acid and butylated hydroxytoluene (BHT) were used as controls. After incubation in the dark for 20 min, the DPPH reduction was measured at a wavelength of 517 nm with the aid of a UV-Vis spectrophotometer. All experiments were carried out in triplicate.

Ferric reducing antioxidant power (FRAP) assay

According to the FRAP assay, the reducing ability of the plant extracts was estimated (Fernande et al., 2016). Different concentrations of the test samples were prepared; 2.5 mL of each concentration was mixed with 2.5 mL phosphate buffer solution and 2.5 mL potassium ferricyanide. The solutions were incubated in a water bath for 30 min at 50°C. After that, trichloroacetic acid (TCA) (2.5 mL) was added to each solution before it was mixed. Next, 2.5 mL distilled water was used to dilute the mixture, after which 0.5 mL FeCl₃ solution was added and allowed to settle for 10 min at room temperature. Absorbance was measured at 700 nm using a UV-Vis spectrophotometer. BHT and ascorbic acid served as positive controls.

6.2.5 Antibacterial Susceptibility Test

Three Gram-positive indicator bacteria, *Bacillus subtilis* ATCC 6653, methicillin-resistant *Staphylococcus aureus* ATCC 43000 and *Mycobacterium smegmatis* mc² 155 and four Gram-negative indicator bacteria, beta-lactam-resistant *Escherichia coli* ATCC 35218, multidrug-resistant *Pseudomonas aeruginosa* ATCC 27853, extended-spectrum beta-lactamase-producing *Klebsiella pneumoniae* ATCC 700603 and the quorum sensing indicator *Chromobacterium violaceum*, were employed to evaluate the antibacterial activity. Three crude extracts of *H. acutatum* and two pure compounds were subjected to antibacterial screening using the agar well diffusion method. The test samples were dissolved in MeOH to a final concentration of 20 mg/mL for the crude extracts and 10 mg/mL for the compounds.

6.2.6 Cytotoxicity Testing

Cell culture

Cryopreserved cells were rapidly thawed in the incubator and centrifuged. The cell pellet was recovered and propagated to 100% confluency in a 25 mL tissue culture flask with the addition of CCM (complete culture medium), which consists of 500 mL DMEM, supplemented with 1% L-glutamine, 1% penicillin-streptomycin-fungizone and 10% FCS, in a humid environment (5% CO₂, 37°C). The media was removed, and the cells were washed thrice with PBS. Trypsin was added to the flasks with Caco-2 and HepG2 cells to remove the cells that had adhered to the flasks. The flask with Hek-293 was agitated to remove the cells that have adhered to it. The cells were resuspended in 2 mL for CCM and counted using the trypan blue method.

Sample preparation

Stock solutions of crude extracts were prepared by dissolving in DMSO and diluted with CCM to a concentration of 10 mg/ml, and eight different concentrations (0-5000 µg/mL) for the MTT assay were prepared from the stock. The final concentration of DMSO in each stock was less than 0.5%.

MTT assay

The viability of Caco-2, HepG2, and Hek-293 cells after exposure to varying concentrations of test samples for 24 h was evaluated using the MTT (tetrazolium salt reduction) assay. 2×10^5 cells in CCM were seeded in 96-well microplates and incubated at 37°C in 5% CO₂ overnight for adherence of cells to the plate. The medium was removed, and 100 µL of test samples prepared in CCM at varying concentrations were added to each well. The wells receiving only media served as the control. Treatment was done in triplicate for each test sample at 24 h. After 24 h, the medium was removed, 20 µL of MTT salt in CCM at a concentration of 5 mg/mL, and 100 µL PBS was added and incubated for 4 h at 37°C. After that, the MTT solution was removed, and the formazan crystals formed solubilized with 100 µL DMSO. The inhibition of cell growth by tested samples was measured using a Bio-Tek µQuant plate spectrophotometer (Winooski, Vermont, United States) at a wavelength of 570 nm. Results were presented as percentage cell viability.

$$\% \text{ cell viability} = \frac{\text{average OD of treated cells}}{\text{average OD of control cells}} \times 100$$

Analysis of mitochondrial membrane potential (MMP)

An increase in depolarization of the mitochondrial membrane with a subsequent decrease in mitochondrial membrane potential could result in the activation of pro-apoptotic factors. JC-10, a water-soluble dye, was used to probe the mitochondrial membrane potential in this assay. Cells

were seeded at 2×10^4 into each well and allowed to adhere to the plate. IC₈₀ and IC₅₀ concentrations were prepared from the stock and added to each well. After 24 h, treatment media was removed and stored for other assays. Each well received 25 µL of JC-10 dye and 50 µL PBS before incubation at 37°C for 1 h in the dark. After 60 min of incubation, the JC-10/PBS solution was removed, and 80 µL PBS was added before the plates were read.

ATP quantification

The intracellular ATP levels were monitored using a CellTiter-Glo[®] reagent (Promega) prepared according to the manufacturer's instructions. After taking the reading of the plate used for the mitochondrial membrane potential assay, 50 µL of PBS was added to each well, followed by 25 µL of CellTiter-Glo[®] reagent. Next, a luminescent reading was done on a Modulus[™] microplate luminometer (Turner Bio-Systems, California, USA).

LDH release assay

LDH is a stable cytoplasmic enzyme found in the plasma of living cells. Release of LDH from the cytoplasm to the surrounding cell culture due to loss of the plasma-wall integrity can be used to quantify cell viability and necrosis *in-vitro*. 50 µL of the treatment media from the mitochondrial membrane potential assay was pipetted into a 96-well plate. Thereafter, 25 µL of the assay buffer (iodonitrotetrazolium (INT) chloride, nicotinamide adenine dinucleotide (NAD) sodium salt, and lithium lactate) was added. Plates were incubated at room temperature in the dark for 30 min. The reaction was stopped by the addition of 12.5 µL stop solution (acetic acid). LDH was quantified by measuring the absorbance at 500 nm using a Biotek µQuant spectrophotometer (Winooski, Vermont, United States).

6.2.7 Statistical Analysis

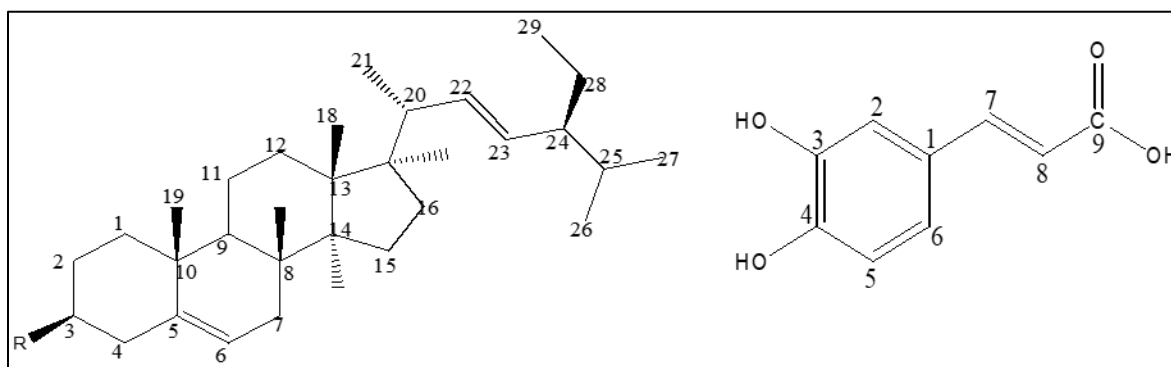
Data were exported to Microsoft Excel for analysis and processed on GraphPad Prism v5.0 (GraphPad Software Inc., San Diego, California, United States). All data were normalized to the untreated control, and the student's t-test was used to determine statistically significant differences ($P < 0.05$). All data were expressed as mean \pm SD ($n = 3$).

6.3 RESULTS

6.3.1 Identification of Isolated Compounds

Three compounds were isolated and elucidated from the roots of *H. actutatum* (Figure 6.1). These include a sterol, a sterol glycoside, and a phenolic acid. The DCM and MeOH extract of the root yielded stigmasterol (compound **C1**). The spectral data compared well to that published in the literature for this compound (Habib et al., 2007). The MeOH extract yielded stigmasterol glucoside (compound **C2**) as confirmed by literature (Khatum et al., 2012). The EtOAc extract yielded caffeic acid (compound **3**). The ^1H NMR and ^{13}C NMR spectral data are consistent with that of cinnamic acid (Silva et al., 2001)) except for resonances in the aromatic region for three protons at δ_{H} 7.05 (H-2), 6.94 (H-6), and 6.79 (H-5), indicating an ABX ring system. The downfield chemical shift (δ_{H} 7.54 (H-7) and 6.23 (H-8)) of deshielded alkenyl hydrogens indicates unsaturation and the high coupling constant (15.9 Hz) indicates a trans arrangement. The HSQC spectrum showed correlations between the carbons at δ_{C} 115.1, 116.5, and 122.8 and the protons at δ_{H} 7.05, 6.79, and 6.94, respectively. Compound **C3** was therefore identified as caffeic acid, which was confirmed by literature data (Jeong et al., 2011).

^1H NMR (MeOD, 400 MHz) δ_{H} : 7.54 (1 H, d, $J = 15.9$ Hz, H-7), 7.05 (1 H, d, $J = 2.0$ Hz, H-2), 6.94 (1 H, dd, $J = 8.2, 2.0$ Hz, H-6), 6.79 (1 H, d, $J = 8.2$, H-5), 6.23 (1 H, d, $J = 15.9$ Hz, H-8).
 ^{13}C -NMR (MeOD, 100 MHz) δ_{C} : 171.0 (C-9), 149.4 (C-4), 147.0 (C-7), 146.8 (C-3), 127.8 (C-1), 122.8 (C-6), 116.5 (C-5), 115.5 (C-8), 115.1 (C-2).



Compound **C1**: R = H

Compound **C3**

Compound **C2**: R = Glucose

Figure 6.1: Compounds **C1-C3** isolated from the root of *H. acutatum*.

6.3.2 Antibacterial Activity

The plant extracts were tested at 0.5 and 1 mg against three Gram-positive bacteria and four Gram-negative bacteria, while the two phytochemicals were tested at 0.25 and 0.5 mg due to limited mass of phytochemicals. No antimicrobial activity was observed against all three Gram-positive and all four Gram-negative indicator organisms with extracts as well as isolated phytochemicals. The following zone diameter criteria were used to assign susceptibility or resistance to compounds tested: Susceptible (S) ≥ 15 mm, Intermediate (I) = 11–14 mm, and Resistant (R) ≤ 10 mm (Chenia, 2013).

6.3.3 Antioxidant Activity

The crude DCM, EtOAc, and MeOH extracts of the roots were subjected to antioxidant testing using DPPH and FRAP. Ascorbic acid and BHT were used as positive controls.

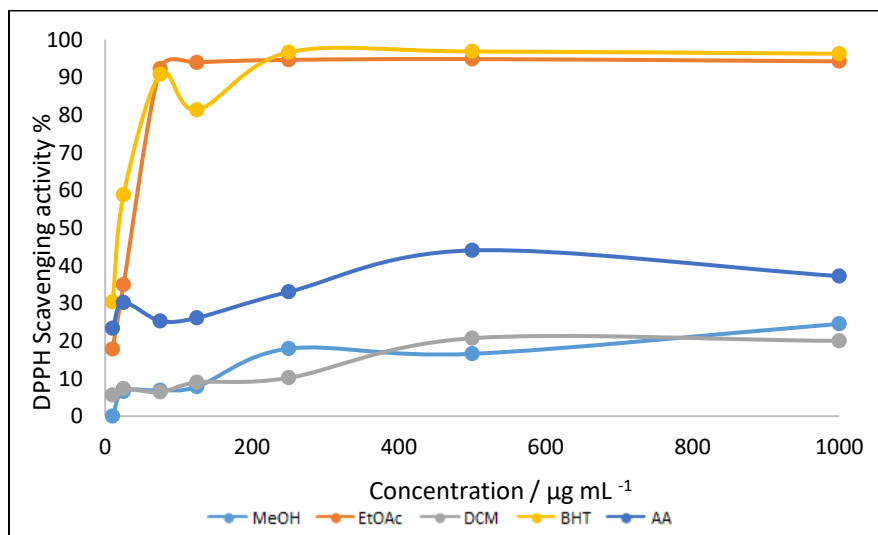


Figure 6.2: Free radical scavenging activity of selected crude extracts measured by DPPH method.

Values represent mean \pm SD (n = 3). MeOH - methanol, EtOAc - ethyl acetate, DCM - dichloromethane, and BHT – butylated hydroxytoluene.

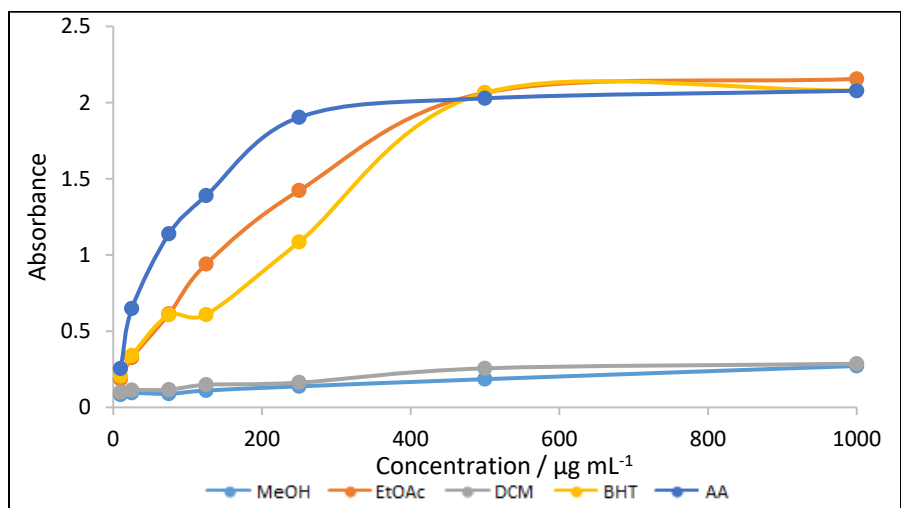


Figure 6.3: Ferric reducing antioxidant power (FRAP) of selected crude extracts.

Values represent mean \pm SD (n = 3). MeOH - methanol, EtOAc - ethyl acetate, DCM - dichloromethane, and BHT – butylated hydroxytoluene.

The results of the radical scavenging activity and reducing power of the crude extracts and the standards, ascorbic acid, and BHT are shown in Figures 6.2 and 6.3. The radical scavenging ability was in the order of BHT > EtOAc > ascorbic acid > MeOH > DCM. For the FRAP assay, the activity of the reference standards swapped and the order of reducing potential was ascorbic acid > EtOAc > BHT > MeOH > DCM.

6.3.4 Cytotoxicity Testing

MTT assay

The different crude extracts were exposed to the tumor cell lines (Caco-2 and HepG2) and the normal human kidney cell line, Hek-293 for 24 h, using the MTT assay to evaluate their cytotoxicity (Figure 6.4). Treatment with 50.12 µg/mL DCM extract decreased cell viability from 100% (control) to 89% in HepG2, 76% in Caco-2, and 62% in Hek-293. At 501.19 µg/mL cell viability decreased 14% for HepG2, 8% for Caco-2, and 52% for Hek-293. IC₅₀ values (in µg/mL) were 126.9, 165.55, and 699.6 for Caco-2, HepG2, and Hek-293, respectively.

Exposure to the EtOAc extract (50.12 µg/mL) stimulated cell growth from 100% (control) to 105% and 114% in HepG2 and Hek-293, respectively, while there was no change in Caco-2. Differently, at 100 µg/mL, there was a sharp decrease in cell viability to 53% for Caco-2 and a slight decrease to 101% for HepG2 and Hek-293. Between 100- 501.19 µg/mL, no significant decrease in cell viability was observed in Caco-2 and Hek-293, but a decrease was recorded for HepG2 from 101% (100 µg/mL) to 77% (501.19 µg/mL). The results showed that the extract has no effect on Hek-293 compared to Caco-2 and HepG2.

Treatment with the MeOH extract produced a stimulatory effect at a concentration of 50.12 µg/mL in HepG2, increasing viability from 100% (control) to 114%. The exact concentration decreased

viability in Caco-2 from 100% (control) to 87%; no change in viability was observed in Hek-293. Between 50.12-1000 $\mu\text{g/mL}$, no significant change in viability was observed across all three cell lines. However, a sharp decrease in cell viability was observed in Caco-2 and HepG2 after 1000 $\mu\text{g/mL}$.

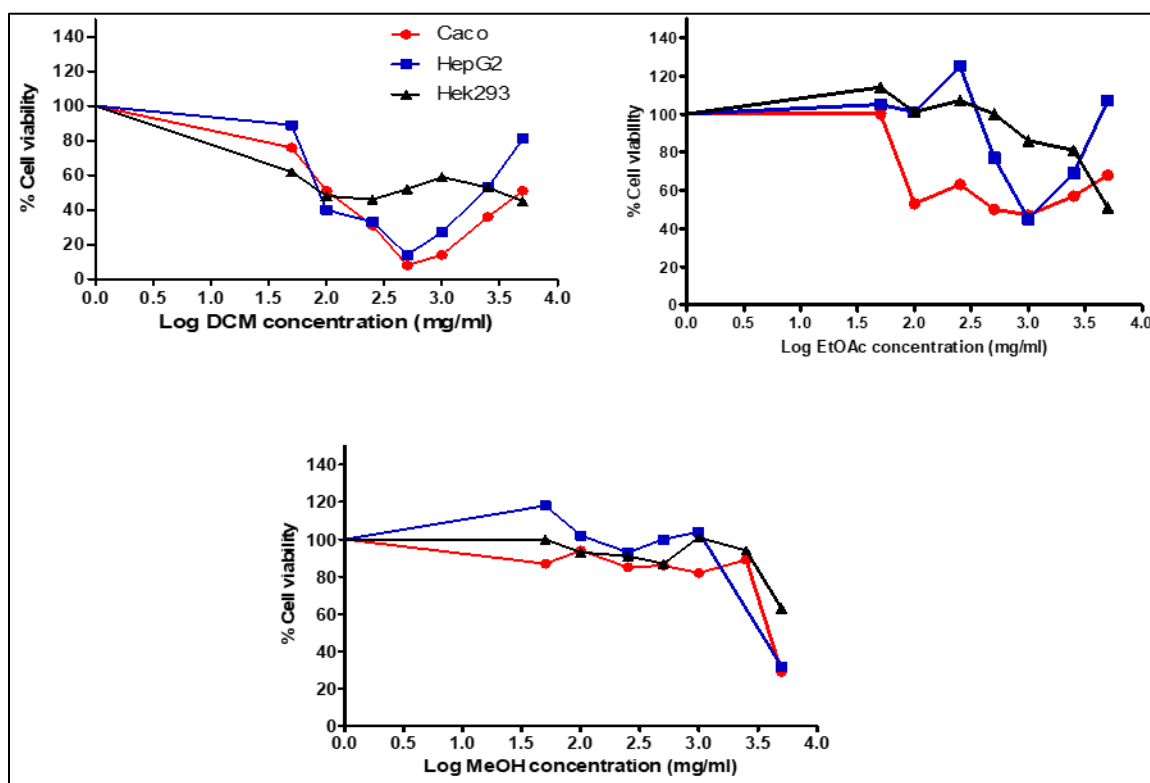


Figure 6.4: MTT graphs; Effect of different concentrations of *H. acutatum* extracts on the viability of three cell lines; Caco-2, HepG2 and Hek293.

DCM - dichloromethane, EtOAc - ethyl acetate, and MeOH - methanol.

LDH release assay

The quantification of LDH released was used to determine cytotoxicity and necrosis. IC_{80} and IC_{50} concentrations of the DCM extract (Figure 6.5) increased LDH released by 1.27 and 1.38-fold in Caco-2; 1.33 and 1.35-fold decrease ($P < 0.05$) was observed for HepG2; 1.06 and 1.04-fold

increase for Hek-293 cell lines. Treatment with IC₈₀ and IC₅₀ concentration of the EtOAc extract caused a 1.36 and 1.65-fold increase ($P < 0.05$) in LDH released in Caco-2; 2.0-fold decrease for IC₈₀ and 1.14-fold increase for IC₅₀ in HepG2; and 1.67 and 1.61-fold decrease ($P < 0.05$) in Hek-293 cell lines. A 1.22 and 1.93-fold increase in LDH released was observed in Caco-2 after exposure to IC₈₀ and IC₅₀ concentrations of the MeOH extract; a 1.20 and 1.14-fold decrease was observed for HepG2 at IC₈₀ and IC₅₀ treatments, and a 1.49-fold decrease for IC₈₀ treatment and 1.22-fold increase for IC₅₀ treatment was observed for Hek-293.

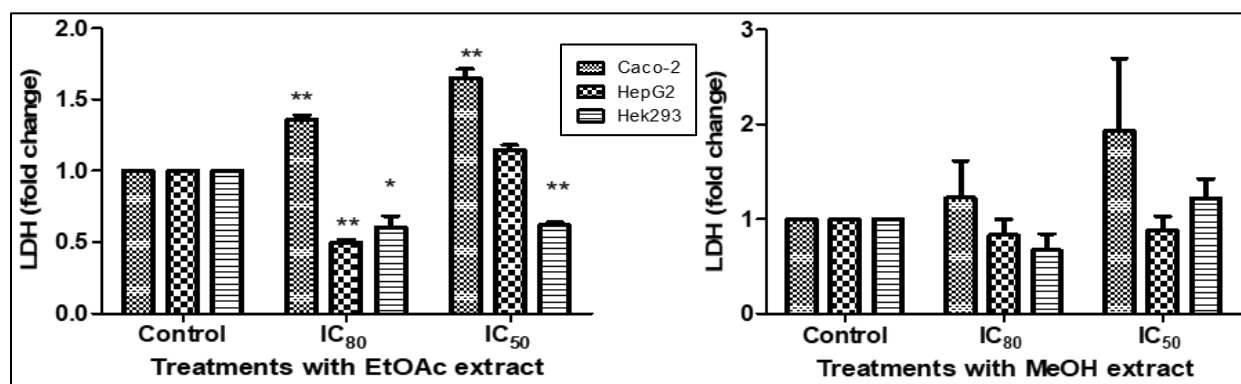


Figure 6.5: LDH graphs; Effect of IC₈₀ and IC₅₀ concentrations of *H. acutatum* extracts on the plasma membrane of Caco-2, HepG2 and Hek-293 cell lines.

DCM - dichloromethane, EtOAc - ethyl acetate, and MeOH - methanol.

Mitochondrial membrane potential (MMP) assay

Depolarization of the mitochondria that leads to the release of pro-apoptotic proteins was probed using JC-10 dye. Exposure of the different cell lines to the IC₈₀ and IC₅₀ values of the DCM extract (Figure 6.6) showed a 1.35 and 1.33-fold decrease ($P < 0.05$) in mitochondrial membrane potential in Caco-2, 1.42 and 1.82-fold increase ($P < 0.05$) in HepG2, and 1.09 and 2.22-fold increase ($P < 0.05$) in Hek-293 cell lines.

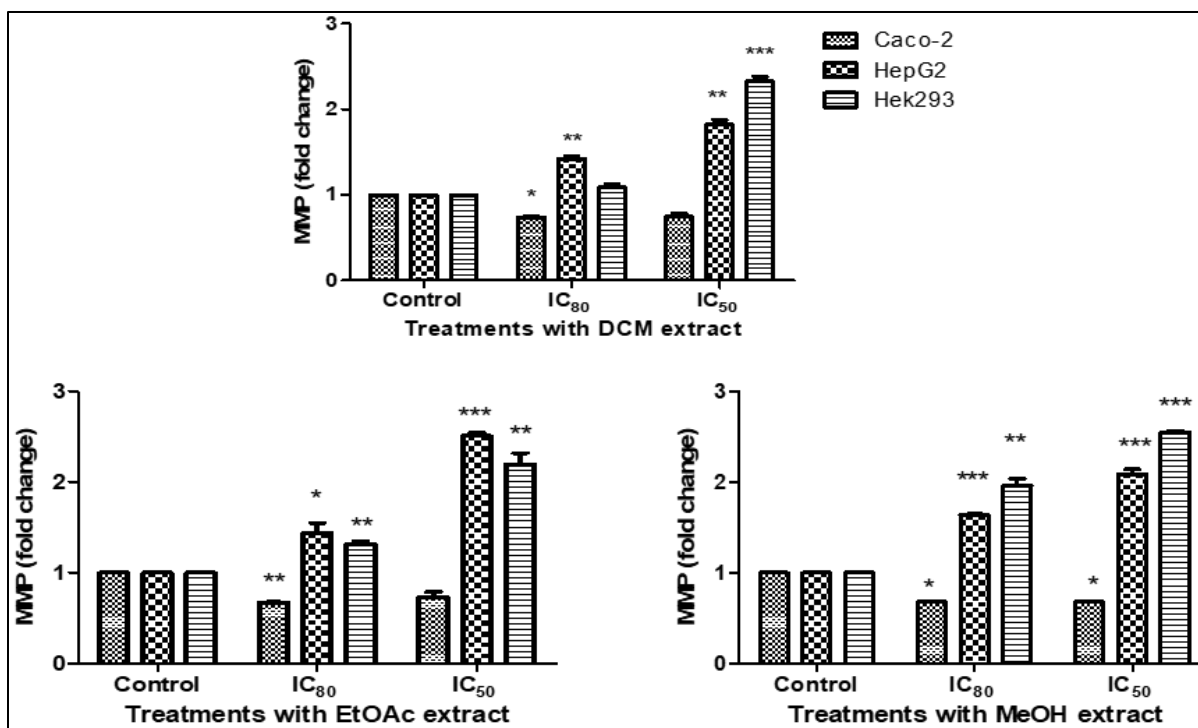


Figure 6.6: MMP graphs; Effect of IC₈₀ and IC₅₀ concentrations of *H. acutatum* extracts on the mitochondrial membrane potential of Caco-2, HepG2 and Hek-293 cell lines.

DCM - dichloromethane, EtOAc - ethyl acetate, and MeOH - methanol.

Treatment with IC₈₀ and IC₅₀ concentrations of the EtOAc extract resulted in 1.49 and 1.34-fold decrease ($P < 0.05$) in Caco-2, 1.44 and 2.51-fold increase ($P < 0.05$) in HepG2, and 1.32 and 2.33-fold increase ($P < 0.05$) in Hek-293 cell lines. The IC₈₀ and IC₅₀ values of the MeOH extract caused a 1.47-fold decrease ($P < 0.05$) for Caco-2, 1.64 and 2.09 increase in HepG2, and 1.96 and 2.55-fold increase ($P < 0.00001$) in Hek-293 cell lines. Treatment with the MeOH extract produced similar results to the EtOAc extract. The general trend was a decrease in mitochondrial membrane potential in Caco-2 and an increase in HepG2 and Hek-293 cell lines for all tested samples.

ATP assay

The amount of intracellular energy (ATP) was used to quantify cell viability and mitochondrial function. ATP was increased by 1.14-fold in Caco-2 after exposure to the IC₈₀ value of the DCM extract (Figure 6.7), but decreased by 1.72-fold ($P < 0.05$) with the IC₅₀ treatment. For the same extract, a 1.20 and 1.67-fold decrease was observed in HepG2 with the IC₈₀ and IC₅₀ treatments respectively, while a 3.25 and 1.79-fold increase ($P < 0.05$) was observed in Hek-293 cell lines.

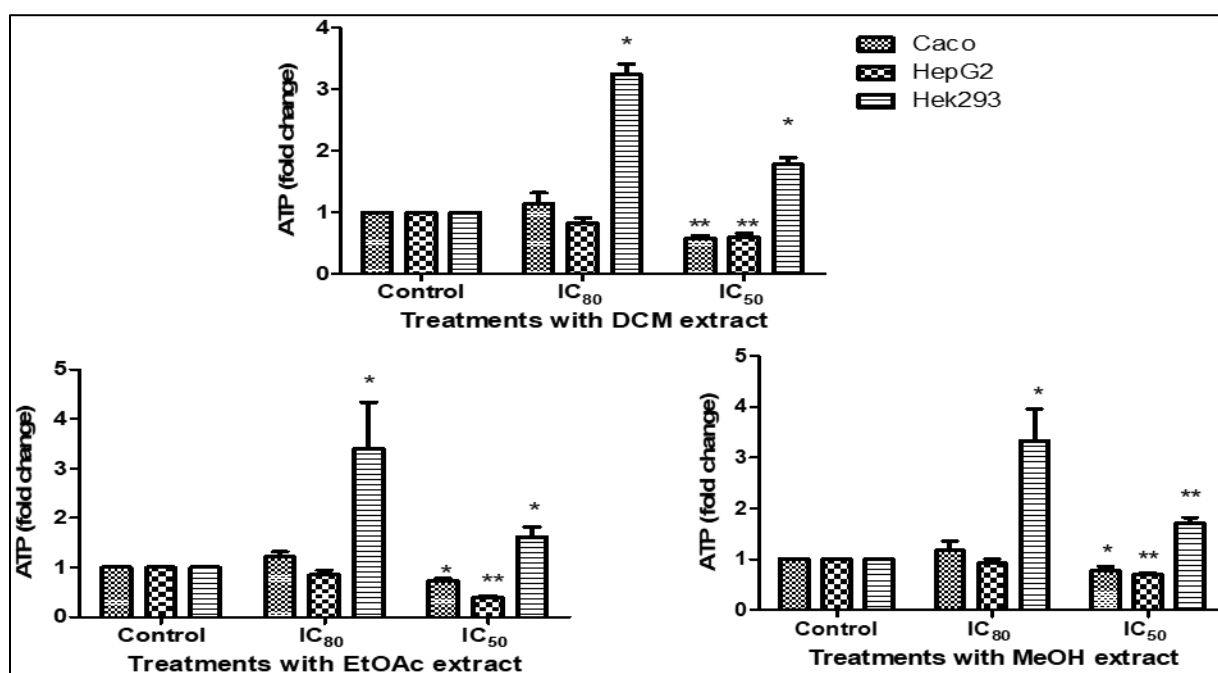


Figure 6.7: ATP graphs. Effect of IC₈₀ and IC₅₀ concentrations of *H. acutatum* extracts on ATP levels of Caco-2, HepG2 and Hek-293 cell lines.

DCM - dichloromethane, EtOAc - ethyl acetate, and MeOH - methanol.

Treatment with IC₈₀ and IC₅₀ concentrations of the EtOAc extract increased ATP by 1.22-fold and decreased it by 1.39-fold ($P < 0.05$) in Caco-2, respectively. In HepG2, a 1.18 and 2.56-fold decrease in ATP was observed at IC₈₀ and IC₅₀ concentrations of the EtOAc extract, respectively. In contrast, there was a 3.40 and 1.62-fold increase ($P < 0.05$) in Hek-293 at IC₈₀ and IC₅₀ values,

respectively. Exposure to IC₈₀ concentration of the MeOH extract increased ATP by 1.17-fold in Caco-2 cell, and decreased it by 1.28-fold ($P < 0.05$) at the IC₅₀ concentration. ATP was decreased by 1.09 and 1.43-fold in HepG2 cell lines at IC₈₀ and IC₅₀ values of MeOH extract, while a 3.32 and 1.71-fold increase was observed in Hek-293, respectively.

6.4 DISCUSSION

The phytochemical investigation of the roots of *H. acutatum* led to the isolation of a sterol (stigmasterol) (Habib et al., 2007), a sterol glucoside (stigmasterol glucoside) (Khatum et al., 2012) and a phenolic compound (caffeic acid) (Jeong et al., 2011). Diterpenes, chalcones and phloroglucinol have been reported from the roots and aerial parts of *H. acutatum* but these three compounds have not previously been isolated from the plant (Bohlman and Abraham, 1979). Caffeic acid is naturally present in many fruits and this compound and its derivatives have been known to possess antioxidant, anticancer and antibacterial activities. These activities are mainly attributed to the free phenolic acid that has high bioavailability and good water solubility, the position of the OHs in the catechol moiety and the double bond in the carbonic chain (Espindola et al., 2019)

This study showed *H. acutatum* to have relatively good antioxidant activity compared to the standards. The strong antioxidant activity demonstrated by the EtOAc extract could be due to the presence of caffeic acid, which has been reported to be a good free radical scavenger (Magnani et al., 2004). Other *Helichrysum* species reported to have good antioxidant activity include *H. longifolium* that demonstrated good radical scavenging activity (Aiyegoro and Okoh, 2010), *H. teretifolium*, and *H. arenarium* (Popoola et al., 2015).

H. acutaum demonstrated poor antibacterial activity. Our results are consonant with the findings for the chloroform extract from *H. acutatum* by Lourens et al., (2011) that demonstrated low antibacterial activity against Gram-positive bacteria, and yeast strains, and the acetone extracts from *H. acutatum*, *H. glomeratum* and *H. pilosellum* that showed no effect against both Gram-negative and Gram-positive bacteria (Matheka and Meyer, 1998). However, some plants in the genus have shown promising antimicrobial activity such as the acetone extract from *H. candolleanum*, *H. herbaceum*, *H. melanacme*, *H. psilolepis*, *H. rugulosum*, *H. simillimum* and *H. umbraculigerum* that significantly inhibited microorganism proliferation with MIC values of 0.10 mg/mL ((Kutluk et al., 2018; Maheka and Meyer, 1998). In addition, *H. caespitosum* showed good activity against four WHO *N. gonorrhea* strains (F, O, N, G) within the range 0.037-0.33 mg/ mL (Mamabolo et al., 2018).

The cytotoxicity of the plant extracts using the MTT assay showed that they are less toxic against the two tumor cell lines (Caco-2 and HepG2), and the normal cell line (Hek-293) with IC₅₀ values within the range of 126-4533 µg/mL and 165-4719 µg/mL for Caco-2 and HepG2 cell lines, respectively. A previous study showed the chloroform: methanol extract (1:1) of *H. acutatum* to have cytotoxic activity against the cancerous cell line, MCF-7 (Lourens et al., 2011). This shows the selective cytotoxicity of *H. acutatum*. Plants in the genus that demonstrated good cytotoxic activity include *H. petiolare* that was cytotoxic to B16F10 and MeWo skin melanoma cell lines in a dose dependent manner (Sagbo and Otang-Mbeng, 2020). The results from our study suggest that *H. acutatum* is potentially safe for human consumption due to its low cytotoxicity towards the normal cell line tested. Despite showing relatively good antioxidant activity, the EtOAc extract demonstrated poor cytotoxic activity towards the two tumor cell lines tested. This contrasts with the results obtained for the EtOAc extract of the flowers of *H. plicatum* that showed good

antioxidant activity and cytotoxicity against K562 and PC3 cell lines with IC₅₀ values of 25.9 and 39.2 µg/mL, respectively (Bigovic et al., 2011).

Mitochondria have been known to play an important role in the maintenance of cell health and could be used to monitor cell viability (Sivandzade et al., 2019). A decrease in the mitochondrial membrane potential has been reported to be the first step in apoptosis, and apoptosis has been reported to require an increase in energy (Zamaraeva, 2005). In cytotoxicity evaluations, cells either undergo an apoptotic or necrotic death (Leist et al., 1997). In necrosis, cells swell, lose membrane integrity, and release their intracellular content into the external environment. LDH, a soluble enzyme found in the cell cytoplasm, is released when the cell membrane is compromised. The amount of LDH released can be used to quantify cell death.

Table 6.1: Results obtained for the cytotoxicity assays (LDH, MMP and ATP) after treatment with the IC₈₀ and IC₅₀ concentrations of the extracts (DCM, EtOAc and MeOH) using the cell lines, Caco-2, HepG2 and Hek-293.

Cell Lines	Assay	Extracts at IC ₈₀ concentration			Extracts at IC ₅₀ concentration		
		DCM	EtOAc	MeOH	DCM	EtOAc	MeOH
Caco-2	<i>LDH</i>	increase	increase	increase	increase	increase	increase
	<i>MMP</i>	decrease	decrease	decrease	decrease	decrease	decrease
	<i>ATP</i>	increase	increase	increase	decrease	decrease	decrease
HepG2	<i>LDH</i>	decrease	decrease	decrease	decrease	increase	decrease
	<i>MMP</i>	increase	increase	increase	increase	increase	increase
	<i>ATP</i>	decrease	decrease	slight decrease	decrease	decrease	decrease
Hek-293	<i>LDH</i>	no change	decrease	decrease	no change	decrease	increase
	<i>MMP</i>	decrease	increase	increase	increase	increase	increase
	<i>ATP</i>	increase	increase	increase	increase	increase	increase

LDH - Lactate dehydrogenase, MMP – Mitochondrial membrane potential, ATP - Adenosine triphosphate;

DCM – Dichloromethane, EtOAc – Ethyl acetate, MeOH - Methanol

At the IC₈₀ concentrations, all three extracts showed an increase in LDH release, a decrease in the mitochondrial membrane potential and increased ATP levels in Caco-2 cell lines (Table 6.1). While at the IC₅₀ concentrations, increase in LDH release, decrease in mitochondrial membrane potential, and decrease in ATP levels were observed for the same cell lines (Table 6.1). Generation of ATP takes place in the mitochondria, a disruption in mitochondrial membrane potential could lead to depletion of intracellular ATP and this was the case after treatment of Caco-2 tumor cell lines with IC₅₀ concentrations of the tested extract. These changes are concentration dependent and depletion of cellular ATP has been shown to switch cell death from apoptosis to necrosis. Apoptosis is a programmed cell death that requires energy (ATP), while necrosis is accidental cell death that does not require energy (Leist et al. 1997). The effect of concentration on the mode of cell death was observed when MCF-7 was treated with the aqueous extract of *Lepidium sativum* extracts; apoptosis was induced in the cell when treated with 25 and 50% of the extract but at a higher concentration of 75%, necrosis was induced (Mahassni and Al-Reemi, 2013). At both concentrations, the plasma membrane was disrupted leading to the release of LDH in Caco-2 cell lines. The high increase in LDH release observed for some extracts, is an indication of the extent of membrane damage, while those with slight increases in the release of LDH indicates minimal membrane damage.

Exposure of HepG2 cell lines to the IC₈₀ and IC₅₀ concentrations of the different extracts caused no depolarization in mitochondrial membrane potential nor was the plasma membrane disrupted but a depletion in ATP levels were observed. The cytotoxic activity of the extract towards HepG2 was through depletion of intracellular energy without effect on the plasma membrane.

From the results obtained, it is evident that the plant possesses the ability to initiate both apoptotic and necrotic cell death, depending on the concentration and the cell lines. Some plant extracts that

have decreased mitochondrial membrane potential with subsequent release of cytochrome c for apoptotic pathway initiation are *Murraya koenigii*, *Annona reticulate*, *Moringa oleifera*, *Hibiscus sabdariffa*, *Lablab purpureus*, and *Euphorbia hirta* (Verma and Singh, 2020).

6.5 CONCLUSION

Three compounds were successfully isolated from the roots of *H. acutatum* and this study is the first report of these compounds from the plant. The findings show *H. acutatum* extracts to have better antioxidant activity compared to antibacterial and anticancer activity for the microbes and cell lines tested, respectively. This study has been able to establish a toxicity profile and scientific basis for the use of *H. acutatum* as an antioxidant in traditional medicine and confirms its safety for human consumption. The study also highlights the lack of antibacterial activity of the species compared to others in the genus, which are well known for their use in traditional medicine in treating different infectious diseases.

REFERENCES

- Aiyegoro, O. A., & Okoh, A. I. (2010). Preliminary phytochemical screening and *In vitro* antioxidant activities of the aqueous extract of *Helichrysum longifolium* DC. *BMC COMPLEMENTARY AND ALTERNATIVE MEDICINE*, 10,21. doi:10.1186/1472-6882-10-21.
- Bigović, D., Savikin, K., Janković, T., Menković, N., Zdunić, G., Stanojković, T., & Djurić, Z. (2011). Antiradical and cytotoxic activity of different *Helichrysum plicatum* flower extracts. *NATURAL PRODUCT COMMUNICATIONS*, 6(6), 819–822.
- Bohlmann, F., Abraham, W.-R., 1979c. Neue Diterpene aus *Helichrysum acutatum*. *PHYTOCHEMISTRY* 18, 1754–1756.
- Espíndola, K., Ferreira, R. G., Narvaez, L., Silva Rosario, A., da Silva, A., Silva, A., Vieira, A., & Monteiro, M. C. (2019). Chemical and pharmacological aspects of caffeic acid and its activity in hepatocarcinoma. *FRONTIERS IN ONCOLOGY*, 9, 541. doi:10.3389/fonc.2019.00541
- Fernandes, R. P., Trindade, M. A., Tonin, F. G., Lima, C. G., Pugine, S. M., Munekata, P. E., Lorenzo, J. M., & de Melo, M. P. (2016). Evaluation of antioxidant capacity of 13 plant extracts by three different methods: cluster analyses applied for selection of the natural extracts with higher antioxidant capacity to replace synthetic antioxidant in lamb burgers. *JOURNAL OF FOOD SCIENCE AND TECHNOLOGY*, 53(1), 451–460. doi:10.1007/s13197-015-1994-x.
- Habib M. R., Nikkon, F., Rahman, M., Haque, M. E., & Karim, M. R. (2007) Isolation of stigmasterol and beta-sitosterol from methanolic extract of root bark of *Calotropis gigantea* (Linn). *PAKISTAN JOURNAL OF BIOLOGICAL SCIENCES: PJBS*. 10(22), 4174-4176. DOI:10.3923/pjbs.2007.4174.4176.

- Hayyan M., Hashim M. A., Al-Nashef I. M. (2016). Superoxide ion: Generation and chemical implications. *CHEMICAL REVIEWS*. 116 (5), 3029–85.
- Hilliard, O. M. (1983). *Flora of Southern Africa, Part 7 Inuleae, Fascicle 2 Gnaphaliinae*. Government Printer, Pretoria, South Africa.
- Jakupovic, J., Kuhnke, J., Schuster, A., Metwally, M.A., Bohlmann, F., (1985). Phloroglucinol derivatives and other constituents from South African *Helichrysum* species. *PHYTOCHEMISTRY* 25, 1133–1142.
- Jeong, C. H., Jeong, H. R., Choi, G. N., Kim, D. O., Lee, U., & Heo, H. J. (2011). Neuroprotective and anti-oxidant effects of caffeic acid isolated from *Erigeron annuus* leaf. *CHINESE MEDICINE*, 6, 25. <https://doi.org/10.1186/1749-8546-6-25>.
- Khatun, M., Billah, M., & Quader, M. A. (2012). Sterols and sterol glucoside from *Phyllanthus* species. *DHAKA UNIVERSITY JOURNAL OF SCIENCE*, 60(1). doi:10.3329/dujs.v60i1.10327.
- Kutluk, I., Aslan, M., Orhan, I. E., & Özçelik, B. (2018). Antibacterial, antifungal and antiviral bioactivities of selected *Helichrysum* species. *SOUTH AFRICAN JOURNAL OF BOTANY*, 119, 252–257. doi: 10.1016/j.sajb.2018.09.009.
- Leist, M., Single, B., Castoldi, A. F., Kühnle, S., & Nicotera, P. (1997). Intracellular adenosine triphosphate (ATP) concentration: A switch in the decision between apoptosis and necrosis. *THE JOURNAL OF EXPERIMENTAL MEDICINE*, 185(8), 1481–1486. doi:10.1084/jem.185.8.1481.

- Lourens, A. C. U., Van Vuuren, S. F., Viljoen, A. M., Davids, H., & Van Heerden, F. R. (2011). Antimicrobial activity and *in vitro* cytotoxicity of selected South African *Helichrysum* species. SOUTH AFRICAN JOURNAL OF BOTANY, 77(1), 229–235. doi: 10.1016/j.sajb.2010.05.006.
- Lourens, A. C. U., Viljoen, A. M., & van Heerden, F. R. (2008). South African *Helichrysum* species: A review of the traditional uses, biological activity and phytochemistry. JOURNAL OF ETHNOPHARMACOLOGY, 119(3), 630–652. doi: 10.1016/j.jep.2008.06.011.
- Magnani, C., Isaac, V. L. B., Correa, M. A., & Salgado, H. R. N. (2014). Caffeic acid: a review of its potential use in medications and cosmetics. ANALYTICAL METHODS, 6(10), 3203–3210. doi:10.1039/c3ay41807c.
- Mahassni, S. H., & Al-Reemi, R. M. (2013). Apoptosis and necrosis of human breast cancer cells by an aqueous extract of garden cress (*Lepidium sativum*) seeds. SAUDI JOURNAL OF BIOLOGICAL SCIENCES, 20(2), 131–139. doi: 10.1016/j.sjbs.2012.12.002.
- Mamabolo, M. P., Muganza, F. M., Olivier, M. T., Olaokun, O. O., & Nemutavhanani, L. D. (2018) Evaluation of anticonorrhea activity and cytotoxicity of *Helichrysum caespitium* (DC) Harv. whole plant extracts. BIOLOGY AND MEDICINE (Aligarh) 10: 422. DOI: 10.4172/0974-8369.1000422.
- Mathekga, A. D. M., & Meyer, J. J. M. (1998). Antibacterial activity of South African *Helichrysum* species. SOUTH AFRICAN JOURNAL OF BOTANY, 64(5), 293–295. doi:10.1016/s0254-6299(15)30903-0.
- Popoola, O., Marnewick, J., Rautenbach, F., Ameer, F., Iwuoha, E., & Hussein, A. (2015). Inhibition of oxidative stress and skin aging-related enzymes by prenylated chalcones

- and other flavonoids from *Helichrysum teretifolium*. MOLECULES, 20(4), 7143–7155. doi:10.3390/molecules20047143.
- Rajendra Prasad, N., Karthikeyan, A., Karthikeyan, S., & Venkata Reddy, B. (2010). Inhibitory effect of caffeic acid on cancer cell proliferation by oxidative mechanism in human HT-1080 fibrosarcoma cell line. MOLECULAR AND CELLULAR BIOCHEMISTRY, 349(1-2), 11–19.
- Rajurkar, N. S., & Hande, S. M. (2011). Estimation of phytochemical content and antioxidant activity of some selected traditional Indian medicinal plants. INDIAN JOURNAL OF PHARMACEUTICAL SCIENCES, 73(2), 146–151. <https://doi.org/10.4103/0250-474x.91574>.
- Sagbo, I. J., & Otang-Mbeng, W. (2020). Anti-proliferative and genotoxic activities of the *Helichrysum petiolare* Hilliard & B.L. Burt. SCIENTIA PHARMACEUTICA, 88(4), 49. doi:10.3390/scipharm88040049.
- Silva, A. M. S., Alkorta, I., Elguero, J., & Silva, V. L. M. (2001). A ¹³C NMR study of the structure of four cinnamic acids and their methyl esters. JOURNAL OF MOLECULAR STRUCTURE, 595(1-3), 1–6. doi:10.1016/s0022-2860(01)00486-0.
- Sivandzade, F., Bhalerao, A., & Cucullo, L. (2019). Analysis of the mitochondrial membrane potential using the cationic JC-1 dye as a sensitive fluorescent probe. BIO-PROTOCOL, 9(1). doi:10.21769/bioprotoc.3128.
- Verma, A. K., & Singh, S. (2020). Phytochemical analysis and *in vitro* cytostatic potential of ethnopharmacological important medicinal plants. TOXICOLOGY REPORTS, 7, 443–452. <https://doi.org/10.1016/j.toxrep.2020.02.016>.

Zamaraeva, M. V., Sabirov, R. Z., Maeno, E., Ando-Akatsuka, Y., Bessonova, S. V., & Okada, Y. (2005). Cells die with increased cytosolic ATP during apoptosis: a bioluminescence study with intracellular luciferase. *CELL DEATH AND DIFFERENTIATION*, 12(11), 1390–1397. doi: 10.1038/sj.cdd.4401661.

CHAPTER SEVEN

OVERALL SUMMARY

Medicinal plants have served mankind for centuries and compounds from natural sources have served as a foundation for new inventions or leads in drug discovery. These active metabolites have either been formulated into drugs or modified for better efficacy. Research on the active constituents and biological potential of plants used in conventional medicine will help in the discovery of chemical compounds with structural diversity and enhanced biological activities that will help solve some of the health issues plaguing the earth. *Scilla nervosa*, *Helichrysum panduratum* and *Helichrysum acutatum* are three South African species commonly used in traditional medicine. They are widely sold at the Muthi market for the treatment of different ailments. The phytochemistry and biological studies of these plants were presented in this study.

Homoisoflavonoids, triterpenes and stilbenes were isolated from the bulbs and leaves of *S. nervosa*. Lanostane-type triterpenes that have been isolated from other *Scilla* species were isolated and reported for the first time. Some homoisoflavonoids and organic crude extracts of the bulbs were evaluated for their antibacterial and anticancer properties. The homoisoflavonoids demonstrated low antibacterial activity compared to other classes of flavonoids but have good anticancer activity against Caco-2 and HepG2 tumor cell lines. Synergistic effects were observed in the anticancer activity of the methanol extract of the bulbs against Caco-2 and HepG2 cell lines. Molecular docking studies on the homoisoflavonoids showed that modification of the molecular structure could improve their antibacterial potential. Modification could also improve selectively towards normal cell lines because they showed high toxicity towards normal cell lines as well as tumor cell lines.

The phytochemical investigation of the leaves and stems *H. panduratum* led to the isolation of triterpenes, a sterol and sterol glycoside, a phenol glycoside and one homoisoflavonoid. This is the first report of homoisoflavonoids from *Helichrysum* species. The homoisoflavonoid was isolated from both the polar extracts of the stem but was not found in the leaves. Our study showed that the leaves are rich in α -arbutin more than the stems. The result from the antibacterial susceptibility testing showed that the test samples did not demonstrate any notable antimicrobial activity at 400 and 800 $\mu\text{g/mL}$. The quorum sensing inhibition assay using *Chromobacterium violaceum* ATCC 12472 as a bioindicator showed that the methanol extract of the leaves was the most effective at inhibiting both short and long-chain N-acyl homoserine lactone -mediated quorum sensing. The methanol extract of the leaves also demonstrated the ability to inhibit autoinducer-2. The test samples demonstrated low or medium cytotoxicity towards Caco-2 and HepG2 tumor cell lines and high cytotoxicity towards the normal cell line, Hek-293.

Three compounds were isolated from *H. acutatum*, one of it was caffeic acid. The ethyl acetate extract showed good antioxidant activity that was comparable to reference standards. The cytotoxicity assay showed that the plant is safe for use. Other plant in the genus have demonstrated good antibacterial activity, but *H. actutaum* showed no activity towards both Gram-positive and Gram-negative bacteria.

CONCLUSION

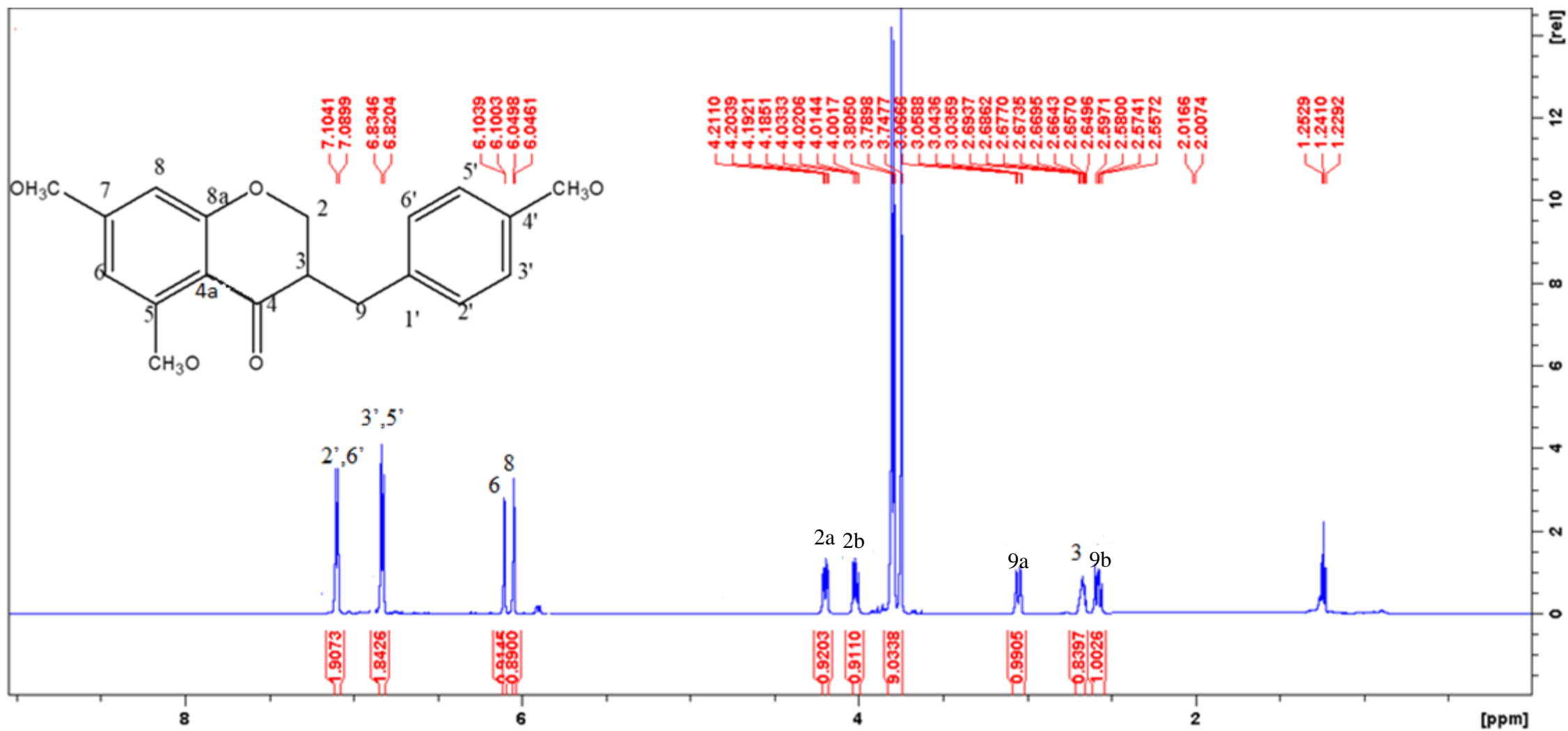
This study described the phytochemistry and biological activities of three plants used in South Africa traditional medicine, *S. nervosa*, *H. panduratum* and *H. acutatum*. Lanostane triterpenes was isolated from *S. nervosa* and reported for the first time. The homoisoflavonoids showed

potential as cytotoxic agents. Homoisoflavonoids though limited in their occurrence in nature was isolated for the first time from *H. panduratum*, which shows high diversity in secondary metabolites from this genus. The most significant finding from *H. panduratum* was the high yield of α -arbutin, a tyrosinase inhibitor, which provides a new natural source of this active biomolecule for inclusion in skincare formulations to treat hyperpigmentation. There is no record of the ethnomedicinal use of *H. acutatum* in literature. Therefore, this study provides a record and scientific justification for its use as a result of its potent antioxidant properties.

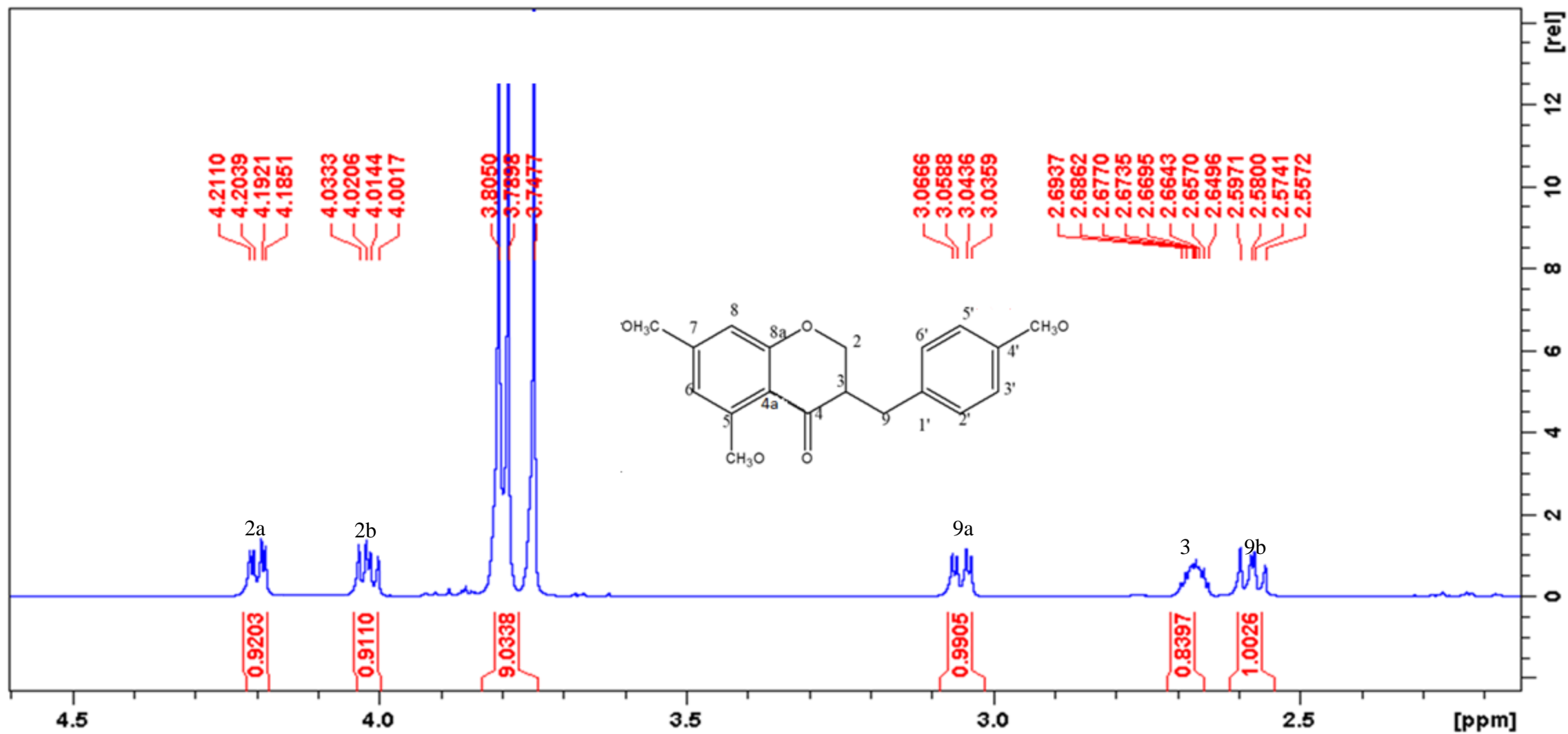
RECOMMENDATIONS FOR FUTURE WORK

- Evaluation of the anticancer properties of different homoisoflavonoids isolated from *S. nervosa* for better understanding of their structure-activity relationships.
- Phytochemical and biological study of the aerial parts of *H. acutatum* to establish a relationship between bioactive compounds present in the roots and the aerial parts of the plant.
- *H. panduratum* leaves are rich in α -arbutin; therefore, evaluation of its tyrosinase inhibitory potential is recommended as it has potential for use as a raw material of this biomolecule from a natural source.

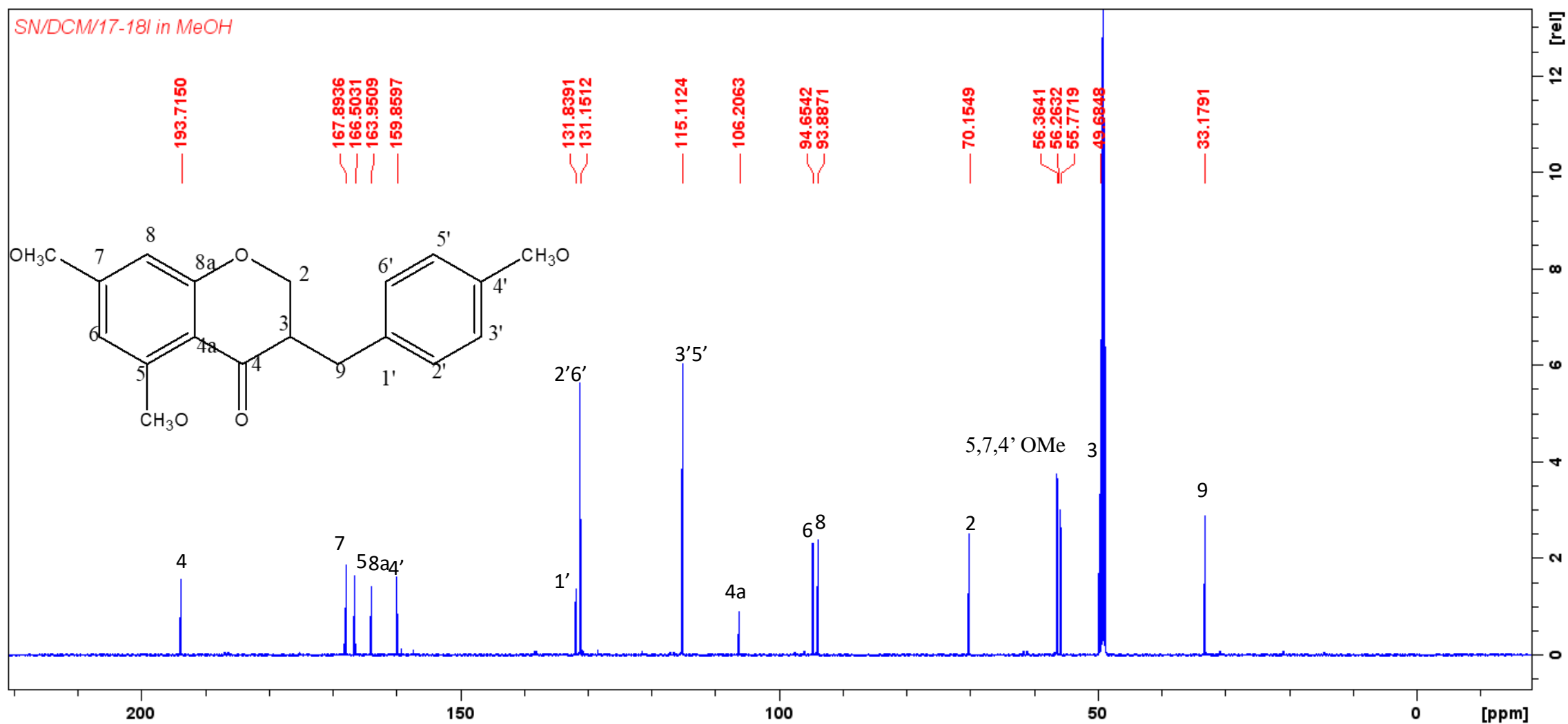
APPENDICES



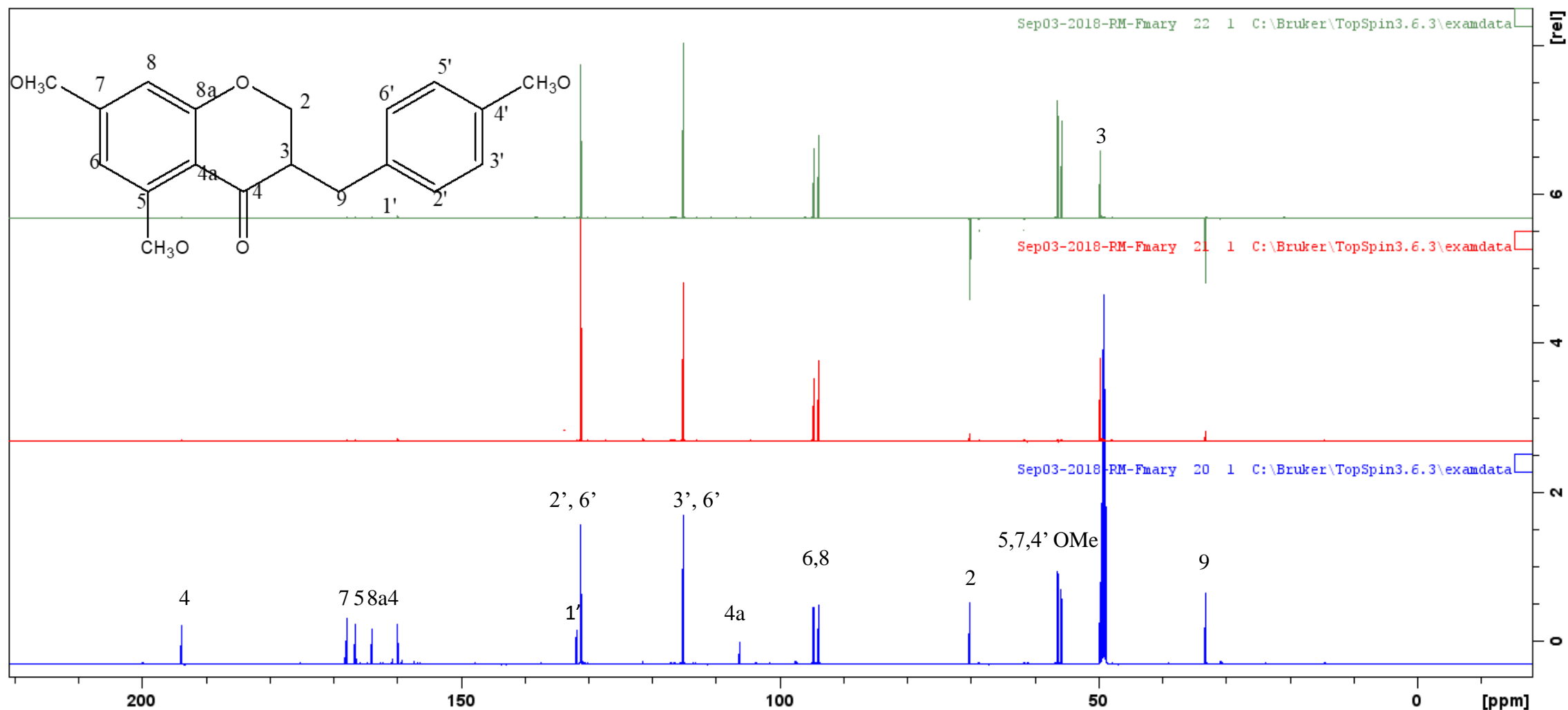
¹H NMR of compound **A1** 3-(4-methoxybenzyl)-5,7-dimethoxychroman-4-one

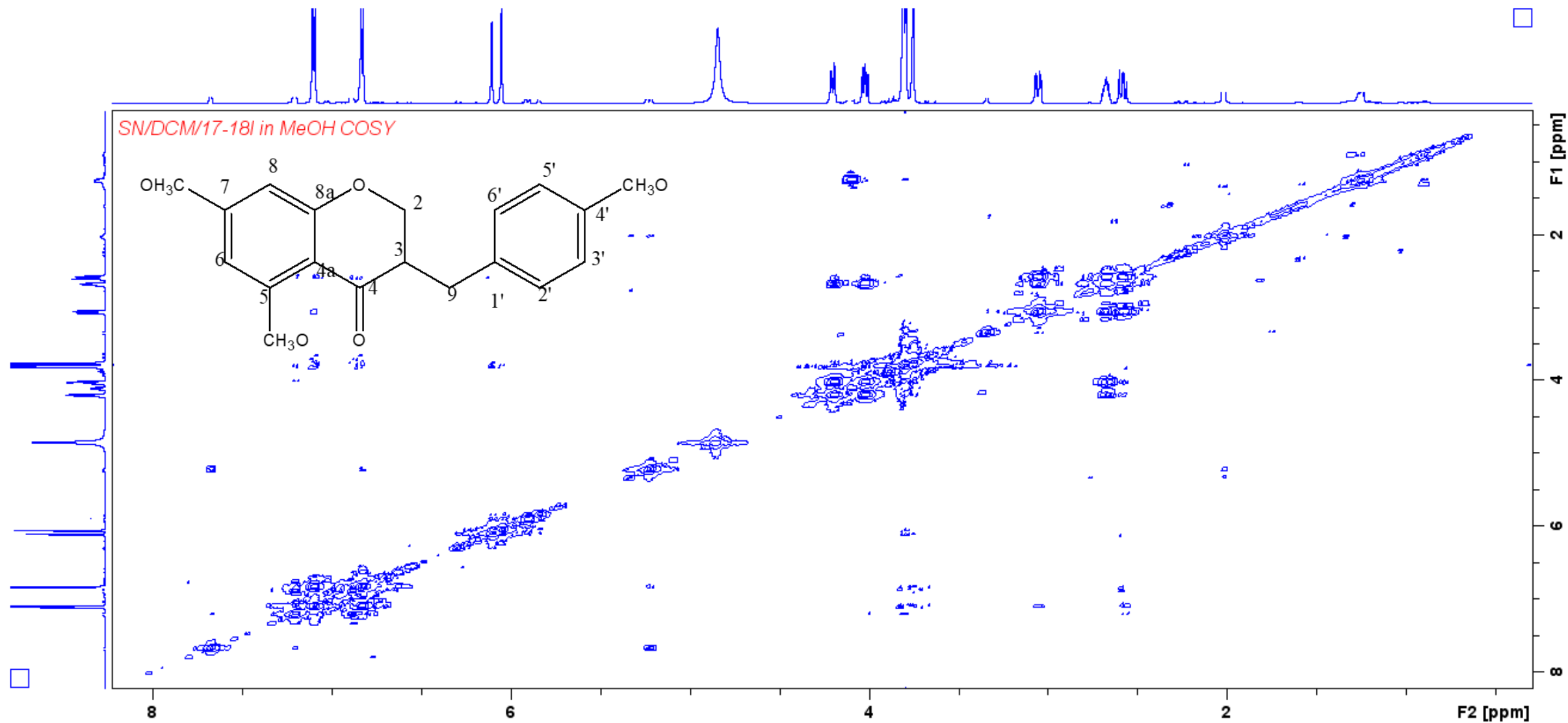


Expanded ^1H NMR of compound **A1** 3-(4-methoxybenzyl)-5,7-dimethoxychroman-4-one

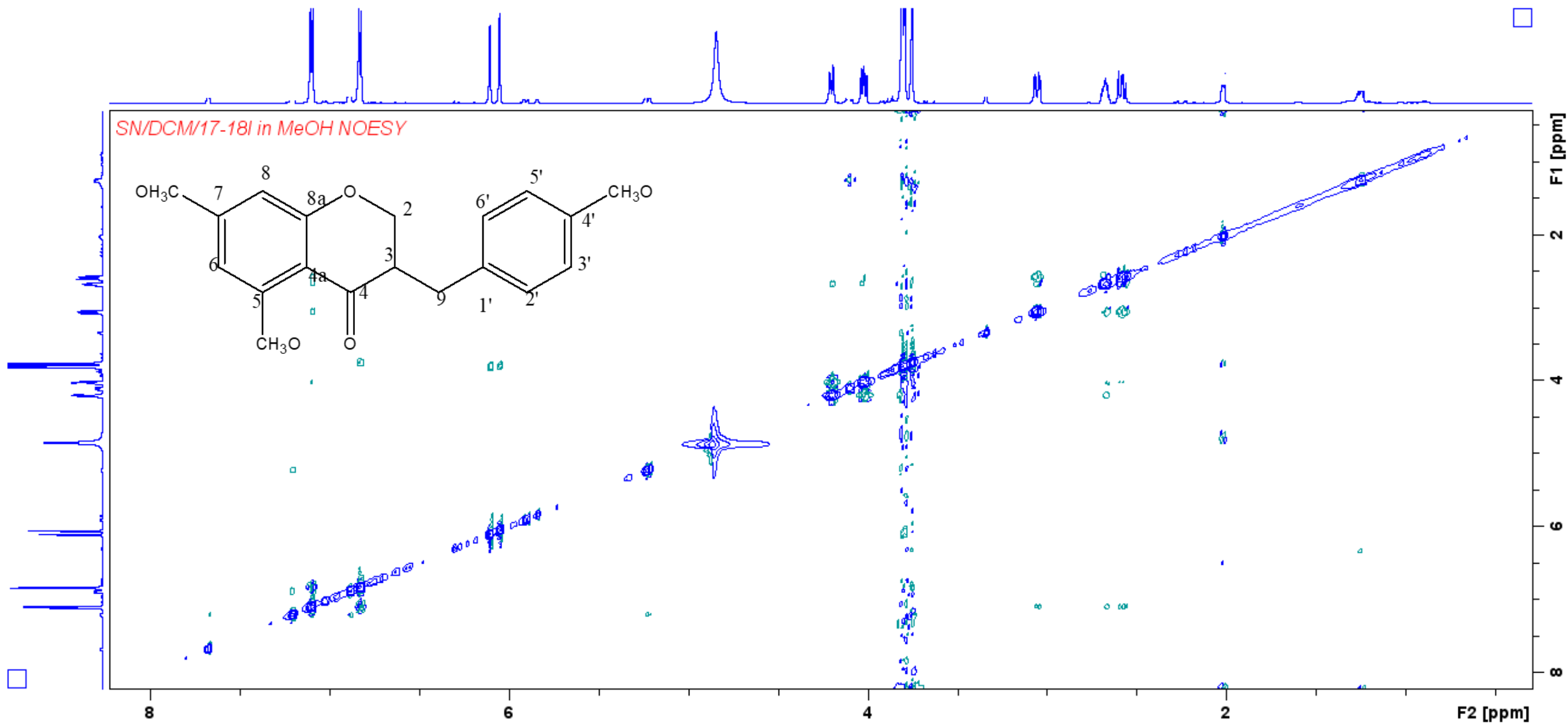


¹³C NMR of compound **A1** 3-(-4-methoxybenzyl)-5,7-dimethoxychroman-4-one

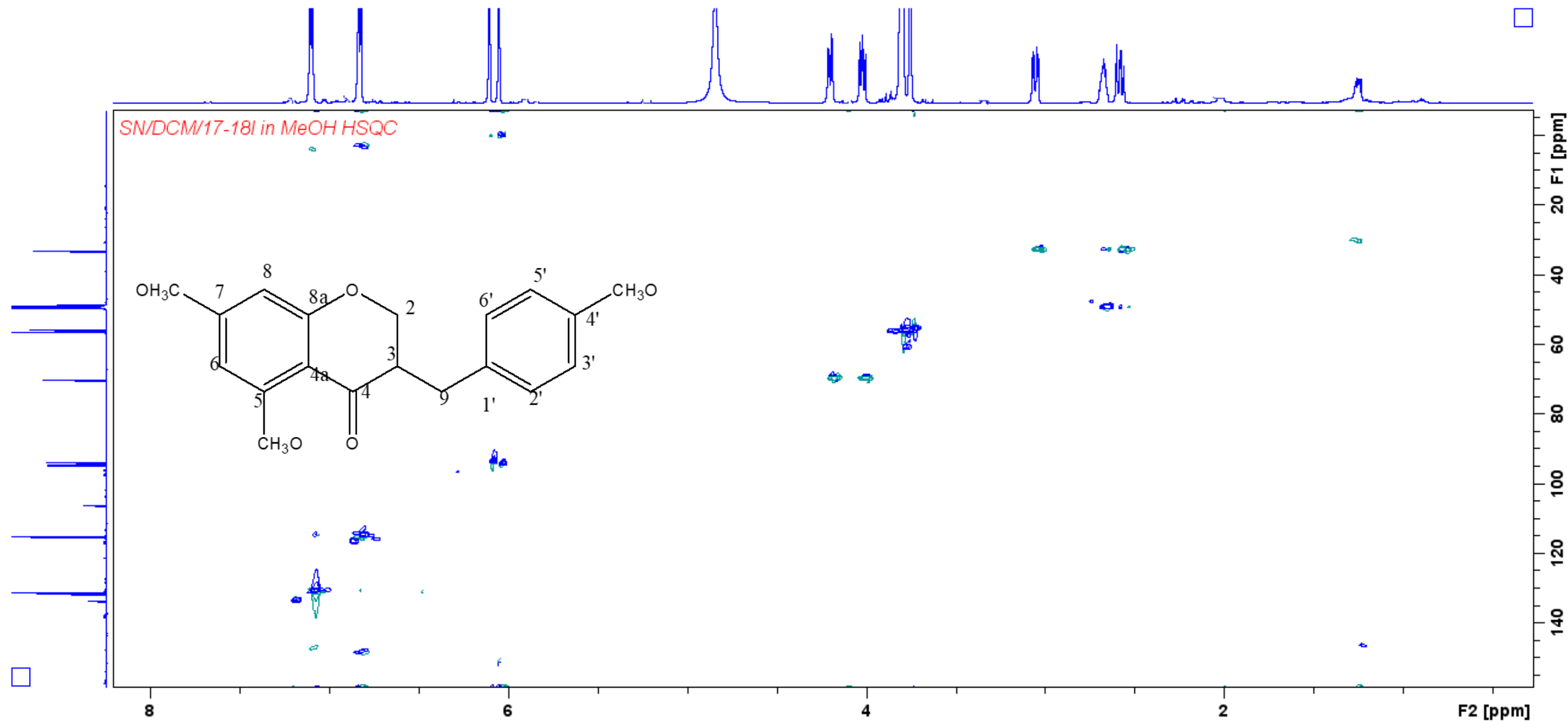
DEPT of compound **A1** 3-(-4-methoxybenzyl)-5,7-dimethoxychroman-4-one



COSY of compound **A1** 3-(4-methoxybenzyl)-5,7-dimethoxychroman-4-one



NOESY of compound **A1** 3-(4-methoxybenzyl)-5,7-dimethoxychroman-4-one



HSQC of compound **A1** 3-(4-methoxybenzyl)-5,7-dimethoxychroman-4-one

Monoisotopic Mass, Even Electron Ions

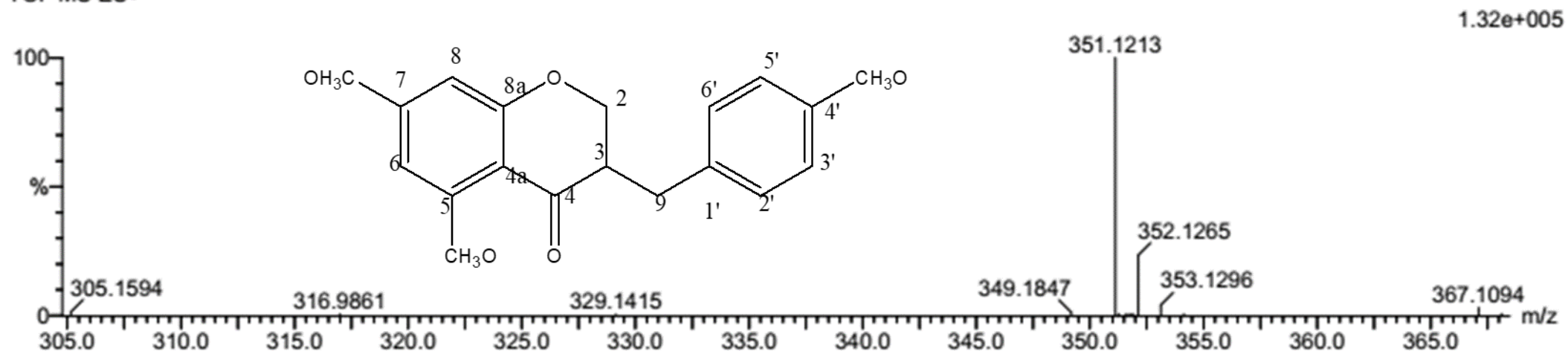
4 formula(e) evaluated with 1 results within limits (all results (up to 1000) for each mass)

Elements Used:

C: 15-20 H: 20-25 O: 0-5 Na: 1-1

SN_DCM_17-18L 2 (0.034) Cm (1:61)

TOF MS ES+



Minimum: -1.5

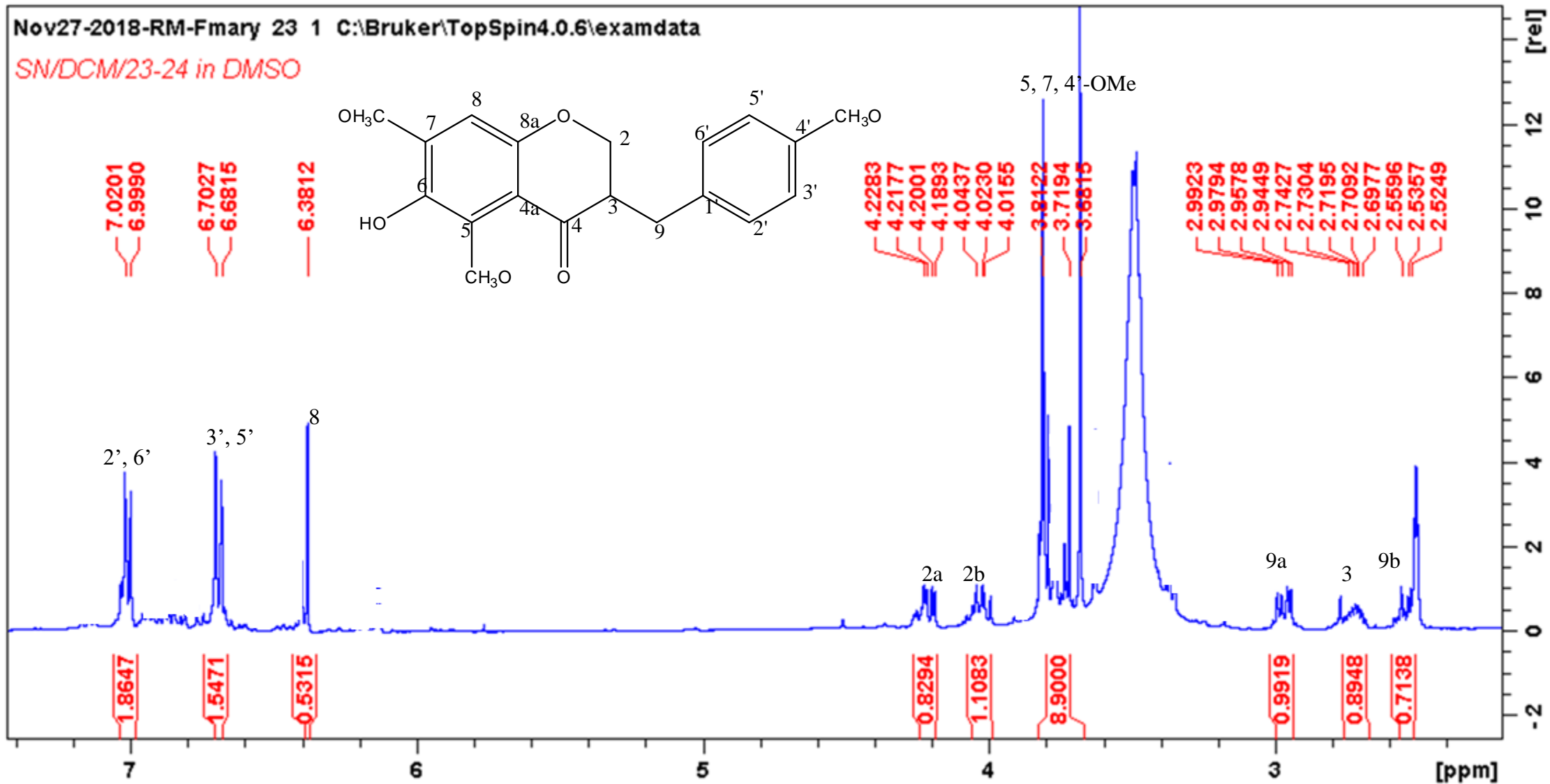
Maximum: 5.0 5.0 50.0

Mass	Calc. Mass	mDa	PPM	DBE	i-FIT	i-FIT (Norm)	Formula
351.1213	351.1208	0.5	1.4	9.5	119.1	0.0	C19 H20 O5 Na

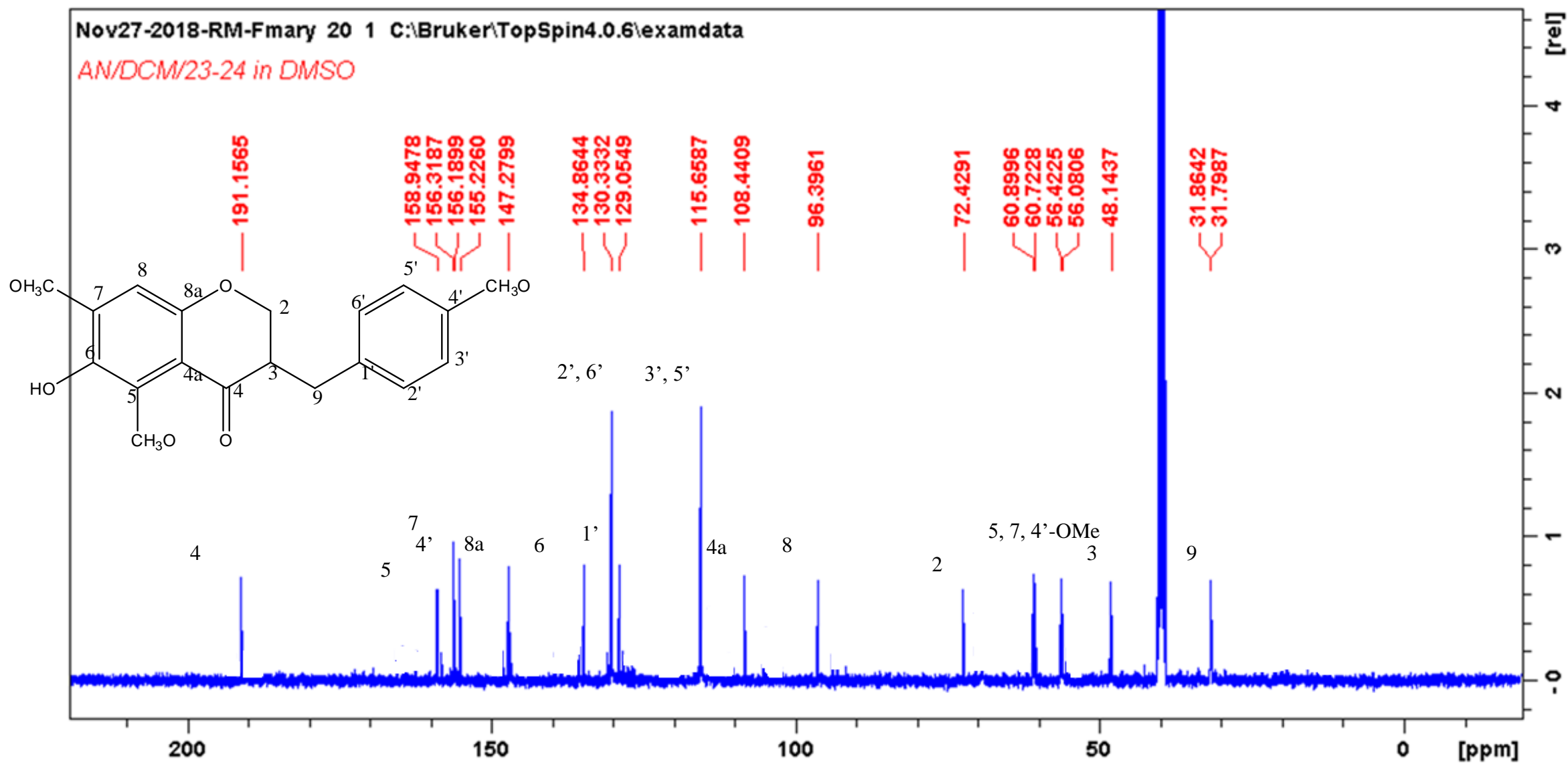
HRMS of compound **A1** 3-(4-methoxybenzyl)-5,7-dimethoxychroman-4-one



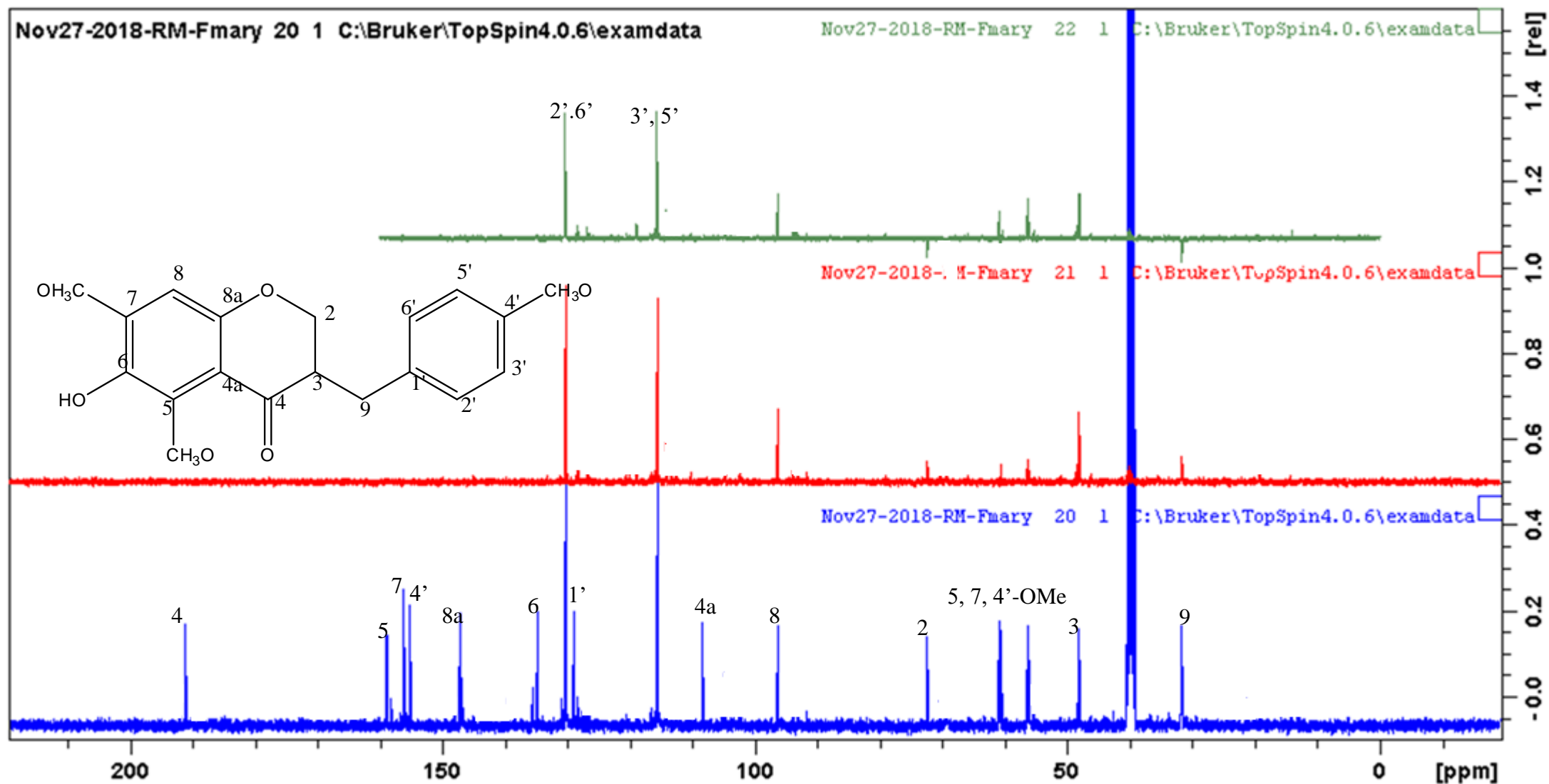
IR of compound A1 3-(4-methoxybenzyl)-5,7-dimethoxylchroman-4-one

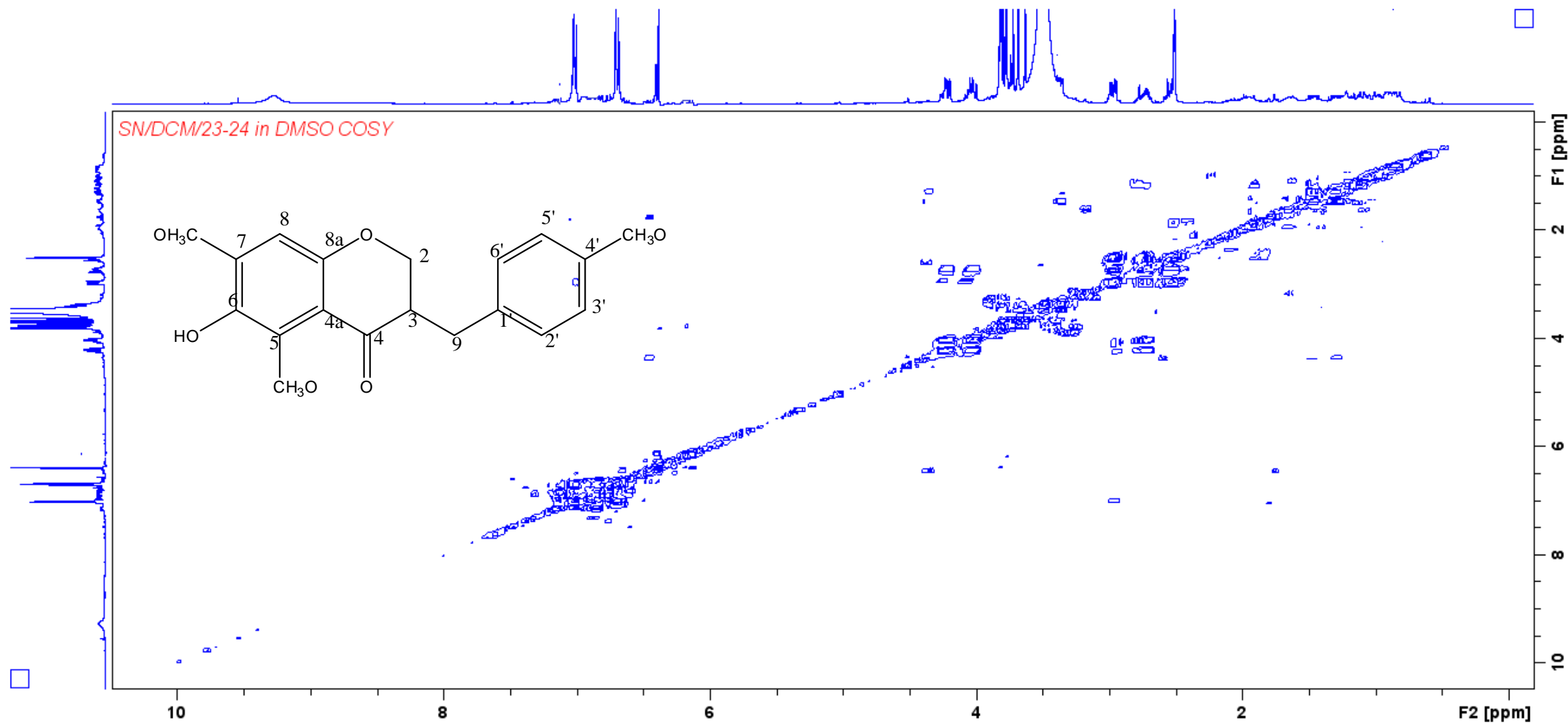


¹H NMR of compound **A2** 3-(4-methoxybenzyl)-6-hydroxy-5,7-dimethoxychroman-4-one

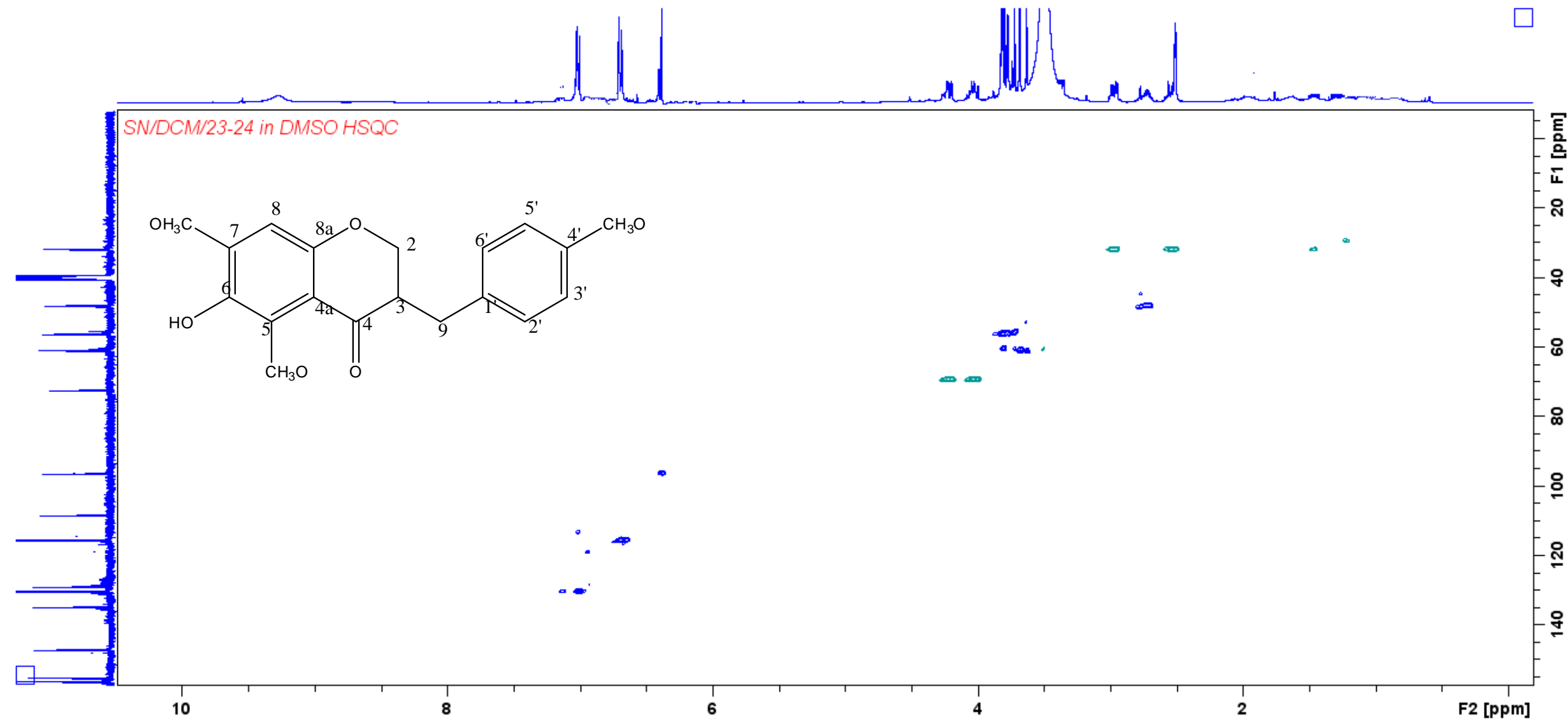


¹³C of compound **A2** 3-(4-methoxybenzyl)-6-hydroxyl-5,7-dimethoxychroman-4-one

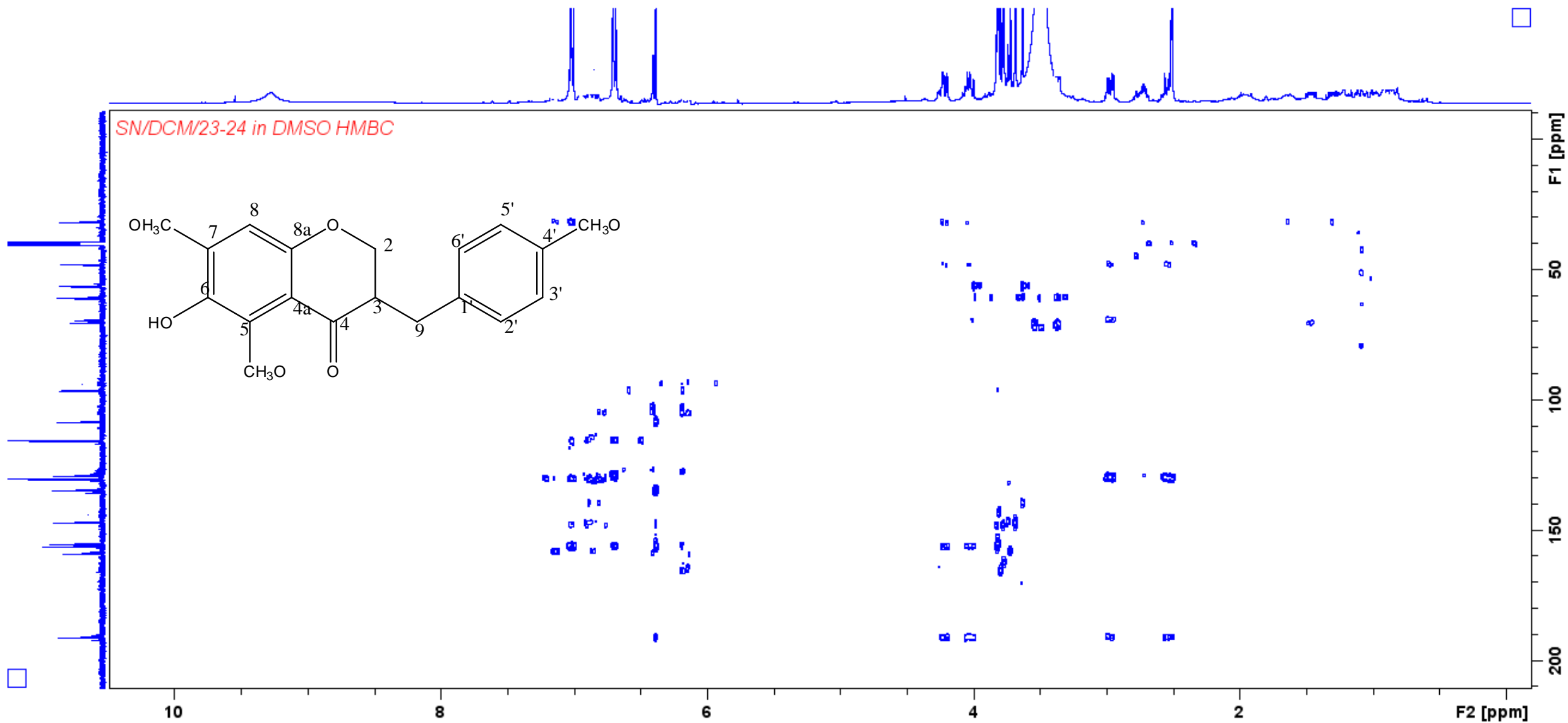
DEPT of compound **A2** 3-(4-methoxybenzyl)-6-hydroxyl-5,7-dimethoxychroman-4-one



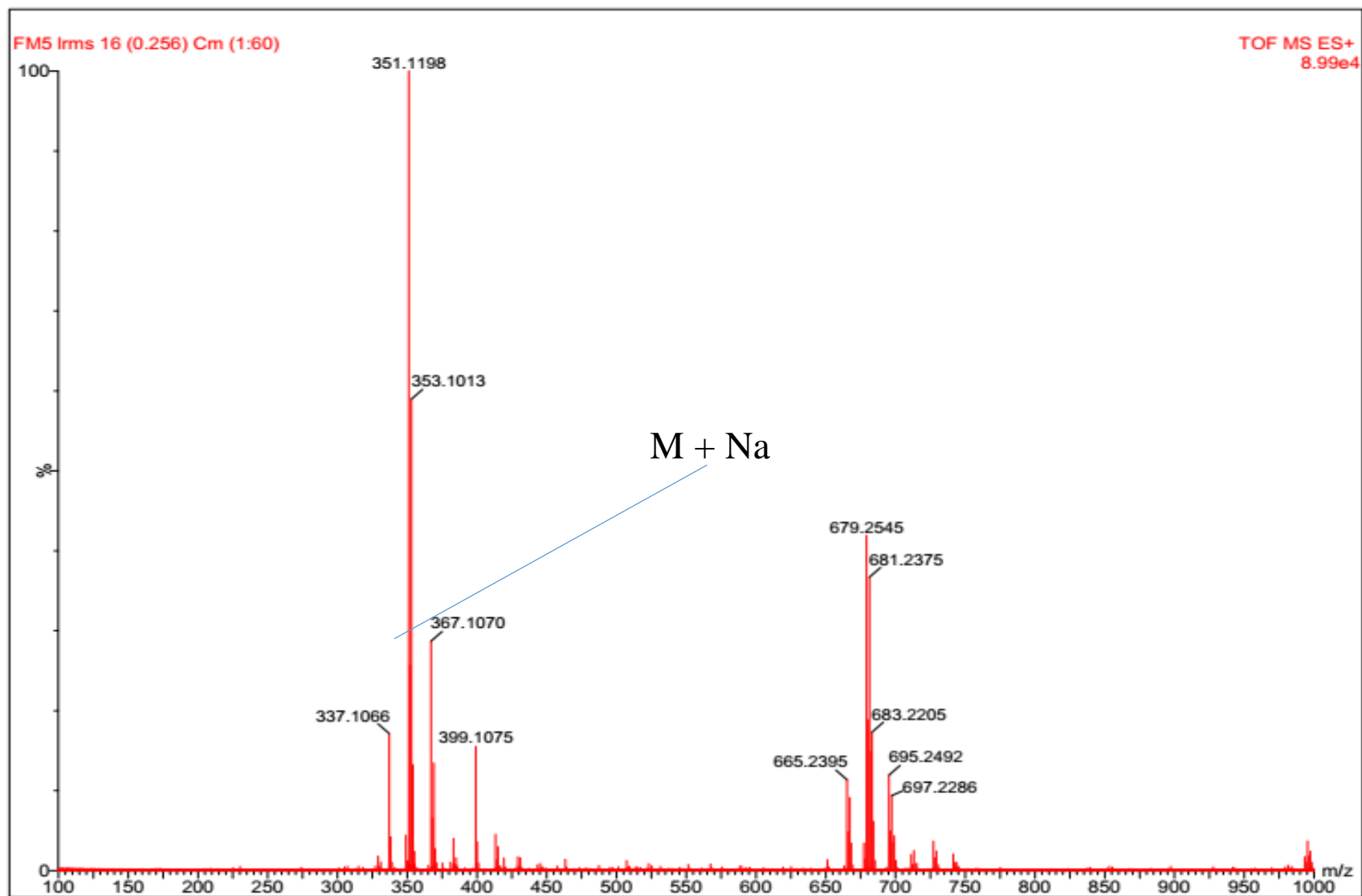
COSY of compound **A2** 3-(4-methoxybenzyl)-6-hydroxyl-5,7-dimethoxychroman-4-one



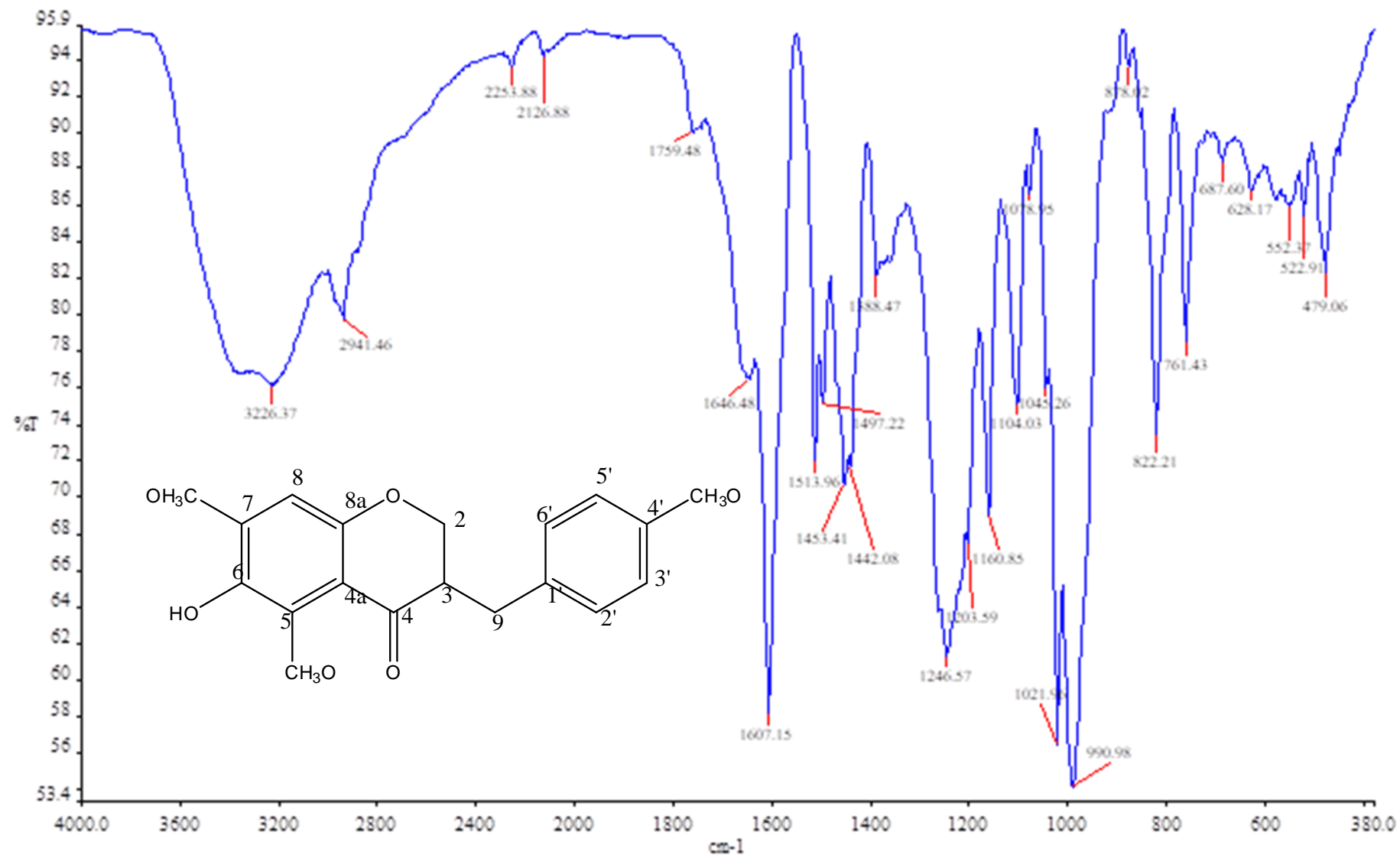
HSQC of compound **A2** 3-(4-methoxybenzyl)-6-hydroxy-5,7-dimethoxychroman-4-one



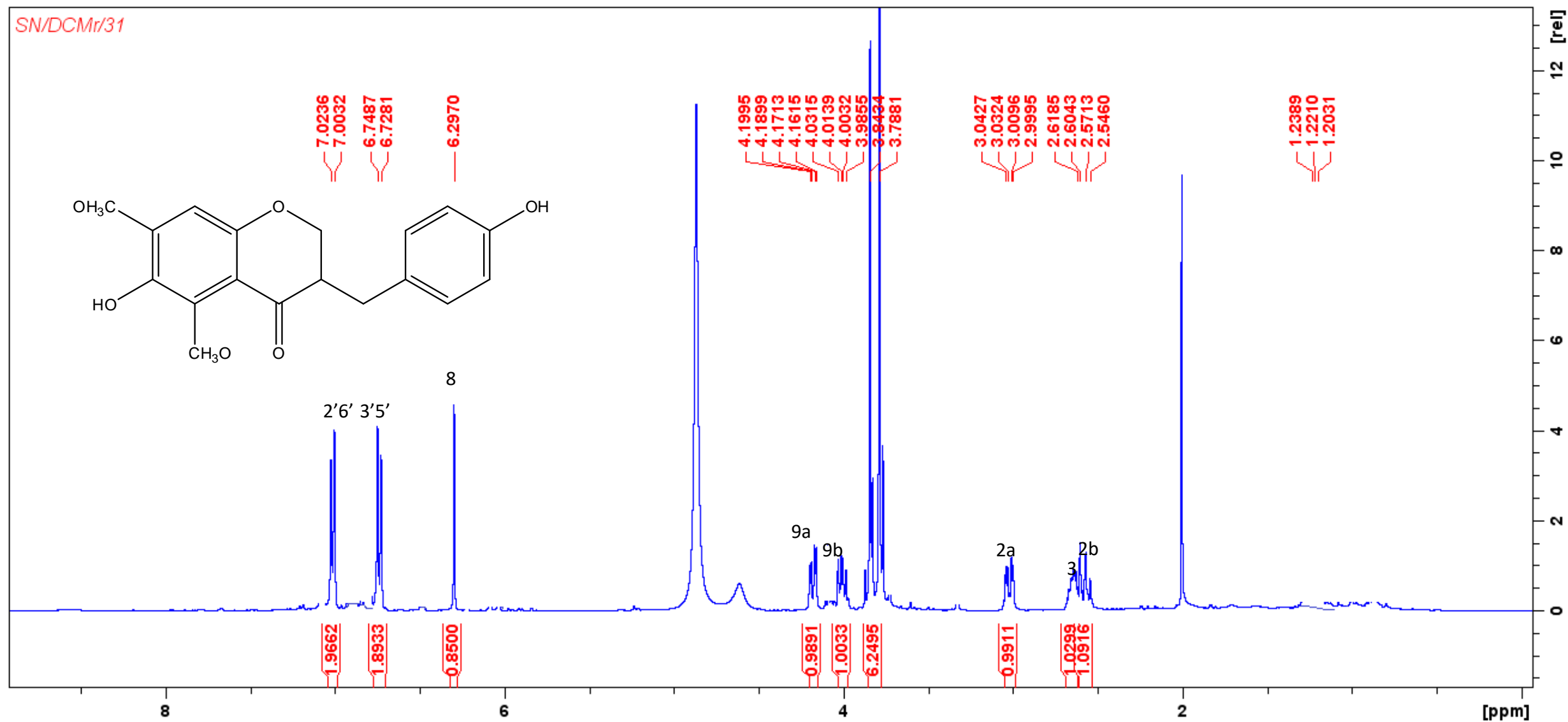
HMBC of compound **A2** 3-(4-methoxybenzyl)-6-hydroxy-5,7-dimethoxychroman-4-one



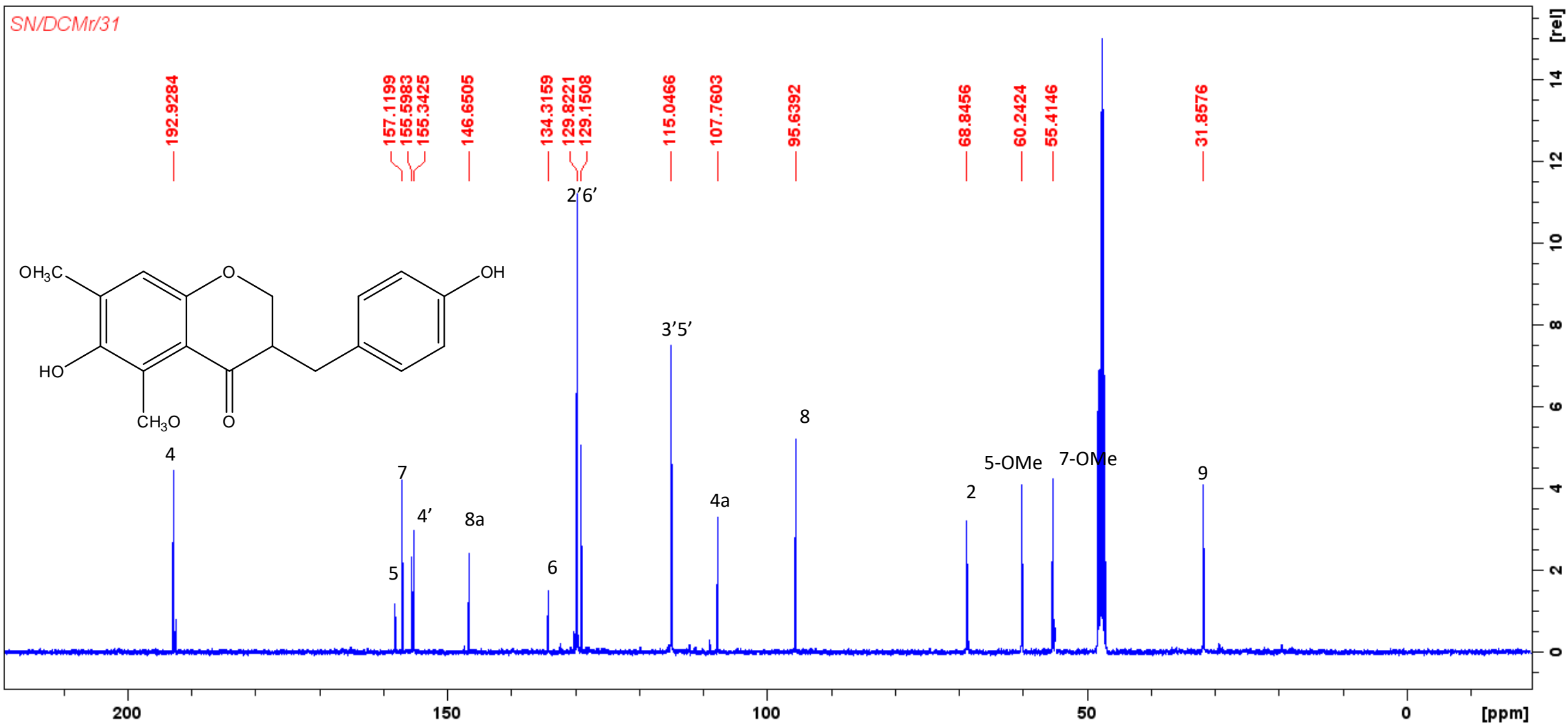
Mass spectrum of compound **A2** 3-(4-methoxybenzyl)-6-hydroxyl-5,7-dimethoxychroman-4-one



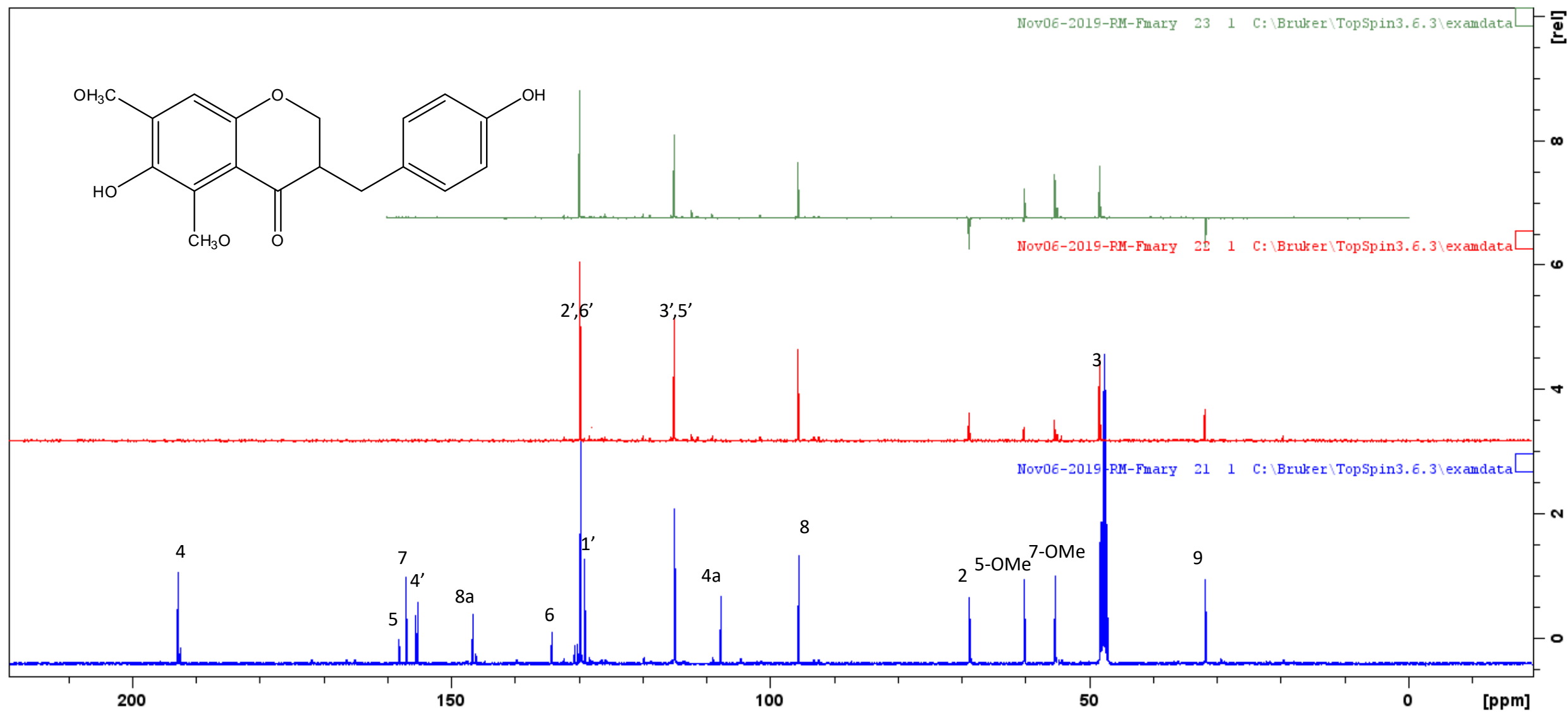
IR of compound **A2** 3(-4-methoxybenzyl)-6-hydroxyl-5,7-dimethoxychroman-4-one



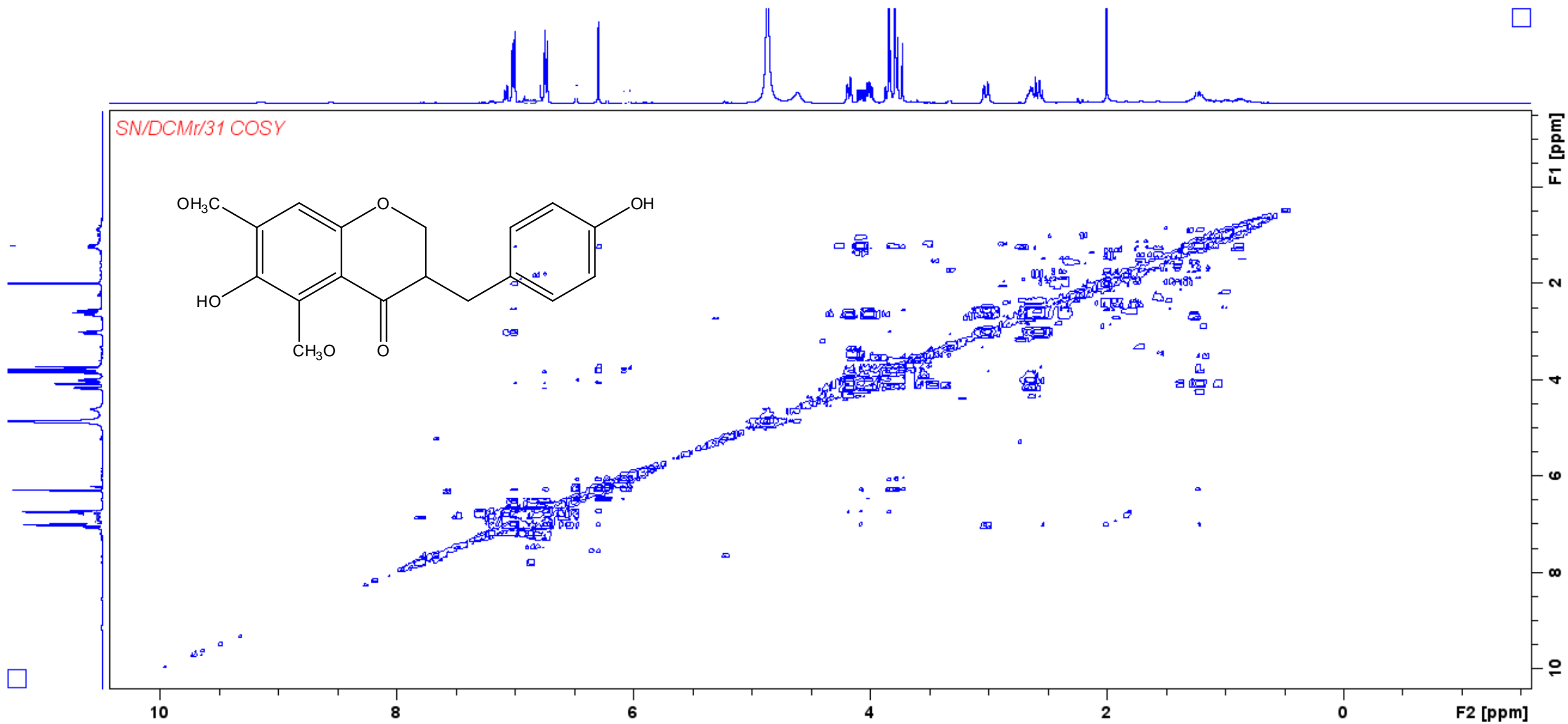
¹H NMR of compound **A3** 3(3-hydroxybenzyl)-6-hydroxyl-5,7-dimethoxychroman-4-one



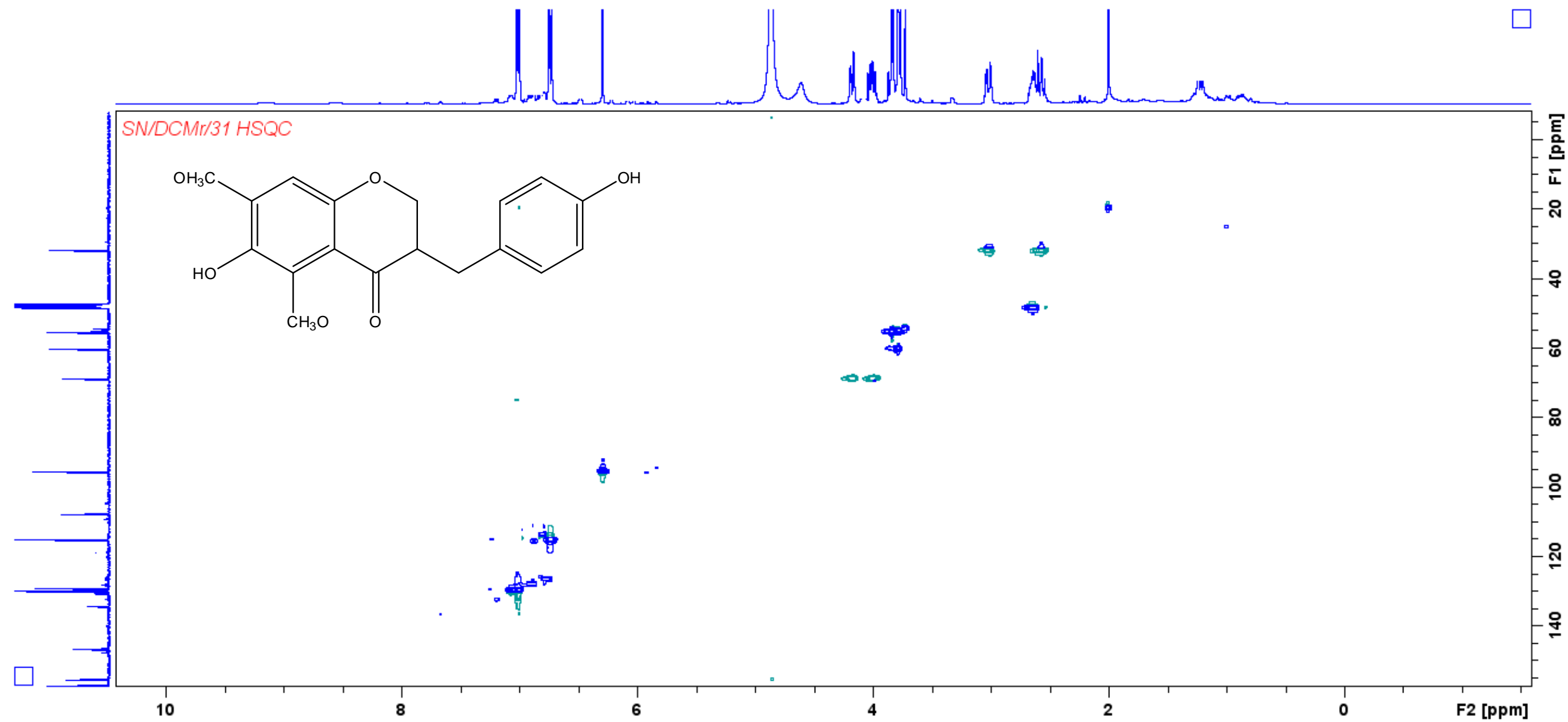
Expanded ¹³CNMR of compound **A3** 3-(3-hydroxybenzyl)-6-hydroxy-5,7-dimethoxychroman-4-one

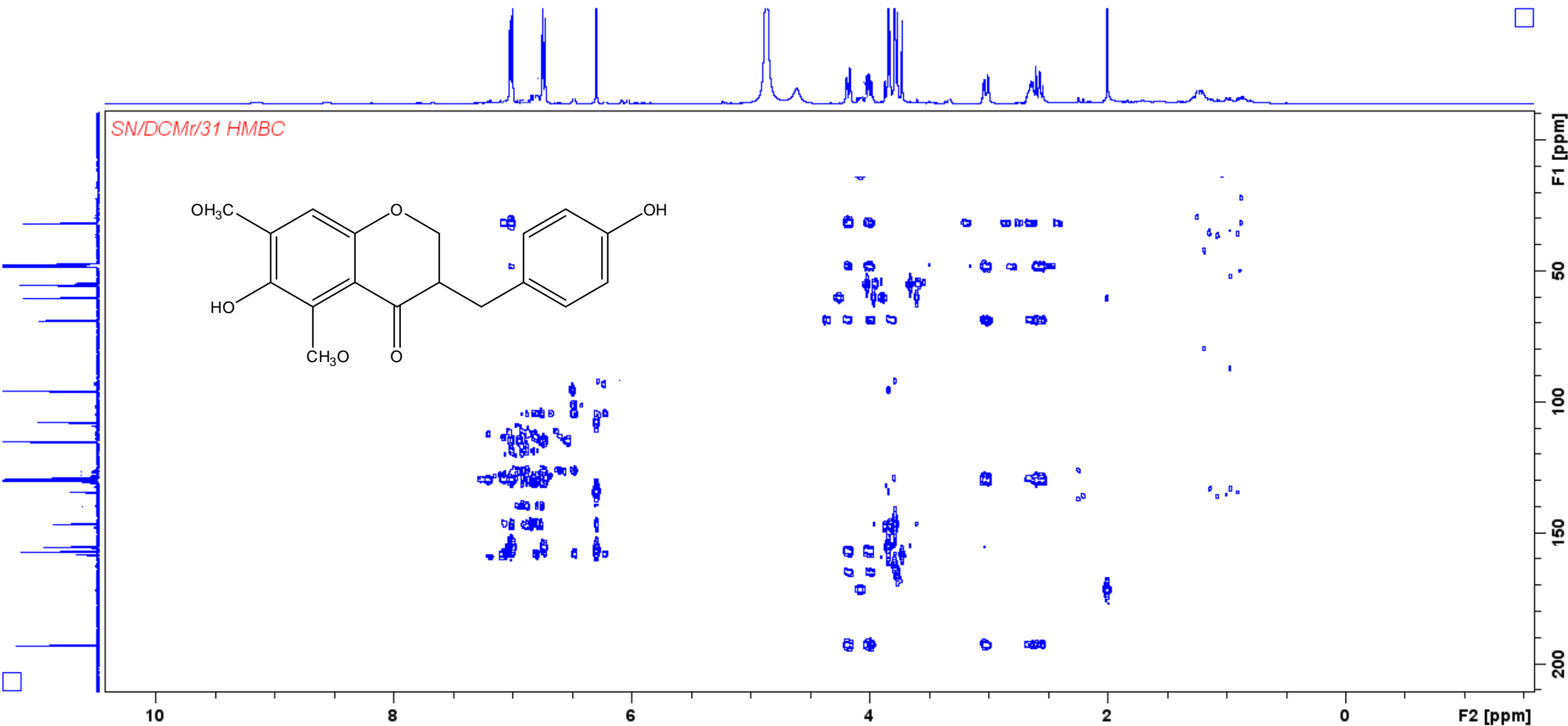


DEPT of compound **A3** 3(3-hydroxybenzyl)-6-hydroxyl-5,7-dimethoxychroman-4-one

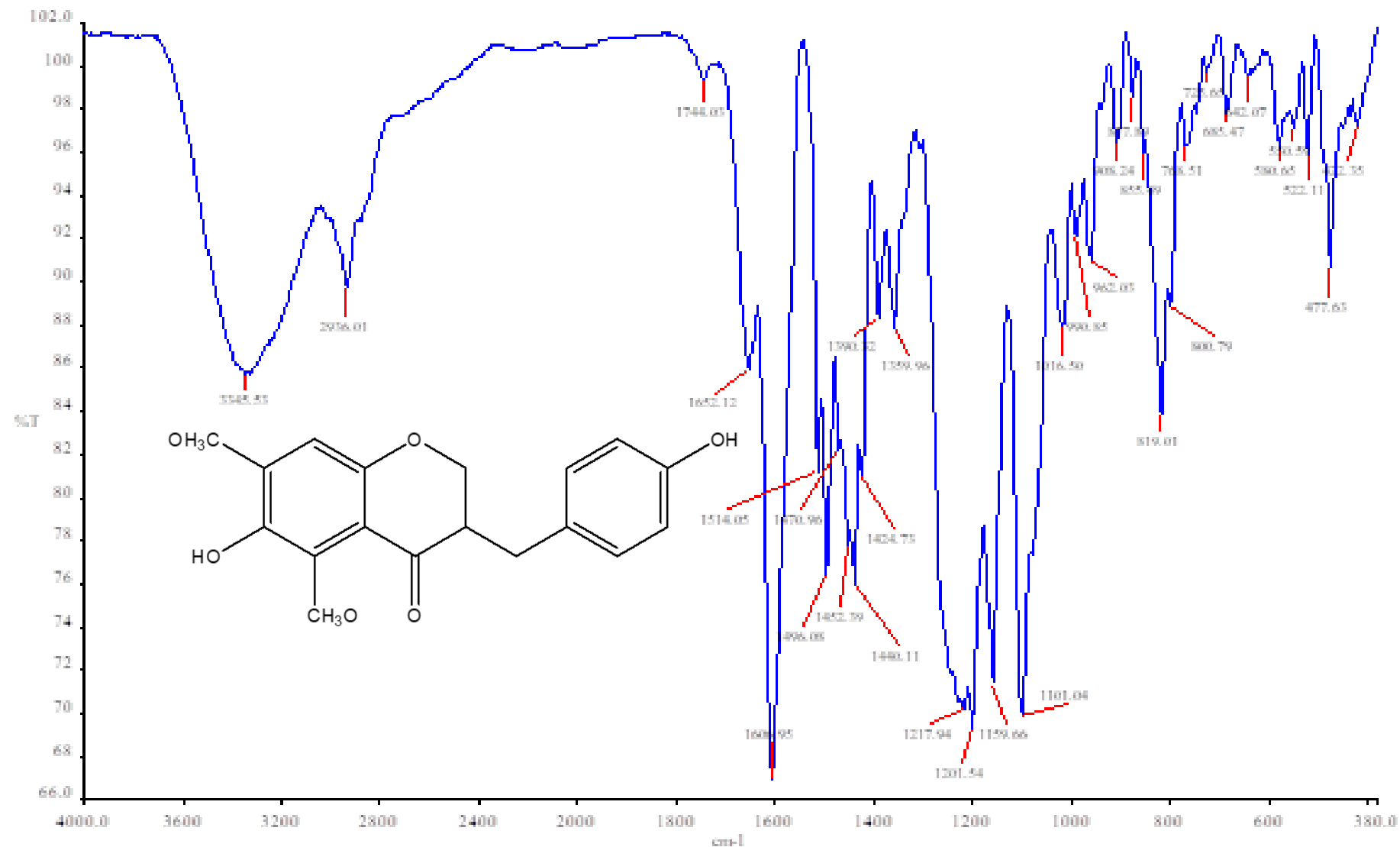


COSY of compound **A3** 3(3-hydroxybenzyl)-6-hydroxyl-5,7-dimethoxychroman-4-one

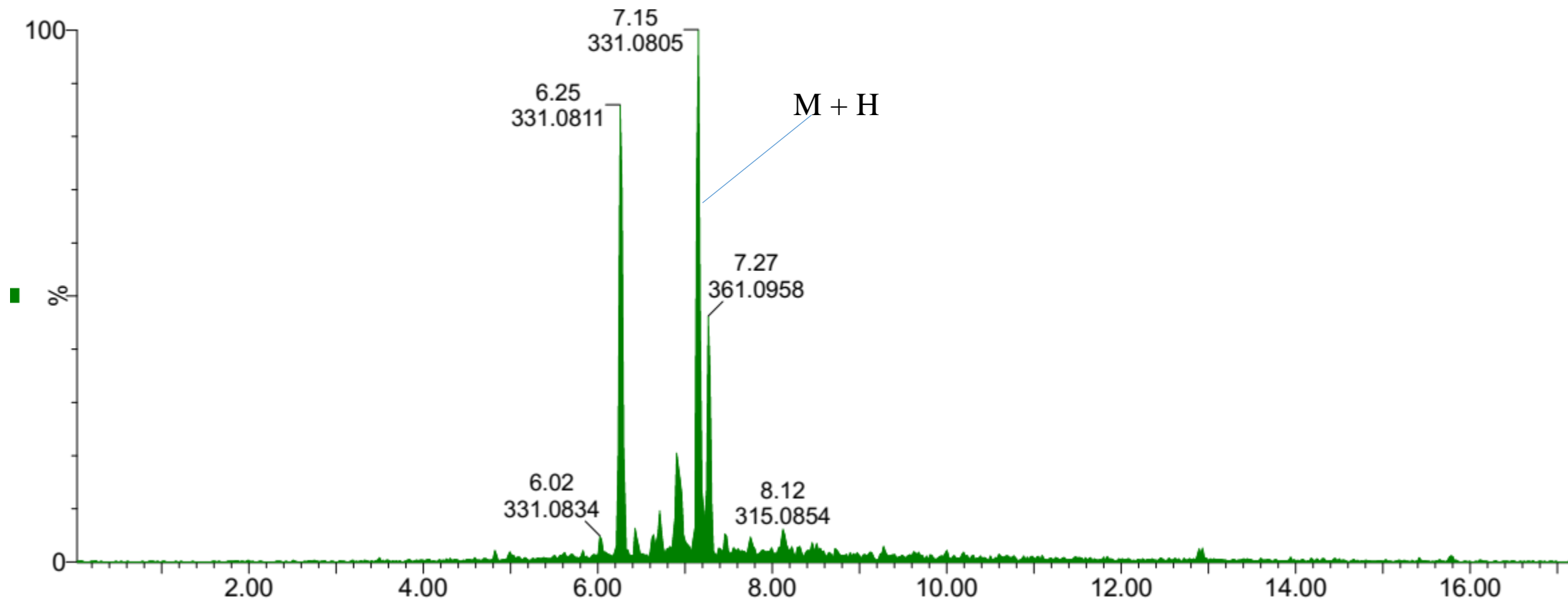
HSQC of compound **A3** 3(3-hydroxybenzyl)-6-hydroxyl-5,7-dimethoxychroman-4-one



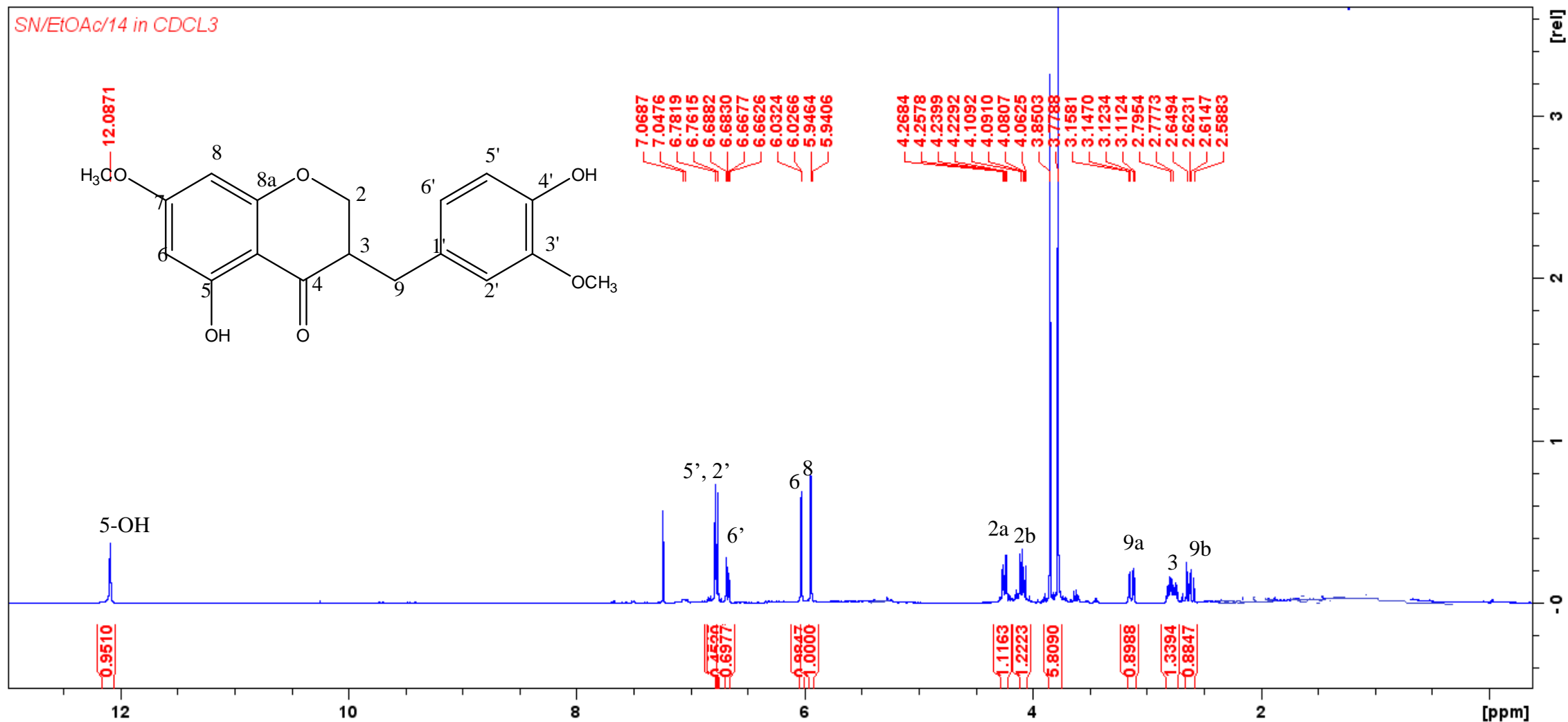
HMBC of compound **A3** 3(3-hydroxybenzyl)-6-hydroxyl-5,7-dimethoxychroman-4-one



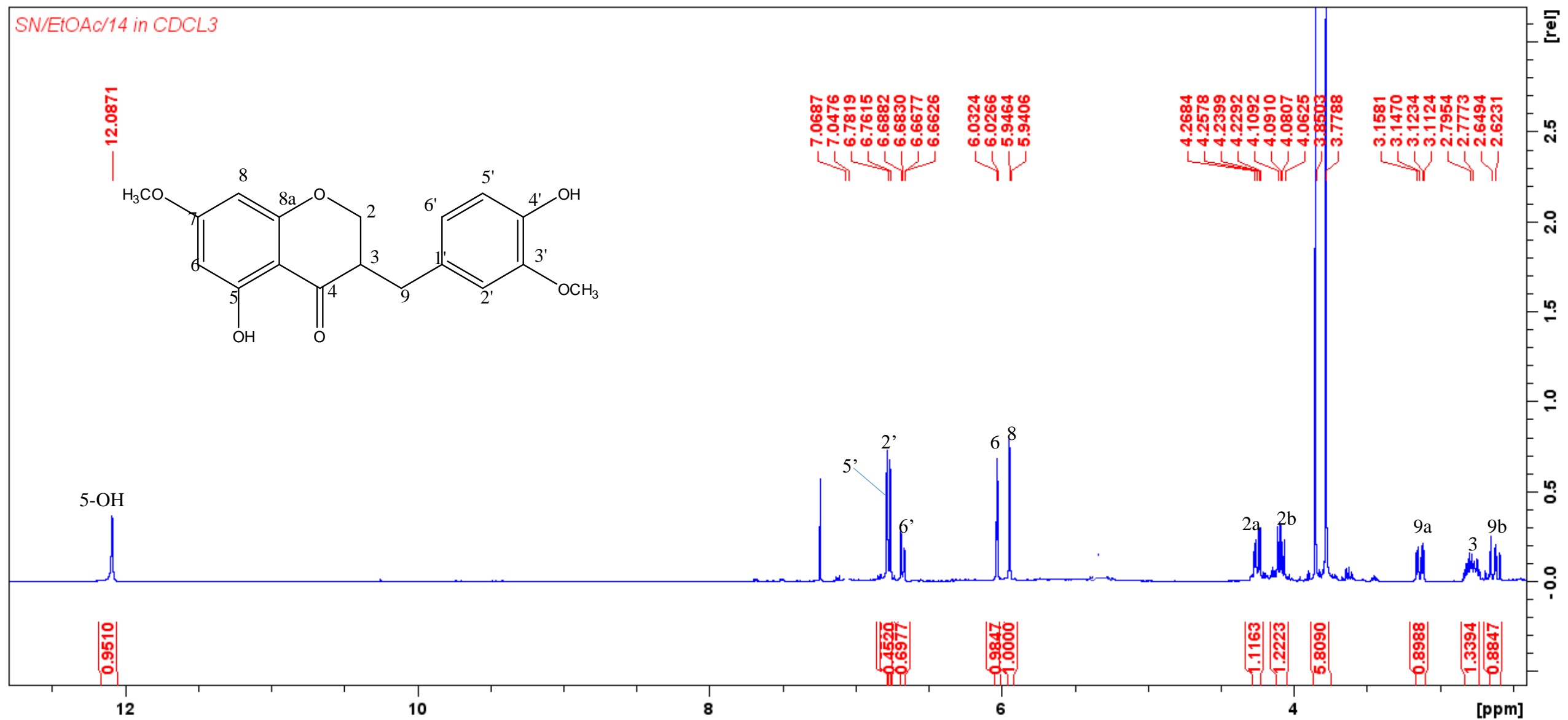
IR of compound **A3** 3-(4-hydroxybenzyl)-6-hydroxy-5,7-dimethoxychroman-4-one



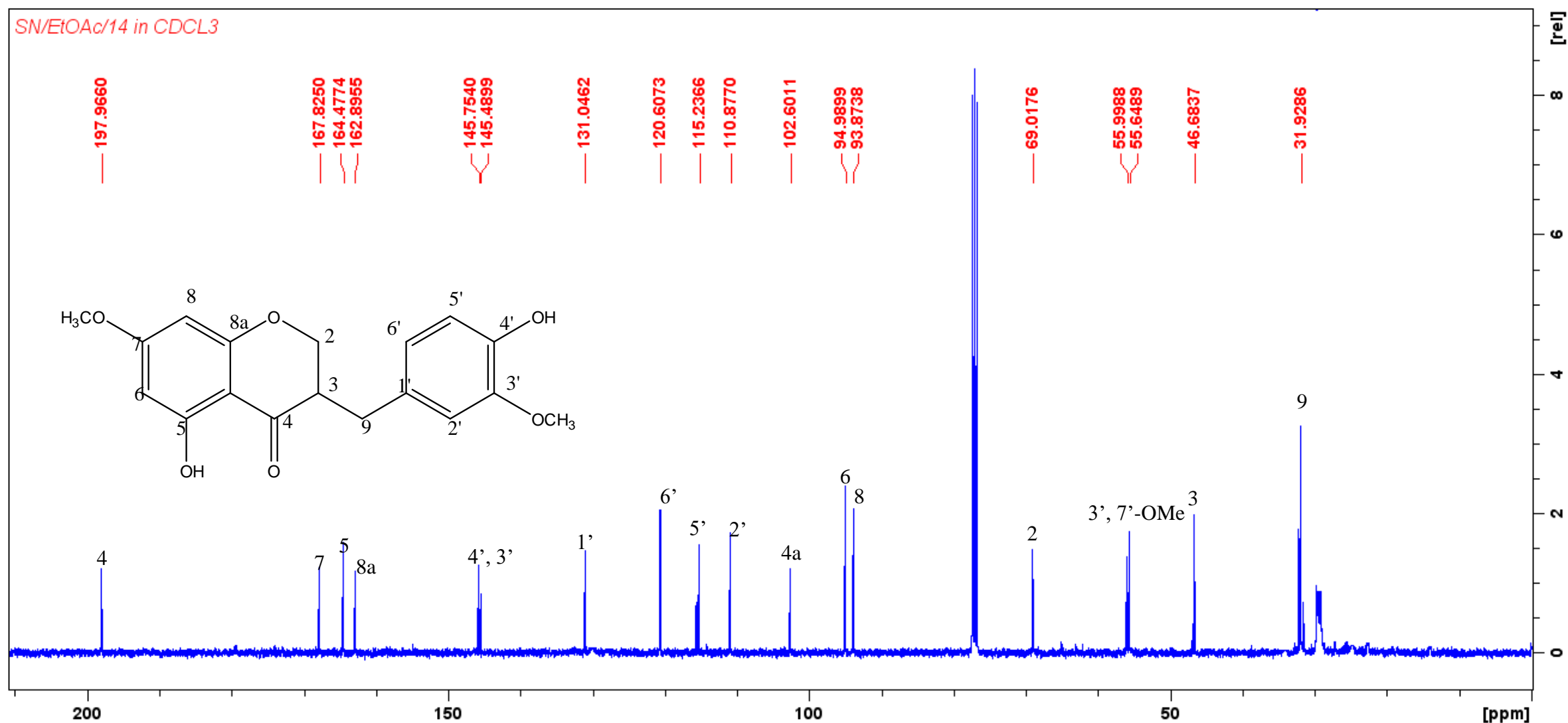
Mass of compound **A3** 3(3-hydroxybenzyl)-6-hydroxyl-5,7-dimethoxychroman-4-one



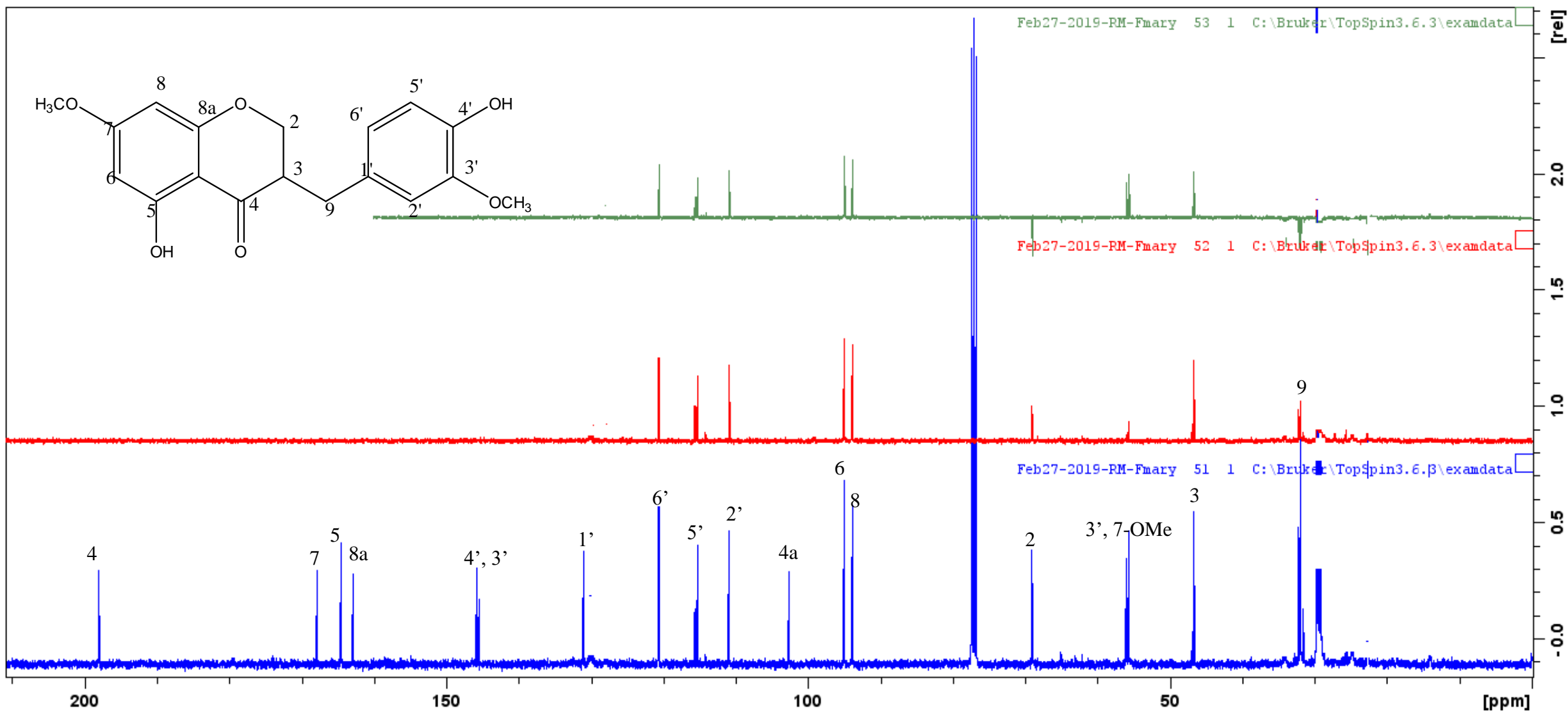
¹H NMR of compound **A4** 3-(4-hydroxy-3-methoxybenzyl)-5-hydroxy-7-methoxychroman-4-one



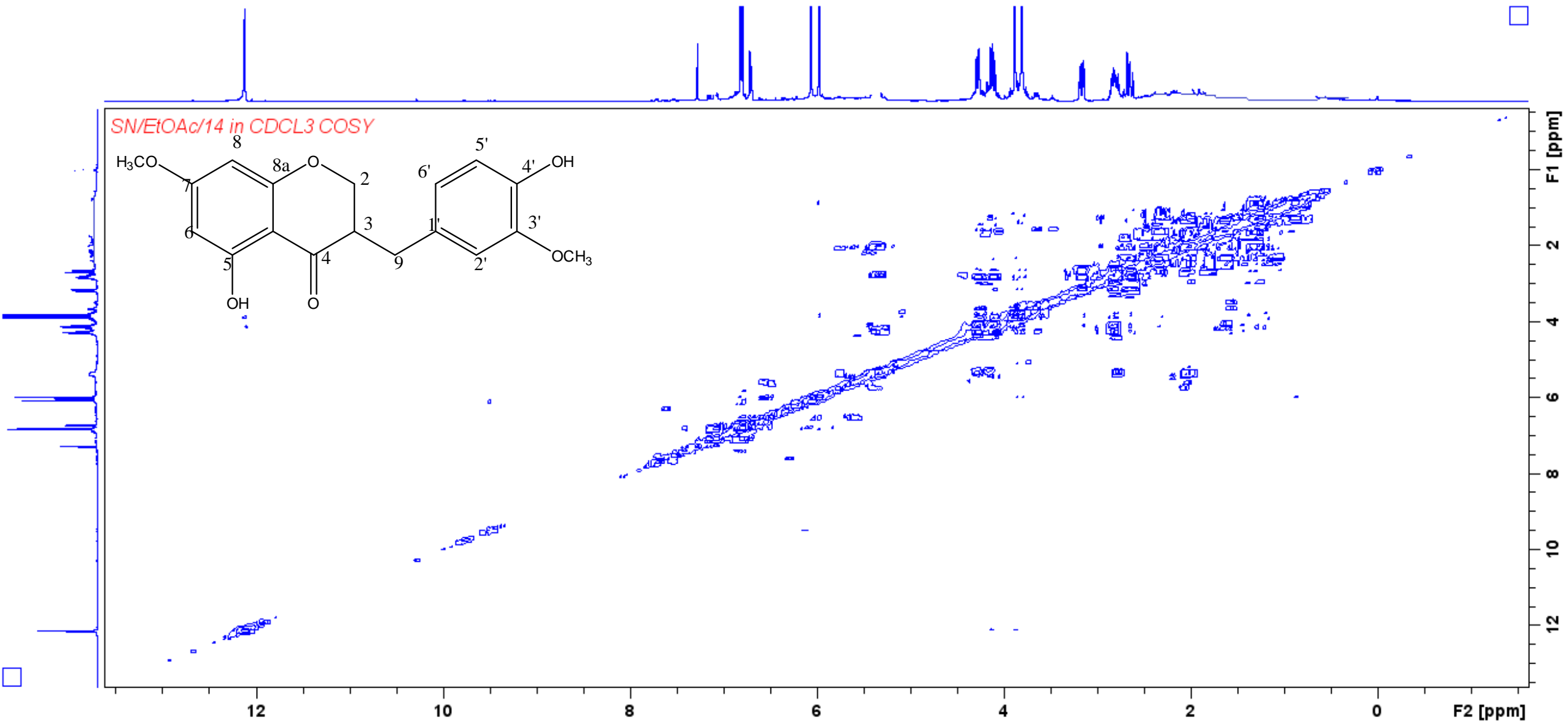
Expanded ¹H NMR of compound **A4** 3-(4-hydroxy-3-methoxybenzyl)-5-hydroxy-7-methoxychroman-4-one



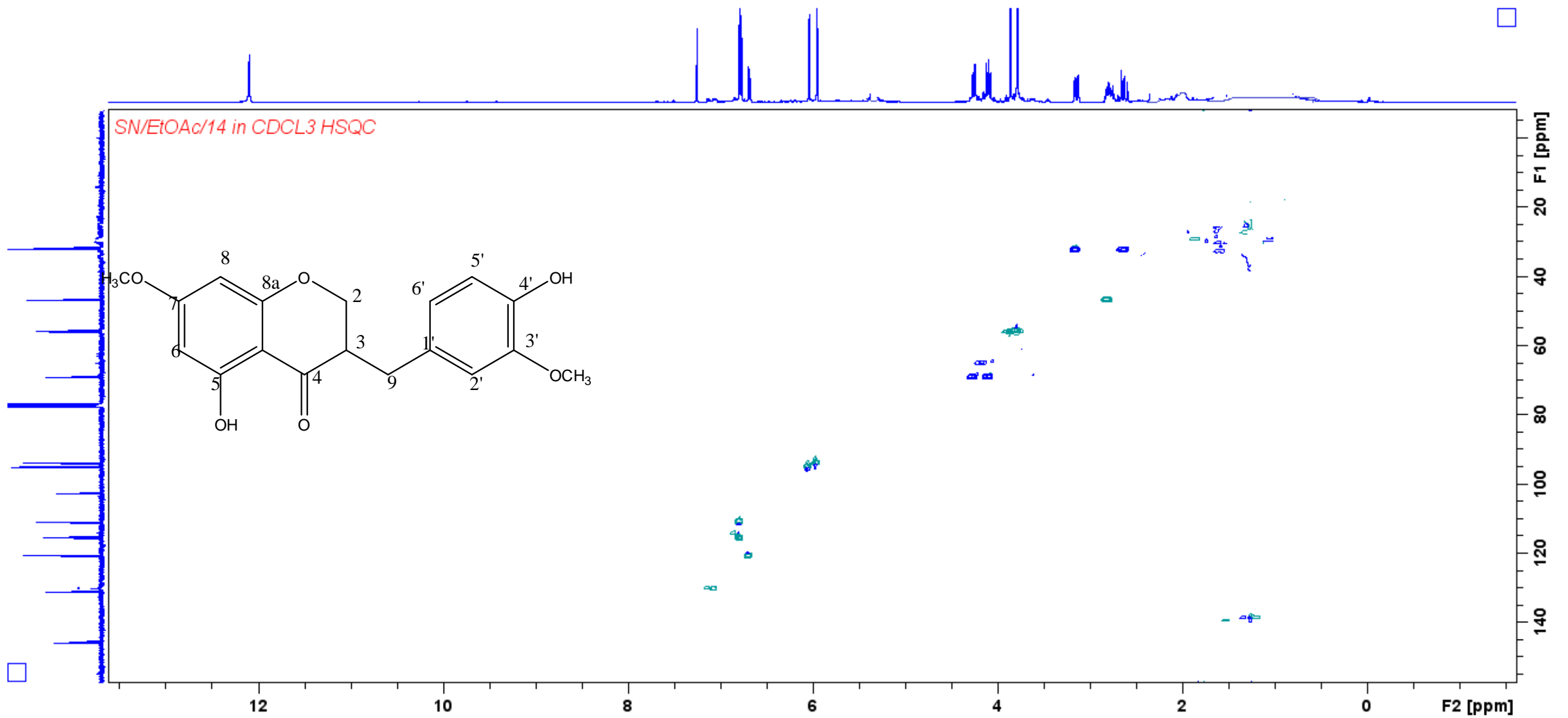
¹³C NMR of compound **A4** 3-(4-hydroxyl-3-methoxybenzyl)-5-hydroxyl-7-methoxychroman-4-one



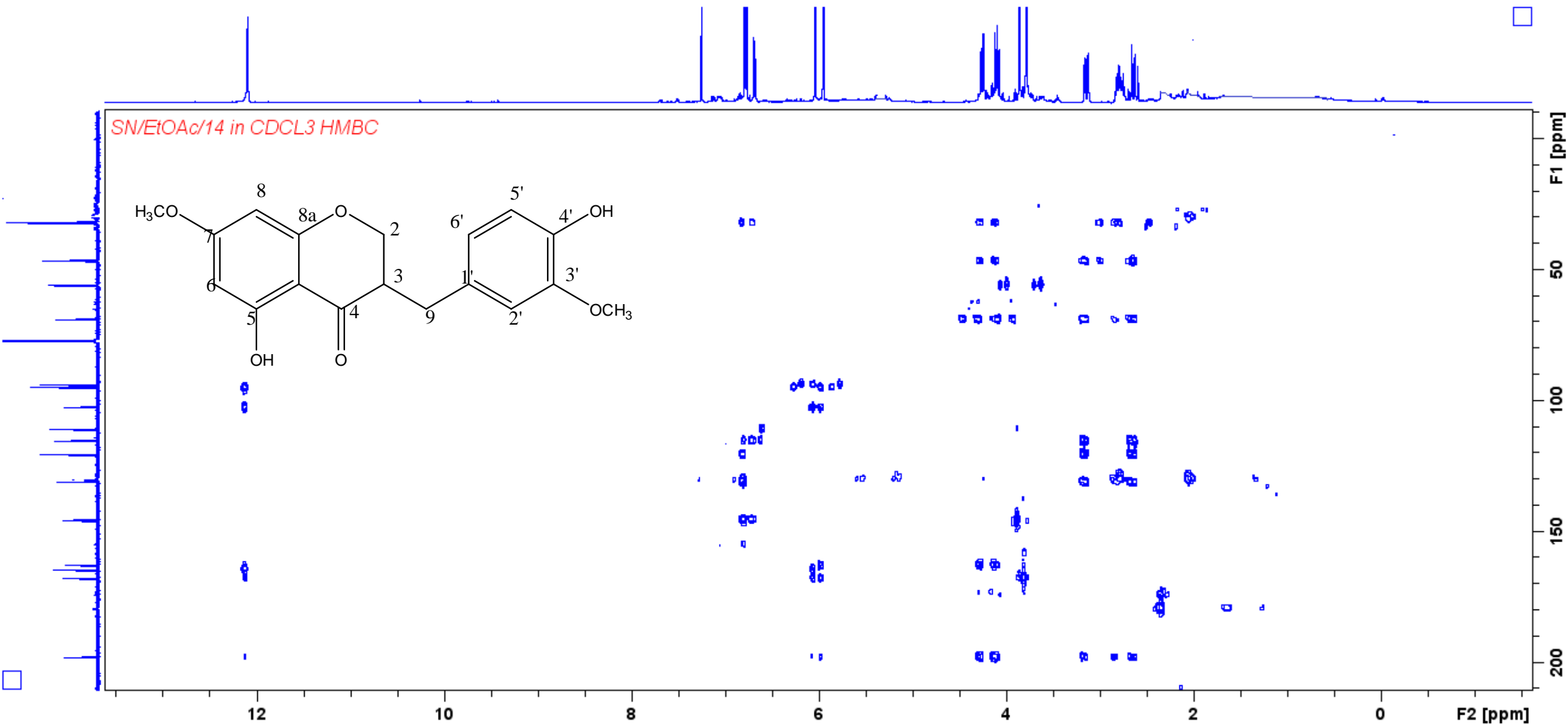
DEPT of compound **A4** 3-(4-hydroxy-3-methoxybenzyl)-5-hydroxy-7-methoxychroman-4-one



COSY of compound **A4** 3-(4-hydroxyl-3-methoxybenzyl)-5-hydroxyl-7-methoxychroman-4-one



HSQC of compound **A4** 3-(4-hydroxyl-3-methoxybenzyl)-5-hydroxyl-7-methoxychroman-4-one



HMBC of compound **A4** 3-(4-hydroxyl-3-methoxybenzyl)-5-hydroxyl-7-methoxychroman-4-one

Monoisotopic Mass, Even Electron Ions

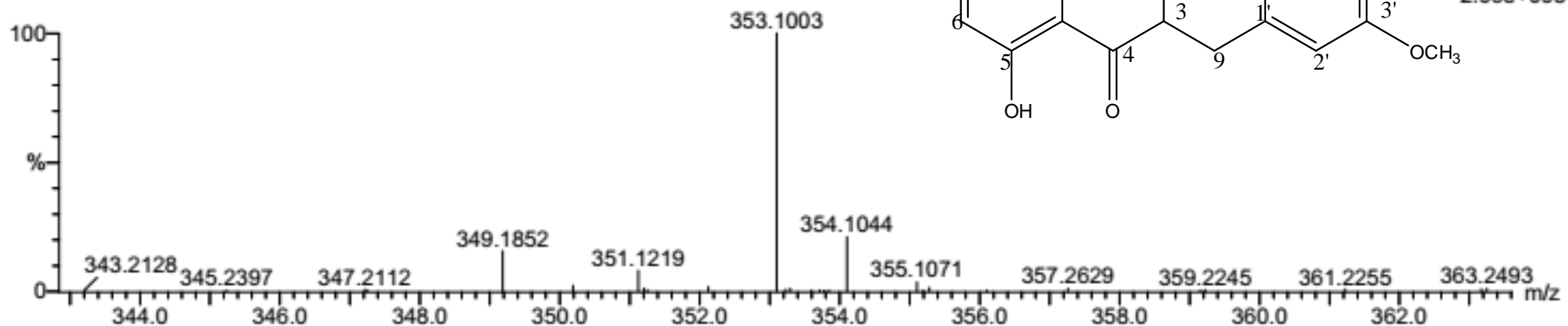
2 formula(e) evaluated with 1 results within limits (all results (up to 1000) for each mass)

Elements Used:

C: 15-20 H: 15-20 O: 5-10 Na: 1-1

SN_DCM_11-12 4 (0.101) Cm (1:61)

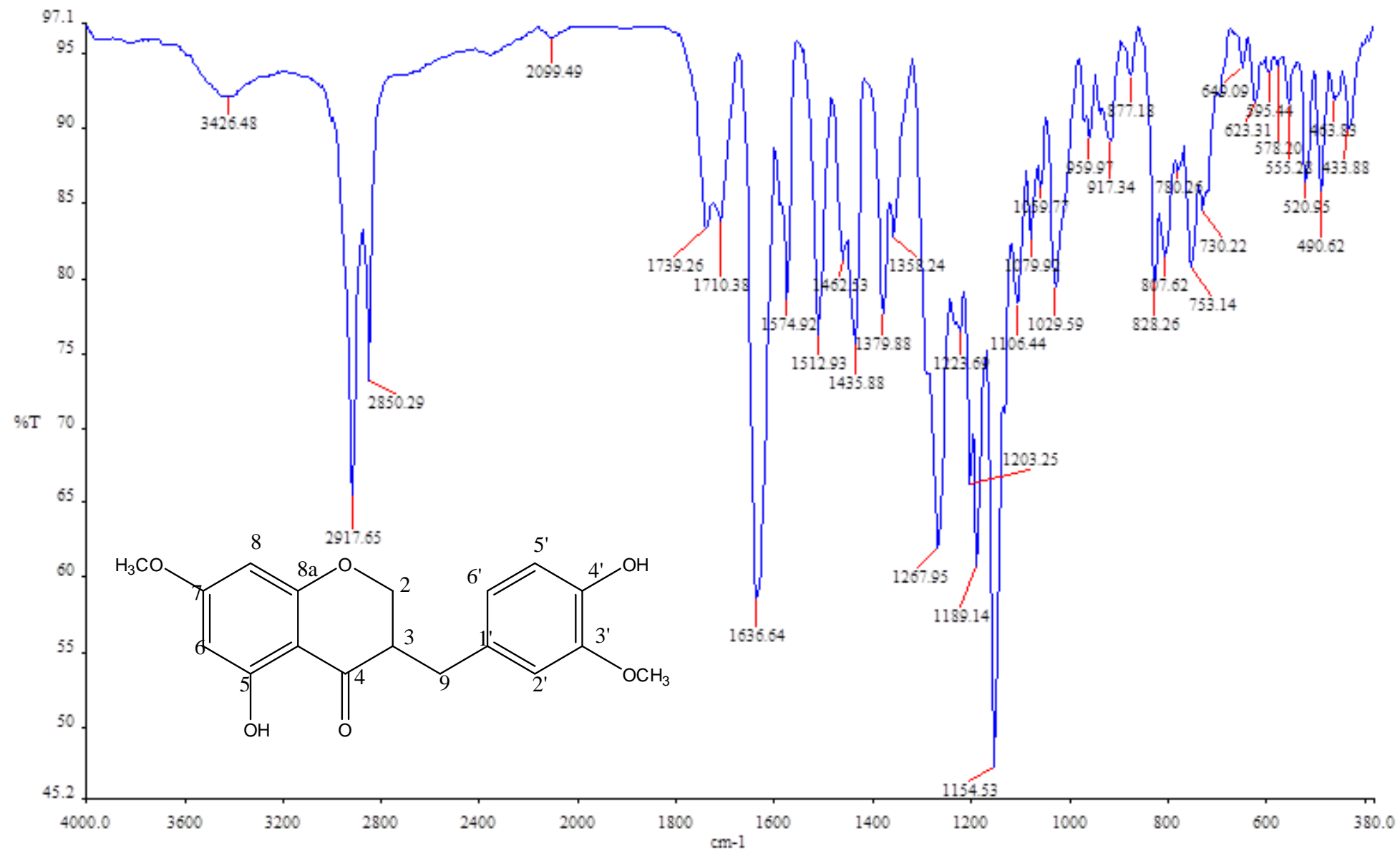
TOF MS ES+



Minimum: -1.5
Maximum: 5.0 5.0 50.0

Mass	Calc. Mass	mDa	PPM	DBE	i-FIT	i-FIT (Norm)	Formula
353.1003	353.1001	0.2	0.6	9.5	127.2	0.0	C18 H18 O6 Na

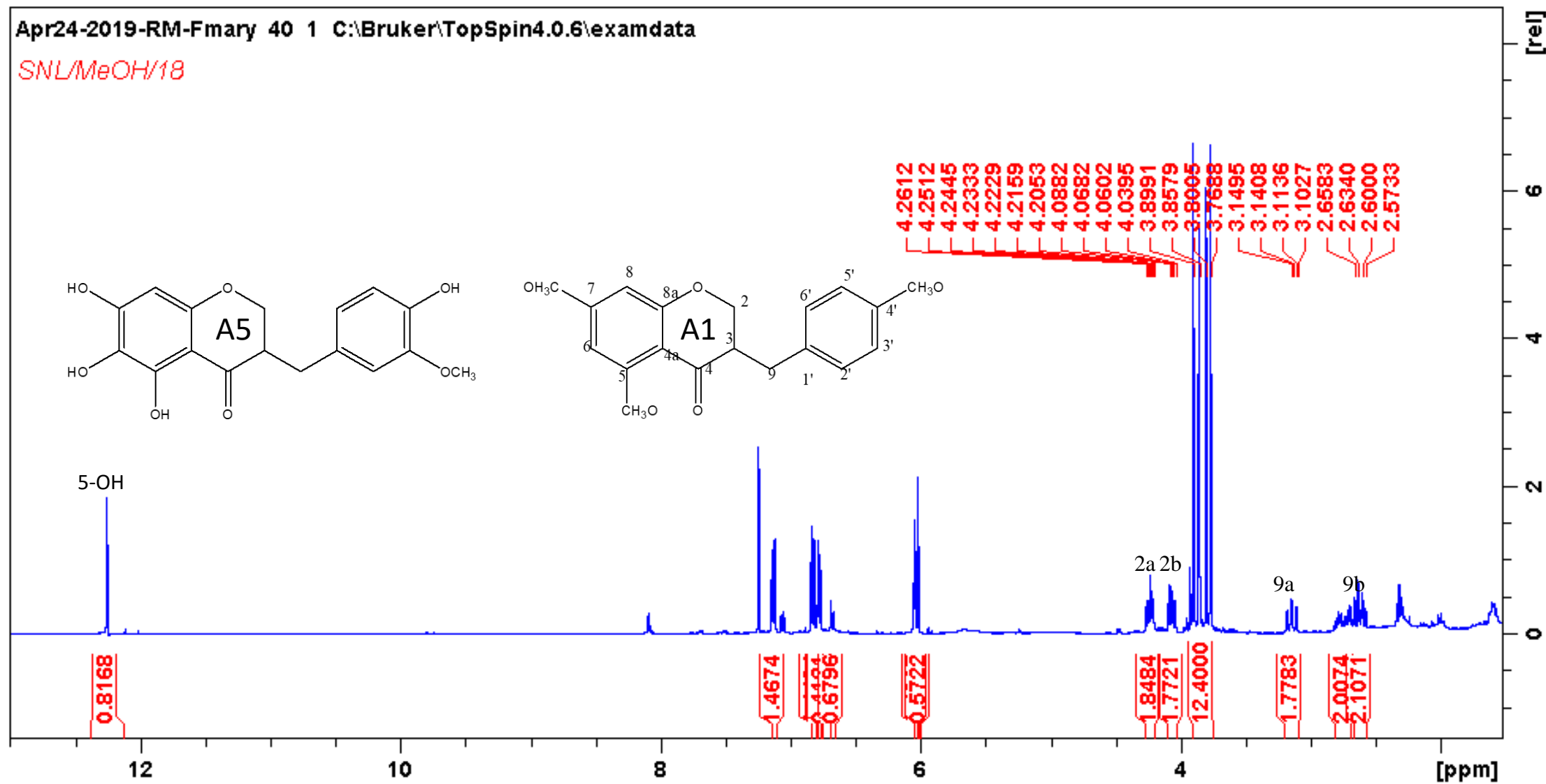
HRMS of compound **A4** 3-(4-hydroxyl-3-methoxybenzyl)-5-hydroxyl-7-methoxychroman-4-one



IR of compound **A4** 3-(4-hydroxyl-3-methoxybenzyl)-5-hydroxyl-7-methoxychroman-4-one

Apr24-2019-RM-Fmary 40 1 C:\Bruker\TopSpin4.0.6\examdata

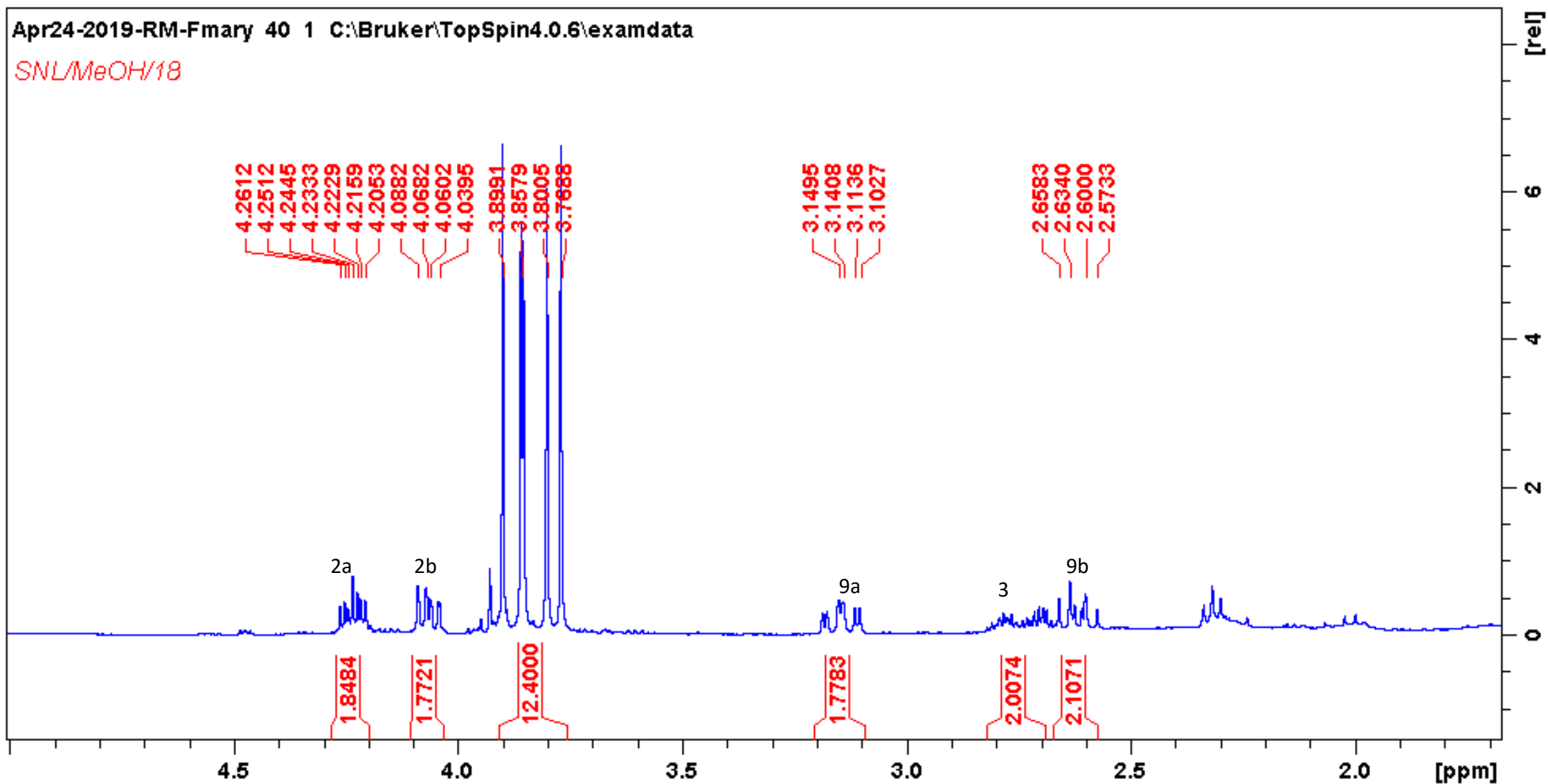
SNL/MeOH/18



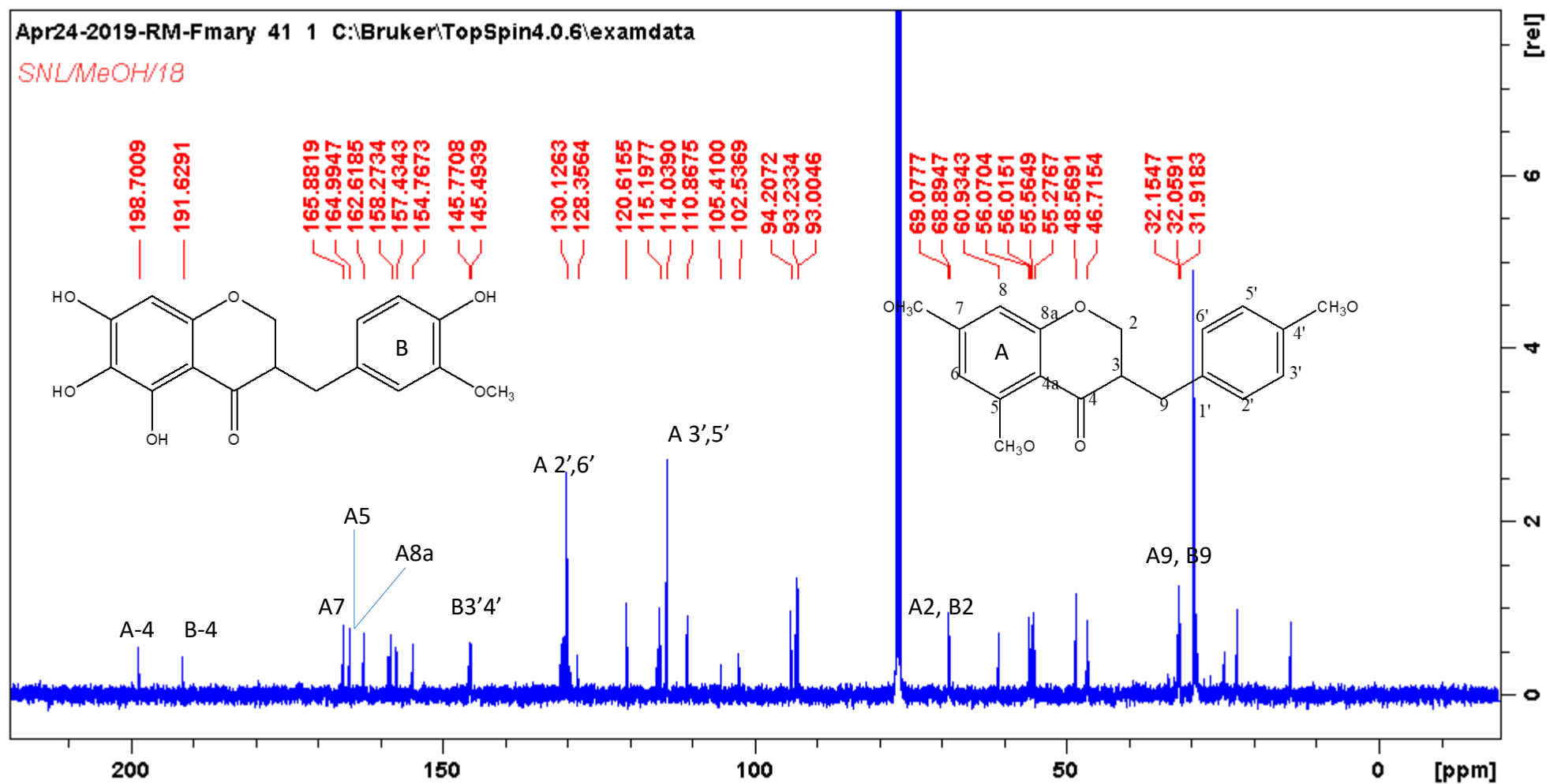
¹H NMR of compound (A1) 3-(4-methoxybenzyl)-5,7-dimethoxychroman-4-one and 5 (A5) 3-(4-hydroxyl-3-methoxybenzyl)-5,6,7-trimethoxychroman-4-one

Apr24-2019-RM-Fmary 40 1 C:\Bruker\TopSpin4.0.6\examdata

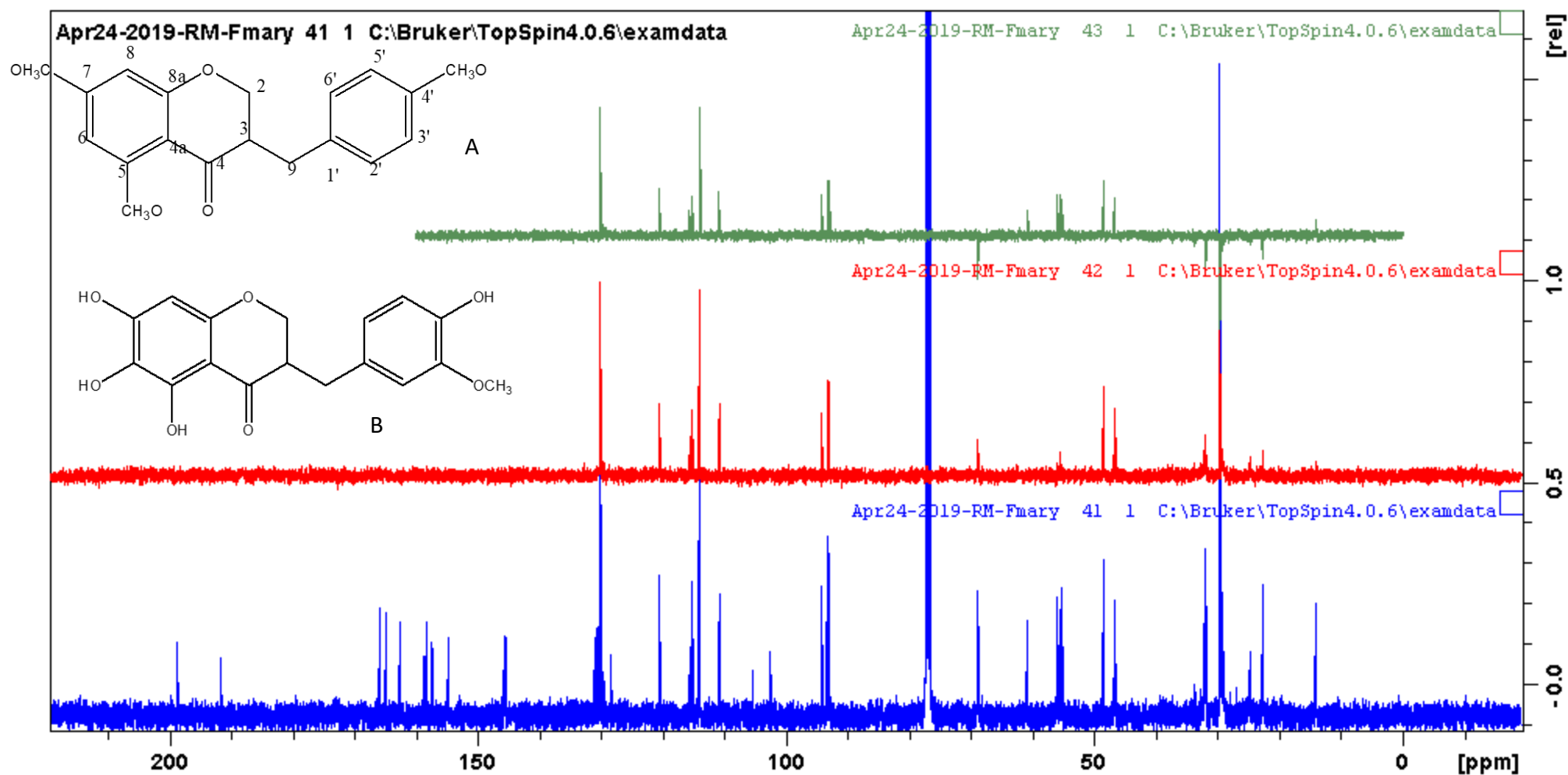
SNL/MeOH/18



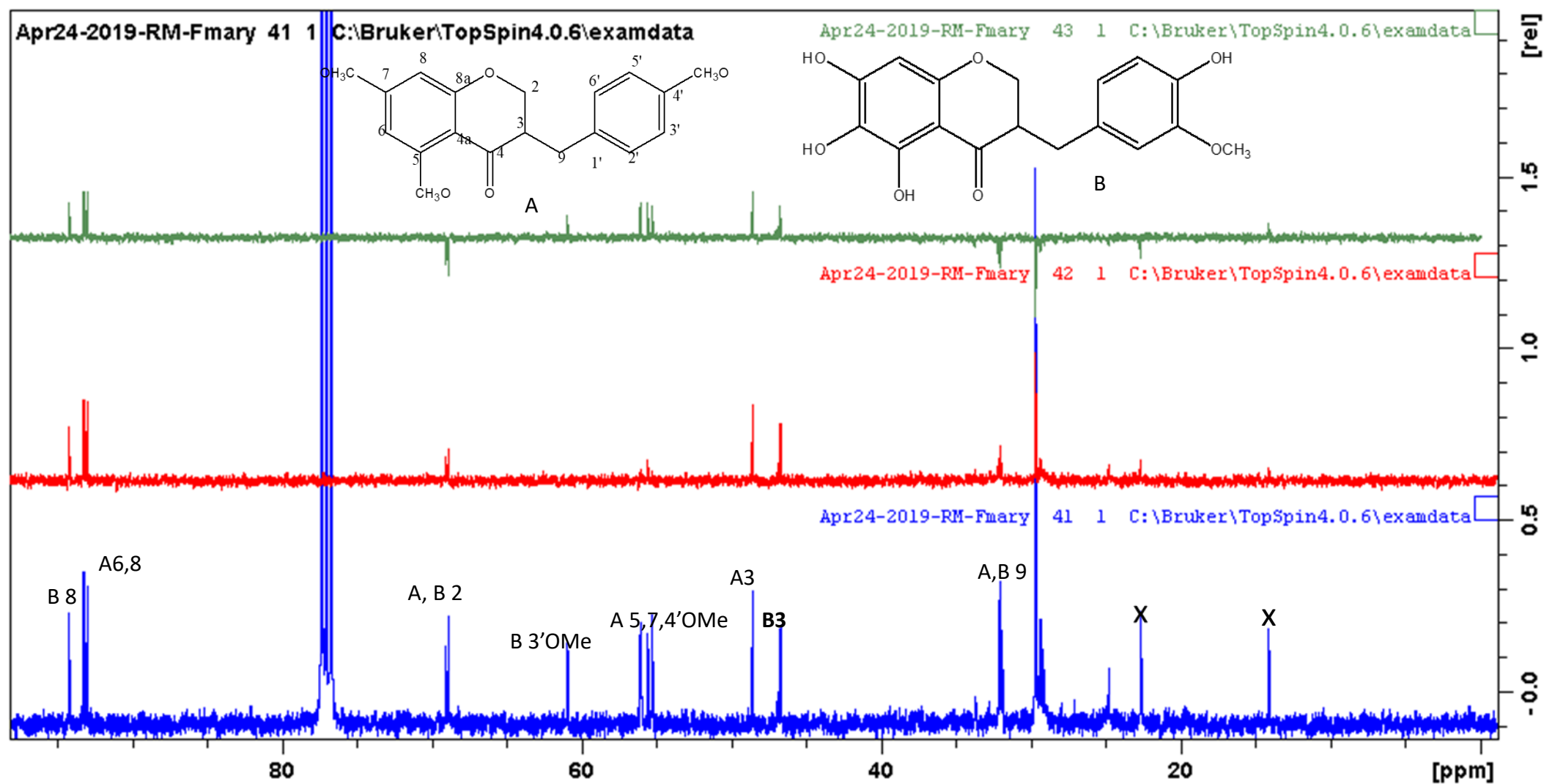
Expanded ^1H NMR of compound **A1** and **A5**



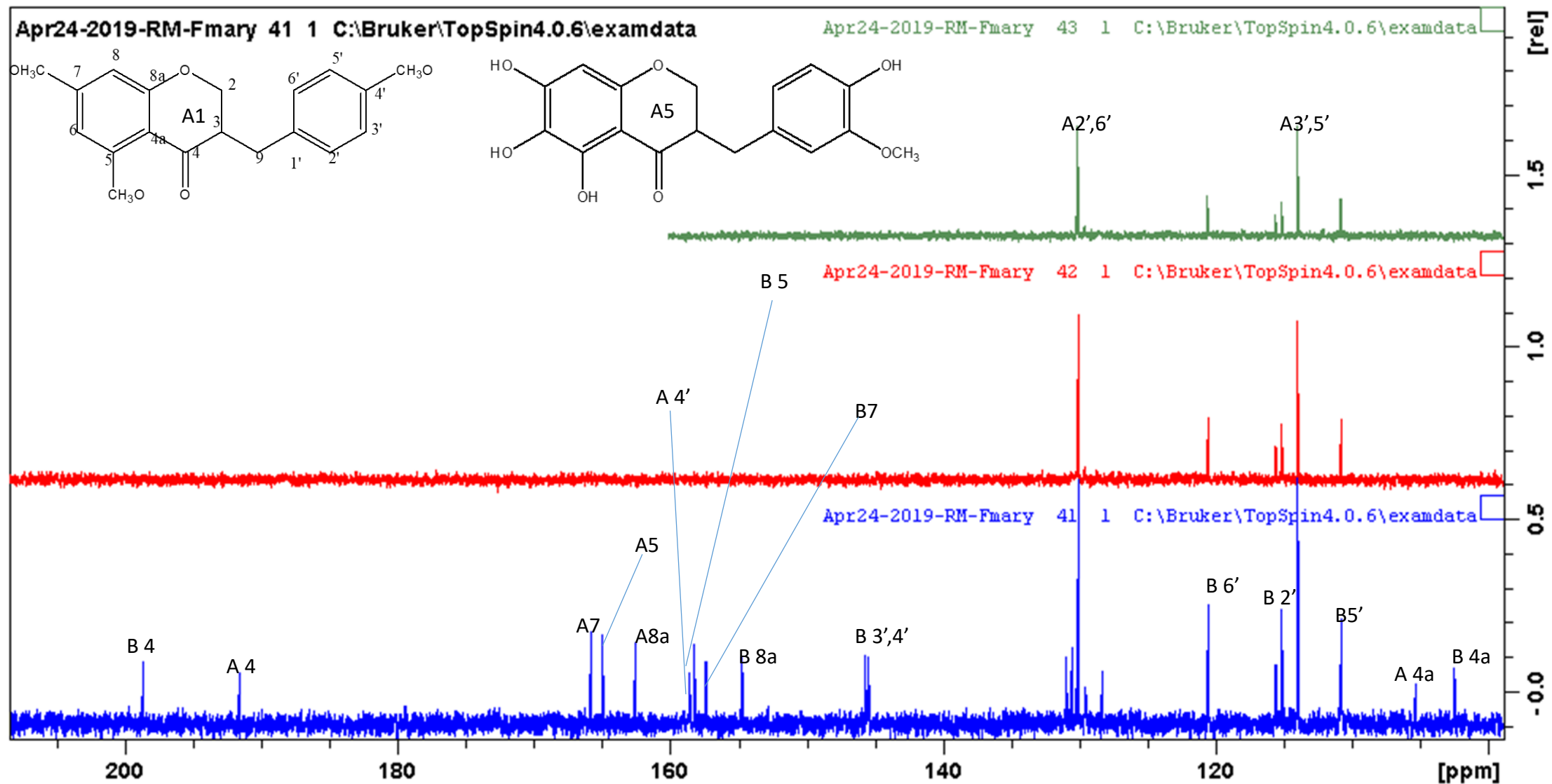
^{13}C NMR of compounds (**A1**) 3-(4-methoxybenzyl)-5,7-dimethoxychroman-4-one and (**A5**) 3-(4-hydroxyl-3-methoxybenzyl)-5,6,7-trimethoxychroman-4-one



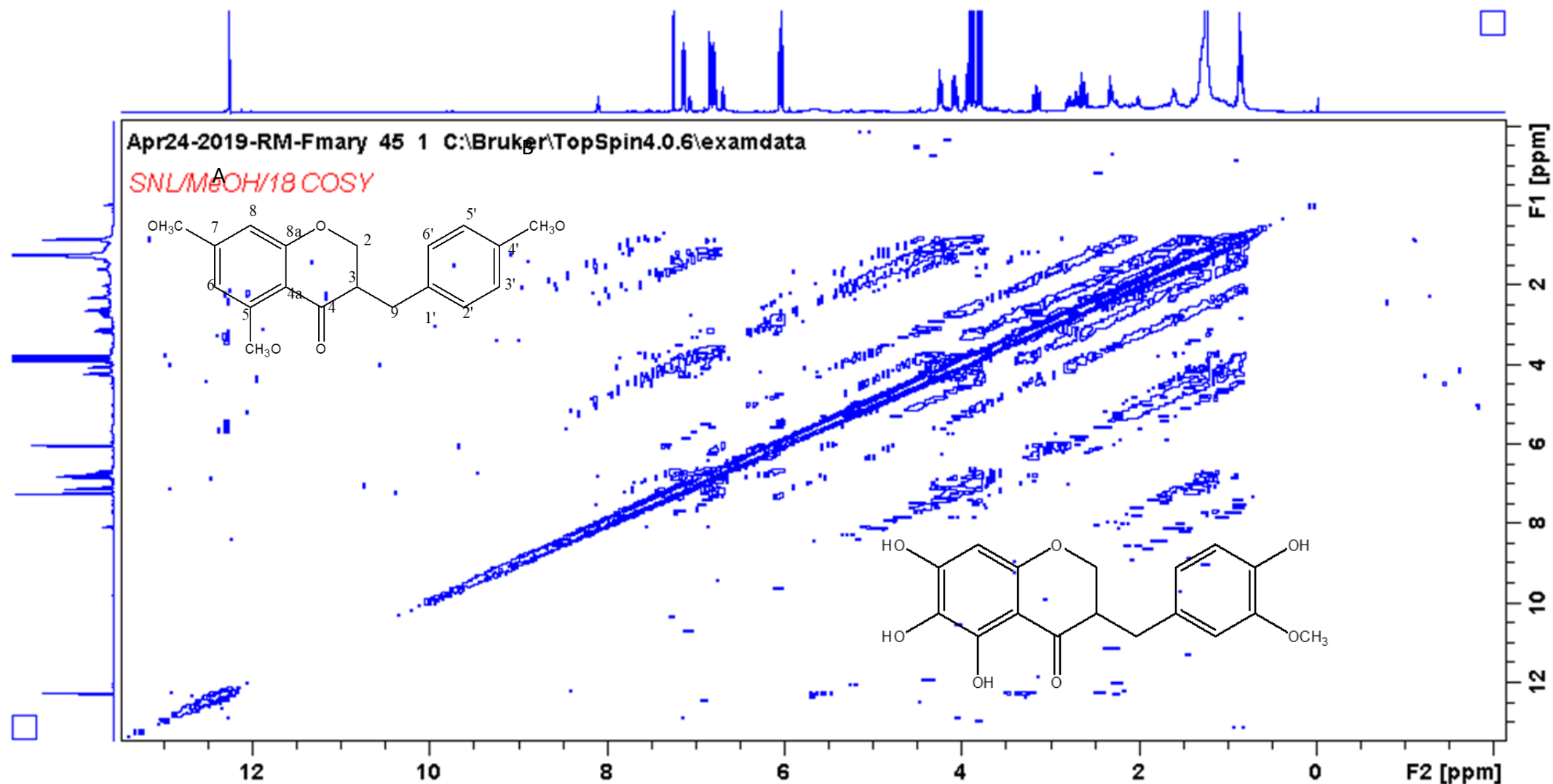
DEPT of compounds (**A1**) 3-(4-methoxybenzyl)-5,7-dimethoxychroman-4-one and (**A5**) 3-(4-hydroxy-3-methoxybenzyl)-5,6,7-trimethoxychroman-4-one



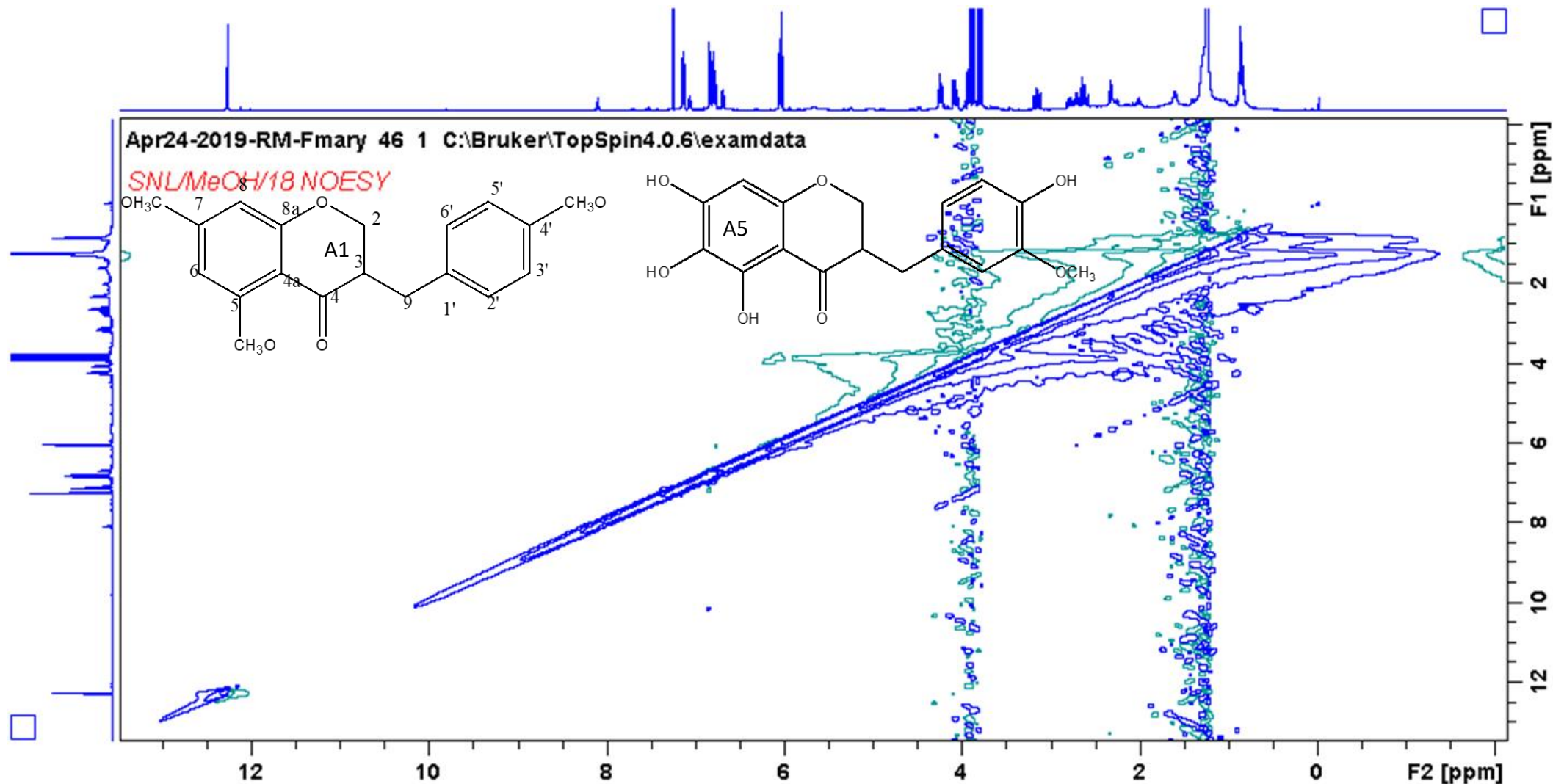
Expanded DEPT of compounds (**A1**) 3-(4-methoxybenzyl)-5,7-dimethoxychroman-4-one and (**A5**) 3-(4-hydroxyl-3-methoxybenzyl)-5,6,7-trimethoxychroman-4-one



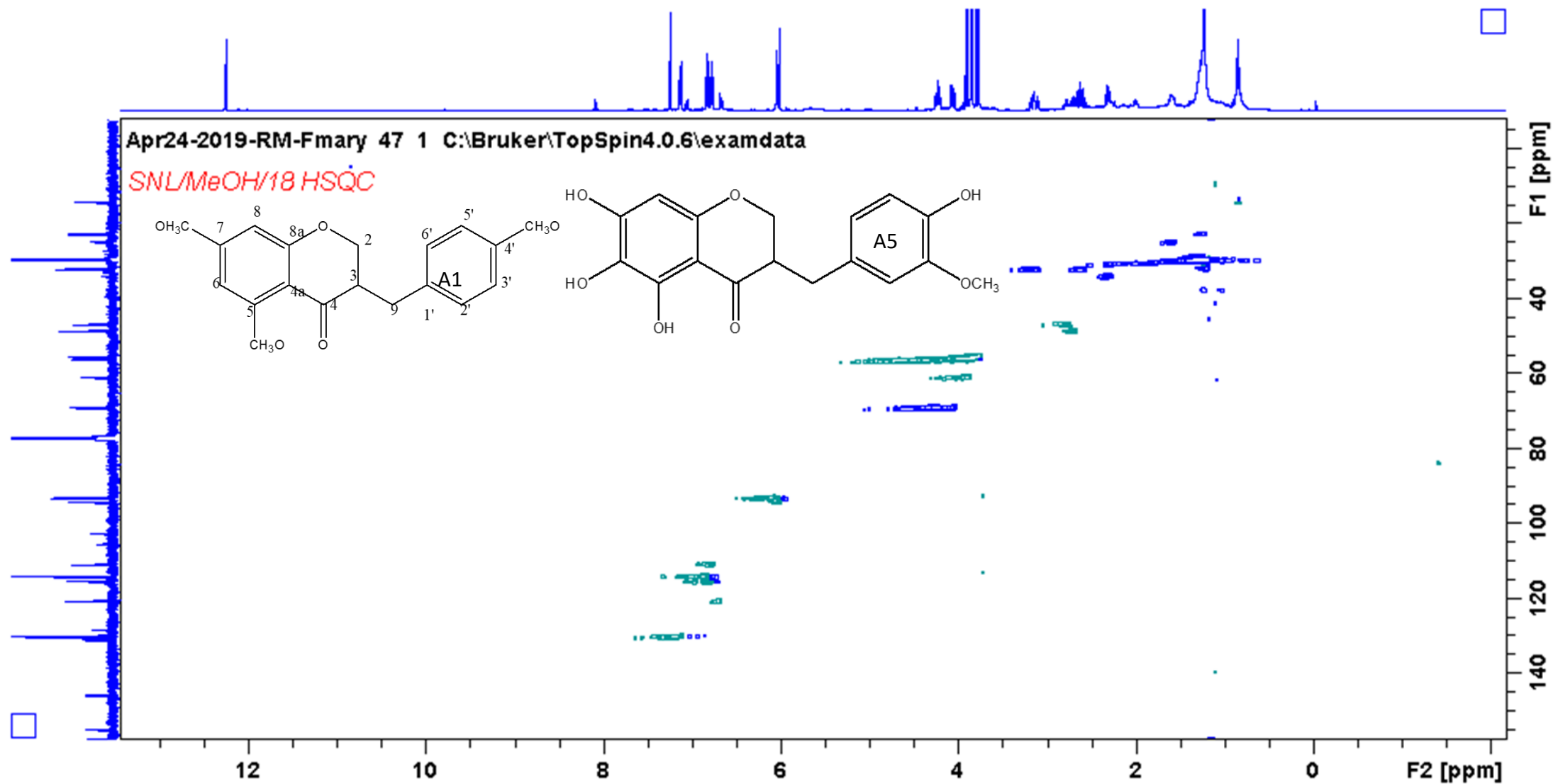
Expanded DEPT of compounds (**A1**) 3-(4-methoxybenzyl)-5,7-dimethoxychroman-4-one and (**A5**) 3-(4-hydroxy-3-methoxybenzyl)-5,6,7-trimethoxychroman-4-one



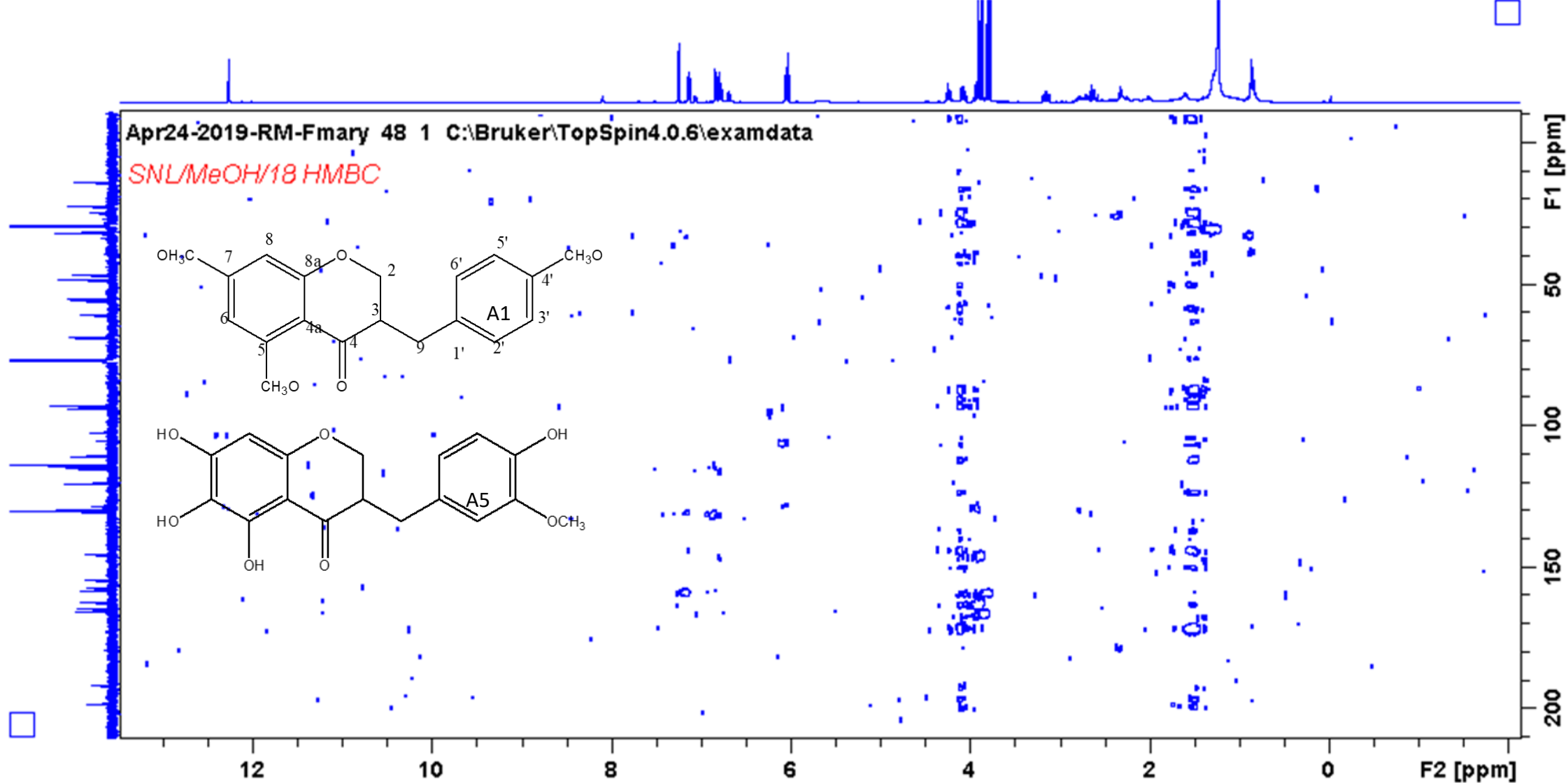
COSY of compounds (A1) 3-(4-methoxybenzyl)-5,7-dimethoxychroman-4-one and (A5)3-(4-hydroxyl-3-methoxybenzyl)-5,6,7-trimethoxychroman-4-one



NOESY of compounds (**A1**) 3-(4-methoxybenzyl)-5,7-dimethoxychroman-4-one and (**A5**) 3-(4-hydroxyl-3-methoxybenzyl)-5,6,7-trimethoxychroman-4-one

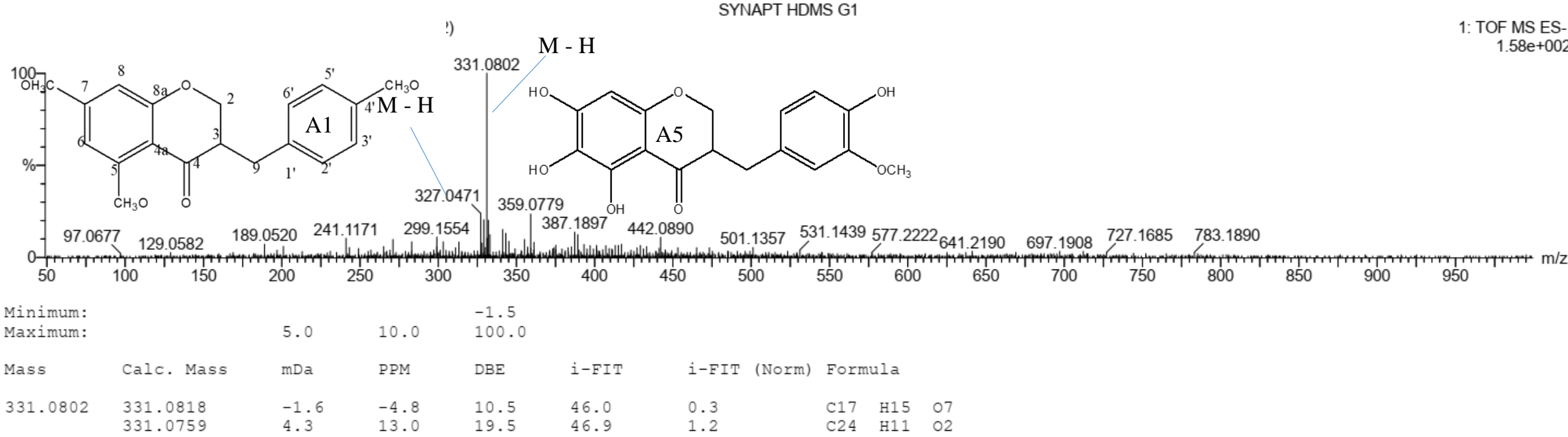


HSQC of compounds (**A1**) 3-(4-methoxybenzyl)-5,7-dimethoxychroman-4-one and (**A5**) 3-(4-hydroxy-3-methoxybenzyl)-5,6,7-trimethoxychroman-4-one

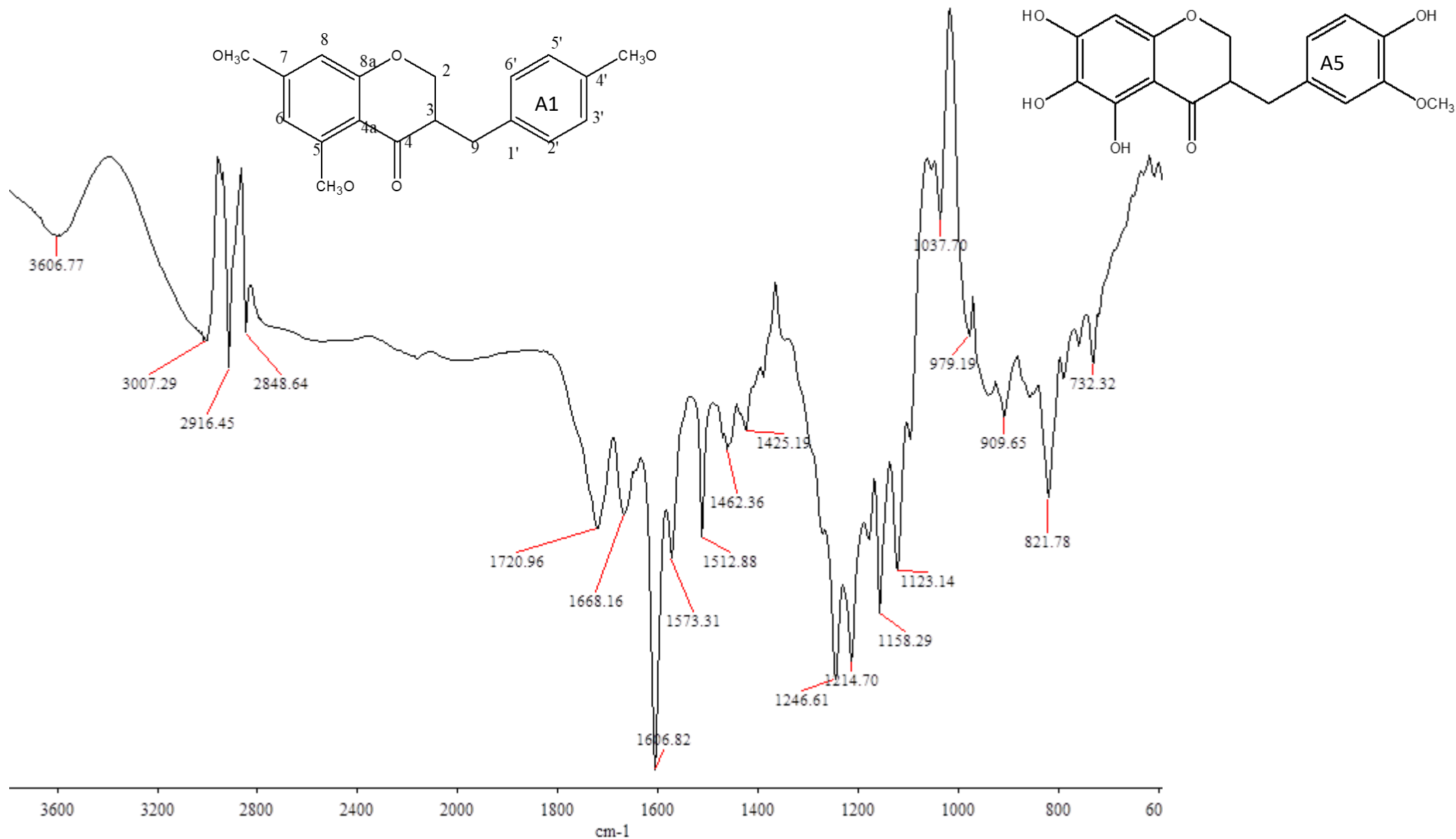


HMBC of compounds **1(A)** 3-(4-methoxybenzyl)-5,7-dimethoxychroman-4-one and **5(B)** 3-(4-hydroxy-3-methoxybenzyl)-5,6,7-trimethoxychroman-4-one

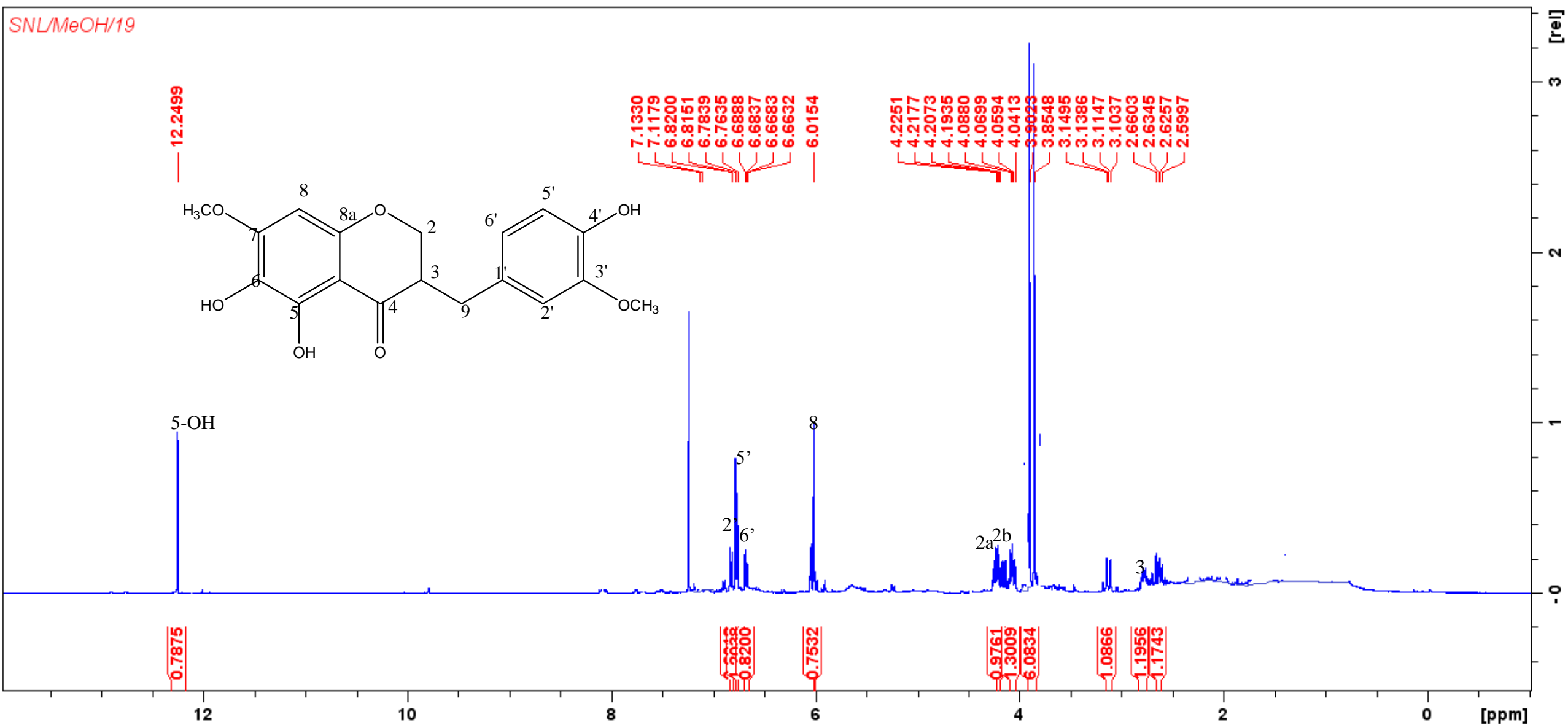
Monoisotopic Mass, Even Electron Ions
31 formula(e) evaluated with 2 results within limits (up to 10 best isotopic matches for each mass)
Elements Used:
C: 1-70 H: 1-100 O: 1-8



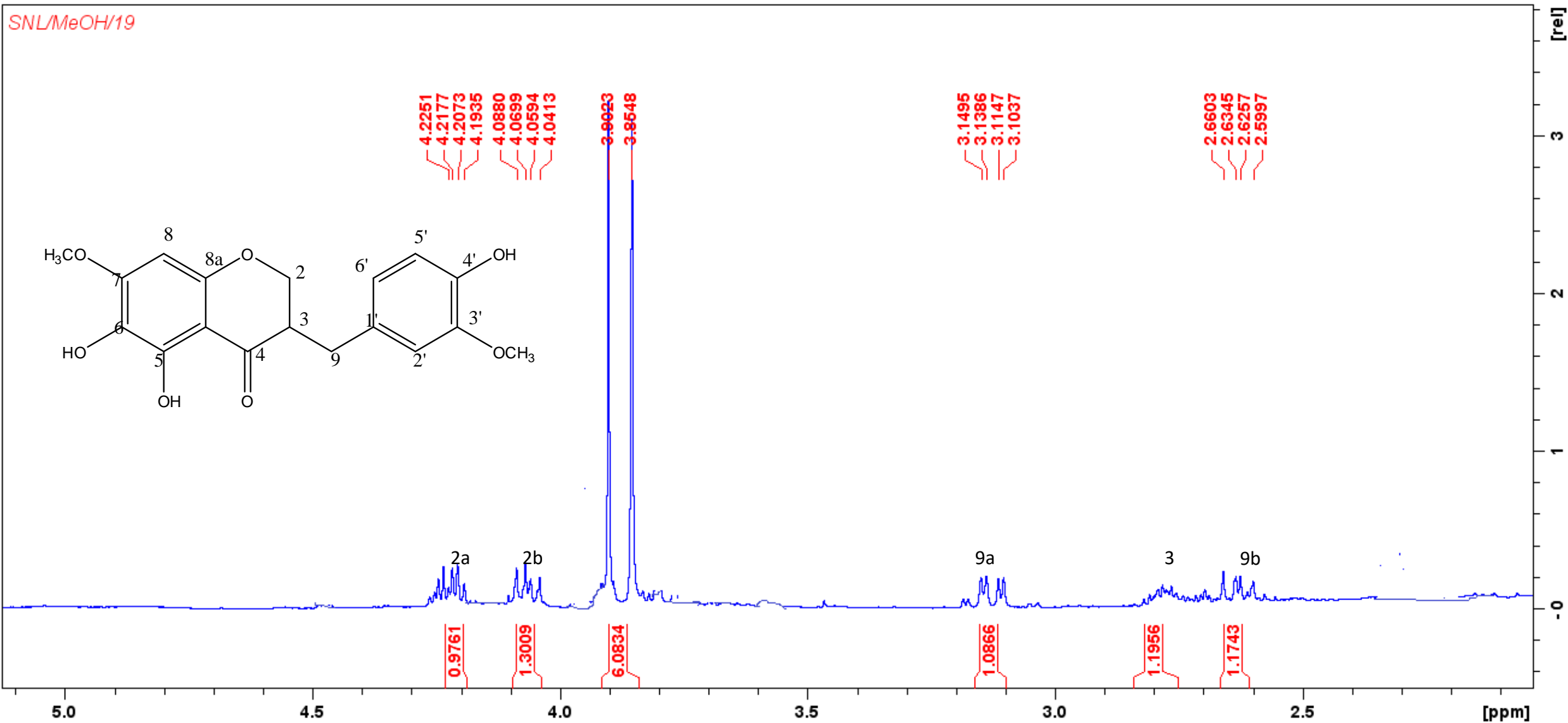
HR-MS of compounds (**A1**) 3-(4-methoxybenzyl)-5,7-dimethoxychroman-4-one and (**A5**)3-(4-hydroxyl-3-methoxybenzyl)-5,6,7-trimethoxychroman-4-one



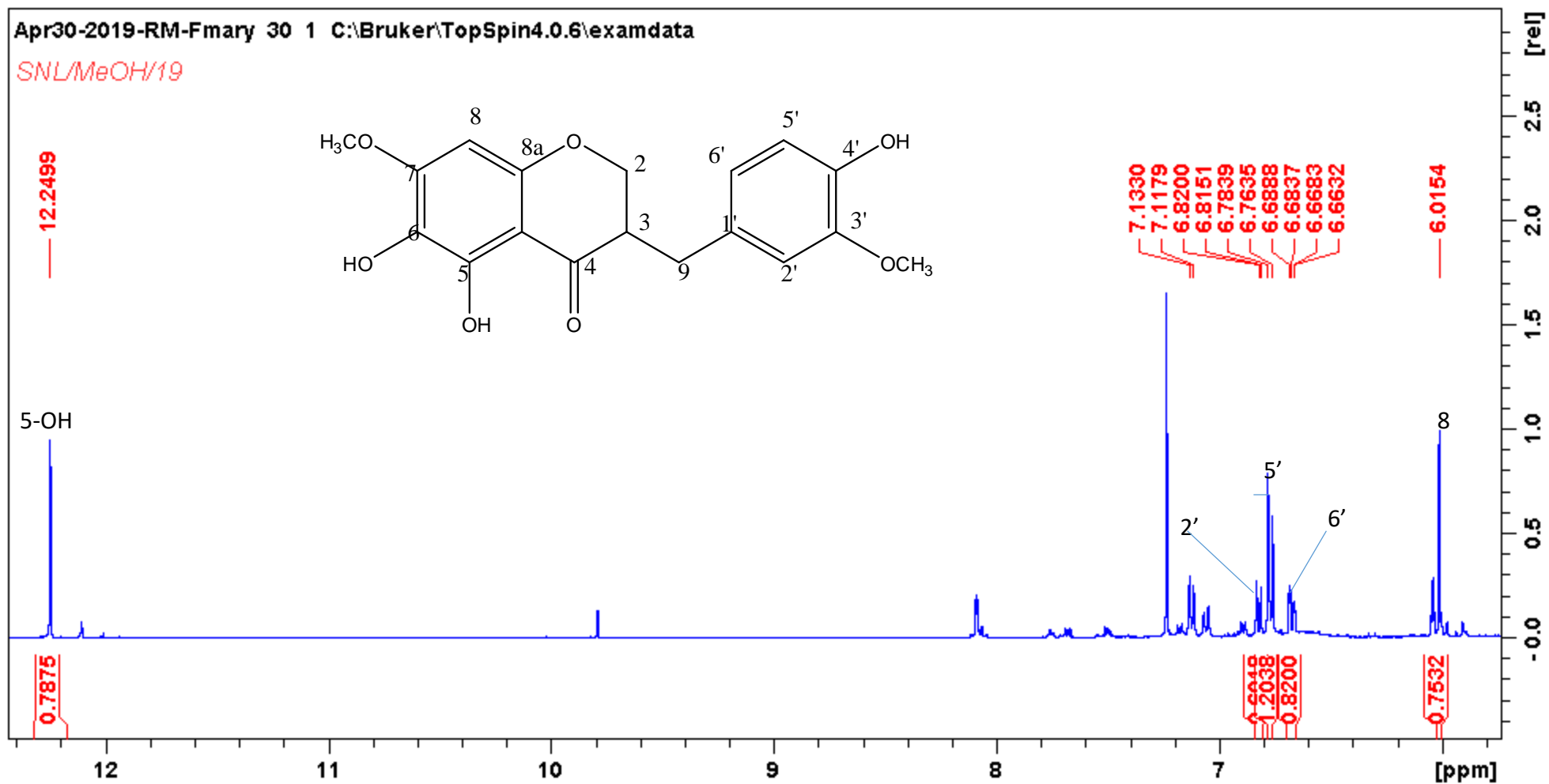
IR of compounds (**A1**) 3-(4-methoxybenzyl)-5,7-dimethoxychroman-4-one and **5(A5)**3-(4-hydroxyl-3-methoxybenzyl)-5,6,7-trimethoxychroman-4-one



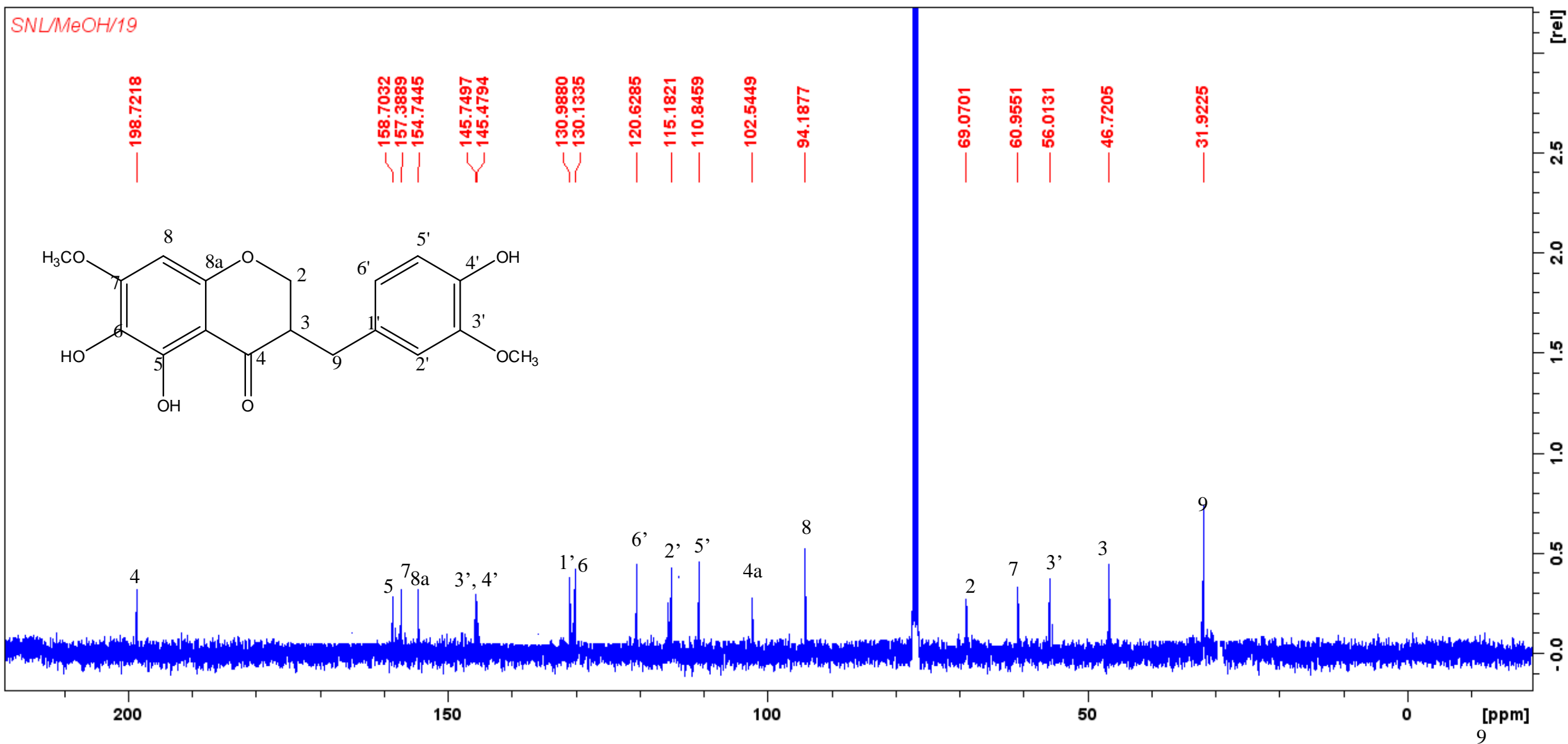
¹H NMR of compound **A6** 3-(4-hydroxyl-3-methoxybenzyl)-5,6-dihydroxy-7-methoxychroman-4-one



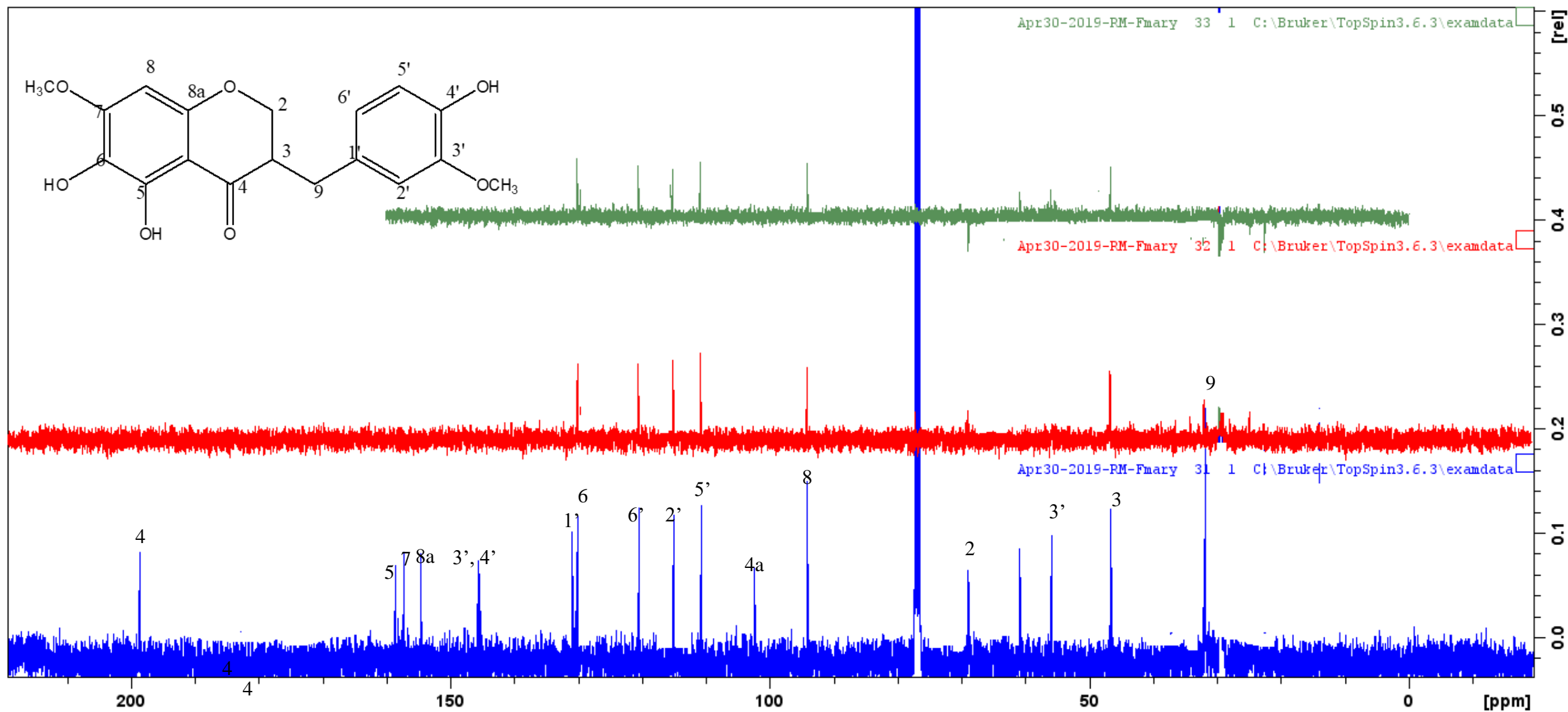
Expanded ¹H NMR of compound **A6** 3-(4-hydroxyl-3-methoxybenzyl)-5,6-dihydroxy-7-methoxychroman-4-one



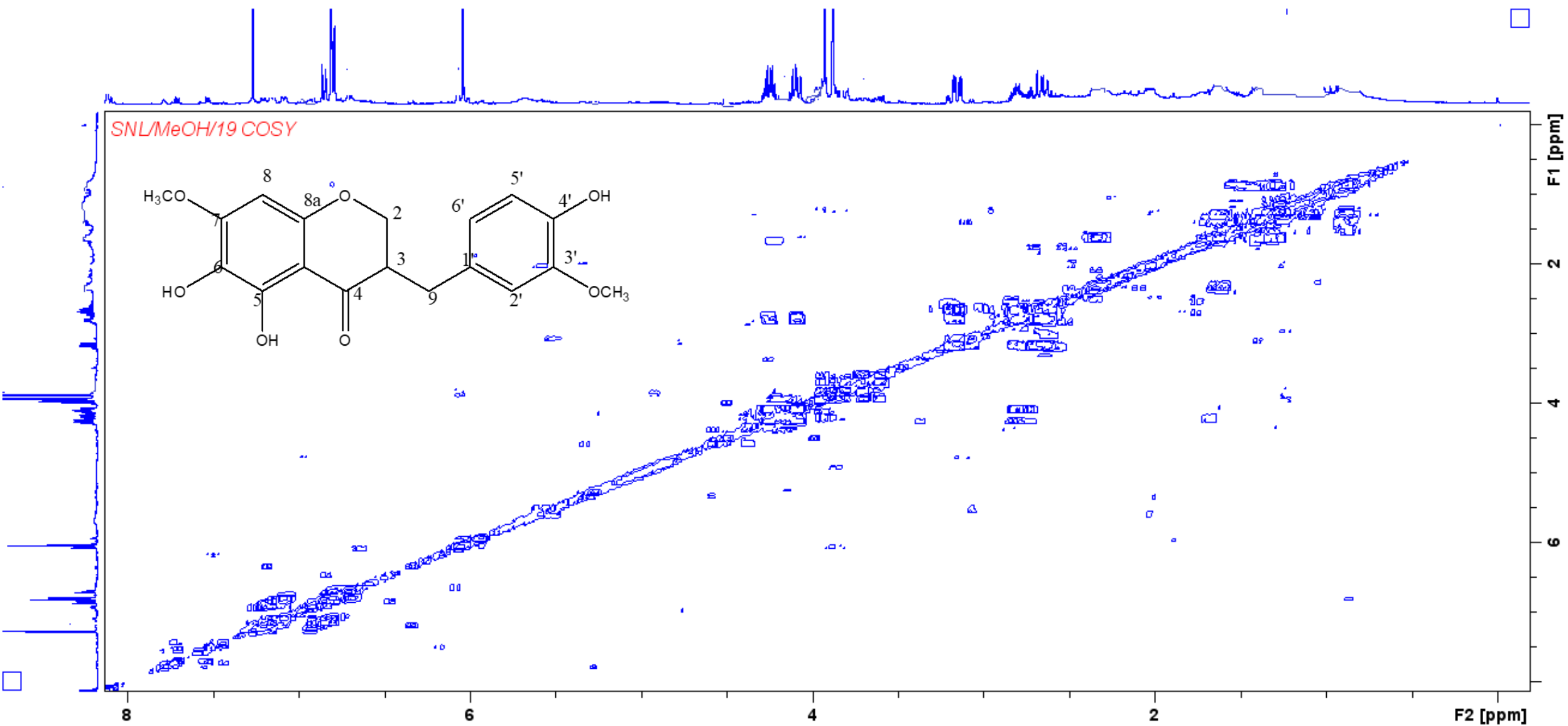
Expanded ¹H NMR of compound **A6** 3-(4-hydroxyl-3-methoxybenzyl)-5,6-dihydroxyl-7-methoxychroman-4-one



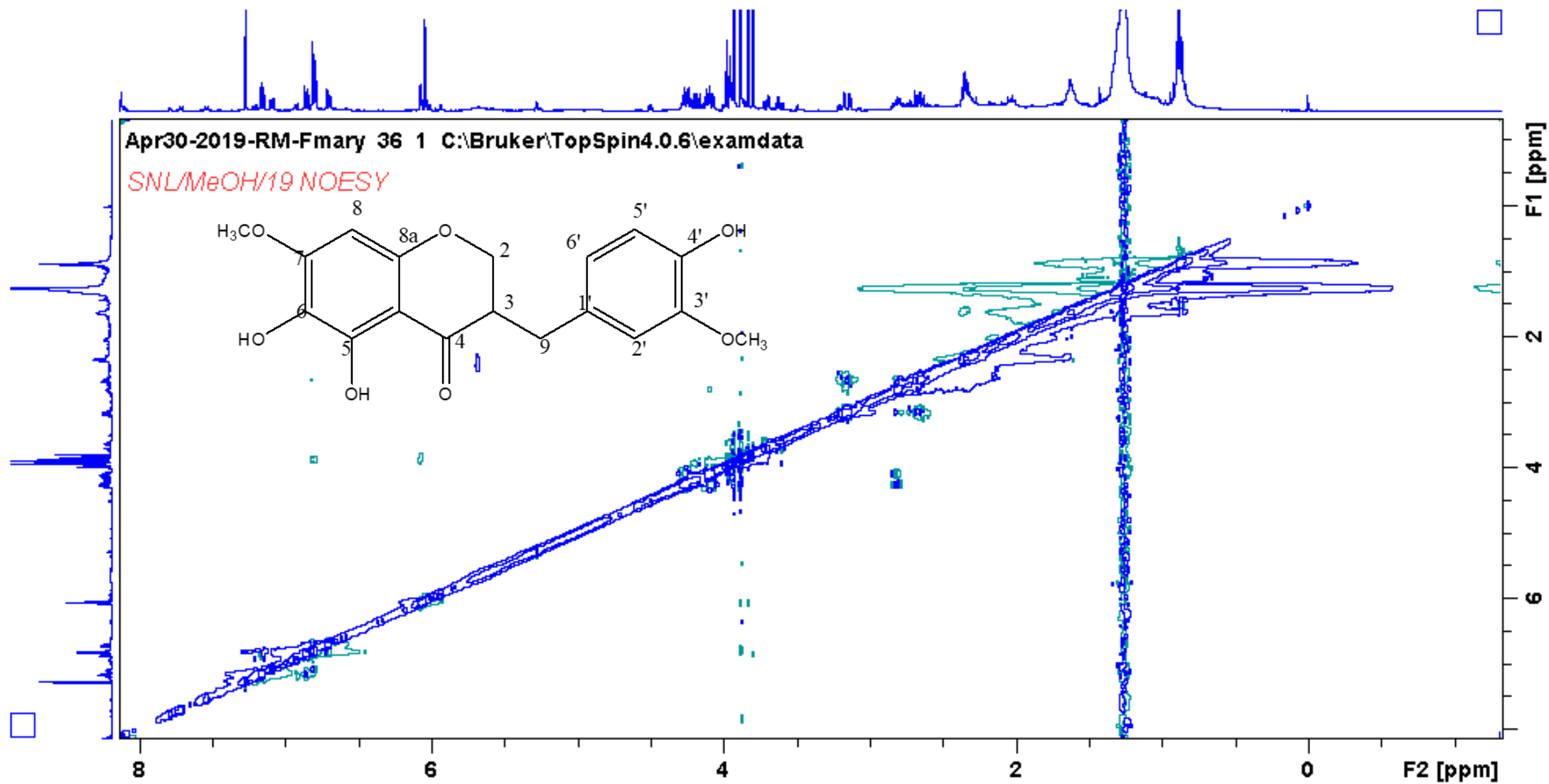
¹³C NMR of compound **A6** 3-(4-hydroxy-3-methoxybenzyl)-5,6-dihydroxy-7-methoxychroman-4-one



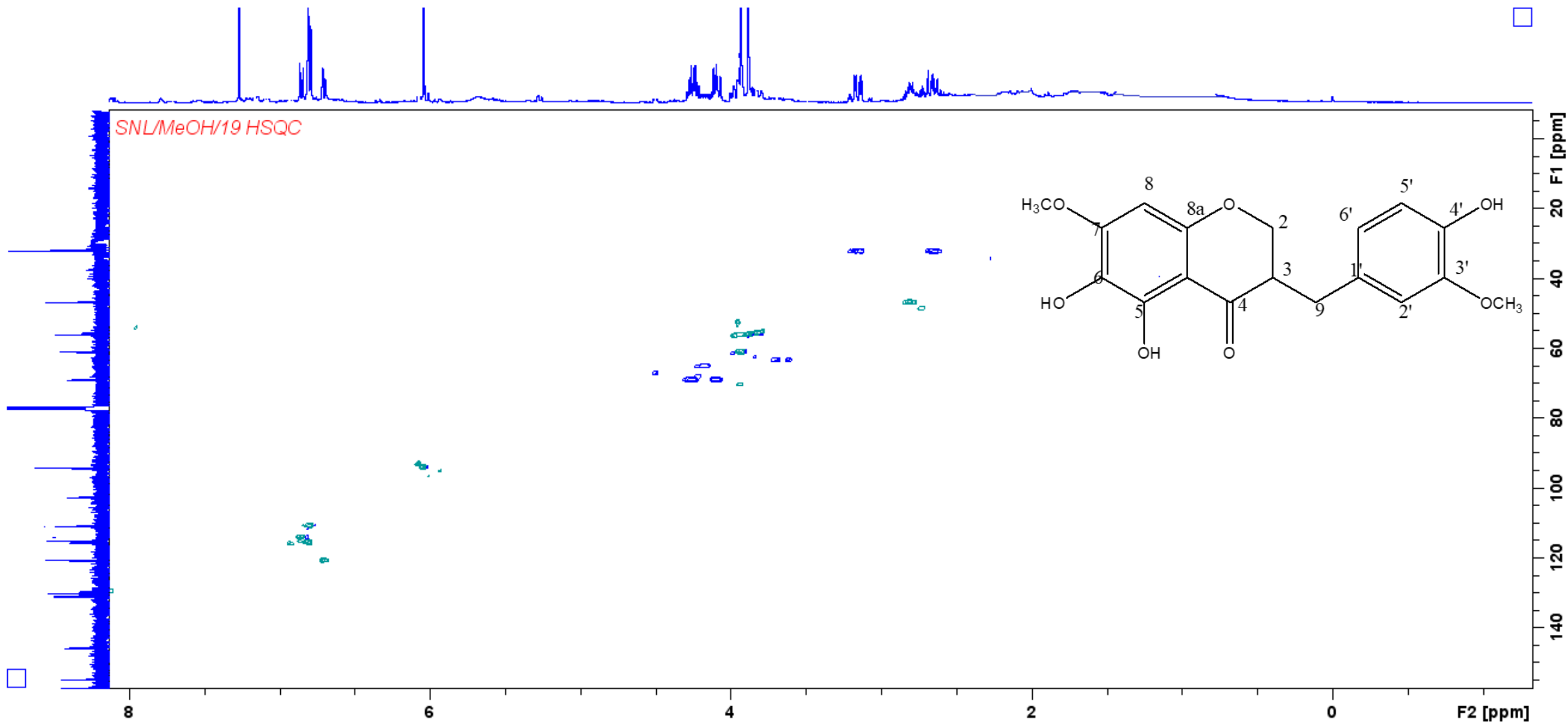
DEPT of compound **A6** 3-(4-hydroxyl-3-methoxybenzyl)-5,6-dihydroxy-7-methoxychroman-4-one



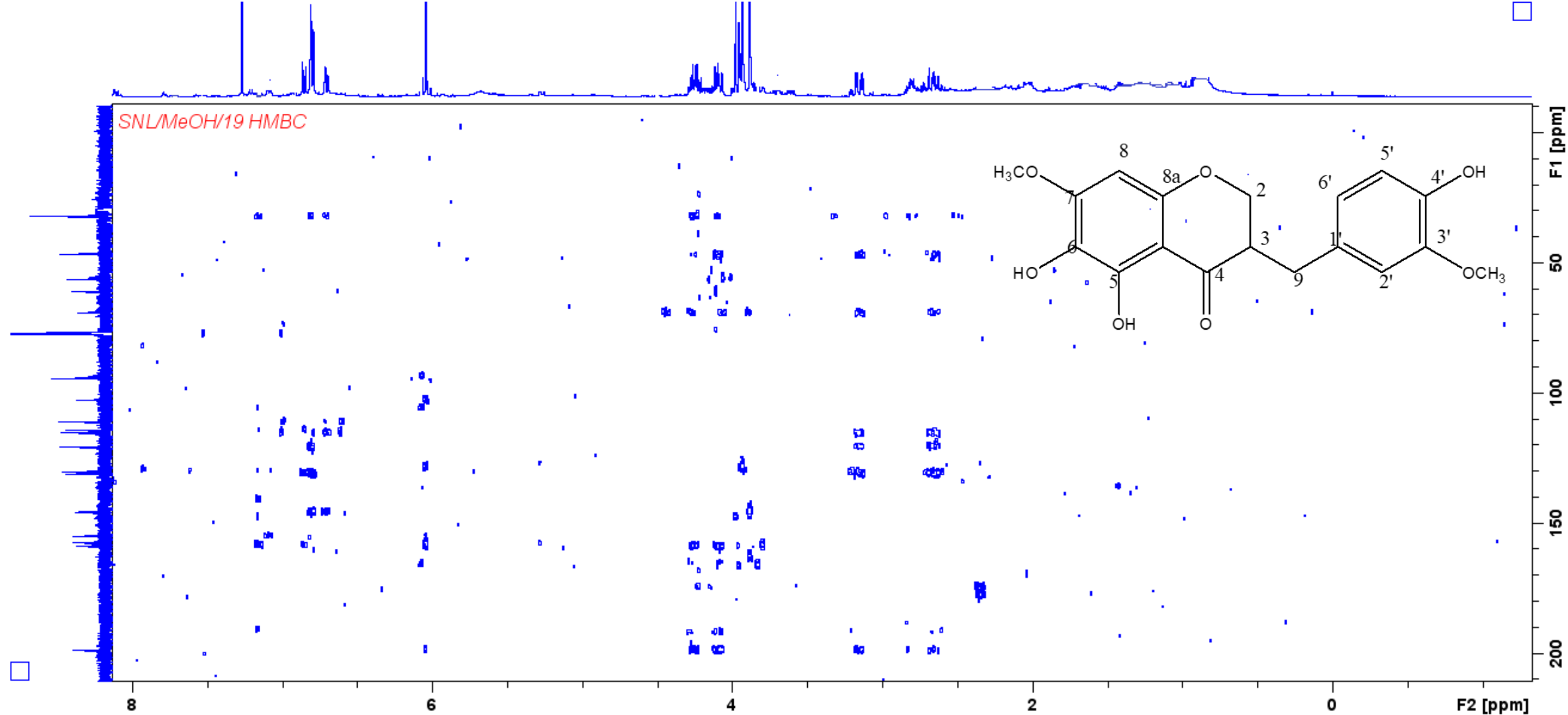
COSY of compound **A6** 3-(4-hydroxyl-3-methoxybenzyl)-5,6-dihydroxy-7-methoxychroman-4-one



NOESY of compound **A6** 3-(4-hydroxyl-3-methoxybenzyl)-5,6-dihydro-7-methoxychroman-4-one

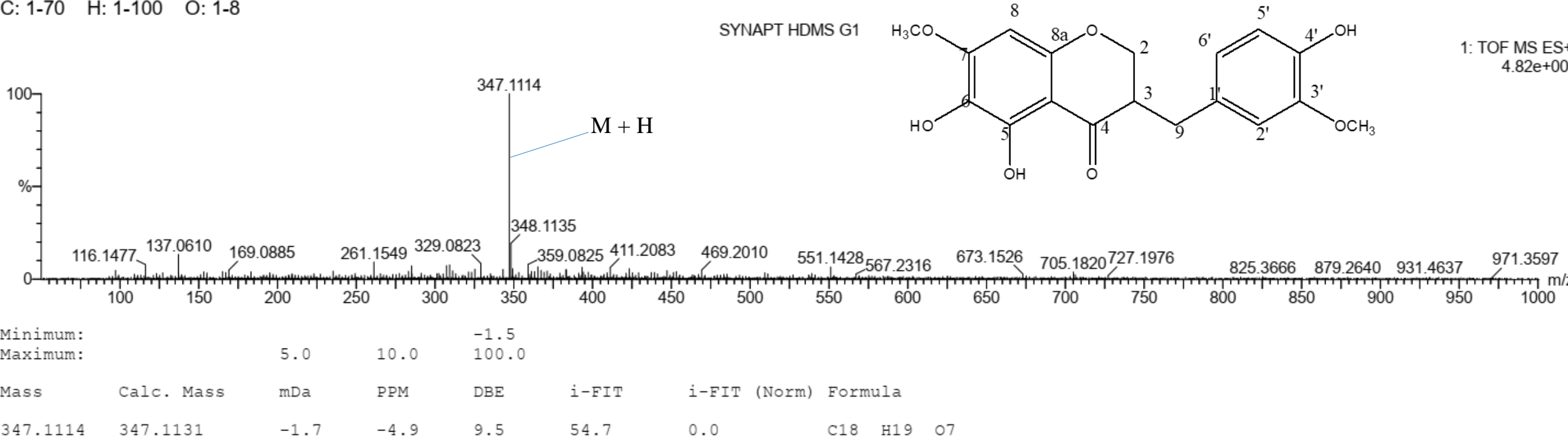


HSQC of compound **A6** 3-(4-hydroxyl-3-methoxybenzyl)-5,6-dihydroxy-7-methoxychroman-4-one

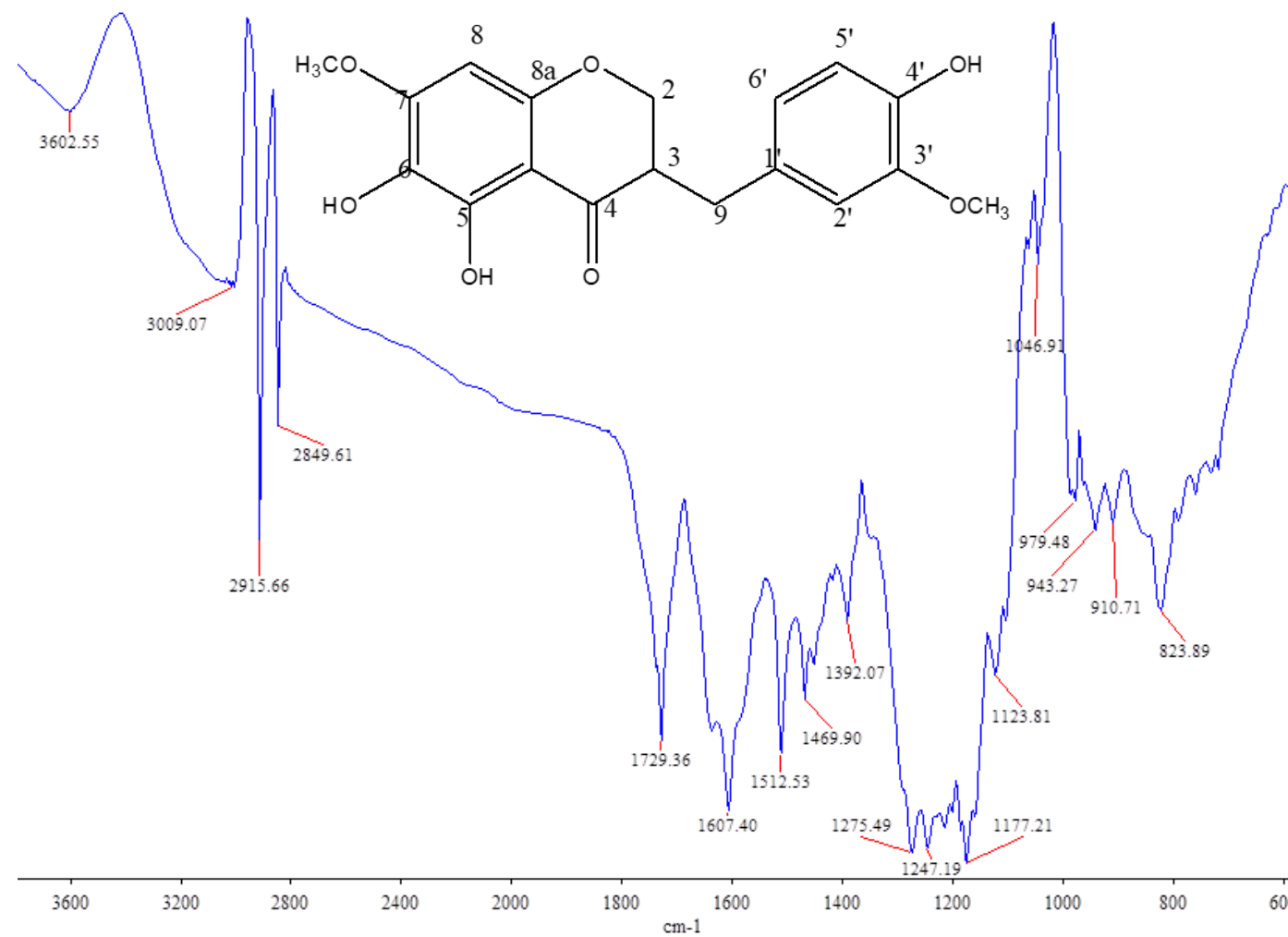


HMBC of compound **A6** 3-(4-hydroxyl-3-methoxybenzyl)-5,6-dihydroxyl-7-methoxychroman-4-one

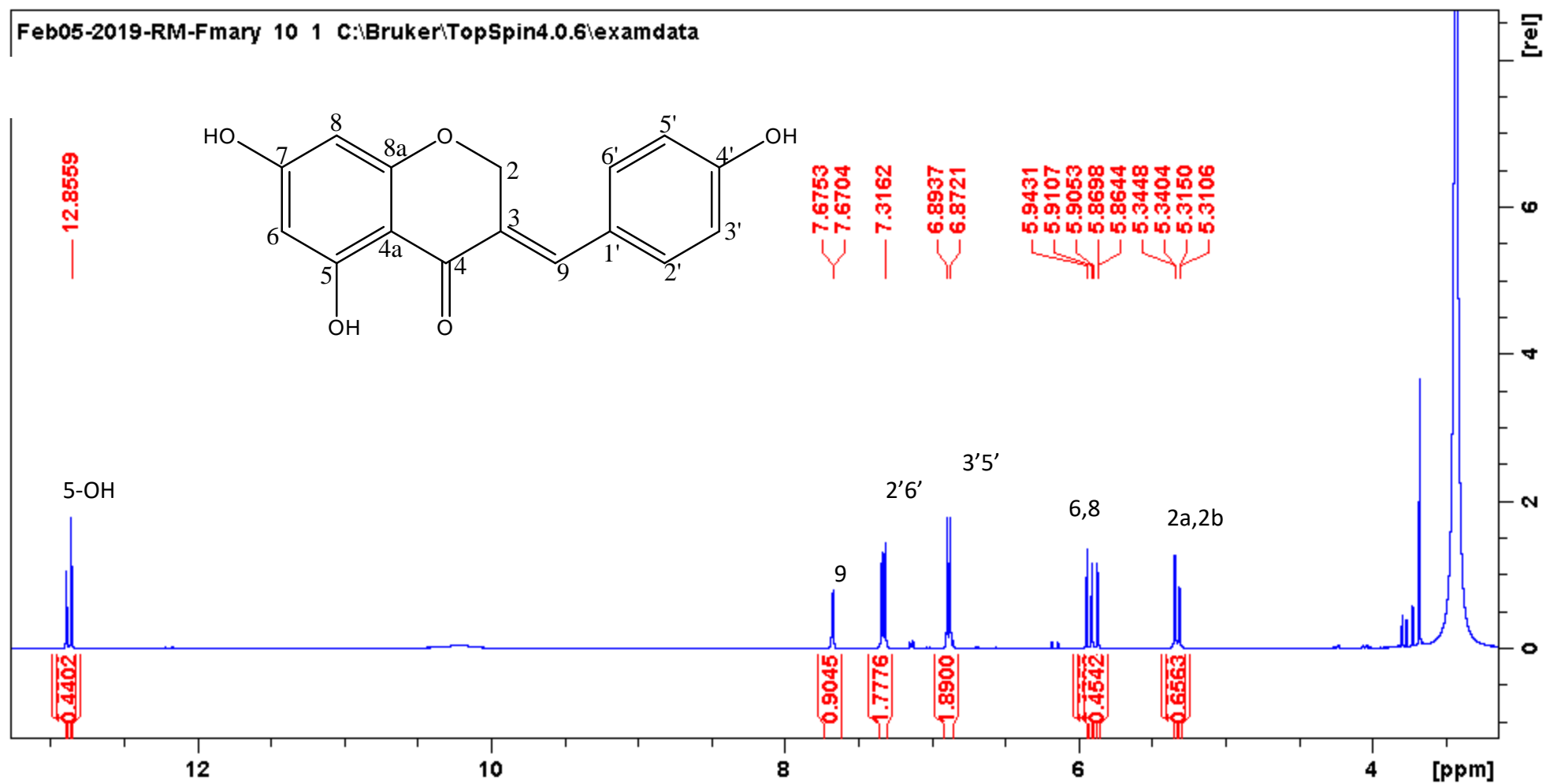
Monoisotopic Mass, Even Electron Ions
33 formula(e) evaluated with 2 results within limits (up to 10 best isotopic matches for each mass)
Elements Used:
C: 1-70 H: 1-100 O: 1-8



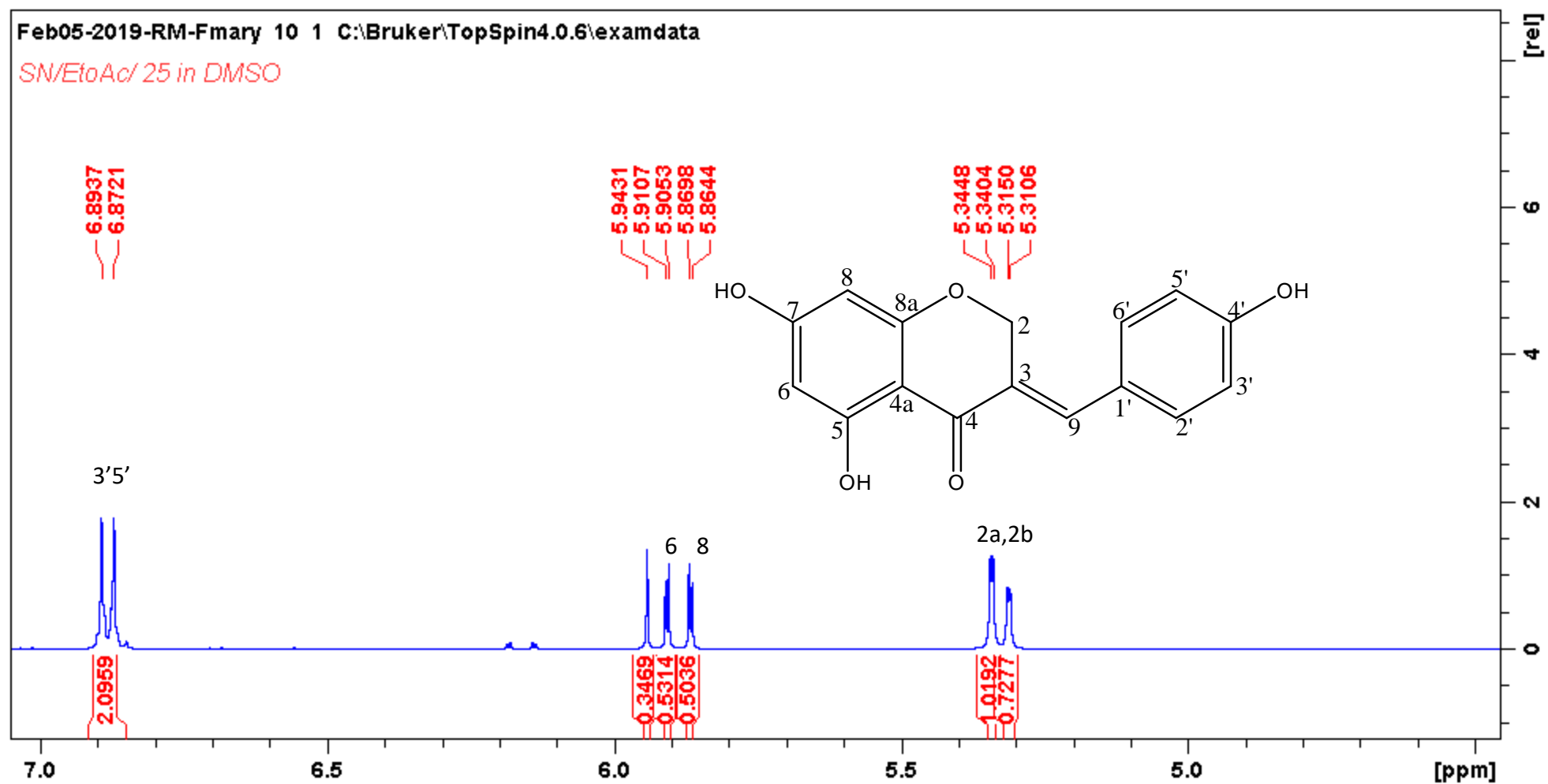
HRMS of compound **A6** 3-(4-hydroxyl-3-methoxybenzyl)-5,6-dihydroxy-7-methoxychroman-4-one



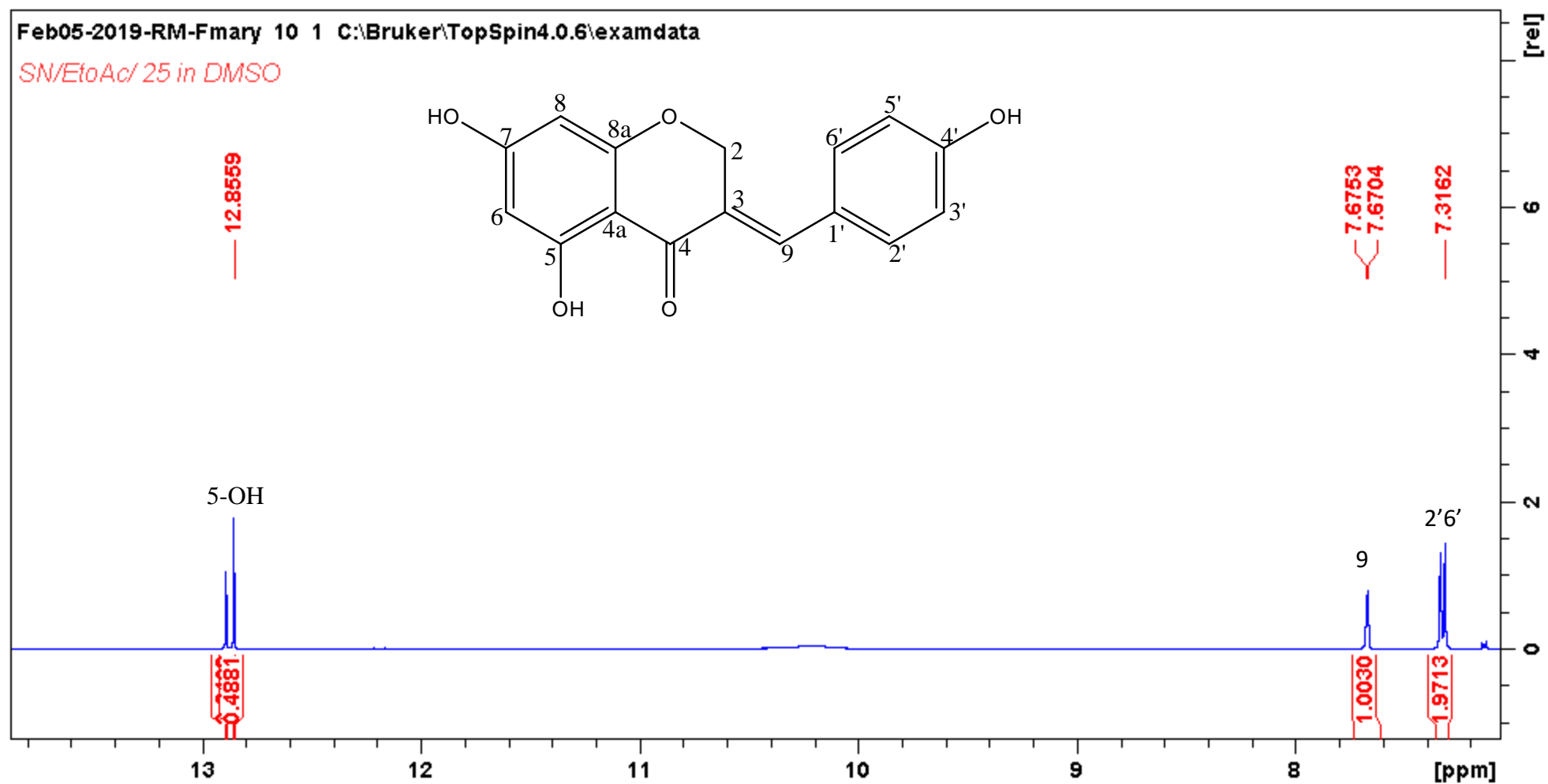
IR of compound **A6** 3-(4-hydroxyl-3-methoxybenzyl)-5,6-dihydro-7-methoxychroman-4-one



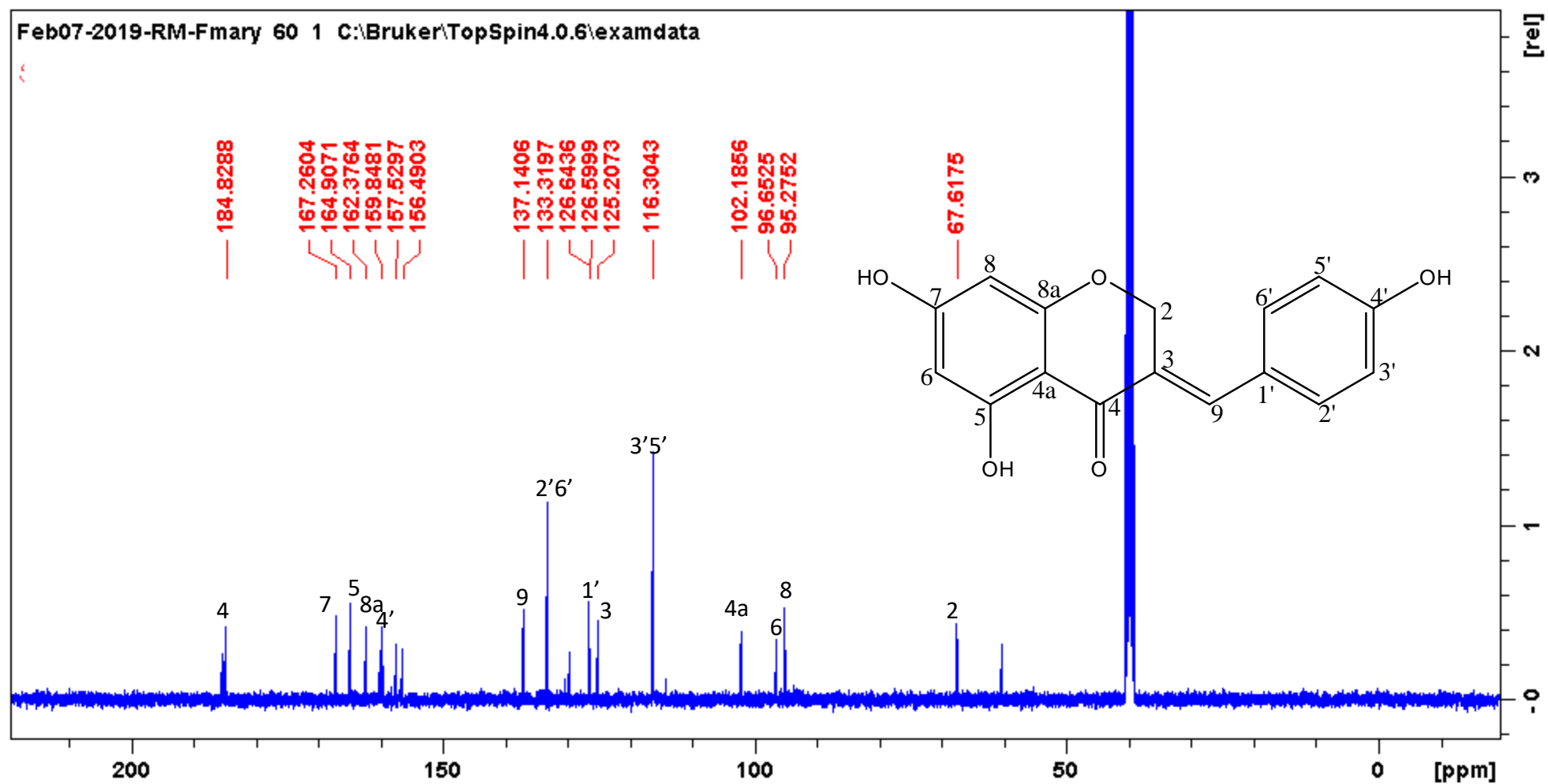
^1H NMR of compound **A7** 3-(4-hydroxybenzylidene)-5,7-dihydroxylchroman-4-one



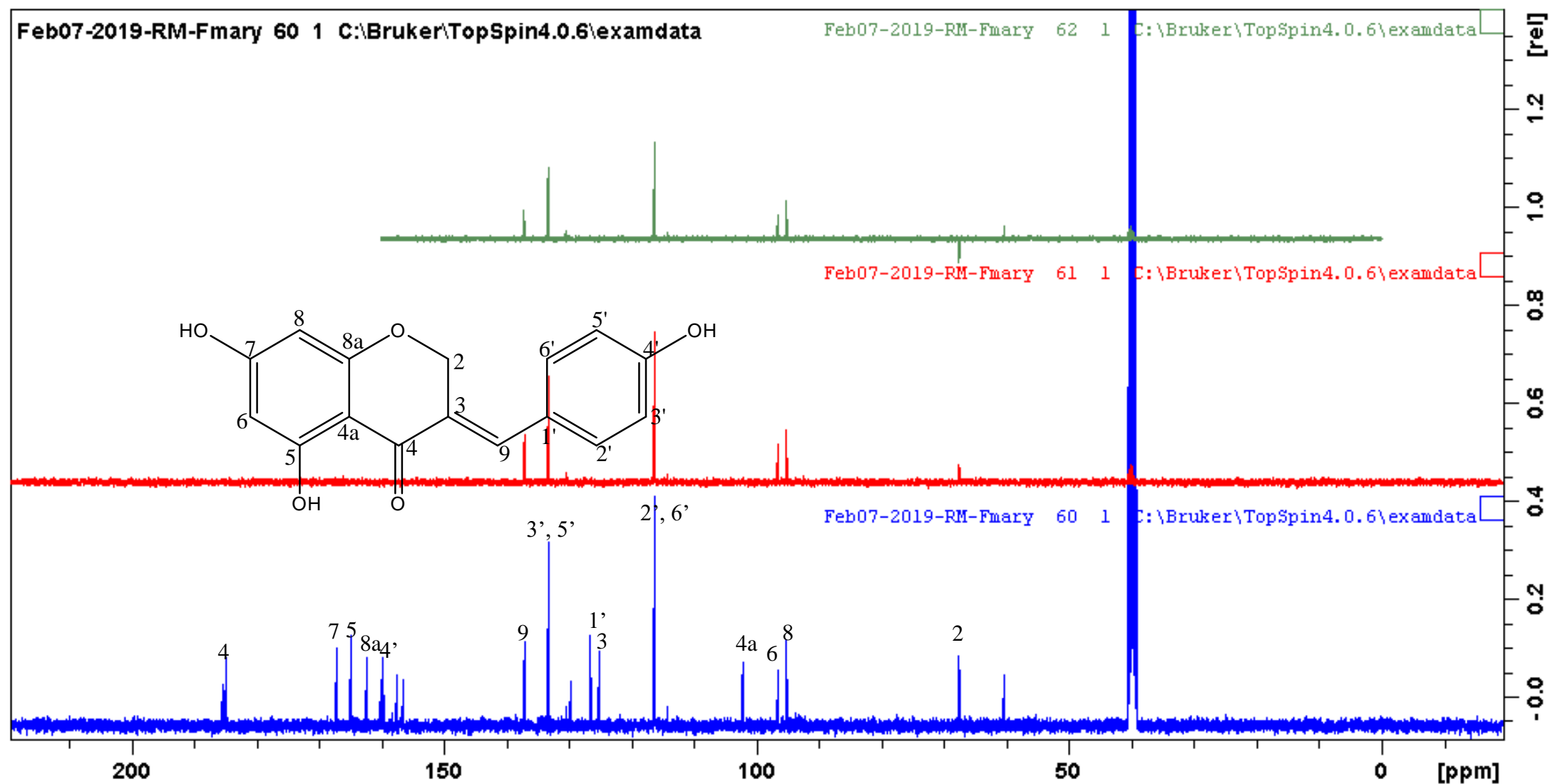
Expanded ^1H NMR of compound **A7** 3-(4-hydroxybenzylidene)-5,7-dihydroxylchroman-4-one

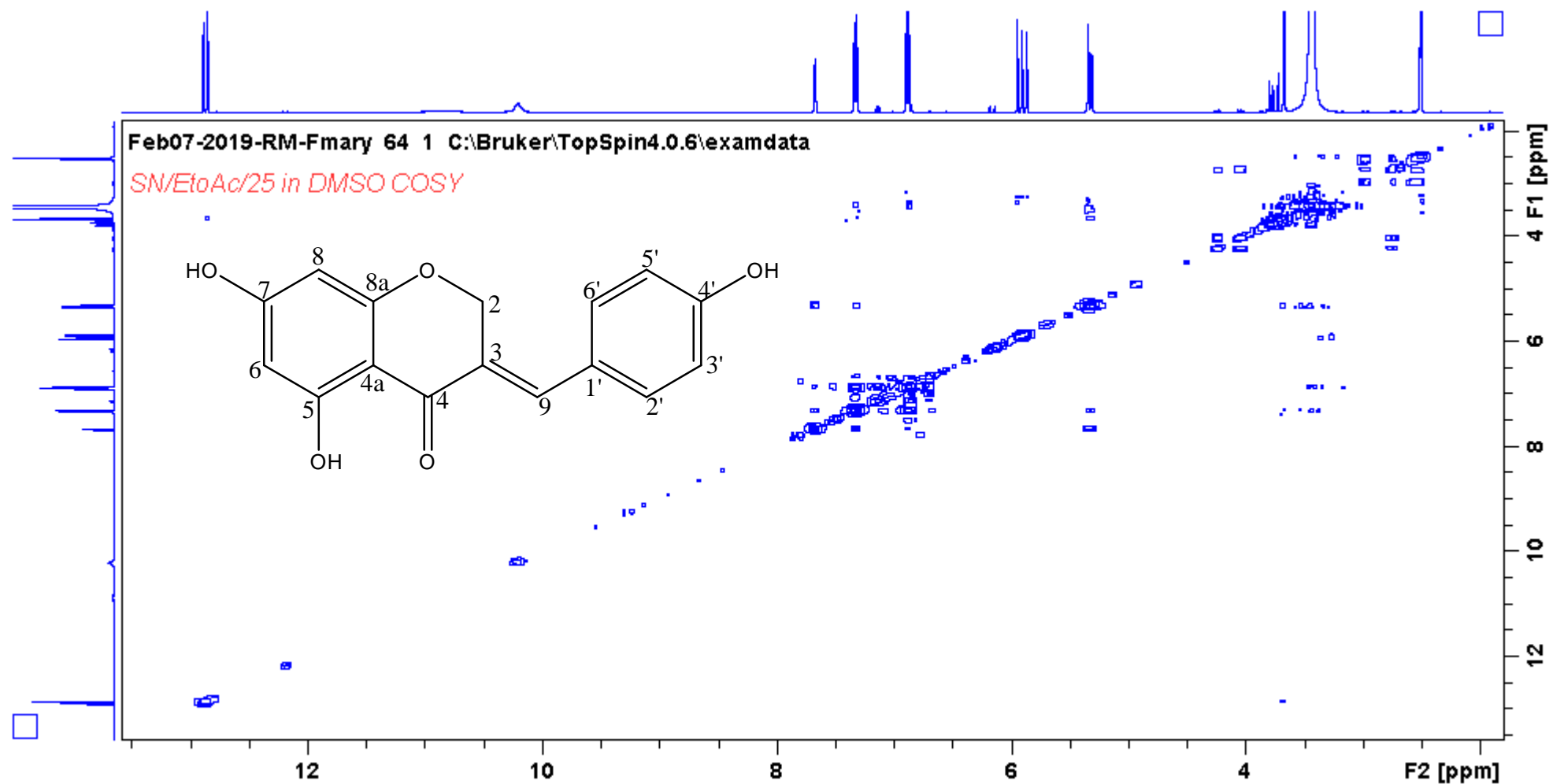


Expanded ¹H NMR of compound **A7** 3-(4-hydroxybenzylidene)-5,7-dihydroxychroman-4-one

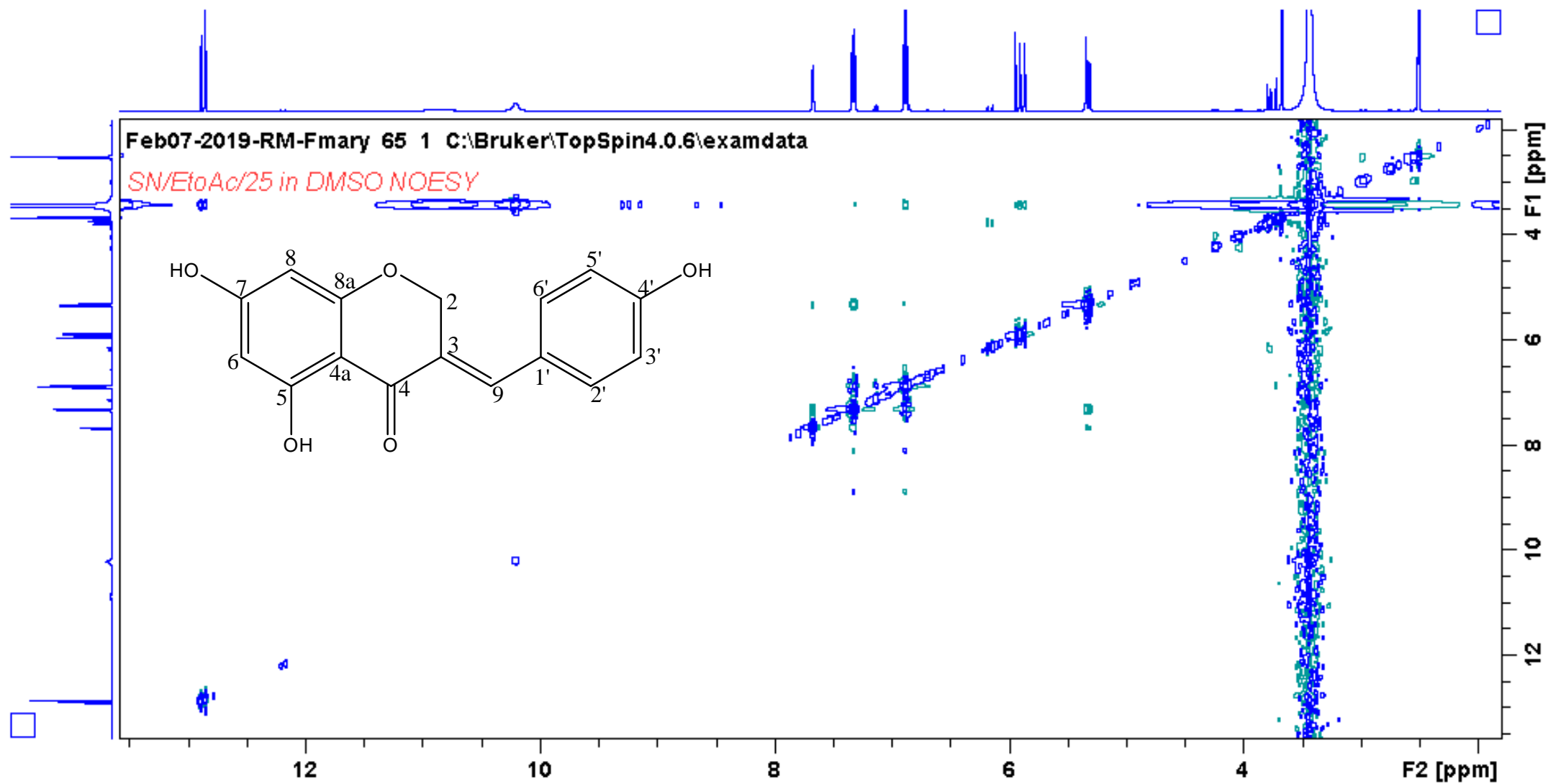


¹³C NMR of compound A7 3-(4-hydroxybenzylidene)-5,7-dihydroxylchroman-4-one

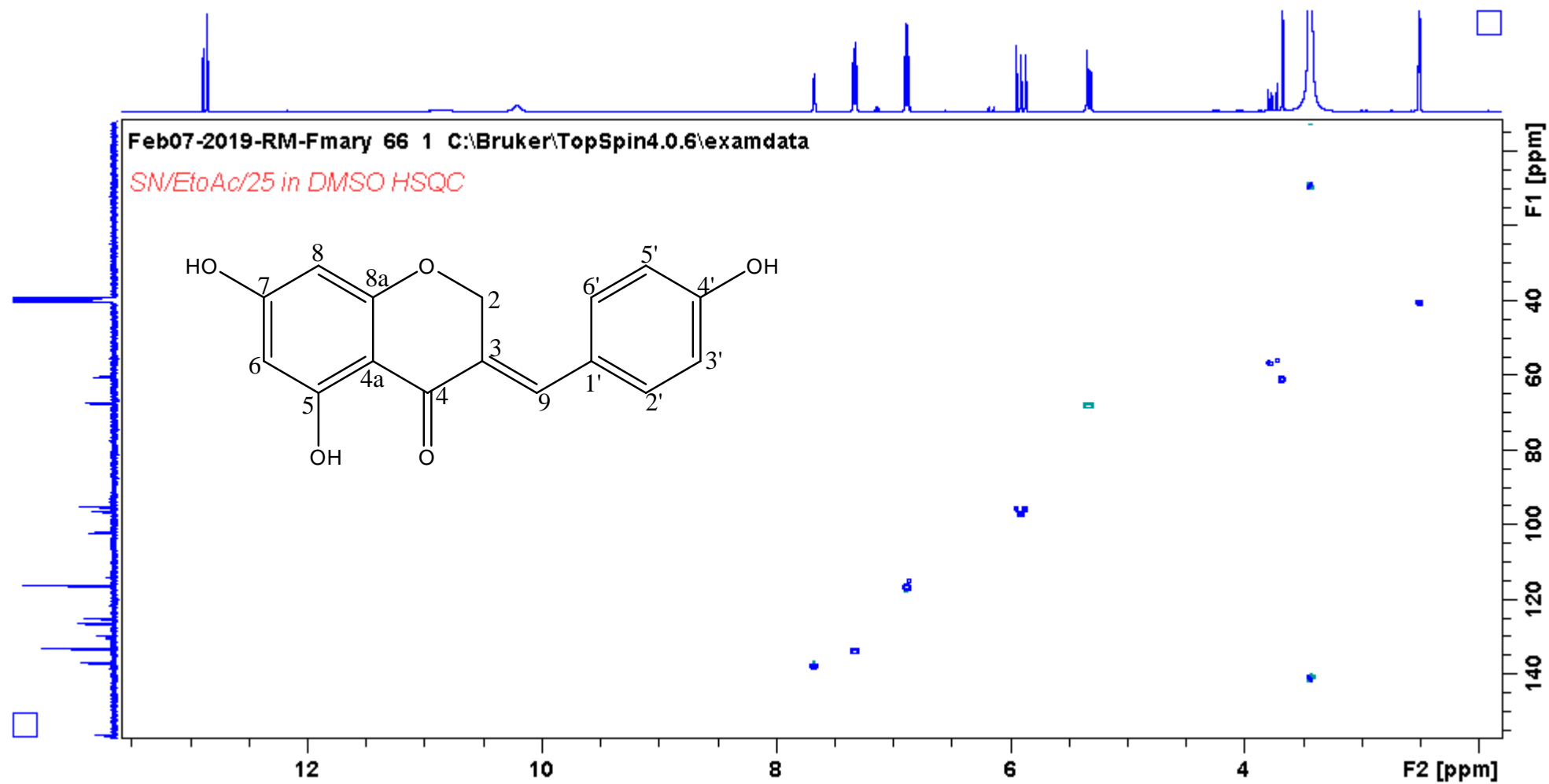




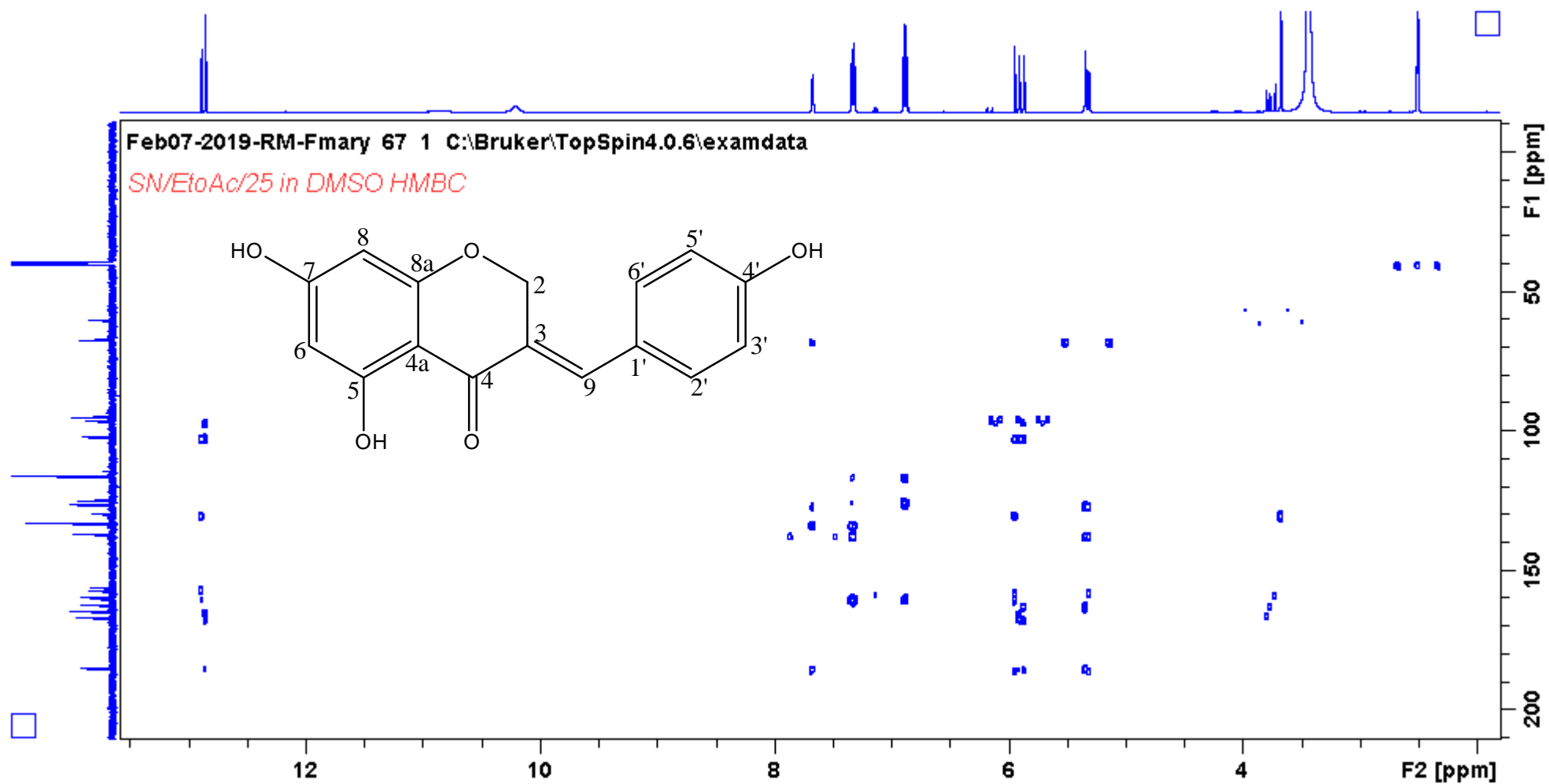
COSY of compound **A7** 3-(4-hydroxybenzylidene)-5,7-dihydroxychroman-4-one



NOESY of compound **A7** 3-(4-hydroxybenzylidene)-5,7-dihydroxychroman-4-one



HSQC of compound **A7** 3-(4-hydroxybenzylidene)-5,7-dihydroxychroman-4-one



HMBC of compound **A7** 3-(4-hydroxybenzylidene)-5,7-dihydroxychroman-4-one

Single Mass Analysis

Tolerance = 5.0 PPM / DBE: min = -1.5, max = 50.0

Element prediction: Off

Number of isotope peaks used for i-FIT = 3

Monoisotopic Mass, Even Electron Ions

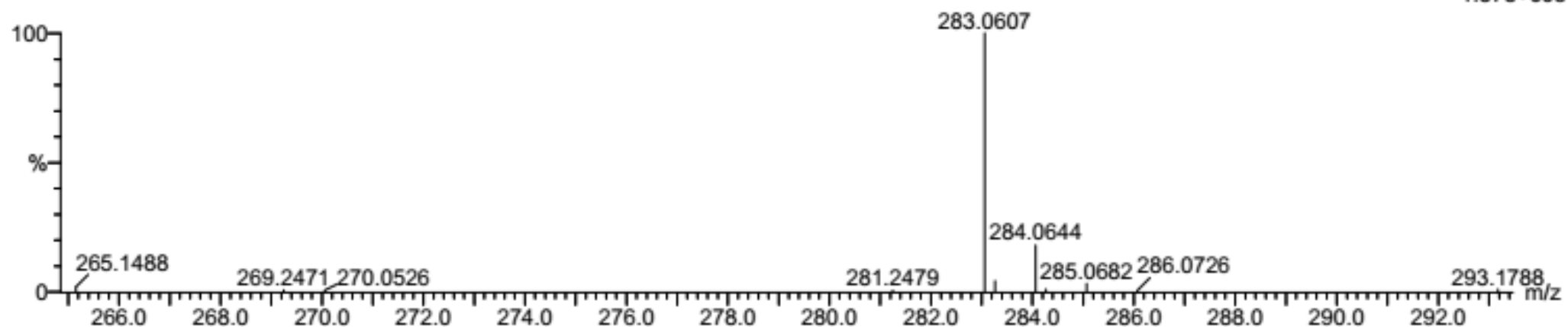
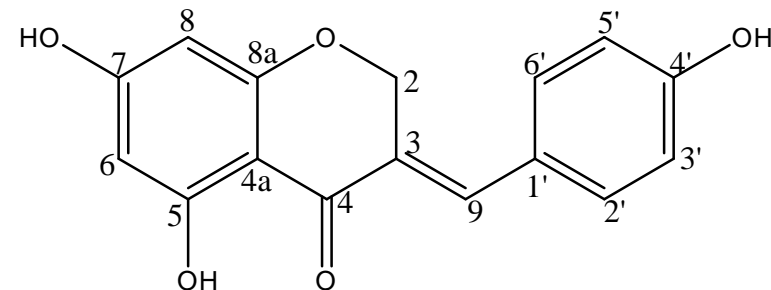
3 formula(e) evaluated with 1 results within limits (all results (up to 1000) for each mass)

Elements Used:

C: 15-20 H: 10-15 O: 0-5

SN_DCM_17-18o 3 (0.068) Cm (1:61)

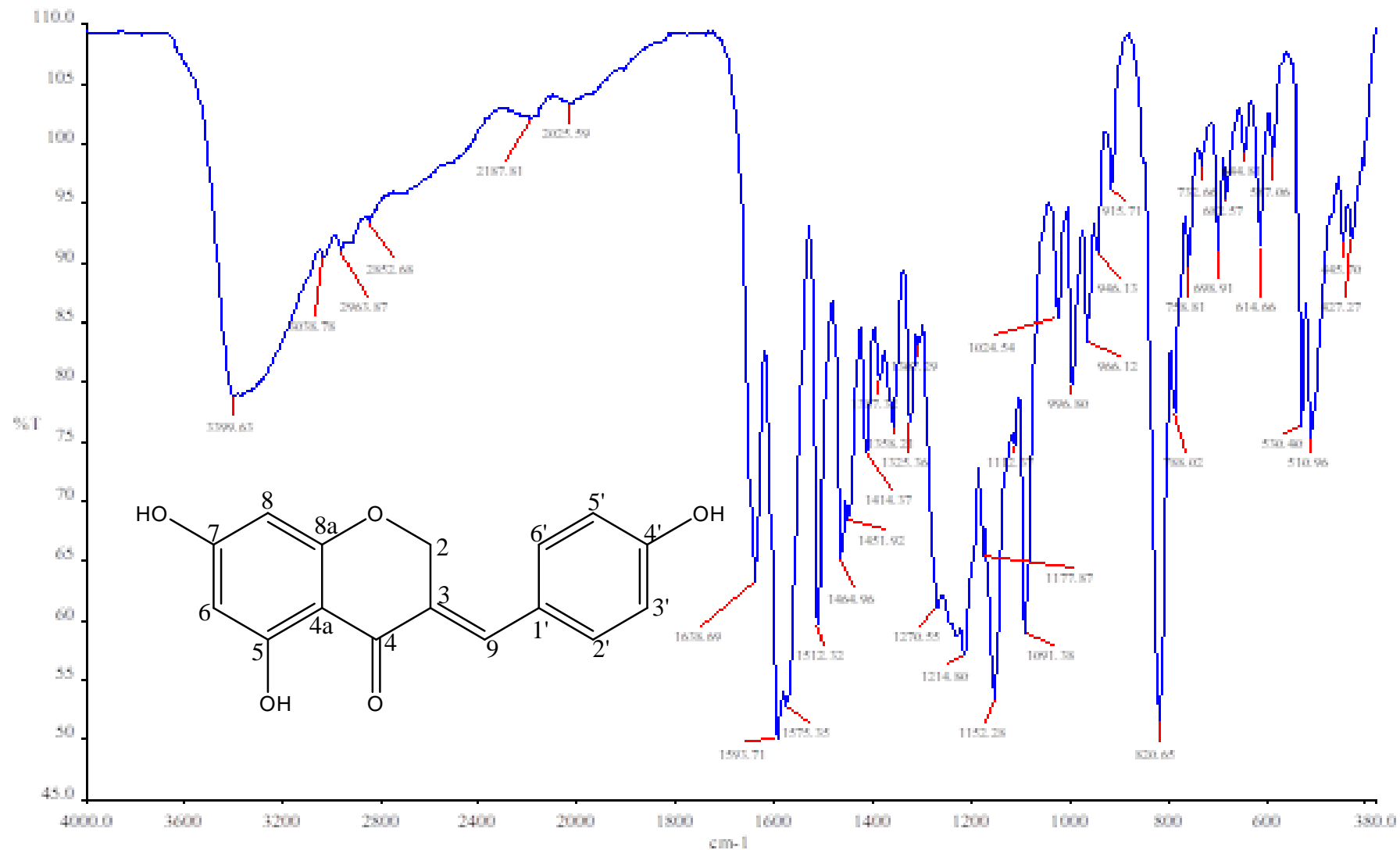
TOF MS ES-



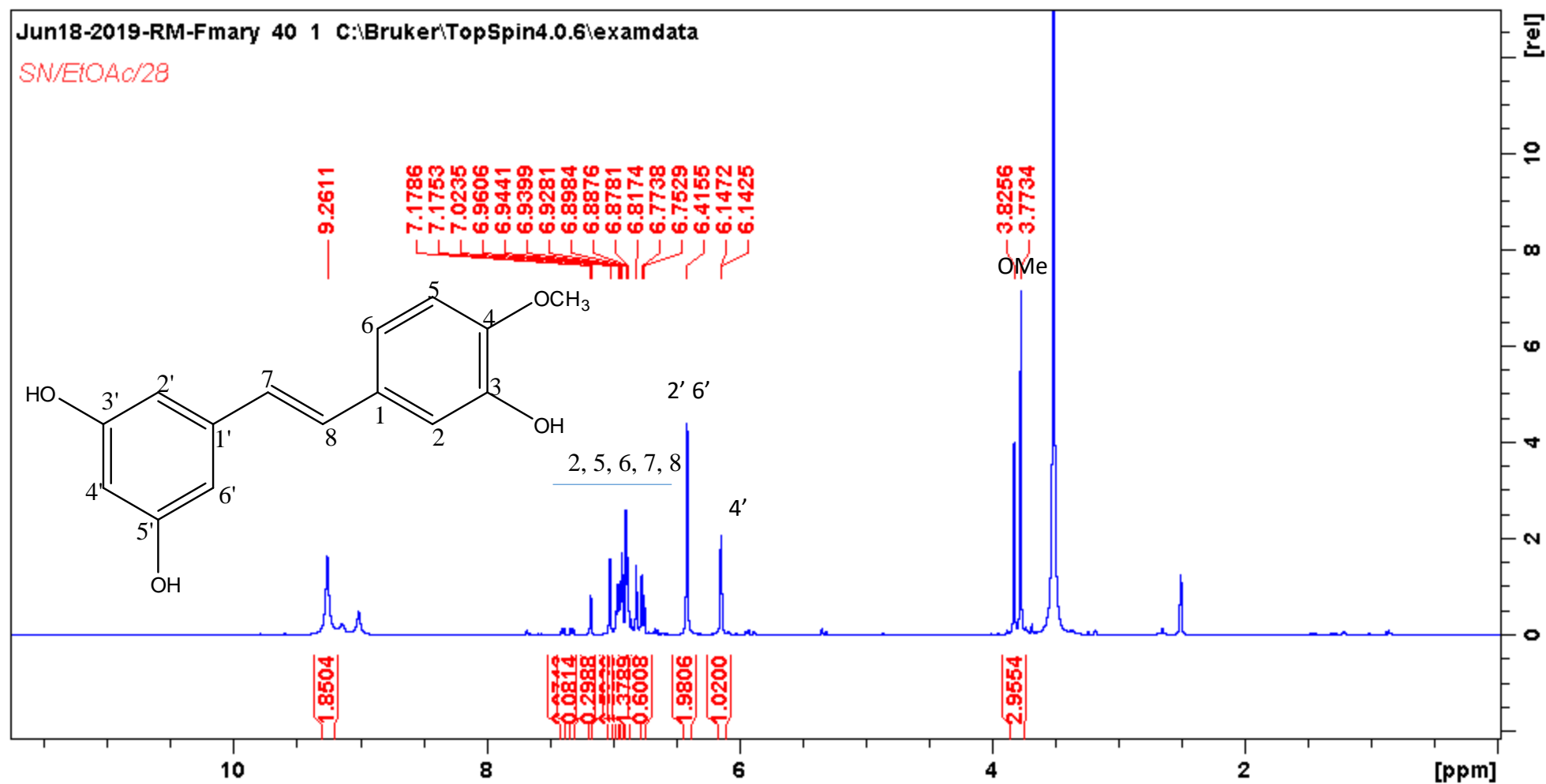
Minimum: -1.5
Maximum: 5.0 5.0 50.0

Mass	Calc. Mass	mDa	PPM	DBE	i-FIT	i-FIT (Norm)	Formula
283.0607	283.0606	0.1	0.4	11.5	49.6	0.0	C16 H11 O5

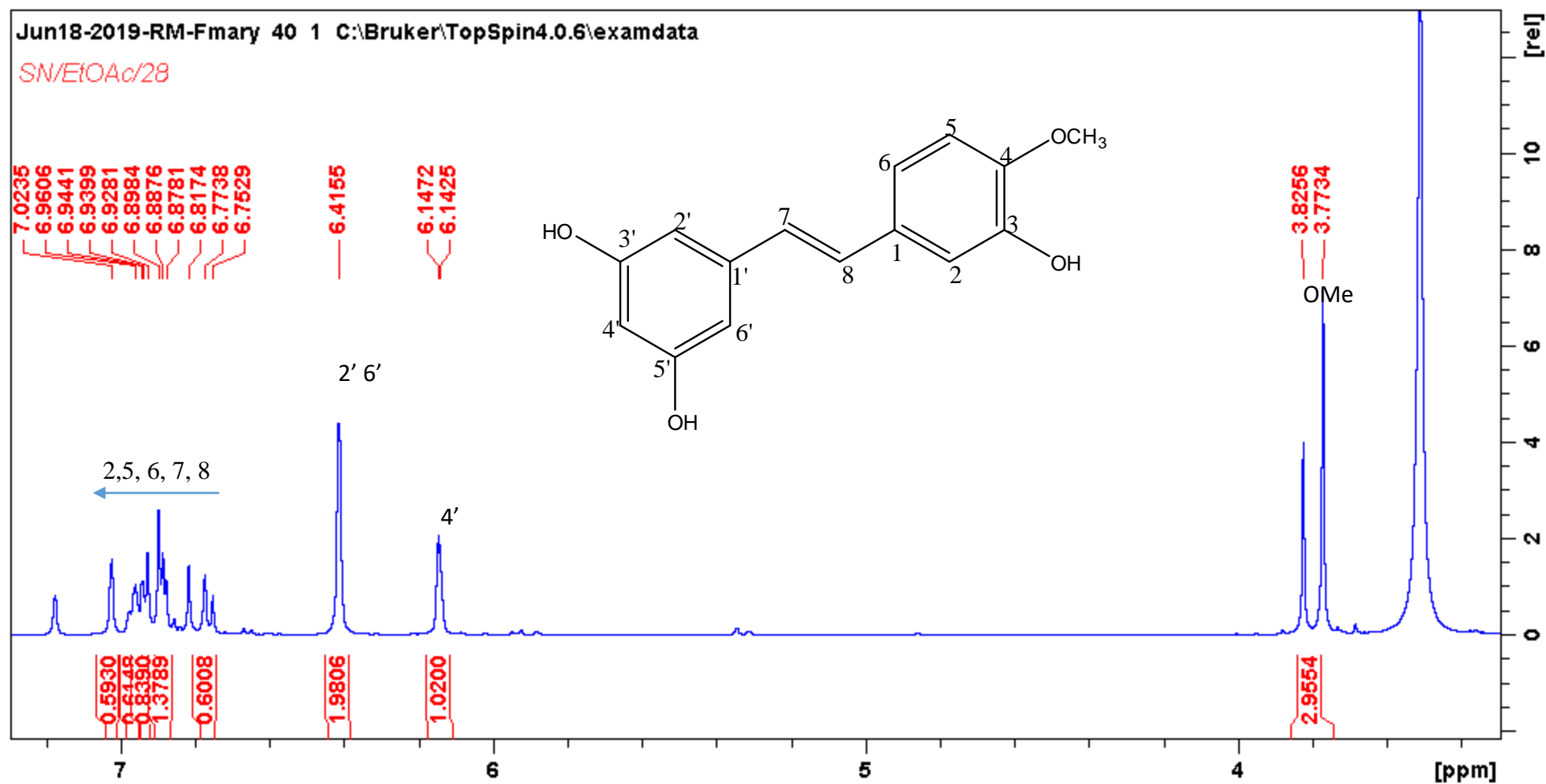
HRMS of compound **A7** 3-(4-hydroxybenzylidene)-5,7-dihydroxychroman-4-one



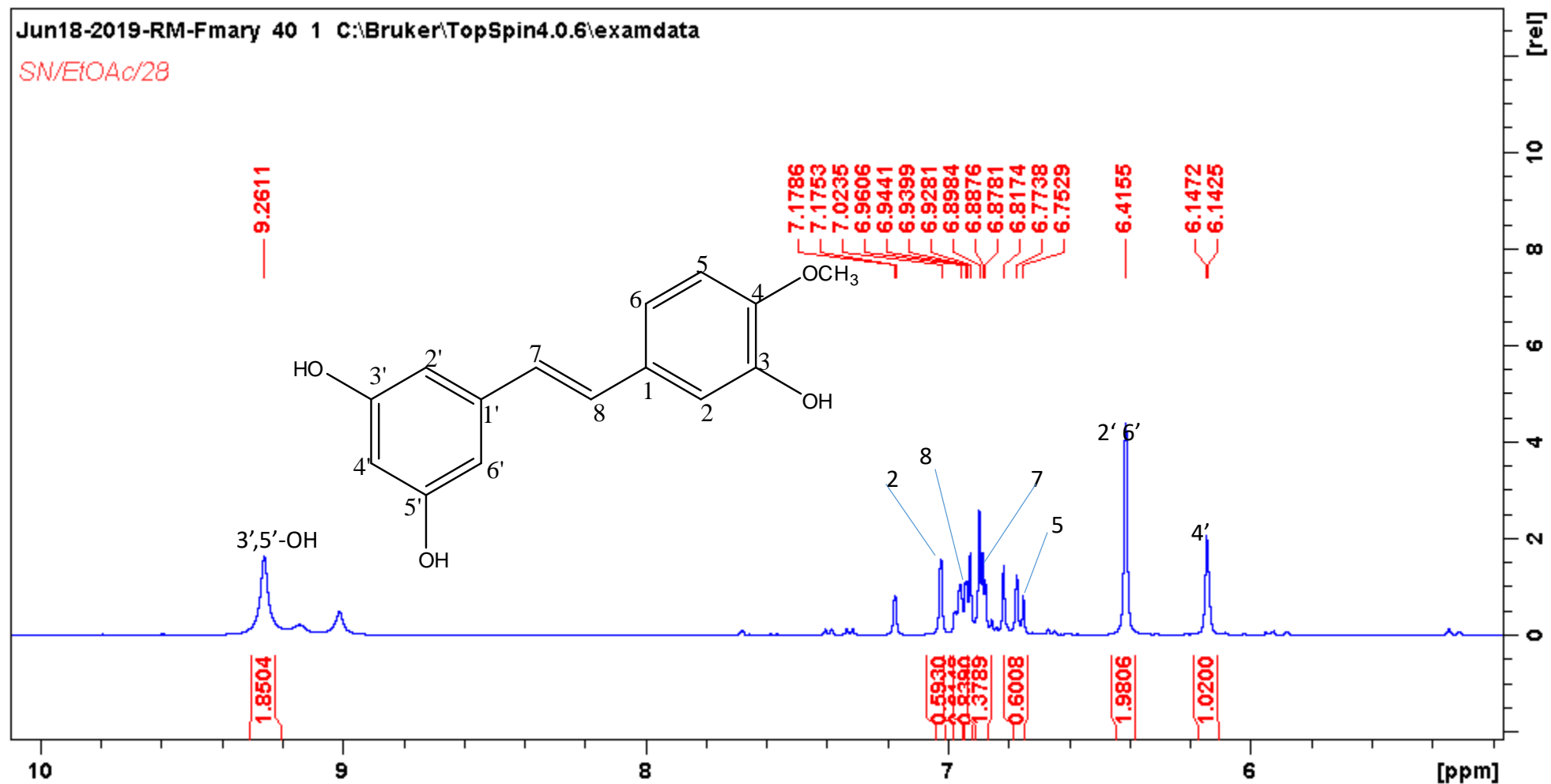
IR of compound **A7** 3-(4-hydroxylbenzylidene)-5,7-dihydroxylchroman-4-one



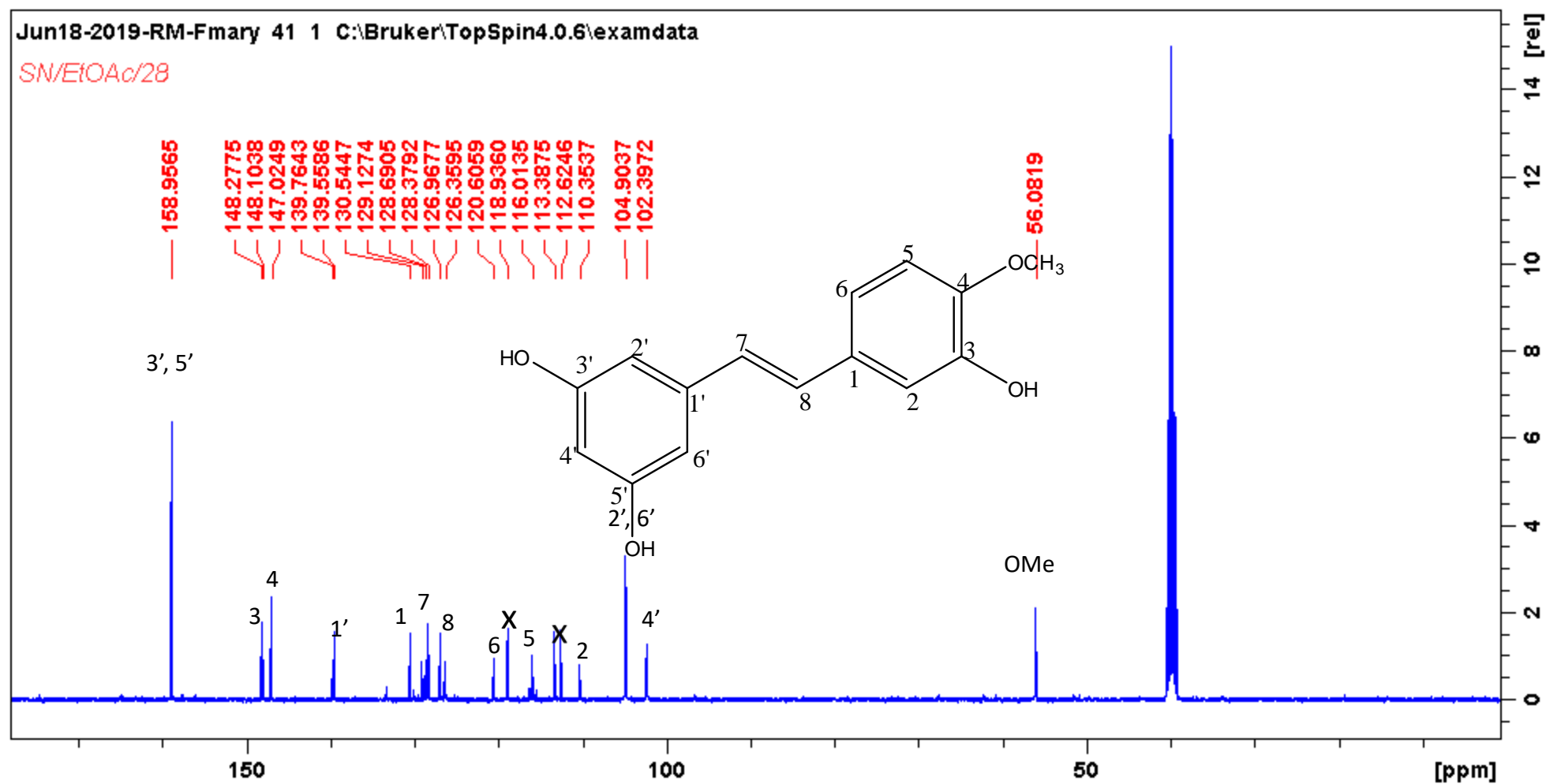
^1H NMR of compound **A8** 3, 3', 5' -Trihydroxy-4-methoxystilbene, Rhapontigenin



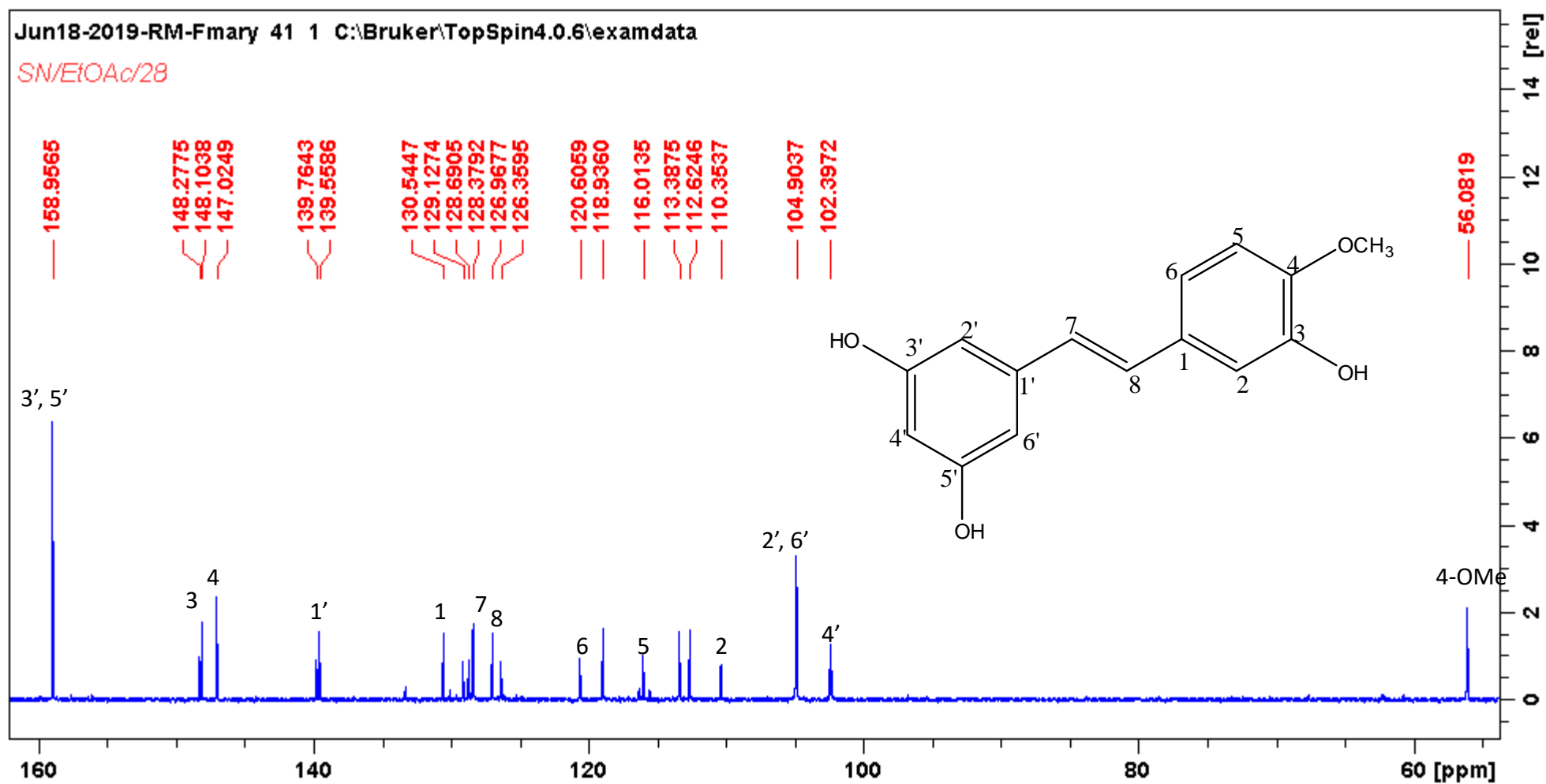
Expanded ^1H NMR of compound **A8** 3, 3', 5' -Trihydroxy-4-methoxystilbene, Rhapontigenin



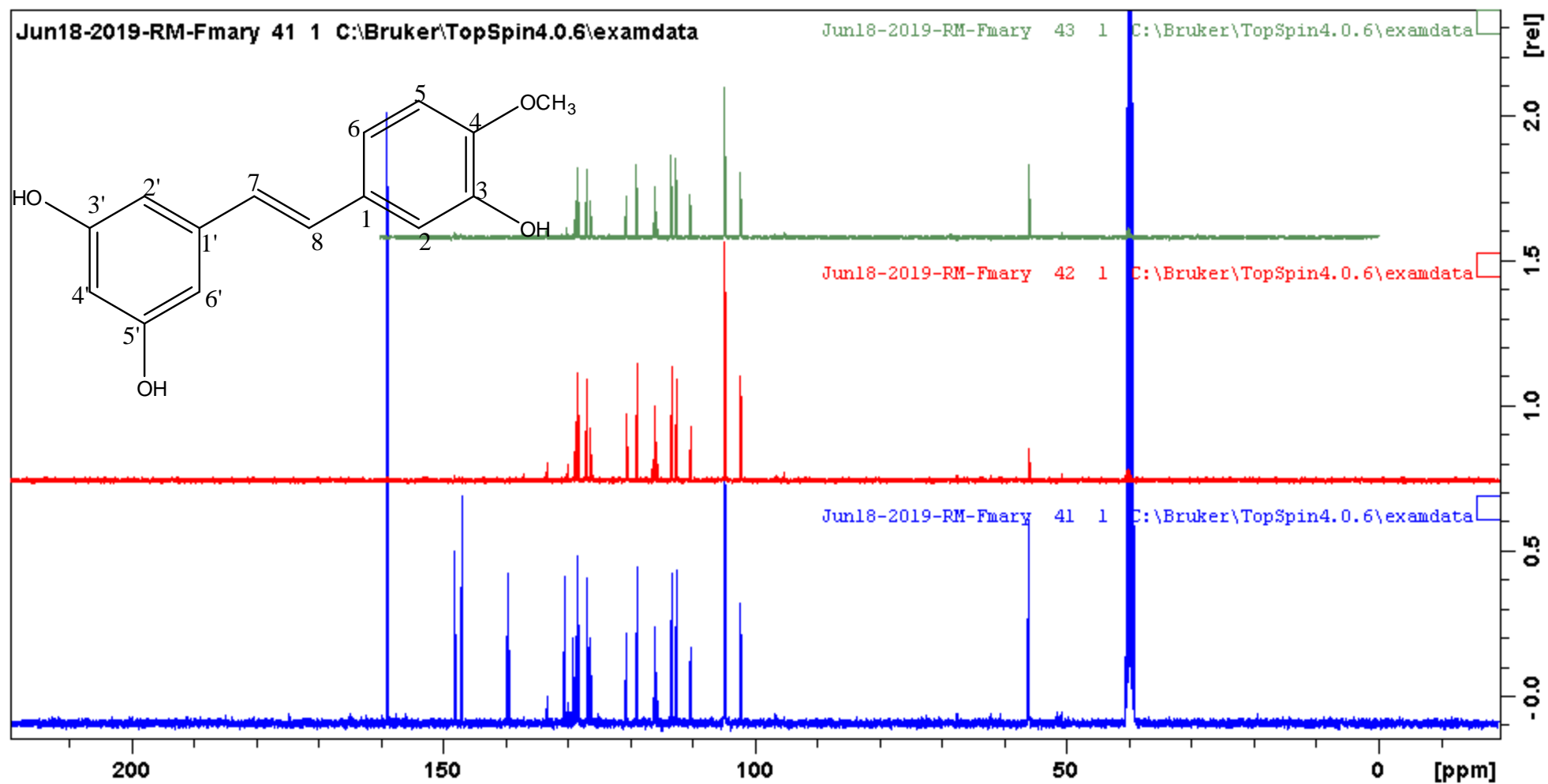
Expanded ^1H NMR of compound **A8** 3, 3', 5' -Trihydroxy-4-methoxystilbene, Rhapontigenin



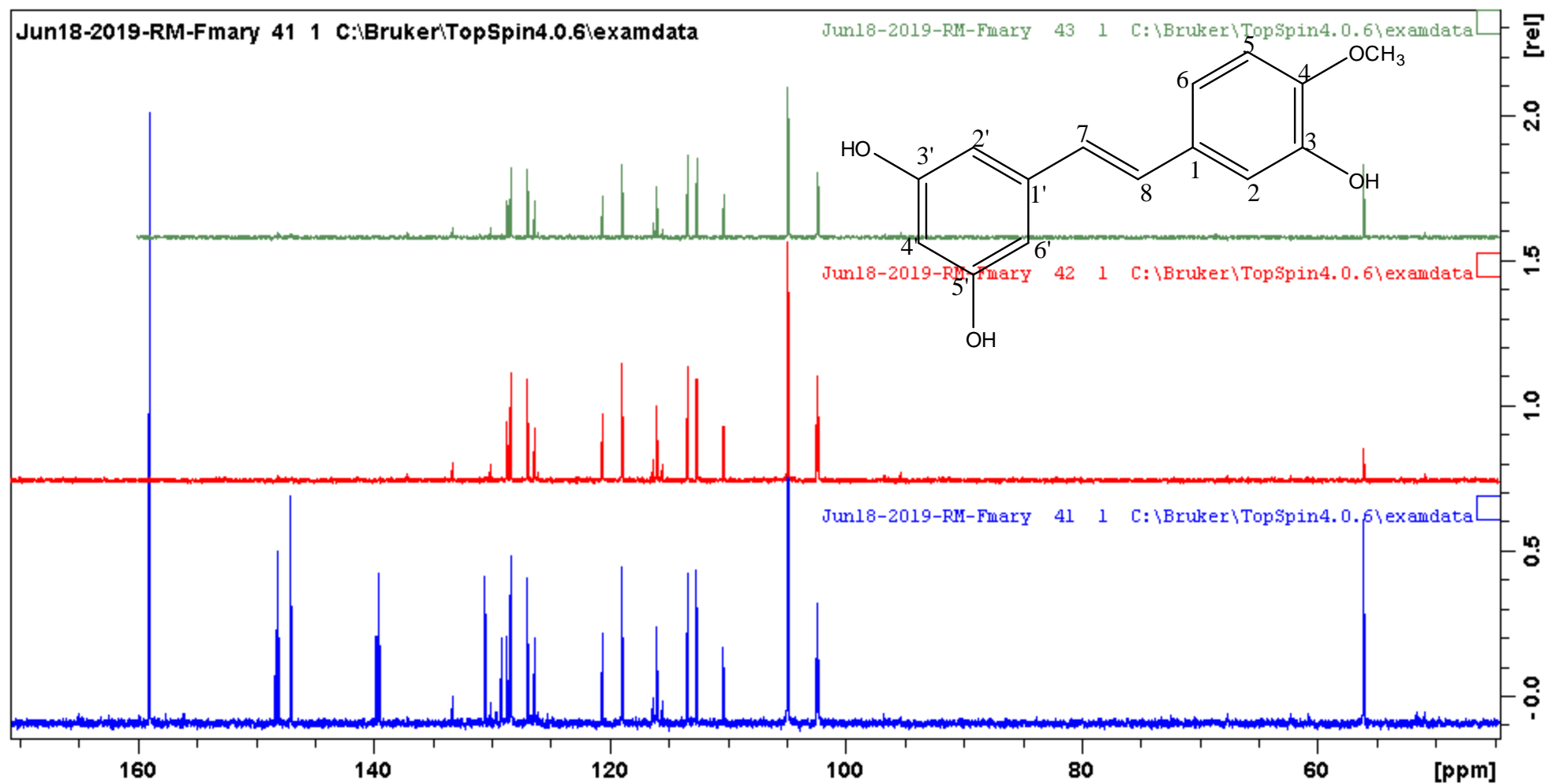
¹³C NMR of compound **A8** 3, 3', 5' -Trihydroxy-4-methoxystilbene, Rhapontigenin



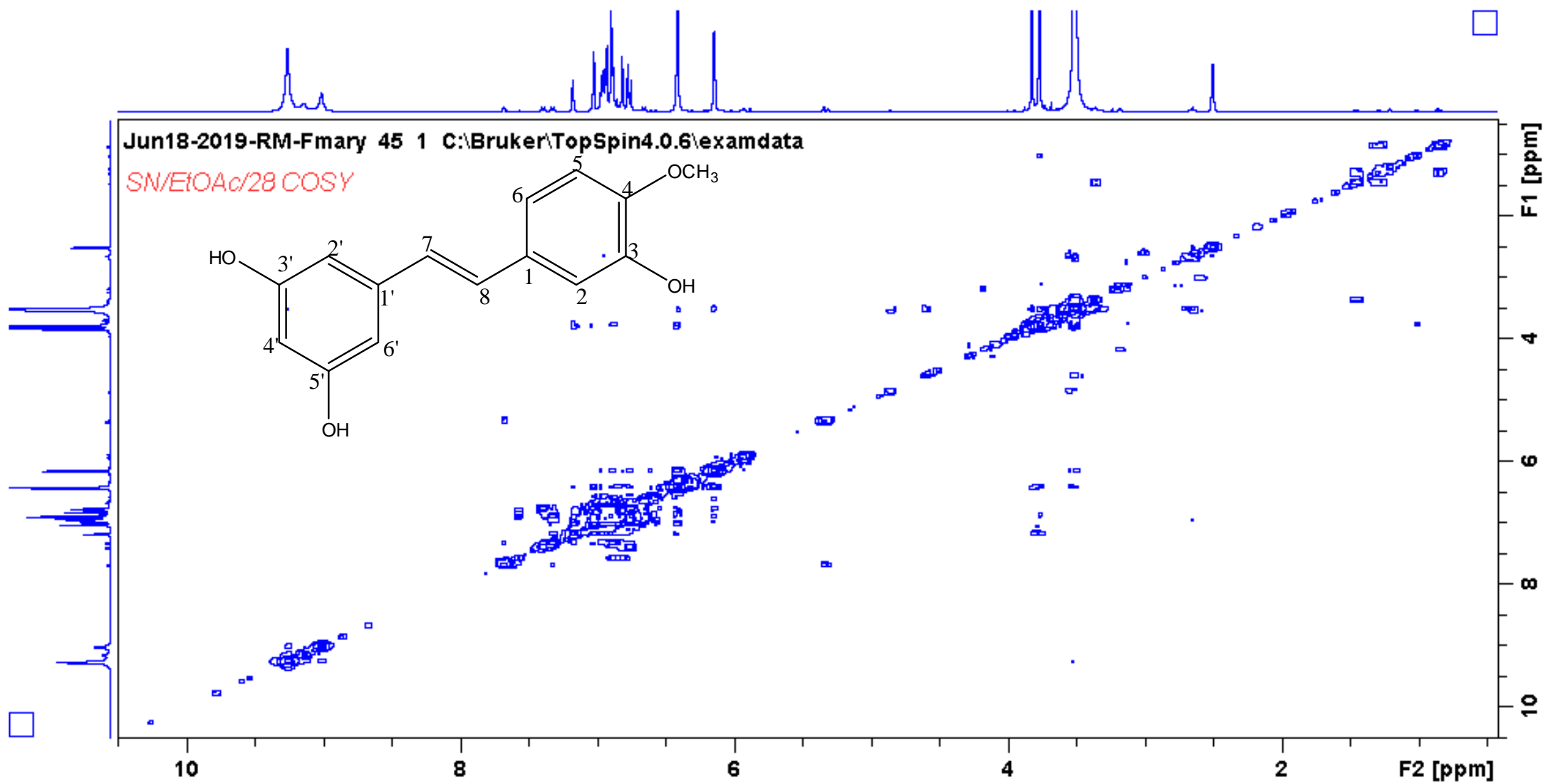
¹³C NMR of compound **A8** 3, 3', 5' -Trihydroxy-4-methoxystilbene, Rhapontigenin



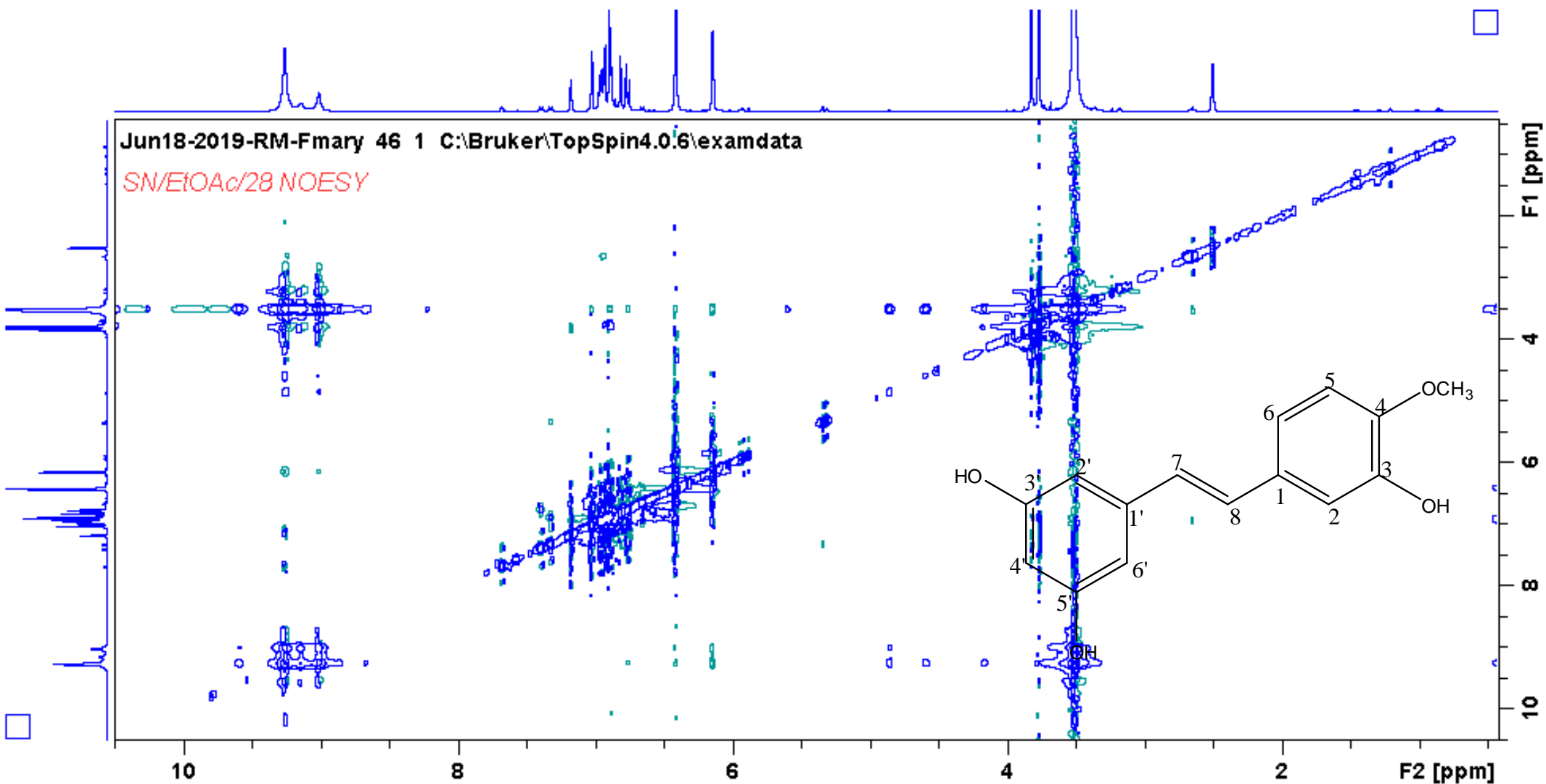
DEPT of compound **A8** 3, 3', 5' -Trihydroxy-4-methoxystilbene, Rhapontigenin



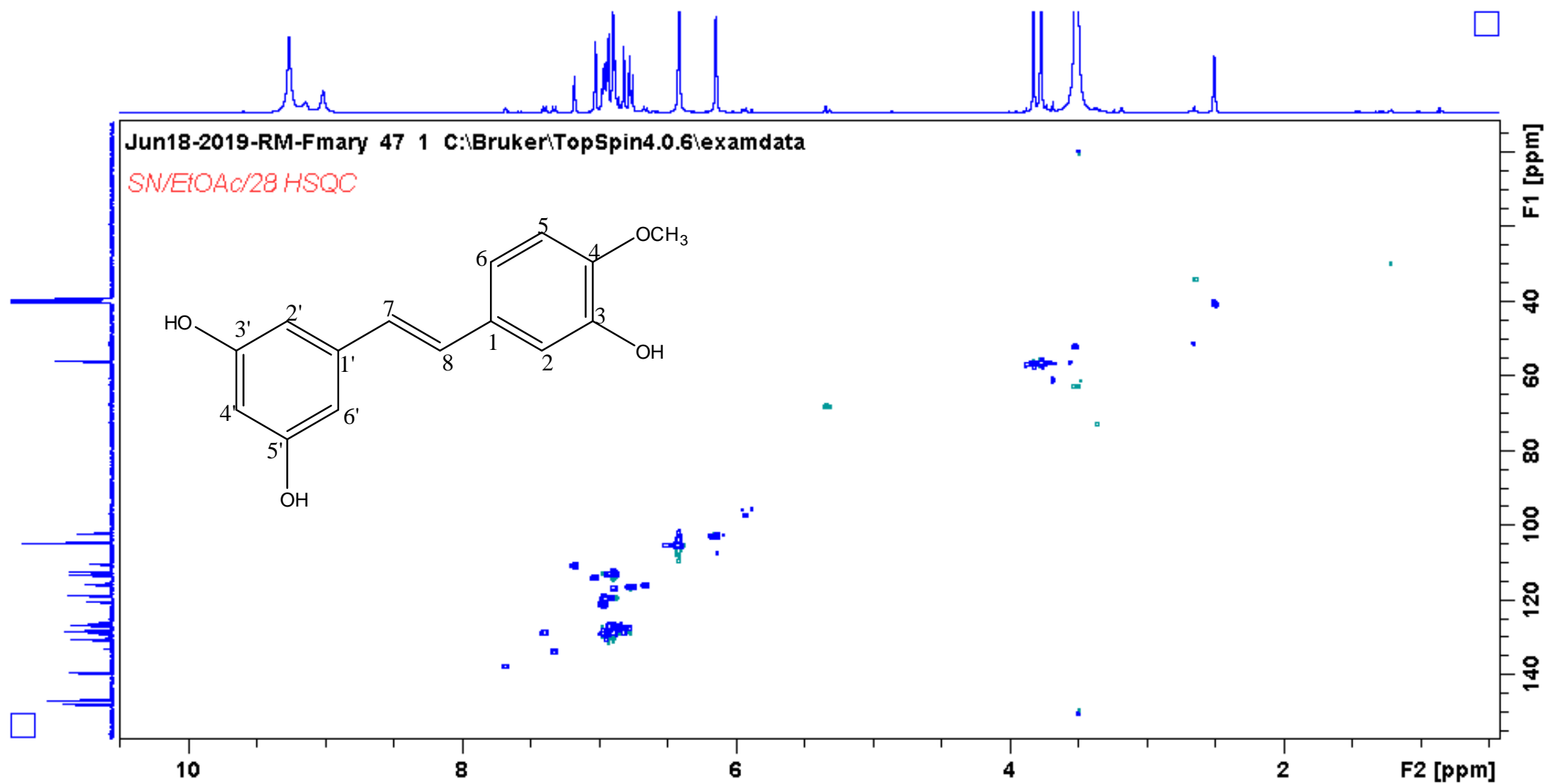
Expanded DEPT of compound **A8** 3, 3', 5' -Trihydroxy-4-methoxystilbene, Rhapontigenin



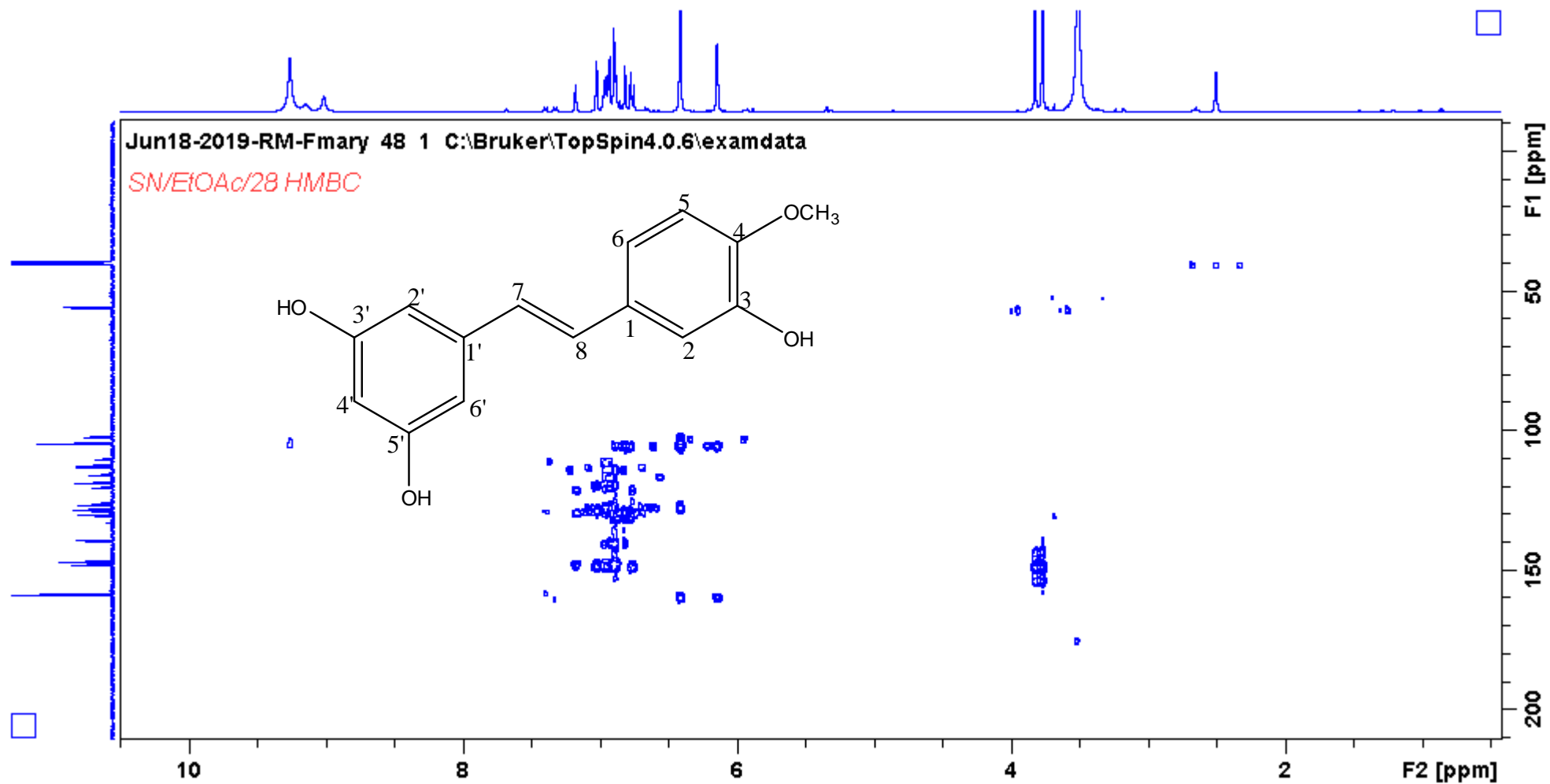
COSY of compound A8 3, 3', 5' -Trihydroxy-4-methoxystilbene, Rhapontigenin



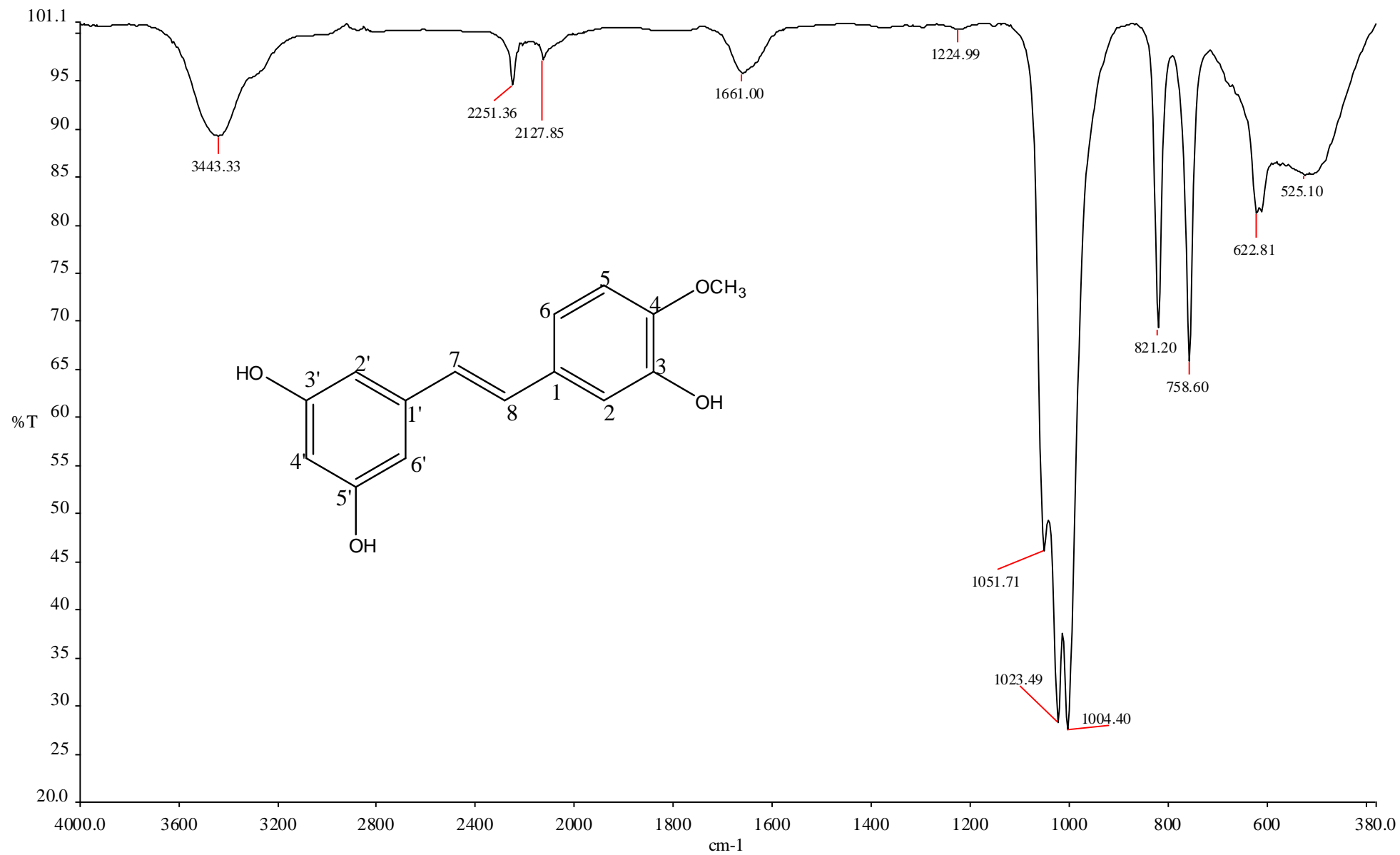
NOESY of compound **A8** 3, 3', 5' -Trihydroxy-4-methoxystilbene, Rhapontigenin



HSQC of compound **A8** 3, 3', 5' -Trihydroxy-4-methoxystilbene, Rhapontigenin



HMBC of compound **A8** 3, 3', 5' -Trihydroxy-4-methoxystilbene, Rhapontigenin



IR of compound **A8** 3, 3', 5'-Trihydroxy-4-methoxystilbene, Rhapontigenin

Monoisotopic Mass, Even Electron Ions

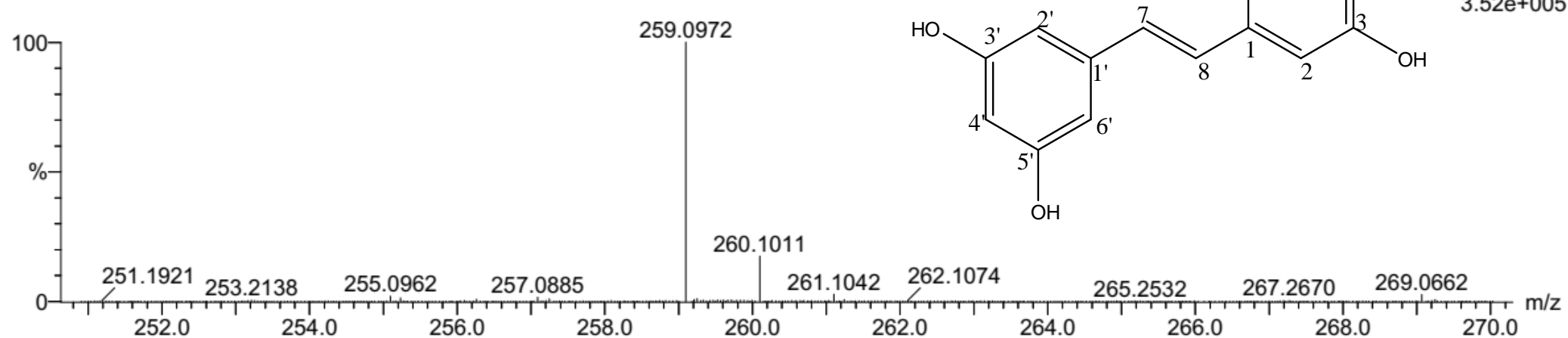
4 formula(e) evaluated with 1 results within limits (up to 50 best isotopic matches for each mass)

Elements Used:

C: 10-15 H: 10-15 O: 0-5

FM4 44 (0.733) Cm (1:119)

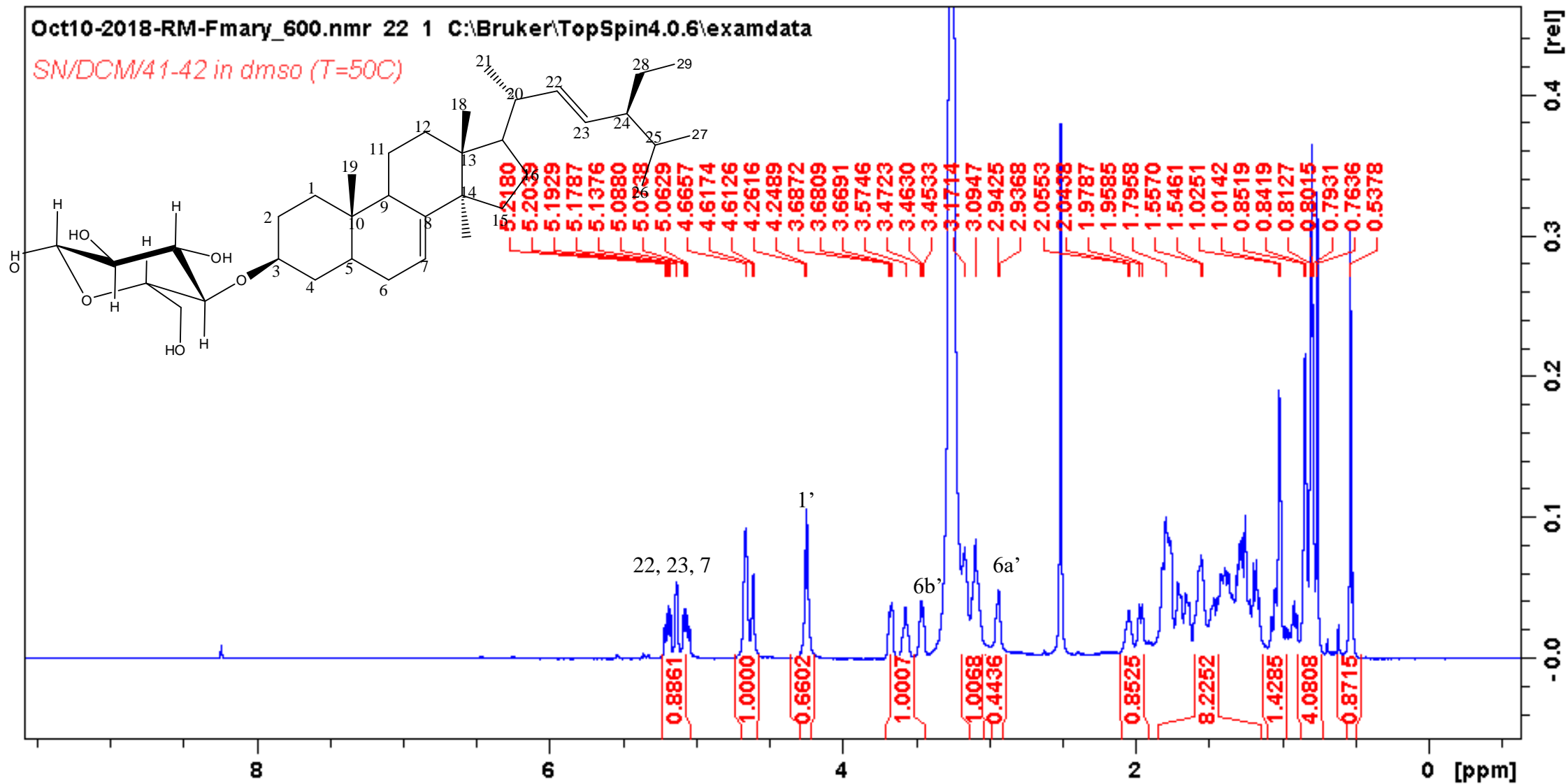
TOF MS AP+



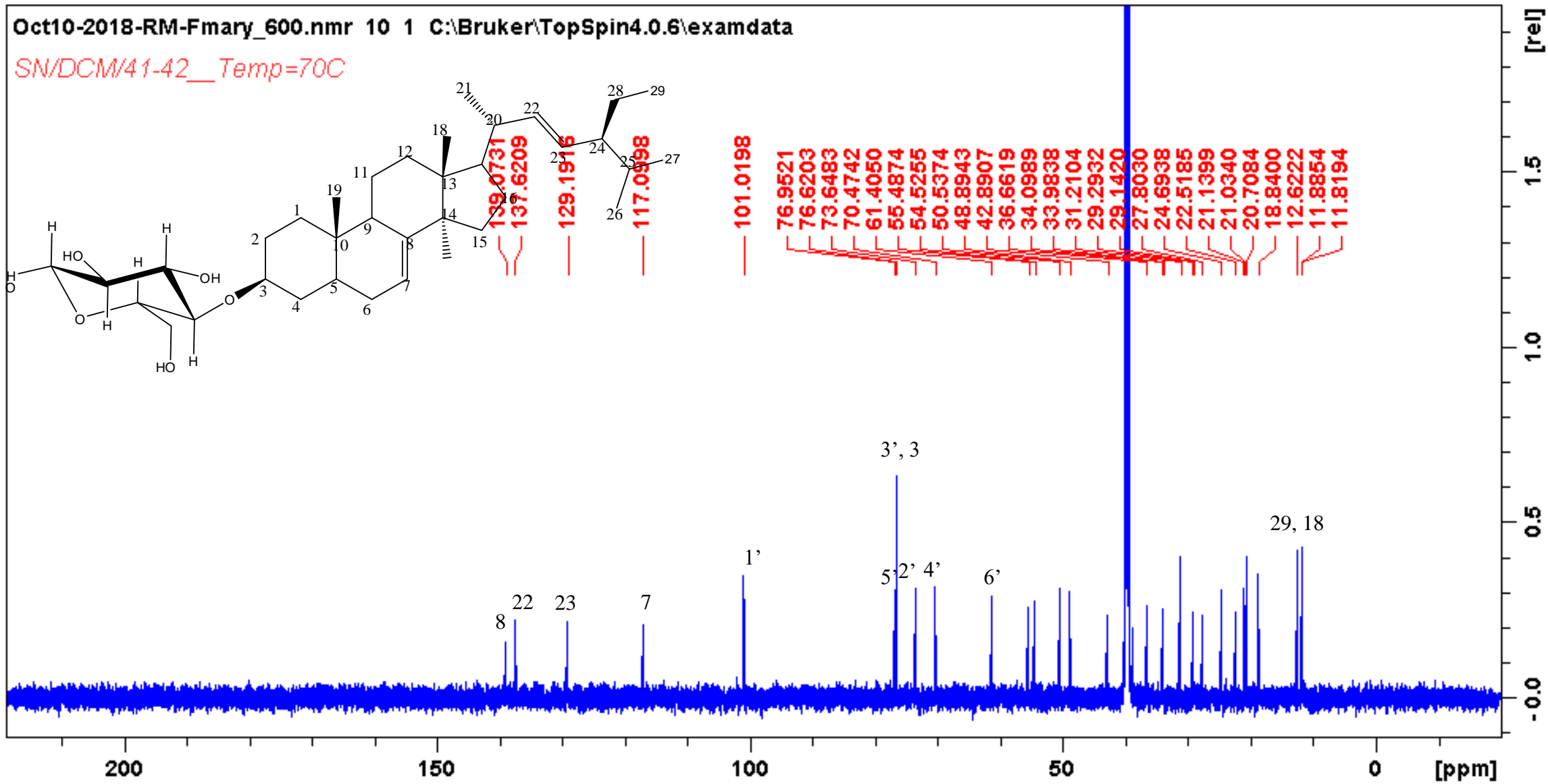
Minimum: -1.5
Maximum: 5.0 5.0 50.0

Mass	Calc. Mass	mDa	PPM	DBE	i-FIT	i-FIT (Norm)	Formula
259.0972	259.0970	0.2	0.8	8.5	746.2	0.0	C15 H15 O4

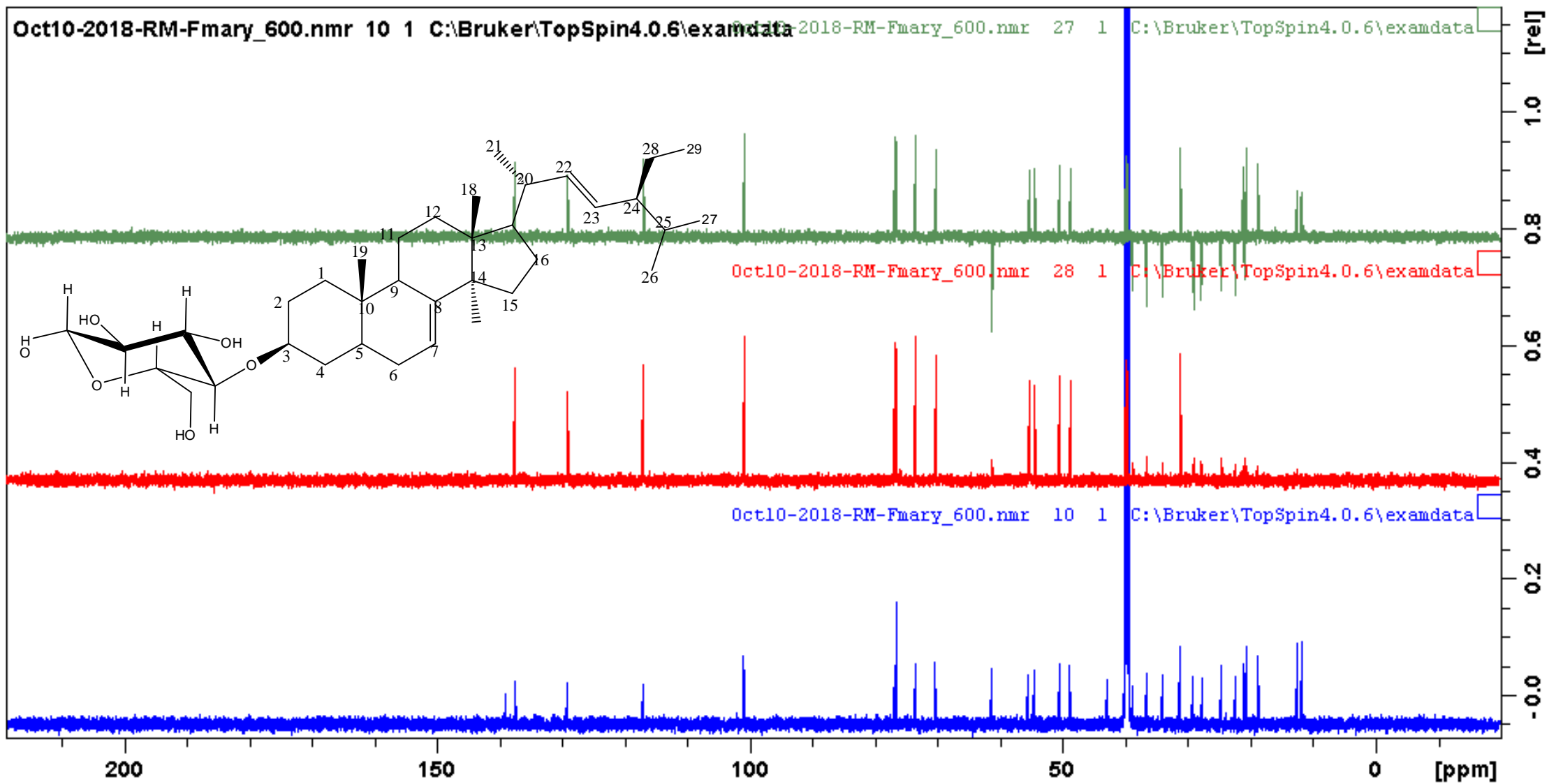
HRMS of compound **A8** 3, 3', 5' -Trihydroxy-4-methoxystilbene, Rhapontigenin



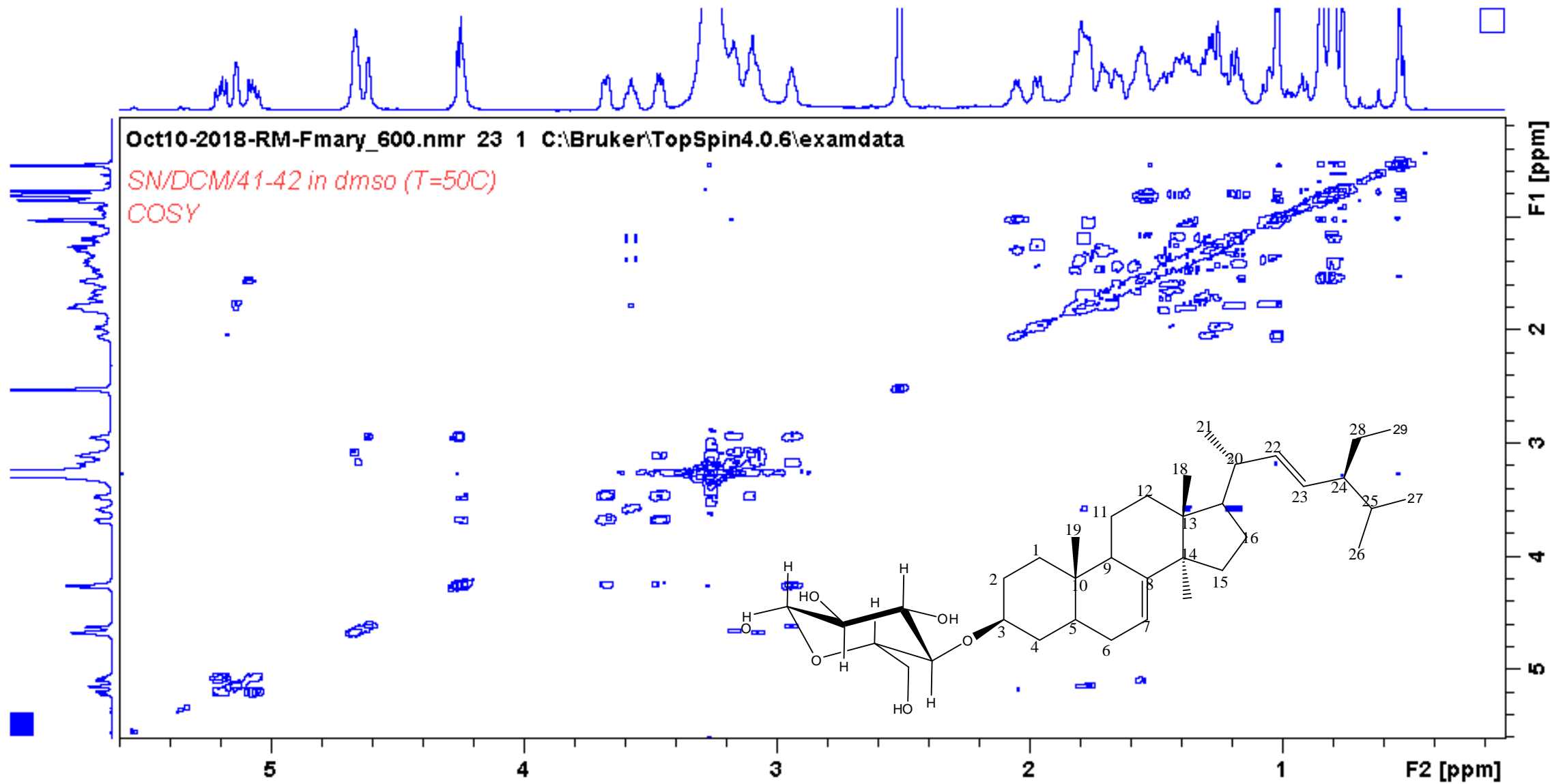
¹H NMR of compound A9 spinasterol glucopyranoside



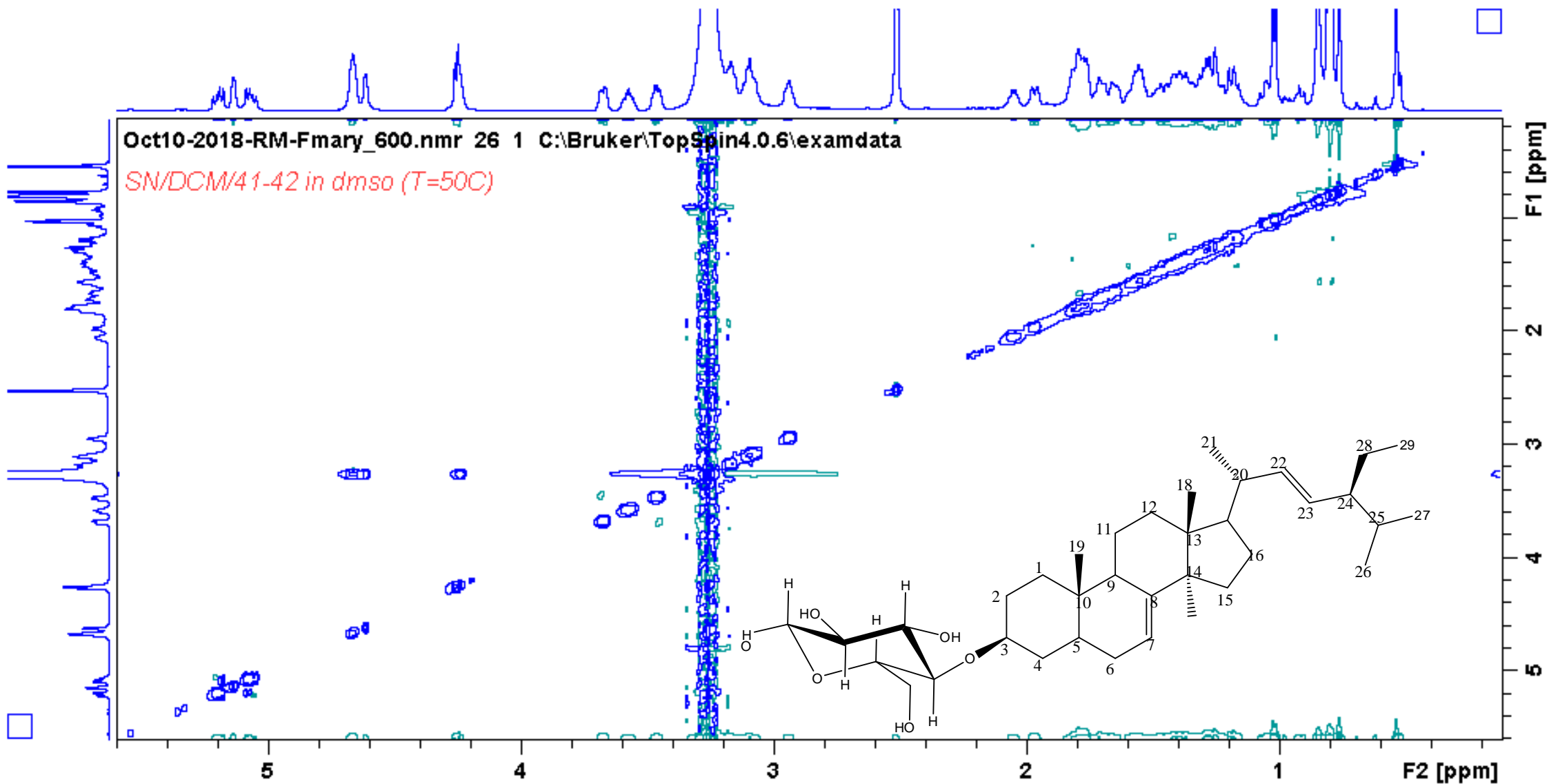
^{13}C NMR of compound **A9** spinasterol glucopyranoside



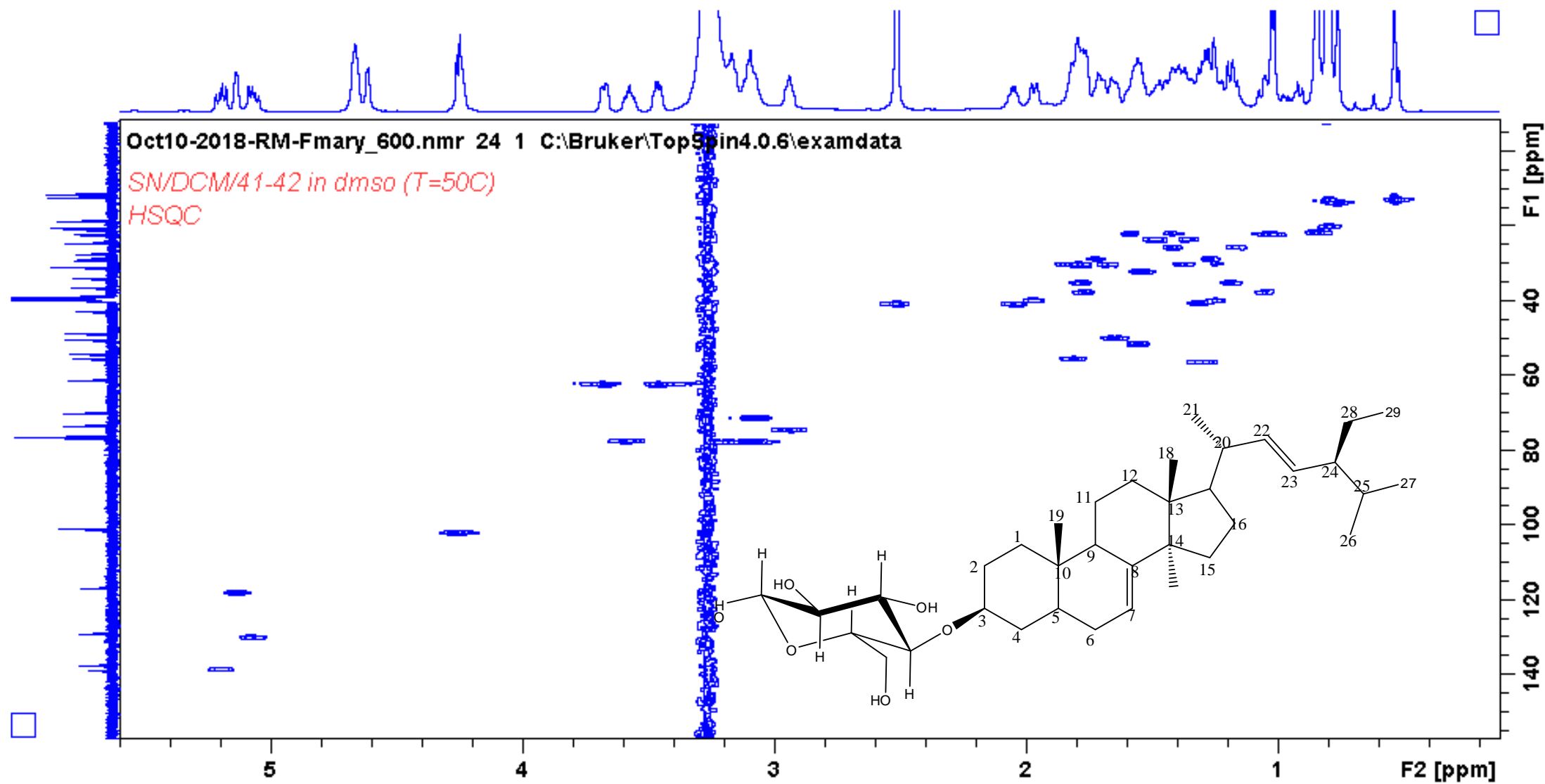
DEPT of compound **A9** spinasterol glucopyranoside



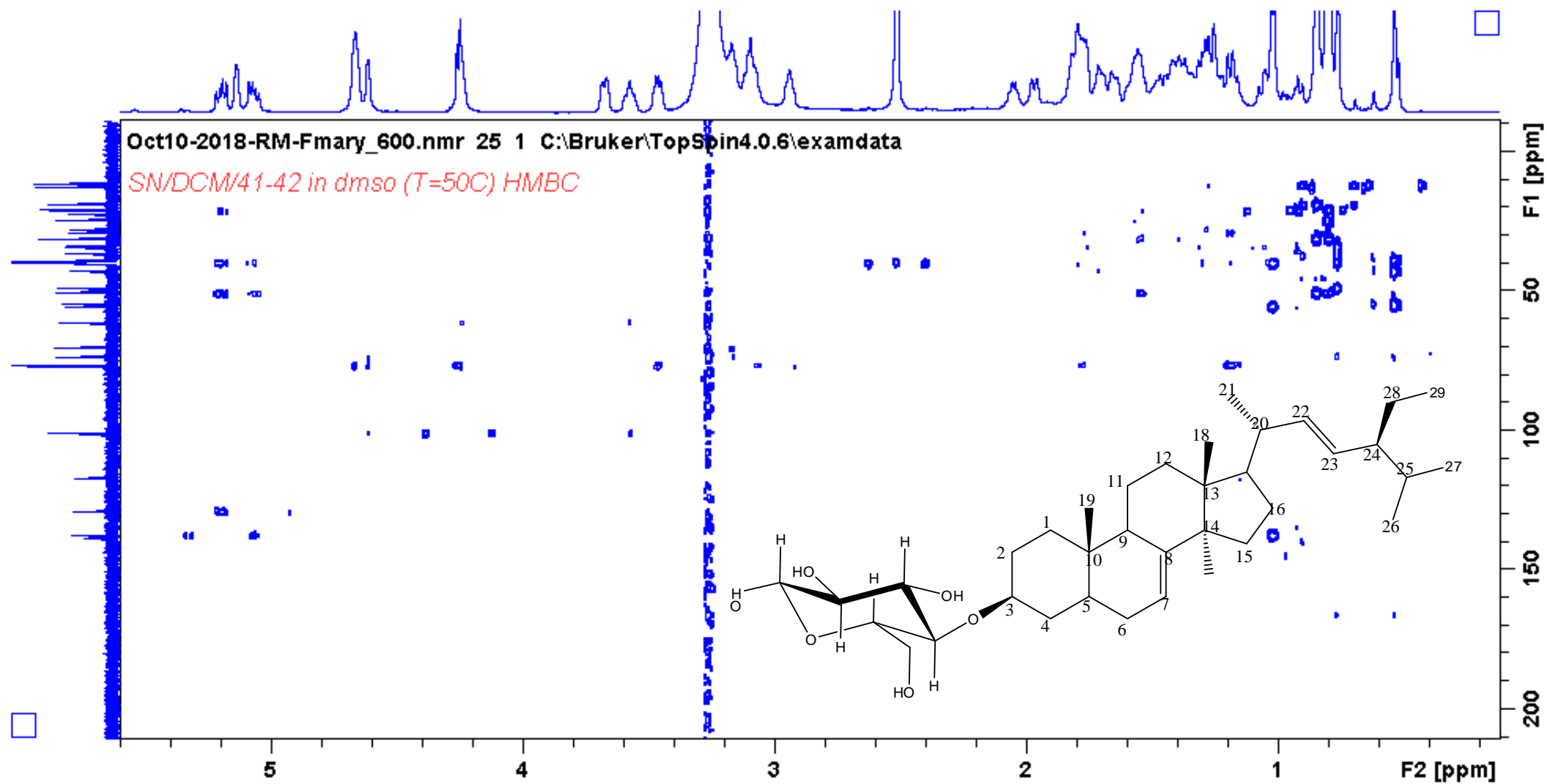
COSY of compound A9 spinasterol glucopyranoside



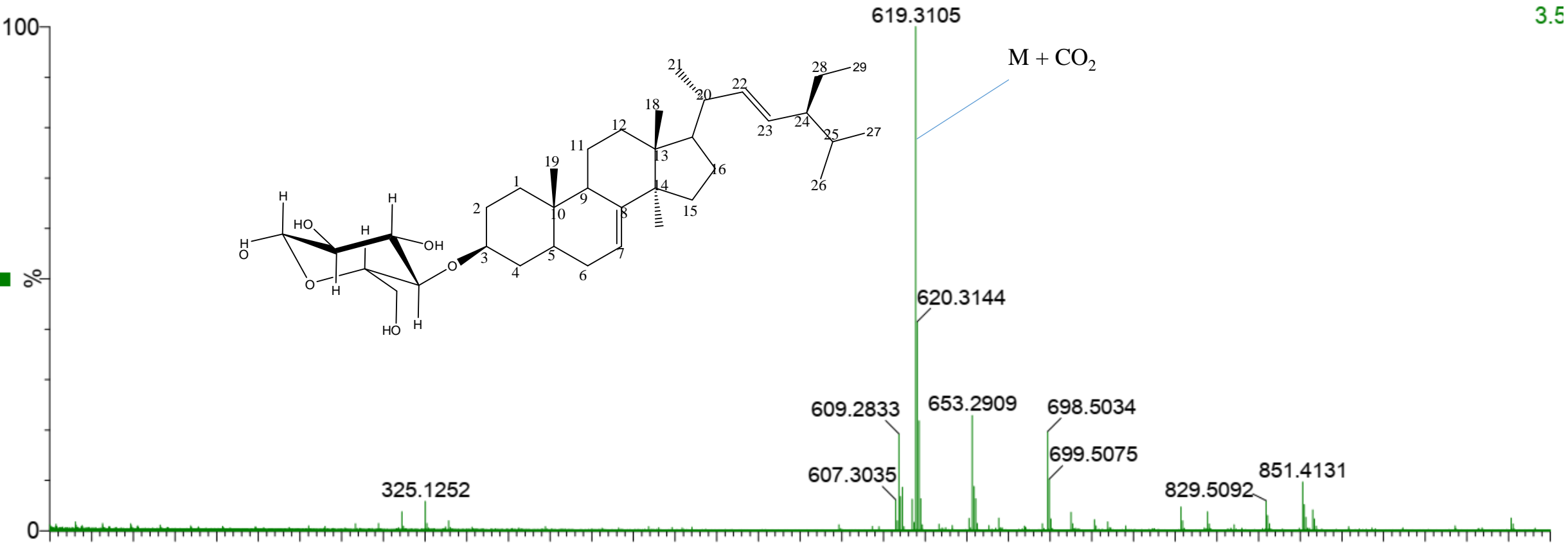
NOESY of compound **A9** spinasterol glucopyranoside



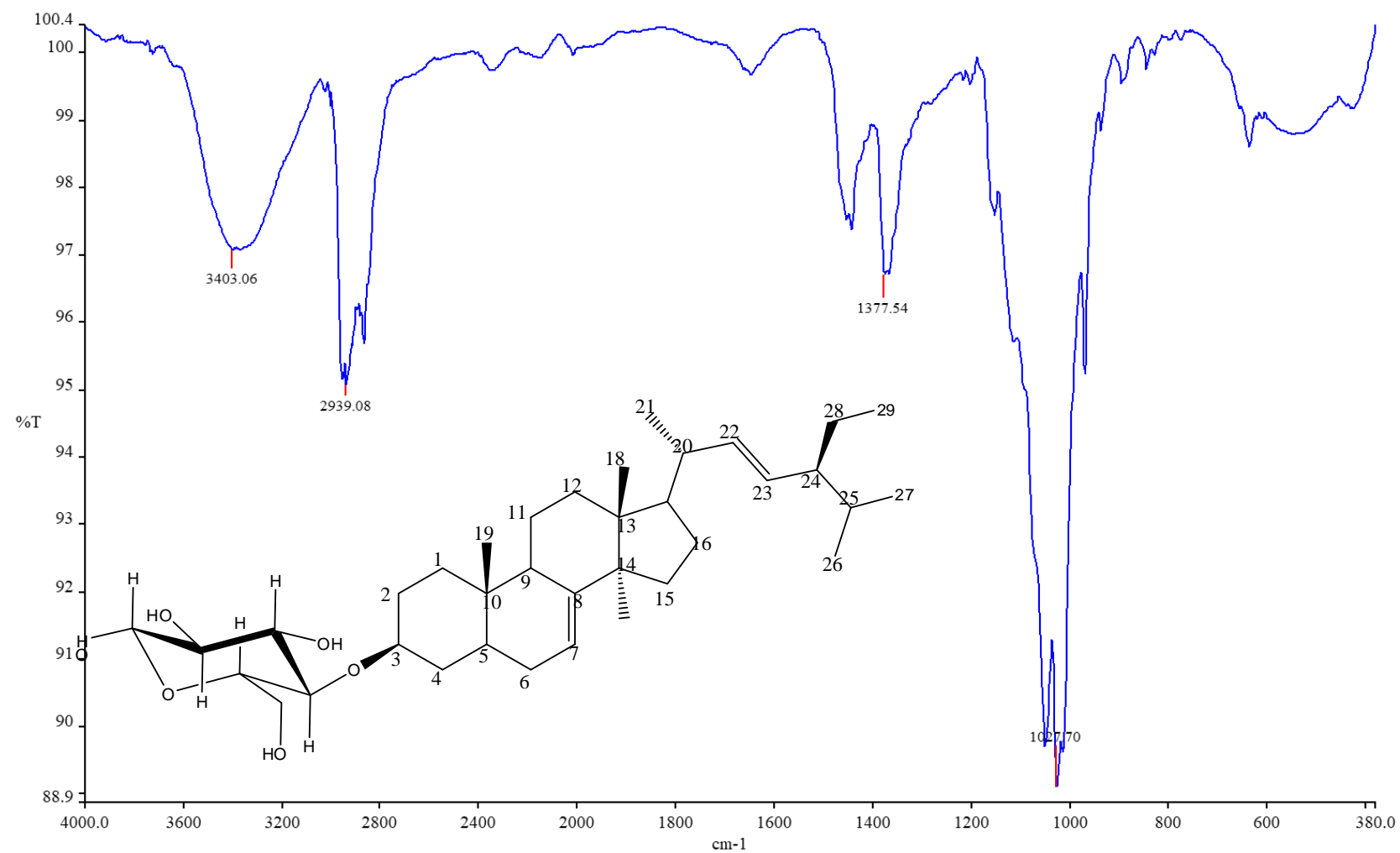
HSQC of compound A9 spinasterol glucopyranoside



HMBC of compound **A9** spinasterol glucopyranoside

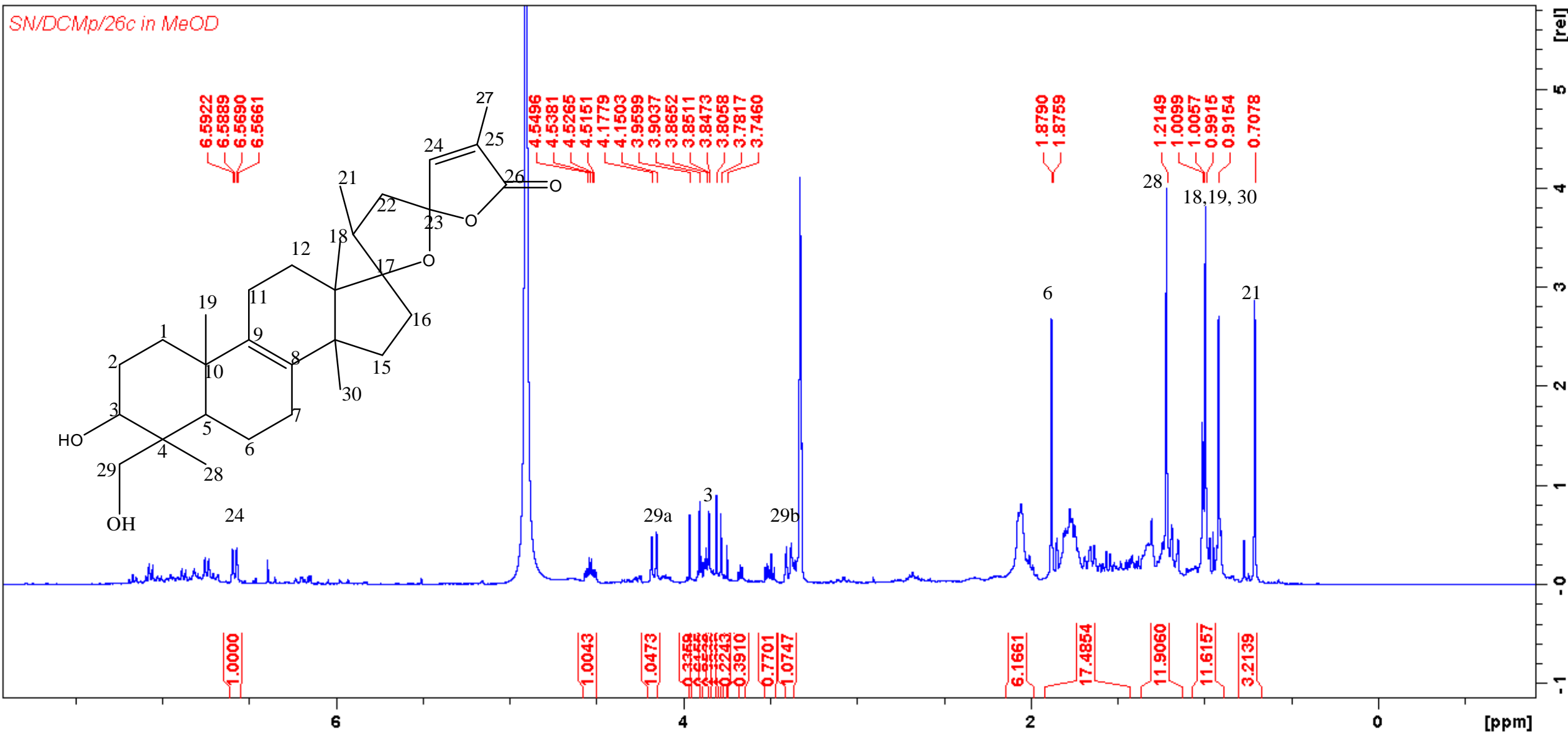


HRMS of compound **A9** spinasterol glucopyranoside

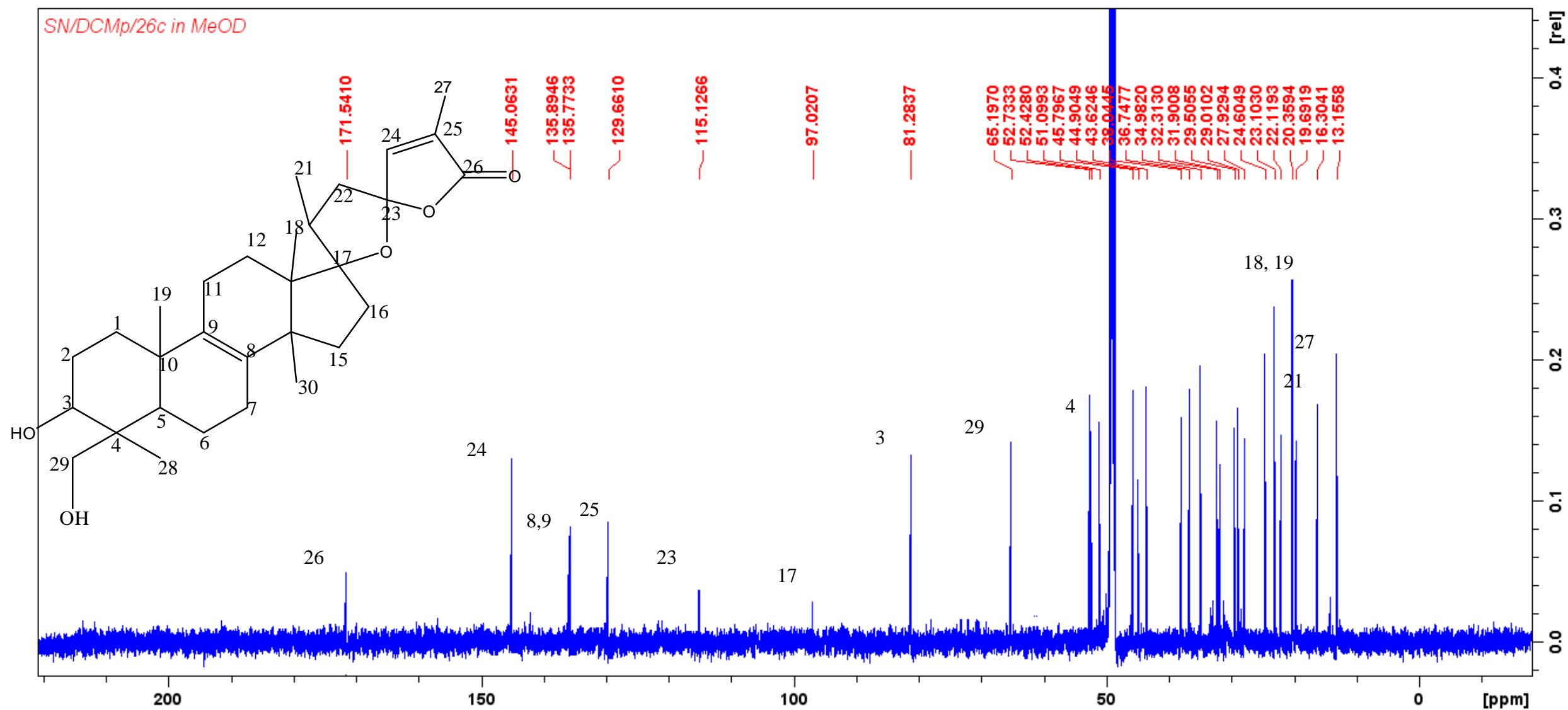


IR of compound **A9** spinasterol glucopyranoside

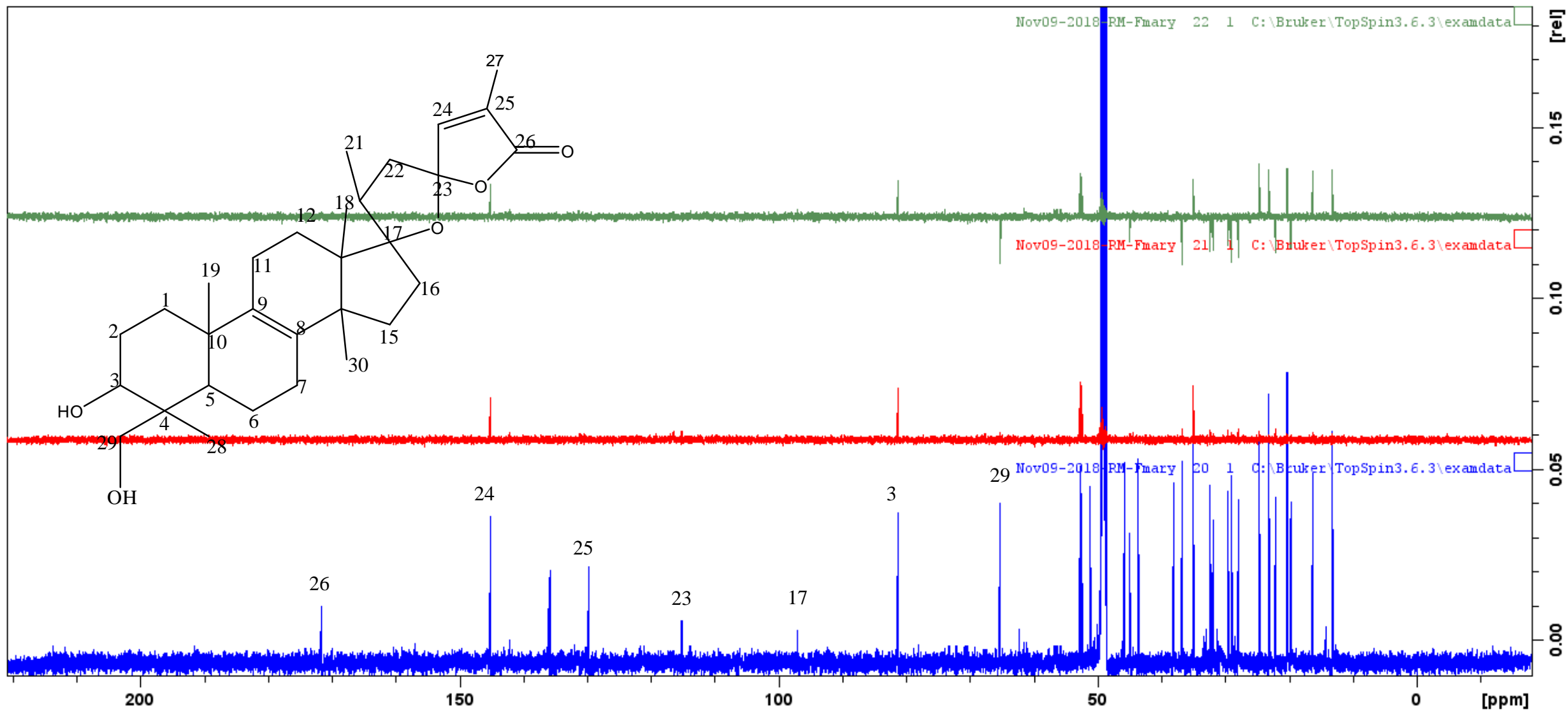
SN/DCMp/26c in MeOD



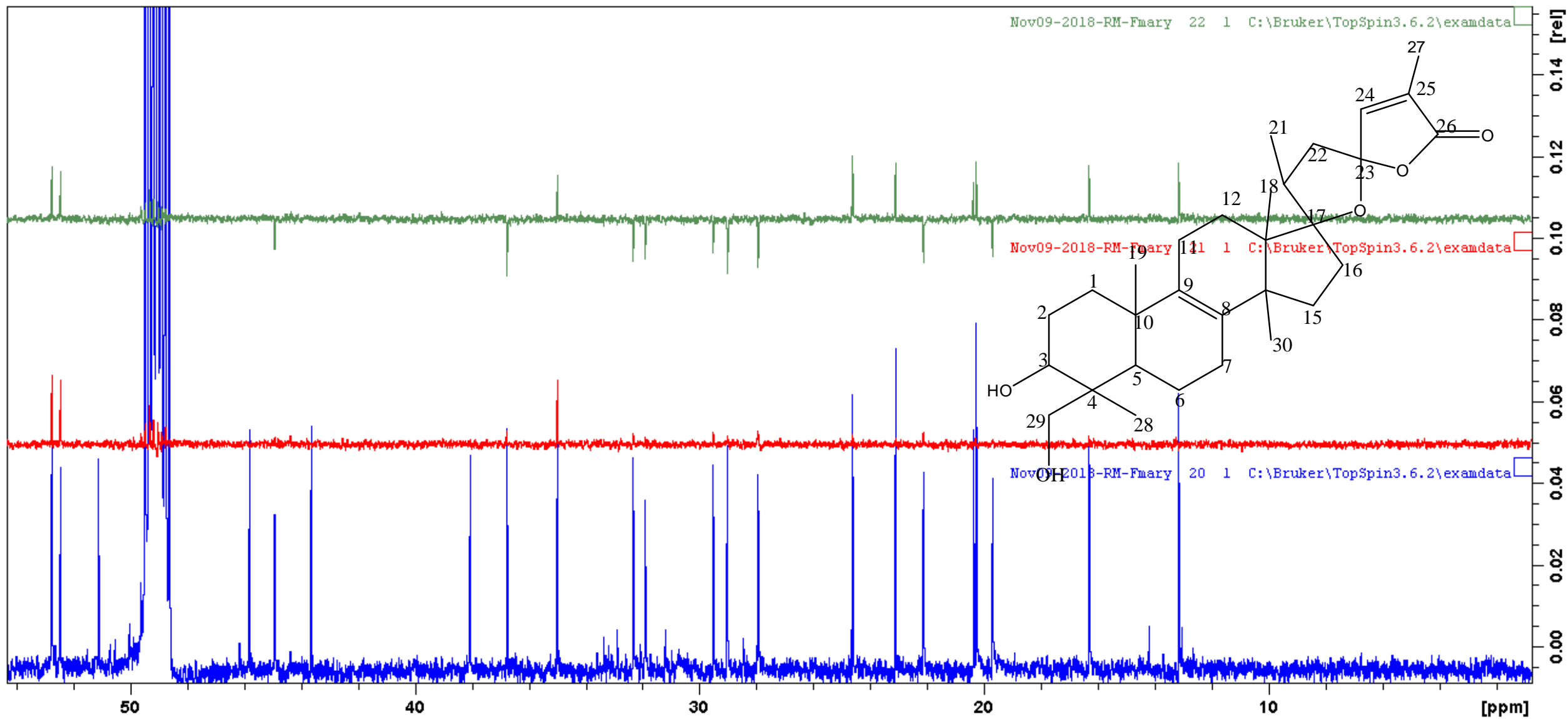
¹H NMR of compound A10 17 α , 23 α -epoxy-3 β ,29-dihydroxyl-nor-lanost-8,24-dien-26-one.



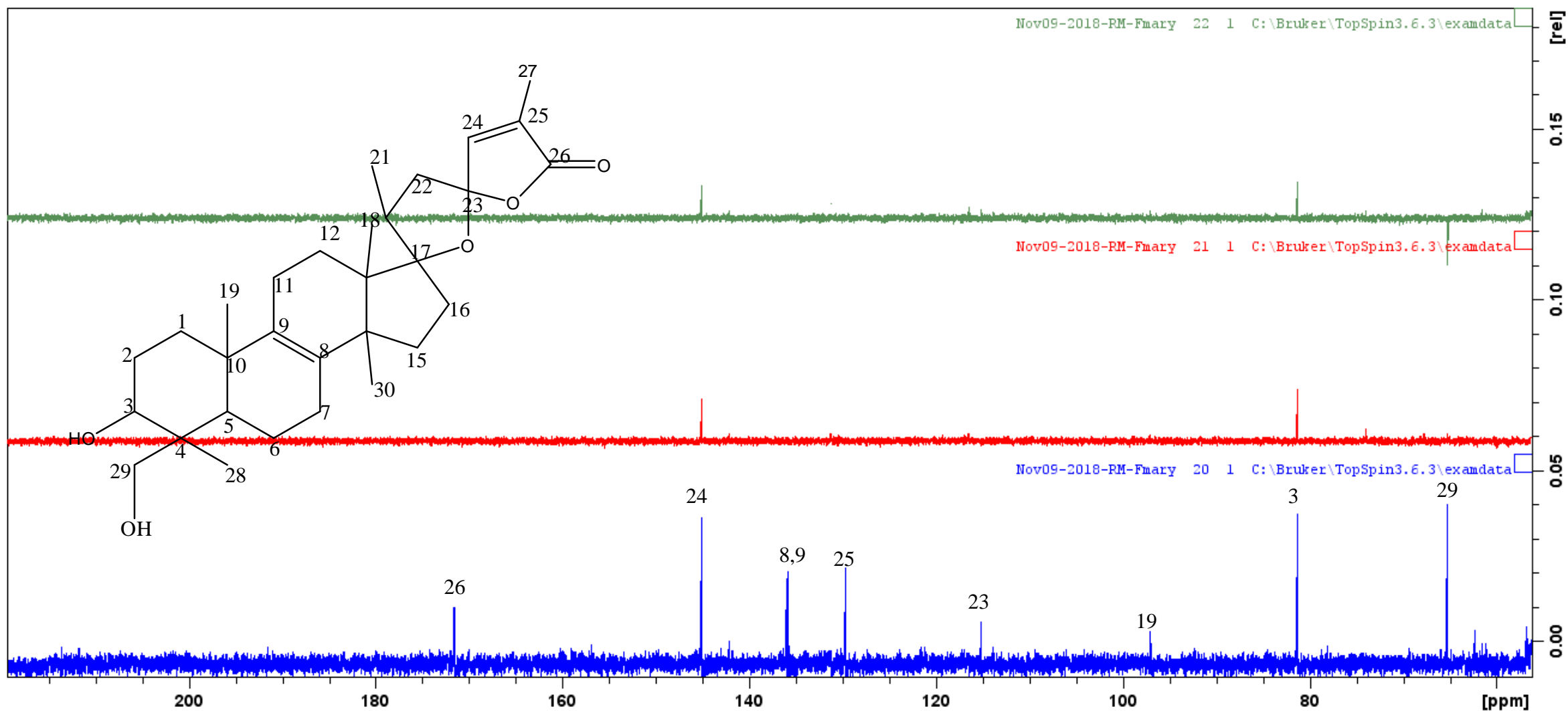
¹³C NMR of compound **A10** 17 α , 23 α -epoxy-3 β ,29-dihydroxyl-nor-lanost-8,24-dien-26-one.



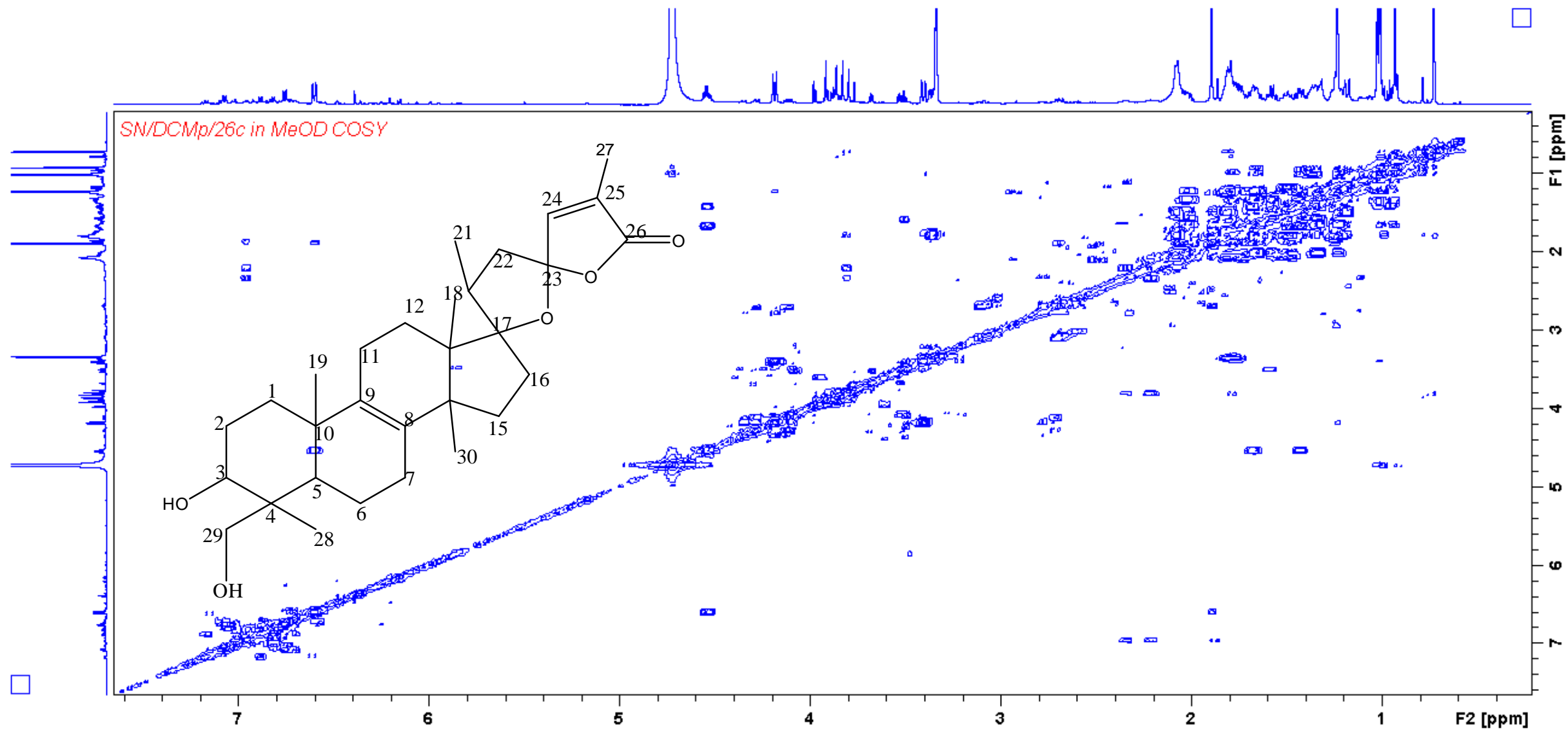
DEPT of compound **A10** 17 α , 23 α -epoxy-3 β , 29-dihydroxyl-nor-lanost-8, 24-dien-26-one.



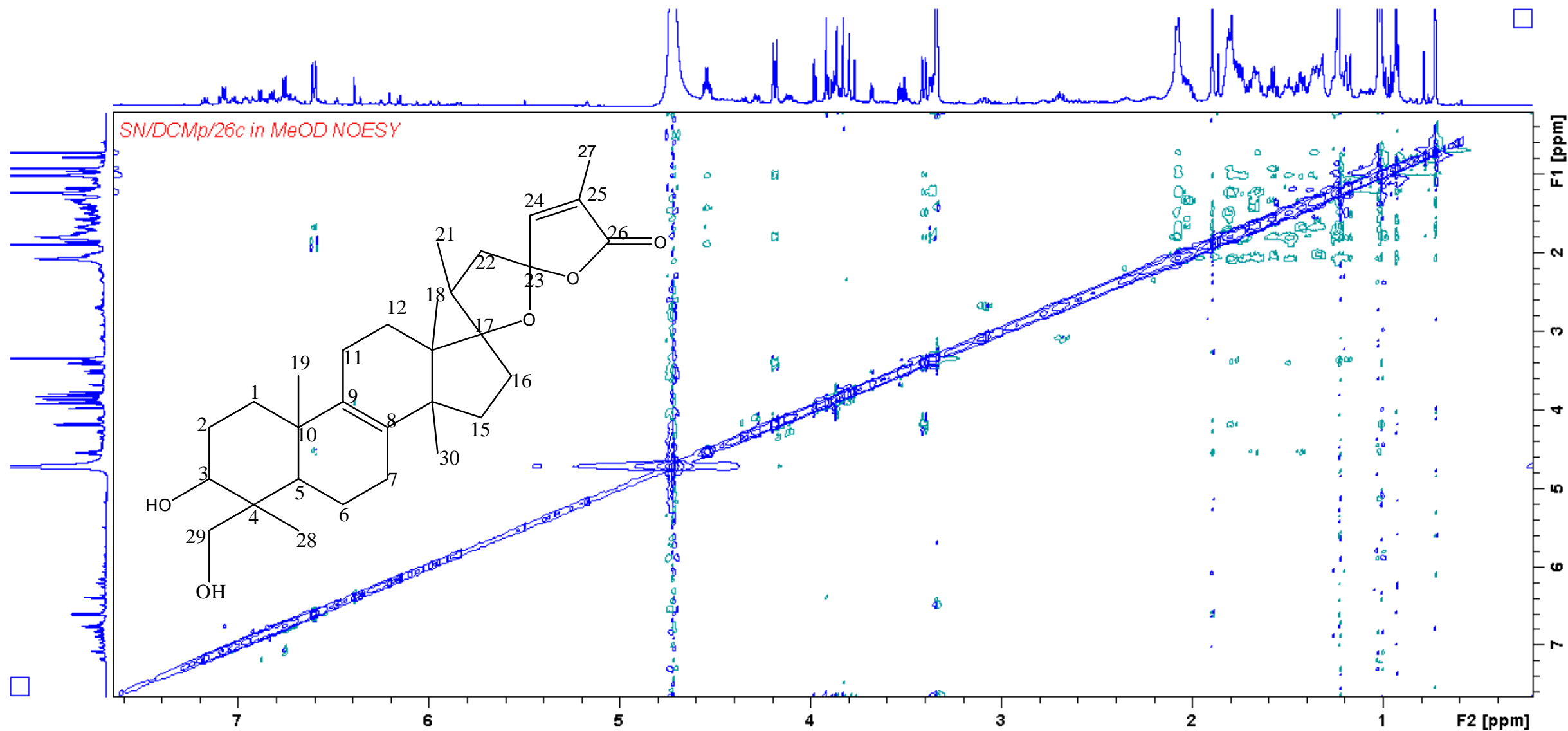
Expanded ^{13}C NMR of compound **A10** 17 α , 23 α -epoxy-3 β ,29-dihydroxyl-nor-lanost-8,24-dien-26-one.



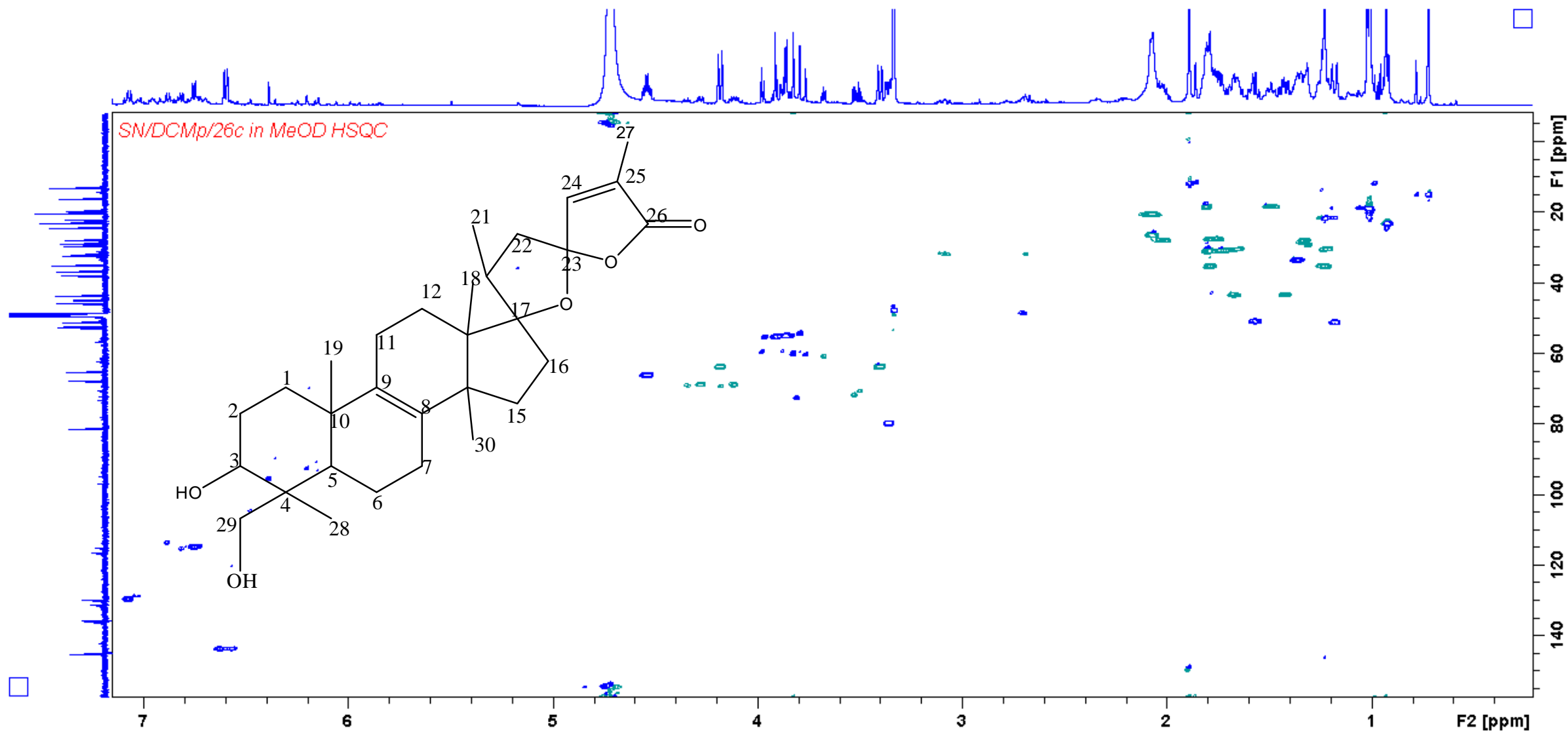
Expanded DEPT of compound **A10** 17 α , 23 α -epoxy-3 β ,29-dihydroxyl-nor-lanost-8,24-dien-26-one.

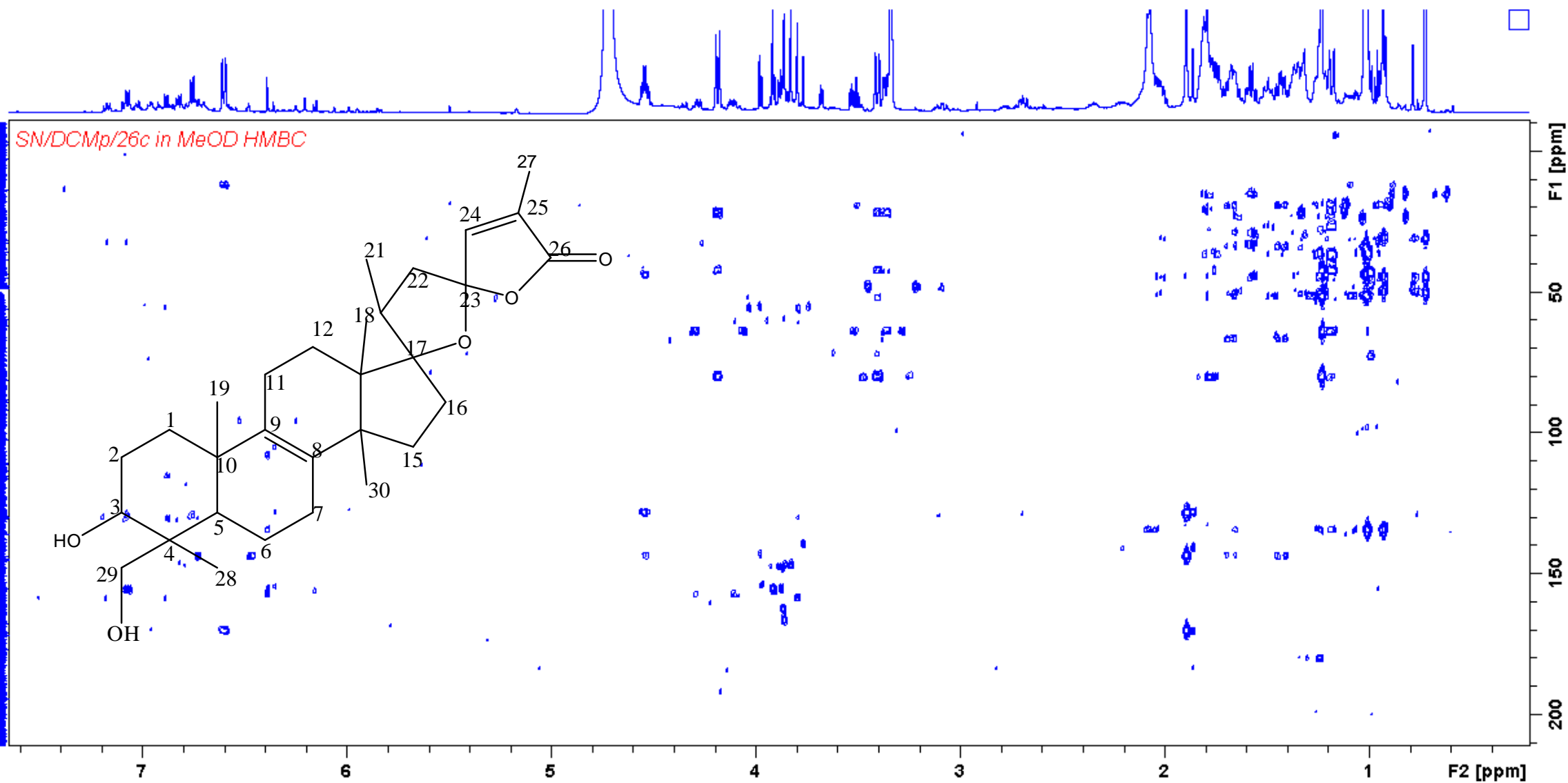


COSY of compound **A10** 17α , 23α -epoxy- 3β , 29 -dihydroxyl-nor-lanost- $8,24$ -dien- 26 -one.

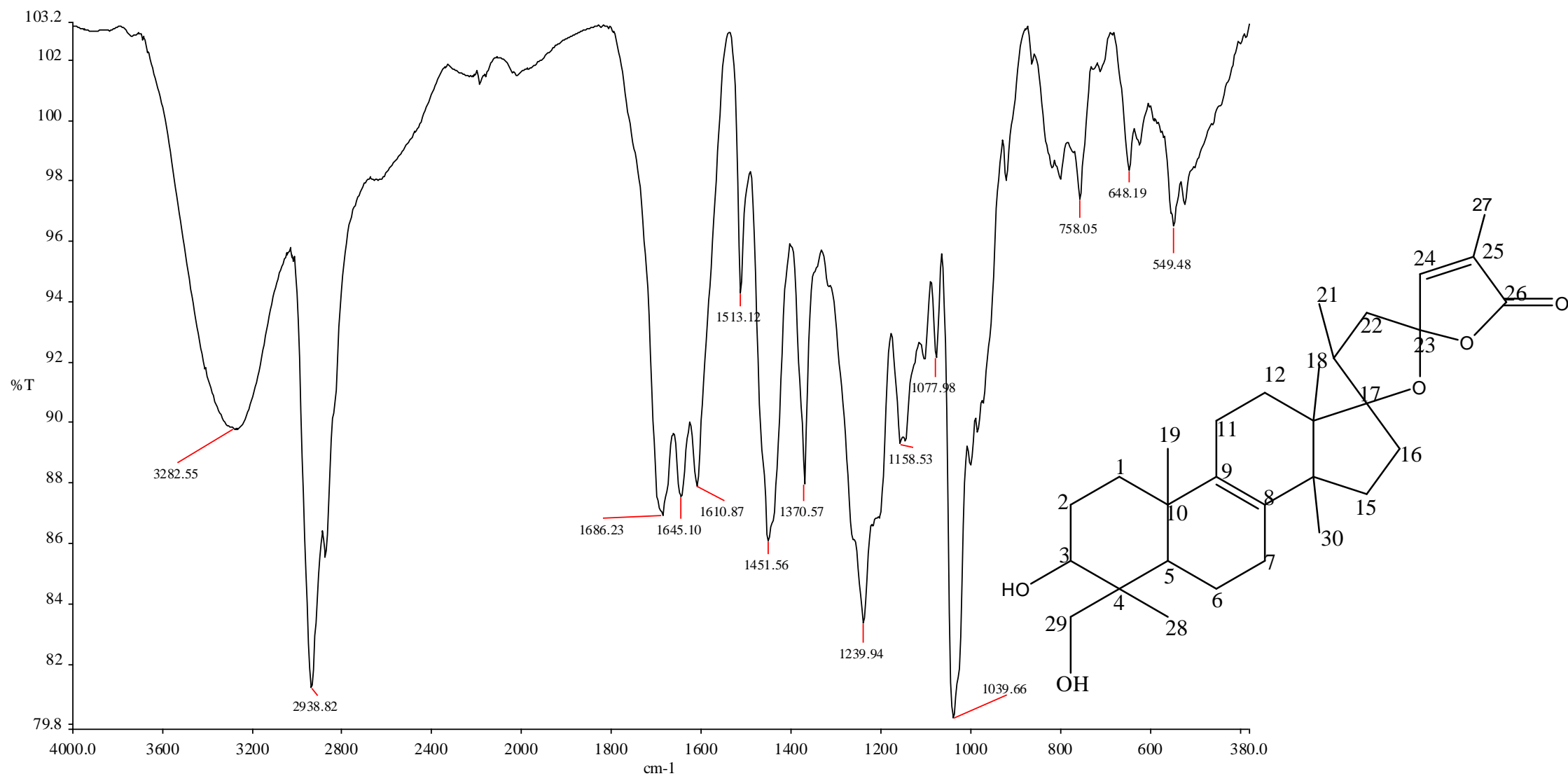


NOESY of compound **A10** 17 α , 23 α -epoxy-3 β ,29-dihydroxyl-nor-lanost-8,24-dien-26-one.





HMBC of compound **A10** 17α , 23α -epoxy- 3β , 29 -dihydroxyl-nor-lanost- $8,24$ -dien- 26 -one.



IR spectrum of compound **A10** 17 α , 23 α -epoxy-3 β ,29-dihydroxyl-nor-lanost-8,24-dien-26-one.

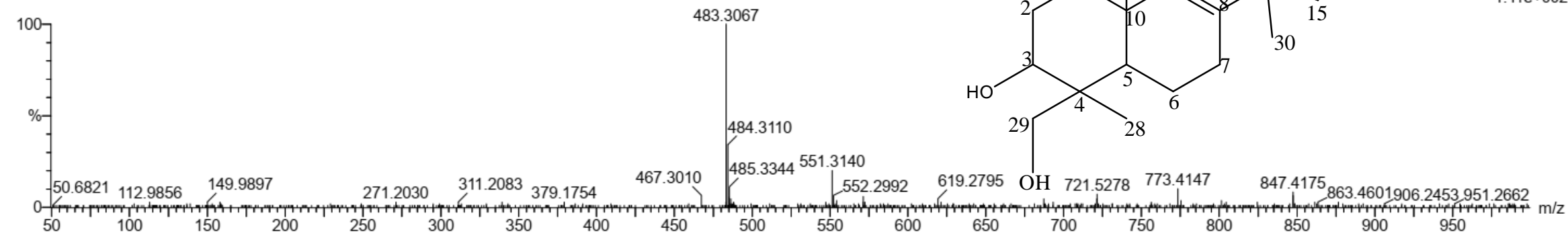
Monoisotopic Mass, Even Electron Ions

45 formula(e) evaluated with 1 results within limits (up to 10 best isotopic matches for each mass)

Elements Used:

C: 1-70 H: 1-100 O: 1-8

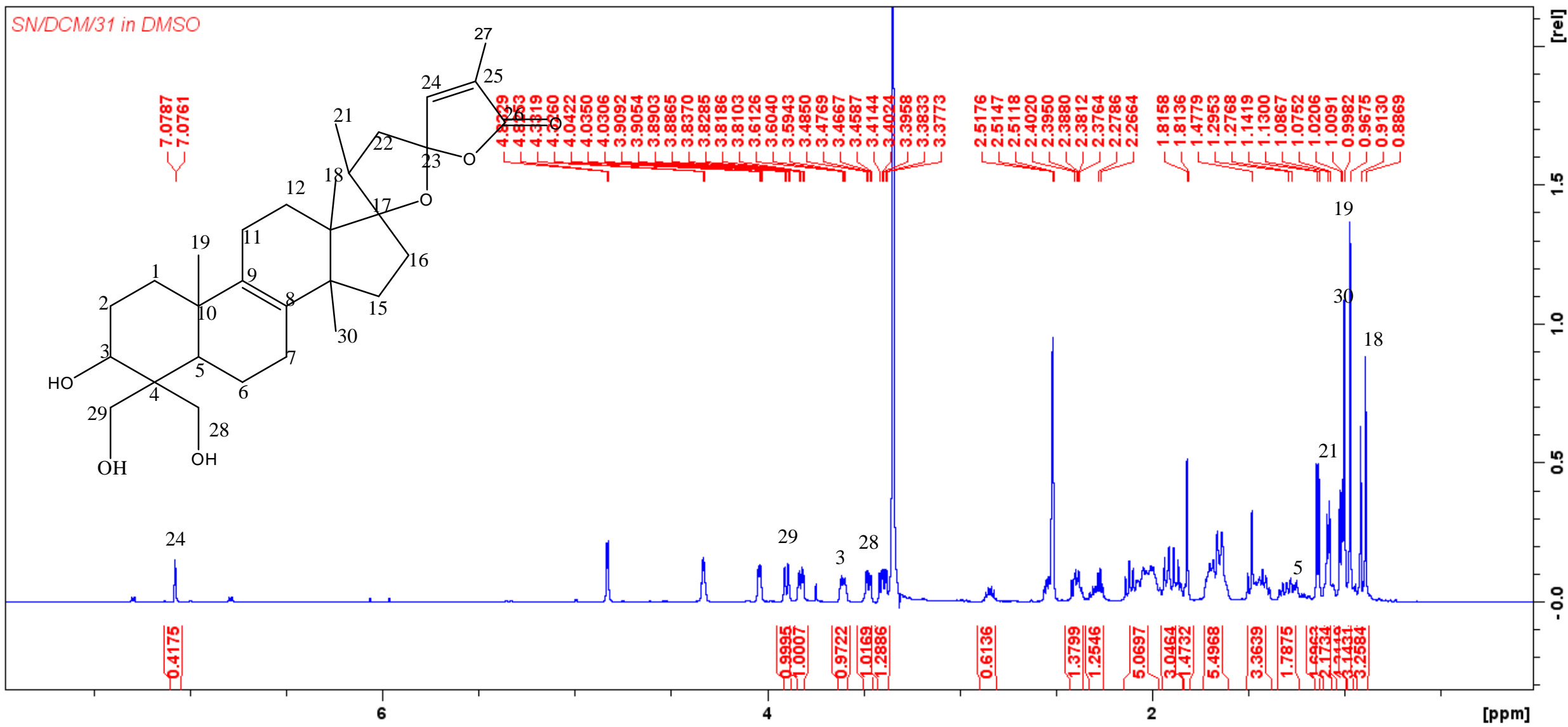
Sample 26a 29 March 2021 UPLC #1b 555 (11.884)



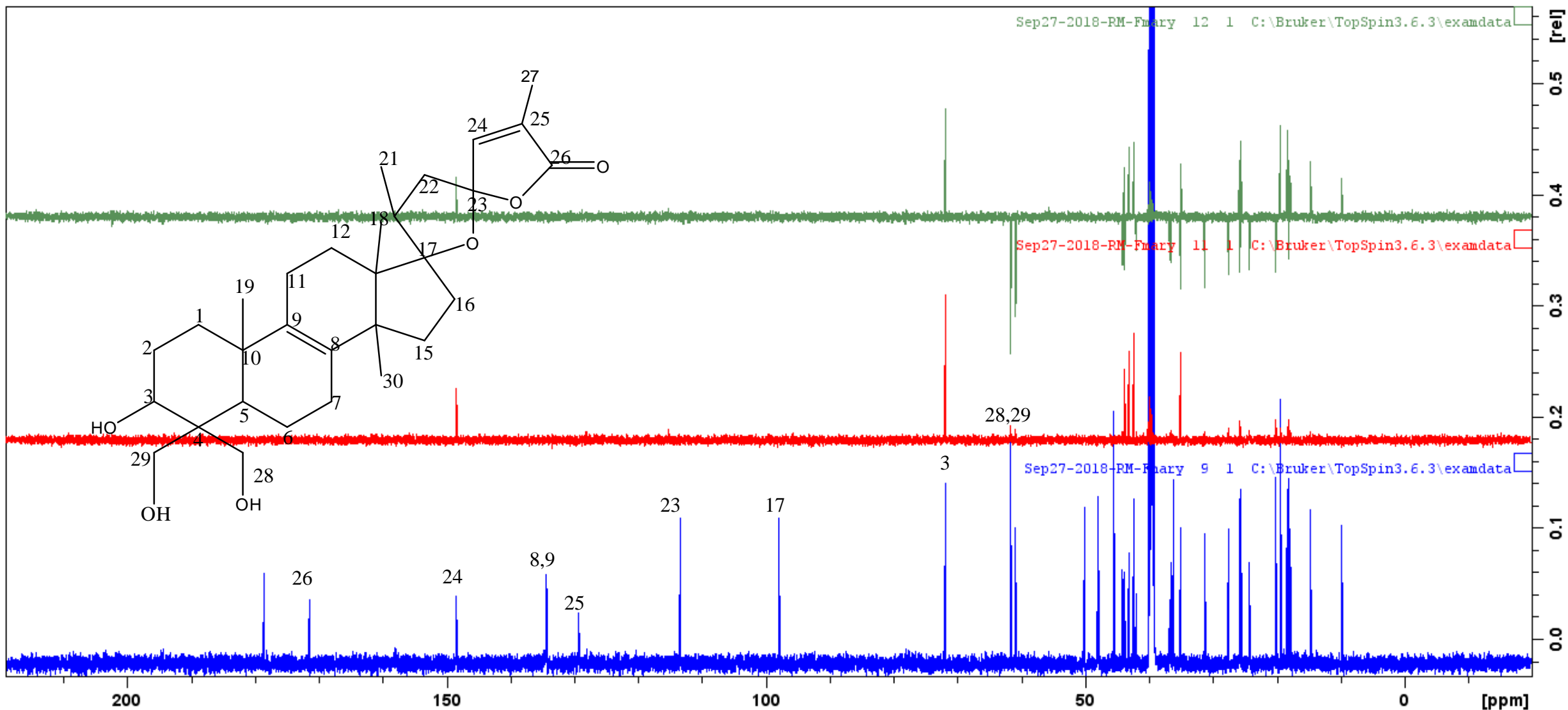
Minimum: -1.5
Maximum: 5.0 10.0 100.0

Mass	Calc. Mass	mDa	PPM	DBE	i-FIT	i-FIT (Norm)	Formula
483.3067	483.3110	-4.3	-8.9	9.5	23.1	0.0	C30 H43 O5

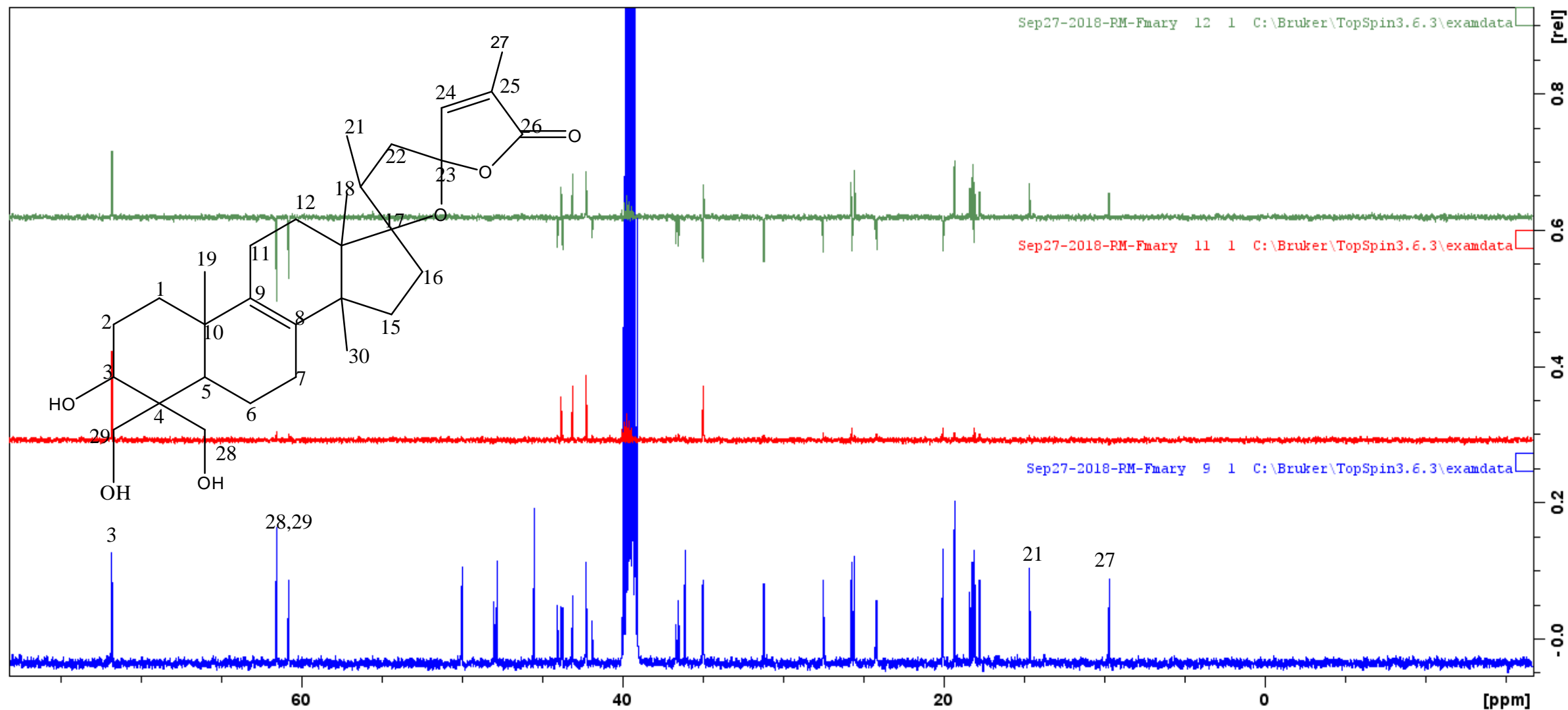
HRMS of compound **A10** 17 α , 23 α -epoxy-3 β ,29-dihydroxyl-nor-lanost-8,24-dien-26-one.



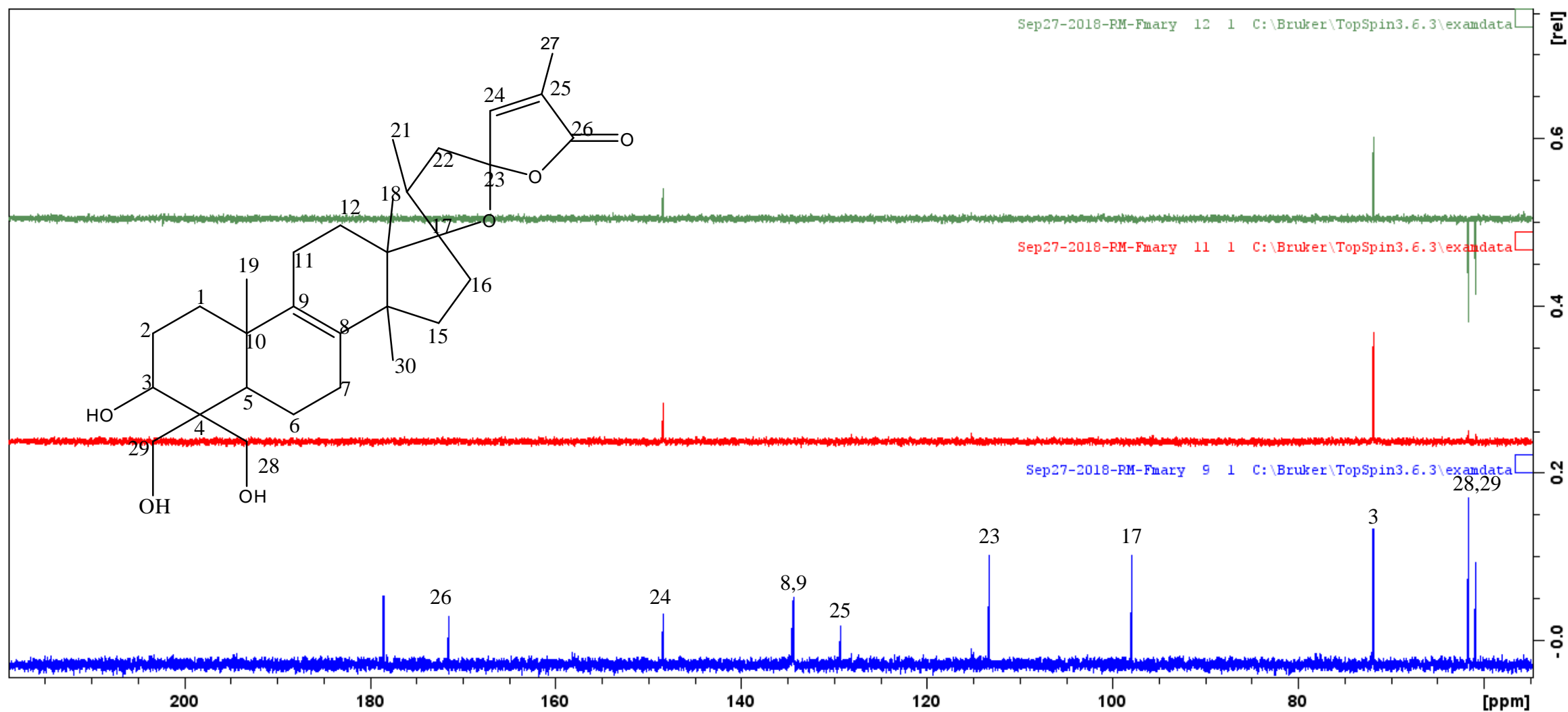
¹H NMR of compound **A11** 17 α , 23 α -epoxy-3 β , 28,29-trihydroxyl-nor-lanost-8,24-dien-26-one.



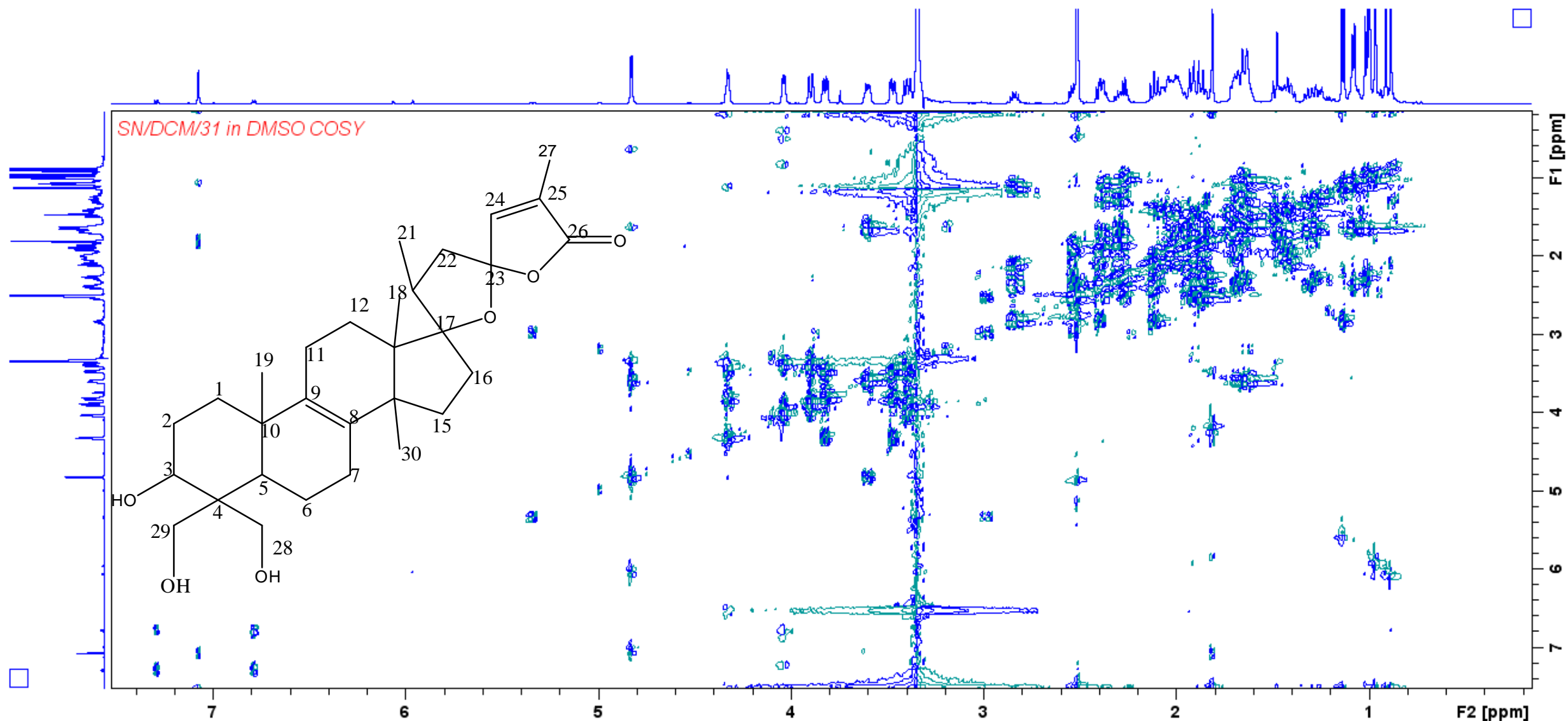
^{13}C NMR of compound **A11** 17 α , 23 α -epoxy-3 β , 28,29-trihydroxyl-nor-lanost-8,24-dien-26-one.



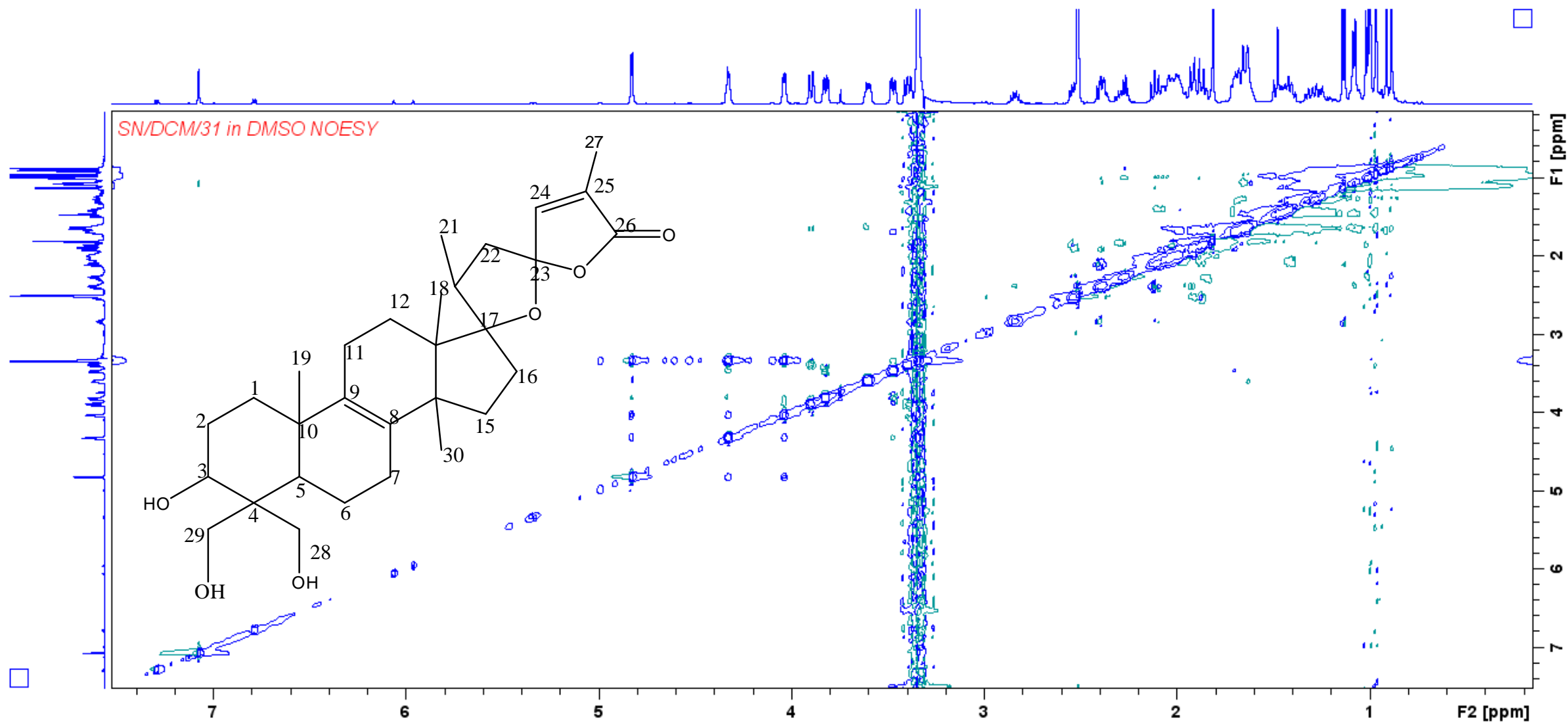
Expanded ¹³C NMR of compound **A11** 17 α , 23 α -epoxy-3 β , 28,29-trihydroxyl-nor-lanost-8,24-dien-26-one



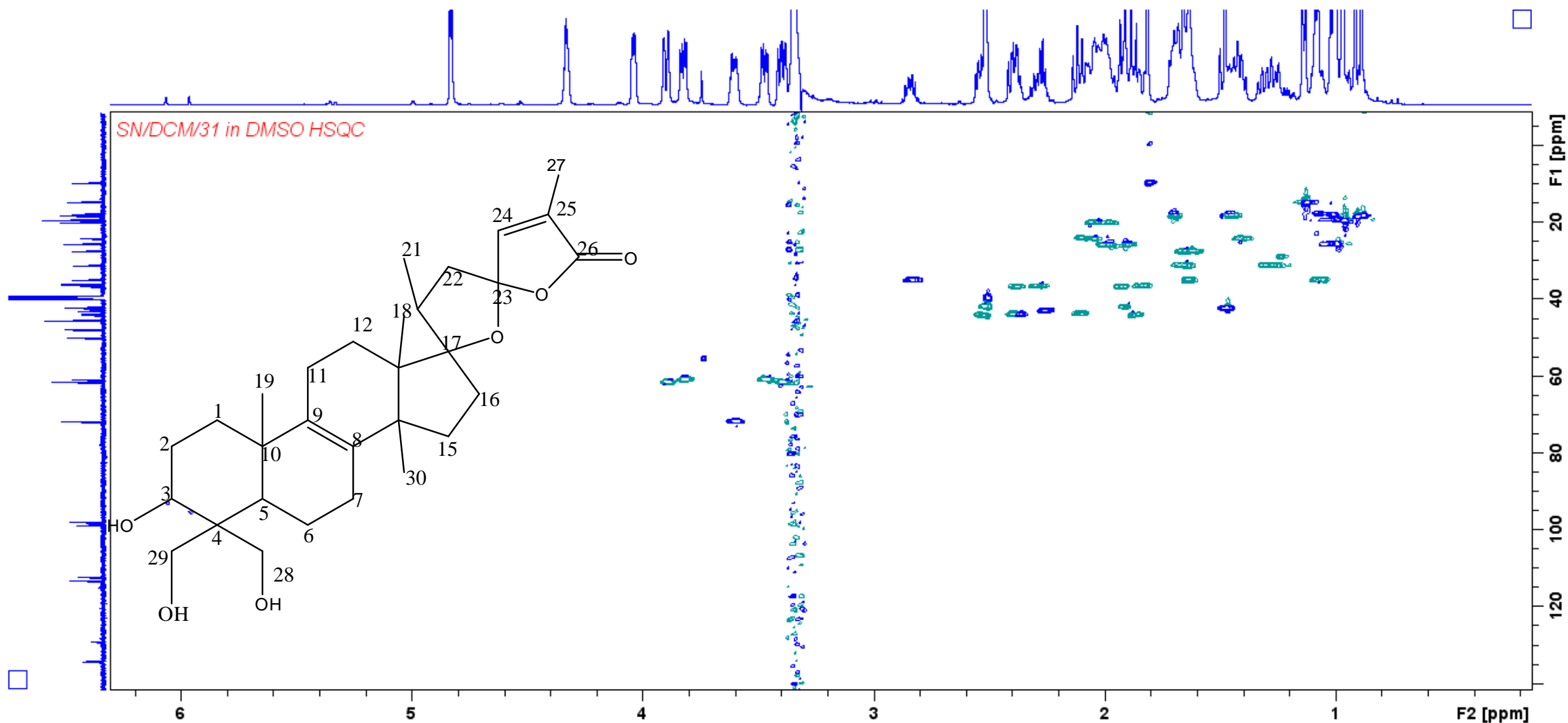
Expanded ^{13}C NMR of compound **A11** 17 α , 23 α -epoxy-3 β , 28,29-trihydroxyl-nor-lanost-8,24-dien-26-one



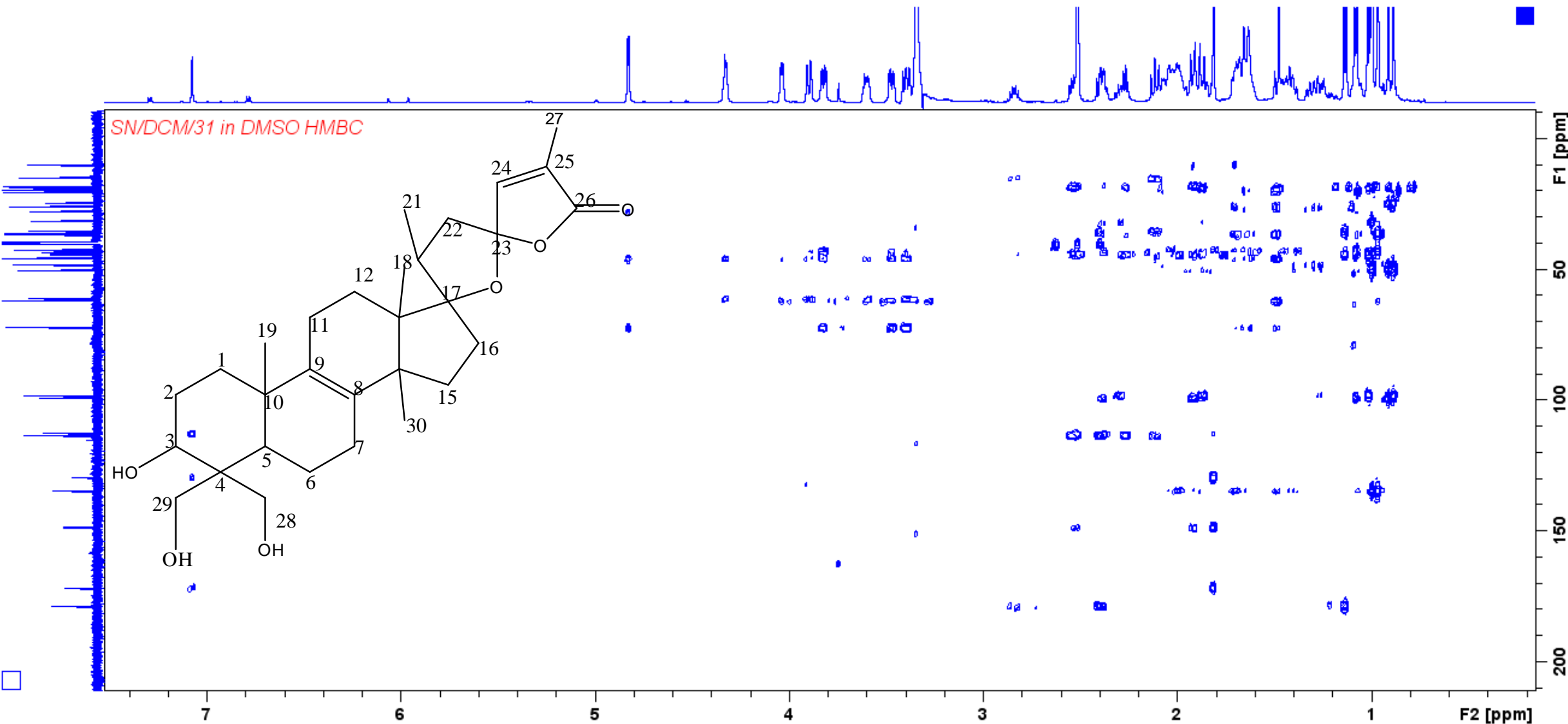
COSY of compound **A11** 17 α , 23 α -epoxy-3 β , 28,29-trihydroxyl-nor-lanost-8,24-dien-26-one



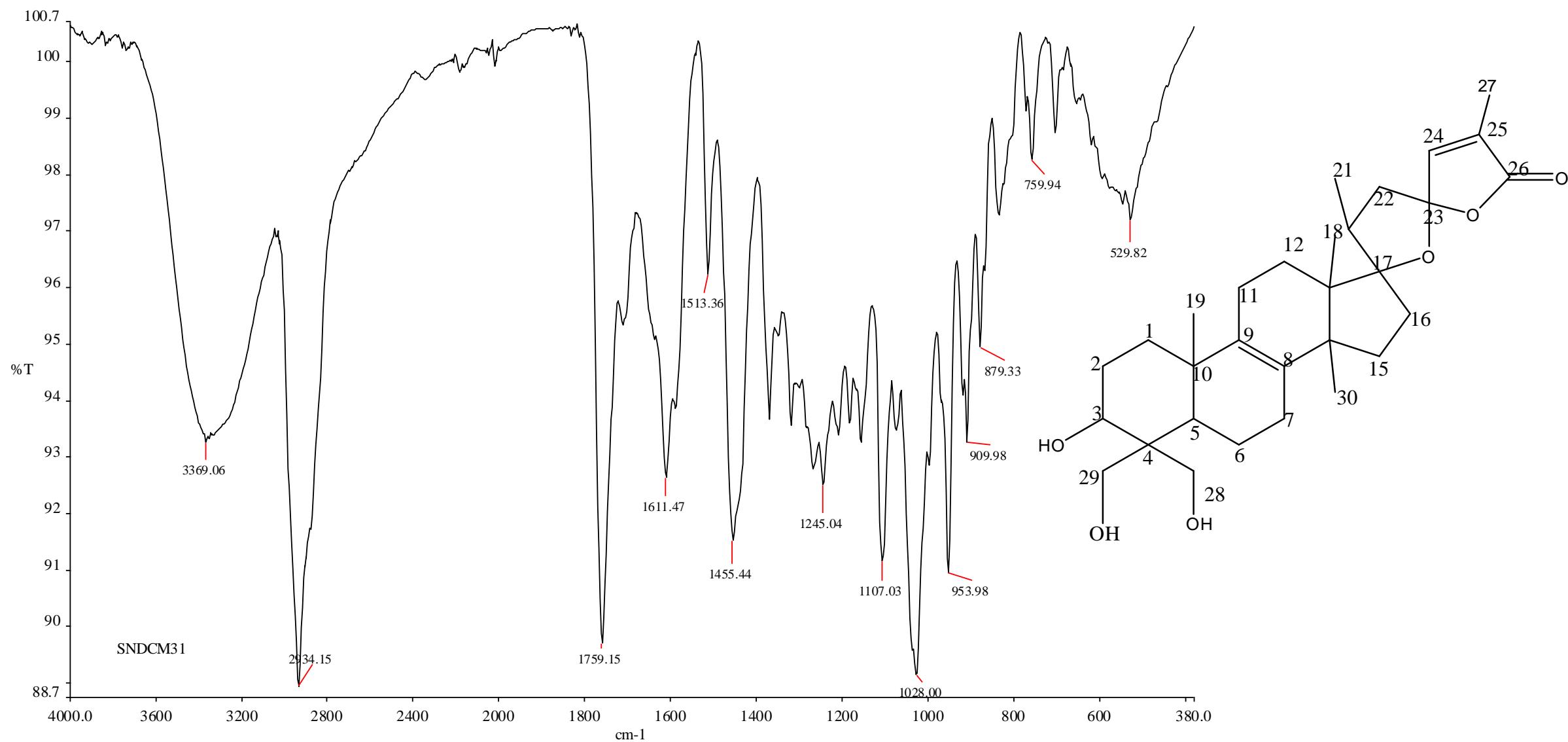
NOESY of compound **A11** 17 α , 23 α -epoxy-3 β , 28,29-trihydroxyl-nor-lanost-8,24-dien-26-one



HSQC of compound **A11** 17 α , 23 α -epoxy-3 β , 28,29-trihydroxyl-nor-lanost-8,24-dien-26-one



HMBC of compound **A11** 17 α , 23 α -epoxy-3 β , 28,29-trihydroxyl-nor-lanost-8,24-dien-26-one

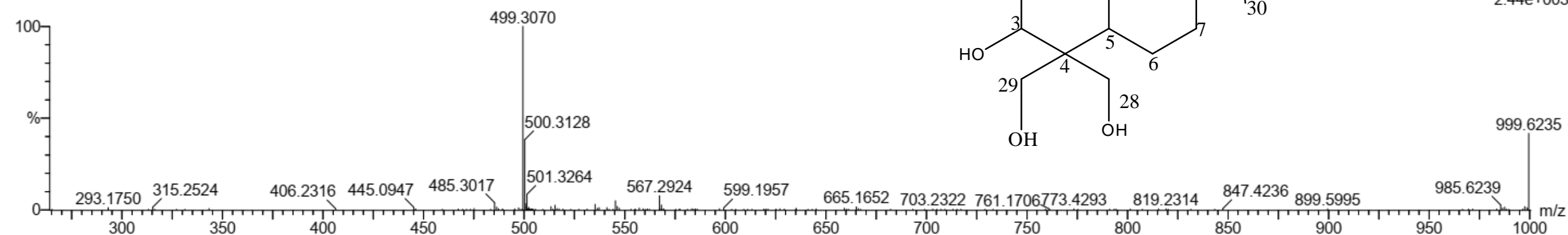


IR spectrum of compound **A11** 17 α , 23 α -epoxy-3 β , 28,29-trihydroxyl-nor-lanost-8,24-dien-26-one

Monoisotopic Mass, Even Electron Ions
 47 formula(e) evaluated with 1 results within limits (up to 10 best isotopic matches for each mass)
 Elements Used:
 C: 1-70 H: 1-100 O: 1-8

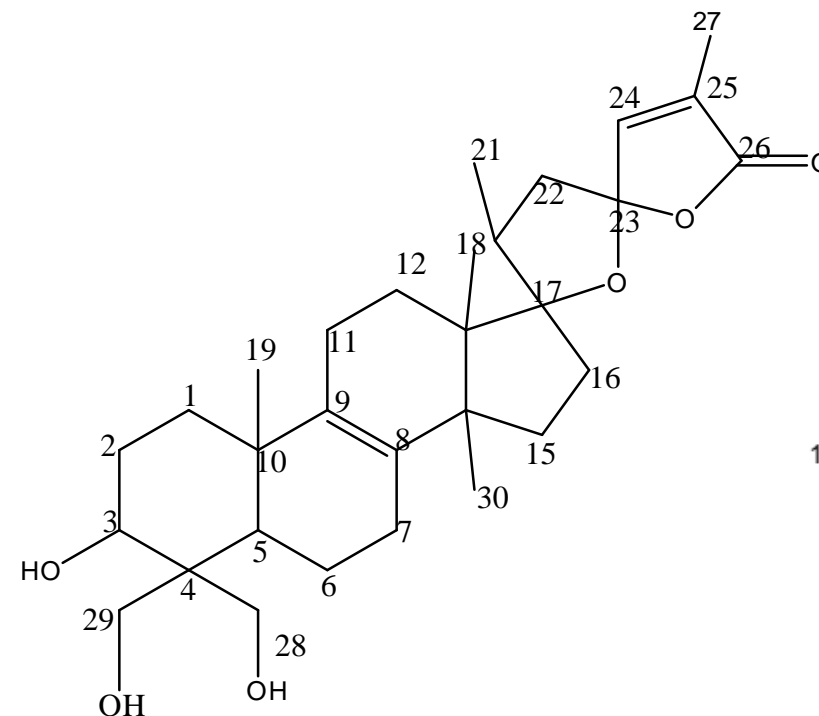
Sample 26b 29 March 2021 UPLC #1b 466 (9.985)

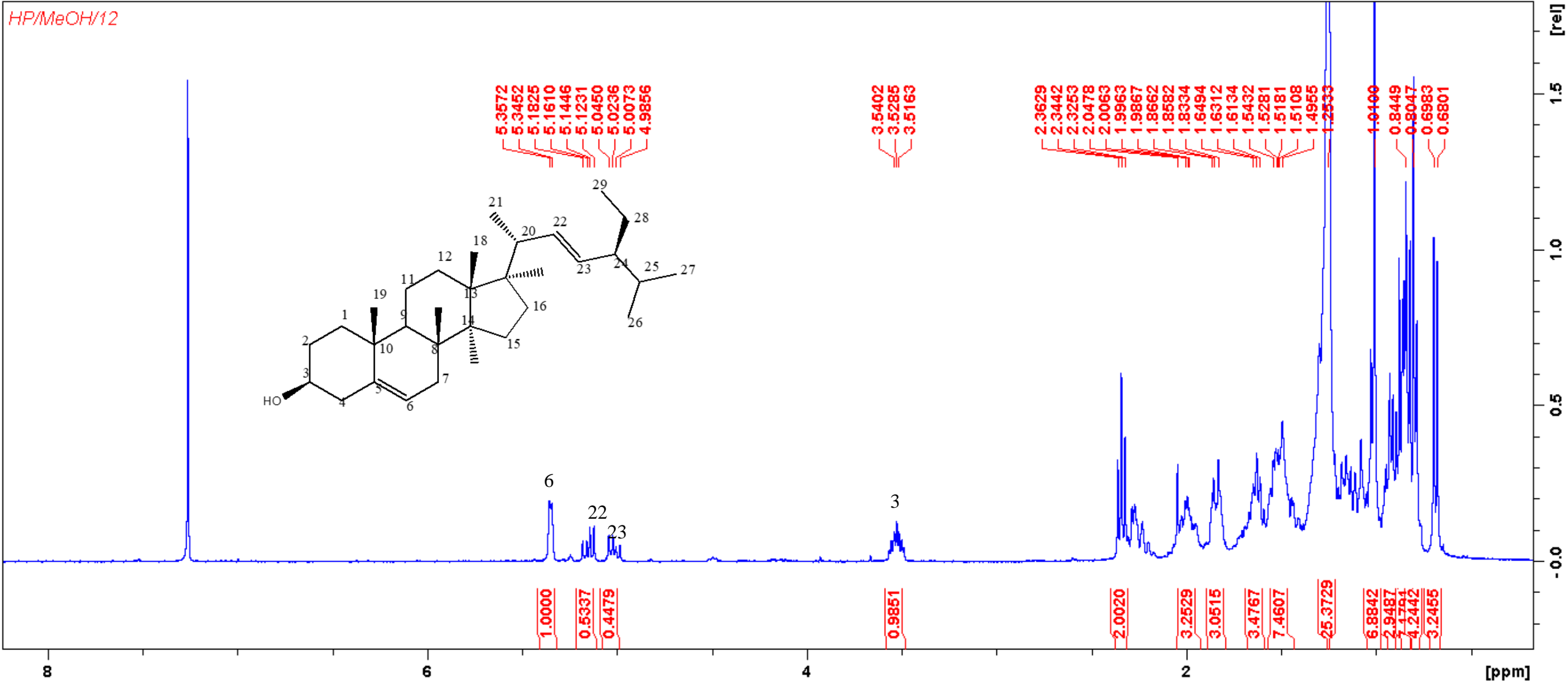
SYNAPT HDMS G1



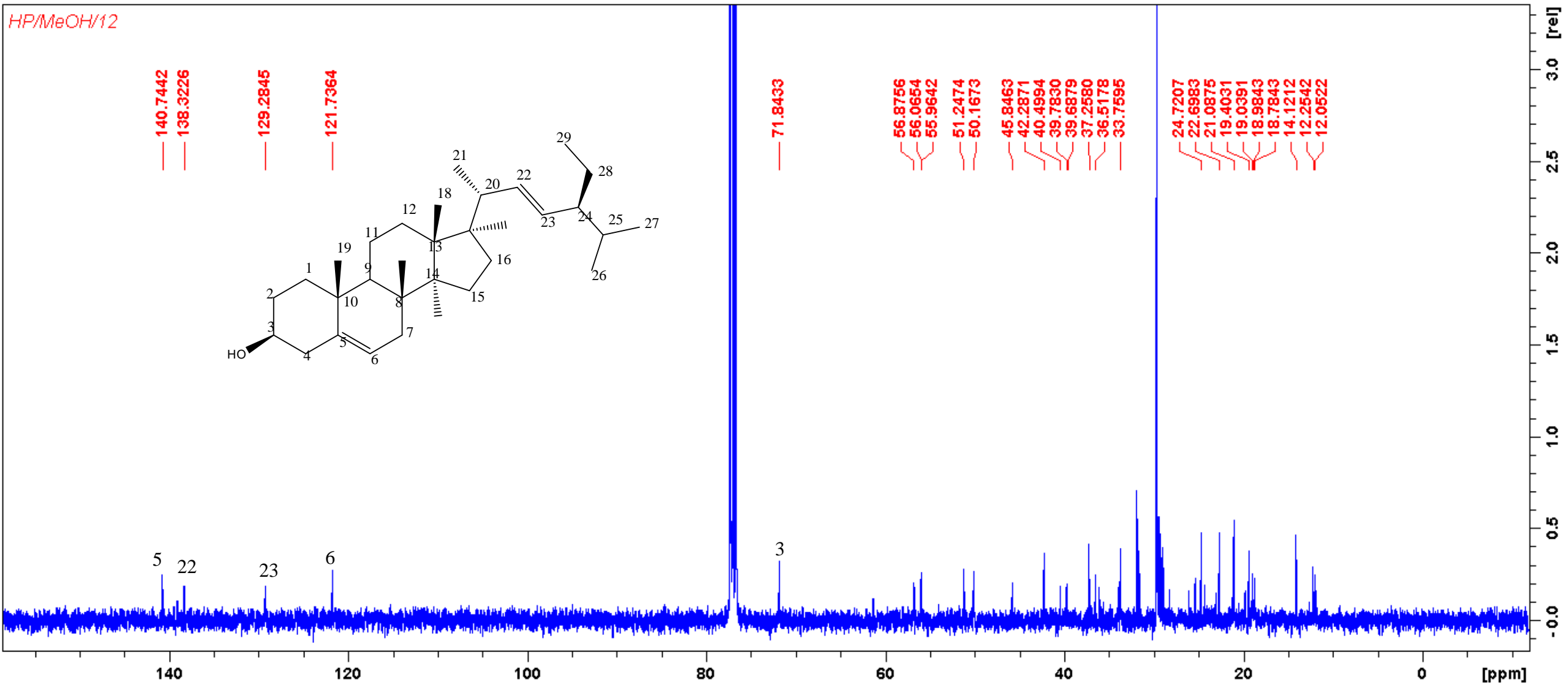
Minimum:				-1.5			
Maximum:	5.0	10.0		100.0			
Mass	Calc. Mass	mDa	PPM	DBE	i-FIT	i-FIT (Norm)	Formula
499.3070	499.3060	1.0	2.0	9.5	40.8	0.0	C30 H43 O6

HRMS of compound **A11** 17 α , 23 α -epoxy-3 β , 28,29-trihydroxyl-nor-lanost-8,24-dien-26-one

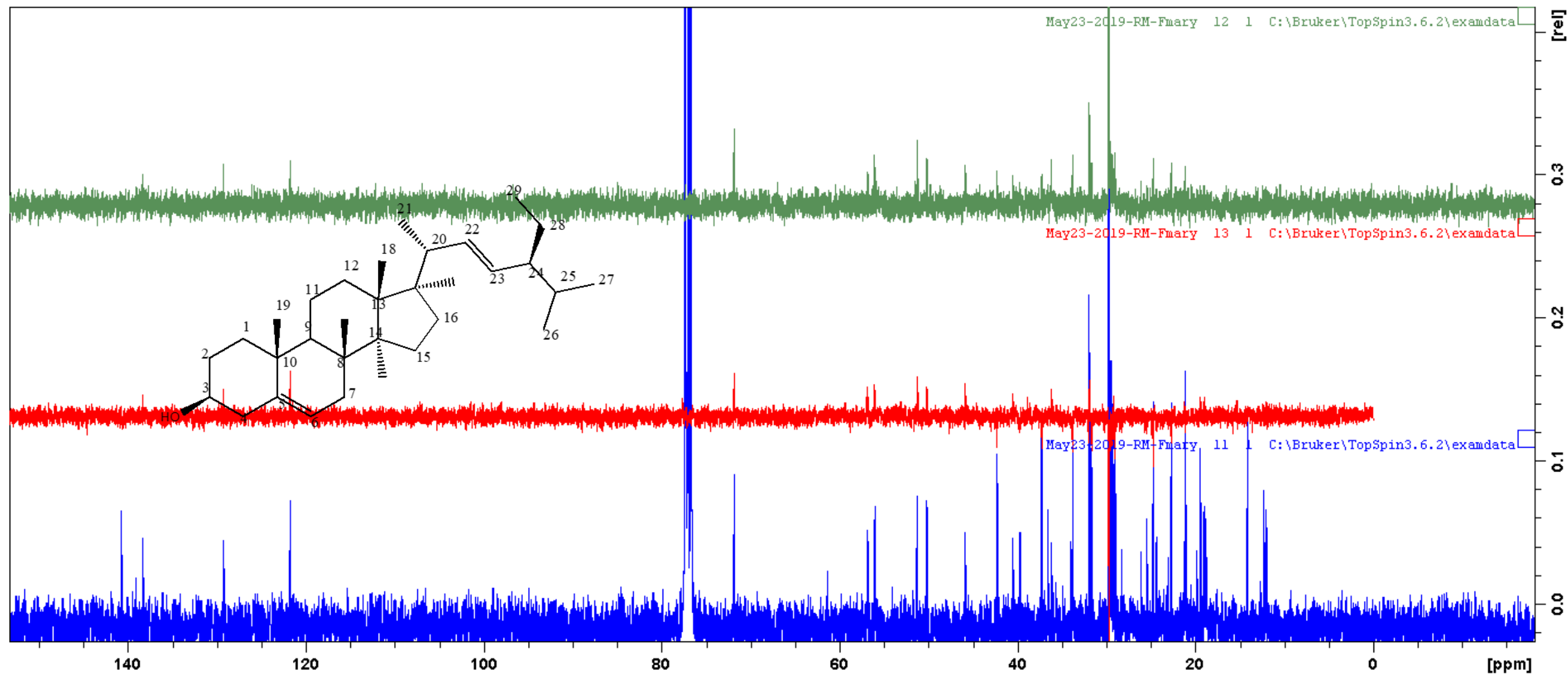




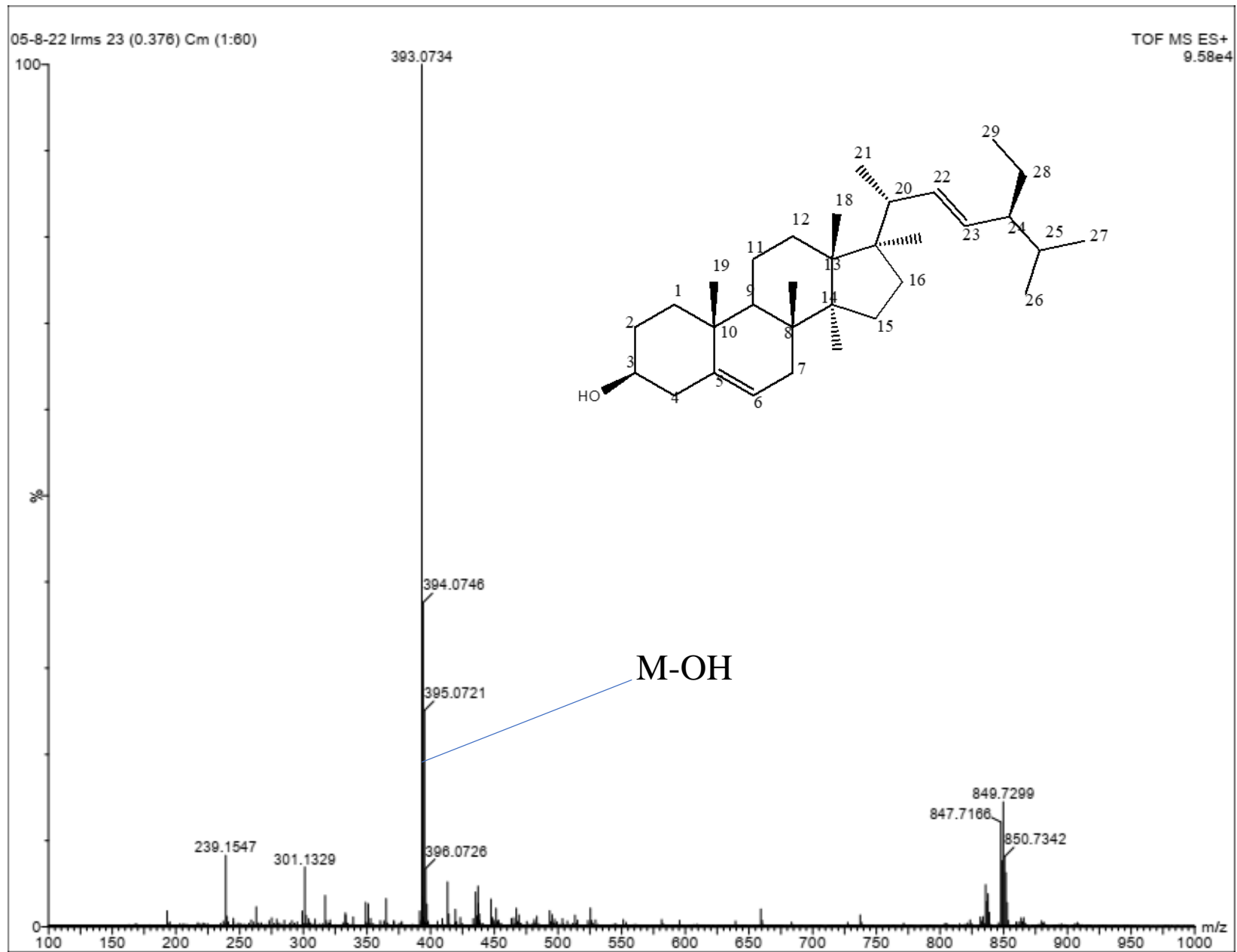
^1H NMR spectrum of **B1** stigmasterol



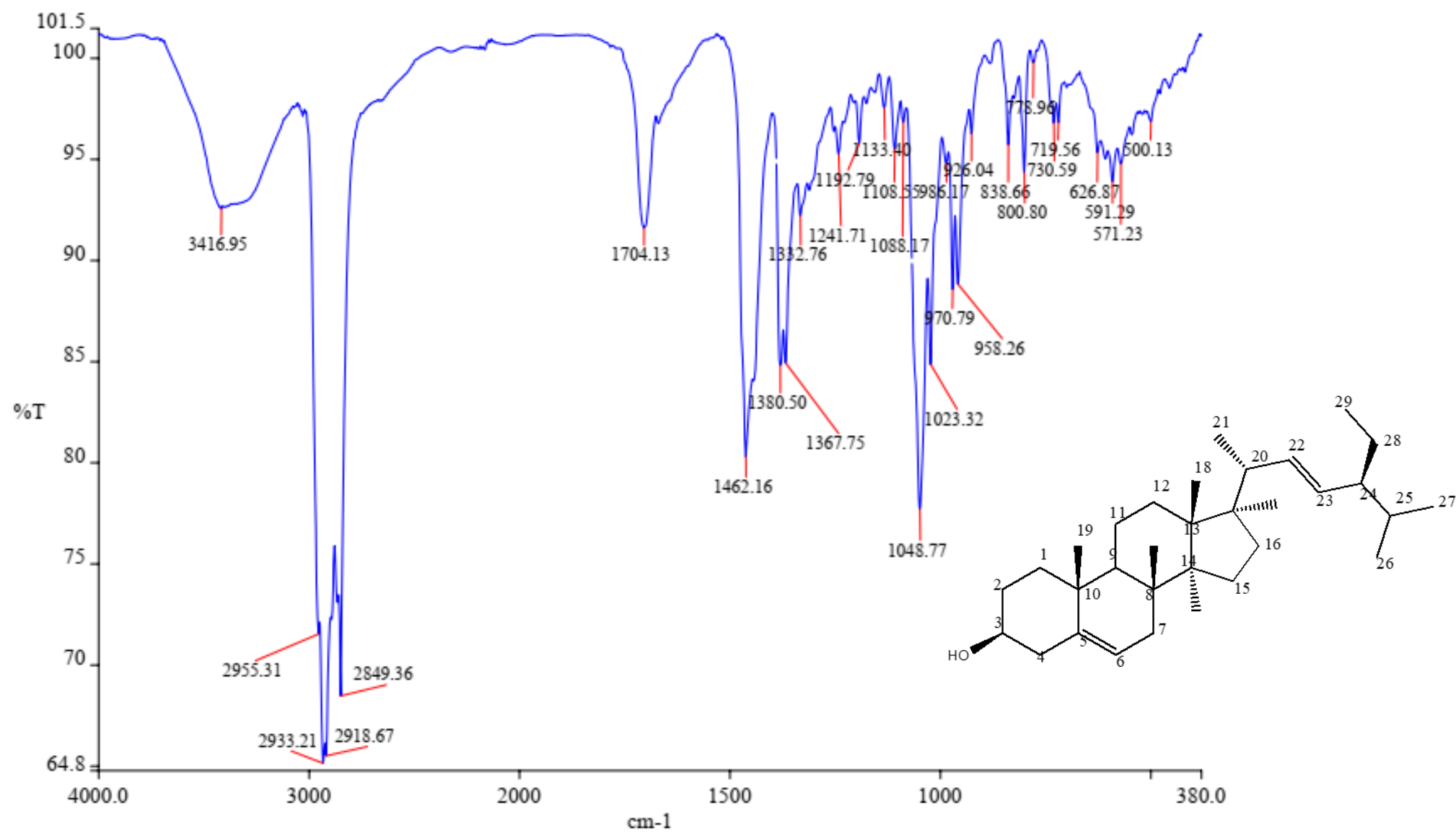
^{13}C NMR spectrum of **B1** stigmasterol



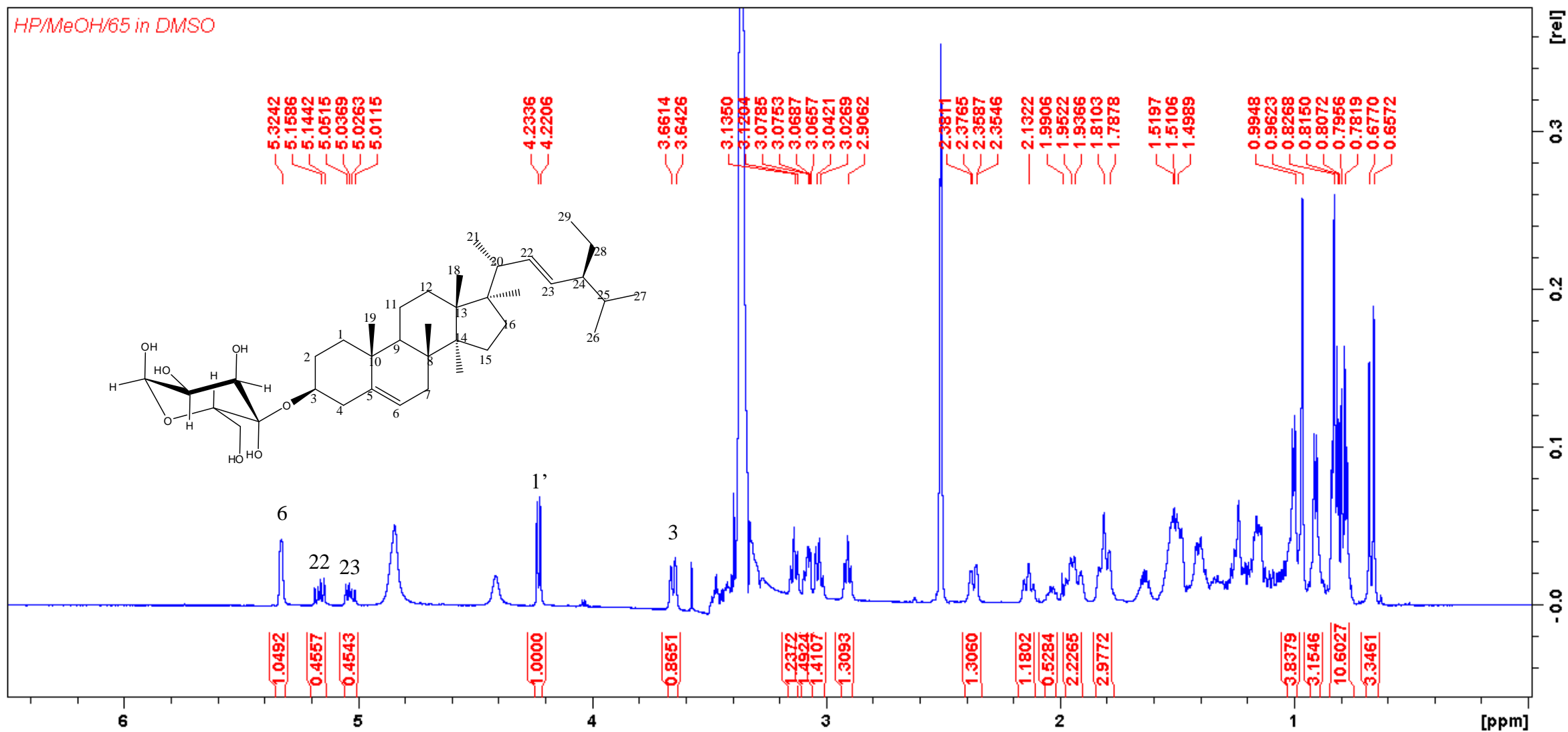
DEPT spectrum of **B1** stigmasterol



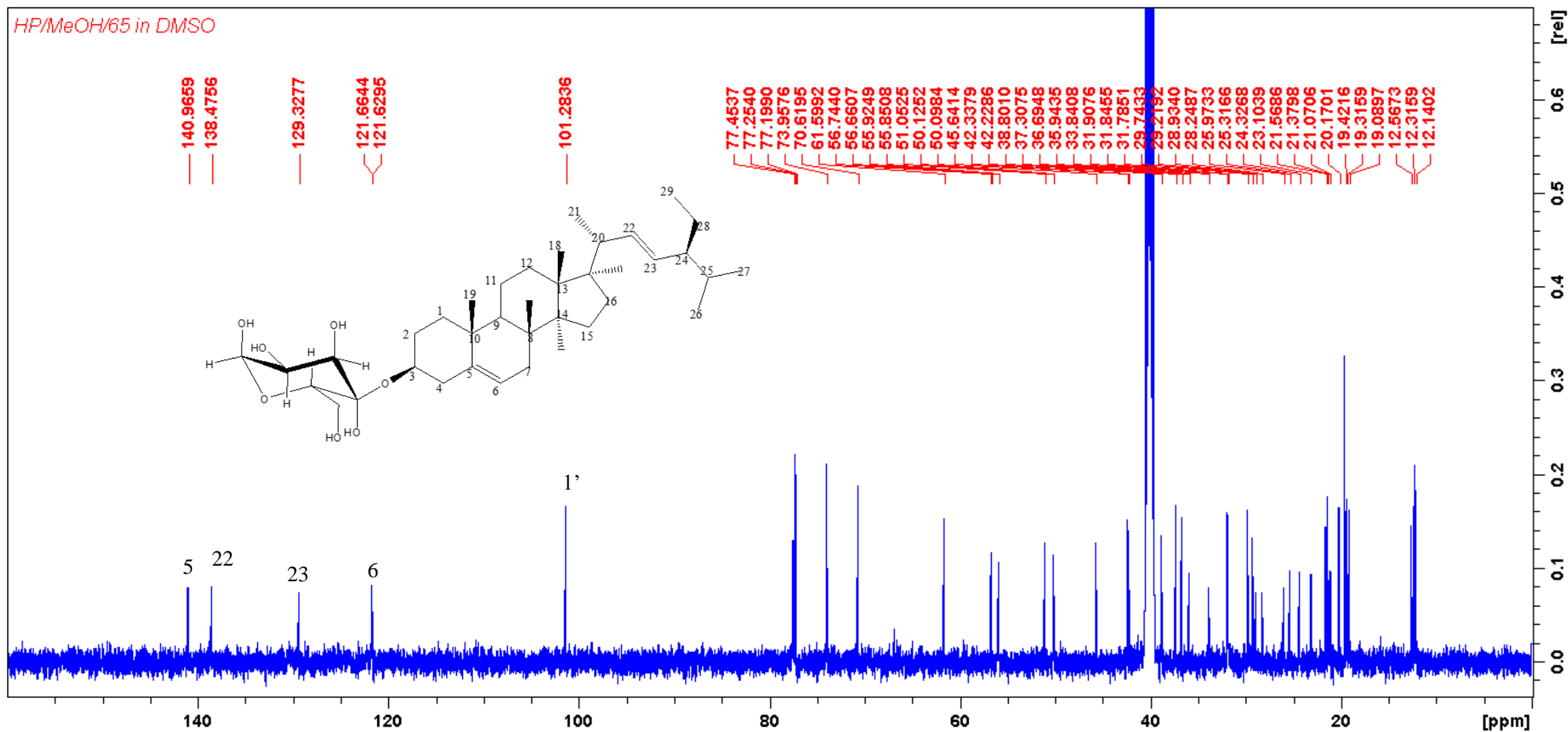
Mass spectrum of **B1** stigmasterol



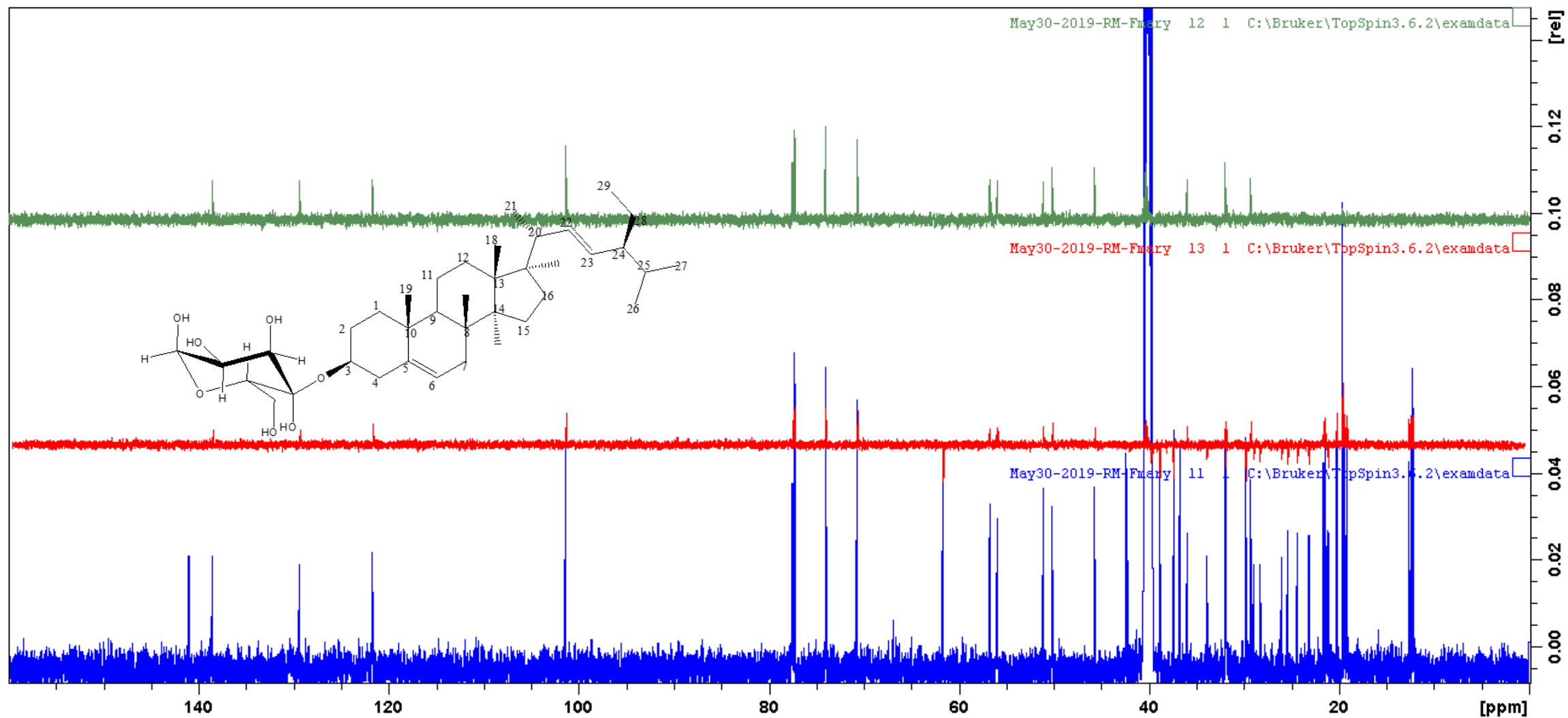
IR spectrum of **B1** stigmasterol



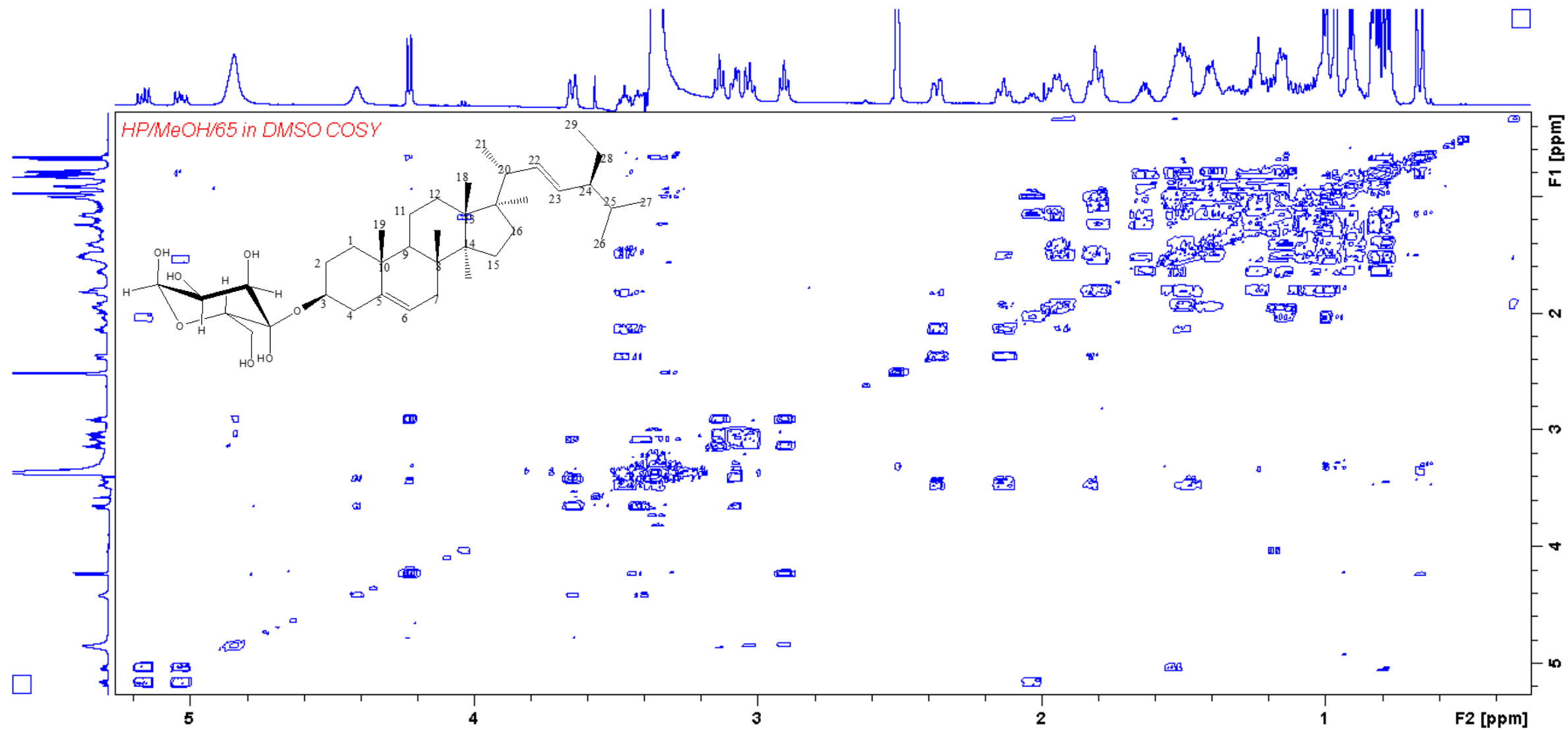
^1H NMR of **B2** stigmasterol glucoside



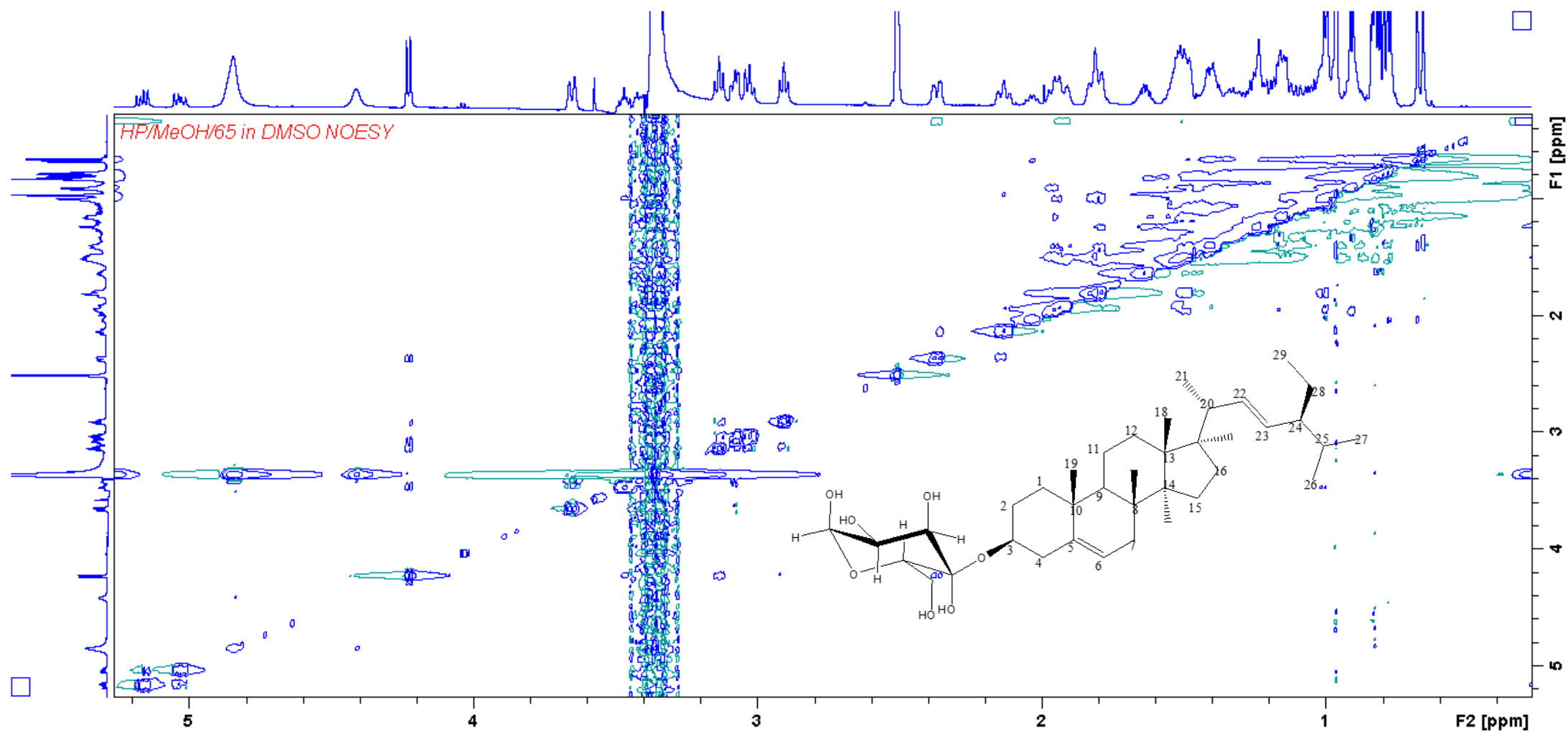
^{13}C NMR of **B2** stigmasterol glucoside



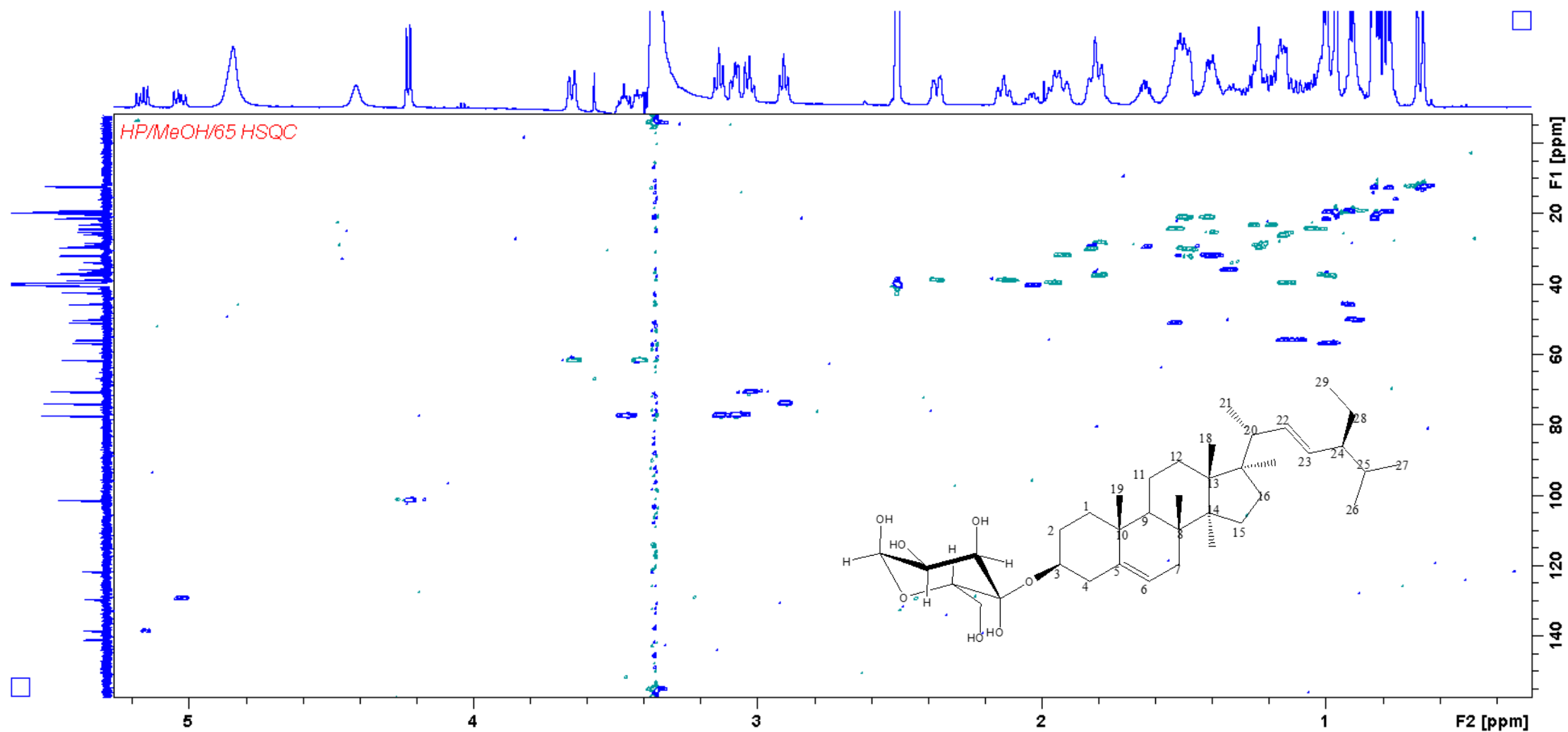
DEPT of **B2** stigmasterol glucoside



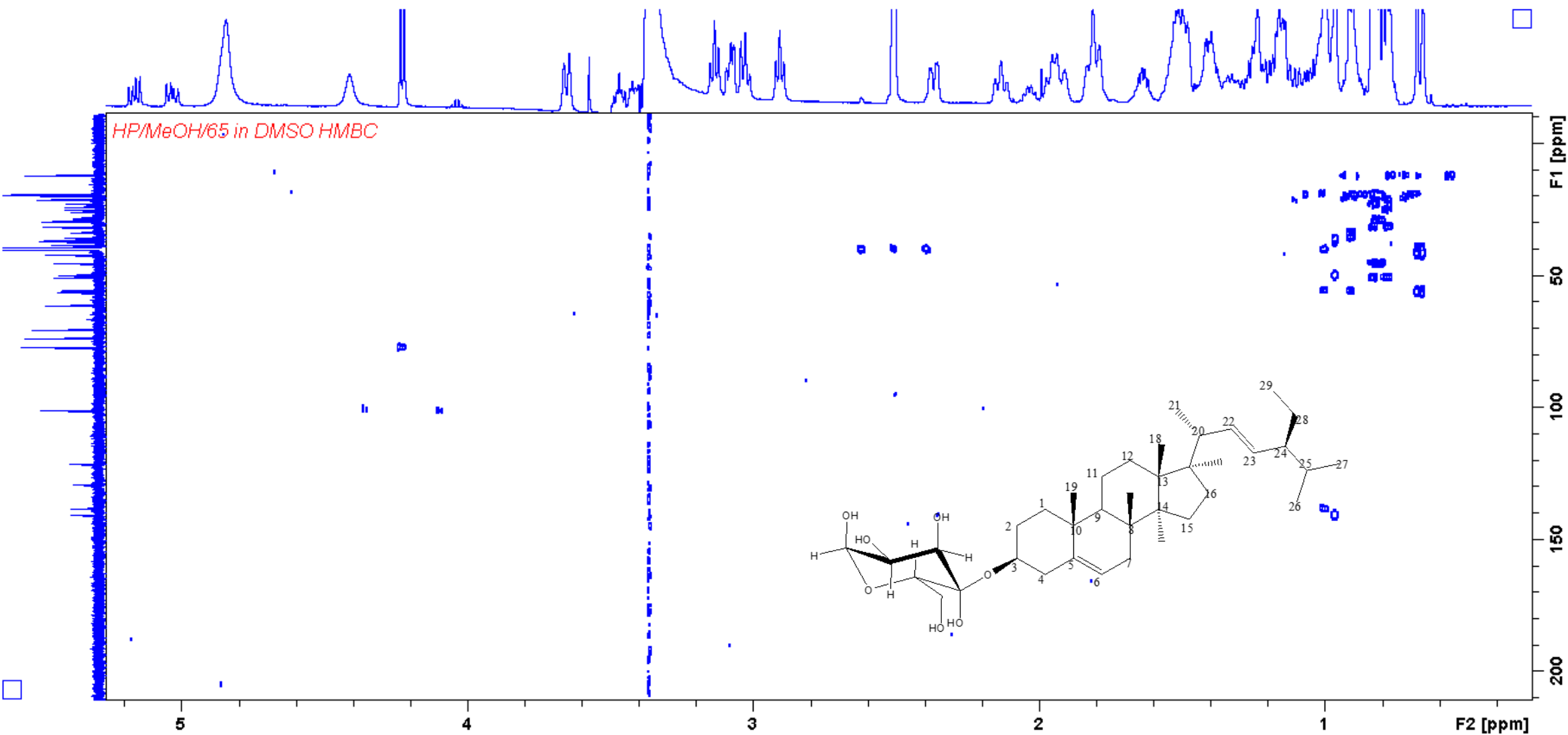
COSY of **B2** stigmasterol glucoside



NOESY of **B2** stigmasterol glucoside



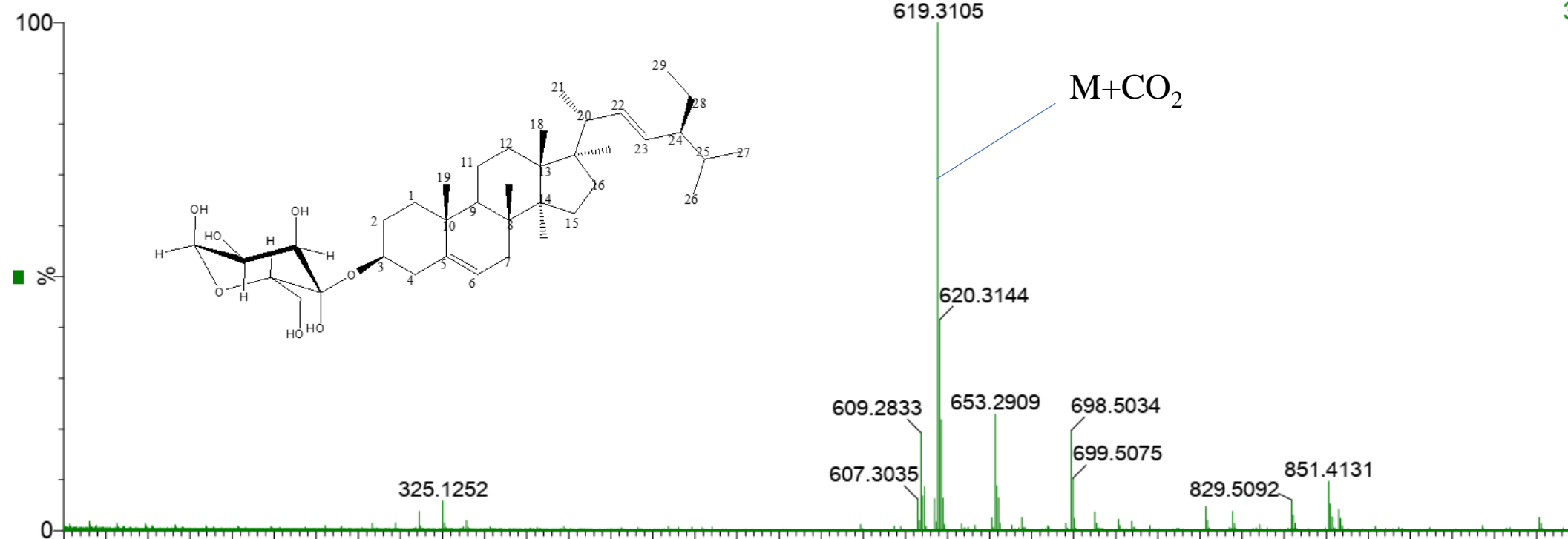
HSQC of **B2** stigmasterol glucoside



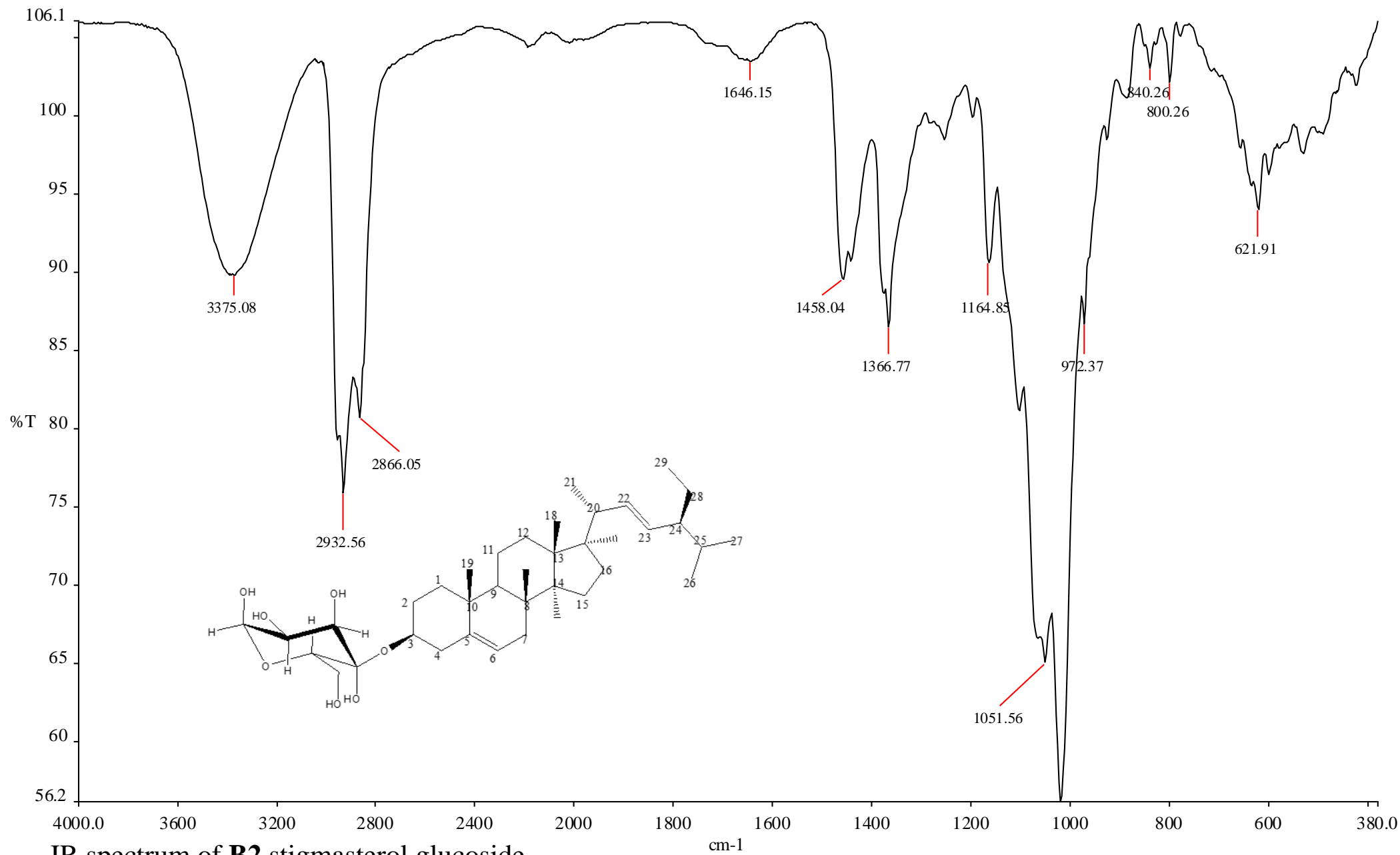
HMBC of **B2** stigmasterol glucoside

=M3 -lrms 15 (0.239) Cm (1:59)

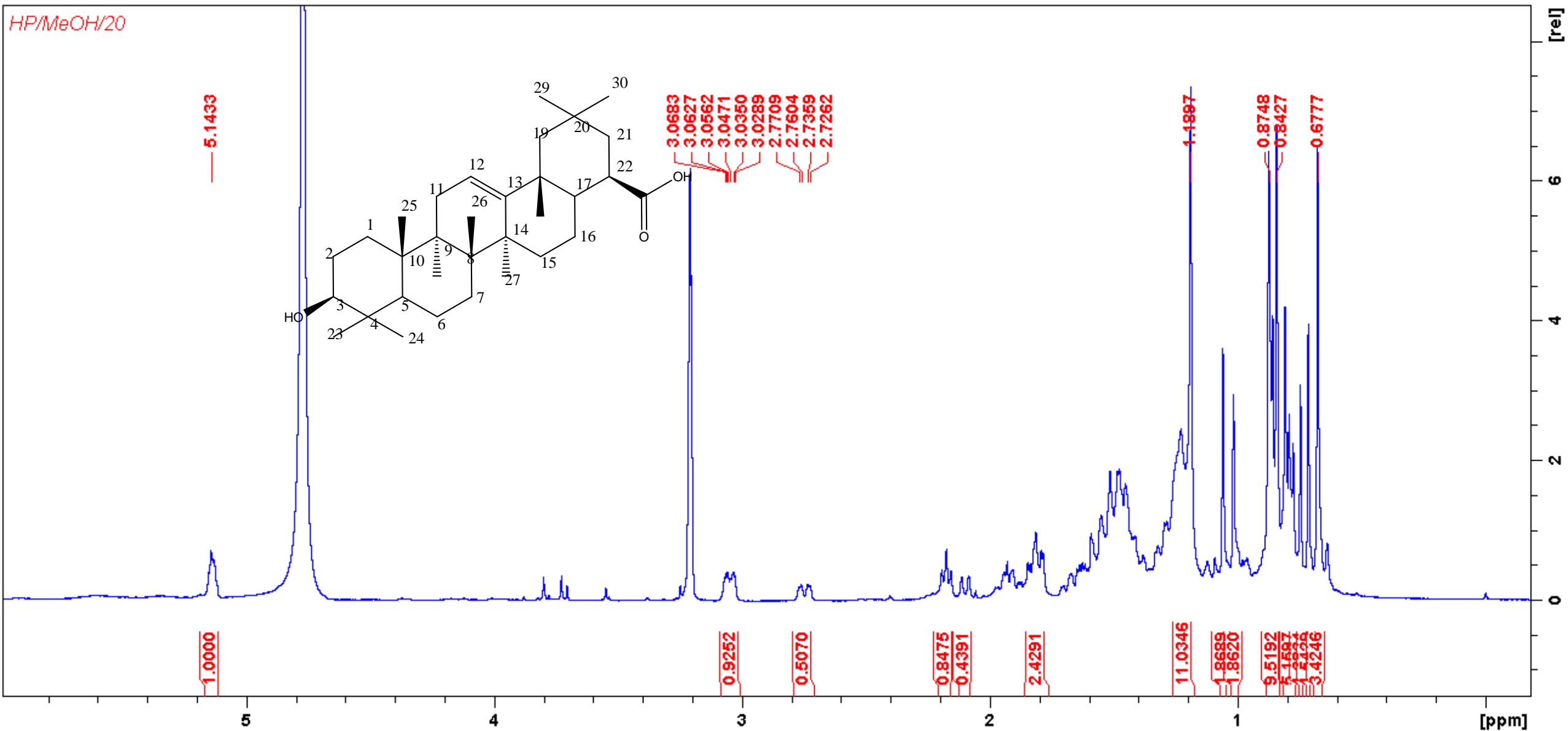
TOF MS ES-
3.54e4



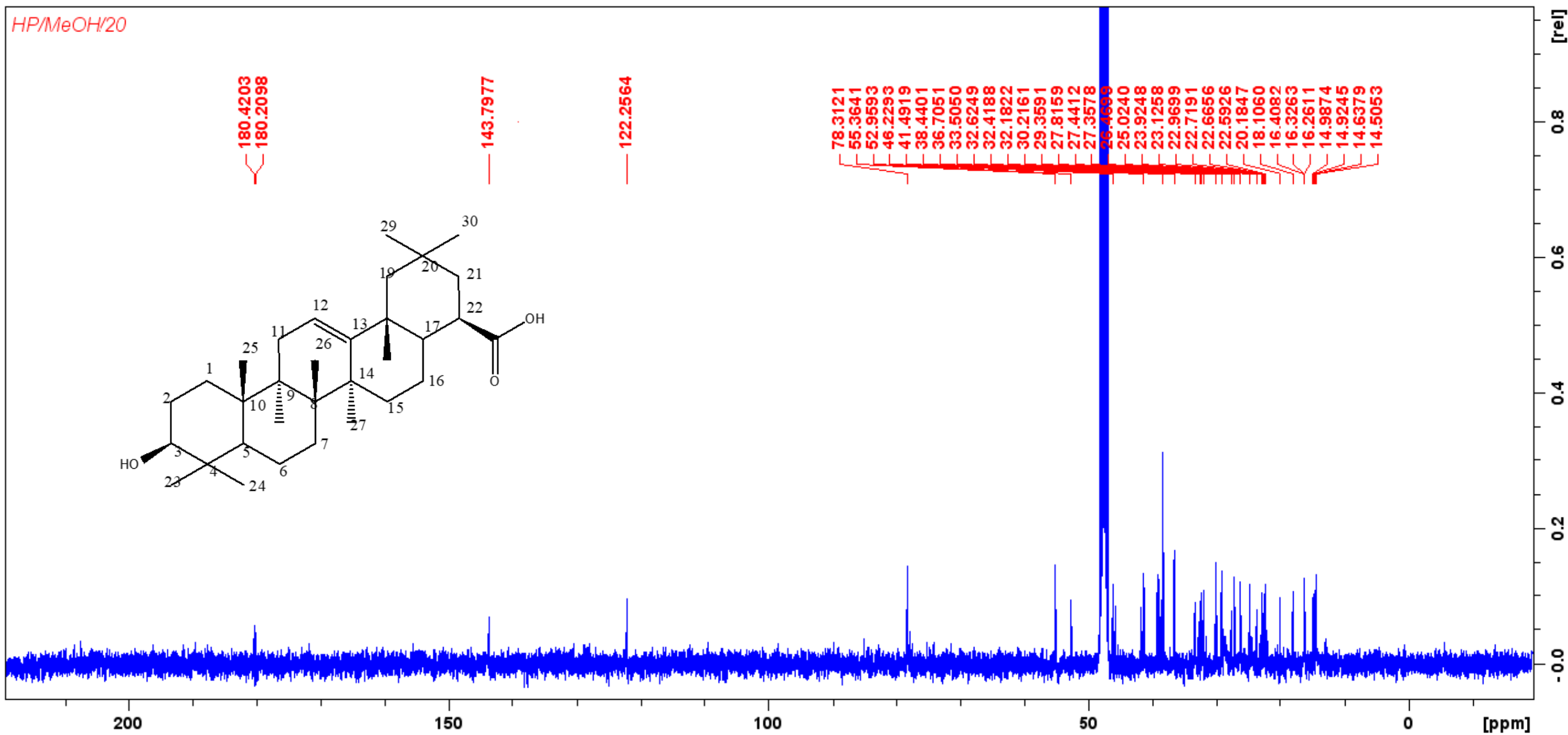
Mass spectrum of **B2** stigmasterol glucoside



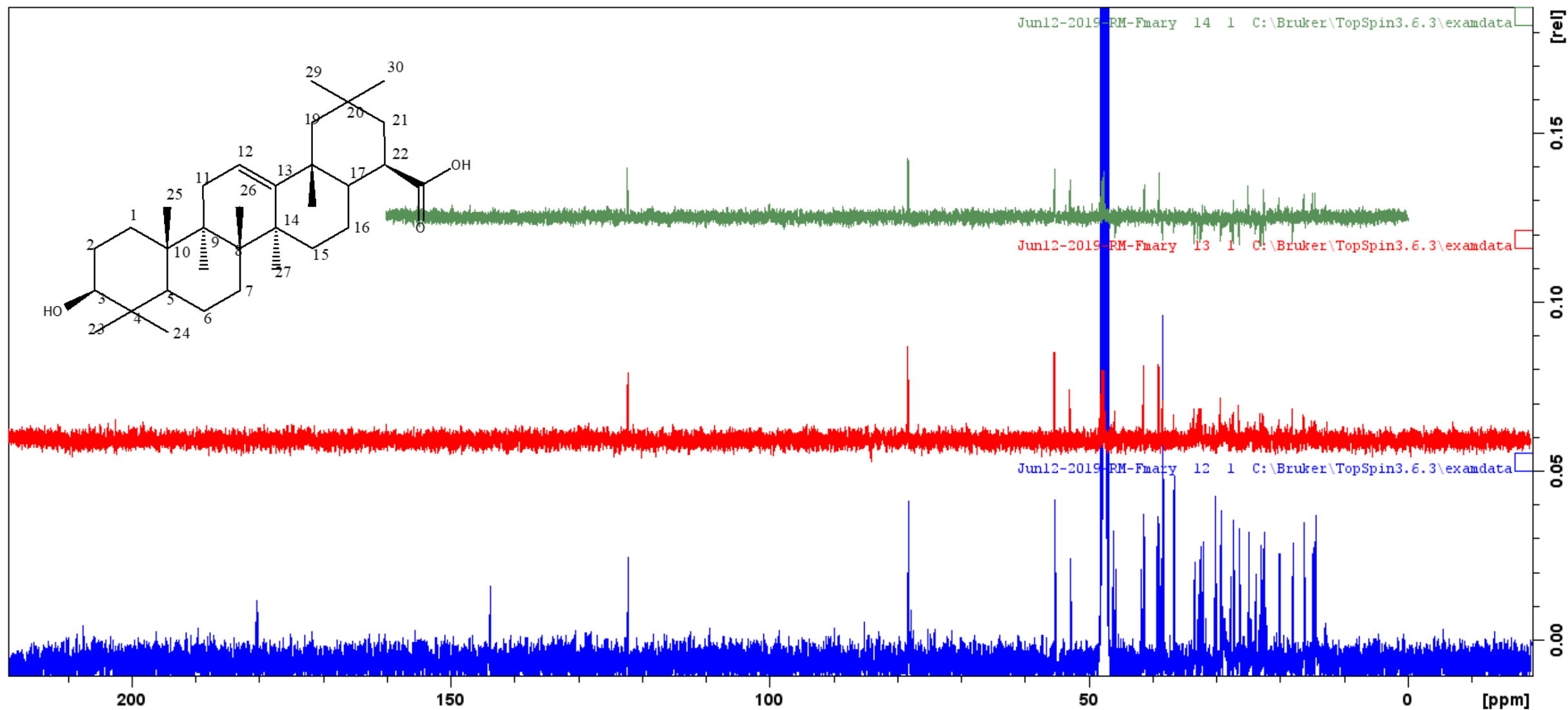
IR spectrum of **B2** stigmasterol glucoside



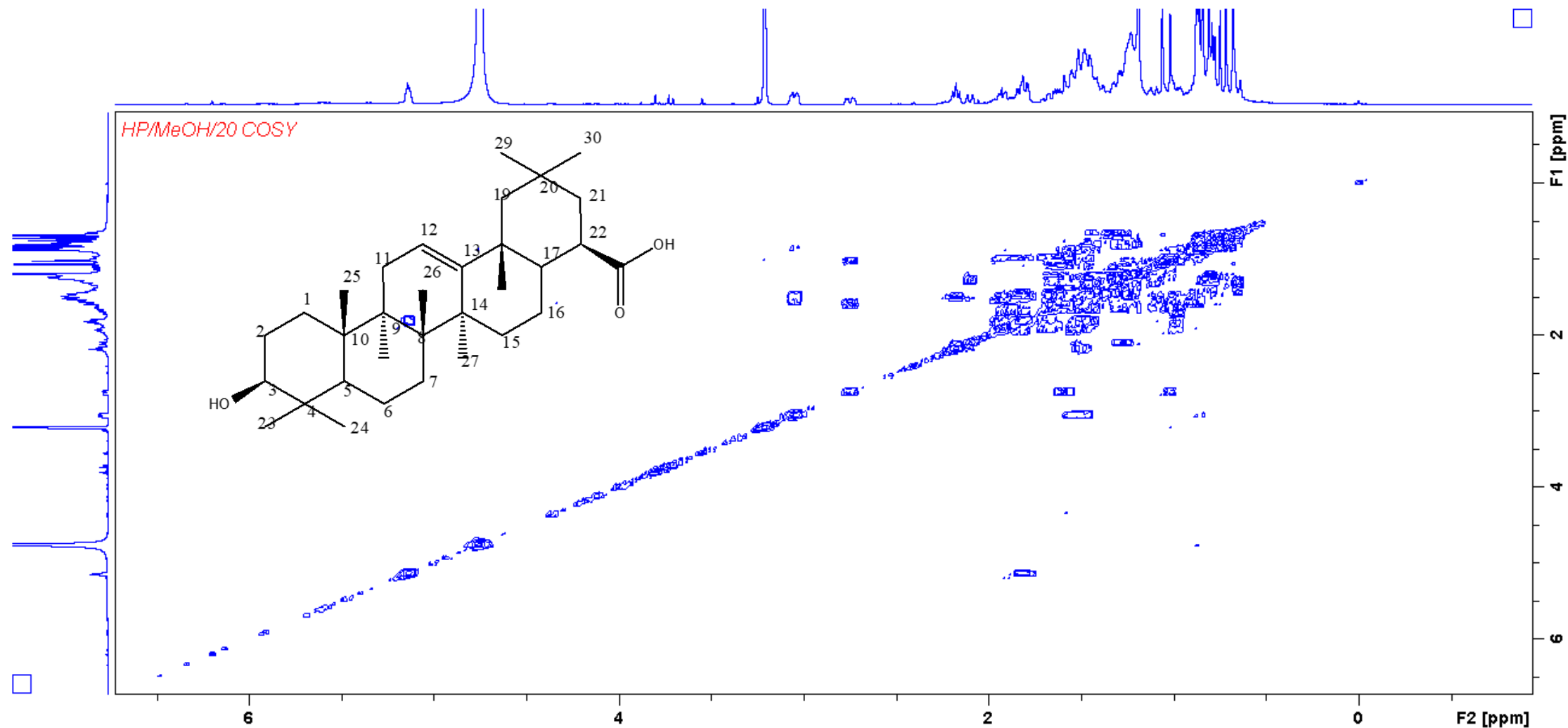
¹H NMR of **B3** oleanolic acid



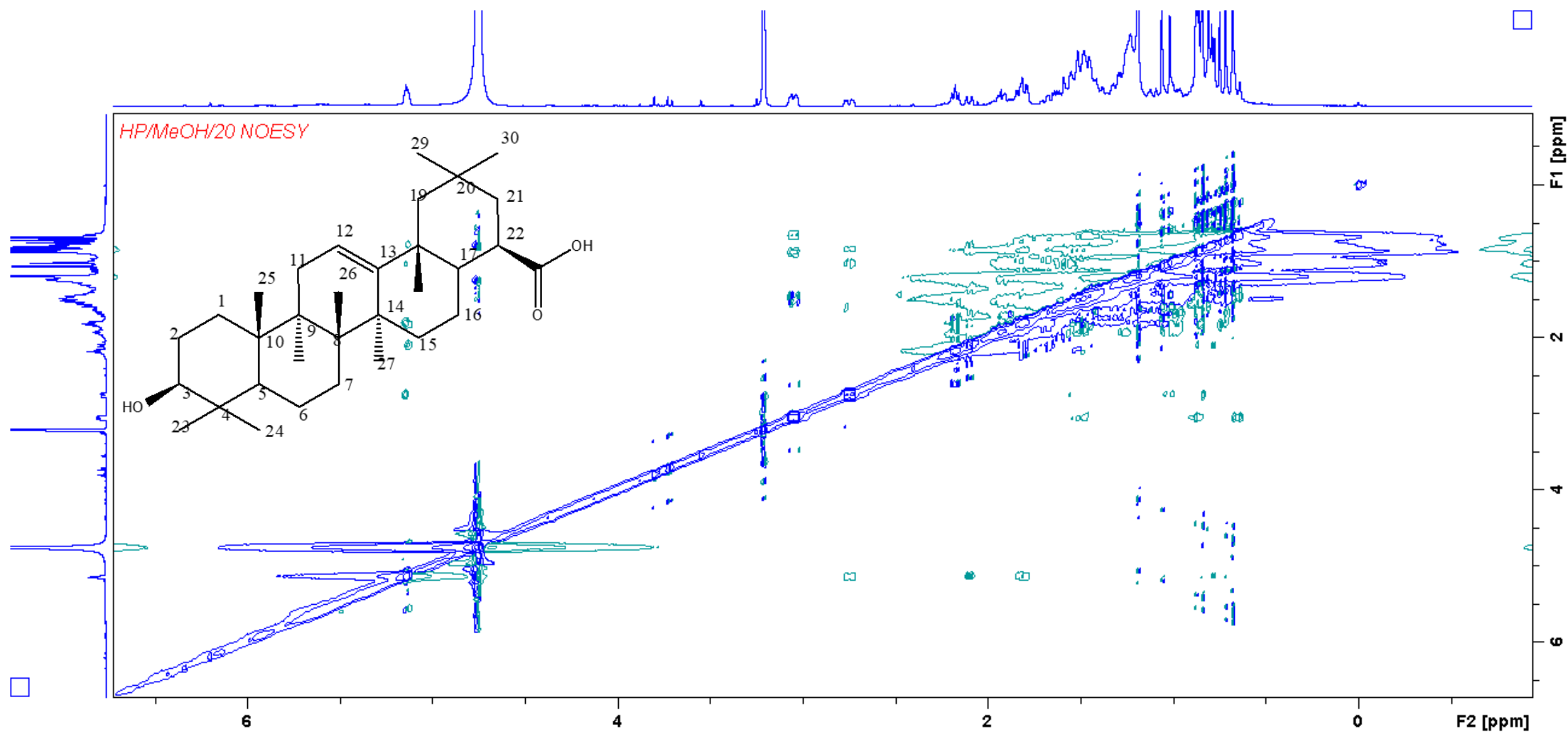
^{13}C NMR of **B3** oleanolic acid



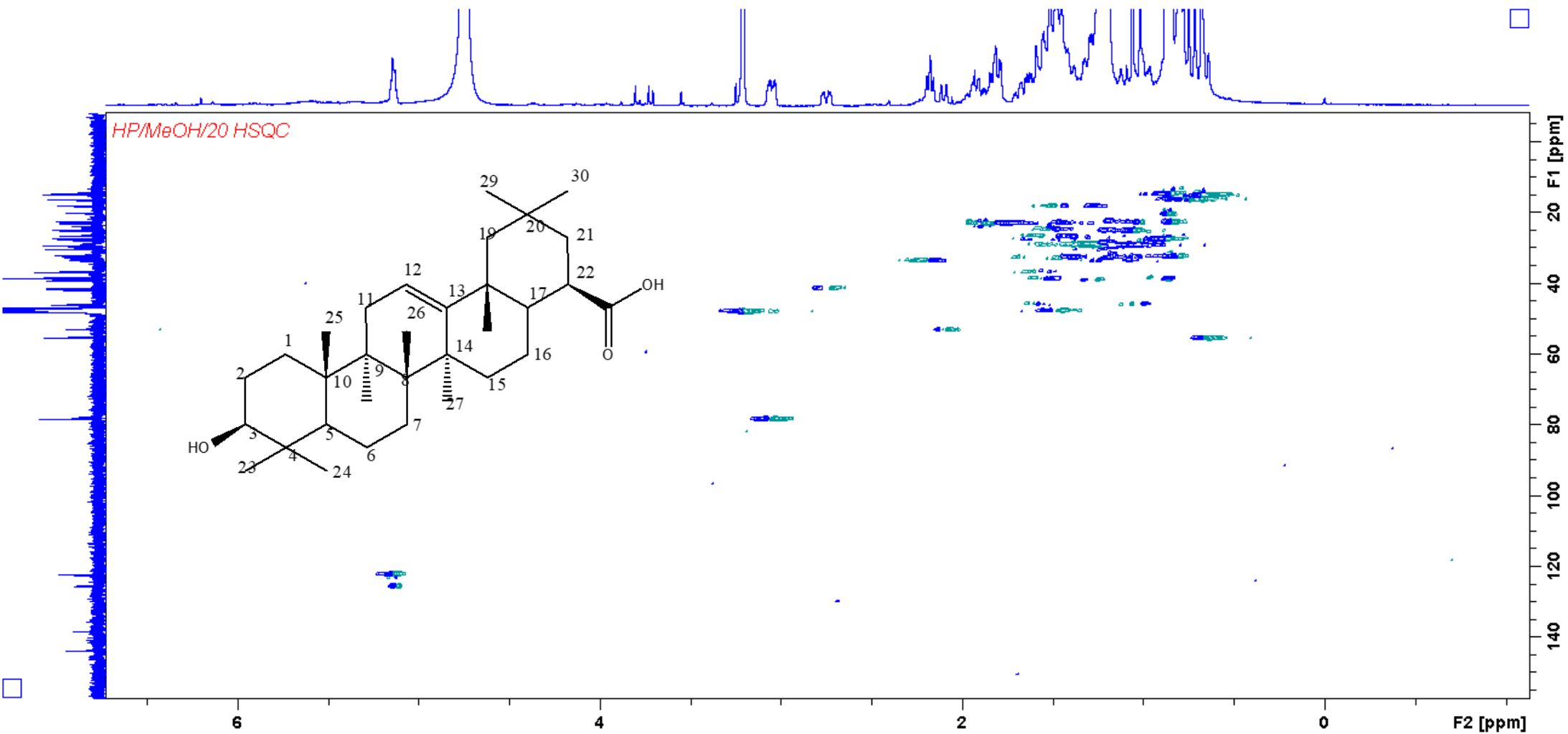
DEPT of **B3** oleanolic acid



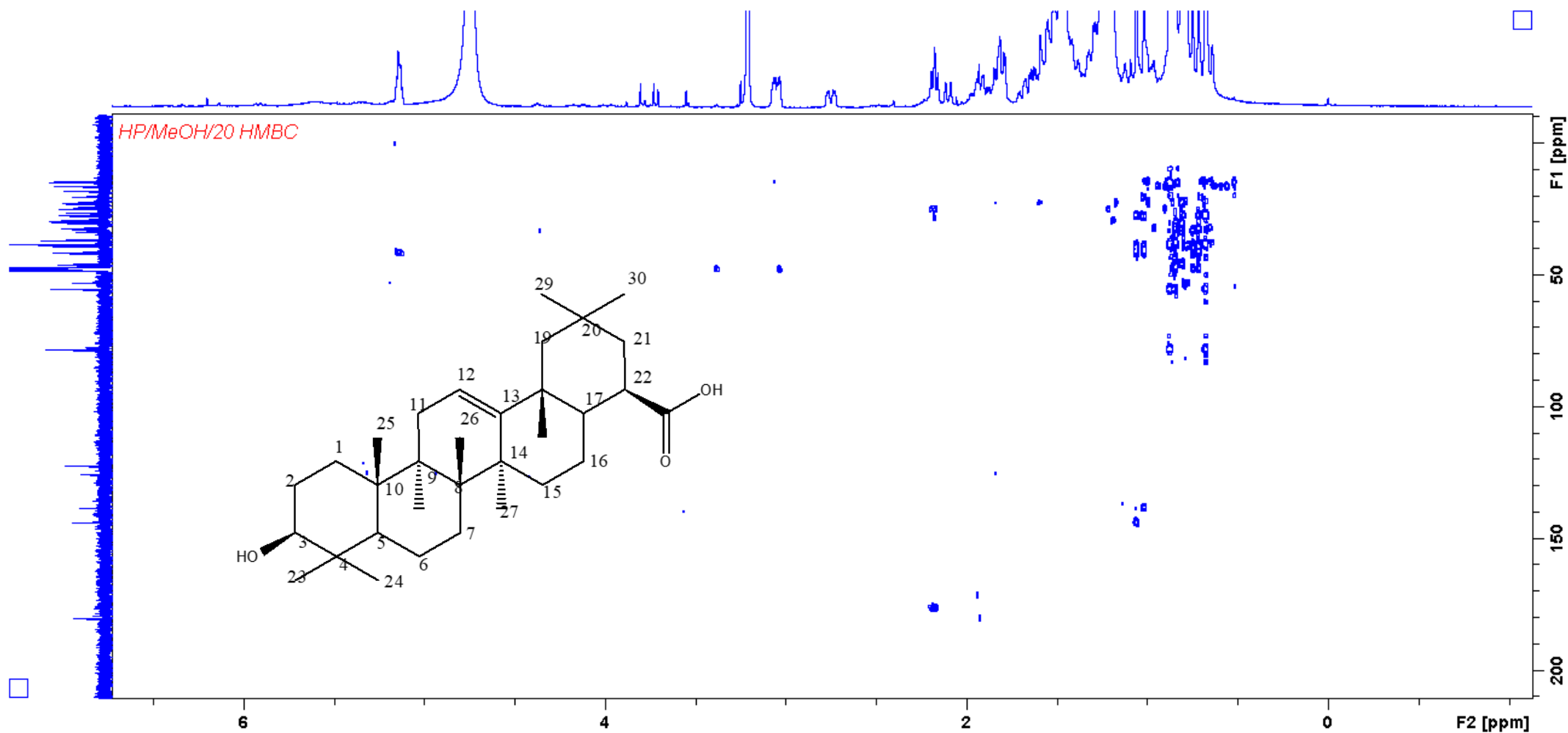
COSY of **B3** oleanolic acid



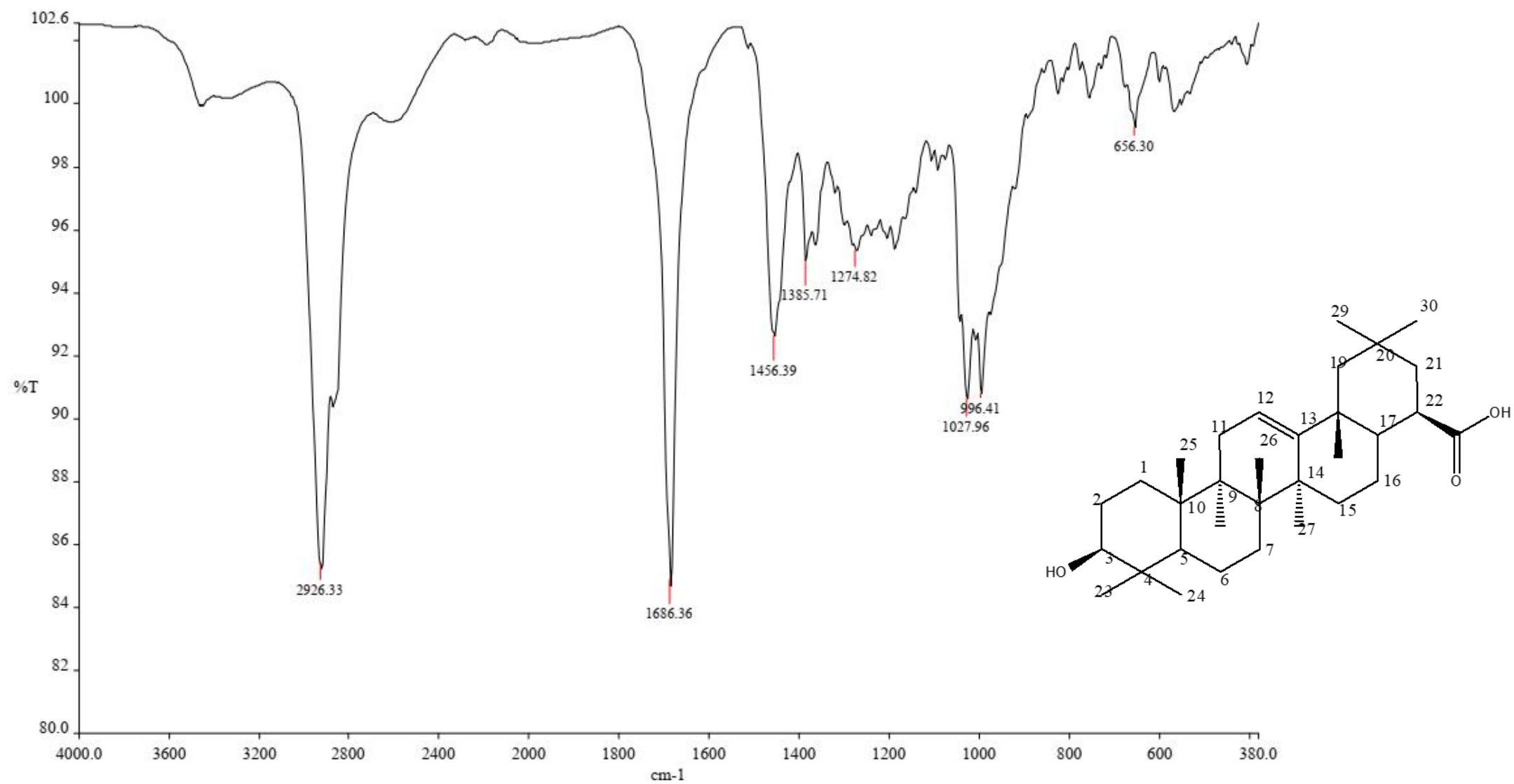
NOESY of **B3** oleanolic acid



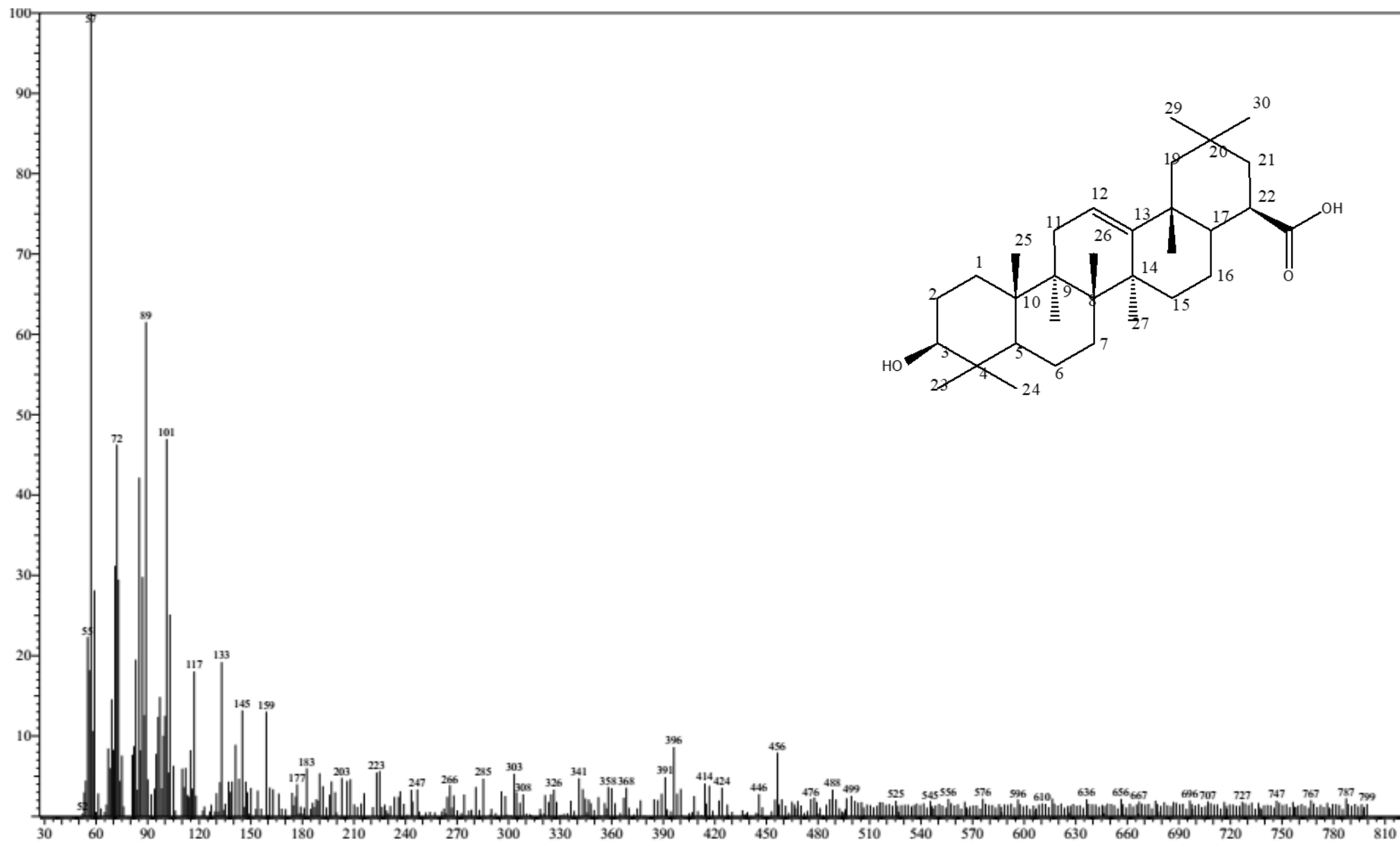
HSQC of **B3** oleanolic acid



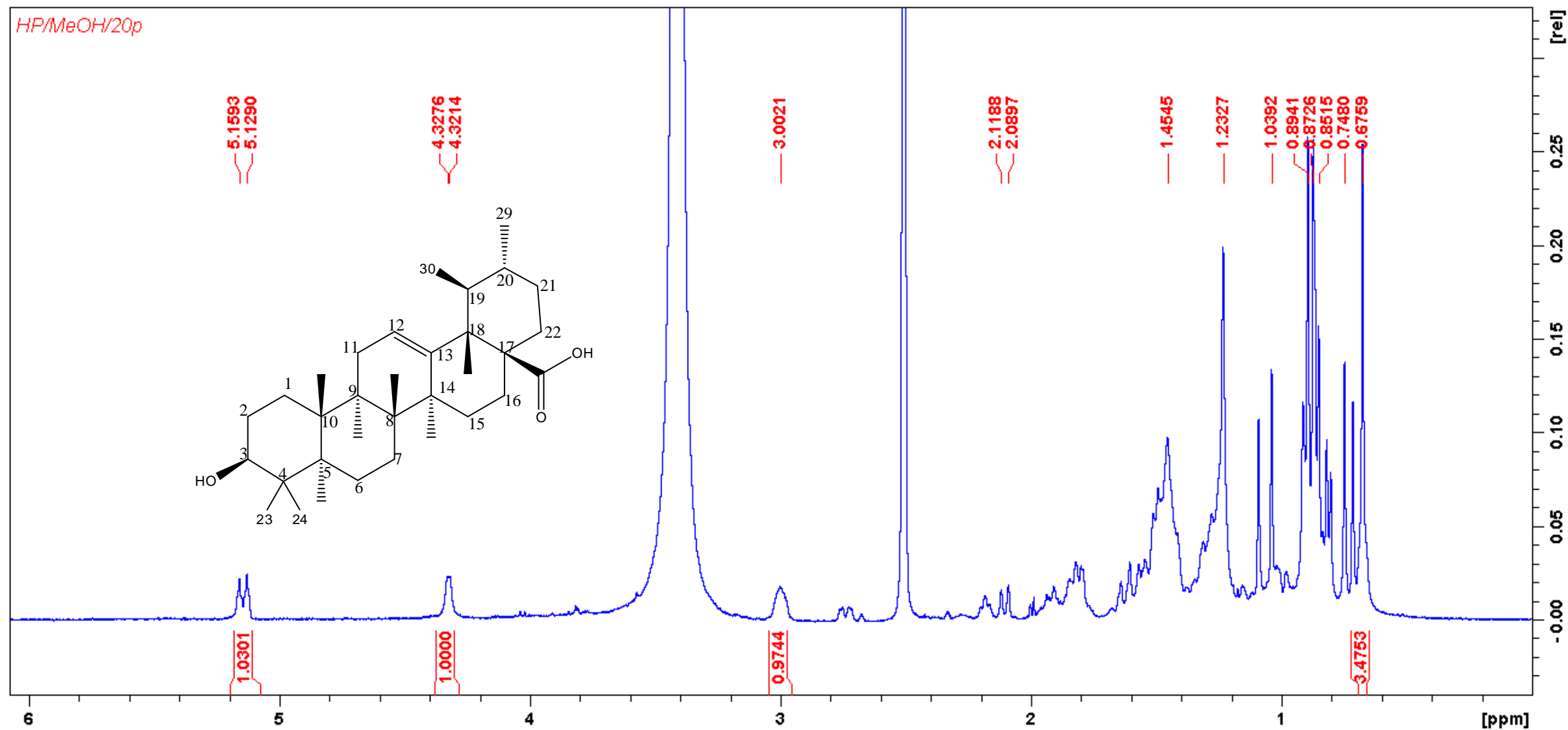
HMBC of **B3** oleanolic acid



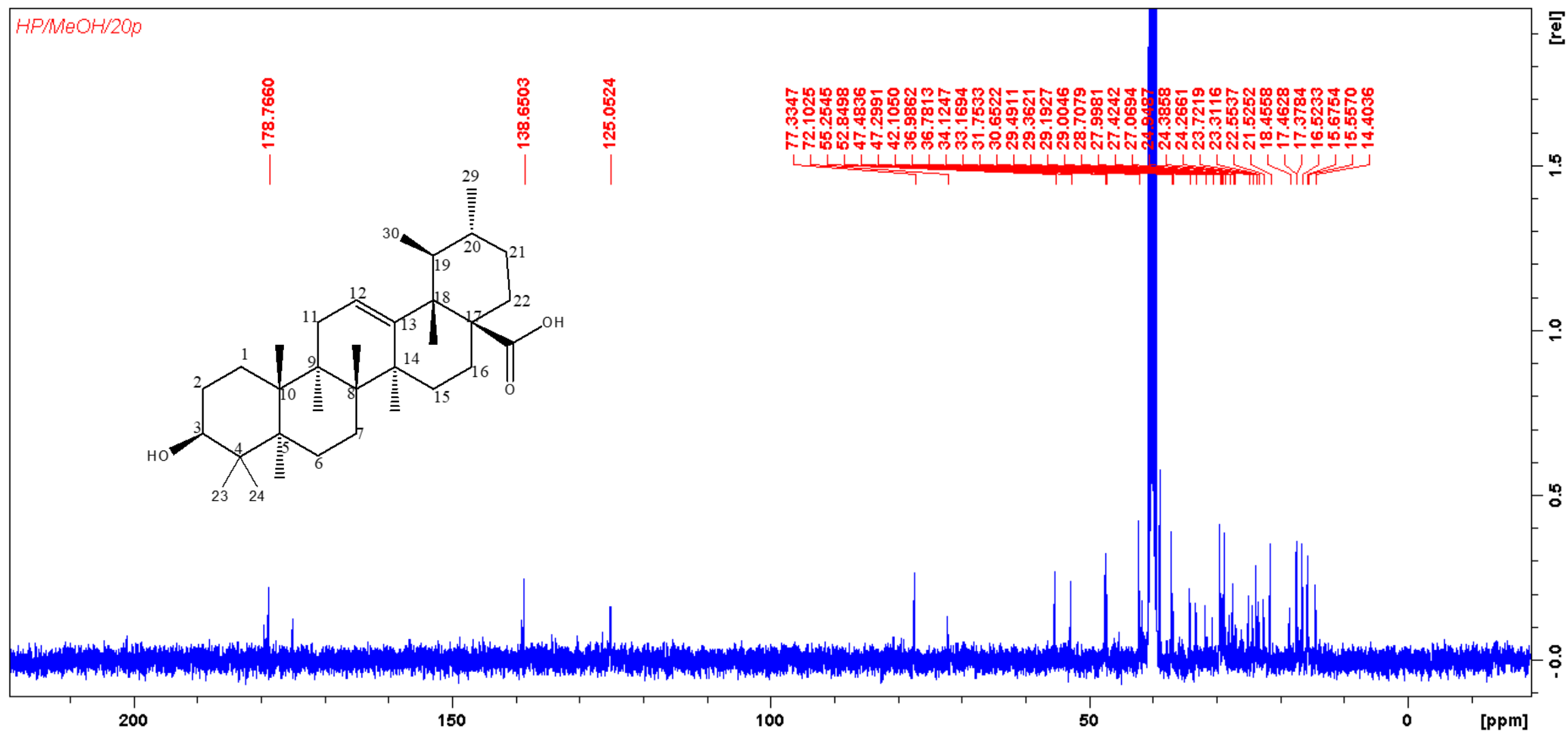
IR spectrum of **B3** oleanolic acid



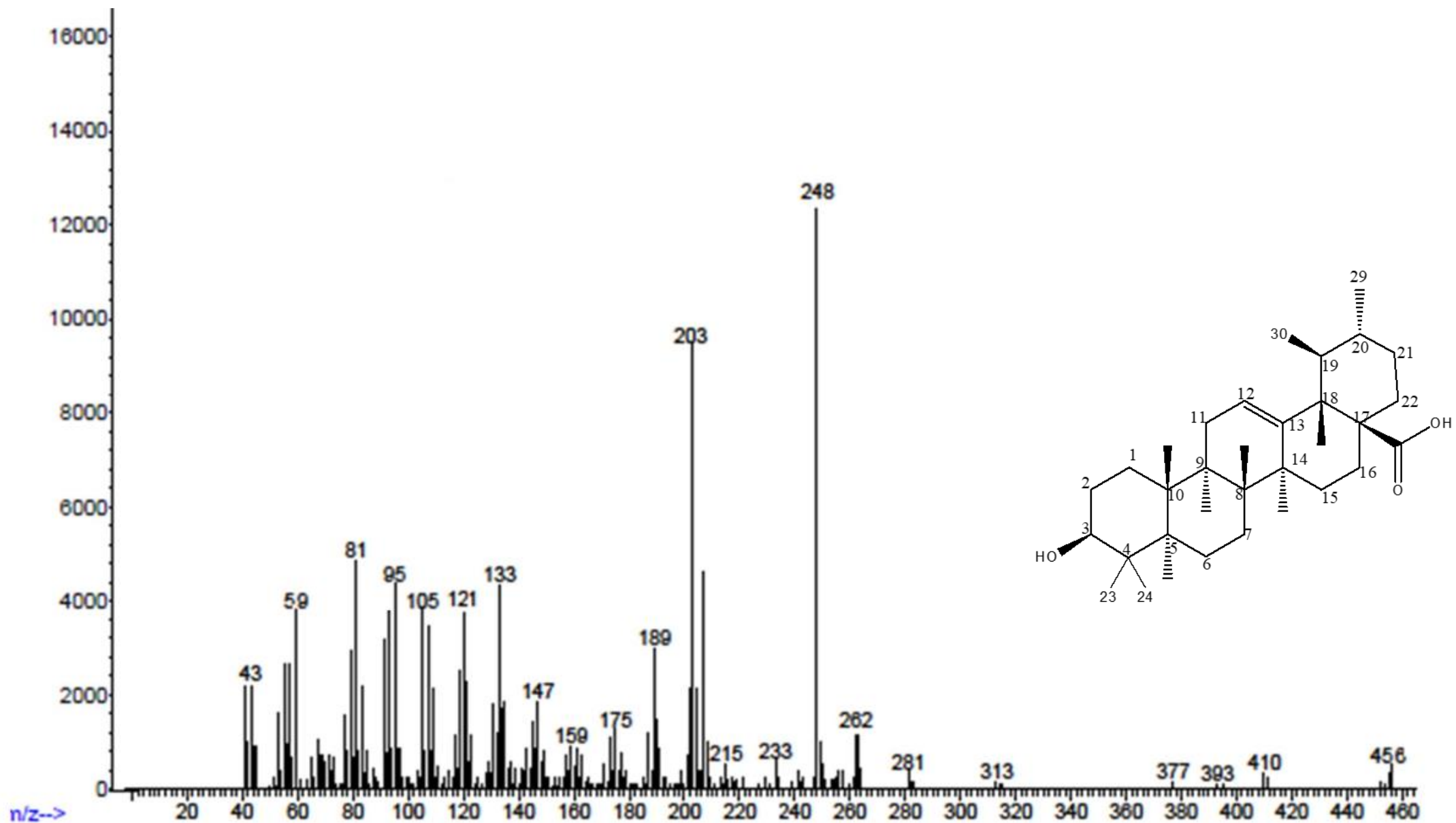
Mass spectrum of **B3** oleanolic



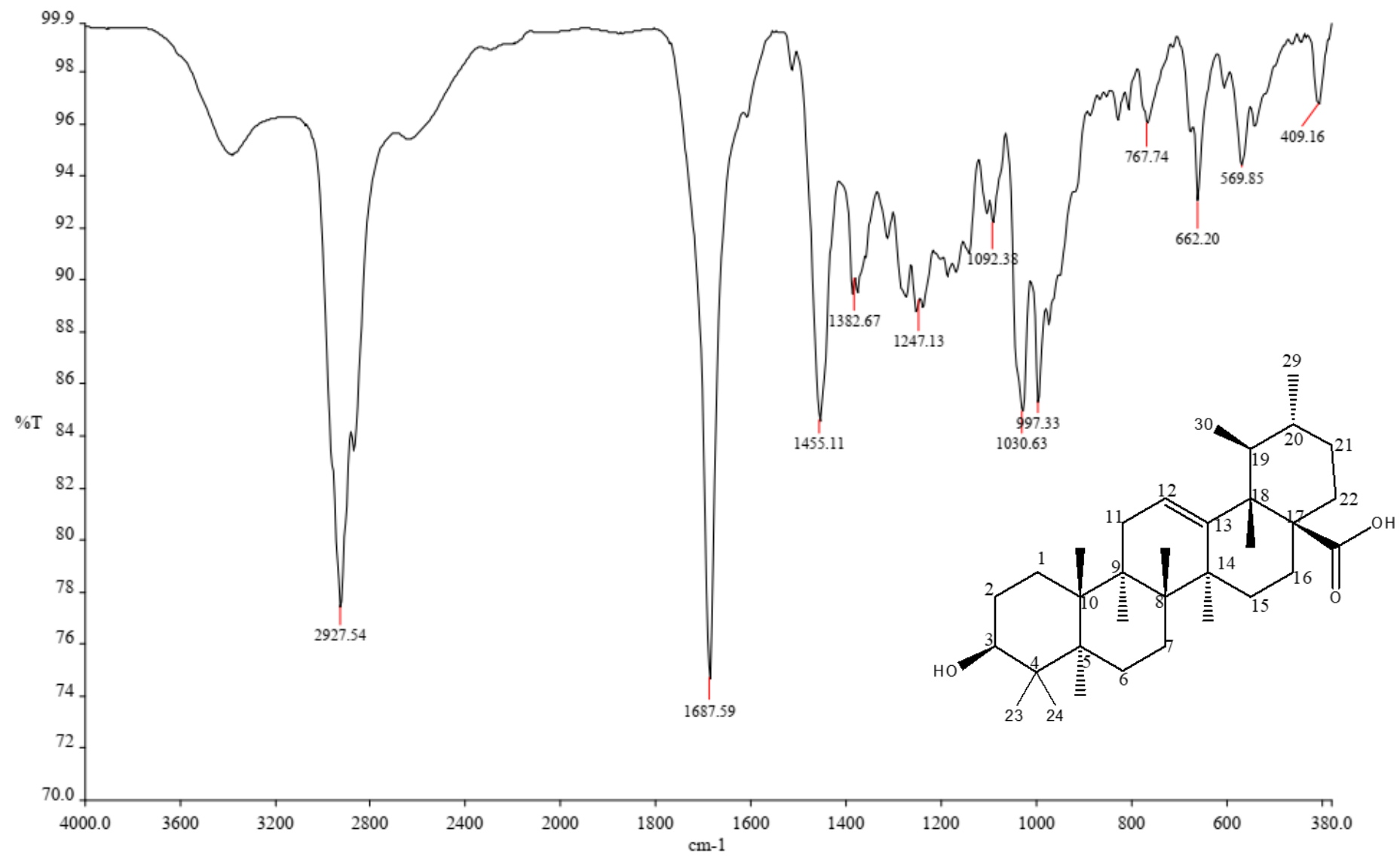
^1H NMR of **B4** Ursolic acid



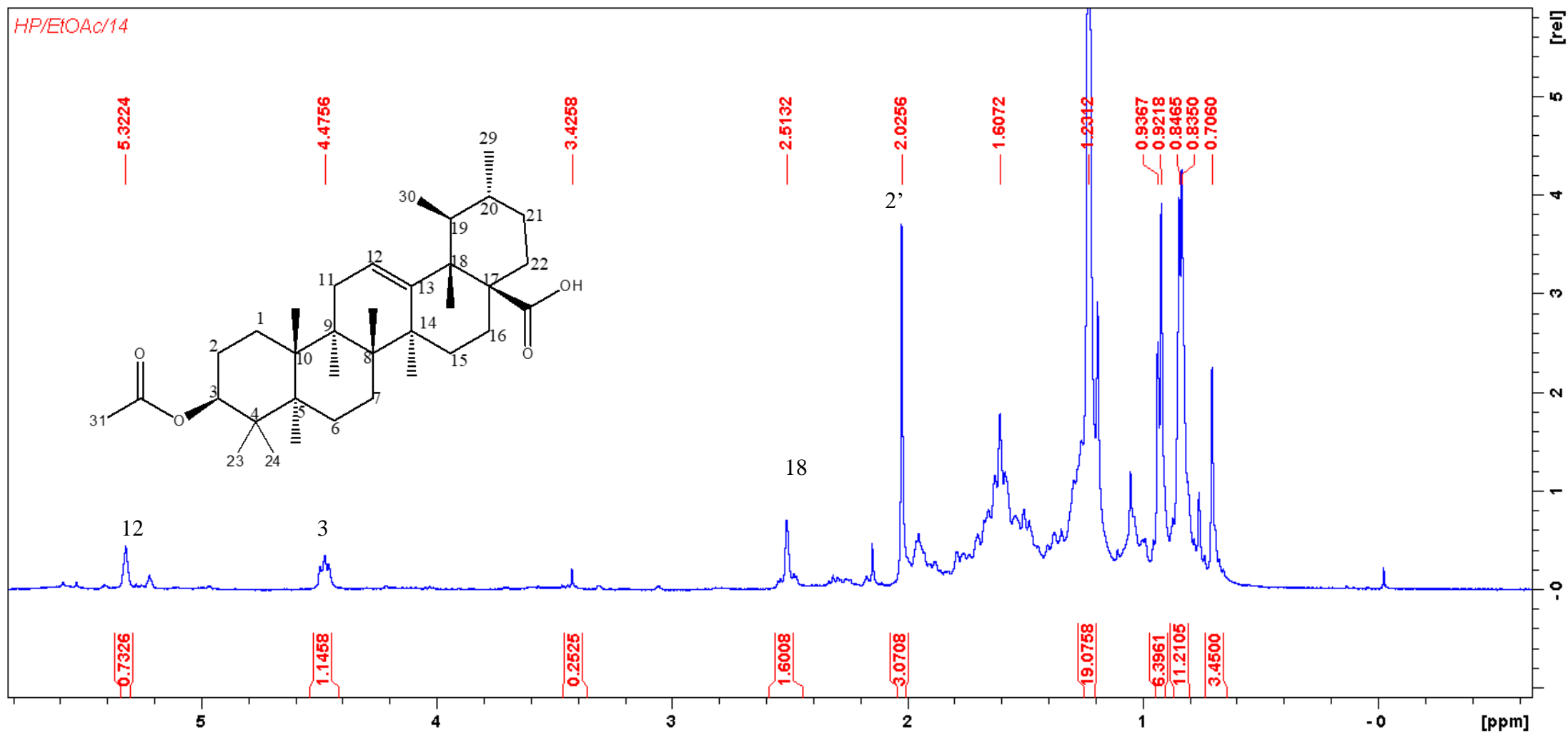
^{13}C NMR of **B4** Ursolic acid



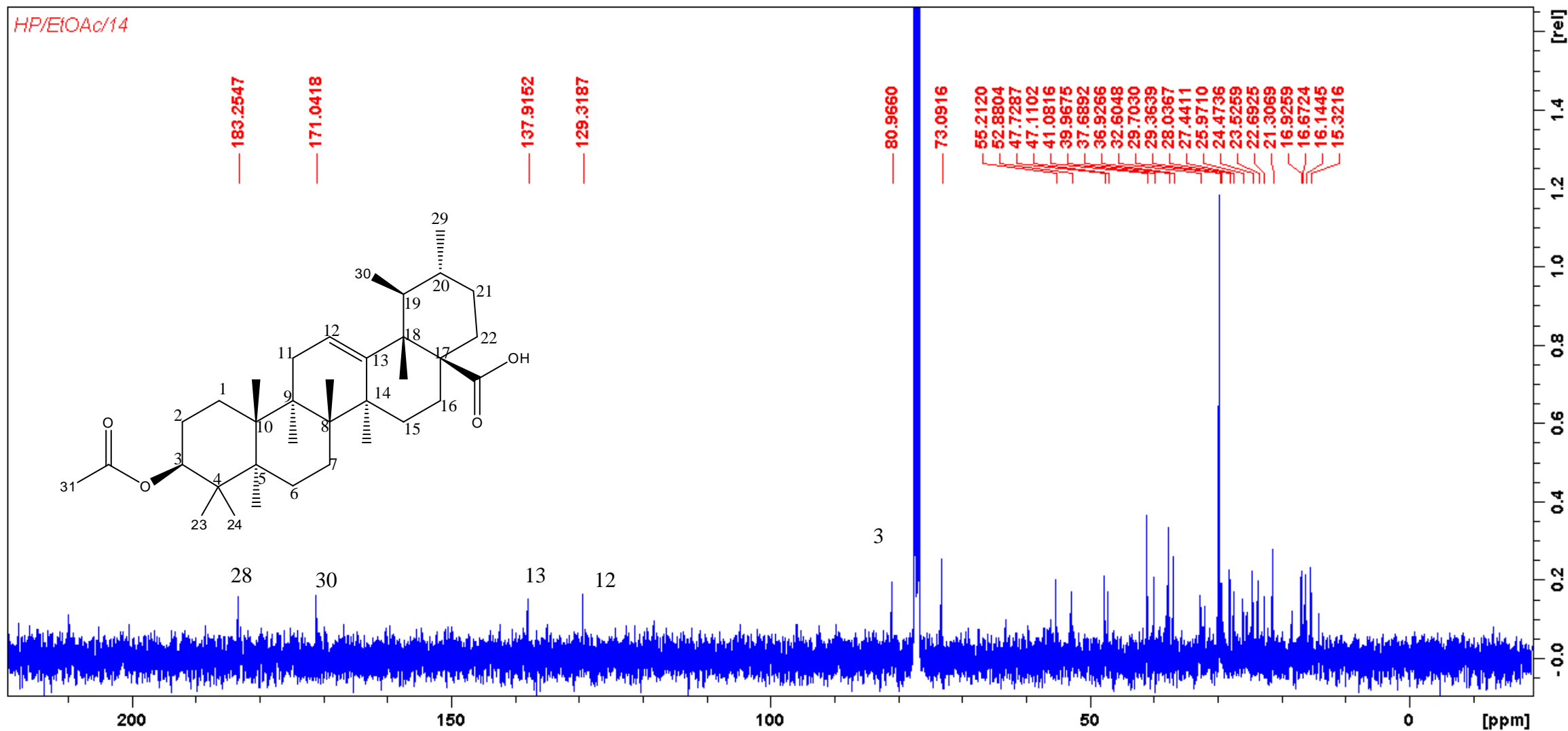
Mass spectra of **B4** Ursolic acid



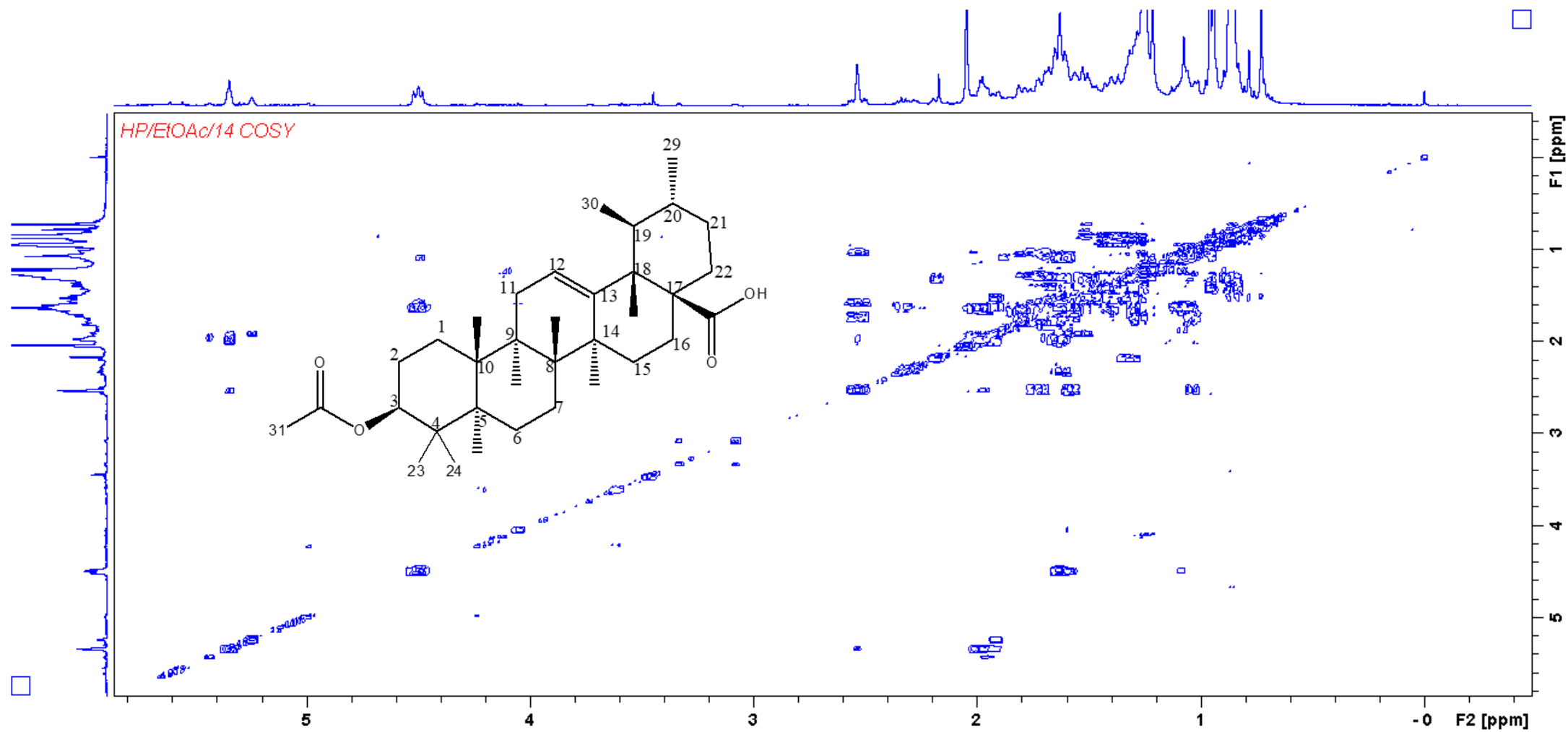
IR spectrum **B4** Ursolic acid



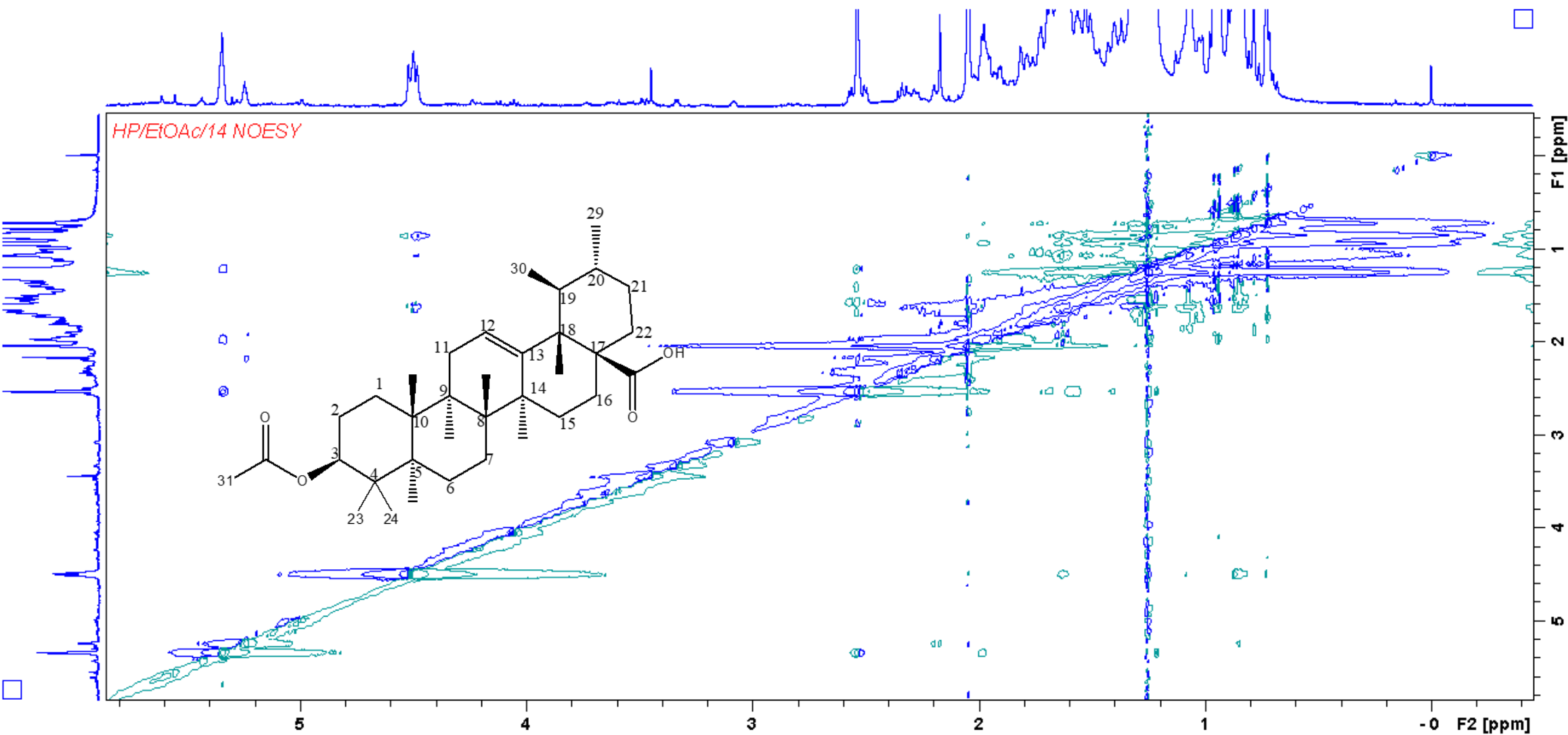
¹H NMR of **B5** 3-acetyl ursolic acid



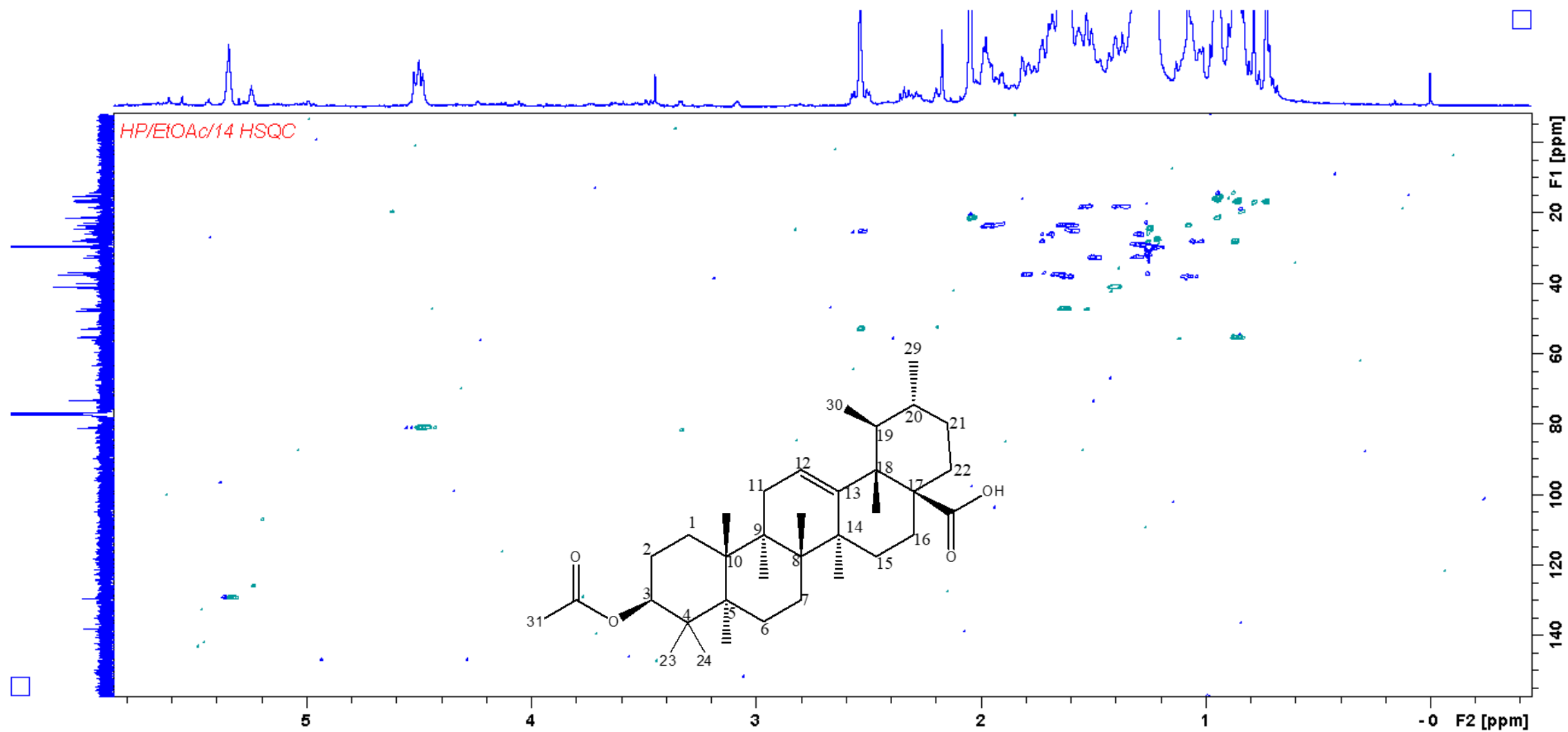
¹³C NMR of **B5** 3-acetyl ursolic acid



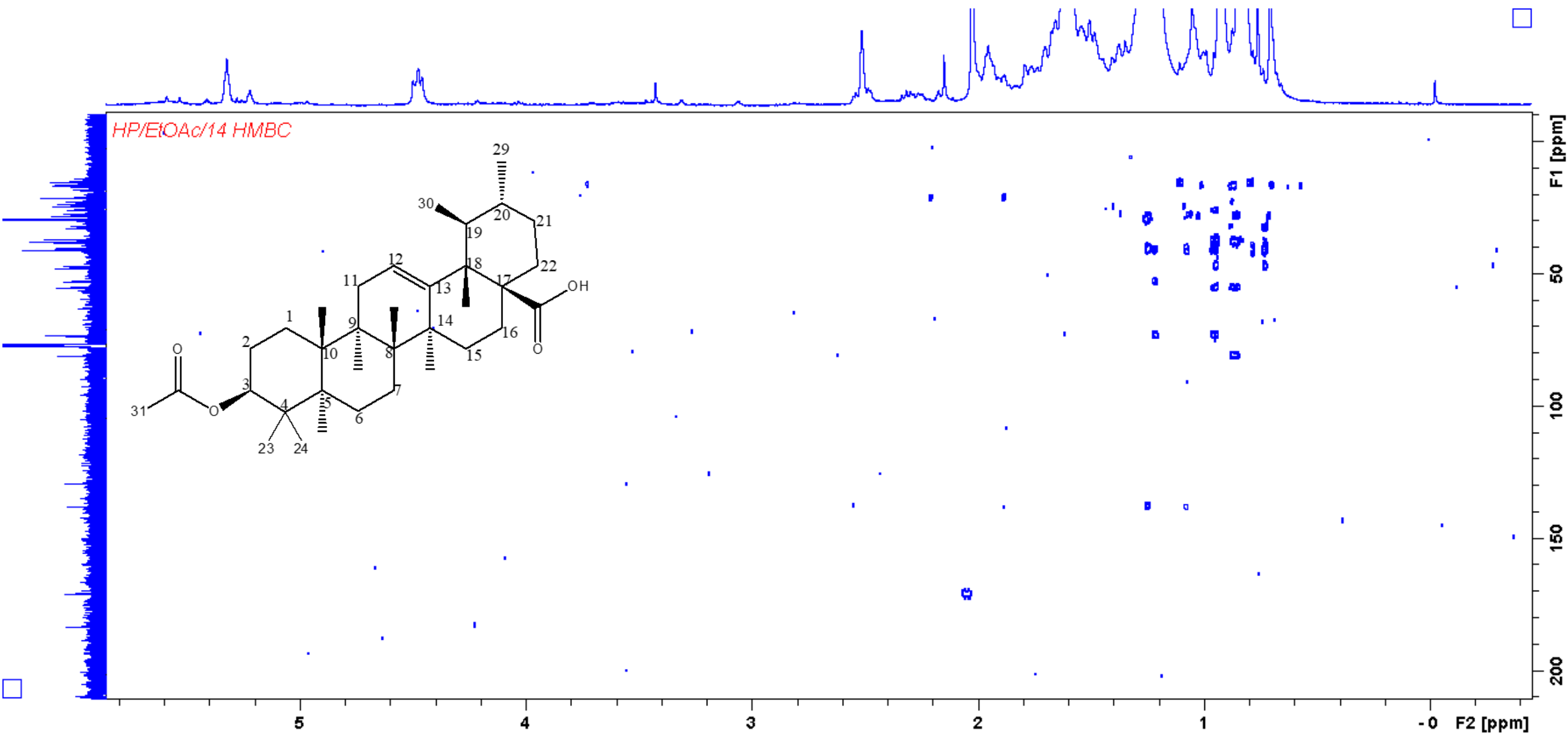
COSY spectrum of **B5** 3-acetyl ursolic acid



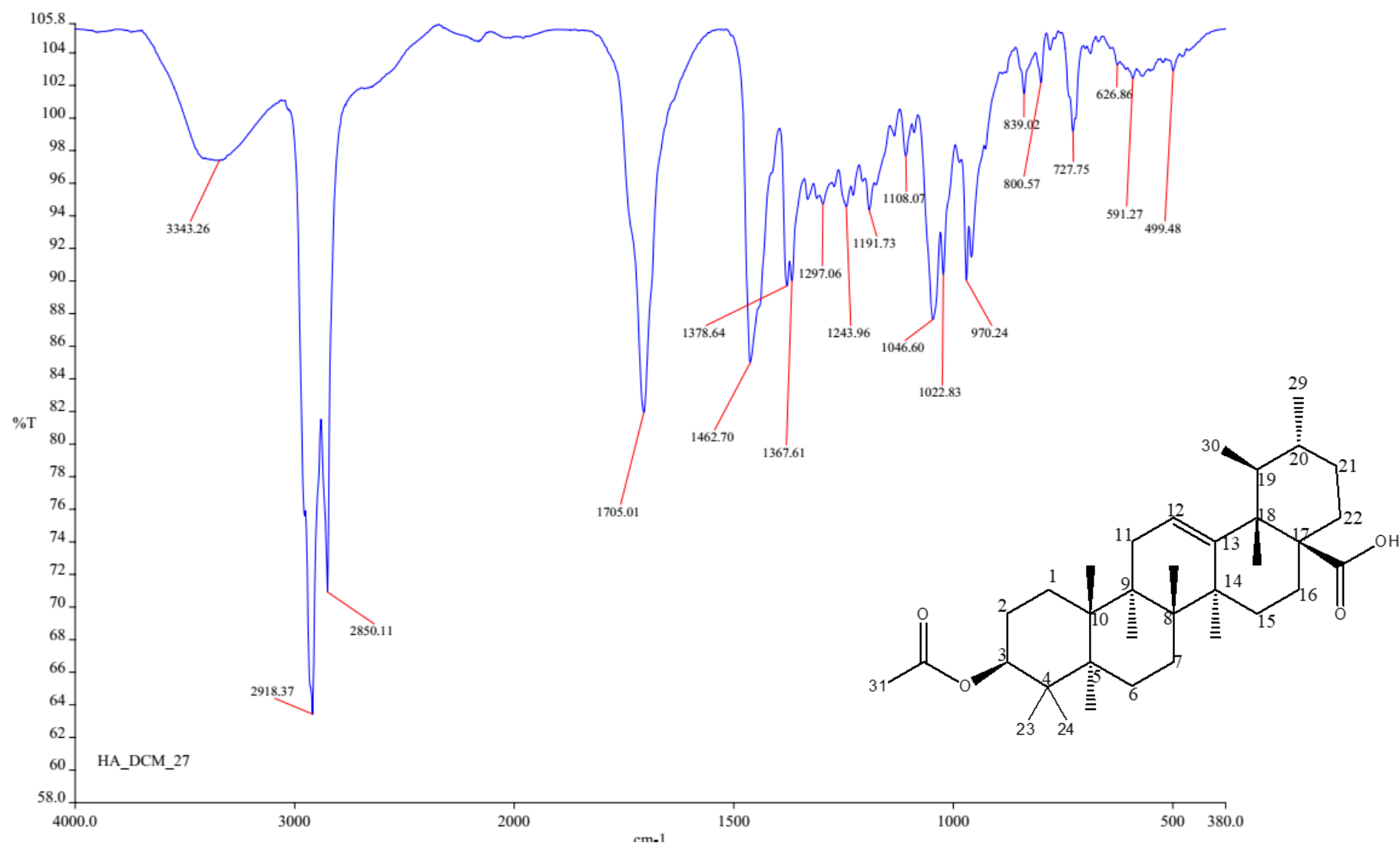
NOESY spectrum of **B5** 3-acetyl ursolic acid



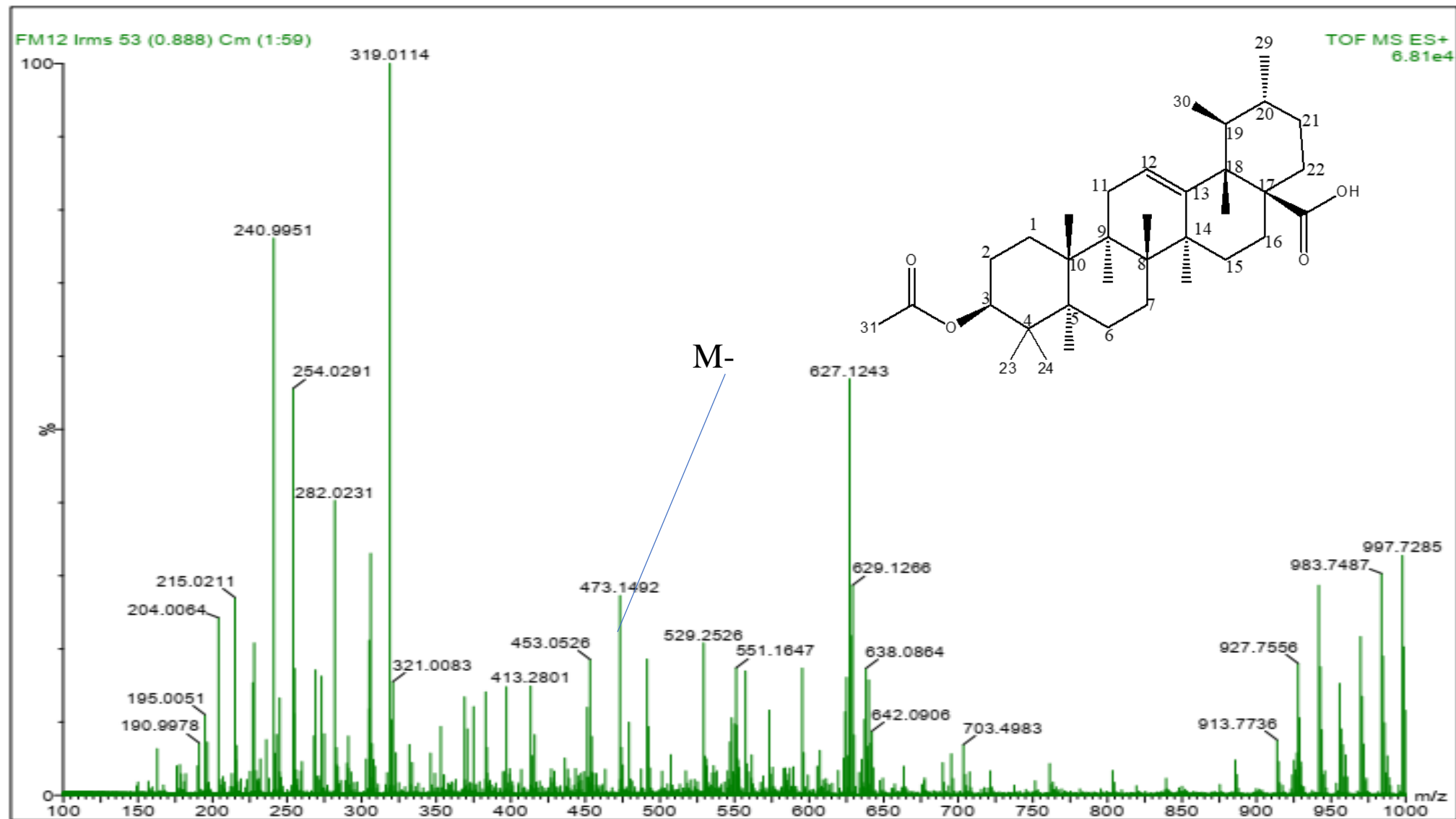
HSQC spectrum of **B5** 3-acetyl ursolic acid



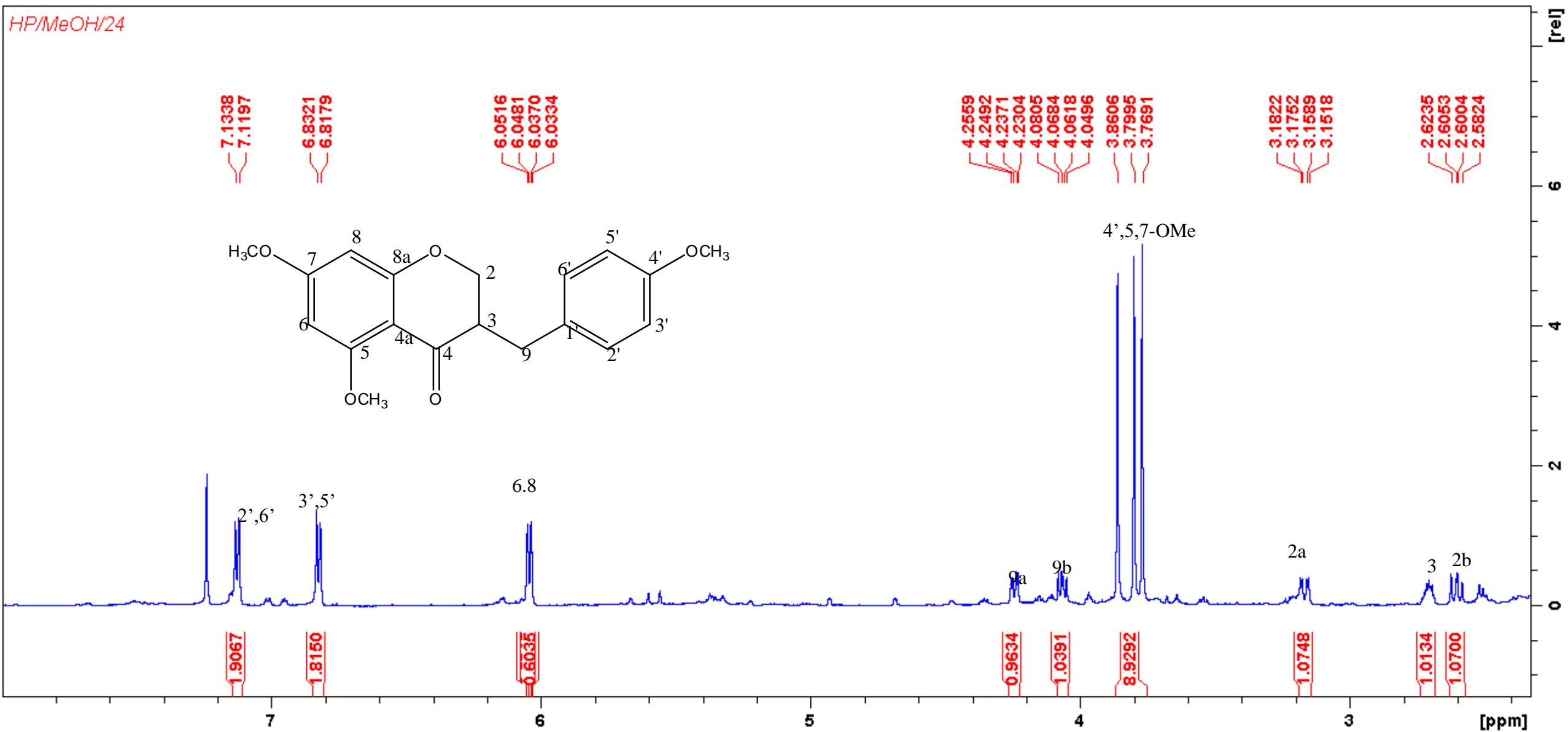
HMBC spectrum of **B5** 3-acetyl ursolic acid



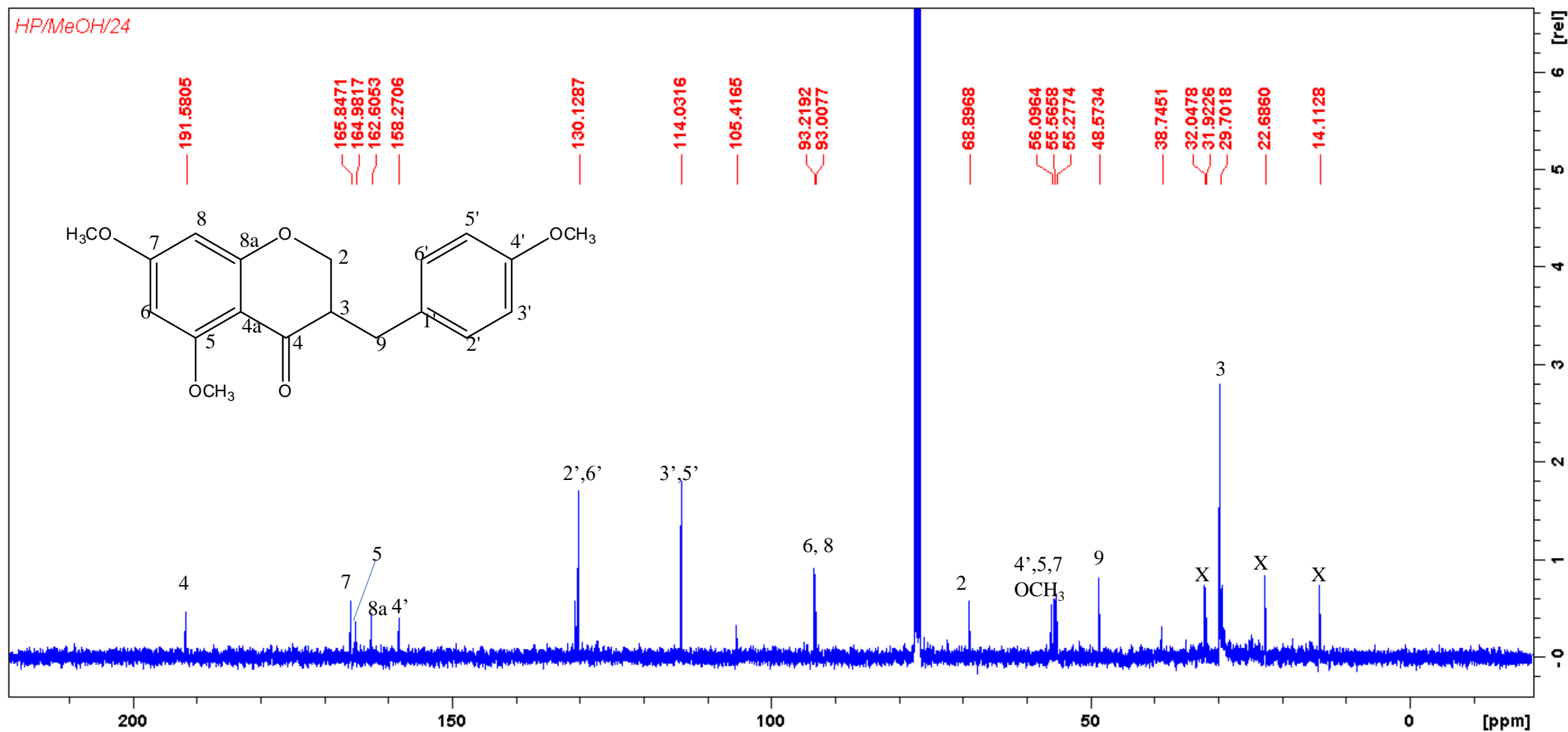
IR spectrum of **B5** 3-acetyl ursolic acid



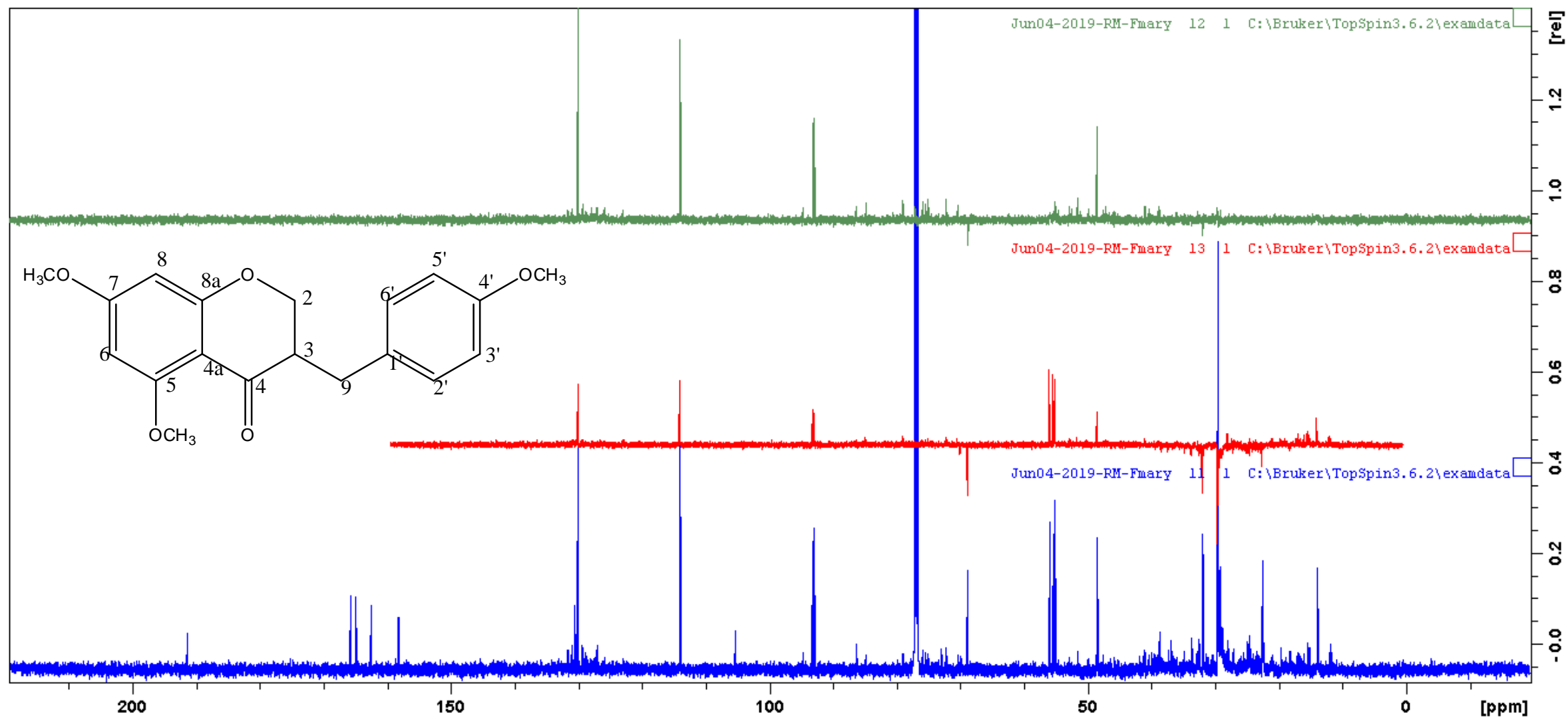
Mass spectrum of **B5** 3-acetyl ursolic acid



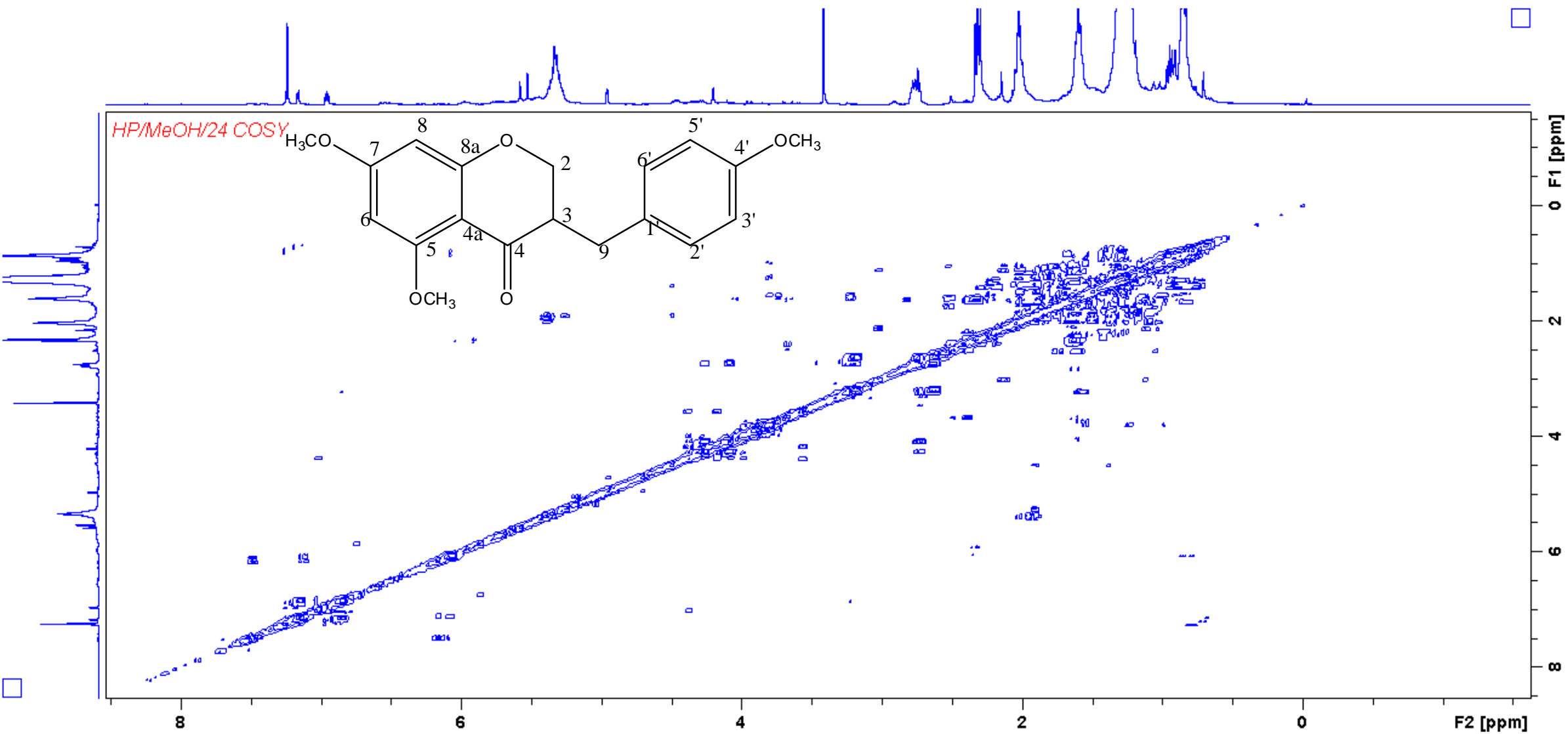
¹H NMR of **B6** 3-(4-methoxybenzyl)-5,7-dimethoxychroman-4-one



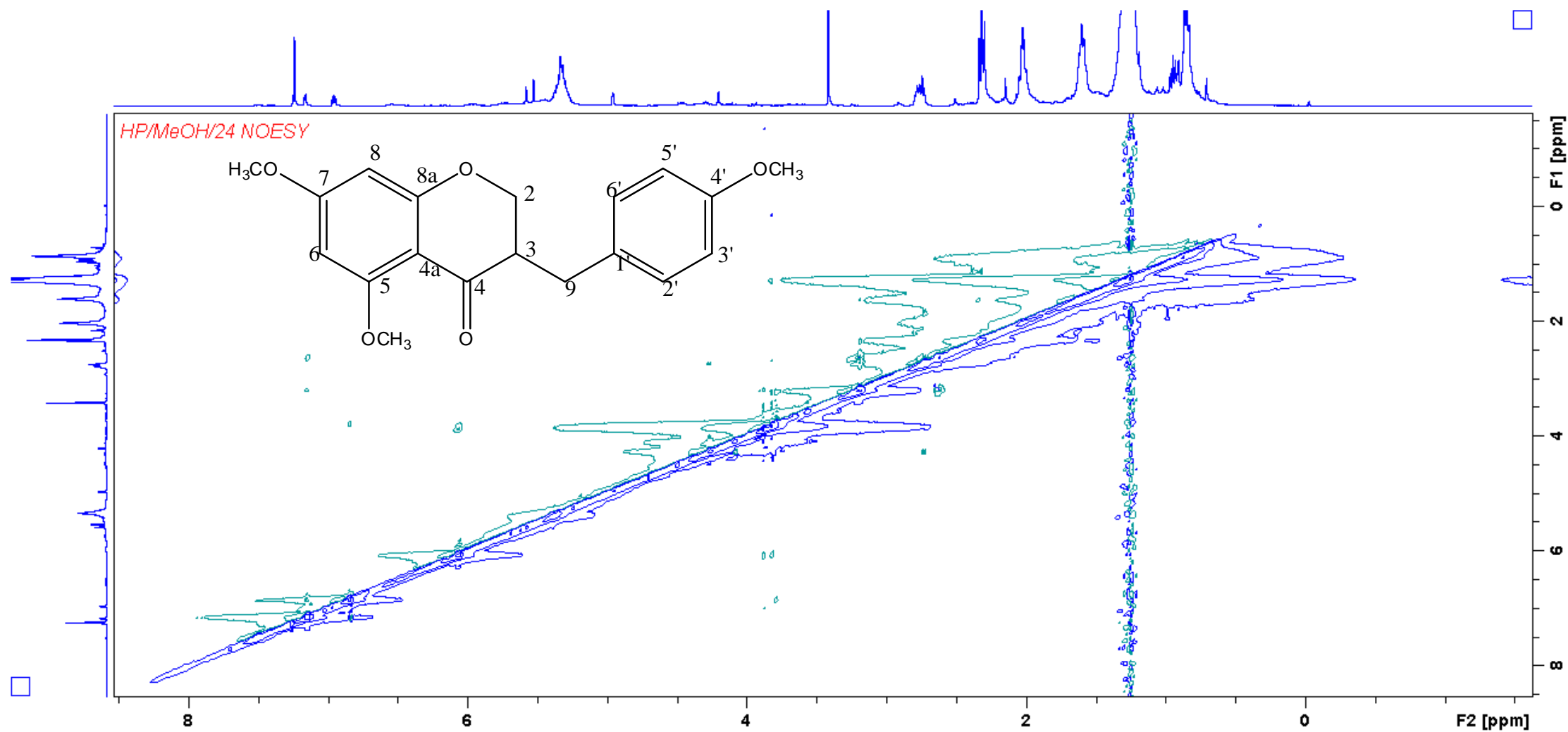
¹³C NMR of **B6** 3-(4-methoxybenzyl)-5,7-dimethoxychroman-4-one



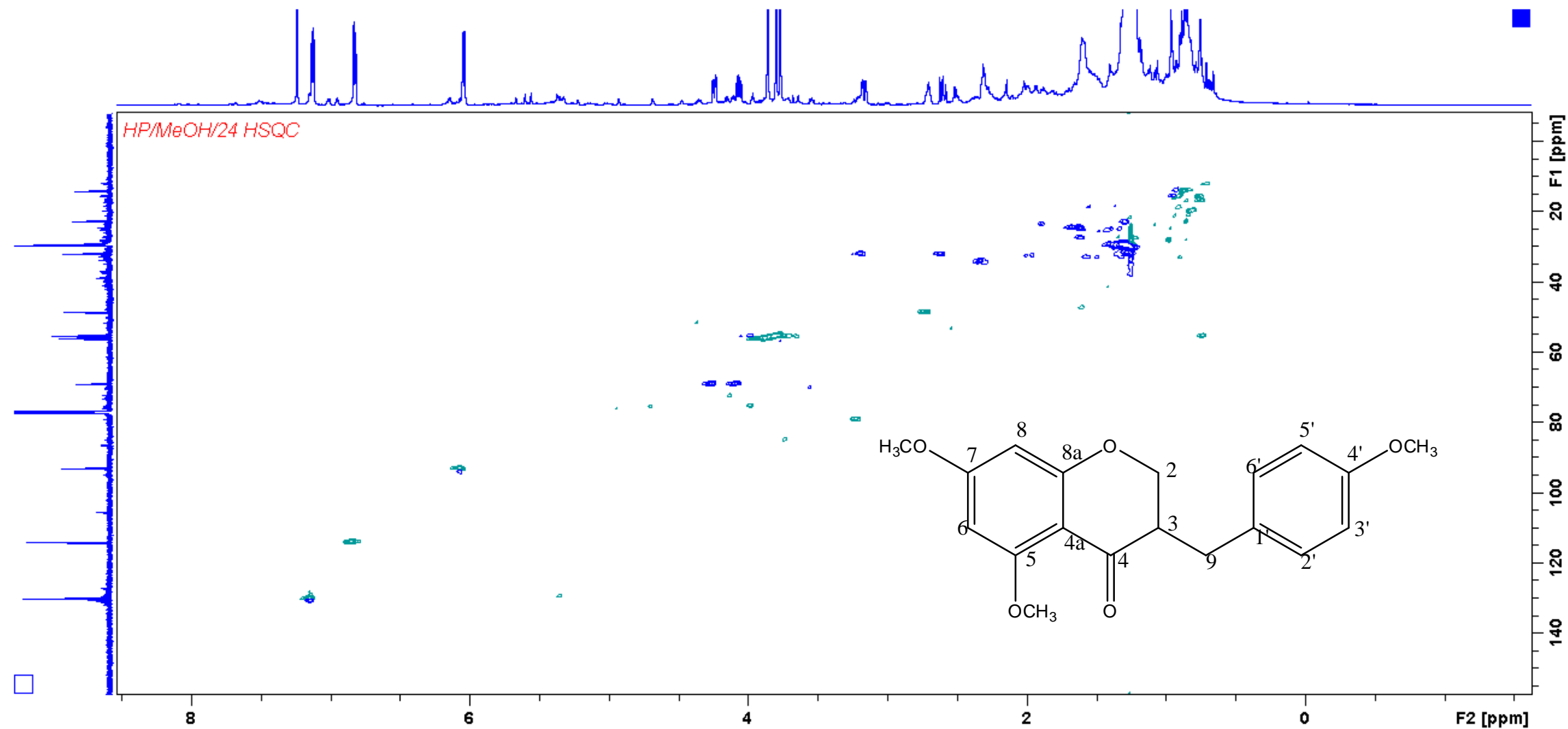
DEPT of **B6** 3-(4-methoxybenzyl)-5,7-dimethoxychroman-4-one



COSY of **B6** 3-(4-methoxybenzyl)-5,7-dimethoxychroman-4-one



NOESY of **B6** 3-(4-methoxybenzyl)-5,7-dimethoxychroman-4-one



HSQC of **B6** 3-(4-methoxybenzyl)-5,7-dimethoxychroman-4-one

Monoisotopic Mass, Even Electron Ions

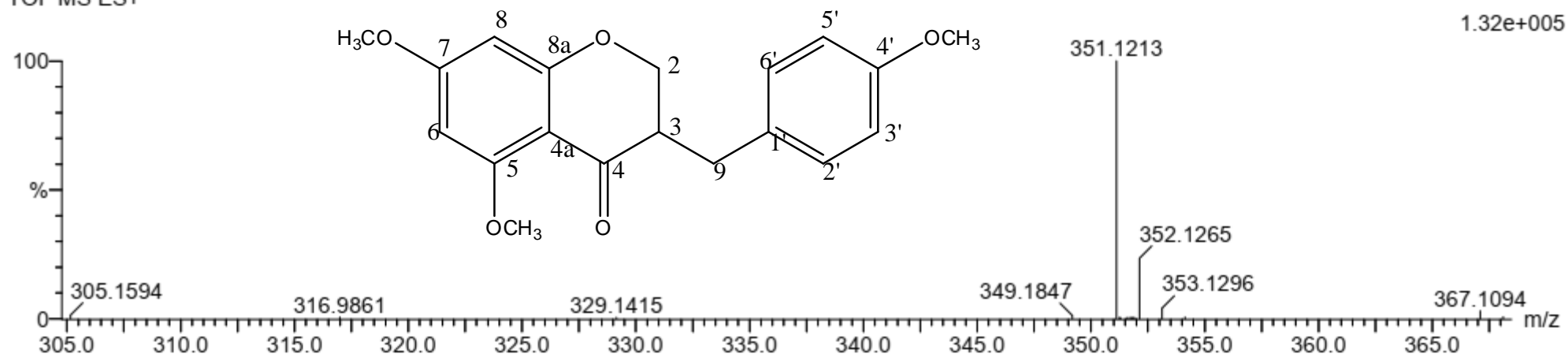
4 formula(e) evaluated with 1 results within limits (all results (up to 1000) for each mass)

Elements Used:

C: 15-20 H: 20-25 O: 0-5 Na: 1-1

SN_DCM_17-18L 2 (0.034) Cm (1:61)

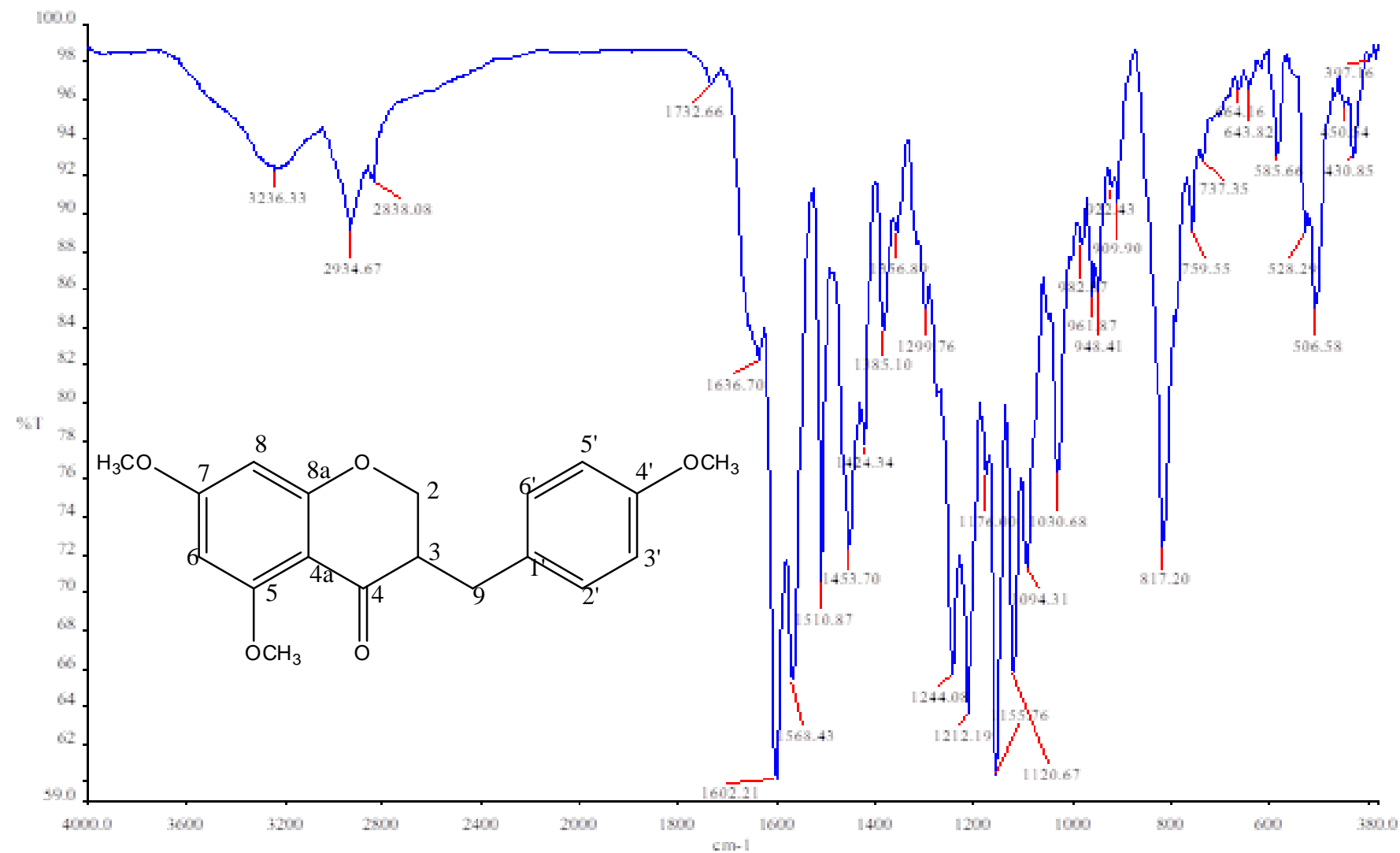
TOF MS ES+



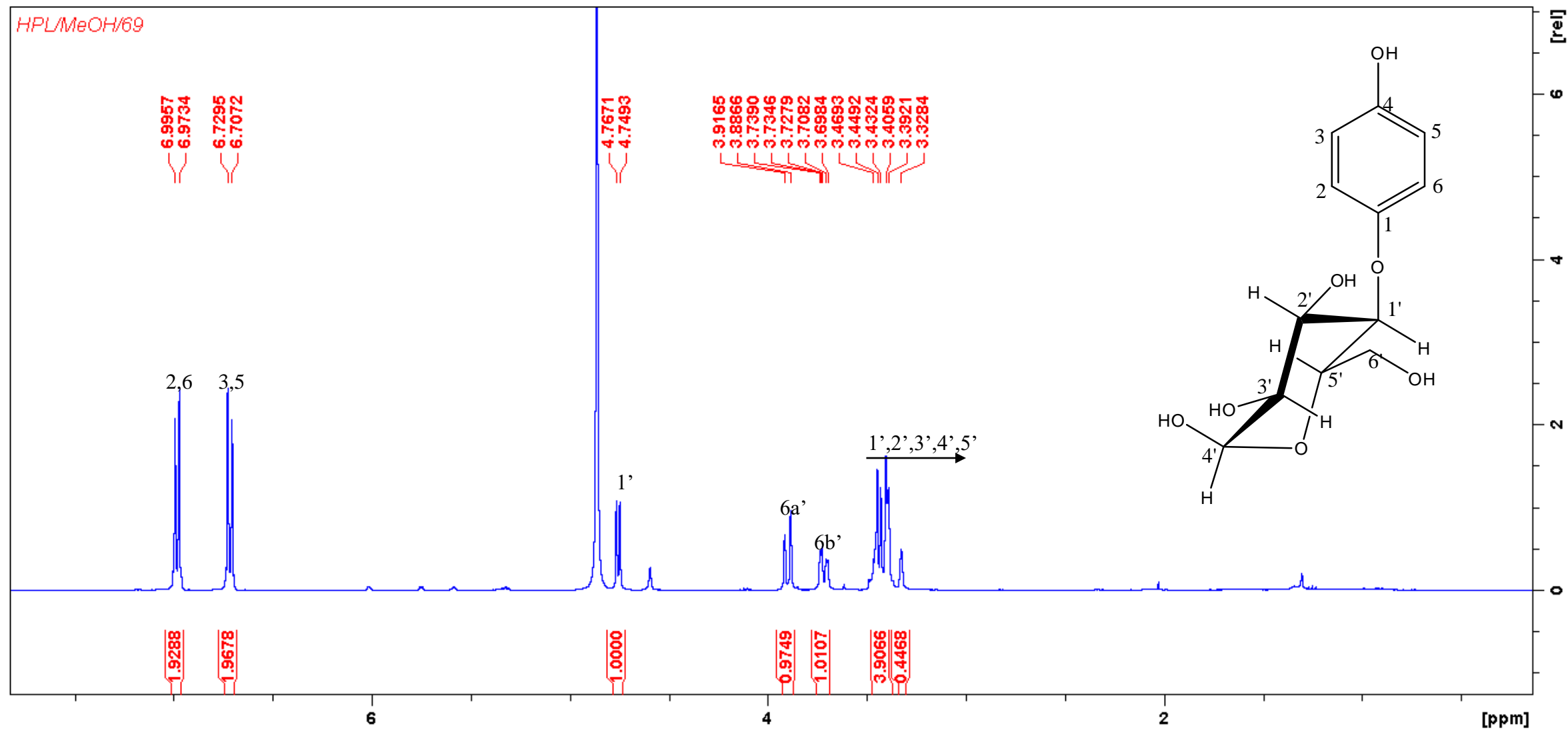
Minimum: -1.5
Maximum: 5.0 5.0 50.0

Mass	Calc. Mass	mDa	PPM	DBE	i-FIT	i-FIT (Norm)	Formula
351.1213	351.1208	0.5	1.4	9.5	119.1	0.0	C19 H20 O5 Na

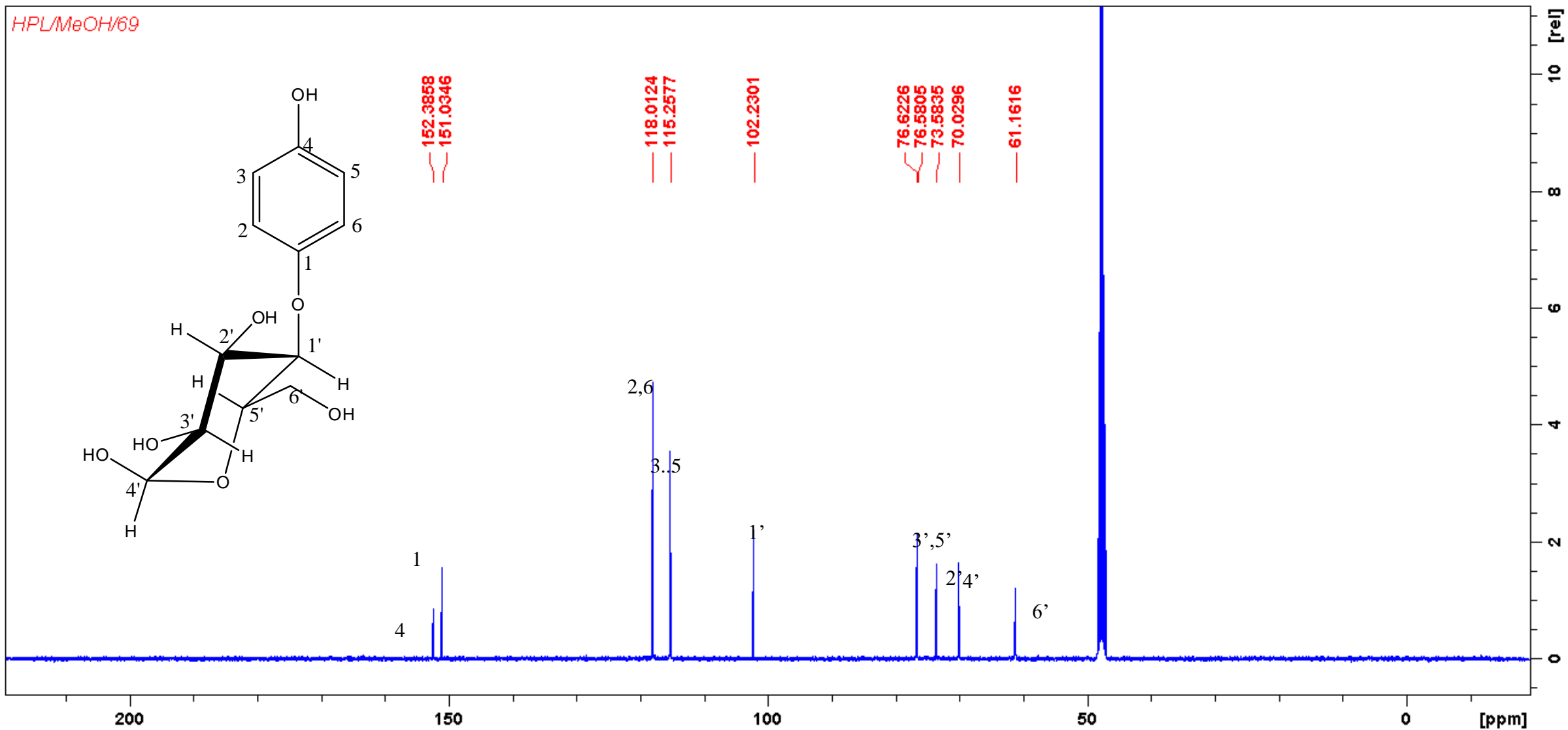
HRMS of **B6** 3-(4-methoxybenzyl)-5,7-dimethoxychroman-4-one



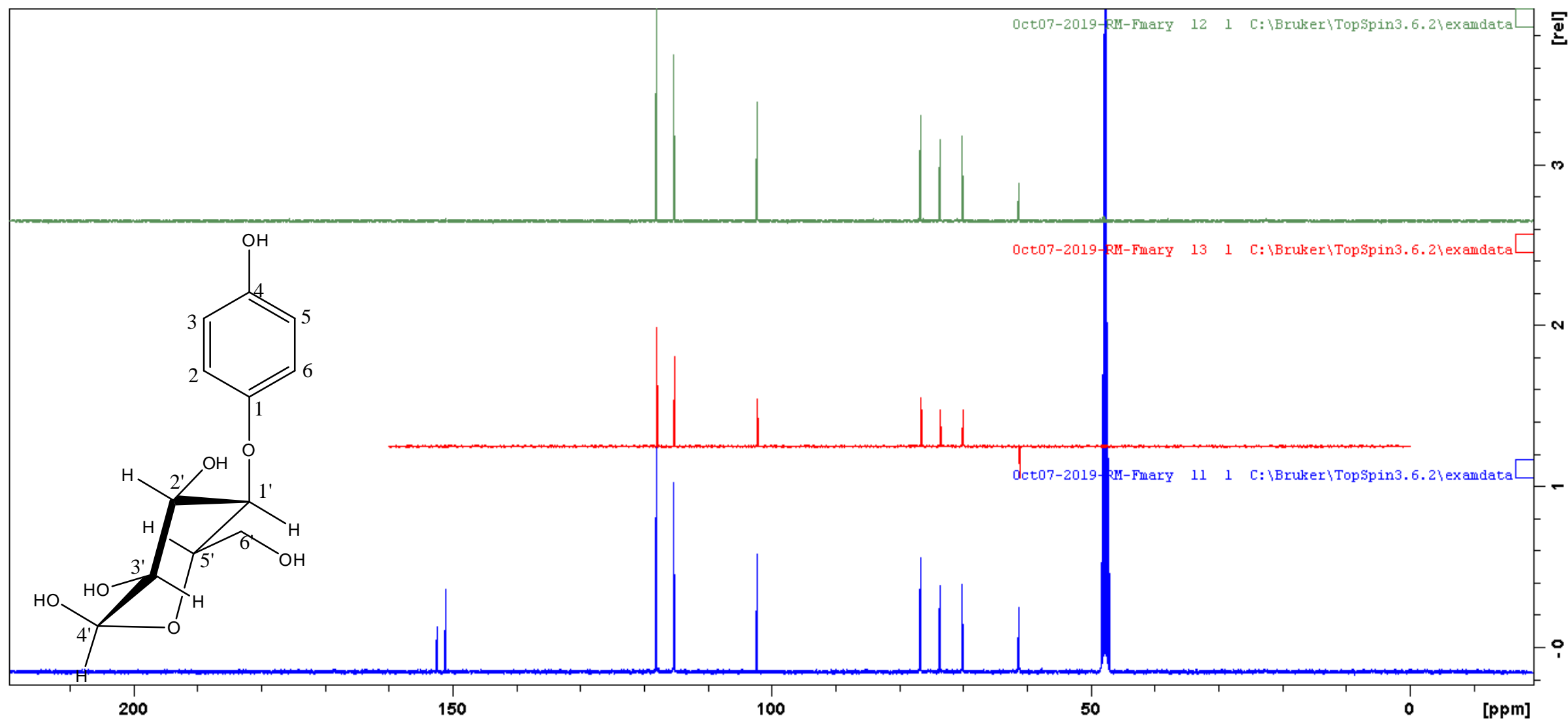
IR of compound **B6** 3-(4-methoxybenzyl)-5,7-dimethoxychroman-4-one (**B6**)



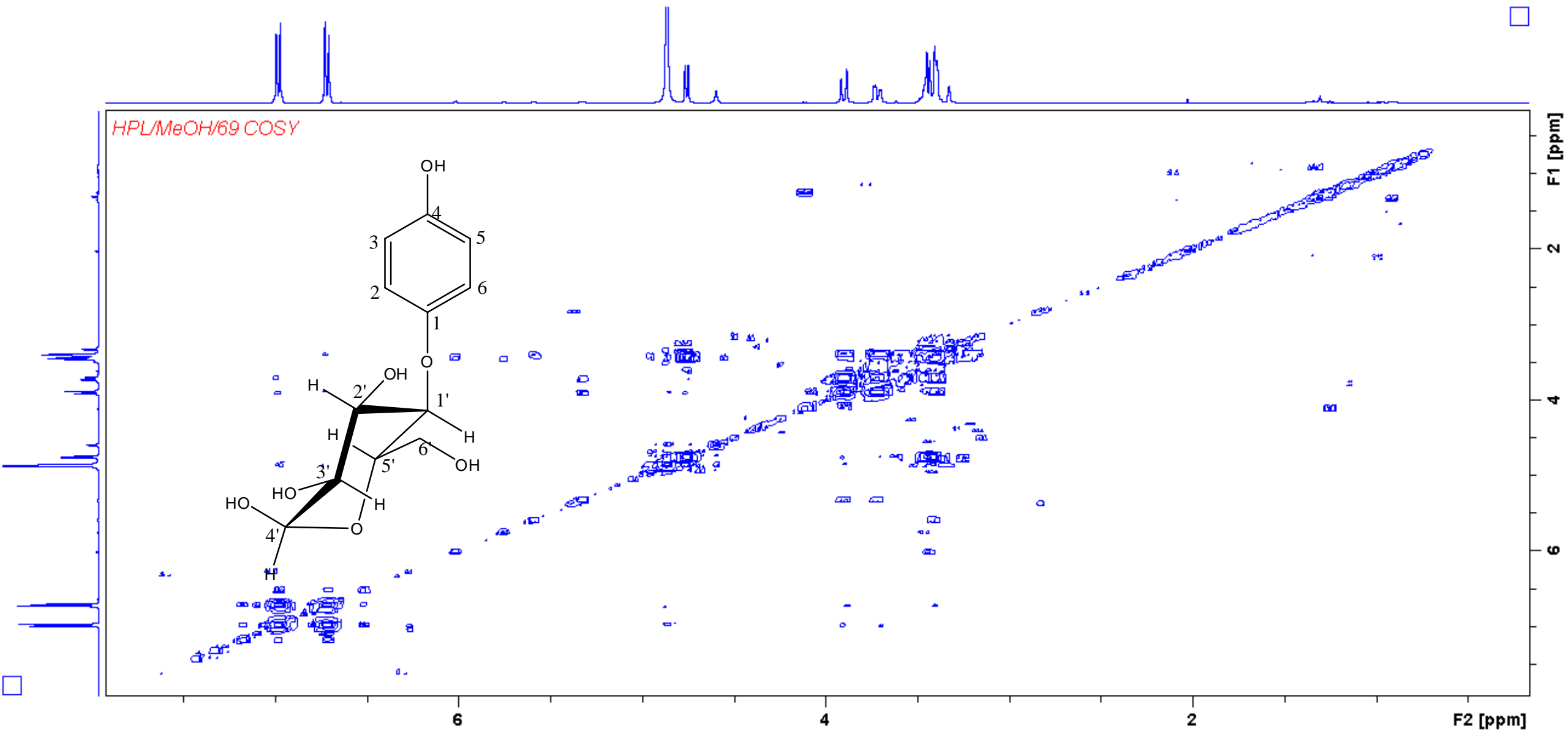
^1H NMR compound **B7** of arbutin



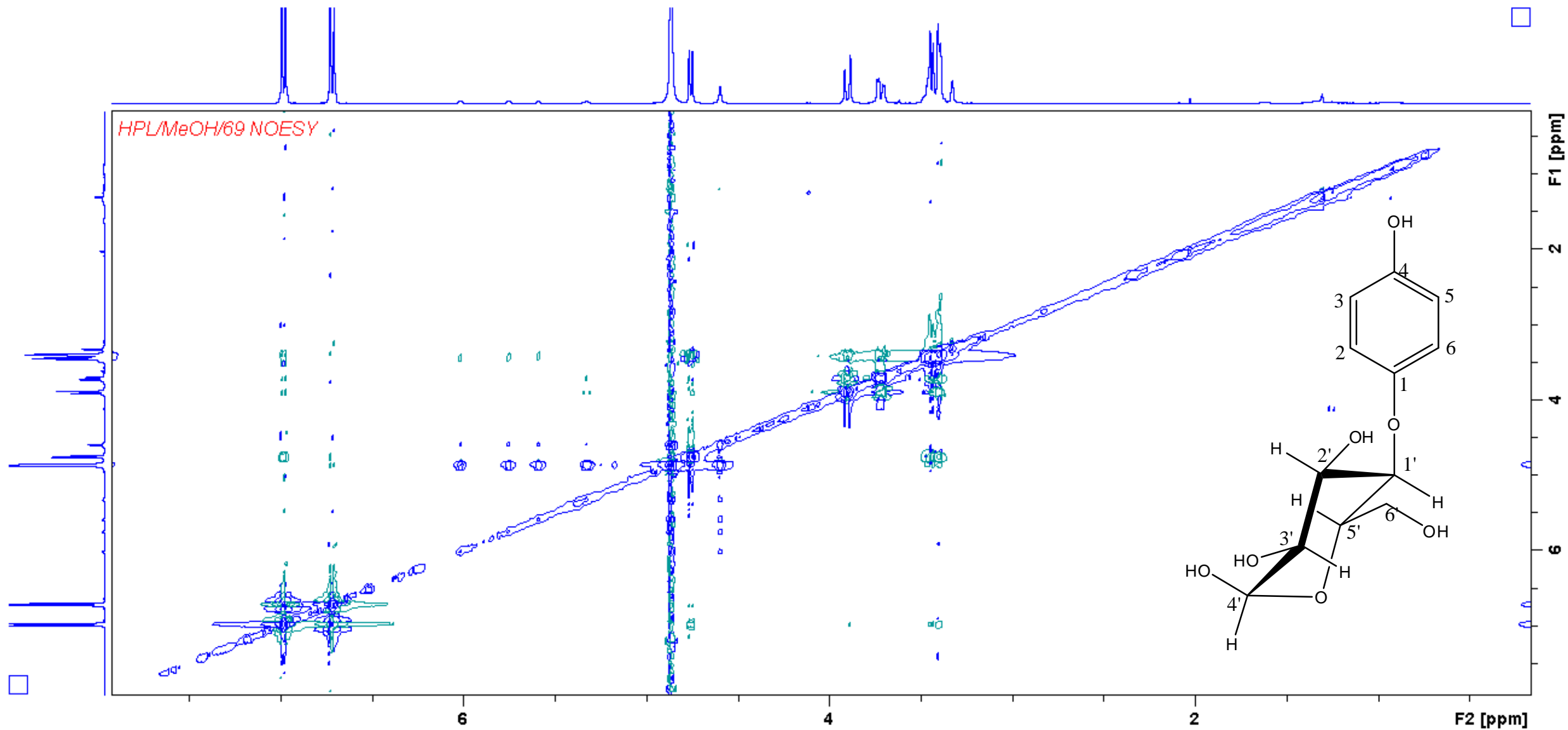
^{13}C NMR of compound **B7** arbutin



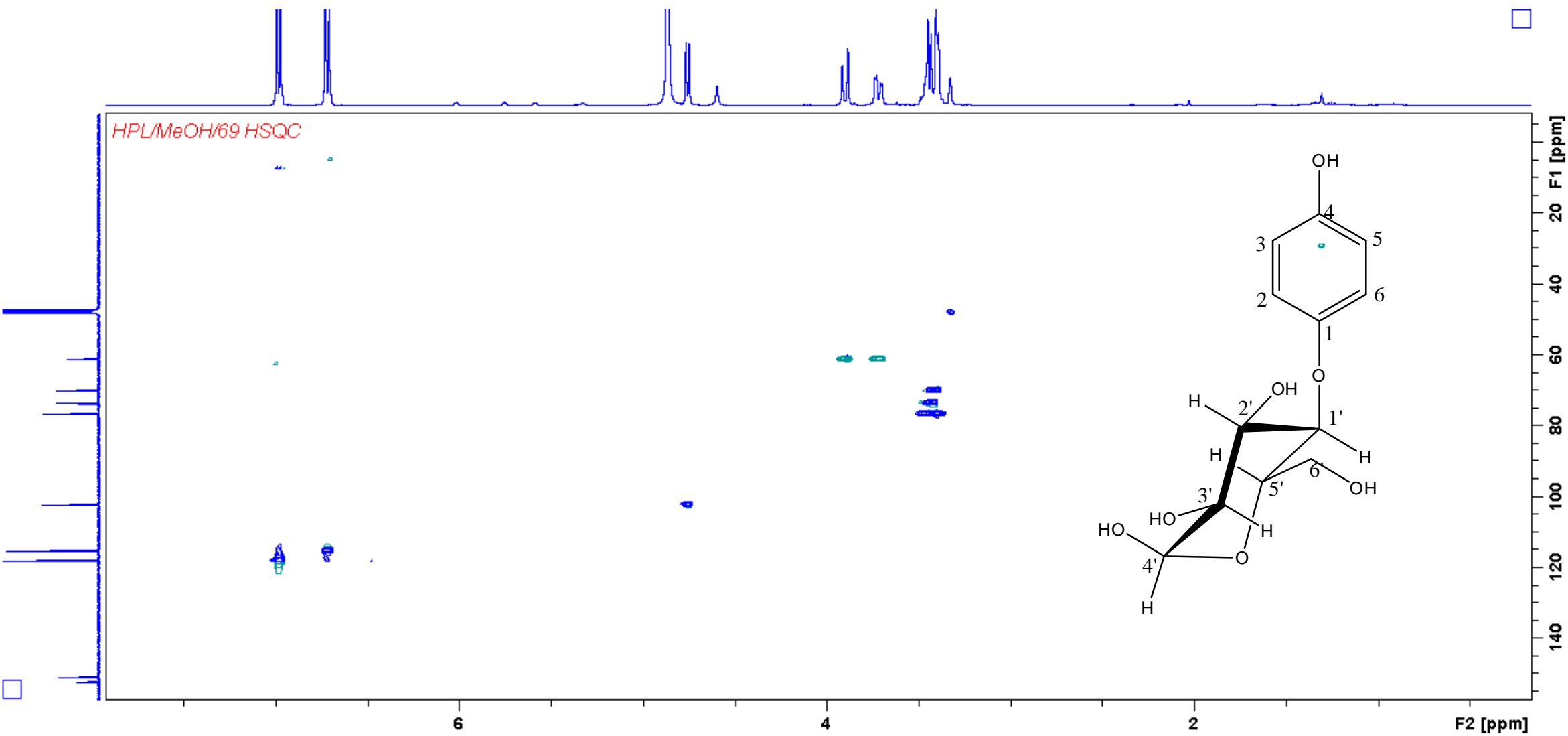
DEPT NMR compound **B7** of arbutin

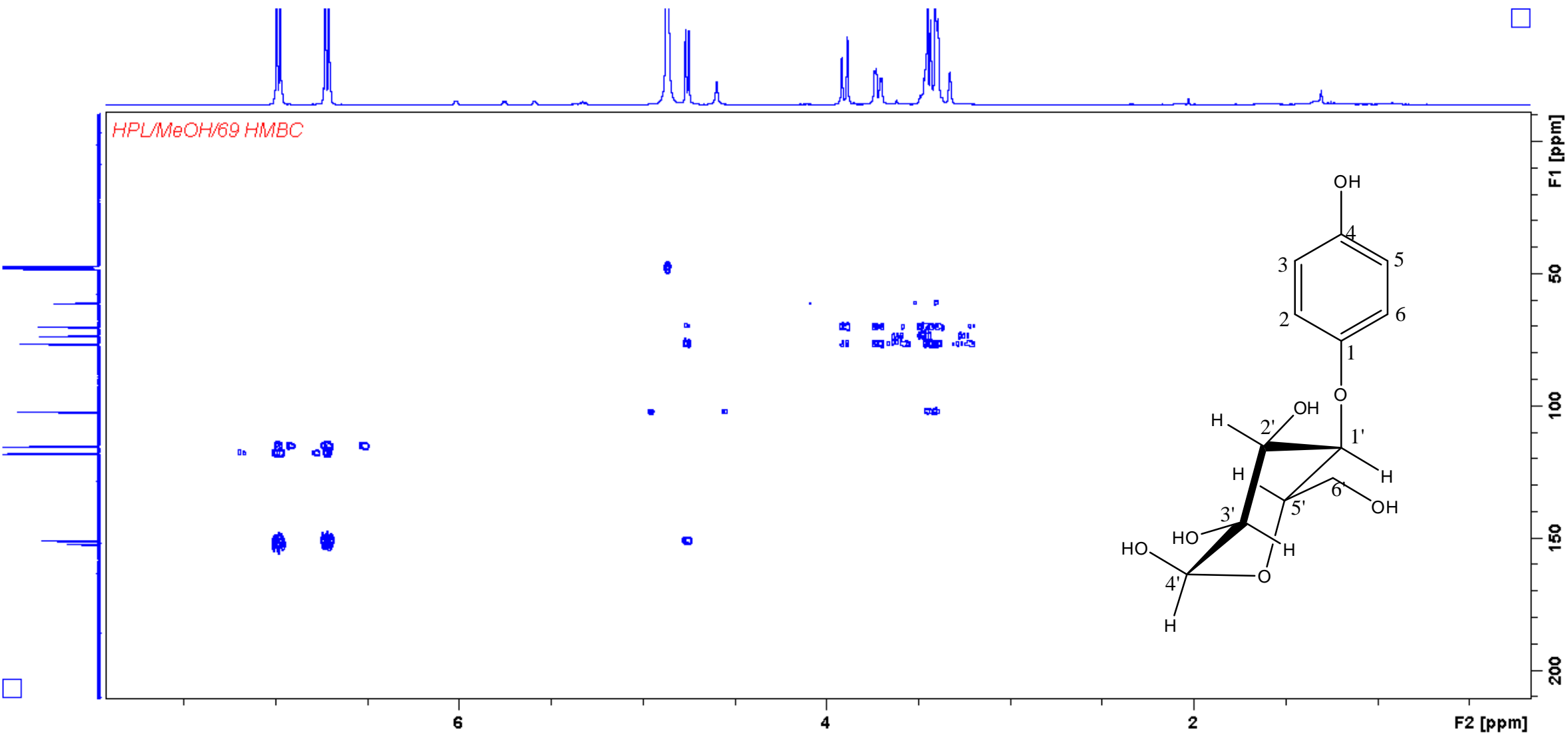


COSY of compound **B7** arbutin



NOESY of compound **B7** arbutin





HMBC of compound **B7** arbutin

Monoisotopic Mass, Even Electron Ions

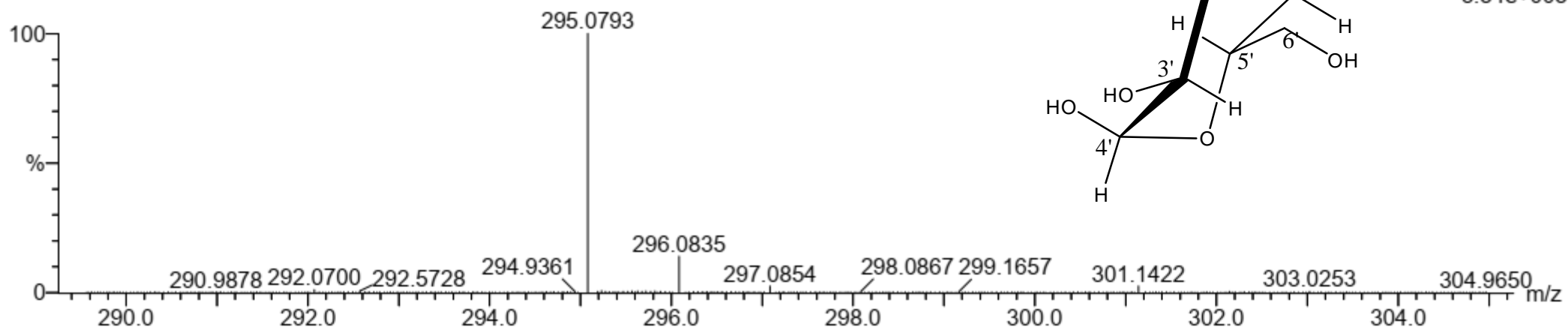
3 formula(e) evaluated with 1 results within limits (up to 50 best isotopic matches for each mass)

Elements Used:

C: 10-15 H: 15-20 O: 5-10 Na: 1-1

FM1 82 (1.380) Cm (1:118)

TOF MS ES+

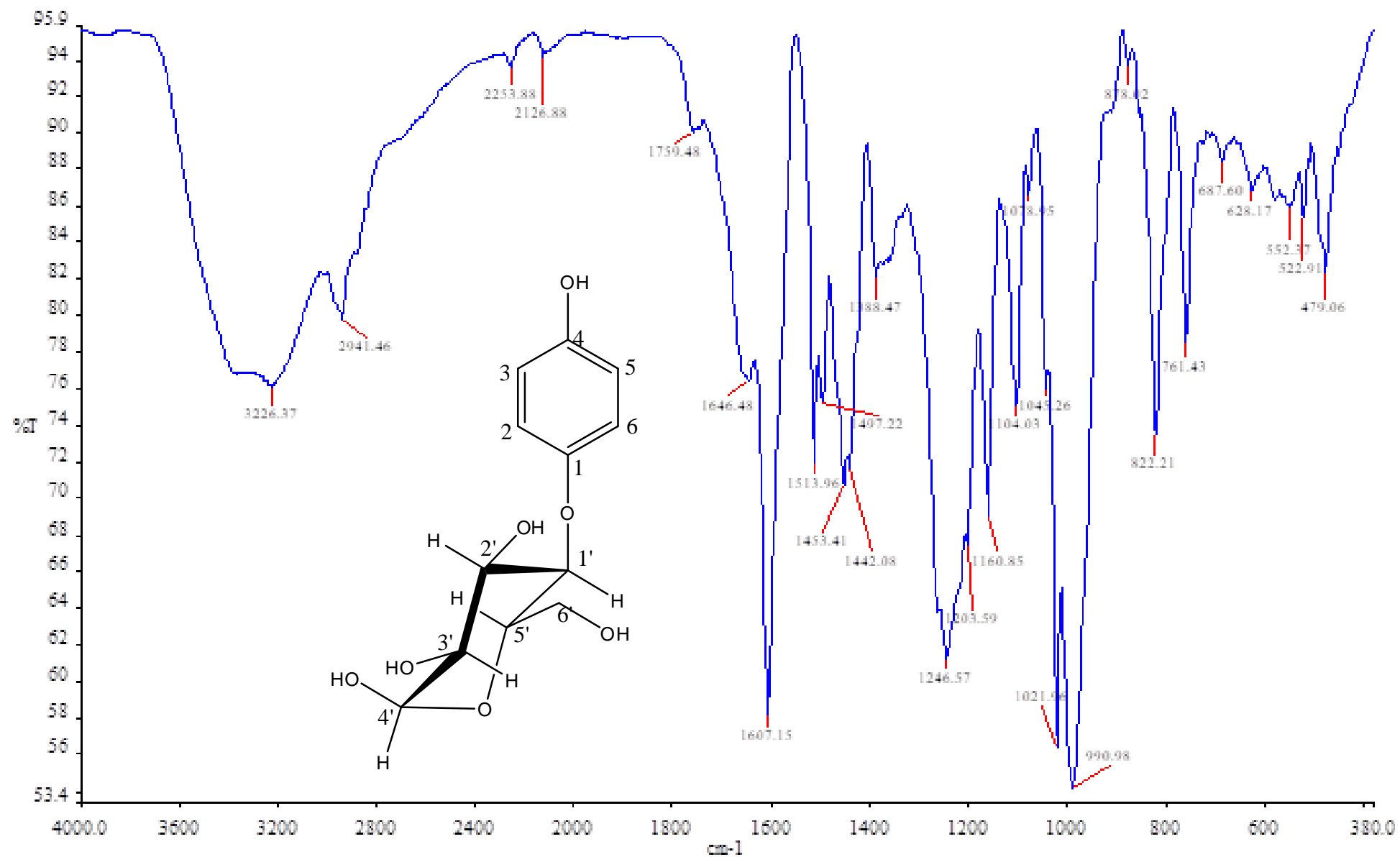


Minimum: -1.5

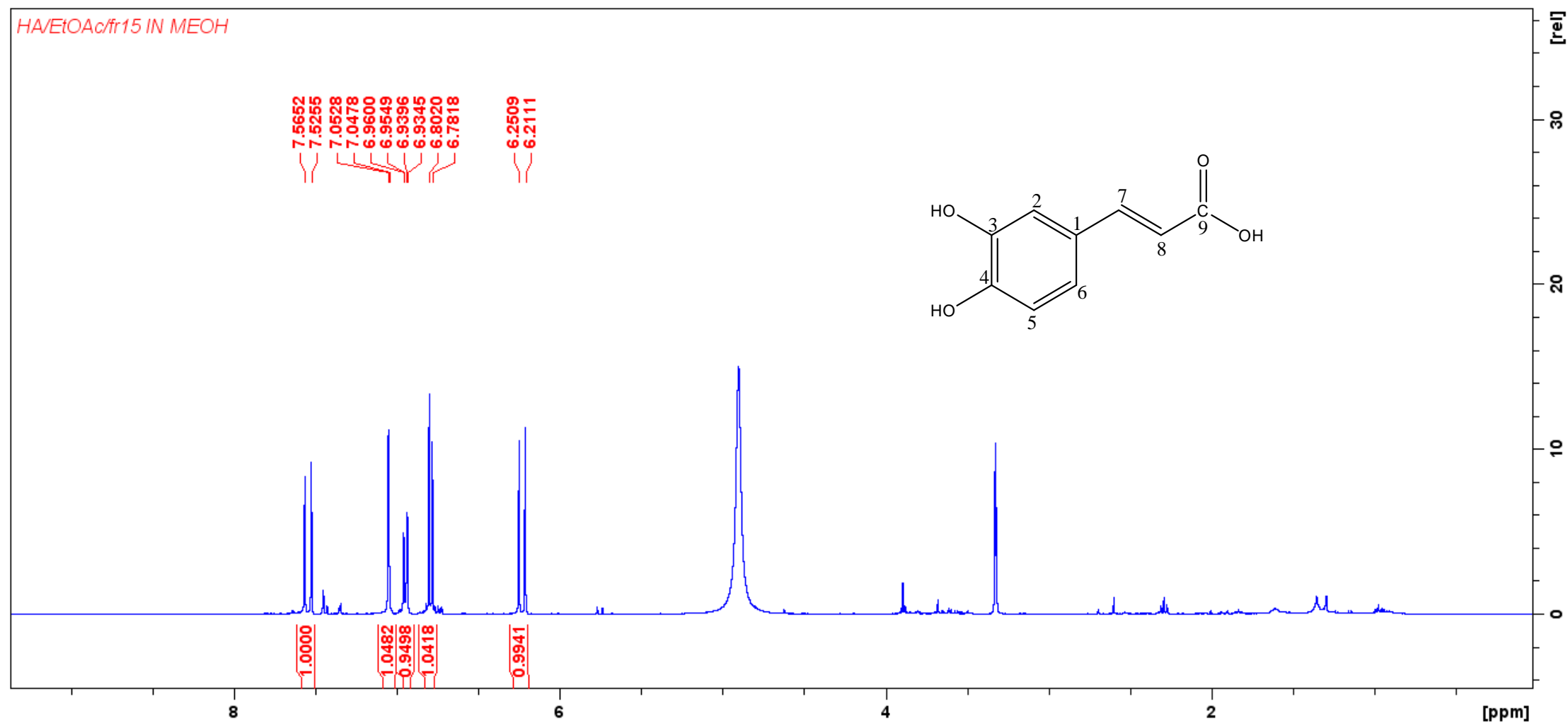
Maximum: 5.0 5.0 50.0

Mass	Calc. Mass	mDa	PPM	DBE	i-FIT	i-FIT (Norm)	Formula
295.0793	295.0794	-0.1	-0.3	4.5	740.4	0.0	C12 H16 O7 Na

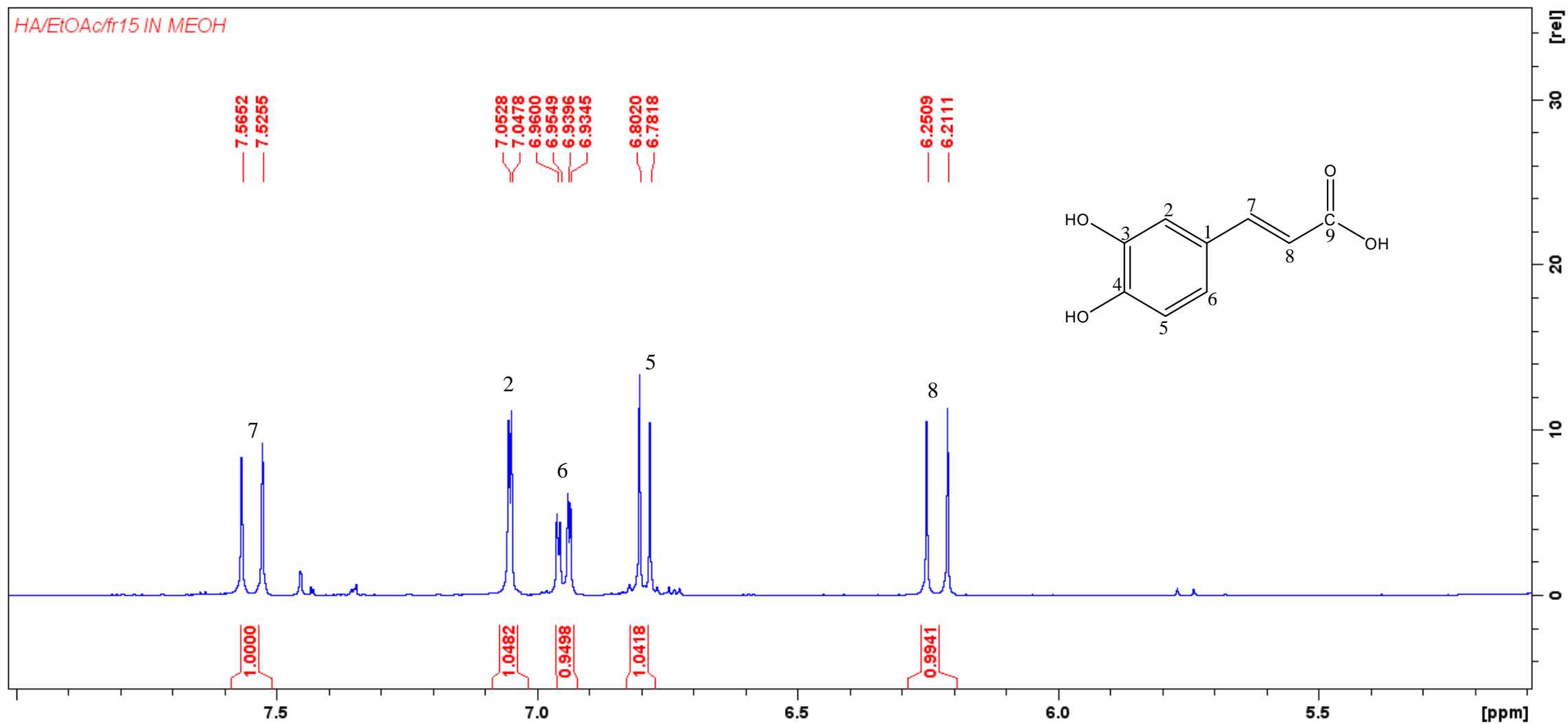
HRMS of compound **B7** arbutin



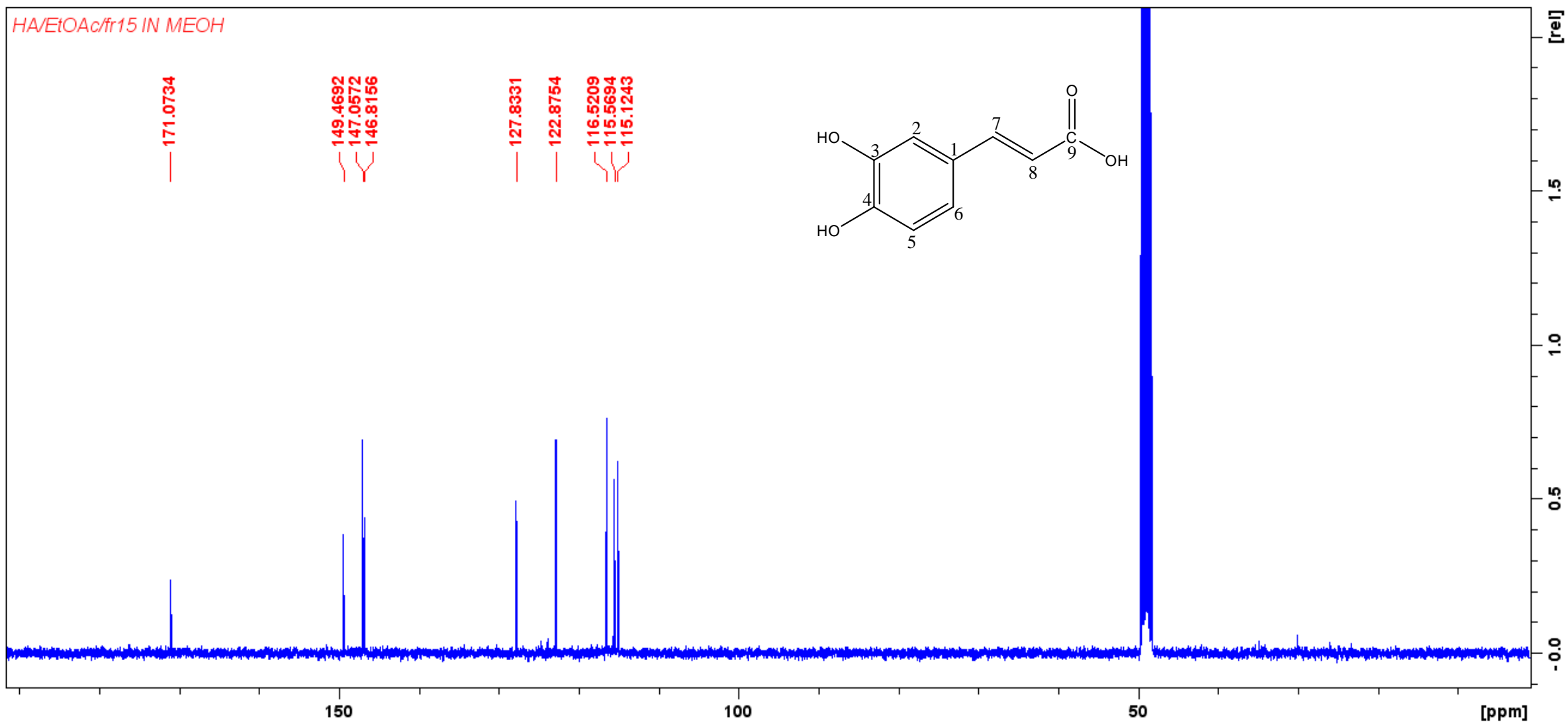
IR of compound **B7** Arbutin



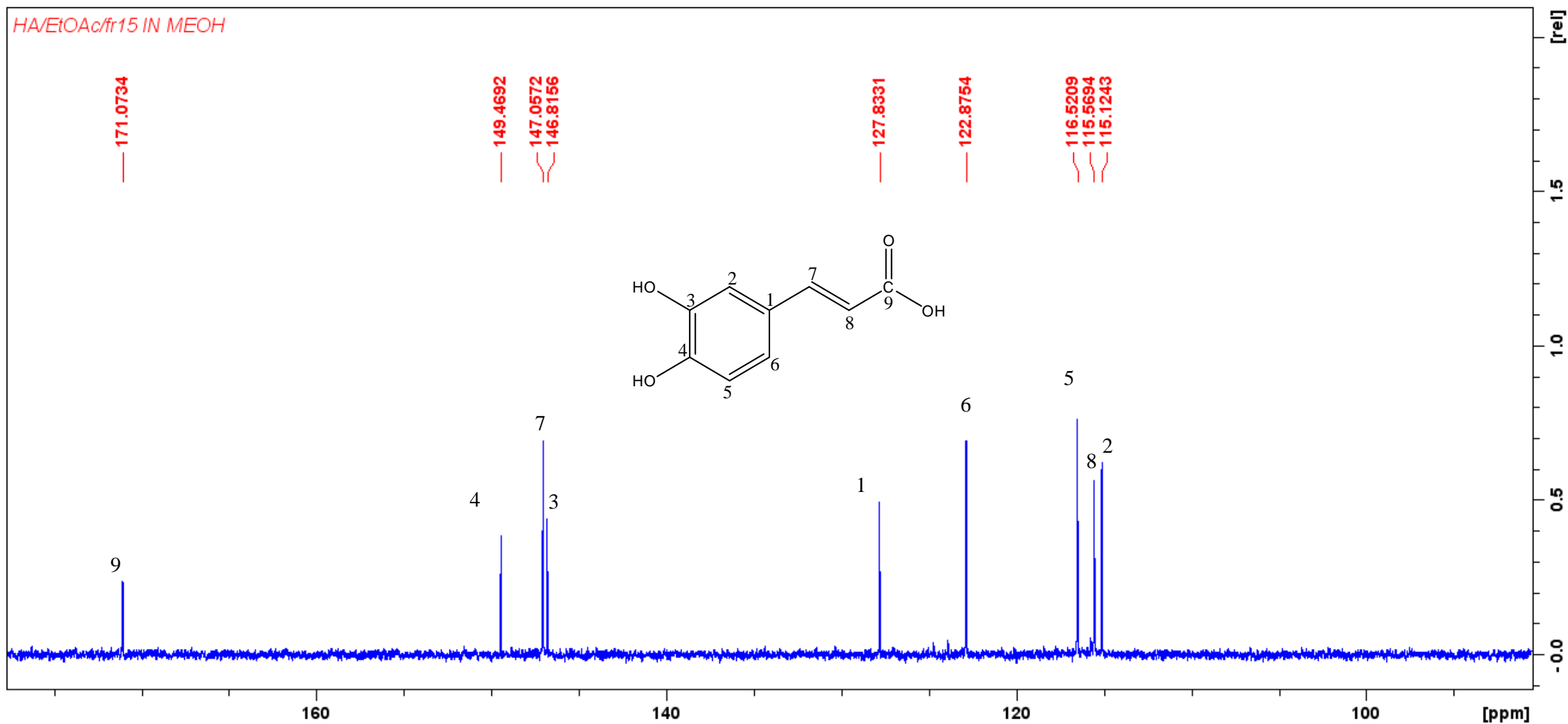
^1H NMR of compound **C3** caffeic acid



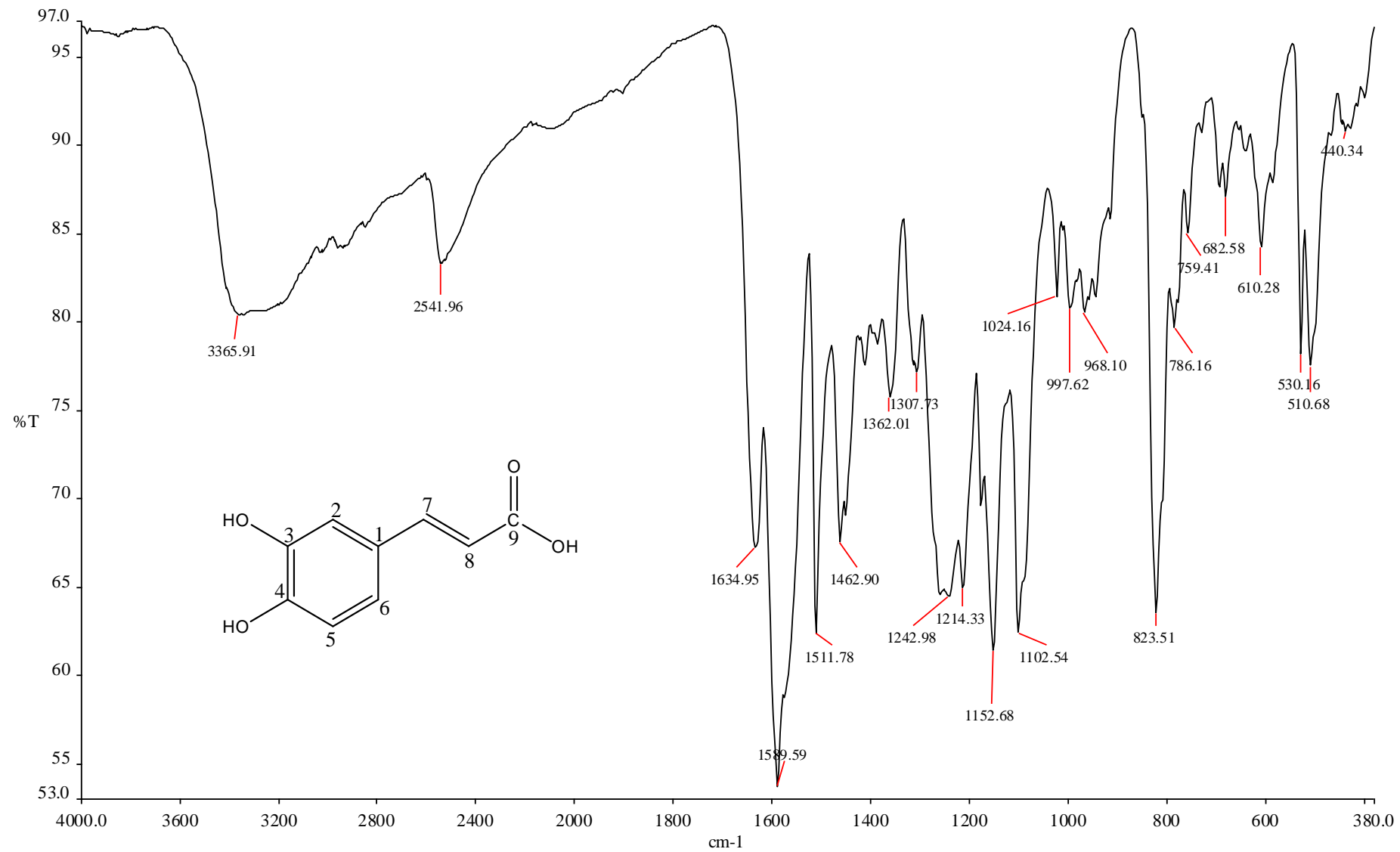
Expanded ^1H NMR of compound C3 caffeic acid



^{13}C NMR of compound C3 caffeic acid



Expanded ^{13}C NMR of compound C3 caffeic acid



IR of compound C3 caffeic acid

Monoisotopic Mass, Even Electron Ions

3 formula(e) evaluated with 1 results within limits (up to 50 best isotopic matches for each mass)

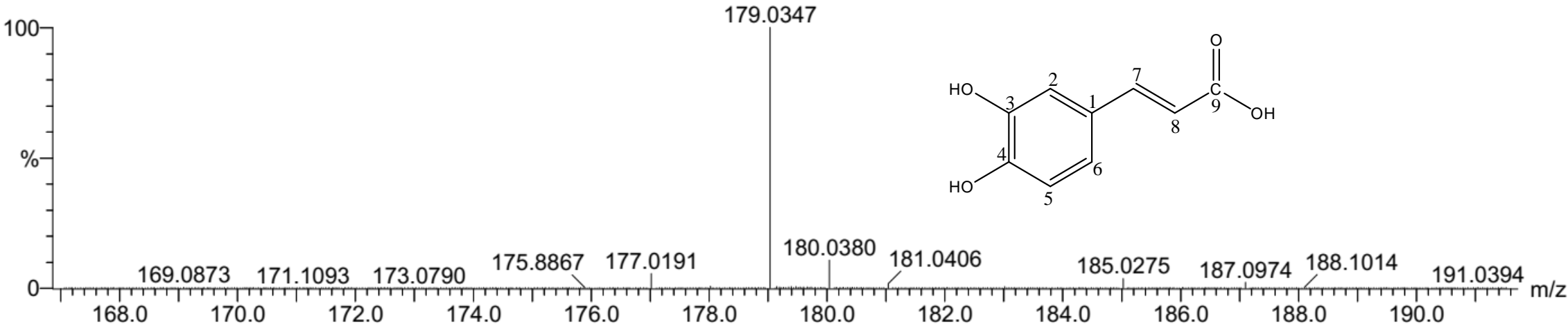
Elements Used:

C: 5-10 H: 5-10 O: 0-5

FM11 72 (1.211) Cm (1:119)

TOF MS ES-

2.01e+005



Minimum: -1.5
Maximum: 5.0 500.0 50.0

Mass	Calc. Mass	mDa	PPM	DBE	i-FIT	i-FIT (Norm)	Formula
179.0347	179.0344	0.3	1.7	6.5	647.5	0.0	C9 H7 O4

HRMS of compound C3 caffeic acid